Argonne NATIONAL LABORATORY

ANL-07/25
ISSN 1931-5007
May 2008

APS SCIENCE 2007

THE ANNUAL REPORT OF THE ADVANCED PHOTON SOURCE AT ARGONNE NATIONAL LABORATORY

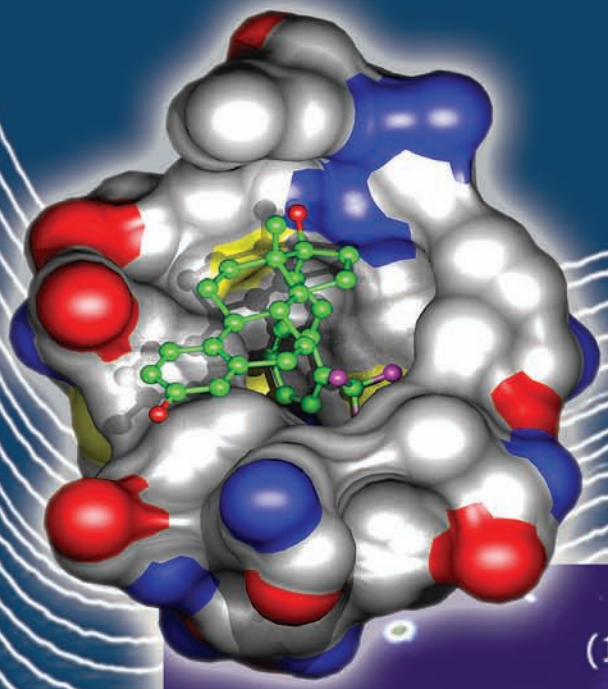

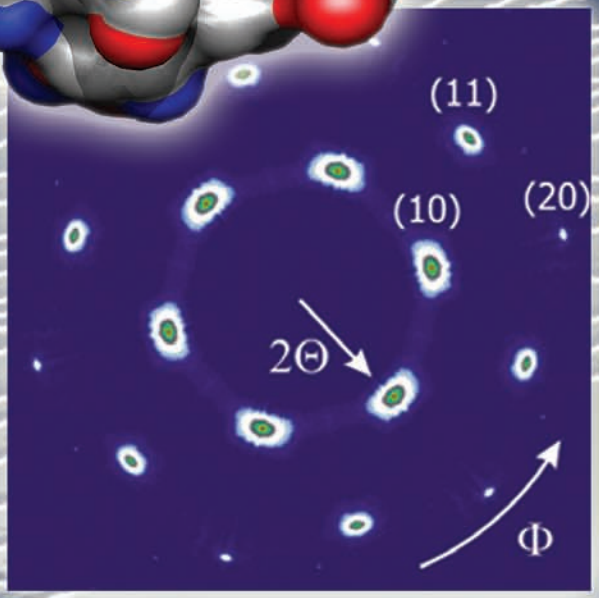

ANL-07/25
ISSN 1931-5015

On the cover: Background: *In situ* x-ray diffraction patterns of $[La_{0.5}Ce_{0.5}]_{64}Al_{16}Ni_5Cu_{15}$ bulk metallic glass under pressure at room temperature (see page 22). Upper figure: Structure of an estrogen receptor ligand-binding domain bound to a novel synthetic estrogen compound, TFMPV-estradiol (see page 102). Lower figure: A scattered intensity data map, in a radial plot to resemble a conventional powder diffraction pattern, showing excellent long-range sixfold orientation of the two-dimensional single crystals of polystyrene-b-2vinyl pyridine (PS-PVP) block copolymer spheres (see page 42).

Argonne is managed by UChicago Argonne, LLC, for the U.S. Department of Energy under contract DE-AC02-06CH11357. The Laboratory's main facility is outside Chicago, at 9700 South Cass Avenue, Argonne, Illinois 60439. For information about Argonne and its pioneering science and technology programs, see www.anl.gov.

The Advanced Photon Source at Argonne National Laboratory is supported by the U. S. Department of Energy, Office of Science, Office of Basic Energy Sciences, under Contract No. DE-AC02-06CH11357.

Availability of This Report:
This report is available at no cost, at http://www.osti.gov/bridge. It is also available on paper to the U.S. Department of Energy and its contractors, for a processing fee, from:
U.S. Department of Energy
Office of Scientific and Technical Information
P.O. Box 62
Oak Ridge, TN 37831-0062
phone (865) 576-8401
fax (865) 576-5728
reports@adonis.osti.gov

Argonne NATIONAL LABORATORY

ANL-07/25
ISSN 1931-5007

APS SCIENCE 2007

The annual report of the Advanced Photon Source at Argonne National Laboratory

The Advanced Photon Source is funded by the U.S. Department of Energy, Office of Science, Office of Basic Energy Sciences

Welcome

Advanced Photon Source Director Murray Gibson (left) and Ali Nassiri (Accelerator Systems Division RF Group Leader) discuss a failed booster rf cavity coupler. The failed component demonstrates our need to anticipate obsolescence, as such a failure had never before occurred in more than 10 years of operations.

Thank you for reading our annual report of research highlights from the Advanced Photon Source (APS). Although these highlights represent less than 10% of the published work from the APS in 2007, they give a flavor of the diversity and impact of user research at our facility. In our strategic planning we aim to foster the growth of existing user communities and foresee new areas of research. This coming year we are engaged in putting together, with our users, a blueprint for the next five years at the APS, and making the case for a set of prioritized investments in beamlines, the accelerator, and infrastructure, each of which will be transformational in terms of our scientific impact. As this is written we are formulating plans for an important user workshop on October 20-21, 2008, to prioritize our strategic plans.

The fruit from past investments can be seen in this report. Examples include the creation of a dedicated beamline for x-ray photon correlation spectroscopy at Sector 8 (e.g., page 10), the evolution of dedicated high-energy x-ray scattering beamlines at sectors 1 and 11 (pages 30 and 124), a dedicated imaging beamline at Sector 32 (page 140), and new beamlines for inelastic scattering and powder diffraction (page 145). A single-pulse facility has been built in collaboration with Sector 14 (BioCARS) and Phil Anfinrud at the National Institutes of Health, which will offer exceptionally high flux for single-pulse diffraction. The nanoprobe at Sector 26, built and operated jointly by the Argonne Center for Nanoscale Materials and the X-ray Operations and Research (XOR) section of the APS X-ray Science Division, has come on line to define the state of the art in nanoscience (page 142).

This year, the commitment to fund a new beamline for intermediate energy x-ray scattering means that only three sectors remain uncommitted. There are strong proposals for all of these sectors.

In the arena of accelerator R&D, we continue to pursue long-term upgrades to the APS, favoring an energy-recovery linac (ERL), and we are engaged in R&D on the key technical issues (page 160). We are also thinking about radically new approaches for future sources made possible by parallel developments, for example, an x-ray laser oscillator (page 163). We continue the development of picosecond short-pulse slicing capability at the APS using crab cavities (page 158).

The accelerator is operating at an unprecedentedly high level of reliability. But I know that this magic comes from the hard work of our engineering support staff. Because of a limited budget, we are challenged to prudently invest our resources in the preventive maintenance—especially of increasingly obsolete systems—that we need in order to maintain a high level of reliability and keep the machine performance at the state of the art. The image on this page shows a component that recently failed, having never failed before, and caused a very unusual downtime of more than 24 hours. We are updating our plans to avoid long down times in the future. But properly executing our plans will require increased resources.

Sir Winston Churchill said that “A pessimist sees the difficulty in every opportunity; an optimist sees the opportunity in every difficulty.” This year, we have suffered budget setbacks that challenge us. The APS is struggling to grow and flourish in a very tough fiscal climate. Even more disappointing is that the early news was good: both houses of Congress, and the Administration, supported increases for the physical sciences and, in particular, for light-source operations. But we need to hang in there. Our review committees have endorsed our current successes and the need for resources to facilitate our future successes. In order to ensure future success, we need the help of our users in advocating to the public the importance of scientific research in general, and the APS in particular. it is imperative that we listen closely to our user needs, and work together to make the case for new investment.

The chairman of our Scientific Advisory Committee, Miles Klein, states, “The high productivity of the APS—a result of the hard work of the staff and management—must be maintained, even with budget problems.” No matter what the budget situation, we must continue to focus on doing things very well, even if that means doing fewer things: operating fewer beamlines for fewer hours, and serving fewer users. We must be ready to do this, but of course it is not the strategy that we are fighting for. We want to expand, not shrink. Our hope is that through the advocacy of our user community we will be able to see the budgets that we need to function properly and serve the broadest community.

In 2007 we were reviewed by The University of Chicago. The committee recognized that the APS is growing in scientific impact, and is now at the world-class level in several areas. In particular, our protein crystallography output exceeds that of any facility in the world, and there are many other high-impact areas, including high-pressure research and high-energy scattering. The integration of former collaborative access teams (CATs) into XOR sectors has been viewed as a success, although finding the resources required to properly staff these sectors and maintain the engagement of previous collaborative access team members remains a challenge.

We have learned some hard lessons this year. A user's near-miss electrical incident has led us to reinforce our user training (page 171). In the short-pulse x-ray project, we experienced setbacks with our plans for room temperature cavities as a short-term solution. We are now focusing on the ultimate solution: superconducting radio-frequency cavities.

The 2007 APSUO Steering Committee. Left to right: Tim Graber (Chair, The University of Chicago), Gene Ice (Oak Ridge National Laboratory), Linda Young (Argonne National Laboratory), David Reis (University of Michigan), Anne Mulichak (The University of Chicago), Paul Evans (University of Wisconsin-Madison), Nadia Leyarovska (Argonne National Laboratory), Paul Fuoss (Argonne National Laboratory), J. Murray Gibson (Argonne National Laboratory), Nino Campobasso (Glaxo SmithKline, Inc.), Simon Mochrie (Yale University), Barbara Golden (Purdue University). Not pictured: Simon Billinge (Columbia University), Millie Firestone (Argonne National Laboratory), Laurence Lurio (Northern Illinois University).

At Argonne, we have many positive developments that will favor APS research, such as the new Argonne Leadership Computation Facility, which will bring petaflop-scale computation to the Laboratory. On the other hand, Department of Energy (DOE) funding shortfalls led to the premature closure of the historic Intense Pulsed Neutron Source, the first DOE-Basic Energy Sciences user facility. We hope to maintain our expertise in neutron scattering at Argonne through collaboration with the Spallation Neutron Source and a proposal for a new Argonne Scattering Imaging and Spectroscopy Institute for tackling grand-challenge problems through innovative software.

The APS has been a key partner in construction of the world's first x-ray laser, the Linac Coherent Light Source (LCLS) at the Stanford Linear Accelerator Center. We have delivered the undulator system on time, and the LCLS anticipates first light in 2008 (see page 165 for "A New Beam Position Monitor System for the LCLS"). We are also involved in other innovative accelerator projects such as the International Linear Collider.

We at the APS are immensely proud of the societal impact of our research. Following are comments from the chairs of our advisory committees.

J. Murray Gibson (jmgibson@aps.anl.gov)

APS User Organization

The year 2007 was an active one for the Advanced Photon Source User Organization (APSUO) Steering Committee. It began on a high note with the organization of Users' Week, a jointly held ANL facilities meeting with participants from the APS, the Center for Nanoscale Materials, the Electron Microscopy Center, and the Intense Pulsed Neutron Source. Each facility individually highlighted their most compelling work, held independent science sessions, and collectively participated in a joint science session followed by 11 cross-disciplinary workshops. In anticipation of the proposed APS upgrade, several workshops emphasized science that would benefit from the improved properties of a fourth-generation source such as an ERL. In recognition of their significant contributions to synchrotron science, Andrzej Joachimiak (Argonne) and Gerold "Gerd" Rosenbaum (Argonne and the University of Georgia) received the biennial Arthur H. Compton Award given by the APS and the APSUO (see page 150).

The APSUO invests considerable effort—and places a high priority on—advocacy for the facility. This was especially

Continued on page 4

The APS Scientific Advisory Committee as of January 3, 2008. Back row (standing) from left: Richard Leapman (National Institutes of Health), Glenn Waychunas (Lawrence Berkeley National Laboratory), Piero Pianetta (Stanford Synchrotron Radiation Laboratory), John Helliwell (University of Manchester), Howard Einspahr (Bristol-Myers Squibb, retired), G. Slade Cargill (Lehigh University), Michael Wasielewski (Northwestern University), Denis Keane (*ex officio*, Northwestern University), Jens Als-Nielsen (Copenhagen University). Middle row (seated) from left: Soichi Wakatsuki (High Energy Accelerator Research Organization [KEK]), Timothy Graber (*ex officio*, The University of Chicago), Dan Neumann (Center for Neutron Research, National Institute of Standards and Technology [NIST], replacing Patrick Gallagher, NIST), Wei Yang (National Institutes of Health). Front row (seated) from left: J. Murray Gibson (Argonne National Laboratory), Miles Klein (Chair, University of Illinois at Urbana-Champaign), Michelle Buchanan (Oak Ridge National Laboratory). Not pictured: Donald Weidner (State University of New York, Stony Brook)

"Welcome" *continued from page 3*

critical given the continuing budget resolution during the 2007 fiscal year and the omnibus budget bill passed by Congress in December of 2007. The APSUO partnered with the American Physical Society and National User Facilities Organization to provide effective advocacy.

It was suggested during the joint APSUO/Partner User Council (PUC) meeting in August that beamline-specific user advisory committees (UACs) be formed for XOR sectors. An ad hoc subcommittee of the APSUO and PUC was convened to define the role of the UAC and draft a charter, which was approved by both the APSUO and PUC at their October 2007 meetings. These committees will work closely with the APS group leaders and beamline scientists at each sector by offering advice on a range of issues from instrumentation to a scientific vision for the sector. Committee membership will be posted appropriately and approved on an ongoing basis by the APSUO Steering Committee. As the APS moves toward a future upgrade of the facility, these committees will play a crucial role by communicating the particular needs of various segments of the community to APS management.

Timothy J. Graber (The University of Chicago), Chair
(graber@cars.uchicago.edu)

Scientific Advisory Committee

The Science Advisory Committee (SAC) meeting for 2007 took place on January 23-25. The SAC members and representatives from the APS were joined by two invited reviewers: Sine Larsen (European Synchrotron Radiation Facility) and Doug Ohlendorf (University of Minnesota). In addition to two days of updates, discussions, and planning, the SAC reviewed and made recommendations to the APS concerning reports of reviews of the ten sectors and beamlines carried out during 2006, eight ongoing partner user programs, two collaborative development team (CDT) proposals, and other issues carried over from the 2006 meeting. The SAC also participated in the Cross-cut Review of Research in Structural Biology, chaired by John Helliwell, which was held in conjunction with the SAC meeting. SAC members chaired and participated in the following additional cross-cut and sector reviews in 2007: SGX-CAT, Sector 31 (Howard Einspahr, chair); Bio-CAT, Sector 18 (Richard Leapman, chair); Biology, Polymers, and Soft Materials Cross-cut (Michael Wasielewski, chair); Time-resolved Science Cross-cut (Glenn Waychunas, chair); Materials Physics,

The APS Partner User Council as of January 18, 2008. Back row from left: Jörg M. Maser (Argonne National Laboratory), John J. Chrzas (University of Georgia), Malcom Capel (Cornell University), Stephen R. Sutton (The University of Chicago), Guoyin Shen (Carnegie Institution of Washington; High Pressure-CAT), Robert A. Gordon (Simon Fraser University), Bruce A. Bunker (University of Notre Dame), Keith Brister (Northwestern University). Front row from left: Lisa J. Keefe (The University of Chicago), Robert F. Fischetti (Argonne National Laboratory), Denis T. Keane (Northwestern University), J. Murray Gibson (Argonne National Laboratory), Vukica Srajer (The University of Chicago). Not pictured: Douglas S. Robinson (Iowa State University), P. James Viccaro (The University of Chicago), Thomas C Irving (Illinois Institute of Technology), Andrzej Joachimiak (Argonne National Laboratory), John P. Hill (Brookhaven National Laboratory), Stephen R. Wasserman (SGX Pharmaceuticals, Inc.), Chris J. Benmore (Argonne National Laboratory), Paul Fenter (Argonne National Laboratory), J. Kent Blasie (University of Pennsylvania).

Materials Science, and Engineering Materials Cross-cut (Slade Cargill, chair); Condensed Matter and Theory Cross-cut (Miles Klein, chair); Geoscience and Magnetism Cross-cut (Miles Klein, chair). *Miles V. Klein (University of Illinois at Urbana-Champaign), Chair (mvklein@uiuc.edu)*

Partner User Council

During 2007, the APS Partner User Council (PUC) continued to fulfill its role as both an advisory group to the Director of the APS, Murray Gibson, and as an advocacy group for its members. The PUC Executive Board meets quarterly with APS management and in executive session, and consists of the Directors of all CATs and CDTs and the chairs of all XOR advisory boards. The PUC meets at least annually, and is made up of the executive board and representatives of all partner users, including the spokesperson of each partner user proposal, the chair of each special interest group, the InterCAT Technical Workgroup chair, and an "at-large" representative from each sector. Two continuing topics of interest to the PUC in 2007 were APS upgrade plans, both mid-term and long-term—especially the proposed ERL, and changes to proprietary charges for work at APS in the wake of recommendations from the DOE Inspector General audit.

Several issues were worked on in concert with the APSUO (sometimes in joint sessions), including a broad-ranging discussion of beam time set-asides on multi-technique beamlines and a proposal for the formation of new XOR user advisory committees. A sub-group of the PUC Executive Board, consisting of the CAT Directors of the structural biology sectors, met several times during the year to produce a document responding to the recommendations from the cross-cut review of structural biology at the APS held in January 2007. Partner User Council representatives met during the year with many of the review committees, in particular at a round-table discussion with The University of Chicago review committee in September and at a luncheon with the DOE review committee in December. In all of these efforts, and in the weekly and monthly interactions between PUC members and APS management, clear lines of communication remain open, and the PUC and the APS work creatively together to improve the APS technically and scientifically. *Denis T. Keane (Northwestern University), Chair (dtkeane@northwestern.edu)*

The Advanced Photon Source facility at Argonne National Laboratory

The APS occupies an 80-acre site on the Argonne campus, about 25 miles from downtown Chicago, Illinois. For directions to Argonne, see www.anl.gov/Visiting/anlil.html.

Access to beam time at the APS

Beam time at the APS can be obtained either as a general user (a researcher not associated with a particular beamline) or as a partner user (e.g., a member of a collaborative access team [CAT], a partner user proposer, or a member of a collaborative development team [CDT]). If you are a CAT or CDT member, contact your CAT or CDT for instructions on applying for CAT/CDT beam time. At minimum, 25% of the time at all operating beamlines is available to general users, but many offer considerably more general user time—up to 80% on X-ray Operations and Research beamlines, for example.

How general users can apply for beam time at the APS:
1) First-time users should read the information for new users found on our Web site at http://www.aps.anl.gov/user/ new_users.html before applying for beam time. Also, certain administrative requirements must be completed. In particular, a user agreement between the APS and each research-sponsoring institution must be in place.

2) To choose the appropriate technique(s) and beamline(s), see the beamlines directory in the "Data" section of this volume or at http://beam.aps.anl.gov/pls/apsweb/beamline_display_pkg.beamline_dir.

3) Submit a proposal via the Web-based system. Proposals are evaluated before each user run. For more information see the proposal system overview at:
http://www.aps.anl.gov/Users/Scientific_Access/General_User/General_User_Proposal/Instructions/Proposer/.

Contact us

For more information about the Advanced Photon Source or to order additional copies of this, or previous, issues of *APS Science*, send an e-mail to apsinfo@aps.anl.gov, or write to APS info, Bldg. 401, Rm. A4115, Argonne National Laboratory, 9700 S. Cass Ave., Argonne, IL 60439.

Table of Contents

APS Science is also available on line in PDF format at http://www.aps.anl.gov/Science/Reports/

For news from, and information about, light sources worldwide, visit www.lightsources.org

APS sectors:

Sectors 1-4: XOR 1-4
X-ray Operations and Research (XOR)

Sector 5: DND-CAT
DuPont-Northwestern-Dow Collaborative Access Team (CAT)

Sector 6: MU/XOR
Midwest Universities/XOR

Sector 7: XOR 7

Sector 8: XOR 8

Sector 9: XOR/CMC
XOR/Complex Materials Consortium

Sector 10: MR-CAT
Materials Research CAT

Sectors 11 and 12: XOR/BESSRC
XOR/Basic Energy Sciences Synchrotron Radiation Center

Sectors 13 through 15: CARS
Center for Advanced Radiation Sources:
GeoSoilEnviroCARS—sector 13
BioCARS—sector 14
ChemMatCARS—sector 15

Sector 16: HP-CAT
High Pressure CAT

Sector 17: IMCA-CAT
Industrial Macromolecular Crystallography Association CAT

Sector 18: Bio-CAT
Biophysics CAT

Sector 19: SBC-CAT
Structural Biology Center CAT

Sector 20: XOR/PNC
XOR/Pacific Northwest Consortium

Sector 21: LS-CAT
Life Sciences CAT

Sector 22: SER-CAT
Southeast Regional CAT

Sector 23: GM/CA-CAT
General Medicine and Cancer Institutes CAT

Sector 24: NE-CAT
Northeastern CAT

Sector 26: CNM/XOR
Center for Nanoscale Materials/XOR

Sector 30: XOR/IXS
XOR/Inelastic X-ray Scattering

Sector 31: SGX-CAT
SGX SGX Pharmaceuticals, Inc.

Sector 32: XOR 32

Sectors 33 and 34: XOR/UNI
XOR/University-National Laboratory-Industry

The Advanced Photon Source (APS), a national synchrotron radiation research facility at the U.S. Department of Energy's (DOE's) Argonne National Laboratory in Illinois, provides this nation's most brilliant x-ray beams for science. Research by APS users extends from the center of the Earth to outer space, from new information on combustion engines and microcircuits to new drugs and nanotechnologies whose scale is measured in billionths of a meter. The APS, which is funded by the DOE Office of Science, Office of Basic Energy Sciences, enhances America's competitiveness in such areas as superconductors, semiconductors, pharmaceuticals, polymers, and catalysts, and promises to have far-reaching impact on our technology, economy, health, and fundamental knowledge of the materials that make up our world.

At the APS, a "sector" comprises the radiation sources (potentially one of the two bending magnets, and one insertion device, although the number of insertion devices in the straight sections of the storage ring can vary), and the beamlines, enclosures, and instrumentation that are associated with a particular storage ring sector. The APS has 35 sectors, 34 of which are dedicated to user science and experimental apparatus. The 35th has limited space for instrumentation and is used primarily for accelerator-related studies.

X-ray Operations and Research sectors comprise those beamlines operated by the APS. Some XOR sectors have historic CAT origins, e.g. XOR/PNC.

Collaborative access team (CAT) sectors comprise beamlines operated by independent groups made up of scientists from universities, industry, and/or research laboratories.

To access the APS as **general users** (GUs), researchers submit proposals that can be active for up to two years. These proposals are reviewed and rated by one of nine proposal review panels comprising scientific peers, generally not affiliated with the APS. Beam time is then allocated by either of two APS Beam Time Allocation Committees.

Those users who propose to carry out research programs beyond the scope of the GU program may apply to become **partner users** on any beamline operated by the APS. Prospective Partner User Proposals are peer reviewed by a subset of the APS Scientific Advisory Committee. Final decisions on the appointment of partner users are made by APS management.

Beamlines, sector designations, disciplines, techniques, radiation source, and general-user status for particular beamlines are displayed with the science highlights that follow. This information can be viewed in whole at :
http://beam.aps.anl.gov/pls/apsweb/beamline_display_pkg.beamline_dir

NOTE: In this PDF version, information in these boxes will link you to the beamline page in the Beamline Directory.

THE ADVANCED PHOTON SOURCE

Sector Allocations & Disciplines

Source Configuration

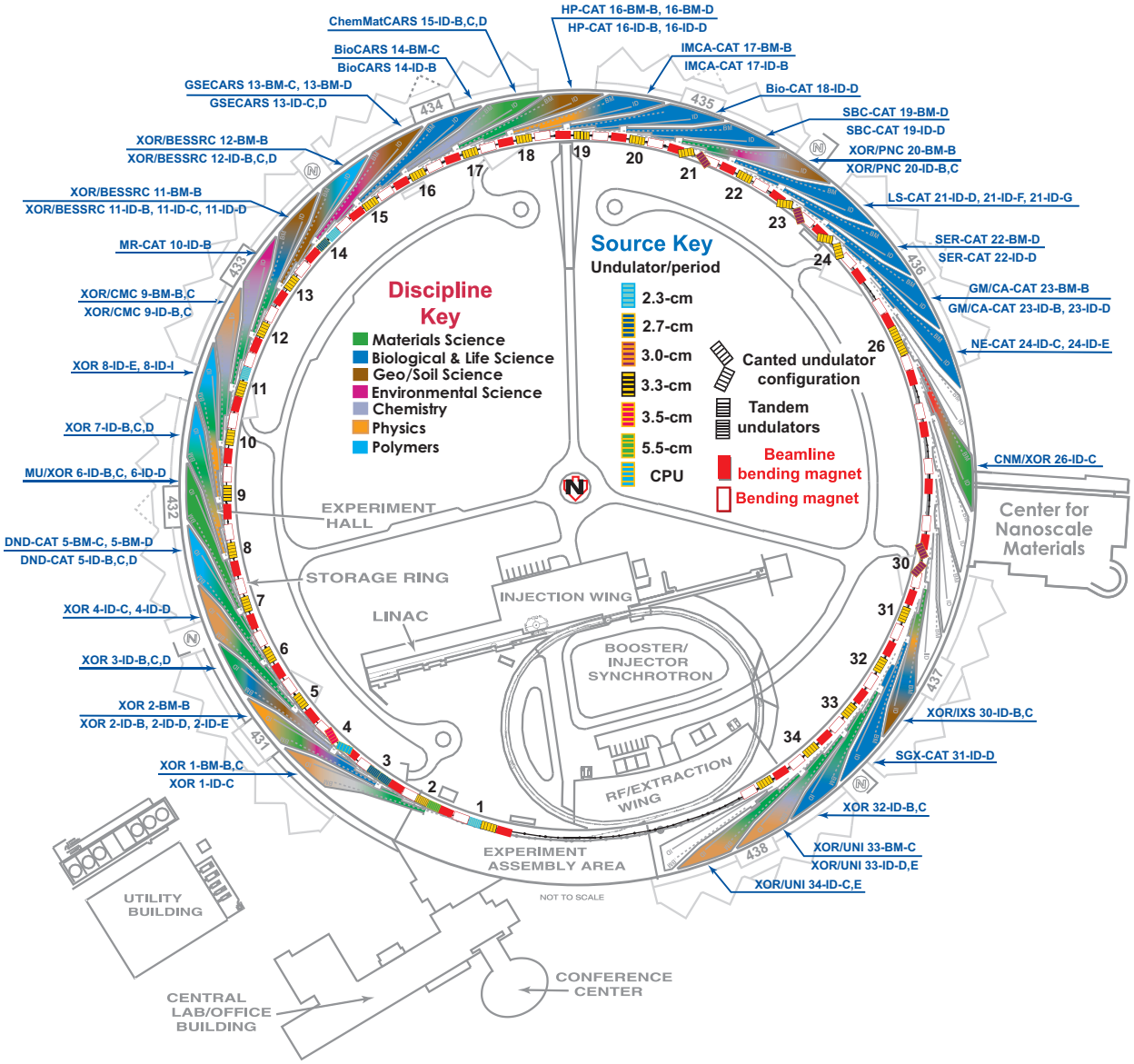

Surprising Low-Temperature Domain Wall Fluctuations in Antiferromagnets

33-ID-D,E • XOR/UNI • Materials science, physics, chemistry • Anomalous and resonant scattering (hard x-ray), diffuse x-ray scattering, x-ray reflectivity, surface diffraction, x-ray standing waves, general Diffraction • 3.3-cm Undulator A • Accepting general users

8-ID-E • XOR • Materials science, polymer science, physics • Intensity fluctuation spectroscopy, x-ray reflectivity, x-ray photon correlation spectroscopy, grazing incidence small-angle x-ray scattering • 3.3-cm Undulator A • Accepting general users

Domain formation is inherent in most types of magnetic materials because of their crystal symmetry. In each domain, all of the electron spins are coupled together in a preferential direction, and thermal fluctuations can cause random movement of the boundary walls between domains. In the case of a ferromagnetic material such as iron, this "thermal noise" can be measured by detecting small jumps in the magnetization by using only a tiny coil of wire placed near a sample of the material. But measuring similar fluctuations in antiferromagnetic materials such as chromium (Cr) had not been possible because the magnetic moments of neighboring atoms point in opposite directions, preventing bulk magnetization and making it impossible to detect fluctuations in the domain walls of an antiferromagnet via the use of conventional magnetization probes. Researchers using a beam of coherent x-rays from XOR beamlines 33-ID-D,E and 8-ID-E discovered a way to eavesdrop on the antiferromagnetic domain walls in chromium.

Researchers from Argonne, The University of Chicago, and University College London, employed x-ray photon correlation spectroscopy (XPCS) to exploit the fact that when a disordered material is illuminated by coherent incident radiation, an interference pattern called a "speckle" pattern is observed. This speckle pattern is uniquely determined by the instantaneous spatial distribution of the disorder in the material; if the spatial distribution changes in time, the corresponding speckle pattern will also change, so it is possible to extract information about the dynamics of a disordered system by analyzing the time correlation of one speckle.

It is known that the antiferromagnetism in Cr arises from its conduction electrons, rather than the localized electrons themselves. The electrons surrounding each Cr atom have a magnetization opposite to those of the nearest Cr neighbors. This results in a sinusoidal magnetic structure called a spin density wave (SDW) of wavelength λ = 6 to 8 nm. Although the x-rays could not probe the SDWs directly, each SDW is accompanied by a commensurate electron charge density wave (CDW). The team scattered a coherent beam of x-rays from a Cr sample, and the resulting speckle pattern (Fig. 1) was captured by using a charge-coupled device camera over a period of several hours. The precise appearance of the speckle pattern is related to the arrangement of CDWs in a tiny portion of the sample. By watching how the speckle changed over time, the group was able to observe changes in the antiferromagnetic domains over distances as small as 1 μm. These results cannot be attributed to drift of the x-ray beam, motion of crystalline defects, or other similar experimental artifacts not related to magnetic domain dynamics because the reference speckle sensitive to these motions is stable over at least ~20,000 s, while the speckles related to domain wall structure are completely uncorrelated after 100 s to 3,000 s.

< Fig. 1. By observing changes in the coherent x-ray speckle pattern, researchers can investigate nanoscale dynamics of antiferromagnetic domain walls and observe a crossover from classical to quantum behavior.

In addition, the group observed that domain fluctuations continued, even at temperatures as low as 4K. This result is quite surprising because domain walls are relatively large structures that require a significant amount of thermal energy to move. To account for this unexpected result, the group used measured relaxation times to construct a simple model of electrons hopping across the domain walls, which suggests that at very low temperatures the walls are moving because of quantum tunneling instead of thermal activation.

Antiferromagnetic materials are currently used in read heads for magnetic storage devices, and they show promise for use in spintronic devices, which could make use of both the spin and charge of the electron to process information. However, any future technologies that rely on the precise location of antiferromagnetic domains would be affected by the instability of the antiferromagnetism. The current findings light the way toward engineering stability in these materials; for example, the introduction of defects or impurities in the antiferromagnetic materials would tend to fix the domain locations.

The researchers are now turning their attention to the study of other magnetic materials, including those that can contain both ferromagnetic and antiferromagnetic domains. They also believe that the XPCS technique could be used to study quantum phase transitions in antiferromagnets and to gain insight into ways in which antiferromagnetic nanoparticles might be engineered into a valuable new class of material, one in which magnetization can be switched quickly and with negligible energy loss, ideal for use in high-frequency electronic devices. — *Luis Nasser*

See: O.G. Shpyrko[1]*, E.D. Isaacs[1,3], J.M. Logan[3], Yejun Feng[3], G. Aeppli[4], R. Jaramillo[3], H.C. Kim[3], T.F. Rosenbaum[3], P. Zschack[2], M. Sprung[2], S. Narayanan[2], and A.R. Sandy[2], "Direct measurement of antiferromagnetic domain fluctuations," Nature **447**, 68 (3 May 2007). DOI: 0.1038/nature05776

Author affiliations: [1]Center for Nanoscale Materials, Argonne National Laboratory; [2]Advanced Photon Source, Argonne National Laboratory; [3]James Franck Institute and Department of Physics, The University of Chicago; [4]London Centre for Nanotechnology and Department of Physics and Astronomy, University College London

Correspondence: *oshpyrko@anl.gov

Use of the Center for Nanoscale Materials and Advanced Photon Source was supported by the U.S. Department of Energy, Office of Science, Office of Basic Energy Sciences. Work at the University of Chicago was supported by the National Science Foundation, while that in London was funded by a Royal Society Wolfson Research Merit Award and the Basic Technologies program of RCUK.

Oxygen Reduction and Superconductivity in *T′*-Structure Cuprates

High-temperature superconductors are typically antiferromagnetic cuprate insulators made up of stacks of conducting CuO_2 planes separated by block layers of charge reservoir. The superconductivity arises when electrons or holes—electron vacancies that behave like positively charged electrons—are doped into the CuO_2 planes. Holes doped into a sample of the cuprate material effectively destroy the antiferromagnetic order in the planes and cause the material to transition into a metallic superconducting state. On the other hand, it is known that in materials such as *T′*-structured R_2CuO_4 (R is Nd, Pr, La, Ce, and so on), electron doping is not enough, and superconductivity is only observed after the sample is annealed in a low-oxygen environment to remove some oxygen from the CuO_2 planes. The exact role played by this annealing process in achieving superconductivity has been a long-standing unsolved question. Now, a group of researchers using two APS beamlines has elucidated the microscopic details of the role played by the annealing process.

Researchers from the University of Tennessee, the National Institute of Standards and Technology, the University of Maryland, Oak Ridge National Laboratory, Brigham Young University, Argonne, and the Central Research Institute of Electric Power Industry employed x-ray and neutron scattering data in tandem with chemical and thermogravimetric analysis (TGA) in single crystals and powders of $Pr_{0.88}LaCe_{0.12}CuO_4$ (PLCCO). The group noted that the appearance of superconductivity after annealing was accompanied by the creation of an epitaxially grown impurity phase of R_2O_3, which is not observed in the as-grown materials. This impurity phase has a cubic structure whose lattice parameter matches the in-plane lattice parameter of the *T′* phase but is about 10% less than the out-of-plane lattice parameter of the *T′* phase; it is therefore easy to predict the location of Bragg reflections from the impurity phase, and to distinguish them clearly from Bragg peaks due to thermal diffuse scattering in the pure as-grown samples.

The single-crystal x-ray diffraction measurements were carried out at room temperature by using 30-keV x-rays at the XOR/BESSRC 11-ID-D beamline at the APS. It was found that as-grown nonsuperconducting (ag-NSC) crystals had only Bragg peaks arising from the ideal crystalline structure, while both reduced superconducting (r-SC) and re-reduced superconducting (r2-SC) crystals both showed peaks at the exact predicted locations for the impurity layer (Fig. 1). The reversibility of the impurity phase was tested by means of x-ray powder diffraction measurements on the XOR 32-ID-B,C beamline at APS. Both r-SC and oxygenated nonsuperconducting (o-NSC) were used, and the reflection peak coming from the impurity phase present in the SC sample was found to be conspicuously absent from the NSC powder. This study provides conclusive evidence of two important points: First, that the impurity phase grows epitaxially, parallel to the cuprate plane of the *T′* structure, reversibly created by oxygen reduction to the SC state and destroyed by oxidation to the NSC state. Second, that the creation of this impurity phase is intimately linked to the appearance of superconductivity in PLCCO.

A way to understand this result is by noting that the observed R_2O_3 impurity phase has a C-type sesquixoidal structure of the kind normally seen when a slightly Cu-deficient *T′* material phase separates into a Cu-perfect *T′* majority phase and a Cu-free minority phase. This is relevant because, as a result of Cu evaporation during the high-temperature synthesis process, a small amount of Cu deficiency was found to be present in the as-grown PLCCO crystals. In this sense, removing oxygen also removes copper deficiencies and creates oxygen vacancies in the materials. The annealing process then serves the dual role of repairing disorder in the copper oxide plane and providing itinerant carriers for superconductivity. By putting to rest this long-standing materials question, these results suggest that the fundamental mechanism for superconductivity in hole- and electron-doped copper oxides is the same. — *Luis Nasser*

See: Hye Jung Kang[1,2,3]*, Pengcheng Dai[1,4]**, Branton J. Campbell[5], Peter J. Chupas[6], Stephan Rosenkranz[6], Peter L. Lee[7], Qingzhen Huang[2], Shiliang Li[1], Seikil Komiya[8], and Yoichi Ando[8], "Microscopic annealing process and its impact on superconductivity in *T′*-structure electron-doped copper oxides," Nat. Mater. **6**, 224 (March 2007).
DOI: 10.1038/nmat1847

These results suggest that the fundamental mechanisms for superconductivity in hole- and electron-doped copper oxidesis are the same

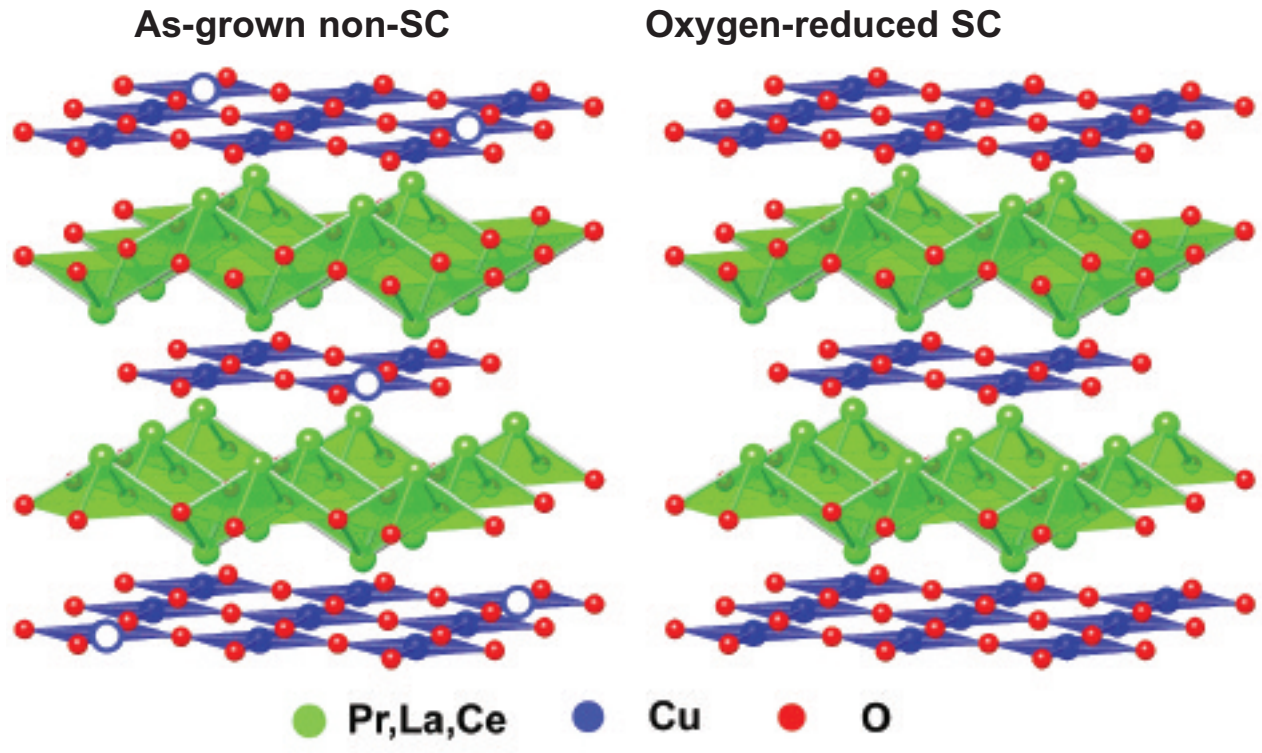

Fig. 1. The crystal structures of an as-grown sample (left), which is non-superconducting, and a superconducting sample after oxygen reduction (right). The as-grown sample has Cu deficiency in the CuO_2 plane, whereas the oxygen-reduced superconducting sample has Cu perfect structure in the CuO_2 plane.

Author affiliations: [1]Department of Physics and Astronomy, The University of Tennessee; [2]NIST Center for Neutron Research, National Institute of Standards and Technology; [3]Department of Materials Science and Engineering, University of Maryland; [4]Neutron Scattering Sciences Division, Oak Ridge National Laboratory; [5]Department of Physics and Astronomy, Brigham Young University; [6]Materials Science Division, Argonne National Laboratory; [7]Advanced Photon Source, Argonne National Laboratory; [8]Central Research Institute of Electric Power Industry
Correspondence:*hkang@nist.gov, **daip@ornl.gov

The x-ray- and neutron-scattering work was supported in part by the U.S. National Science Foundation with grant No. DMR-0453804 and by an award from the Research Corporation. The PLCCO single-crystal growth at the University of Tennessee is supported by the U.S. DOE BES under contract No. DE-FG02-05ER46202. ORNL is supported by U.S. DOE grant No. DE-AC05-00OR22725 through UT/Battelle LLC. The part of the work done in Japan was supported by a Grant-in-Aid for Science provided by the Japan Society for the Promotion of Science. Use of the APS was supported by the U.S. Department of Energy, Office of Science, Office of Basic Energy Sciences, under Contract No. DE-AC02-06CH11357.

11-ID-D • XOR/BESSRC • Chemistry, geoscience, materials science • X-ray absorption fine structure (XAFS), general diffraction, time-resolved XAFS • 3.3-cm Undulator A • Accepting general users

32-ID-B,C • XOR • Materials science, life science • Phase-contrast imaging, ultra-small-angle x-ray scattering, radiography • 3.3-cm Undulator A • Accepting general users

Incommensurate Phases Due to Geometrical Frustration

Many physical phenomena in transition metal oxides, including colossal magnetoresistance and high-temperature superconductivity, are related to charge order (CO), which involves the patterning of charge carriers across a crystal. Using resistivity and differential scanning calorimetry (DSC) measurements, ^{57}Fe Mössbauer spectroscopy, generalized gradient approximation (GGA+U) electronic structure calculations, and x-ray diffraction experiments, a team of researchers used two MU/XOR beamlines at the APS as part of their investigation of the temperature dependence of charge order in Fe_2OBO_3, revealing an unanticipated intermediate phase between room temperature and 340K. Since similar incommensurate phases may occur in other frustrated systems with binary order, the results of the research not only provide the first example of incommensurate phases with ionic (and therefore binary) CO, but have implications for the broader study of geometrical frustration.

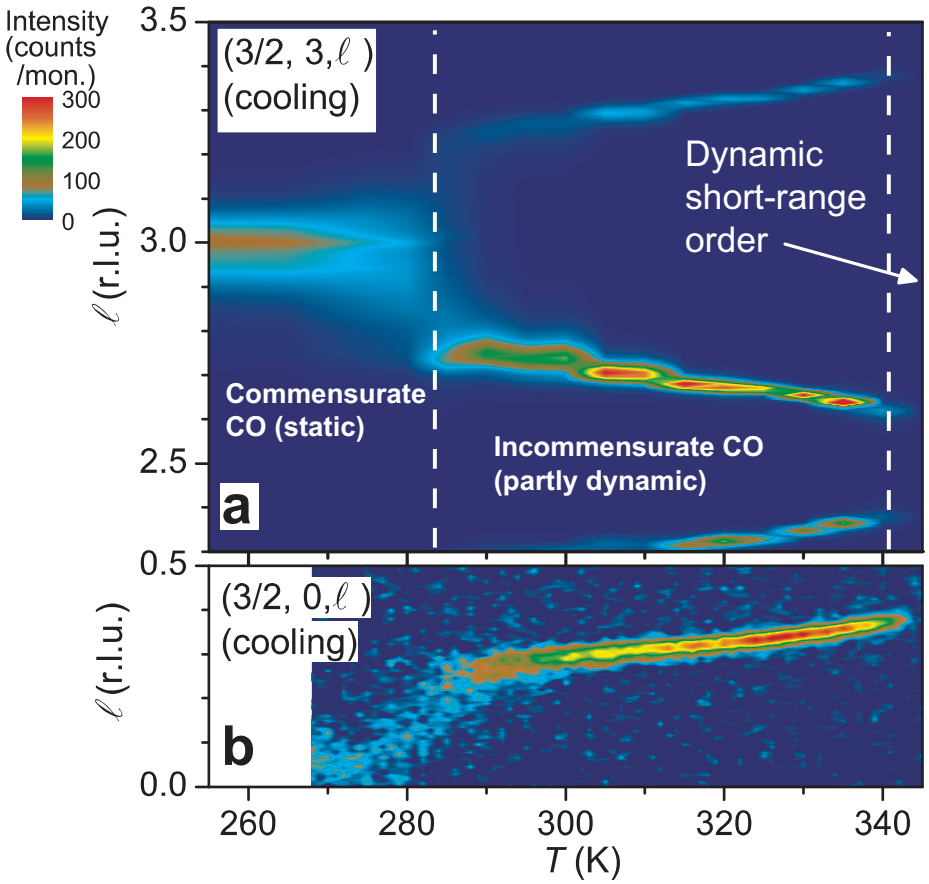

Fig. 1. Incommensurate superstructure reflections from synchrotron x-ray scattering. (a) Scattered intensity at (3/2,3,ℓ) as a function of temperature, measured with a photon energy of 7.05 keV. The phase boundaries of the intermediate temperature phase are indicated by dashed lines. (b) Temperature dependence of intensity at (3/2,0,ℓ), measured with 98-keV photons and a temperature resolution of 1K, showing a *continuous* change of the propagation vector as a function of temperature.

The discovered intermediate phase was characterized by coexisting mobile and immobile carriers and by incommensurate superstructure modulations that propagate in a temperature-dependent fashion. The researchers from Oak Ridge National Laboratory, Forschungszentrum Jülich GmbH, Université de Liège, Ames Laboratory, the University of Massachusetts, the State University of New York at Stony Brook, and North Carolina State University showed how the incommensuration arises from geometrical charge frustration via the proliferation of low-energy antiphase boundaries. That the superstructure is incommensurate in the intermediate phase was established by x-ray diffraction studies carried out at the MU/XOR 6-ID-B,C, and 6-ID-D beamlines at the APS.

Geometrical charge frustration refers to the inability of Coulomb interactions to be simultaneously satisfied due to the geometry of the underlying crystal lattice. Between 250K and 400K, resistivity and DSC data showed two separate, well-defined phase transitions on cooling (and warming) at 340K and 280 (308)K, the former corresponding to the monoclinic-orthorhombic structural transition. The transitions delineate low-, intermediate-, and high-temperature (*T*) phases.

Mössbauer spectra indicated that divalent and trivalent Fe ions were distributed over two structural sites. While there was no discernible hopping of electrons between Fe ions at low *T*, electron hopping was observed at high *T* with a *T*-dependent frequency that remained quite low even above 400K. In the intermediate-*T* phase between the two transitions (e.g., at 325K), contributions with and without electron hopping coexist.

Superstructure reflections observed using x-ray diffraction suggested differently ordered domains in the low-*T* phase. These microdomains corresponded to an imperfect overall CO. In the intermediate phase, superstructure reflections correspond to an incommensurate modulation (Fig. 1a). Above 340K, a long-range ordered superstructure no longer exists, but very weak and broad reflections indicate persistent short-range correlated fluctuations. The correlations are dynamic but relatively slow. To test the incommensurability of the modulations in the intermediate-temperature phase, data were collected in 1K intervals with high-energy x-rays (Fig. 1b). No indications of any ‘‘lock in’’ to commensurate values were visible, showing that the modulations are truly incommensurate with a continuous change of the propagation as a function of temperature.

To understand the microdomain formation at low *T* and the incommensurate CO at intermediate *T*, the researchers considered the relative energies of various CO configurations using GGA+U electronic structure calculations. Electrostatic energy is minimized by having as few same-valence nearest neighbors as possible. This requirement establishes “ordered chains” as the basic CO unit and requires strictly alternating valences within each chain. Geometrically, the two-dimensional lattice of chains consists of two sublattices offset from each other by 1.6 Å. The electrostatic interactions between any two chains not belonging to the same sublattice are geometrically frustrated. Therefore, flipping all valences in all chains (changing their phase) of one sublattice does not change the energy. This twofold degeneracy is lifted by a monoclinic distortion (ribbon tilting); however, the GGA+U calculations showed that the energy gain associated with this distortion is insufficient to prevent the facile formation of domains.

Because of the near degeneracy of configurations with different phase relationships, resulting from a hierarchy of geometrical frustration, the energy cost of creating antiphase boundaries between various CO domains is small. In the intermediate phase, the coherent arrangement of these antiphase boundaries leads to the observed incommensuration. The strong and continuous temperature dependence of the propagation vector then implies that the boundaries move easily in the intermediate phase, and thermal excitations should cause them to fluctuate. Fluctuating boundaries reduce the monoclinic distortion and imply that the Fe ions near the boundaries change their valences by electron hopping. The coexistence of mobile and immobile electrons that are coherently ordered in Fe_2OBO_3 further stabilizes the intermediate phase and enhances the delocalizing influence of the geometrical frustration. — *Vic Comello*

See: M. Angst[1]*, R.P. Hermann[2,3], W. Schweika[2], J.-W. Kim[4], P. Khalifah[5,6], H.J. Xiang[7], M.-H. Whangbo[7], D.-H. Kim[1], B.C. Sales[1], and D. Mandrus[1], “Incommensurate Charge Order Phase in Fe_2OBO_3 Due to Geometrical Frustration,” Phys. Rev. Lett. **99**, 256402 (2007).
DOI: 10.1103/PhysRevLett.99.256402
Author affiliations: [1]Oak Ridge National Laboratory, [2]Forschungszentrum Jülich GmbH, [3]Université de Liège, [4]Ames Laboratory, [5]University of Massachusetts, [6]State University of New York at Stony Brook, [7]North Carolina State University
Correspondence: *angst@ornl.gov

Research at Oak Ridge National Laboratory (ORNL) was sponsored by the Division of Materials Sciences and Engineering, Office of Basic Energy Sciences, U.S. Department of Energy, under Contract DE-AC05-00OR22725 with ORNL; work at North Carolina State University by DOE Grant DE-FG02-86ER45259. Work at Université de Liège: Fonds National de la Recherche Scientifique credit 1.5.064.05. The Midwest Universities sector at the APS is supported by the U.S. Department of Energy, Office of Science, Office of Basic Energy Sciences, through the Ames Laboratory under Contract No. DEACD2 07CH11358. Use of the Advanced Photon Source was supported by the U.S. Department of Energy, Office of Science, Office of Basic Energy Sciences, under Contract No. DE-AC02-06CH11357.

6-ID-B,C • MU/XOR • Physics, materials science • Anomalous and resonant scattering (hard x-ray), liquid scattering, magnetic x-ray scattering, powder diffraction, general diffraction, grazing incidence diffraction, surface diffraction (UHV) • 3.3-cm Undulator A • Accepting general users

6-ID-D • MU/XOR • Physics, materials science • High-energy x-ray diffraction, magnetic x-ray scattering, powder diffraction, pair-distribution function • 3.3-cm Undulator A • Accepting general users

The Effect of Sample Geometry on Magnetization Reversal Dynamics

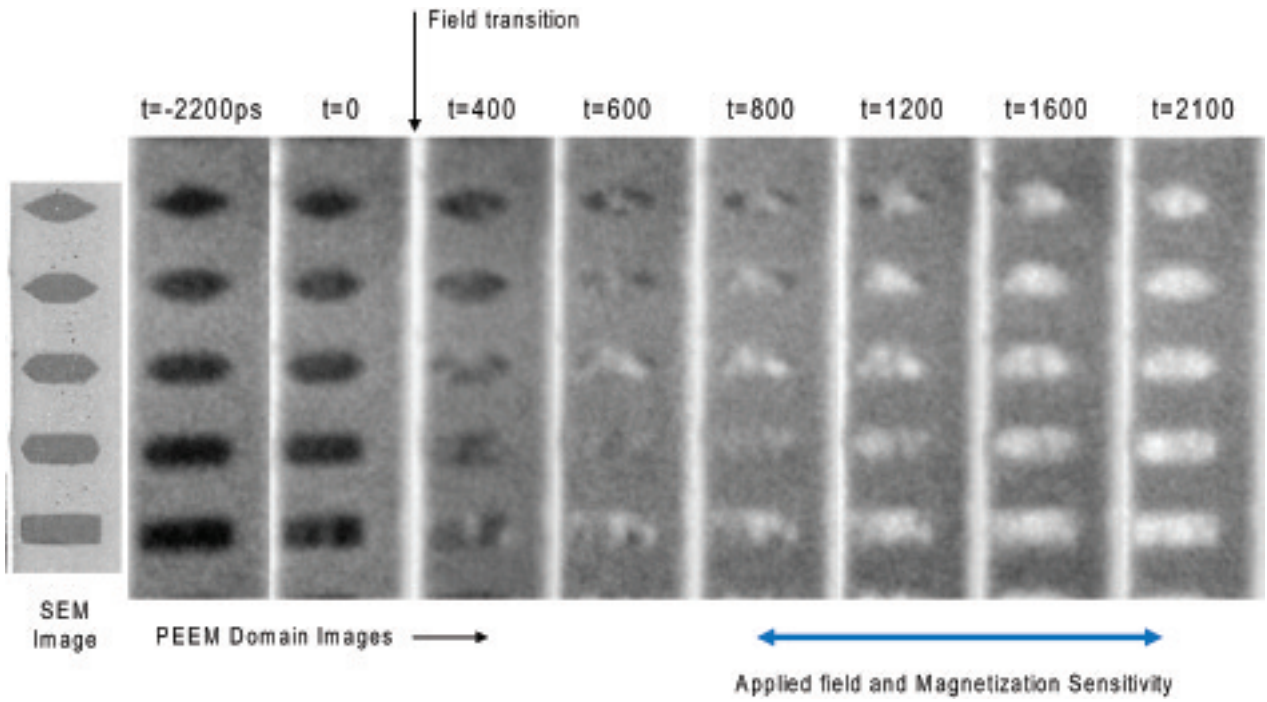

A clear understanding of the dynamics of nanoscale magnetic structures is of crucial importance for the development of new, high-speed magneto-electronic devices. Magnetic random access memory (MRAM), for example, could enable "instant-on" computers that would not require booting with every power cycle. However, there are many unresolved questions concerning the effect that the shape of a nanostructure has on the magnetization reversal process. Understanding this reversal mechanism is essential; this is the process by which information bits are written on the magnetic materials used in computer data storage. In particular, details about the mechanism and the time scale over which magnetization reverses in micron-size circuit lithographs are two of the biggest questions awaiting an answer. Researchers working at XOR beamline 4-ID-C at the APS, have produced new insights into the properties that affect the magnetization reversal process.

The experimental and theoretical results clearly show that subtle variations in shape can be used to tailor the properties of magnetic nanostructures

In these small, patterned structures, long-range magnetostatic interactions introduce strong effects that depend on the shape of the sample. These effects, in turn, lead to the formation of magnetic vortices and local regions of magnetic instability that have significant impact upon the sample's switching and dynamics. Rectangular dots have been amply studied in this connection because their shape anisotropy has the effect of producing a stable ground state. The sharp edges of the dots, on the other hand, produce strong demagnetizing fields that are problematic in a magnetic storage device. To overcome this difficulty, tapered edges have been suggested to "soften" this effect, and magnetic force microscopy (MFM) studies on the influence of end tapering on the static magnetization domains have been amply reported in the literature. However, the intermediate domain patterns during reversal have not been studied, which means the dynamical effect of shape-dependent variations of the magnetic stability has not been established. To this end, time-resolved magnetic domain imaging of the intermediate states formed during reversal is key to obtaining a clear picture of how the competition between demagnetizing, anisotropy, and exchange energies affects the magnetization reversal process.

Researchers from Argonne, Katholieke Universiteit Leuven, and Universitat Autònoma de Barcelona, working at the XOR beamline 4-ID-C at the APS, used time-resolved photoemission electron microscopy (PEEM) to image magnetic reversal in a series of tapered, permalloy ($Ni_{80}Fe_{20}$), needle-like dots with different end shapes. The permalloy shapes were lithographically patterned on a Au coplanar waveguide driven by high-speed bipolar current pulses synchronized to the APS storage ring with an adjustable delay time Δt. The images were obtained by taking the difference between left and right circularly polarized light at the Ni L_3 resonance (852.7 eV); the intensity in the difference images is proportional to the projection of the magnetization vector along the direction of light propagation. These images were taken with a spatial resolution of 300 nm, approximately every 100 ps. The team established that the shape of the permalloy dot has a strong impact on the magnetic fields needed and the time required for switching; it controls the location of the initial reversal, the subsequent motion of the domain wall, and therefore the total time needed to complete the reversal.

They also found that reversal in needles with rectangular ends occurred due to nucleation and subsequent growth of multiple magnetized domains throughout the structure, as shown in the Figure. On the other hand, in needles with tapered ends, the reversal began from a single domain at the center of the structure and later moved toward the ends. In addition, the group proposed a theoretical model that can be used to predict the location of the onset of the magnetization reversal in structures with different end geometries. The experimental and theoretical results clearly show that subtle variations in shape can be used to tailor the properties of magnetic nanostructures. — *Luis Nasser*

< Fig. 1. Scanning electron microscopy (SEM) and selected time-resolved PEEM images of five permalloy needles with varying taper angles. A 2.5-mT field is applied by the waveguide in the horizontal direction and reverses sign in between t = 0 and 400 ps. The PEEM images are sensitive to the horizontal component of the local magnetization, such that dark areas indicate magnetization to the left, and light areas are to the right. In the needle with rectangular ends (bottom structure), reversal of magnetization occurs at multiple points within the structure. With highly tapered ends (top structure), the reversal only initiates in the structure's interior. A crossover between these two behaviors is observed as the taper angle increases.

See: X.F. Han[1], M. Grimsditch[2], J. Meersschaut[2,3], A. Hoffmann[2], Y. Ji[2,4], J. Sort[5], J. Nogués[5], R. Divan[4], J.E. Pearson[2], and D.J. Keavney[1]*, "Magnetic Instability Regions in Patterned Structures: Influence of Element Shape on Magnetization Reversal Dynamics," Phys. Rev. Lett. **98**, 147202 (2007). DOI: 10.1103/PhysRevLett.98.147202

Author affiliations: [1]Advanced Photon Source, Argonne National Laboratory; [2]Materials Science Division, Argonne National Laboratory; [3]Instituut voor Kern- en Stralingsfysica and INPAC, Katholieke Universiteit Leuven; [4]Center for Nanoscale Materials, Argonne National Laboratory; [5]Institució Catalana de Recerca i Estudis Avançats (ICREA) and Departament de Física, Universitat Autònoma de Barcelona

Correspondence: *keavney@aps.anl.gov

Work at Argonne was supported by the U.S. Department of Energy, Office of Science, Office of Basic Energy Sciences under Contract No. DE-AC02-06CH11357. Work at Universitat Autònoma de Barcelona was supported by grant No. 2005SGR-00401, the No. MAT-2004-01679 research projects, and the Institut Català de Nanotecnologia. Use of the APS was supported by the U.S. Department of Energy, Office of Science, Office of Basic Energy Sciences, under Contract No. DE-AC02-06CH11357.

4-ID-C • XOR • Physics, materials science • X-ray photoemission electron microscopy, x-ray photoemission spectroscopy, magnetic circular dichroism (soft x-ray), x-ray magnetic linear dichroism, magnetic x-ray scattering, anomalous and resonant scattering (soft x-ray) • Circularly polarized undulator • Accepting general users

Transport Across Domain Walls in Anti-Ferromagnetic Materials

The number of studies that focus on antiferromagnetic domain imaging has been growing in recent years, in large part due to the increased importance of hybrid magnetic structures for advanced electronics. Notable examples include magnetic bilayers, in which an antiferromagnetic thin film causes a shift in the soft magnetization curve of a ferromagnetic film. This is known as the exchange-bias effect, and it is of great importance in magnetic recording. However, as more hybrid applications of this type are developed, detailed knowledge of the effects on transport of antiferromagnetic domain structure, both at the micro and macro scales, becomes increasingly important. Recently an international group of researchers have performed a combined electrical transport and x-ray imaging study of single chromium (Cr) crystals to address this issue. By comparing the thermal hysteresis observed in the longitudinal and Hall resistivities with that observed with real-space domain imagery, the researchers were able to isolate the transport signatures of the antiferromagnetic domain walls themselves. In particular, they were able to deduce the electrical resistance of a single antiferromagnetic domain wall. This work is an important contribution to the nascent science of antiferromagnetic domain walls and suggests new directions of inquiry into their potential applications in electronic devices.

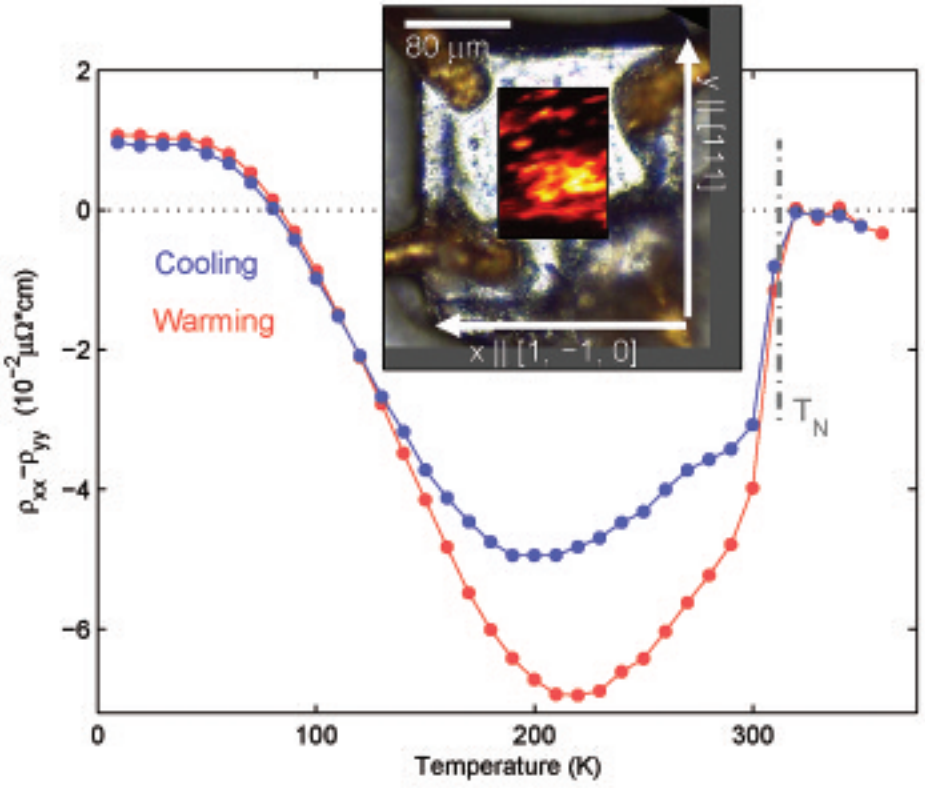

Magnetic domains are volumes where the magnetic fields of a large number of atoms are grouped together and aligned, giving rise in a ferromagnet to a net local magnetization. These domains are separated by domain walls, whose thickness depends on the type of magnetic material used; across these walls, the orientation of the magnetization changes from one domain to its neighbor. In a ferromagnet, each domain is characterized by a single magnetization vector. The formation, motion, and electron scattering properties of these domain structures are exploited in the design of devices ranging from transformers to magnetic memory storage. On the other hand, antiferromagnetic materials are described by a pair of vectors that specify the orientation of the local magnetic moments as well as how those moments are modulated in space within a given domain. While this richness of structure is tantalizing, the lack of a net magnetic moment has complicated the study of antiferromagnetic domains, which in turn has held back the development of possible applications.

The electronic properties of the domain walls are governed by how readily electrons can scatter between the different Fermi surfaces of neighboring domains. The ease with which electrons perform this trick depends strongly on the ratio of the domain wall width R to the electron mean-free path l. For conventional ferromagnetic materials this ratio is large. The transport across domain walls is therefore diffusive, and the resistivity of an individual wall is very small. By contrast, for antiferromagnetic Cr the ratio R/l is of order unity. In this case quantum scattering effects are expected to dominate the transport of spin and charge across the domain wall, and the resistance of a single wall should be large. In order to isolate the transport signatures of this interesting domain structure the researchers in this study—from The University of Chicago, Argonne, the University of Wisconsin-Madison, and University College London—prepared crystals that were small enough to allow only a finite number of domains, yet large enough to be fully in the bulk regime. These crystals exhibited a pronounced thermal hysteresis in their electrical transport properties that was attributed to evolution of the antiferromagnetic domains with temperature.

The actual behavior of the domains themselves was then elucidated via the x-ray microprobe at XOR beamline 2-ID-D, where direct images of the domain structure at various points around the thermal hysteresis loop could be obtained (Fig. 1). Combining macroscopic and mesoscopic experimental probes in this way made it possible to pinpoint the effect of the antiferromagnetic domain walls on electron transport, as well as to begin to understand their thermodynamics. By contrasting transport results taken on samples with different domain orientations, the group was able to deduce that a single antiferromagnetic domain wall has an interface resistance of about 5×10^{-5} $\mu\Omega$ cm^2. This large value indeed corresponds to the R/l ~1 limit and confirms the notion of transport across domain walls in Cr as the scattering of electrons between volumes with mismatched gaps on their Fermi surfaces. In addition to making an important contribution to the nascent science of antiferromagnetic domain walls, this work points toward new directions of inquiry into their potential applications in electronic devices. What remains is to obtain a first-principles theoretical calculation for electron scattering from antiferromagnetic domain walls, exploring their full potential to modulate charge and spin transport. — *Luis Nasser*

< Fig. 1. Anisotropic resistivity $\rho_{xx} - \rho_{yy}$ measured on the imaged sample around a thermal hysteresis loop, showing clear evidence for magnetic domain reconfiguration and hysteresis with thermal cycling. The inset color map shows the population of one domain type as measured at the x-ray microprobe beamline 2-ID-D. The sample micrograph and x-ray image are to scale (but do not represent the same sample), allowing comparison of the current path lengths to the typical domain dimensions.

See: R. Jaramillo[1], T.F. Rosenbaum[1]*, E.D. Isaacs[2], O.G. Shpyrko[2], P.G. Evans[3], G. Aeppli[4], and Z. Cai[5], "Microscopic and Macroscopic Signatures of Antiferromagnetic Domain Walls," Phys. Rev. Lett. **98**, 117206 (16 March 2007).
DOI: 10.1103/PhysRevLett.98.117206
Author affiliations: [1]The James Franck Institute and Department of Physics, The University of Chicago; [2]Center for Nanoscale Materials, Argonne National Laboratory; [3]Department of Materials Science and Engineering, University of Wisconsin-Madison; [4]London Centre for Nanotechnology and Department of Physics and Astronomy, University College London; [5]Advanced Photon Source, Argonne National Laboratory
Correspondence: *t-rosenbaum@uchicago.edu

The work at the University of Chicago was supported by the National Science Foundation Grant No. DMR-0534296. R.J. gratefully acknowledges additional financial support from the NSF. The work in London was funded by the Royal Society and the Basic Technologies program of RCUK. Use of the Advanced Photon Source was supported by the U.S. Department of Energy, Office of Science, Office of Basic Energy Sciences, under Contract No. DE-AC02-06CH11357.

2-ID-D • XOR • Life science, materials science, environmental science • Microfluorescence (hard x-ray), microdiffraction, micro-x-ray absorption fine structure • 3.3-cm Undulator A • Accepting general users

Phonons Go Ballistic: Explaining Thermal Transport on the Nanoscale

Thermal properties of microelectronic and optoelectronic materials are crucial in the operation of current technologies, such as solid-state lighting and high-power radio-frequency devices, and gallium arsenide (GaAs) is considered a model system for studying the physics of heat transport in crystals. Phonons are the primary contributor to thermal conductivity of a solid material. A major challenge to understanding thermal transport of nanoscale materials has been the difficulty of probing beneath the surface layer to determine the contribution of phonons to heat transport in the buried layers. Measurements at the picosecond scale using time-domain thermoreflectance (TDTR) can accurately detect thermal changes at the surface of nanomaterials, but not in deeper structures. To fill in this information gap, researchers using the XOR 7-ID-B,C,D beamline at APS explored the contribution of ballistic phonons to heat conduction in the buried layers of an alloy of GaAs coated with a thin aluminum film. By comparing temperatures of the Al layer with and without a ballistic channel, they determined that ballistic phonons account for 20% of heat flow to the buried layer. This new technique represents a major breakthrough in the quest to understand thermal transport in nanoscale materials.

This new technique represents a major breakthrough in the quest to understand thermal transport in nanoscale materials

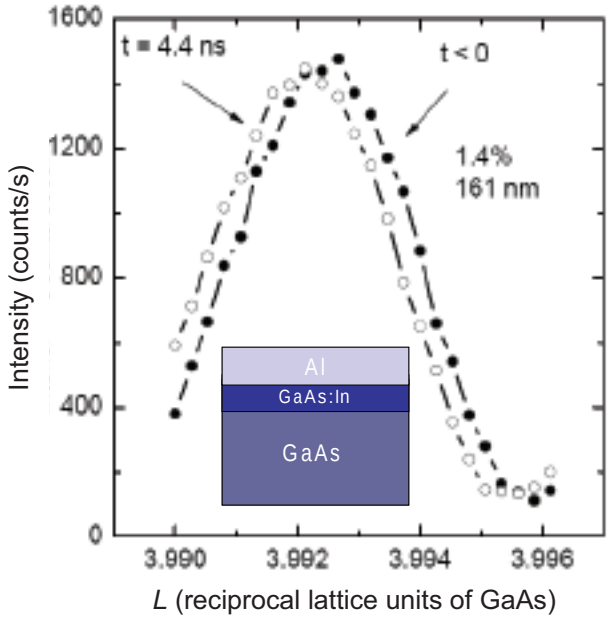

Fig. 1. Thermal expansion of the indium-doped buried layer (1.4% InAs in GaAs) provides a time-resolved thermometer.

The researchers from the University of Illinois at Urbana-Champaign and Argonne grew 120-nm to 250-nm layers of GaAs doped with indium to form the alloy $(GaAs)_{1-x}(InAs)_x$ on a GaAs substrate. Indium doping gives the buried layer a lattice strain. Magnetron sputtering was used to apply a 100-nm-thin film of aluminum on the alloy layer. Three samples were prepared at thicknesses of 126 nm, 161 nm, and 246 nm. The thickest sample lies at the threshold of thickness that would induce partial relaxation of strain, thus eliminating the possible contribution of phonon scattering to heat exchange.

In the first experiment, TDTR was used to measure thermal decay of the Al film at a time resolution of picoseconds. A radio-frequency lock-in amplifier (phase-sensitive detector) was used to measure small changes in the reflectivity produced by changes in temperature of the Al film; these data allow the researchers to determine the thermal conductivity (Λ) of the buried layers and thermal conductance (G) of the interface between layers. In the second suite of experiments, time-resolved x-ray diffraction (TRXRD) was used to measure thermal expansion of the lattice in the buried layer. This expansion is an indication of temperature change (Fig. 1).

When the distance that phonons travel between scattering events—the mean free path—is greater than the thickness of the alloy layer, the phonons are considered ballistic. In large-scale materials, it is possible to apply the diffusion equation to determine the thermal transport because the mean free path is small relative to the scale of the material. At the nanoscale and at very short time scales, however, the diffusion equation does not yield accurate information about heat transport because of the very short length and time scales being probed.

As the researchers tried to fit the data from TDTR using a single-channel thermal model with data obtained with TRXRD, they found discrepancies in the thermal conductance of the interface and the thermal conductivity of the buried layers. The single-channel model assumes that the thermal transport through the buried layer is diffusive. By applying a new, two-channel model they were able to determine that there are actually two channels for heat propagation: diffusive and ballistic. — *Elise LeQuire*

See: M. Highland[1], B.C. Gundrum[1], Yee Kan Koh[1], R.S. Averback[1], David G. Cahill[1]*, V.C. Elarde[2], J.J. Coleman[2], D.A. Walko[3], and E.C. Landahl[3], "Ballistic-phonon heat conduction at the nanoscale as revealed by time-resolved x-ray diffraction and time-domain thermoreflectance," Phys. Rev. B **76** 075337 (2007). DOI: 10.1103/PhysRevB.76.075337

Author affiliations: [1]Frederick Seitz Materials Research Laboratory and Department of Materials Science and Engineering, University of Illinois at Urbana-Champaign; [2]Department of Electrical and Computer Engineering, University of Illinois at Urbana-Champaign; [3]Advanced Photon Source, Argonne National Laboratory
Correspondence: *d-cahill@uiuc.edu

This work was supported by DOE Grant No. DEFG02-91ER45439. Sample characterization used the Central Facilities of the Frederick Seitz Materials Research Laboratory at UIUC, which is partially supported by DOE Grant No. DEFG02-91ER45439. Use of the Advanced Photon Source was supported by the U.S. Department of Energy, Office of Science, Office of Basic Energy Sciences, under Contract No. DE-AC02-06CH11357.

7-ID-B,C,D • XOR • Materials science, atomic physics, chemistry • Time-resolved x-ray scattering, radiography, time-resolved x-ray absorption fine structure • 3.3-cm Undulator A • Accepting general users

Around the Experiment Hall

Art and Science Join Together

Scientists at the APS are collaborating with colleagues from the Art Institute of Chicago and Northwestern University to investigate the casting technology and inner structure of ancient bronzes from early Chinese dynasties (1700-221 BCE). Argonne researchers Dean Haeffner and Jon Almer (both with the Argonne X-ray Science Division) are working with Professor David Dunand and post-doctoral researcher Marcus Young from Northwestern University, and Francesca Casadio and Suzanne Schnepp from the Art Institute of Chicago, to understand the creation and corrosion of ancient Chinese bronzes.

X-ray beams from the APS are being used for diffraction studies, as well as for phase-enhanced imaging for higher contrast than traditional x-ray absorption methods, at XOR beamline 1-ID-C. One of the things this technique permits is imaging the texture of the grains in the material. If the bronze was cast in ingots, there should be very little texture in the grains; metals usually get texture from mechanical processing, such as rolling. So the group gets clues as to how the object was made, what sort of technology was used, and what tools were available. Being able to sample a number of small spots all over the vessel at one time provides comprehensive results, which helps lead to a more thorough understanding of how the bronze was worked and shaped.

The researchers found that the vessel's outer corrosion layer, which is visible optically, is very thin and consists of cuprite and cassiterite. The bulk of the vessel remains uncorroded and is composed of a lead phase and a copper-tin intermetallic phase, which was observed as large, untextured grains, indicating that the vessel was produced by casting, rather than by cold- or hot-working. Results from an earlier study on an ancient Chinese bronze fragment can be found in Applied Physics A **83**, 163 (2006). DOI: 10.1007/s00339-006-3504-5. Use of the APS was supported by the U.S. Department of Energy, Office of Science, Office of Basic Energy Sciences, under Contract No. DE-AC02-06CH11357.

The high-energy x-ray diffraction measurements of a Chinese wine vessel (Shang Dynasty 14-13 century BCE) are explained to members of the Northwestern/Art Institute/Argonne collaboration.

Metallic Glass Morphs under Pressure

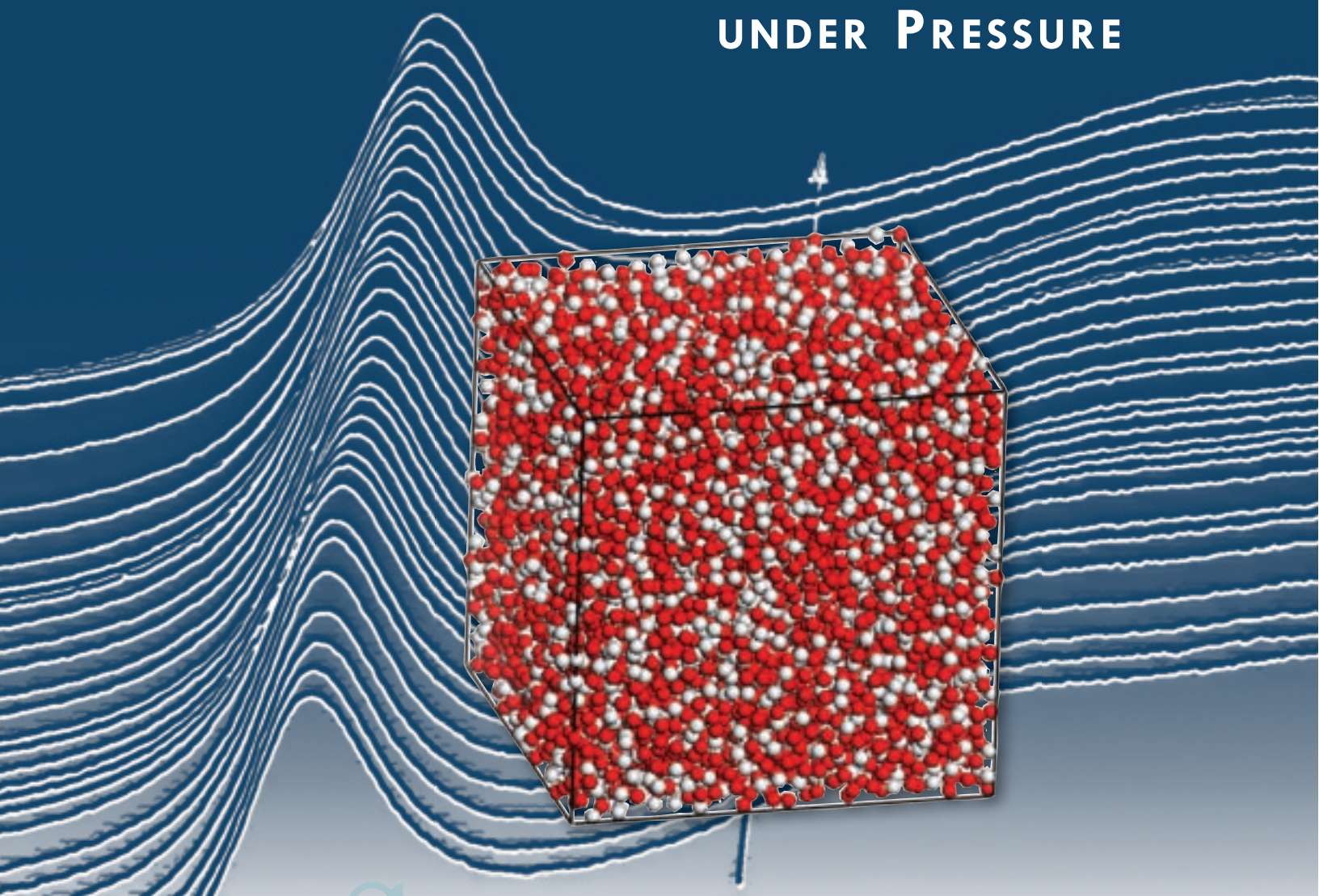

Solids such as ice, carbon, silicon, and silicon dioxide are not always shining examples of regular, crystalline substances. Under particular conditions of temperature and pressure they can form highly irregular, amorphous forms. However, there are several more complex materials, as opposed to these elemental or simple molecular materials, that can also form amorphous solids. One of these is a novel class of materials known as bulk metallic glasses (BMGs), which could be the basis for new engineering applications not possible with conventional metals, alloys, or ceramics. Now, an international team of researchers working on HP-CAT beamline 16-ID-B at the APS is revealing the shifting structures of BMGs, which could help materials scientists create designer structures with specific physical, electrical, and magnetic properties for products including recording heads, sensors and transducers, motors, sports equipment, and power transformer cores. Above: Amorphous state; a three-dimensional atomic configuration for a BMG. Background: *in situ* x-ray diffraction patterns of $[La_{0.5}Ce_{0.5}]_{64}Al_{16}Ni_5Cu_{15}$ BMG under pressure at room temperature.

Researchers are discovering that BMGs have properties unlike any of their component metallic elements. Bulk metallic glasses are, for instance, usually much stronger than metals, are tougher than ceramics, and can be stretched to great lengths without snapping. Some amorphous solids also have hidden talents and can, if squeezed, undergo a transition in which their internal amorphous structure rearranges into an entirely different amorphous form. Such a transition can cause a change in the physical, electrical, magnetic, and optical properties of the material.

The existence of such amorphous polymorphs has led scientists to imagine that novel BMGs may also exist that can be switched between two amorphous states. Such a property might lead to switchable engineered materials.

The researchers in this study, from Zhejiang University, the Chinese Academy of Sciences, and the Carnegie Institution of Washington, have carried out high-pressure x-ray diffraction experiments—as well as low-temperature resistivity and magnetization experiments—on one such BMG, a complex solid containing the heavy metals lanthanum and cerium, having the chemical formula $La_{32}Ce_{32}Al_{16}Ni_5Cu_{15}$. Materials scientists have known for decades that the metal cerium, the first element in the lanthanide series in the Periodic Table, has some unique properties. For instance, it has a single 4f electron, which makes it behave as a paramagnet, an antiferromagnet, or a superconductor depending on its temperature and pressure. The team suspected that locking cerium's uniqueness into a BMG might reveal yet other strange properties. The results did not disappoint.

The team applied pressure to the material using a diamond anvil cell held in the x-ray diffraction instrument so that they could take direct *in situ* measurements. Their results revealed that this particular BMG, as anticipated, can undergo a sudden change in its compressibility at 14 GPa—approximately 140,000 times atmospheric pressure. The sudden change in compressibility may indicate the occurrence of an "amorphous-to-amorphous" phase transition in these types of materials (Fig. 1). Amorphous solids, of which metallic glasses constitute one example, have long confounded scientists who seek to characterize them. Unlike crystalline solids, which possess a regular long-range atomic order, amorphous materials consist of atoms arranged randomly, making their behavior much harder to predict.

The material also undergoes an incredible leap in its resistivity at 12K. The diffraction patterns also suggest that there is an unusual change in the electronic structure of the cerium atoms that occurs at 14 GPa. Changes in how the electrons interact as the material switches from one amorphous form to the other are thought to underlie both this and the leap in resistivity.

In general, the superior fracture strength and toughness, the excellent corrosion and wear resistance, and improved plasticity of bulk metallic glasses may lead to more applications in the future. — *David Bradley*

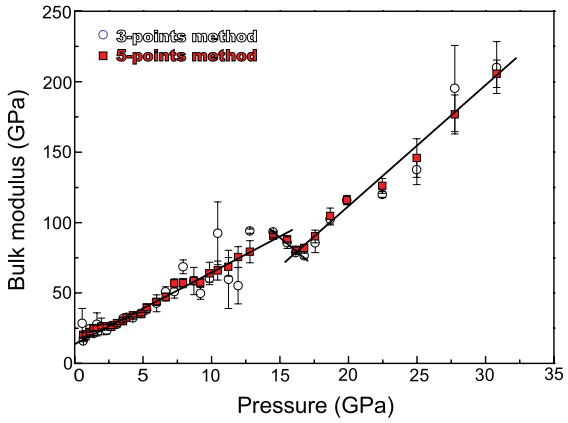

Fig. 1. A distinct break in bulk modulus occurs at 14 GPa, suggesting that the material undergoes an amorphous-to-amorphous transition at this pressure.

See: Q.S. Zeng[1], Y. C. Li[3], C.M. Feng[1,2], P. Liermann[4,6], M. Somayazulu[4,6], G.Y. Shen[4,6], H.-k. Mao[1,4,6**], R. Yang[5], J. Liu[3], T.D. Hu[3], and J.Z. Jiang[1*] "Anomalous compression behavior in lanthanum/cerium-based metallic glass under high pressure," Proc. Natl. Acad. Sci. USA **104**(34), 13565 (August 21, 2007). DOI: 10.1073pnas.0705999104

Author affiliations: [1]International Center for New-Structured Materials and Laboratory of New-Structured Materials, Department of Materials Science and Engineering, and [2]Analysis and Testing Centre, Zhejiang University; [3]Institute of High Energy Physics, Chinese Academy of Sciences; [4]High Pressure Collaborative Access Team and [5]X-ray Science Division, Advanced Photon Source, Argonne National Laboratory; and [6]Geophysical Laboratory, Carnegie Institution of Washington

Correspondence: *jiangjz@zju.edu.cn, **h.mao@gl.ciw.edu.

Use of HP-CAT was supported by the U.S. Department of Energy, Basic Energy Sciences; the Department of Energy, National Nuclear Security Administration; the NSF; the Department of Defense, Tank Automotive and Armaments Command; the W.M. Keck Foundation; the National Natural Science Foundation of China Grants 50341032, 50425102, and 50601021 (to J.Z.J.); Ministry of Science and Technology of China Grants 2004/249/37-14 and 2004/250/31-01A (to J.Z.J.); Ministry of Education of China Grants 2.005E10 and 2005-55 (to J.Z.J.); the Zhejiang University–Helmholtz Cooperation Fund; and Zhejiang University. Use of the Advanced Photon Source was supported by the U.S. Department of Energy, Office of Science, Office of Basic Energy Sciences, under Contract No. DE-AC02-06CH.

16-ID-B • HP-CAT • Materials science, geoscience • Microdiffraction, powder diffraction, single-crystal diffraction, high-pressure diamond anvil cell • 3.3-cm Undulator A • Accepting general users

Forging the Bonds at Interfaces

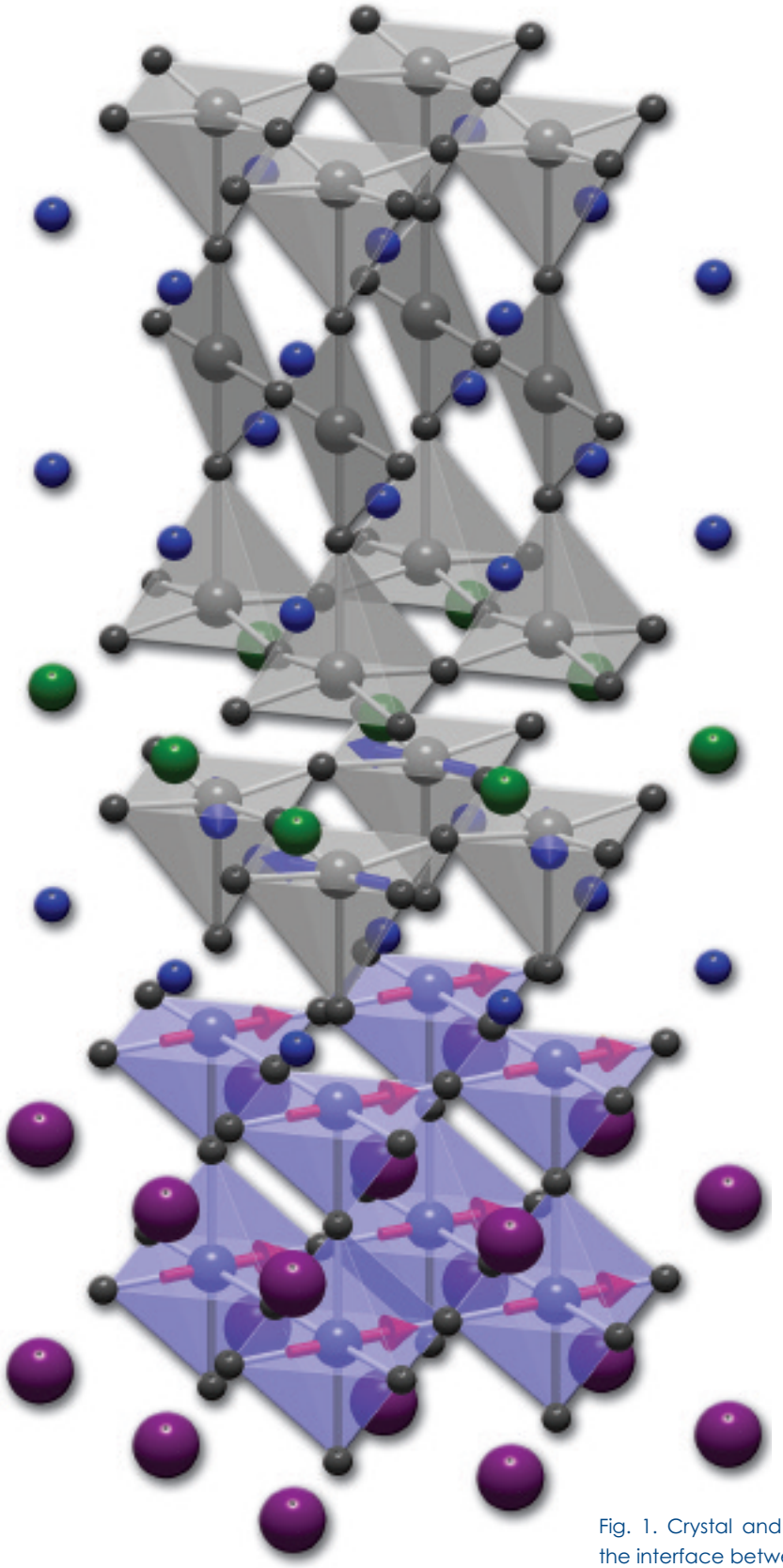

Fig. 1. Crystal and magnetic structure at the interface between a superconducting and ferromagnetic oxide.

In the semiconducting devices that serve as the heart of our modern microelectronic gadgets, most of the action takes place at the interfaces, the region where one type of semiconductor bumps up against another. At this junction, the differences in the electronic properties of each separate material can be used to control and alter the flow of electrons in one direction or another. Because the composition of semiconductors (i.e., their precise materials and structure) directly affects their electronic behavior, the close study of different sorts of semiconductor interfaces provides key information on how to improve and tailor them for various uses. One promising recent development is the creation of abrupt atomic-scale interfaces between some complex oxide structures, which feature a wide variety of exotic electronic and magnetic qualities not attainable in semiconductors and conventional metals. Now, researchers using the XOR 4-ID-C beamline at the APS have uncovered a reconstruction of electronic orbitals confined at an interface between ferromagnetic and superconducting oxides. This insight has important implications for the behavior at interfaces between materials with strongly correlated electrons, and the work was selected as one of the breakthroughs of the year for 2007 by *Science* magazine.

The researchers, from the University of Arkansas, Argonne, the Max Planck Institute, and Northern Illinois University probed the interface between two particular complex oxides: (Y,Ca)$Ba_2Cu_3O_7$ (YBCO), which is a high-temperature superconductor, and $La_{0.67}Ca_{0.33}MnO_3$ (LCMO), a ferromagnetic manganese oxide. Through soft x-ray absorption spectroscopy (XAS) and x-ray linear dichroism (XLD) techniques at the 4-ID-C beamline, the team studied the orbital occupation and electronic structures at the YBCO-LCMO interface (Fig. 1).

Resonant XAS and XLD methods allow precise tuning of the synchrotron x-ray beam to study particular atoms, so that the interference of bulk electrons is kept to a minimum. Here, the beam was tuned to investigate specific electronic properties of copper and manganese atoms at the interfaces in the total electron yield (TEY) mode. Fluorescence-yield (FY) bulk-sensitive data were also obtained. Studies of x-ray absorption and with x-ray polarization parallel and perpendicular to the interface provided information about the symmetry (shape) of orbitals of the atoms.

When the bulk-sensitive data are compared with the interface-sensitive data, the interfacial absorption peak is found to be shifted to a lower energy level by ~0.4 eV, indicating a change in valence of copper atoms in the interface and a transfer of charge across the interface, forming a charged double layer. This is accompanied by a reduction in the YBCO hole density at the interface, which along with the absorption peak shift indicates a change in structure of the CuO_2 layer next to the interface. This shows an orbital reconstruction where some of the YBCO holes now occupy the $3d^3_{z^2-r^2}$ orbitals in the interface, an orbital which in the bulk material is normally fully occupied and inactive. Examination at different temperatures shows that peak position and polarization remain unaffected.

The team considered several possible mechanisms to account for this orbital reconstruction. One involved a change in the energy level of the $3d^3_{z^2-r}$ orbital due to the arrangement of atoms, but this was considered unlikely. Instead, the researchers suggested that a more plausible scenario would involve hybridization between Mn and Cu orbitals that would create a covalent bond capable of bridging the YBCO-LCMO interface. They confirmed this model by performing numerical exact-diagonalization calculations on a $MnCuO_{10}$ atomic cluster, showing that a charge of about –0.2 electron is transferred across the interface from Mn to Cu ions with the formation of a strong covalent chemical bond.

This modification of the CuO_2 layer by orbital reconstruction with covalent bonding explains some of the unusual magnetic properties observed at these oxide heterostructure interfaces in previous experimental work. Even more important, the ability to closely examine the detailed behavior of electrons at complex oxide interfaces will eventually make it possible to design correlated nanomaterials that will allow highly controlled interactions to more exacting specifications and precise functions than previously possible. The potential for ever more sophisticated and versatile electronic devices is practically limitless. — *Mark Wolverton*

See: J. Chakhalian[1,2]* J.W. Freeland[3]**, H.-U. Habermeier[2], G. Cristiani[2], G. Khaliullin[2], M. van Veenendaal[3,4], and B. Keimer[2], "Orbital Reconstruction and Covalent Bonding at an Oxide Interface," Science **318**, 1114 (16 November 2007).
DOI: 10.1126/science.1149338
Author affiliations: [1]University of Arkansas; [2]Max Planck Institute for Solid State Research; [3]Advanced Photon Source, Argonne National Laboratory; [4]Department of Physics, Northern Illinois University
Correspondence: *jchakhal@uark.edu, **freeland@anl.gov

M.v.V. was supported by the U.S. Department of Energy, No. DE-FG02-03ER46097. J.C. was supported by the U.S. Department of Defense–Army Research Office under Contract No. 0402-17291. Use of the Advanced Photon Source was supported by the U.S. Department of Energy, Office of Science, Office of Basic Energy Sciences, under Contract No. DE-AC02-06CH11357.

4-ID-C • XOR • Physics, materials science • X-ray photoemission electron microscopy, x-ray photoemission spectroscopy, magnetic circular dichroism (soft x-ray), x-ray magnetic linear dichroism, magnetic x-ray scattering, anomalous and resonant scattering (soft x-ray) • Circularly polarized undulator • Accepting general users

Building a Better SAM

Organosilicon technology—combining carbon and silicon atoms in unique ways to create devices for use in applications as varied as biosensors, implantable batteries, and molecular electronics—has been the subject of intense research, accelerated by the ever-increasing capability to design and create materials on the molecular scale. Much of this research has focused on the characterization of self-assembled monolayers (SAMs) on silicon and how to tailor their terminal reactive groups (moieties). Because of the reactive nature of these terminal moieties, they can complicate matters by attaching themselves to the SAM's silicon substrate, interfering with the SAM's intended functionality. While the moiety can be protected and subsequently deprotected during SAM formation to avoid this, hindrances created by the spatial arrangement of atoms in the SAM can limit this process. How, then, to create a handy Si SAM with useful functional terminal moieties without such complications? Aided by the DND-CAT 5-ID-B,C,D beamline at the APS, researchers from Northwestern University have discovered a way around this dilemma by finding a molecular SAM structure with a terminal moiety that does not need chemical protection during the formation process.

Employing 4-bromostyrene molecules provides a "handle" for the useful attachment of other molecules onto the SAM monolayer without the troublesome attachment of the terminal moiety to the substrate. But facilitating the practical development and design of such SAMs requires the ability to fully understand and control their molecular structure.

The Northwestern team first hydrogen-passivated Si(111) substrates, upon which 4-bromostyrene SAMs were grown photochemically. The researchers then set out to extensively characterize the structure of a terminally functionalized 4-bromostyrene SAM through a variety of complementary techniques, including atomic force microscopy along with several x-ray methods. At the DND-CAT 5-ID-B,C,D undulator station, the experimenters performed x-ray standing wave (XSW) measurements to examine the distribution of bromine (Br) atoms relative to the underlying Si lattice, and x-ray fluorescence studies to examine the coverage of the Br layers upon the SAM. X-ray photoelectron spectroscopy revealed the chemical bonding of the SAM structure, while electron density measurements obtained with x-ray reflectivity revealed the molecular packing density and thickness of the SAM. These two latter x-ray studies were carried out at Northwestern University. Density functional theory modeling was applied to the data gathered from these various modalities. Because Br is a fluorescent x-ray tag, it readily lends itself to analysis by a range of complementary x-ray techniques. This array of techniques allowed the experimenters to characterize the SAMs with submolecular resolution.

The studies revealed a densely packed 4-bromostyrene SAM on the Si(111) substrate with a thickness of 8.5 Å. The 4-bromostyrene molecules are tilted at 17° around the [111] axis in the direction of the Si T4 site, with the Br atoms directly above these sites, and a packing density of about 0.5 ML. Most significantly, the team's detailed characterization of the 4-bromostyrene SAMs demonstrates that the Br atoms retain their functionality at the adlayer, so that further substitutional chemistry can be performed with them. This proven effectiveness of 4-bromostyrene SAMs, as well as the close definition of the SAM's molecular structure demonstrated in this work, holds great importance for the further development of useful and versatile organosilicon devices.

— Mark Wolverton

See: Rajiv Basu, Jui-Ching Lin, Chang-Yong Kim, Matthew J. Schmitz, Nathan L. Yoder, Joshua A. Kellar, Michael J. Bedzyk, and Mark C. Hersam*, "Structural Characterization of 4-Bromostyrene Self-Assembled Monolayers on Si(111)," Langmuir **23**, 1905 (2007). DOI: 10.1021/la062759f

Author affiliation: Department of Materials Science and Engineering, Northwestern University
Correspondence: *m-hersam@northwestern.edu

This work was supported by the Nanoscale Science and Engineering Initiative of the NSF (EEC-0118025, DMR-0134706, and ECS-0506802), the NASA Institute for Nanoelectronics and Computing (NCC2-1363), and an ONR Young Investigator Award (N00014-05-1-0563). M.C.H. also acknowledges an Alfred P. Sloan Research Fellowship. Northwestern University Central Facilities supported by the MRSEC program of the NSF (DMR-050513). DND-CAT is supported in part by the State of Illinois. Use of the APS was supported by the U.S. Department of Energy, Office of Science, Office of Basic Energy Sciences, under Contract No. DE-AC02-06CH11357.

5-ID-B,C,D • DND-CAT • Materials science, polymer science • Powder diffraction, x-ray reflectivity, small-angle x-ray scattering, surface diffraction, wide-angle x-ray scattering, x-ray standing waves, x-ray optics development/techniques • 3.3-cm Undulator A • Accepting general users

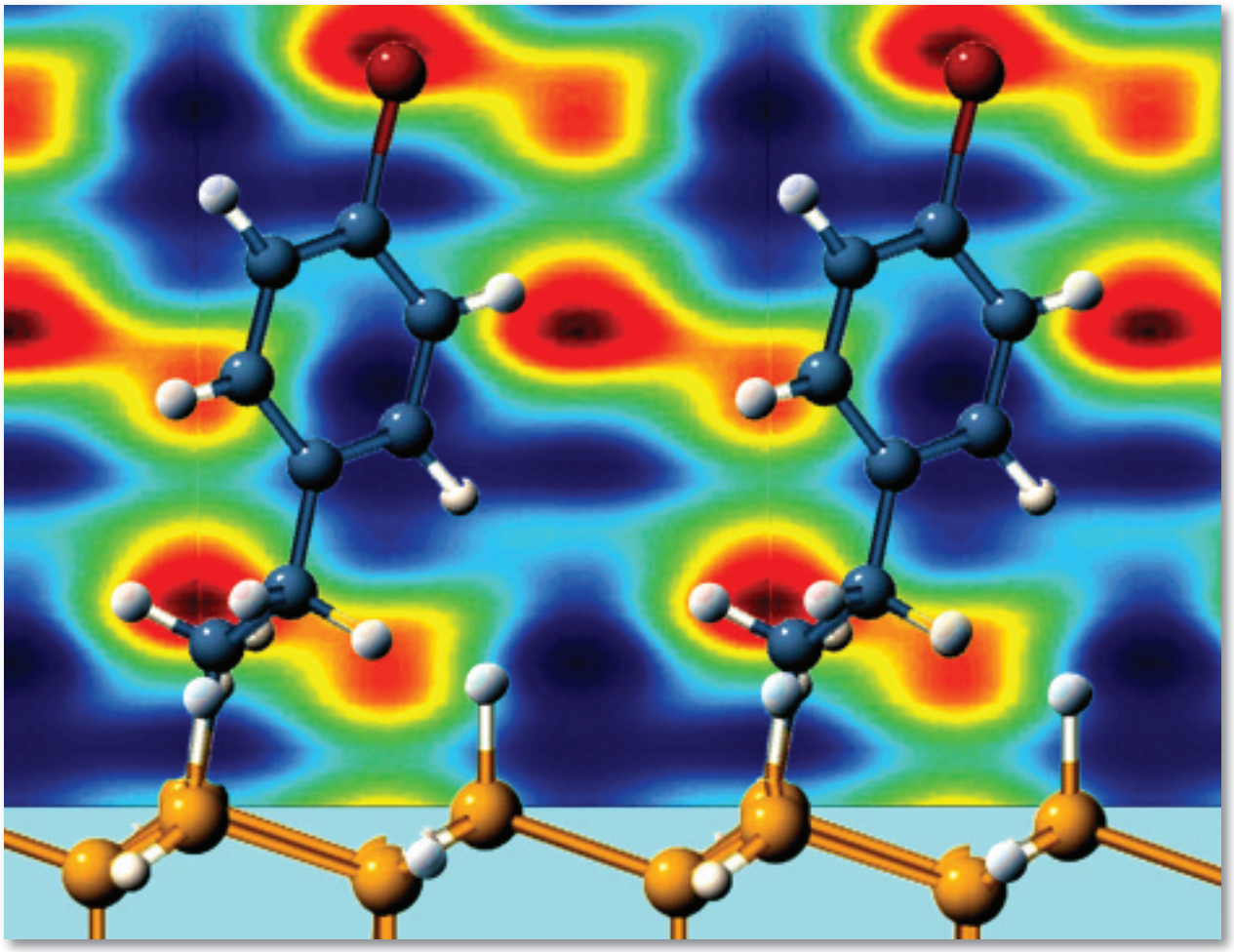

Fig. 1. Calculated structure (foreground) and x-ray standing wave image (background) for a 4-bromostyrene monolayer on the Si(111) surface.

A More-Perfect Thermal Insulator from Dense, Solid Tungsten Diselenide

A new insulating material with the lowest thermal conductivity ever measured for a fully dense solid has been created and evaluated by researchers from the University of Oregon, the University of Illinois at Urbana-Champaign, the Rensselaer Polytechnic Institute, and Argonne, and studied with x-ray diffraction measurements taken at the XOR/UNI 33-BM-C beamline at the APS. While far from having immediate application, the principles involved, once understood, could lead to improved insulation for a wide variety of uses, including improved insulation materials for conserving energy, and in converting between different forms of energy, such as in thermoelectric energy conversion.

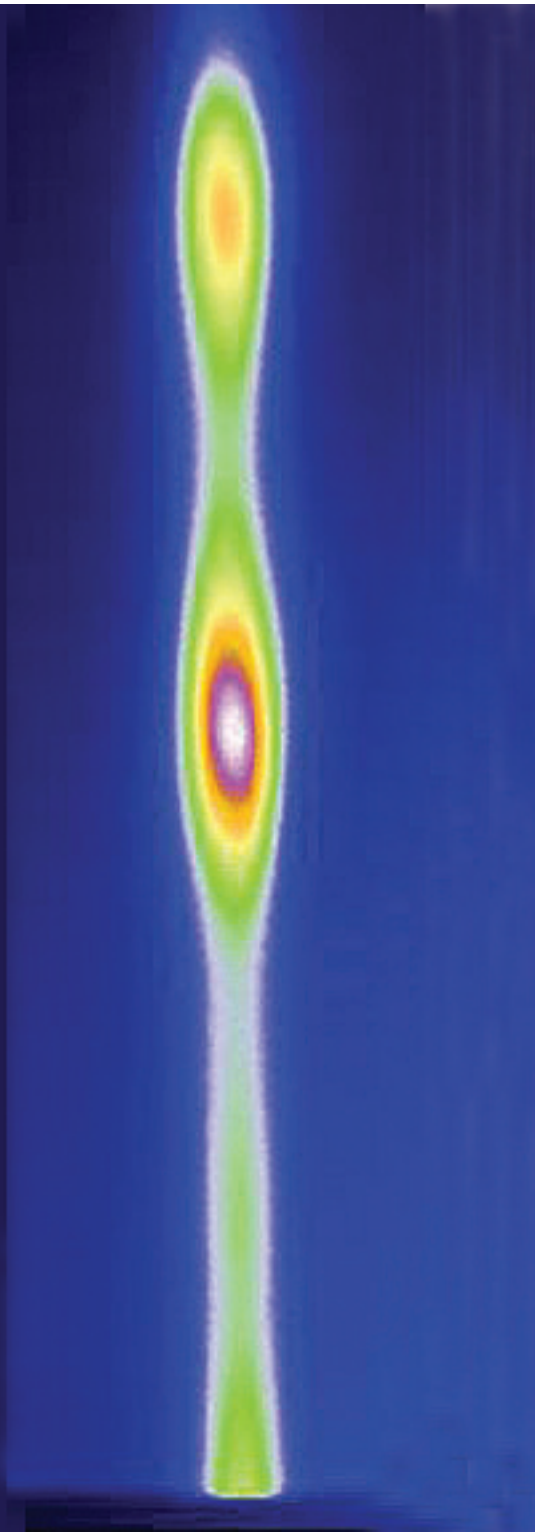

Fig. 1. X-ray diffraction data for a 32.5-nm-thick tungsten-diselenide film using 18.5-keV photons. After deposition, the film was annealed for 1 h at 650° C in a nitrogen gas atmosphere. The false-color depiction of the x-ray diffraction intensities was collected by the area detector in the vicinity of the (1 0 3) and (1 0 5) reflections. The horizontal direction is in the plane of the sample, and the vertical direction is normal to the sample surface.

Thermally insulating materials such as amorphous solids and glasses with disordered structures are usually the poorest conductors of heat, with a specific value for their minimum lattice thermal conductivity. However, the researchers in this study have found a way to evade this minimum and produce a new thermal insulating material with a cross-plane thermal conductivity six times smaller than the minimum lattice thermal conductivity, sometimes called its theoretically computed minimum amount.

The University of Oregon scientists synthesized thin films of crystalline tungsten diselenide (WSe_2) structures from several different thicknesses of alternating layers of tungsten (W) and selenium (Se). They attained ultralow thermal conductivity by using a new synthetic method called modulated elemental reactant (MER), which the collaborators have been developing. The MER preparatory method generally involves chemical deposition of several layers of elements, followed by annealing at relatively high temperatures. Within their experiment, the special method controls the thermal pathways—specifically, the ordering and disordering—of the WSe_2 thin films. This was found to be the best way to produce the desired ultralow thermal conductivity. The researchers contend that the extremely low thermal conductivity of this nanocrystalline material is due to localization of lattice vibrations brought about by the random stacking of two-dimensional sheets of crystalline tungsten diselenide. The researchers believe that the final material prepared in the University of Oregon laboratory is the closest thing to a dense solid made into a perfect thermal insulator. While this material would not be practical for insulating a refrigerator, the wall of a house, or parts inside a turbine engine, the new physical properties displayed might some day point the way toward methods of creating more effective practical insulations.

The researchers deposited sequential layers of tungsten and selenium onto unheated silicon (100) [Si (100)] wafers within an ultrahigh vacuum chamber. Various thicknesses of the resulting thin films were then annealed for 1 h at high temperatures—at various points between 200° and 650° C (392° and 1,202° F)—in a nitrogen (N_2) gas atmosphere in order to form the desired tungsten diselenide (Fig. 1). The WSe_2 is a sheet-like hexagonal structure with normally strong covalent bonds within the structure's *a-b* planes but with characteristically weak bonds in the cross-plane (*c*-axis surface between the layers, perpendicular to the *a-b* planes). The properties of the material were measured in a University of Illinois laboratory. Then, synchrotron x-ray diffraction data were collected from the microstructure of the WSe_2 thin films at the XOR/UNI 33-BM-C beamline at the APS, employing photons with an energy of 18.5 keV. Computational simulations and molecular modeling of the layered crystals were carried out by researchers at Rensselaer Polytechnic Institute.

Under standard laboratory conditions, the resulting textured nanocrystalline material—from a thin film with thickness of 62 nm measured at 300K—had a cross-plane thermal conductivity of 0.048 ($Wm^{-1}K^{-1}$)—the lowest thermal conductivity found within the experiment. This result for the WSe_2 thin film was about 30 times smaller than that for a single crystal of WSe_2.

The researchers found that the conductivity of the 62-nm-thick film was smaller than the conductivity of both the thinner 24-nm film and the thicker 343-nm film. Why this difference occurs is not yet fully understood by the group. They speculate that the physical processes behind the difference involve certain variations in the degree of crystallographic ordering along the thickness of the thin films, which provides for a large degree of localization of the lattice vibrations.

Unexpectedly, the researchers found that when creating a fully disordered structure—by irradiating the films with ion beams to disrupt the order in the two-dimensional planes—the action actually increased thermal conductivity.

Further research and computational studies by the scientists are ongoing in order to better understand the disorder in the stacking of the WSe_2 sheets. Experimentation with other disordered layered crystals is also planned. Once the physical principles behind the discovery are better understood, the technique used by the researchers could lead to improved insulation materials for conserving energy and for converting between different forms of energy, such as in thermoelectric energy conversion. — *William Arthur Atkins & Jim Barlow*

See: Catalin Chiritescu[1], David G. Cahill[1]*, Ngoc Nguyen[2], David Johnson[2], Arun Bodapati[3], Pawel Keblinski[3], and Paul Zschack[4], "Ultralow Thermal Conductivity in Disordered, Layered WSe_2 Crystals," Science **315**, 351 (January 19, 2007). DOI: 10.1126/science.1136494

Author affiliations: [1]Department of Materials Science and Engineering, Frederick Seitz Materials Research Laboratory, University of Illinois at Urbana-Champaign; [2]Department of Chemistry, University of Oregon; [3]Department of Materials Science and Engineering, Rensselaer Polytechnic Institute; [5]Advanced Photon Source, Argonne National Laboratory
Correspondence: *d-cahill@uiuc.edu

This work supported by Office of Naval Research grants N00014-05-1-0250 and N00014-96-0407. Research was performed in the Laser and Spectroscopy Facility and the Center for Microanalysis of Materials of the Frederick Seitz Materials Research Laboratory, University of Illinois, which is partially supported by the U.S. Department of Energy under grant DEFG02-91-ER45439. Use of the APS was supported by the U.S. Department of Energy, Office of Science, Office of Basic Energy Sciences, under Contract No. DE-AC02-06CH11357.

33-BM-C • XOR/UNI • Materials science, physics, chemistry • Anomalous and resonant scattering (hard x-ray), diffuse x-ray scattering, powder diffraction, x-ray reflectivity, general diffraction, grazing incidence diffraction • Bending magnet • Accepting general users

Bulk Phase Strains During Ultra-High Carbon Steel Deformation

Ultrahigh-carbon steel (UHCS) is a family of super-strong and yet ductile steels with very high carbon content. After the application of heat treatment, UHCS forms an *in situ* composite consisting of a matrix of soft, ductile ferrite (iron, α-Fe) containing strong particles of brittle cementite (iron carbide, Fe_3C) reinforcement. The composite possesses a wide range of desirable physical properties, such as being extremely strong, very hard, and highly resistant to wear, while at the same time being quite flexible, ductile, and superplastic (at elevated temperatures). Researchers using XOR beamline 1-ID-C at the APS carried out the first high-energy synchrotron x-ray diffraction (SXRD) study of the progression of lattice strain during uniaxial tensile loading of UHCS and measured the bulk phase strains (instead of near-surface strains) during deformation of UHCS, thus determining how load is partitioned between the ferrite and cementite phases and pointing toward future UHCS optimized for strength and ductility.

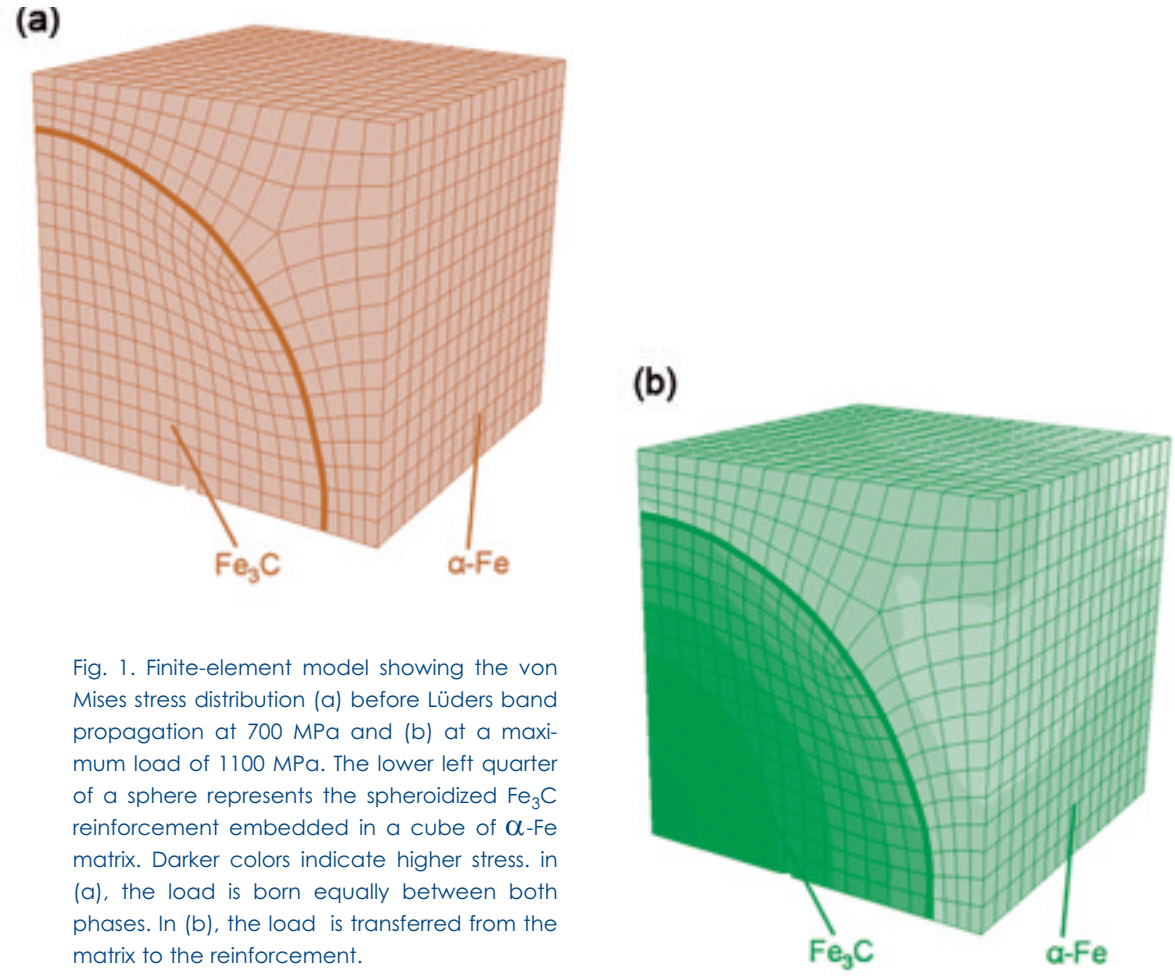

Fig. 1. Finite-element model showing the von Mises stress distribution (a) before Lüders band propagation at 700 MPa and (b) at a maximum load of 1100 MPa. The lower left quarter of a sphere represents the spheroidized Fe_3C reinforcement embedded in a cube of α-Fe matrix. Darker colors indicate higher stress. in (a), the load is born equally between both phases. In (b), the load is transferred from the matrix to the reinforcement.

The bulk strains were measured at beamline 1-ID-C as a function of applied stress, crystallographic orientation, and rolling direction, then compared to finite-element model computations (Fig. 1). The reinforcement cementite phase precipitated within the ferrite matrix consisted of micron-sized, spheroidized particles, 34% by volume, which is almost twice the volume fraction of previous neutron studies. Lattice elastic strains, which were volume-averaged for various crystallographic planes of the ferrite and cementite, were measured for a range of uniaxial tensile stresses up to the point of steel fracture.

The researchers from Northwestern University, Queen's University, and Argonne studied a UHCS with a carbon content of 1.8% by weight. Before sample loading, synchrotron x-ray diffraction measurements were carried out to characterize the preloading composite texture. The group observed that, unlike results seen in prior *ex situ* composite experiments, residual stresses (which occur after cooling from the processing temperatures) are not present in the UHCS because strain differences resulting from thermal expansion (which produce compressive strains) and allotropic transformation (which produce tensile stresses) nearly cancel each other out.

In situ uniaxial tensile testing was performed with the load maintained at a constant level at regular intervals, while phase strains were measured by SXRD. The steel was elastic up to a stress of 720 MPa, followed by plastic deformation with strain hardening up to a failure stress failure at 1060 MPa and a strain of 6.1%.

The researchers found that in the steel elastic range of deformation, the lattice strains are almost the same for both phases; therefore, load transfer did not occur to any appreciable degree between the ferrite matrix and cementite reinforcement because both phases had nearly the same elastic constants [Fig.1(a) and Fig. 2]. This result is in contrast to prior studies on other metal matrix composites, which typically exhibit load transfer in their elastic range.

In the steel plastic deformation range, the researchers found strong load transfer from the matrix to the reinforcement, with the increase in load-carrying capacity of the steel being almost exclusively accounted for by the cementite phase [Fig. 1(b) and Fig. 2]. In addition, matrix load transfer is observed more in the normal direction than in the transverse direction. This observation may be attributed to a deformation difference between the core and the surface of the steel sample resulting from rolling, which was observed in the preloading texture.

The predictions made by finite-element modeling for phase lattice strains of both matrix and reinforcement phases agree with the experimental SXRD data over the range of steel elastic and plastic deformations (Fig. 2). This agreement may allow for the rational design of future UHCS optimized for strength and ductility. — *William Arthur Atkins*

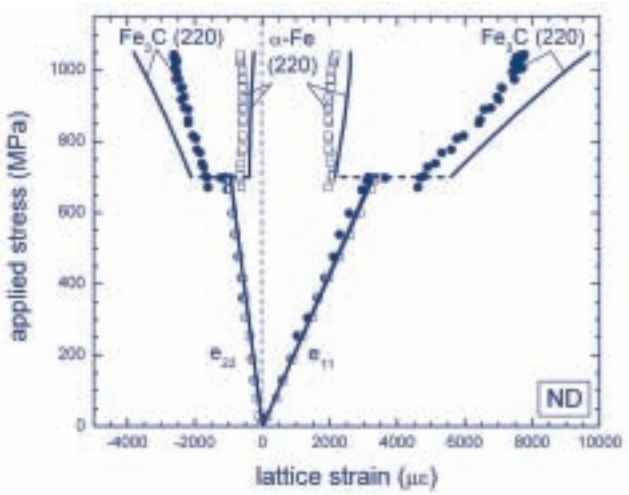

Fig. 2. Applied stress vs. lattice strain (e_{22} perpendicular and e_{11} parallel to the applied stress) for the α-Fe (220) and Fe_3C (220) reflections for sample oriented with rolling normal direction (ND) parallel to beam. The values of the slopes for the α-Fe (220) and Fe_3C (220) reflections are based on best fit of the experimental data. Average finite-element modeling is shown as solid lines.

See: M.L. Young[1,2], J.D. Almer[2], M.R. Daymond[3], D.R. Haeffner[2], and D.C. Dunand[1]*, "Load partitioning between ferrite and cementite during elasto-plastic deformation of an ultrahigh-carbon steel," Acta Mater. **55**, 1999 (2007). DOI: 10.1016/j.actamat.2006.11.004

Author affiliations: [1]Department of Materials Science and Engineering, Northwestern University; [2]Advanced Photon Source, Argonne National Laboratory; [3]Department of Mechanical and Materials Engineering, Queen's University
Correspondence: *dunand@northwestern.edu

Use of the APS was supported by the U.S. Department of Energy, Office of Science, Office of Basic Energy Sciences, under Contract No. DE-AC02-06CH11357.

1-ID-C • XOR • Materials science, physics, chemistry • High-energy x-ray diffraction • 3.3-cm Undulator A • Accepting general users

Polyamorphism in $Ce_{55}Al_{45}$ Metallic Glasses

Metallic glasses—metallic materials containing non-directional metallic bonds, unlike most metals that are crystalline with a highly ordered atomic structure—are a new group of substances with a highly disordered atomic structure. Atoms in metallic glasses are randomly but tightly packed. Polyamorphic phase transitions have been reported only in non-metallic glasses, involving directional changes in bonding. Until recently, it was unknown whether pressure-induced polyamorphic phase transitions could occur in metallic glasses. Researchers using HP-CAT beamline 16-ID-B and XOR beamline 1-ID-C at the APS obtained the first *in situ* x-ray diffraction (XRD) patterns as a function of hydrostatic pressure with respect to abrupt transitions between two distinct polyamorphs in the metallic glass $Ce_{55}Al_{45}$. This work provides information that is important for future research into the state of matter in metallic materials. Further studies could lead to metallic glasses with enhanced properties, fostering new commercial development and applications.

The researchers, from Johns Hopkins University, the Carnegie Institution of Washington, Harbin Institute of Technology, the Chinese Academy of Sciences, and Argonne, used the single-roller melt spinning technique to prepare a sample of $Ce_{55}Al_{45}$ metallic glass. The melt spinning technique is used to rapidly cool liquids via the use of a rotating wheel, which causes rapid solidification. The sample is about 30 μm in thickness and approximately 5 mm in width.

Three of four sets of *in situ* high-pressure XRD experiments were done at beamline 16-ID-B; the fourth took place at beamline 1-ID-C.

The XRD patterns of the $Ce_{55}Al_{45}$ metallic glass show different intensity peaks with varying pressure (Fig. 1). The patterns obtained *in situ* during compression describe gradual movement from 2.0 GPa to 13.5 GPa, with the first sharp diffraction peak shifting to higher momentum transfer at a relatively fast rate. The patterns at 30 GPa are distinctly different from those at lower pressures, which shows that a different amorphous phase has resulted without any crystallization taking place.

However, during decompression an abrupt change in pressure is observed at around 2 GPa. The gradual shift to lower momentum transfer is slow over a wide pressure range, and only speeds up in the first stage of decompression. Thus, by comparing the XRD patterns during compression and decompression, the researchers found that decompression did not duplicate compression over this observed range of pressures.

The researchers also compared the specific volume versus pressure of the $Ce_{55}Al_{45}$. With increasing pressure—greater than 2 GPa—a rapid decrease of volume occurred, with a distinct deviation from equation of state predictions. At 13.5 GPa and above, however, the volume coincides with that expected for the same glass, assuming the *f*-electrons are delocalized. Electronic bond shortening, rather than coordinate or directional changes (resulting from externally applied pressure), is the most likely cause of the large volume decreases.

The results suggest that the researchers observed a polyamorphic transition of the $Ce_{55}Al_{45}$ from a low-density to a high-density state. On decompression, the volume closely followed the prediction for the high-density phase, suggesting that the *f*-electrons remained largely delocalized, until the pressure approached 2 GPa, which caused a rapid return to the low-density phase. The return to original density after decompression suggests the absence of crystallization.

The researchers also analyzed $Ce_{55}Al_{45}$ metallic glass to show that the two amorphous phases—with their large density differences—are structurally different and correspond to the low-density/high-density states modeled upon the *f*-electrons. The large density difference found by the researchers is attributed to different atomic and electronic structures found in the two polyamorphs (in particular, to the bond shortening revealed by *ab initio* modeling of the effects of *f*-electron delocalization).

They compared the compressed low-density state (at 2.6 GPa) with the decompressed high-density state (at 2.9 GPa, just before the abrupt density drop). The researchers found that XRD first-peak positions, along with other features, are distinctly different. The experimental structure factors agree well with those calculated for the low-density and high-density glasses that have different atomic and electronic structures.

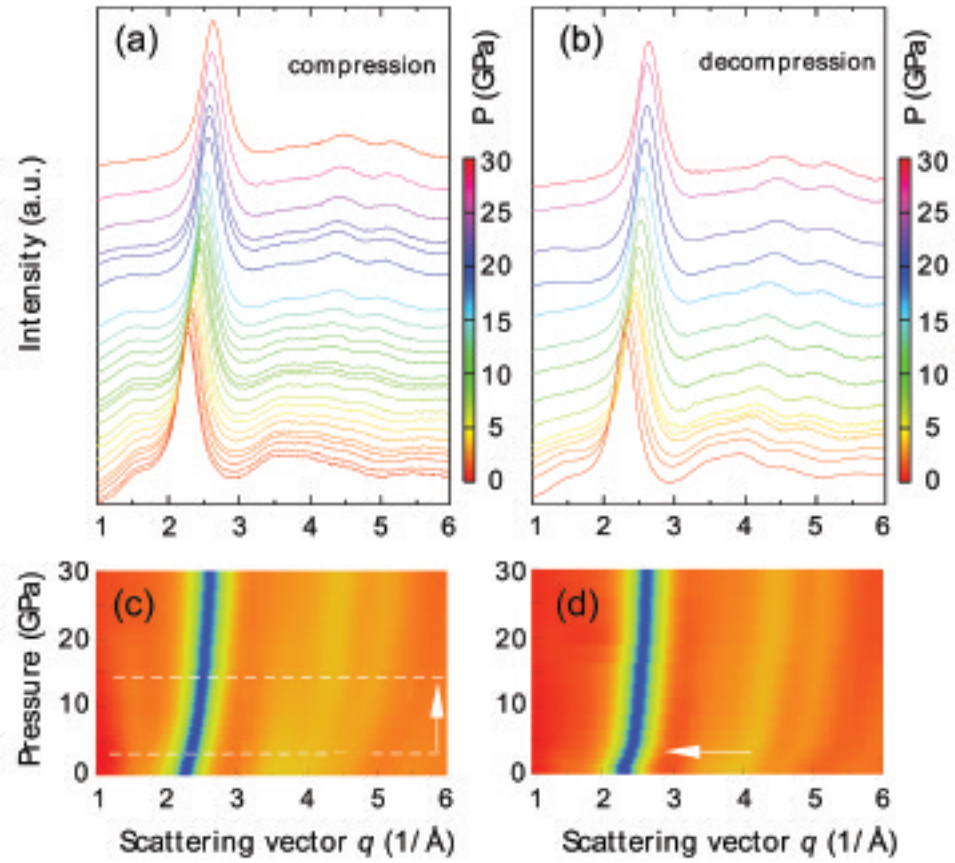

Fig. 1. X-ray diffraction patterns of the $Ce_{55}Al_{45}$ metallic glass in a diamond anvil cell. The display of the XRD patterns—as seen in (a) and (b)—is obtained *in situ* during the compression and decompression experiments, respectively. The bottom panels—as seen in (c) and (d)—highlight and contrast the different behaviors of the XRD intensity peak shift with pressure. The arrow in (c) illustrates a gradual movement during compression in the pressure range from 2.0 to 13.5 GPa (marked with dashed lines), whereas the arrow in (d) marks the abrupt shift toward lower *q*, at around 2 GPa, during decompression.

This work provides a unique analysis of the amorphous state of metals, which helps to foster a better understanding of the structure, evolution, and general properties of metallic glasses and related liquids. This information is especially important for research into the prevention of corrosion and cracking of materials, as well as for materials related to electronic applications. Further research could lead to metallic glasses with enhanced properties and, thus, new commercial development and applications. — *William Arthur Atkins*

See: H.W. Sheng[1]*, H.Z. Liu[2,3], Y.Q. Cheng[1], J. Wen[4], P.L. Lee[5], W.K. Luo[1], S.D. Shastri[5], and E. Ma[1]**, "Polyamorphism in a metallic glass," Nat. Mater. **6**, 192 (March 2007). DOI: 10.1038/nmat1839

Author affiliations: [1]Department of Materials Science and Engineering, Johns Hopkins University; [2]HP-CAT and Geophysical Laboratory, Carnegie Institution of Washington; [3]Center for the Condensed Matter Science and Technology, Harbin Institute of Technology; [4]Institute of Metal Research, Chinese Academy of Sciences; [5]XOR, Advanced Photon Source, Argonne National Laboratory
Correspondence: *hwsheng@jhu.edu; **ema@jhu.edu

This work was supported by the U.S. Department of Energy, Office of Science, Office of Basic Energy Sciences, Division of Materials Sciences and Engineering, under contract No. DE-FG02-03ER46056. The HP-CAT facilities are supported by DOE-BES, DOE-NNSA (CDAC), NSF, DOD-TACOM and the W.M. Keck Foundation. Use of the APS was supported by the U.S. Department of Energy, Office of Science, Office of Basic Energy Sciences, under Contract No. DE-AC02-06CH11357.

1-ID-C • XOR • Materials science, physics, chemistry • High-energy x-ray diffraction • 3.3-cm Undulator A • Accepting general users

Finding the Beats in Film Growth

Sometimes unexpected patterns can show up in the oddest places. When a thin film is being grown atom by atom on a surface, one expects a certain degree of stochastic phenomena. There's always some randomness in just how the film layer grows and where it begins to thicken first. A few atoms or molecules more or less spread at random over a particular area might not matter much on the macro scale, but devices that rely on these thin-layer structures increasingly function on the nanoscale, where a few molecules or atoms can indeed make a huge difference. So, understanding how "roughness" develops during film growth is critical in designing and building these tiny but vital structures. Now a research team working at the XOR/UNI 33-ID-D,E beamline at the APS has found that the buildup of roughness in thin-film deposition might not be quite as random as generally thought. The experimenters have found that examining x-ray diffraction from a thin film at the anti-Bragg points shows a curious beating pattern. The beating modulates diffraction oscillations so that separate growth domains in the "rough" areas of film growth can be identified.

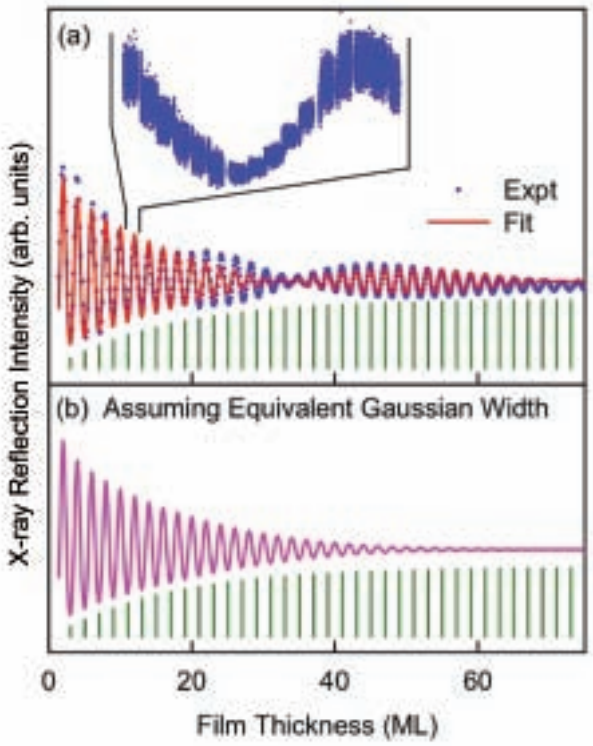

Fig. 1. X-ray intensity at the anti-Bragg position (0, 0, ½) as a function of the average film thickness of TiN deposited on a sapphire substrate. (a) The circles are data, and the curve is a fit. The vertical bars, with a bilayer period, show the oscillation phase reversal in crossing the first node. (b) Calculated intensity pattern assuming a Gaussian roughness with the same standard deviation as the fitting results. It shows no beating.

The team, comprising researchers from the University of Illinois at Urbana-Champaign, National Tsing Hua University, Oak Ridge National Laboratory, and Seagate Technology, used pulsed laser deposition to create TiN films on commercial sapphire substrates. Atomic force microscopy (AFM) was used to image the film step structure, but the experimenters found that the growth domains were too large and few in number for AFM to provide reliable statistical data of the roughness qualities. Examining film deposition in real time via x-ray reflectivity at the anti-Bragg point of the TiN lattice shows rapid oscillations in intensity, corresponding to changes in film thickness.

As the film layer grows, roughness appears when a minor domain with a different atomic layer thickness from the major domain develops and the x-ray oscillation amplitudes from each become out of phase, partially canceling each other out. As the minor domain area becomes equal to the major domain area with further deposition, the net oscillation amplitude becomes zero. This can be seen as a node in the x-ray intensity envelope (Fig. 1). As more domains form under continuing film deposition, the process repeats and another node is formed when two more domains are added that are equal in area. The period of the beating pattern depends on the film roughness, or difference in thickness among different domains, while the oscillation period is governed by the average film thickness, with the oscillation amplitude approaching zero as roughness increases.

If the model is made to fit a Gaussian curve for the roughness, the beating effect diminishes, indicating that the pattern is extremely sensitive to subtle differences in film roughness. But because the self-organizing and diffuse nature of the increasing roughness buildup is not stochastic, it tends to deviate from a Gaussian distribution. The team's work shows that measuring x-ray diffraction at anti-Bragg points is a sensitive enough technique to detect these patterns, which would normally remain undetected and unexpected because of the stochastic effects that are generally assumed to govern the deposition of atoms on thin films. The technique can detect different growth domains separated by only one atomic layer of thickness, allowing them to be reliably counted.

Apart from its academic interest, the research team's work demonstrates that roughness buildup is not an entirely random continuum stochastic phenomenon, but can be characterized and modulated. This opens the intriguing possibility that roughness in thin films can be minimized and controlled.

— Mark Wolverton

See: Y.-R. Lee[1,2,3], A. Gray[1,2], J. Tischler[4], P. Czoschke[5], H. Hong[1], S.-L. Chang[3], and T.-C. Chiang[1,2]*, "Quantum Oscillations and Beats in X-Ray Diffraction during Film Growth," Phys. Rev. Lett. **99**, 156103 (12 October 2007). DOI: 10.1103/PhysRevLett.99.156103

Author affiliations: [1]Department of Physics, University of Illinois at Urbana-Champaign; [2]Frederick Seitz Materials Research Laboratory, University of Illinois at Urbana-Champaign; [3]National Tsing Hua University; [4]Division of Materials Science and Technology, Oak Ridge National Laboratory; [5]Seagate Technology
Correspondence: *Chiang@mrl.uiuc.edu

This work is supported by the U. S. Department of Energy (Grant No. DE-FG02-07ER46383). The Petroleum Research Fund, administered by the American Chemical Society, and the U.S. National Science Foundation (Grant No. DMR-05-03323) are acknowledged for partial support of personnel and the beamline facilities. Use of the Advanced Photon Source was supported by the U.S. Department of Energy, Office of Science, Office of Basic Energy Sciences, under Contract No. DE-AC02-06CH11357.

33-ID-E • XOR/UNI • Materials science, physics, chemistry • Anomalous and resonant scattering (hard x-ray), diffuse x-ray scattering, x-ray reflectivity, surface diffraction, x-ray standing waves, general diffraction • 3.3-cm Undulator A • Accepting general users

Around the APS

HENAAC Honors Two at APS

The Hispanic Engineer National Achievement Awards Conference, or HENAAC, recognized an APS user and an APS employee for their professional contributions and accomplishments.

Juan Carlos Campuzano, an Argonne Distinguished Fellow and APS user, was the recipient of a 2007 Outstanding Technical Achievement Award from HENAAC.

The HENAAC Awards, presented annually for the past 18 years, recognize some of the nation's top engineers, scientists, and technologists of Hispanic heritage. The winners are selected, in part, based on their professional accomplishments and potential as a role model for young people in the Hispanic community. HENAAC (www.henaac.org) was established in 1989 as a means of identifying, honoring, and documenting the contributions of outstanding Hispanic American science, engineering, technology, and math professionals. Campuzano and other 2007 award winners were be honored at the 19th annual HENAAC conference, held on October 11-13 in San Diego, California.

Campuzano, who works in the Synchrotron Radiation Studies Group in Argonne's Materials Science Division, is credited with landmark advances in the field of high-temperature superconductivity. Together with Peter Abbamonte (University of Illinois at Urbana-Champaign) and James Allen (University of Michigan), Campuzano is leading the development of a new sector at the APS, the intermediate energy x-ray scattering (IEX) beamline. The IEX beamline, which will occupy one of the last four open sectors at the APS, will bring to the APS user community a brilliant source of polarized soft x-rays that will be useful for studies of buried electronic structures.

Mariana Varotto, of the Controls Group in the APS Engineering and Support Division, was recognized as a role model for technology professionals by HENAAC. According to the HENAAC Web site, "The Role Model of the Week highlights world-class Hispanic engineers, scientists, and technology professionals from across the employment spectrum. Role Models are selected from the hundreds of nominees submitted for the HENAAC awards."

Varotto was nominated by Ned Arnold, Controls Group leader, who said "Mariana is responsible for dozens of applications related to the APS control systems and is frequently sought out for her expeditious and accurate response to customer requests. The attribute which most compelled me to nominate Mariana for this award was her ability to learn about a new technology or system independently and quickly. She has made significant contributions to our system software, our relational database applications, and numerous on-line systems that are operational 24/7. In addition to her technical capabilities, Mariana has demonstrated a keen interest in promoting engineering and science careers to young women through her involvement in laboratory outreach programs."

Juan Carlos Campuzano

Mariana Varotto

Collapsed Monolayers at the Vapor/Water Interface

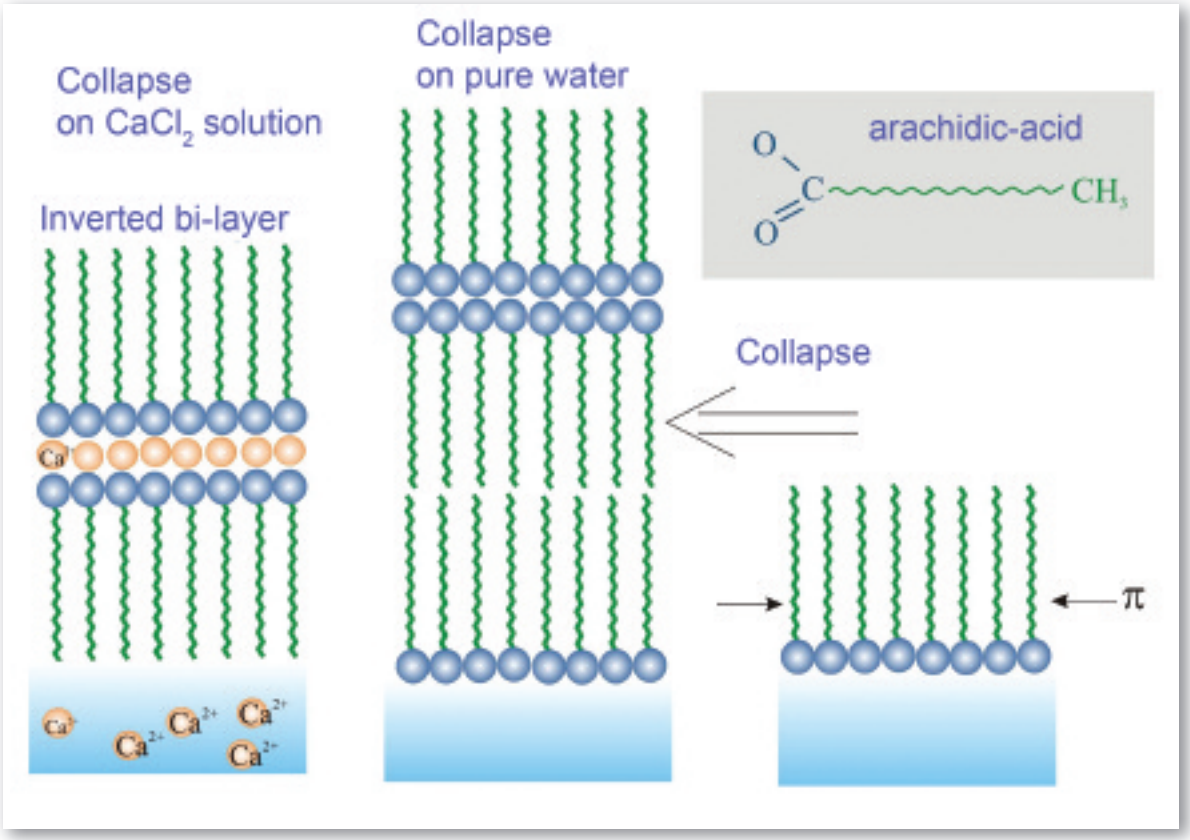

Fig. 1. Compression of arachidic-acid (see box) to collapse (i.e., beyond the molecular cross section) results in the formation of a trilayer structure when the monolayer is manipulated on pure water and to the formation of an inverted bilayer when spread on Ca2+ solution. The collapsed films possess a high degree of in-plane ordering in both cases.

When insoluble monolayers at the gas/water interface (known as Langmuir monolayers) are subjected to controlled pressure and temperature, they can exhibit several phases, from gaseous through liquid to solid. As the pressure on a monolayer increases, causing it to compress, the monolayer becomes a multilayer owing to the fracturing and/or folding that occurs as the pressure passes a critical point. This process is called "collapse," and it is the primary source of monolayer surface-pressure relaxation. The study of collapsed monolayers and its causes (and whether or not that process is reversible) has grown in recent years as science seeks a better understanding of surface tension regulation in the lungs and biological processes, such as the response of membranes to stress, membrane fusion and fission, and other cell membrane processes. Researchers using the MU/XOR 6-ID-B,C beamline at the APS have studied the structure of calcium (Ca^{2+}) Langmuir monolayers, revealing new insights about their genesis and structure.

The researchers, from Iowa State University and the National Institute of Standards and Technology, employed neutron reflectivity, synchrotron x-ray reflectivity, and grazing incidence x-ray diffraction techniques to determine the structure of Langmuir monolayers, which are 1-molecule-thick layers spread at the aqueous/vapor interface. Their experiments show that collapsed films form distinct structures depending on whether the monolayers are compressed on pure water or on solutions containing calcium ions. The researchers also theorize that collapsed structures have lower thermodynamic free energies when compared with other potential structures, and they speculate that these collapsed structures may form spontaneously under specific conditions.

The x-ray measurements at gas/water interfaces were performed on the Ames Laboratory liquid surface diffractometer at beamline 6-ID-B,C. Arachidic-acid monolayers (shown in the box of Fig. 1) were spread at gas/water interfaces in a thermostatic, solid Teflon Langmuir trough. The monolayers and the films undergoing induced collapse were kept under a water-saturated helium environment and under controlled surface-tension and temperature conditions. When the monolayers were manipulated on pure water, the collapsed film was found to consist primarily of a stable crystalline trilayer structure (shown schematically in Fig. 1), with an in-plane ordering closely resembling the three-dimensional crystal structure of fatty acids. Although other experimenters inferred the trilayer structure after collapse from studies of transferred films on a solid support, this is the first known *in situ* detailed experimental evidence of the trilayer structure. This study allows a very precise determination of the ordered crystalline structure.

For arachidic-acid monolayers spread on Ca^{2+} solutions, the collapsed film forms structures consisting of an inverted bilayer (shown schematically in Fig. 1) and trilayer mixtures with a final composition ratio that depends on the collapse protocol. The collapse of arachidic-acid monolayers spread on Ca^{2+} solutions is suggestive of a broad range of very slow relaxation times; monolayer collapse is generally a non-equilibrium process. Quite remarkably, under a specific compression protocol, a pure inverted bilayer can be produced with no measurable trilayer structure present. The inverted bilayer consists of stretched di-arachidate, such that its hydrophobic tails are in contact with aqueous solution (Fig.1). The inverted bilayer is well-ordered, with a crystalline slab of calcium oxalate monohydrate situated between two acyl chains.

Unknown variables still remain regarding collapsed monolayer structures, such as the dependence of collapsed structures on ion specificity, the variables that determine the structures depending on the monolayer collapse protocol, and how collapse regimes may change for molecules with longer molecular chains. The authors are confident that further experimental and theoretical work will help resolve these important issues, which are relevant for the understanding of biological, chemical, and physical processes in living cell membranes. — *William Arthur Atkins*

See: David Vaknin[1]*, Wei Bu[1], Sushil K. Satija[1,2], and Alex Travesseet[1], "Ordering by Collapse: Formation of Bilayer and Trilayer Crystals by Folding Laugmuir Monolayers," Langmuir **23**, 1888 (2007). DOI: 10.1021/la062672u

Author affiliations: [1]Ames Laboratory and Department of Physics and Astronomy, Iowa State University; [2]NIST Center for Neutron Research, National Institute of Standards and Technology

Correspondence: *vaknin@ameslab.gov

The Midwest Universities Collaborative Access Team (MU/XOR) sector at the APS was supported by the U.S. Department of Energy, Basic Energy Sciences, through the Ames Laboratory under Contract No. W-7405-Eng-82. The work of A.T. has been supported by NSF-DMR-0426597. Use of the APS was supported by the U.S. Department of Energy, Office of Science, Office of Basic Energy Sciences, under Contract No. DE-AC02-06CH11357.

6-ID-B,C • MU/XOR • Physics, materials science • Anomalous and resonant scattering (hard x-ray), liquid scattering, magnetic x-ray scattering, powder diffraction, general diffraction, grazing incidence diffraction, surface diffraction (UHV) • 3.3-cm Undulator A • Accepting general users

Do Nanoparticles Dance in Polymer Thin Films?

One of the challenges in studying physics on the nanoscale—not to mention applying physics to the development of useful nano-technological applications—is the fact that, in the nanoworld, things don't always work in quite the same way as at larger scales. One example is the dispersion, behavior, and kinetics of metal particles dispersed in thin polymer matrices. The behavior of such metal nanoparticles in thin polymer films not only provides insight into molecular dynamics at nanometer length scales, but is of prime importance in nanotechnology, particularly in designing and controlling the formation of nanocomposite thin polymer films for various applications. But, how to peer into the dynamics of particles at such small scales? Researchers from Argonne and Northwestern University came up with a novel solution that combines x-ray photon correlation spectroscopy (XPCS) and resonance-enhanced grazing-incidence small-angle x-ray scattering (GISAXS). Using XOR beamlines 8-ID-E and and 8-ID-I at the APS, they measured the intermediate structure factor $f(q,t)$ and probed the slow molecular dynamics and kinetics of nanoparticles in thin nanocomposite films *in situ* for the first time, overcoming the limitations of XPCS at nanometer-length scales.

When dispersed particles are larger than the length scale of the matrix, colloidal theory can describe their characteristics. But when particles are smaller than the radius of gyration (*Rg*), at the nanometer scale or smaller, the descriptions no longer suffice. Such small disordered systems display only very weak scattering intensity, and this, coupled with a relatively low coherent x-ray flux, has restricted the amount of useful data obtainable in previous studies.

Polymer thin films are spun-cast onto silicon substrates coated with a high-electron density material (like palladium) to generate x-ray standing waves under total external reflection from the palladium interface. At certain discrete incidence angles, the electric field intensity inside the film relative to the incident beam intensity is enhanced by a factor of 20 or more due to wave guiding effect. Three samples of gold/polystyrene (PS) nanocomposite thin films were prepared on Si(100) substrates coated with 50 nm of palladium, each film of a different molecular weight and, hence, a different R*g*: 120 kg/mol (R*g*~ 10 nm), 65 kg/mol (R*g* ~ 7 nm), and 30 kg/mol (R*g* ~ 5 nm). The critical molecular weight (M_C) for PS above which the effects of polymer chain entanglements are seen is ca. 36 kg/mol. Thereby, for $M_W < M_C$ (30 kg/mol sample), the polymer film behaves like a viscous fluid whereas for $M_W > M_C$ (65 and 120 kg/mol), the polymer chains face entanglements and thereby has additional elastic properties emanating due to the polymer chain network. The films were 70 nm in thickness. X-ray reflectivity studies were done to obtain electron density profiles and thereby the electric field intensity (EFI) distribution inside the film, along with XPCS and GISAXS experiments (Fig. 1). All work was done at the 8-ID beamlines at an x-ray energy of 7.35 keV.

By performing the measurements at an incident angle just below the PS/nanoparticle critical angle, the penetration of the x-ray beam was limited, giving a four-fold gain in the EFI. This, along with resonance enhancement resulting from the diffusely scattered beam due to wave guiding effect, allows XPCS measurements at wave vectors larger than previously possible. In all the as-prepared samples, the Au nanoparticles are distributed over a 5-nm depth with an average diameter of 3 nm.

Non-equilibrium kinetics was studied by using GISAXS at a temperature of 180° C (glass transition temperature of PS is 100° C), showing a very slow structural evolution of the in-plane nanoparticle distribution over time in all three samples. No out-of-plane changes were observed in the entangled 120-kg/mol and 65-kg/mol films, but in the 30-kg/mol sample, the vertical distribution of Au nanoparticles doubled from 5 to 10 nm over 60 min, attributed to lower viscosity and fewer polymer chain entanglements.

Dynamics studies probing the relaxation time τ vs. the lateral wave vector q_R show a $1/q_R$ dependence (ballistic motion of the nanoparticles) in the entangled samples, while

This study probed the slow molecular dynamics and kinetics of nanoparticles in thin nanocomposite films *in situ*, overcoming the limitations of XPCS at nanometer-length scales

the dynamics of the unentangled sample are more similar to those of a viscous fluid.

The viscoelastic effects observed in entangled polymer melts by the experimenters are quite different from those in colloidal systems that can be explained in terms of Stokes-Einstein-Brownian theories. Without entanglements, there are no elastic effects arising from the polymer matrix, and thus the nanoparticle dynamics are more similar to hydrodynamic interactions in viscous fluid, with van der Waals interactions playing a dominant role.

This research demonstrates that XPCS can be used to examine nanoscale dynamics even in low-electron-density polymer matrices. Further work along these lines will provide more data to allow more accurate molecular dynamics nanoscale simulations, which will lead to the development of better quality nanocomposite materials.

— *Mark Wolverton & Suresh Narayanan*

See: Suresh Narayanan[1]*, Dong Ryeol Lee[1], Aleta Hagman[1,2], Xuefa Li[1], and Jin Wang[1], "Particle Dynamics in Polymer-Metal Nanocomposite Thin Films on Nanometer-Length Scales," Phys. Rev. Lett. **98**, 185506 (2007).
DOI: 10.1103/PhysRevLett.98.185506

Author affiliations: [1]Advanced Photon Source, Argonne National Laboratory; [2]Department of Materials Science and Engineering, Northwestern University
Correspondence: *sureshn@aps.anl.gov

This work and use of the APS was supported by the U.S. Department of Energy, Office of Science, Office of Basic Energy Sciences, under Contract No. DE-AC02-06CH11357.

8-ID-E • XOR • Materials science, polymer science, physics • Intensity fluctuation spectroscopy, x-ray reflectivity, x-ray photon correlation spectroscopy, grazing incidence small-angle scattering • 3.3-cm Undulator A • Accepting general users

8-ID-I • XOR • Polymer science, materials science, physics • Intensity fluctuation spectroscopy, coherent x-ray scattering, small-angle x-ray scattering, x-ray photon correlation spectroscopy • 3.3-cm Undulator A • Accepting general users

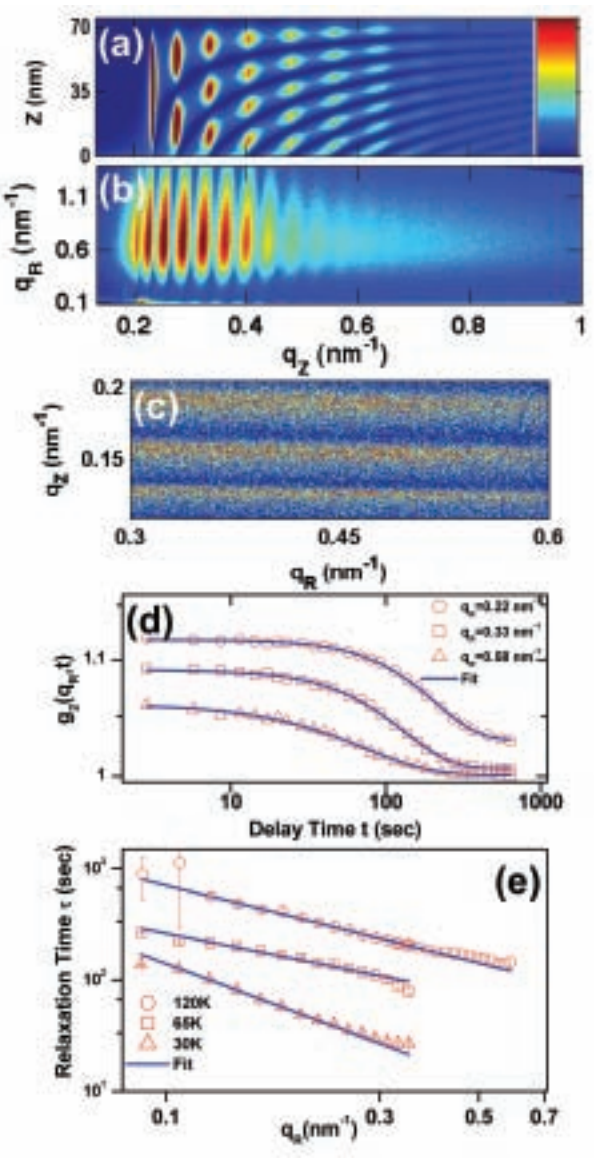

Fig. 1. (a) Two-dimensional (2-D) EFI as a function of depth from the air-polymer interface (Z = 0) and out-of-plane wave vector q_Z, showing enhancement of the EFI at a certain q_Zs due to the waveguiding effect. (b) 2-D GISAXS reciprocal space map (q_Z-q_R) measured at an incidence angle below the critical angle of the PS thin film, showing enhanced diffuse scattering at the q_Zs where EFI enhancement takes place. (c) Snapshot of a speckled scattering pattern from a 120-kg/mol sample shown as a 2-D q_Z-q_R map. (d) Measured autocorrelation functions (g_2) (open circles) at three in-plane wave vectors at 180° C for the 70-nm-thick PS thin film of M_w = 120 kg/mol. Solid lines are best fits to a stretched/compressed exponential form for the intermediate scattering function. (e) Relaxation time (τ) for M_ws of 120, 65, and 30 kg/mol for a PS film with a thickness of 70 nm with a 0.4-nm dispersion of Au, plotted vs q_R on a log-log scale. Solid lines are best fits to a power law form.

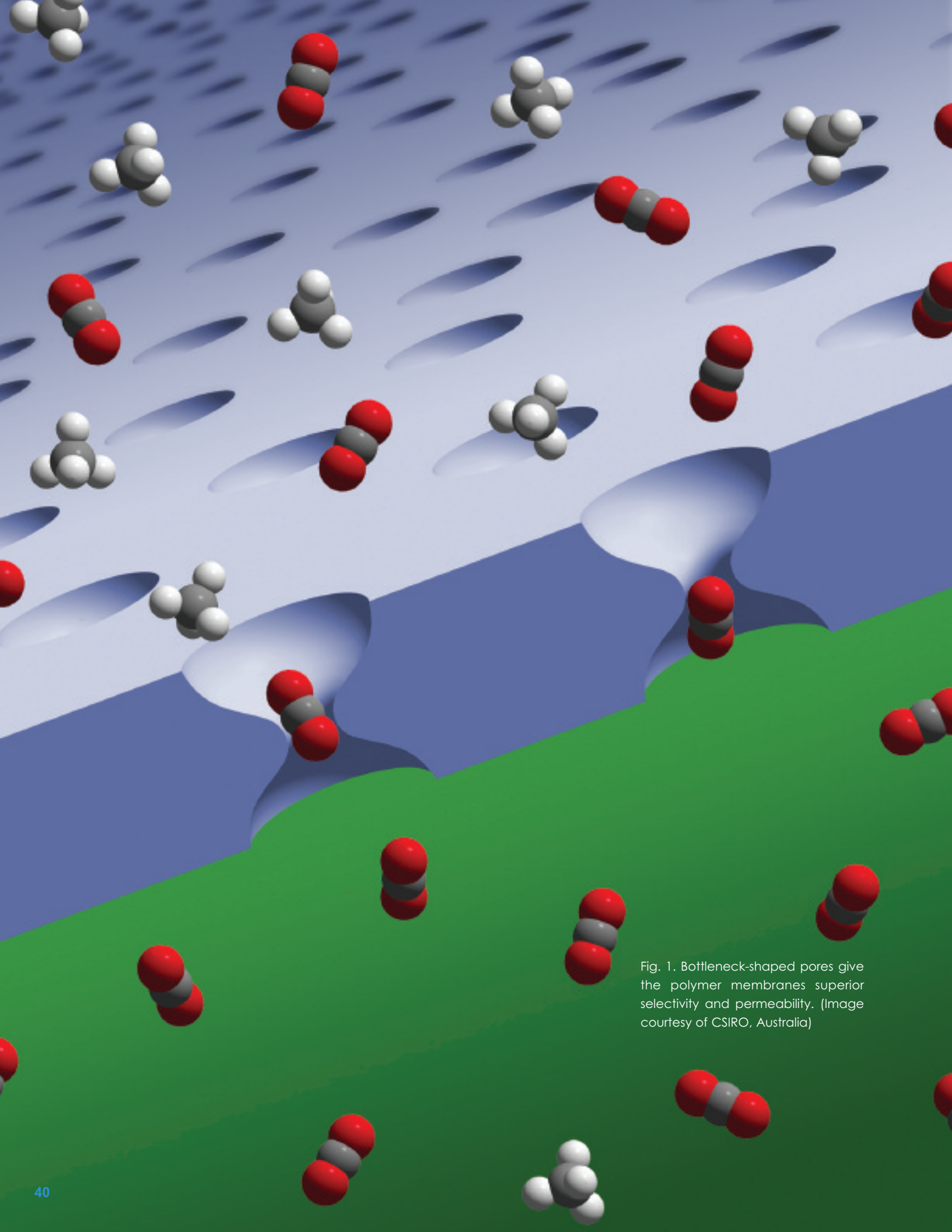

Fig. 1. Bottleneck-shaped pores give the polymer membranes superior selectivity and permeability. (Image courtesy of CSIRO, Australia)

New Polymers for Fast Selective Transport of Small Molecules and Ions

With the aid of small-angle x-ray scattering (SAXS) measurements made at the ChemMatCARS 15-ID-B,C,D beamline at the APS, researchers demonstrated that cavities in dense vitreous polymers can be tailored to give the polymers outstanding molecular and ionic transport and separation characteristics that surpass those of conventional polymers. This rational tailoring of cavity architecture provides an approach for preparing high-performance polymers that is suitable for molecular-scale membrane separation processes in chemicals production, as well as energy conversion and storage. Potential applications for these "super" polymers run the gamut from gas separation membranes and pharmaceuticals to organic batteries and fuel cells.

Small gas molecules and ions diffuse through polymers by traveling inside cavities formed by random, thermally stimulated motion of the flexible organic chains. The mean cavity radius (r) of the most selective polymers, such as polyimides, polysulfones, and polycarbonates, is 0.3 nm or less, with each polymer exhibiting a broad range of cavity radii, as measured by positron annihilation lifetime spectroscopy (PALS). The small cavity size and relatively low connectivity among the cavities make for low gas permeability. Conversely, the most permeable polymer, poly(1-trimethylsilyl-1-propyne), exhibits an approximately bimodal cavity size distribution centered at around r = 0.3 nm and r = 0.6 to 0.7 nm. In this case, the high concentration of large cavities and the high degree of connectivity among the cavities make the polymer highly permeable but unable to separate small molecules. Generally speaking, most polymers have cavities that vary greatly in size, which prevents them from providing both high permeability and high selectivity.

Using PALS, SAXS, and other techniques, the researchers from Hanyang University, the University of Texas at Austin, the Commonwealth Scientific and Industrial Research Organization (CSIRO), and the Australian Synchrotron Research Program at Argonne demonstrated an ability to fabricate polymers yielding both high permeability and high selectivity. These polymers were characterized as having an intermediate cavity size, a narrow cavity size distribution, and bottleneck-type cavities connecting adjacent larger chambers (Fig. 1). Central to their approach in preparing these intermediate-sized cavities is controlled cavity formation through spatial rearrangement of rigid polymer chain segments in the glassy phase. For this purpose, aromatic polymers interconnected with heterocyclic rings were used because the phenylene-heterocyclic ring units in such materials have a flat, rigid-rod structure with high torsional energy barriers to rotation between two rings. The stiff, rigid ring units in such flat topologies pack efficiently, leaving very small penetrant-accessible cavities. These materials meet the demand for polymers that are thermally and chemically stable, but their lack of solubility in common solvents prevented them from being prepared as thin membranes by solvent casting, which is the most widely practiced method for membrane preparation. The researchers circumvented this problem through post-fabrication polymer-modifying reactions. The greatest benefit of these polymers is the ability to tune cavity size and distribution for specific gas applications with one starting material, by using various templating molecules and heat treatments. — *Vic Comello*

See: Ho Bum Park[1,2], Chul Ho Jung[1], Young Moo Lee[1]*, Anita J. Hill[3], Steven J. Pas[3], Stephen T. Mudie[3], Elizabeth Van Wagner[2], Benny D. Freeman[2], and David J. Cookson[4], "Polymers with Cavities Tuned for Fast Selective Transport of Small Molecules and Ions," Science **318**, 254 (12 October 2007). DOI: 10.1126/science.1143719

Author affiliations: [1]School of Chemical Engineering, Hanyang University; [2]Center for Energy and Environmental Resources and Department of Chemical Engineering, The University of Texas, Austin; [3]The Commonwealth Scientific and Industrial Research Organization, Materials Science and Engineering; [4]Australian Synchrotron Research Program at Argonne

Correspondence: *ymlee@hanyang.ac.kr

Work supported by the Carbon Dioxide Reduction and Sequestration Center funded by the Ministry of Science and Technology in Korea, the Australian Research Council (ARC) Centers of Excellence program through the ARC Center for Electromaterials Science, and CSIRO's Water for a Healthy Country Flagship and the Division of Materials Science and Engineering in CSIRO. H.B.P. and B.D.F. acknowledge support of the U.S. Department of Energy (DE-FG03-02ER15362) and the National Science Foundation (CTS-0515425). Use of the Advanced Photon Source was supported by the U.S. Department of Energy, Office of Science, Office of Basic Energy Sciences, under Contract No. DE-AC02-06CH11357.

15-ID-B,C,D • ChemMatCARS • Materials science, chemistry • Anomalous and resonant scattering (hard x-ray), liquid scattering, microdiffraction, single-crystal diffraction, small-angle x-ray scattering, surface diffraction, wide-angle x-ray scattering • 3.3-cm Undulator A • Accepting general users

How Perfect are Two-Dimensional Block Copolymer Single Crystals?

Keeping things in order is important, particularly on the nanoscale. Even a single atom out of place can make the difference between a molecular structure being useful in a practical application or being only a molecular curiosity. Block copolymers self-assemble into nanoscale domains. In the semiconductor industry, two-dimensional (2-D) layers are being considered as an inexpensive method for patterning nanoscale features. Diminished translational order in block copolymer crystals is a serious problem if these systems are used to template devices such as high-density data disks, because proper data storage is impossible without precise domain positioning on the disk. A better understanding of the domain positioning in a 2-D block copolymer crystal is crucial for engineers and scientists attempting to design and build such devices. Researchers used XOR beamline 8-ID-E at the APS to examine how 2-D block copolymer single crystals achieve order.

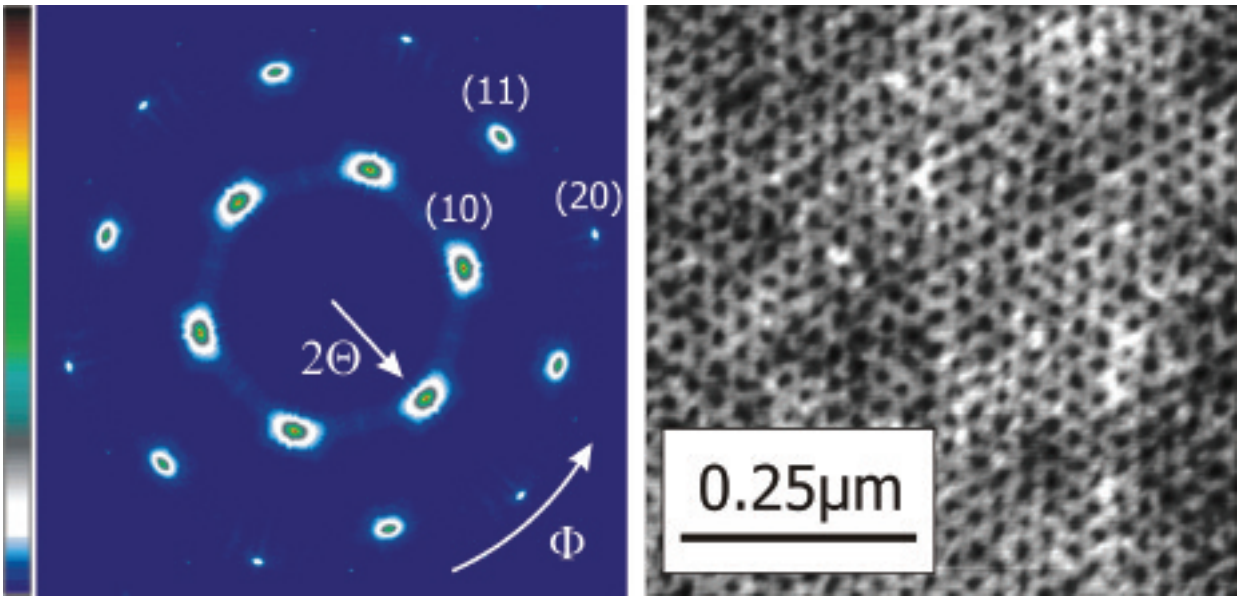

Fig. 1. (Left) A scattered intensity data map, in a radial plot to resemble a conventional powder diffraction pattern, showing excellent long-range sixfold orientation of the 2-D single crystals. (Right) SFM micrograph of the PS-PVP block copolymer spheres.

GISAXD as a probe of single-crystal 2-D block copolymers allows such structures to be better designed for use in practical applications and devices

By using grazing-incidence small-angle x-ray diffraction (GISAXD), the team of researchers from the University of California, Santa Barbara, and Argonne studied the structure of 2-D single crystals of polystyrene-b-2vinyl pyridine (PS-PVP) block copolymer spheres. The single crystals were templated by lateral confinement in 12-μm-wide hexagonal wells; this width is more than 400 times larger than the periodicity of the crystal itself. While a previous study attempted to characterize such structures via scanning force microscopy (SFM), the present experimenters chose the GISAXD technique because it promised a much more accurate look than does SFM, which is limited by distortions caused by thermal drift and also suffers from poor statistics due to the small sampling area it provides for analysis. By analyzing the shape of the Bragg diffraction peaks with the KTNHY (Kosterlitz-Thouless-Halperin-Nelson-Young) theory, which provides the best current description of two-dimensional phase behavior, the experimenters were able to calculate the decay exponent η.

At the 8-ID-E beamline, the PS-PVP copolymer sample was measured with a 7.5-keV x-ray beam at a wavelength of 0.1675 nm. The samples were rotated in-plane and data collected at each rotation angle to demonstrate that single crystals were successfully templated. The data were then compiled to build scattered intensity data maps $I(2\Theta,\phi)$: translational order was determined by analyzing the intensity as a function of the in-plane scattering angle 2Θ, and the orientation of the crystal was determined from the in-plane rotation angle ϕ. The orientation of the crystal was perfect to within 1º, demonstrating excellent long-range orientation of the 12-μm-wide 2-D single crystals (Fig. 1). The translational order was found to decay algebraically with a decay exponent η = 0.2. (A "perfect" crystal has η = 0.)

The KTNHY decay exponent η depends on the 2-D lattice's elastic constants, decreasing inversely as the shear modulus. Simulations using self-consistent field theory provide a way to estimate the elastic properties of the lattice and are in reasonable agreement with experiment [1]. The researchers also note that the decay exponent is temperature dependent, meaning that by controlling the temperature during growth of the block copolymer crystal, it should be possible to manipulate and improve the 2-D positional order despite the disruption caused by phonons.

The team's examination of 2-D block copolymer single crystals with GISAXD shows long-range orientational order. Their interpretation of the data using KTNHY theory shows that this long-range order decays algebraically, with a translational decay exponent of 0.2, and also confirms scaling predictions while providing an estimate of shear modulus. The work demonstrates the usefulness of GISAXD as a tool to probe the single-crystal structure of 2-D block copolymers, an important capacity that will allow such structures to be better and more efficiently designed for use in practical applications and devices. — *Mark Wolverton*

Reference

[1] G.E. Stein, W.B. Lee, G.H. Fredrickson, E.J. Kramer, X. Li, and J. Wang, Macromolecules **40**(16), 5791 (2007).

See: G.E. Stein[1], E.J. Kramer[1,2*], X. Li[3], and J. Wang[3], "Single-Crystal Diffraction from Two-Dimensional Block Copolymer Arrays," Phys. Rev. Lett. **98**, 086101 (23 February 2007). DOI: 10.1103/PhysRevLett.98.086101

Author affiliations: [1]Department of Chemical Engineering, University of California, Santa Barbara; [2]Department of Materials, University of California, Santa Barbara; [3]Advanced Photon Source, Argonne National Laboratory
Correspondence: *edkramer@mrl.ucsb.edu

This work was supported by the NSF DMR Polymers Program Grant No. DMR0307233. This work benefited from use of the facilities of the UCSB MRL, which is supported by the MRSEC Program of the NSF under Grant No. DMR05-20415, and from use of the nanofabrication facilities, which is supported by the NSF-NNIN under Grant No. 44771-7475. Use of the APS was supported by the U.S. Department of Energy, Office of Science, Office of Basic Energy Sciences, under Contract No. DE-AC02-06CH11357.

8-ID-E • XOR • Materials science, polymer science, physics • Intensity fluctuation spectroscopy, x-ray reflectivity, x-ray photon correlation spectroscopy, grazing incidence small-angle scattering • 3.3-cm Undulator A • Accepting general users

Shaking and Sticking in Molten Polymer Thin Films

Much work has been done in recent years on the dynamics of entangled chains of polymer melts that can have properties superior to those of the individual polymer components. Entangled polymer chains are used in a wide range of applications, from polyester and polypropylene films employed in the wrapping and hermetic sealing of foodstuffs and the production of audio and computer tapes, to man-made fibers and industrial resins. But relatively little research has been conducted on the surface dynamics of polymer melts adsorbed on thin films, such as the factors that affect viscosity, elasticity, and other characteristics. An understanding of such phenomena is necessary for further development of these films for new applications, but examining and explaining surface dynamics on thin-film polymer melts are not easy tasks. Researchers have taken on this challenge by using x-ray photon correlation spectroscopy (XPCS) at the XOR beamlines 8-ID-E and 8-ID-I at the APS. Their research shows, for the first time, that the conventional model of capillary waves on a viscous liquid needs modification in order to account for scattering data obtained from ultrathin polymer films.

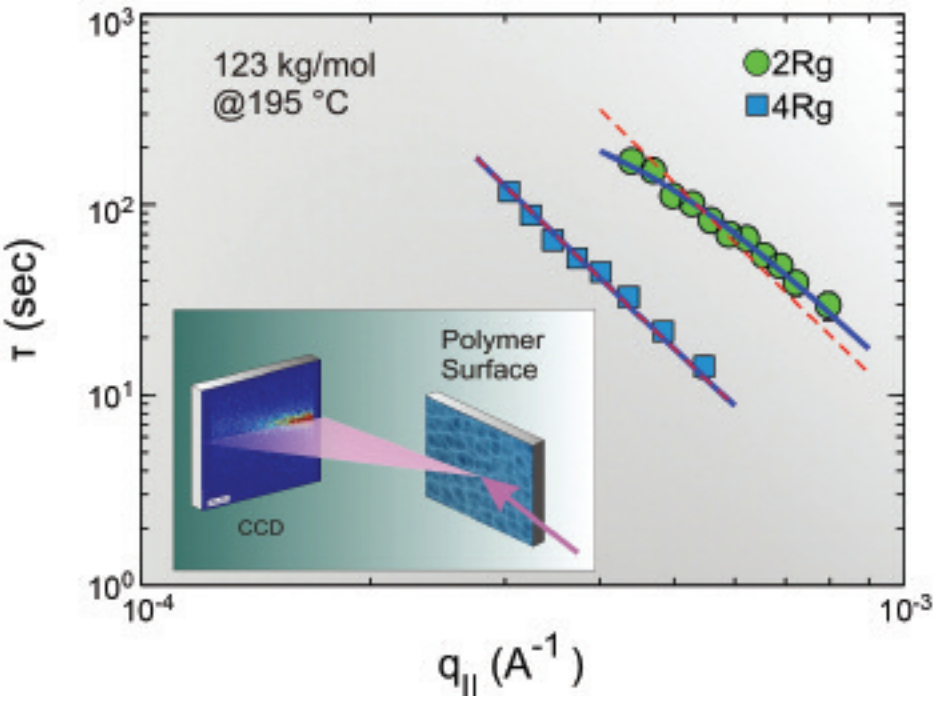

In this technique, the coherent portion of an undulator beam is utilized, resulting in a speckle pattern that fluctuates as the scattering atoms move. The autocorrelation function of the resulting speckle intensities as a function of time allows one to obtain the relaxation times for fluctuations of different wavelengths propagating across the surface of the film. The team's work studies viscoelastic and shear modulus effects in molten polymer films of varying thicknesses.

The experimenters, from the University of California, San Diego; Sogang University; Northern Illinois University; SUNY at Stony Brook; and Los Alamos National Laboratory looked at spun cast polystyrene (PS) films of several different molecular weights (Mw): 65k, 123k, 400k, and 650k g/mol, at film thicknesses h at the radius of gyration (R_g), $2R_g$, $4R_g$, and beyond. Because the XPCS technique does not allow a precise measurement of the shear modulus, the samples were first examined with transverse diffuse scanning, which features a much broader in-plane scattering (q||) window. This work was done at the 8-ID-E beamline by using various temperatures for each sample. These observations showed that the shear modulus did not fit the models for a simple viscous liquid (Fig. 1).

The XPCS work was performed at the 8-ID-I beamline. The researchers found that although in their previous work with films at thicknesses greater than $8R_g$ normal hydrodynamic theory had explained the capillary wave fluctuations very well, this was no longer the case when thicknesses decreased to $2R_g$ and less. In the current experiment, the surface dynamics of the $4R_g$ film can be explained with a simple viscous model, but at lesser thicknesses, the shear modulus comes into play. In principle, a normal liquid shows no resistance to shear; however, it appears that for thin molten polymer films, the adsorption to the substrate and entanglements between the polymer chains give rise to a shear modulus. Viscoelastic effects are seen that increase the surface wave relaxation time. This was seen in $2R_g$ films even of different molecular weights, but not at all in $4R_g$ films, indicating that the ratio of the film thickness to the R_g is the important factor determining whether the shear modulus will affect capillary wave relaxation times.

< Fig. 1. Surface fluctuation relaxation time vs. in-plane wave vector measured by using XPCS on molten PS films of molecular weight 123 kg/mol at 195° C with two different relative thicknesses, $2R_g$ and $4R_g$. The red dashed lines and blue solid lines are best fits to the viscous model and the viscoelastic model, respectively. It is clear that for the $2R_g$, the conventional viscous model for simple liquids, failed, and it is necessary to add the effects of a shear modulus, while for the $4R_g$ film, it is sufficient to describe the experiment data. The inset shows the experiment setup.

The experimenters found that the XPCS scattering data from the various samples examined are best explained by modifying the usual models of capillary wave behavior in viscous liquids to take into account the viscoelastic effects caused by elastic shear modulus in molten polymer films less than $4R_g$ in thickness. These thinner films show suppressed surface dynamics down to $1R_g$, where no such dynamics are observed. Above film thicknesses of $4R_g$, or greater, normal viscous phenomena are seen.

The team's use of XPCS on molten polymer thin films has provided the first evidence of these effects, showing that the typical models are not universally applicable in all cases. The work also demonstrates how viscoelastic effects are dependent on various film characteristics, such as thickness and molecular weight. Such research is essential to perfecting the capacity to create and tailor polymer films for specific jobs and purposes. — *Mark Wolverton*

See: Zhang Jiang[1], Hyunjung Kim[2], X. Jiao[3], H. Lee[2], Y.-J. Lee[2], Y. Byun[2], S. Song[2], D. Eom[2], C. Li[4], M.H. Rafailovich[4], L.B. Lurio[3], and S.K. Sinha[1,5]*, "Evidence for Viscoelastic Effects in Surface Capillary Waves of Molten Polymer Films," Phys. Rev. Lett. **98**, 227801 (2007).
DOI: 10.1103/PhysRevLett.98.227801

Author affiliations: [1]Department of Physics, University of California, San Diego; [2]Department of Physics and Interdisciplinary Program of Integrated Biotechnology, Sogang University; [3]Department of Physics, Northern Illinois University; [4]Department of Materials Science and Engineering, SUNY Stony Brook; [5]LANSCE, Los Alamos National Laboratory
Correspondence: *ssinha@physics.ucsd.edu

This work was supported by NSF Grant No. DMR-0209542, the International Cooperation Program of the Korean Ministry of Science and Technology (M60401000157), Seoul Research and Business Development Program (10816), and a 2007 Sogang Research Grant. Use of the APS was supported by the U.S. Department of Energy, Office of Science, Office of Basic Energy Sciences, under Contract No. DE-AC02-06CH11357.

8-ID-E • XOR • Materials science, polymer science, physics • Intensity fluctuation spectroscopy, x-ray reflectivity, x-ray photon correlation spectroscopy, grazing incidence small-angle scattering • 3.3-cm Undulator A • Accepting general users

8-ID-I • XOR • Polymer science, materials science, physics • Intensity fluctuation spectroscopy, coherent x-ray scattering, small-angle x-ray scattering, x-ray photon correlation spectroscopy • 3.3-cm Undulator A • Accepting general users

Probing Excited Porphyrins

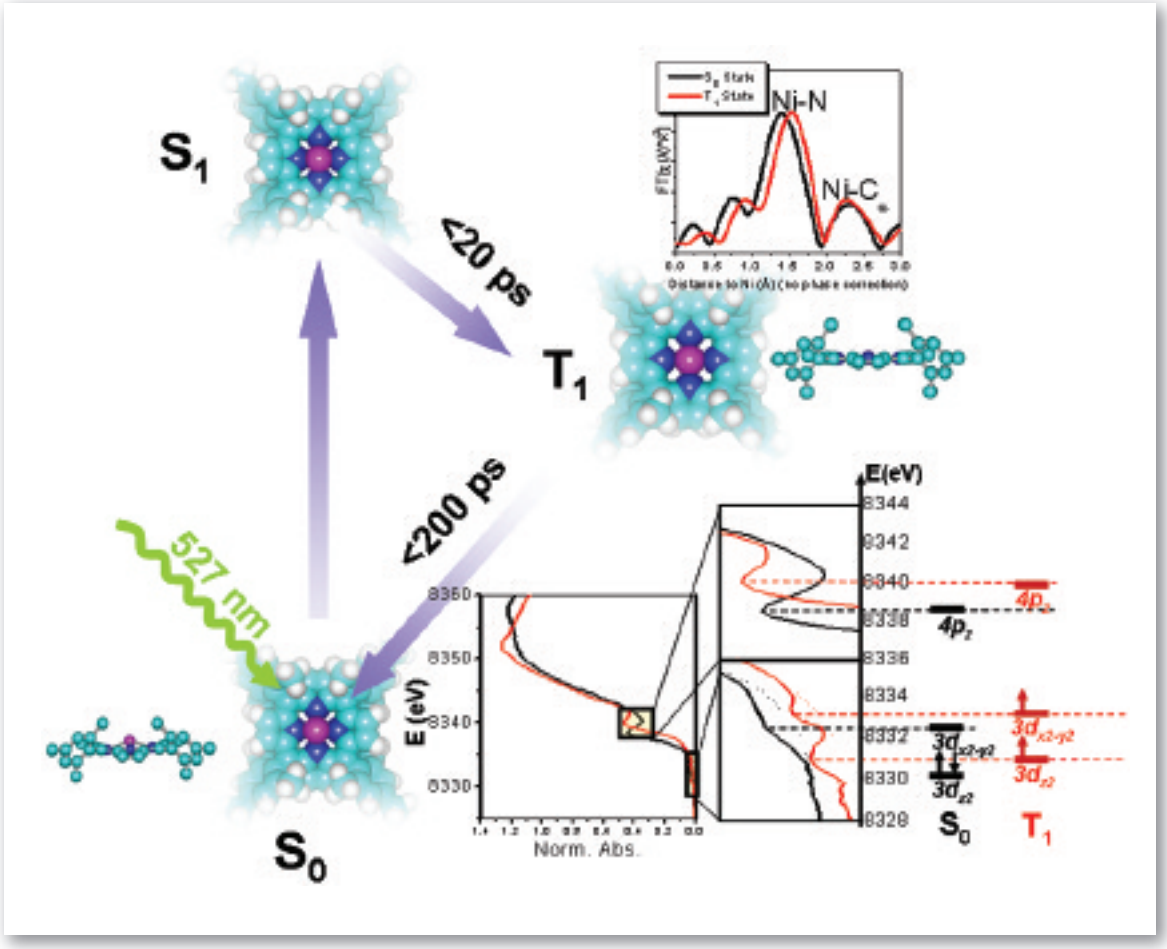

Fig. 1. The photoexcitation pathway and conversion rates for NiTMP. The upper right panel shows Ni-N distance elongation from the XAFS spectra, while the lower right panel shows the XANES spectra where the molecular orbital energy levels are mapped for the unexcited, or ground, state and the vibrational relaxed excited state. The "S1" excited state can be studied only by laser transient absorption spectroscopy, but its structure could be captured when shorter x-ray pulses become available in the future.

11-ID-D • XOR/BESSRC • Chemistry, geoscience, materials science • X-ray absorption fine structure (XAFS), general diffraction, time-resolved XAFS • 3.3-cm Undulator A • Accepting general users

New x-ray studies of the photochemical behavior of molecules found in the cores of several biological systems could shed light on how photosynthesis in plants works and one day lead to synthetic units for converting sunlight. Porphyrin molecules are analogs of chlorophylls at the core of several molecular biological systems. Most notably, the general structure forms the light-trapping units in green plants. Other molecules with the general porphyrin structure at their heart include the iron-bearing heme groups found in hemoglobin and the cobalt-centered vitamin B12, as well as the nickel-based Factor F430 found in certain kinds of methane-producing bacteria. The detailed structure of the organic porphyrin component may differ, but these biological systems have one thing in common: a metal ion at the core. Until the advent of facilities such as the APS, where researchers can run powerful x-ray and related experiments, the metal ions at the core of porphyrins remained a "dark" mystery, their optical characteristics invisible or masked by stronger signals from the rest of the photoreaction system. The work of researchers using the XOR/BESSRC 11-ID-D beamline at the APS sheds new light on the metal centers, bolstering earlier theoretical studies with experimental results.

Metalloporphyrins are chemically versatile compounds that can be used to drive photochemical reactions. They can also allow electrons to be shuffled and energy exchanged between different reactants, triggering useful chemical processes. Chemists have spent many years making and testing metalloporphyrins as photocatalysts and seeking to emulate in the laboratory the incredible efficiency of photosynthesis for making sugars, or fuel, with light, water, and carbon dioxide. However, understanding the way metalloporphyrins function has been incomplete without direct experimental observations of their structures during photochemical reactions. Previous researchers have used ultrafast laser spectroscopy to gain insights into the energetics and kinetics of metalloporphyrin-excited states.

Until now, the information obtained has been limited because the optical signals from the metal center are overshadowed by other stronger signals. The many metal centers are also optically silent or lack optical signatures. Finally, no direct geometric information can be extracted using optical spectroscopy because the wavelengths used are much longer than the atomic scale. Chemists would like to understand what specific structural factors affect these excited states so they can control them in the design of tailored metalloporphyrins with specific photochemical properties.

Researchers from Argonne and North Carolina State University investigated the excited-state properties of a nickel porphyrin molecule—nickeltetramesitylporphyrin (NiTMP)—which exists only fleetingly, for less than 0.2 billionths of a second. The researchers used beamline 11-ID-D to employ x-ray transient absorption spectroscopy (XTA) in tracking the whereabouts of the electrons and atoms in the photoexcited metalloporphyrin. The XTA technique, also known as laser-initiated time-resolved x-ray absorption spectroscopy, allowed the researchers to tease out details of NiTMP on a time scale lasting just 100 ps. In contrast to laser photon techniques, XTA can probe deep into the heart of the nickel center, exciting electrons from the core to the valence levels and higher.

Laser transient absorption spectroscopy demonstrated its prowess as a powerful tool in obtaining the energetics and kinetics of the reaction. Similarly, x-ray transient absorption spectroscopy can provide more accurate information on electron occupations and molecular geometry during a photochemical reaction than is possible with other techniques. As such, XTA combined with ultrafast laser transient absorption spectroscopy allowed the team to obtain detailed and accurate structural and kinetic information for metalloporphyrin in various states of excitation or relaxed excitation.

The nickel-porphyrin system rushes down an energy cascade, spitting out excess energy from different excited states that make the molecule vibrate in previously unseen "vibrationally hot states." These hot states shake the molecular structure, leading to the molecular equivalent of shape-shifting with resulting geometric changes. The distances between the nickel ion and the carbon and nitrogen atoms lengthen, consistent with an overall expansion of the porphyrin ring in the excited state. — *David Bradley*

See: Lin X. Chen[1]*, Xiaoyi Zhang[1,2], Erik C. Wasinger[1], Klaus Attenkofer[2], Guy Jennings[2], Ana Z. Muresan[3], and Jonathan S. Lindsey[3], "Tracking Electrons and Atoms in a Photoexcited Metalloporphyrin by X-ray Transient Absorption Spectroscopy," J. Am. Chem. Soc. **129**, 9616 (2007). DOI: 10.1021/ja072979v

Author affiliations: [1]Chemistry Division and [2]X-ray Science Division, Argonne National Laboratory; [3]Department of Chemistry, North Carolina State University
Correspondence: *lchen@anl.gov

This work is supported by the Division of Chemical Sciences, Office of Basic Energy Sciences, U.S. Department of Energy under contracts DE-AC02-06CH11357 (L.X.C., X.Z., E.C.W., K.A., and G.J.) and DE-FG02-96ER14632 (J.S.L. and A.Z.M.). Use of the Advanced Photon Source was supported by the U.S. Department of Energy, Office of Science, Office of Basic Energy Sciences, under Contract No. DE-AC02-06CH11357.

Molecular Squares in a Flap

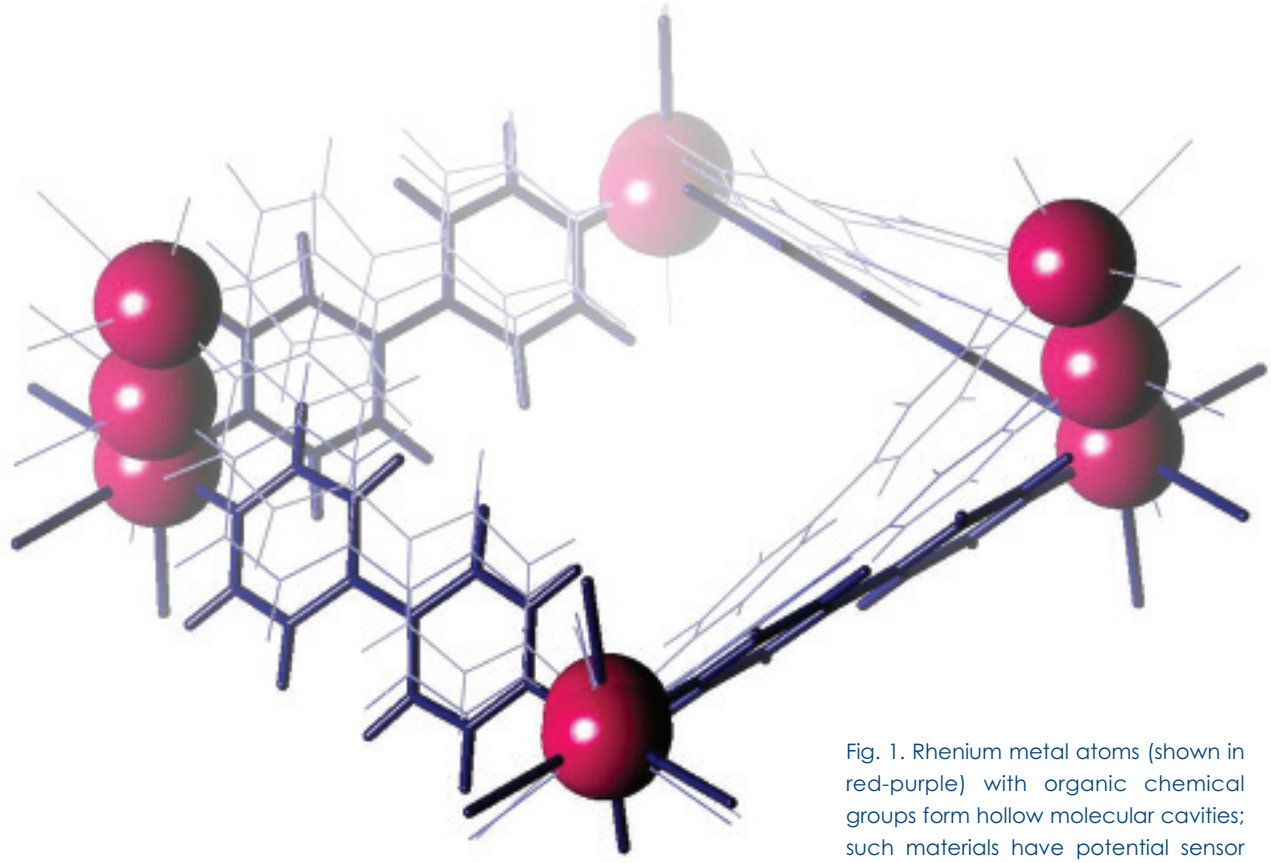

Fig. 1. Rhenium metal atoms (shown in red-purple) with organic chemical groups form hollow molecular cavities; such materials have potential sensor and catalytic applications.

The shape of a given molecule determines how it fits into a reaction and what the end products might be. So it follows that controlling shape is central to controlling reactions. In the area of coordination chemistry, where metal atoms link up with organic ligands and other small molecules, chemists have spent much of the past decade constructing supramolecules that take the shapes of squares, rectangles, triangles, and polyhedra. These building blocks can be linked together to form supramolecules in the form of hollow molecular cavities. While overall shape is important, it is the edges of small molecular units that dictate how they might be linked together. Forming a cavity large enough for another small molecule to fit within forms the basis of concepts in catalysis such as nanoscopic reaction vessels akin to biological enzymes. Understanding the exact structure of such molecules is crucial to understanding and fine-tuning their reactivity and tailoring them to particular applications. Researchers using two beamlines at the APS have obtained new, highly detailed information about supramolecular structures that could have important implications for advancing the art of supramolecule assembly.

Researchers using two APS beamlines have obtained new, highly detailed information about supramolecular structures that could have important implications for advancing the art of supramolcule assembly

Synthetic skills have recently reached the point where it is possible to construct almost any given polyhedral shape from 0.5 nm to 3.5 nm in size, with defined chemical functionality along the edges, and then assemble these blocks to form useful hollow molecules (Fig. 1). Sensor molecules that can trap only molecules of a specific size and shape are also possible based on hollow supramolecular assemblies. In studying the structures of supramolecules, chemists face several obstacles. First, solid-state crystallographic studies are often precluded because these assemblies are loath to crystallize. Second, standard analytical techniques, including nuclear magnetic resonance, infrared, ultraviolet-visible spectroscopy, and elemental analysis, are limited because they cannot generally differentiate between aggregates of individual molecules that might form ring-shaped trimers or tetramers, for instance. Finally, mass spectrometry and chromatography provide some relief in terms of obtaining pure samples and absolute mass information, but none of these techniques provides the fine detail of an x-ray study.

Employing 20-keV, 0.62-Å radiation, a MAR™ charge-coupled device area detector, and wide-angle x-ray scattering at the XOR 12-BM-B and 12-ID-B,C,D beamlines, the researchers from Northwestern University and Argonne obtained detailed characterizations of a range of rhenium-centered compounds built as pyrazine- and bipyridine-edged squares. Their study reveals these molecules to be relatively rigid, even in solution. However, the fine detail made possible by APS x-rays showed what might be described as discrepancies in the bond distances between the rhenium atoms, compared with those obtained for similar compounds using solid-state diffraction techniques. This result, the team suggests, implies that these molecular squares oscillate between two states, much like a butterfly's wings flapping. The team carried out preliminary molecular dynamics calculations on the structure to confirm successfully that such movement was theoretically possible rather than a result of experimental error.

The finding could have important implications for the use of these and related molecules in the construction of supramolecular assemblies. Indeed, these molecular squares are the archetypes of a broad group of related supramolecular structures, the researchers explain. The structures are based on metal coordination chemistry and are more rigid even than conventionally bonded structures. Moreover, the metal atoms, with their high electron density, sit at the corners, connected via relatively simple chemical groups, and so offer a very well-defined framework not only for structural studies but for creating novel molecular capsules and other nanoscopic entities.

The next step is to investigate further the initial strong evidence the team also obtained for ordering of solvent molecules by these supramolecular materials. It seems that a quantitative understanding of this particular phenomenon may arise from studies of host-guest interactions between the host-like cavities and the smaller, guest molecules. The researchers also plan to carry out more sophisticated real-time molecular dynamics studies; these will help shed light on photoinitiated processes that occur in these supramolecules.

— David Bradley

See: Jodi L. O'Donnell[1], Xiaobing Zuo[3], Andrew J. Goshe[3], Lev Sarkisov[2], Randall Q. Snurr[2], Joseph T. Hupp[1], and David M. Tiede[3]*, "Solution-Phase Structural Characterization of Supramolecular Assemblies by Molecular Diffraction," J. Am. Chem. Soc. **129**, 1578 (2007). DOI: 10.1021/ja0659065

Author affiliations: [1]Department of Chemistry, Northwestern University; [2]Department of Chemical and Biological Engineering, Northwestern University; [2]Argonne National Laboratory
Correspondence: *tiede@anl.gov

This work was supported by the Office of Science, U.S. Department of Energy (Grant DE-FG02-01ER15244 to Northwestern and Contract DE-AC02-06CH11357 to Argonne National Laboratory). J.L.O. gratefully acknowledges a fellowship from the Argonne Lab-Grad Program. Use of the APS was supported by the U.S. Department of Energy, Office of Science, Office of Basic Energy Sciences, under Contract No. DE-AC02-06CH11357.

12-BM-B • XOR/BESSRC • Materials science, geoscience, chemistry, polymer science, physics, environmental science • X-ray absorption fine structure, fluorescence spectroscopy, powder diffraction, x-ray reflectivity, general diffraction • Bending magnet • Accepting general users

12-ID-B,C,D • XOR/BESSRC • Chemistry, physics, materials science • Small-angle x-ray scattering, wide-angle x-ray scattering, grazing Incidence small-angle scattering • 3.3-cm Undulator A • Accepting general users

Understanding Li Intercalation into Graphitic Carbon

Carbon exists in various forms. In one form, it is the hardest material known: diamond. In another, it is soccer-ball-shaped molecules—the fullerenes—and nanoscopic tubes. It also exists in a layered form as graphite, sheets of carbon atoms arranged like so many molecular panels making up hexagonal-shaped layers stacked one on top of another. This elegant layered structure makes it very slippery, leading to its application in lubricants, and the fact that the layers can be sloughed from a piece of graphite make it useful in pencil lead. Graphite also displays some unique properties when metal atoms are inserted—or intercalated—between the graphite layers. In fact, lithium-intercalated graphite (LIG) has been widely exploited for commercial high-power and high-energy rechargeable Li-ion batteries, and lithiated graphite is much safer than metallic lithium in batteries. However, these batteries could be made even better with a greater understanding of LIG's electronic structure and the intercalant-host charge transfer. Researchers used XOR/PNC beamline 20-ID-B,C at the APS to probe lithium atoms trapped between layers of graphitic carbon and observe the charge-transfer interaction between lithium and carbon.

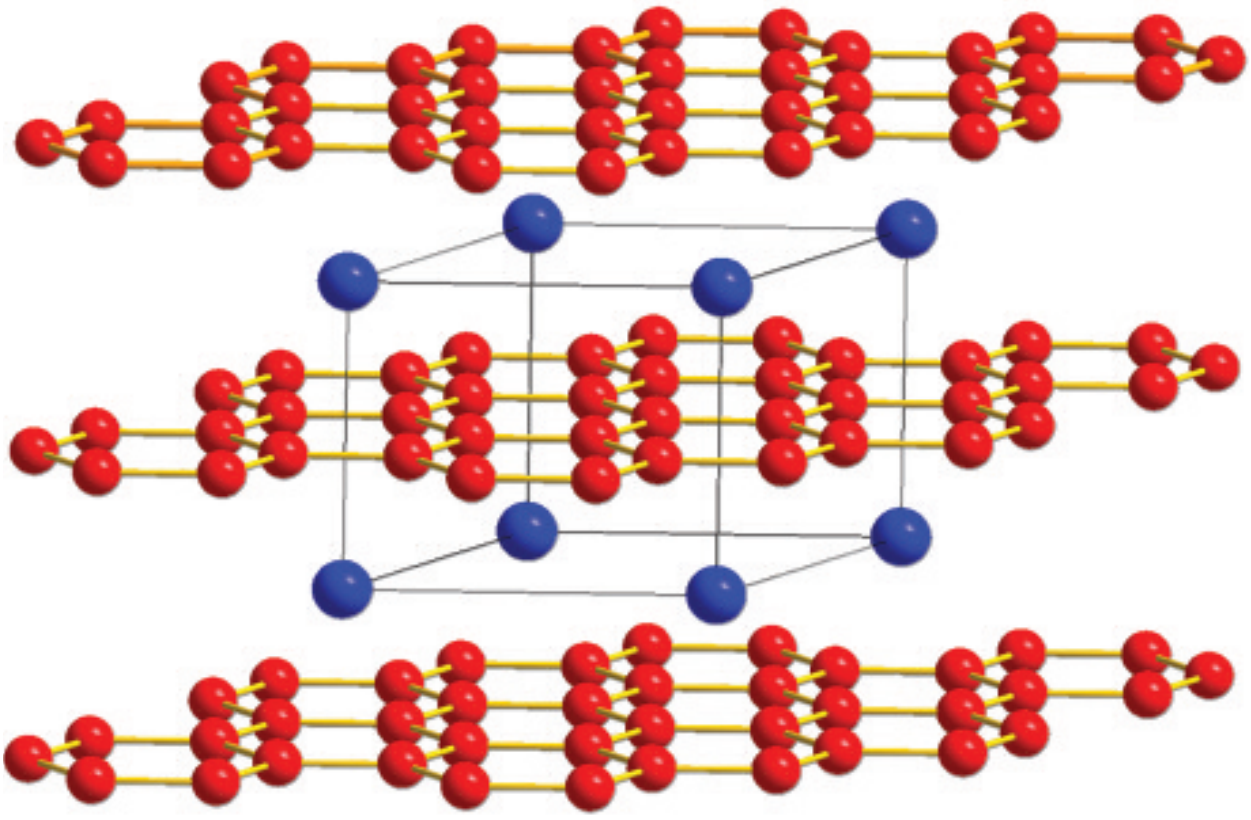

Fig. 1. Lithium (blue) insertion between the graphitic carbon (red) layers.

The researchers, from Argonne, the University of Washington, Washington State University, and the Niels Bohr Institute, prepared test materials of LIG packed with the theoretical amount (at ambient pressure) of lithium atoms between graphite layers (Fig. 1). They used both chemical and electrochemical methods to determine whether or not the preparative technique would influence the final structure. By using hard inelastic x-ray scattering (IXS) with the multielement LERIX spectrometer at 20-ID-B,C, they obtained spectra from the lithium and carbon atoms. One of the contentious issues the researchers hoped to settle with their IXS studies is how charge is transferred between the intercalated Li atoms and the graphite host. This issue is essential to the further development of novel and safe rechargeable lithium batteries. Graphite is almost the ideal candidate for such batteries because it has a very large theoretical capacity for intercalated lithium compared with other materials, it is durable even under repeated discharge and recharge, it is less expensive, and it could make new lithium batteries safer than those containing free-lithium metal as the anode.

Part of the reason for the contention is that LIG is highly sensitive to oxygen and other potential contaminants blighting studies of charge transfer. This type of IXS is unique among the relevant core-shell spectroscopies in having intrinsic bulk-sensitivity and easy compatibility with a wide range of sample environments. The penetration length of about 10-keV x-rays in LIG is well over 2 mm, ensuring a truly bulk-sensitive measurement. Also, this penetrative property of hard x-rays will enable future studies of operating batteries.

The IXS results obtained at Sector 20 have provided strong evidence that in the bulk material substantial charge transfer occurs from the intercalated lithium to the graphite (Fig. 2). More specifically, the evidence points to a positive energy shift of the Li IXS with respect to the lithium metal in both kinds of LIG, whether produced by chemical or electrochemical means. The change in the signal from the carbon IXS is modest but is consistent with an increase in the carbon-carbon bond distance on intercalation. Overall, these behaviors are due to charge transfer from the lithium to the bonds of the graphite sheets. This, explain the researchers, establishes an important baseline from which further studies on "real" operating batteries can be carried out.

— David Bradley

See: M. Balasubramanian[1]*, C.S. Johnson[1], J.O. Cross[1], G.T. Seidler[2], T.T. Fister[2], E.A. Stern[2], C. Hamner[3], and S.O. Mariager[4], "Fine structure and chemical shifts in non-resonant inelastic x-ray scattering from Li-intercalated graphite," Appl. Phys. Lett. **91**, 031904 (2007).

Author affiliations: [1]Argonne National Laboratory; [2]University of Washington; [3]Washington State University; [4]Niels Bohr Institute, University of Copenhagen

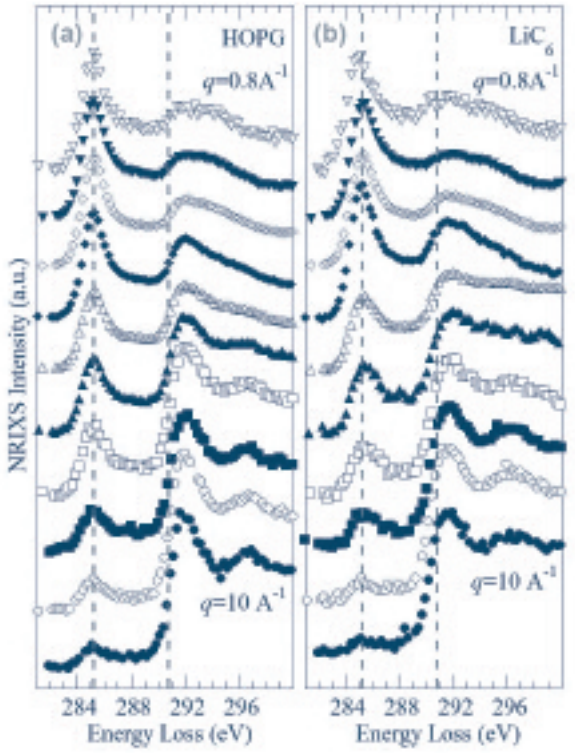

Fig. 2. Comparison of carbon 1s IXS spectra for (a) highly oriented pyrolytic graphite and (b) lithium-intercalated graphite. Shifts in position of electronic states probed in these spectra shed light on the changes in bonding and charge-transfer on lithium intercalation of graphite.

Correspondence: *mali@aps.anl.gov,
**seidler@phys.washington.edu

This research was supported by ONR Grant No. N00014-05-1-0843, and by the Leonard X. Bosack and Bette M. Kruger Charitable Foundation. XOR/ PNC facilities at the APS, and research at these facilities, are supported by the U.S. Department of Energy-Basic Energy Sciences, a major facilities access grant from NSERC, the University of Washington, Simon Fraser University, and the Pacific Northwest National Laboratory. Use of the APS was supported by the U.S. Department of Energy, Office of Science, Office of Basic Energy Sciences, under Contract No. DE-AC02-06CH11357.

20-ID-B,C • XOR/PNC • Materials science, environmental science, chemistry, geoscience • Microfluorescence (hard x-ray), x-ray absorption fine structure (XAFS), surface diffraction, micro-XAFS, x-ray Raman scattering, time-resolved XAFS • 3.3-cm Undulator A • Accepting general users

Making a Molecular Blackberry

Scientists have been making incredibly large molecules from the elements molybdenum and oxygen for nearly 200 years. Initially, it was not known that these large molecules were responsible for the unique color of molybdenum blue solutions, first made in the late 1700s, or indeed the "blue water" of Native American legend. In recent years, however, powerful techniques such as small-angle x-ray scattering (SAXS) have revealed the intricate details of these ions, known as polyoxomolybdates (POMs). Colleagues from Lehigh University and Argonne recently carried out SAXS experiments on the XOR/CMC 9-ID-B,C beamline at the APS to investigate more closely the solution behavior of one of the biggest known POMs: the 2.9-nm-size, soccer-ball-shaped molecule {Mo_{132}} (Fig. 1) Their results could help explain how these large POM macroanions form large, uniform, self-assembled structures in solution; could elucidate the fine control over their size, which is important for fundamental physical chemistry; and could eventually lead to technological applications such as novel inorganic membranes and nanocontainers.

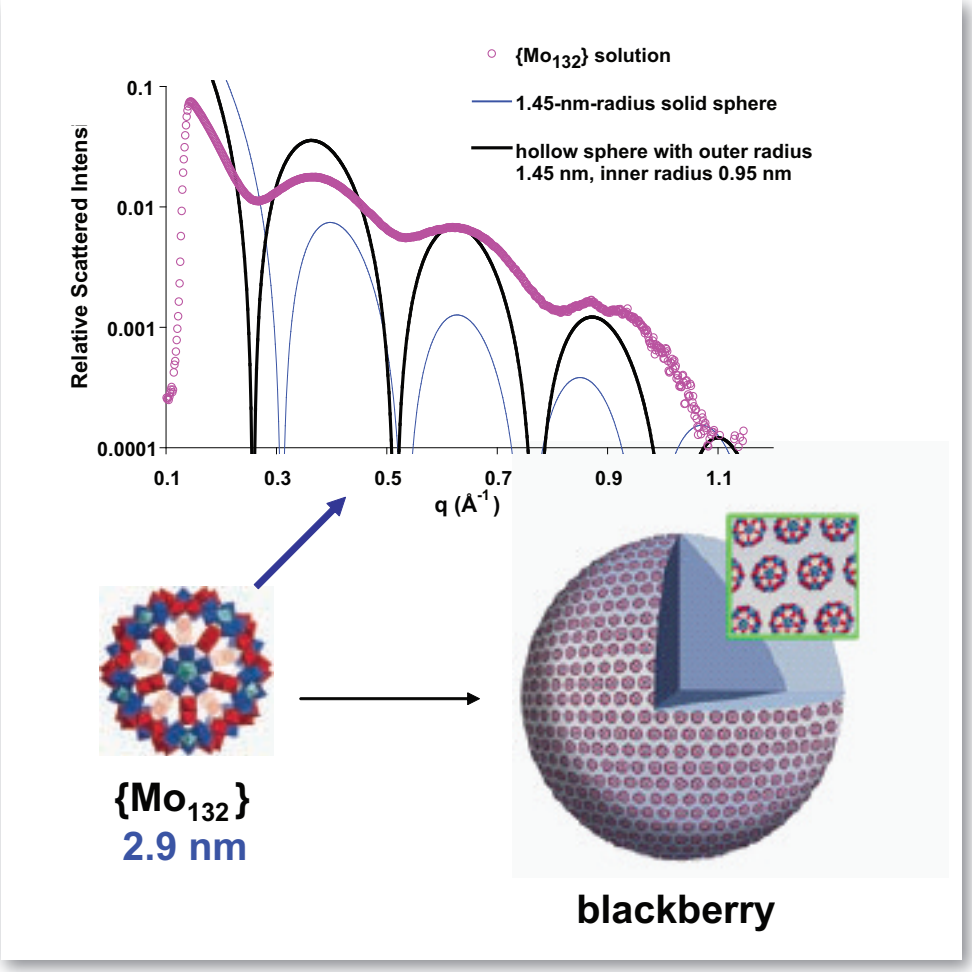

The key discovery is that the electrostatic van der Waals attractions are not the dominant attractive force for the blackberry formation

Polyoxomolybdates are very different from the ions present in simple salts, such as common table salt (sodium chloride). In water, individual positively charged sodium and negatively charged chloride ions float freely, surrounded by a constantly changing entourage of water molecules. Polyoxomolybdates, on the other hand, do not exist as single ions in water. Instead, they clump together to form hollow aggregates with individual bead-like POM capsules aggregated like the individual capsules in a blackberry fruit that make up the berry as a whole.

One almost paradoxical property of these blackberry clusters is that they are stable and remain dissolved in solution despite their size. Scientists understand how simple ions of sodium chloride and many other salts stay in solution. The ions' small size and electrical charge means polar water molecules can surround them, the essence of being dissolved. Much larger chemical entities, such as colloidal particles, on the other hand, are simply too big to be efficiently subsumed by solvent molecules. Above a certain aggregate mass, they begin to form solid particles in the liquid, and they precipitate out of solution.

The researchers in this study suggest that blackberry structures represent a thermodynamically stable state for soluble POM macroanions. The large POM ions have water-loving, hydrophilic surfaces and multiple charges, making them highly soluble in polar solvents. However, the negatively charged POMs tend to attract each other and form very stable, conservative blackberry structures even in dilute solutions. It is important to identify the mysterious attractive forces among the POM macroanions. In its latest study, the team shed new light on this apparently unique behavior, as well as explaining how the blackberries alter with changing solvent quality (in a water/acetone mixed solvent).

The researchers used SAXS to observe the transition from discrete ions to the aggregated blackberry structures in water and acetone, as well as the reverse process. Laser-light scattering studies showed that self-assembled structures based on the $\{Mo_{132}\}$ unit—in which 132 linked molybdenum-oxygen polyhedral units exist in one molecule—can be soluble in both acetone and water. The researchers point out that their blackberries show other unusual properties not commonly seen in inorganic, as opposed to organic, carbon chemistry: They are soft, and they take months to reach an equilibrium state in solution, in stark contrast to other inorganic salts, which can take just seconds to equilibrate.

The key discovery is that the authors proved that the electrostatic van der Waals attractions, which are responsible for many types of aggregation behaviors, are not the dominant attractive force for the blackberry formation. This distinguishes blackberry formation from other types of aggregation/self-assembly processes (surfactant micelles, colloid crystals, etc.). The authors believe that the large $\{Mo_{132}\}$ anions attract each other because of their small counter-ions (mainly ammonium cations). Another key feature revealed is that the size of a molybdenum blackberry can be adjusted simply by tweaking the ratio of acetone to the water in which the anions are dissolved. More acetone means bigger blackberries, with a 3% solution of acetone to water producing 45-nm clusters and a 70% solution leading to 100-nm clusters.

— David Bradley

< Fig. 1. Nanoscopic clusters containing 132 molybdenum atoms linked together by organic chemical groups—$\{Mo_{132}\}$—can form aggregates dubbed "blackberries."

See: Melissa L. Kistler[1], Anish Bhatt[1], Guang Liu[1], Diego Casa[2], and Tianbo Liu[1]*, "A Complete Macroion—'Blackberry' Assembly—Macroion Transition with Continuously Adjustable Assembly Sizes in $\{Mo_{132}\}$ Water/Acetone Systems," J. Am. Chem. Soc. **129**, 6453 (2007). DOI: 10.1021/ja0685809

Author affiliations: [1]Lehigh University, [2]Argonne National Laboratory

Correspondence: *til204@lehigh.edu

T.L. gratefully acknowledges support from the National Science Foundation (NSF-CHE0545983) and Lehigh University (startup fund and FRG). Use of the APS was supported by the U.S. Department of Energy, Office of Science, Office of Basic Energy Sciences, under Contract No. DE-AC02-06CH11357.

9-ID-B,C • XOR/CMC • Physics, materials science • Liquid scattering, inelastic x-ray scattering, resonant inelastic x-ray scattering • 3.3-cm Undulator A • Accepting general users

Synthesizing a Broad Class of Porous, Chalcogenide Materials

Molecular sieves are those materials that selectively sort molecules based on a size-exclusion process. This is due to their highly regular pore structure; the maximum size of the molecular or ionic species that can enter the pores of a molecular sieve is controlled by the diameters of the tunnels. The most common form of molecular sieve has so far been a class of microporous materials, known as zeolites, that are widely used as ion-exchange beds in domestic and commercial water purification, water softening, and other applications. Researchers from Northwestern University, Michigan State University, and Argonne have devised a way to synthesize (and have characterized) broad classes of a new type of inorganic porous material that could potentially offer very different practical applications from those of zeolite molecular sieves.

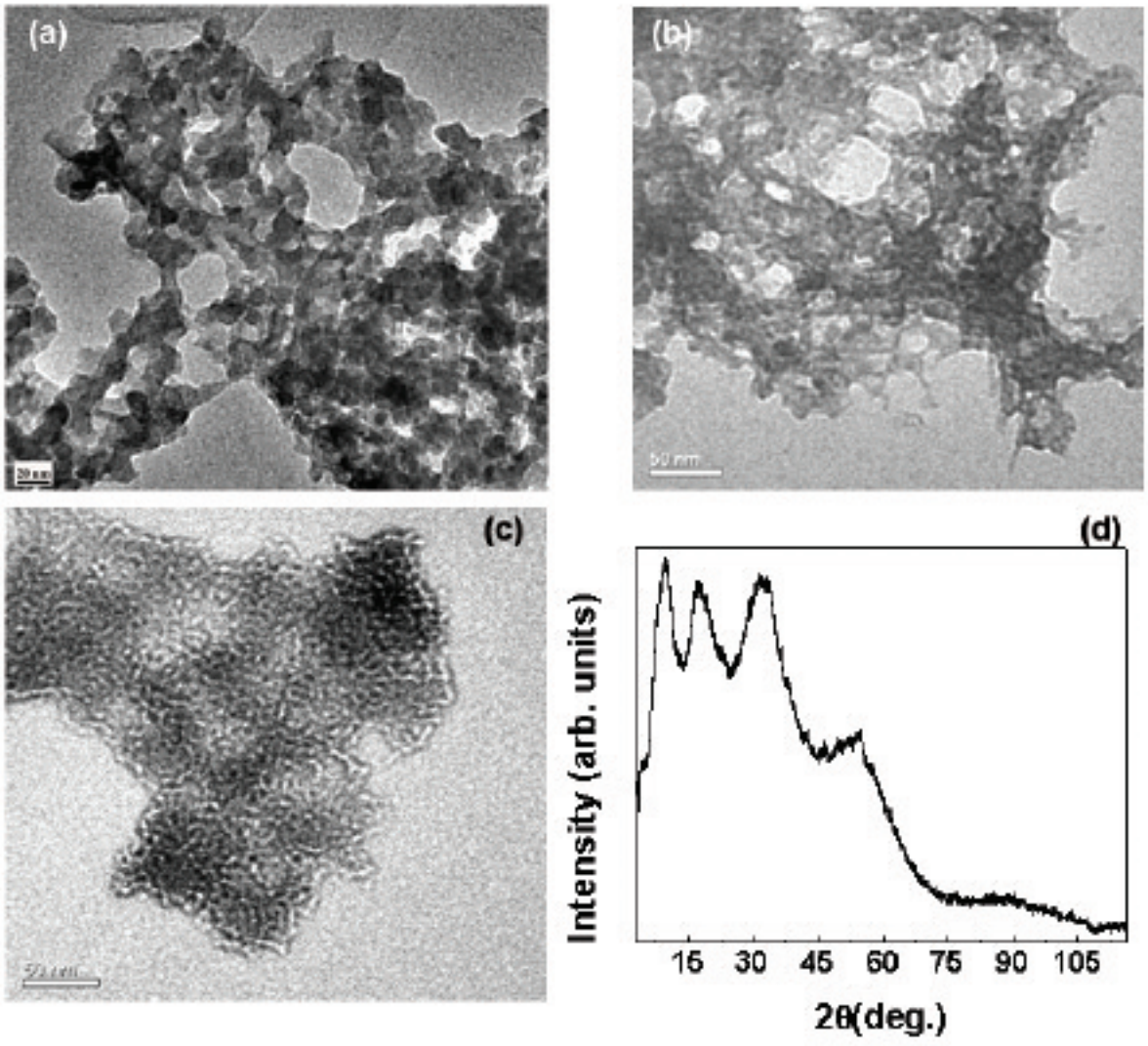

Researchers have synthesized and characterized a new type of material that could offer applications beyond those of zeolite molecular sieves

In chemistry, zeolites are used as filters to separate or trap molecules so they can be analyzed. Of particular interest is that zeolites have the potential for providing precise and specific separation of gases, including the removal of H_2O, CO_2, and SO_2 from low-grade natural gas streams. Other separations include the noble gases N_2, O_2, freon, and formaldehyde. At present, the true potential for improving the handling of such gases in this manner remains unknown. Furthermore, porous inorganic materials are mostly oxides, which can severely limit their range of practical applications.

What sets the new, non-zeolite materials apart from traditional molecular sieves is that they contain heavier sulfides or selenides in place of the oxides; collectively, these materials are known as chalcogenides, or "copper generators." Such materials could in principle combine the electronic properties of chalcogenides with great internal porosity, and the group has recently reported a method that can be used to successfully create highly porous aerogels derived from chalcogenide clusters: a metathesis reaction in aqueous solution capable of linking sulfide or selenide clusters via platinum ions as the metal "glue" to form expanded, polymer-like frameworks. The solvent in the reaction was then removed by supercritical drying using CO_2 to yield a highly porous aerogel.

These aerogels were analyzed using transmission electron microscopy, which revealed empty cylindrical and slit-shaped mesospores with no long-range order that are morphologically similar to the continuous amorphous networks found in silica gels (Fig. 1, a and c). The surface areas of these aerogels were found to range from 108 to 327 m^2/g, depending on the chalcogenide cluster used. Given that their molecular weights are quite high, these surface-area values are considerably higher on a per-mole basis than the corresponding silica values, indicating the possibility of application as efficient catalytic materials or supports for catalytic materials.

Diffraction experiments carried out at the XOR 11-ID-B beamline at the APS yielded data that were the basis for probing the local structure of the amorphous aerogels. The group applied the atomic pair distribution function technique to analyze both diffuse and Bragg scattering by recovering atom-atom correlations in real space in the form of a radial distribution function.

These studies show that the aerogels have a very high capacity for removing heavy metals from contaminated water. Mercury ion levels in water were reduced from 645 ppm to approximately 0.04 ppm by using 10 mg of the chalcogenide aerogel. What's more, unlike mesoporous silicates, these chalcogels did not need to be functionalized with surface-modified thiolate ligands before being applied to the task of Hg^{2+} adsorption. The chalcogels were also shown to be highly effective in absorption of organic hydrophobic aromatic molecules from solution, because the chalcogels present hydrophobic surfaces lined with chalcogen atoms that make them impervious to high humidity, in contrast to unmodified silica aerogels, which tend to have hydrophilic surfaces and are thus unstable under conditions of high humidity.

Spectroscopy measurements revealed that the chalcogels absorbed light in the visible and infrared regions depending on the chalcegonide building blocks used, and they displayed sharp bandgaps from 2 to 8 eV. These tunable bandgaps could potentially make the chalcogels useful as photocatalysts, adding further interest in continued research on these new materials. — *Louis Nasser*

< Fig. 1. (a) and (b) are TEM images of two different chalcogels, clearly showing the disordered pores between the particles; (c) shows a chalcogel without large macropores; (d) is the powder x-ray diffraction profile for the sample in (a), demonstrating the amorphous nature of the chalcogel.

See: Santanu Bag[1,2], Pantelis N. Trikalitis[2]*, Peter J. Chupas[3], Gerasimos S. Armatas[1,2], and Mercouri G. Kanatzidis[1,2,4], "Porous Semiconducting Gels and Aerogels from Chalcogenide Clusters," Science **317**, 490 (27 July 2007). DOI: 10.1126/science.1142535

Author affiliations: [1]Department of Chemistry, Northwestern University; [2]Department of Chemistry, Michigan State University; [3]Advanced Photon Source, Argonne National Laboratory; [4]Materials Science Division, Argonne National Laboratory

Correspondence: *m-kanatzidis@northwestern.edu

Use of the Advanced Photon Source was supported by the U.S. Department of Energy, Office of Science, Office of Basic Energy Sciences, under Contract No. DE-AC02-06CH11357.

11-ID-B • XOR/BESSRC • Chemistry, environmental science, materials science • High-energy x-ray diffraction, pair distribution function • 3.3-cm Undulator A • Accepting general users

What Keeps Bugs from Being Bigger?

Above: Fig. 1. Tracheal tubes are visible in this synchrotron x-ray phase contrast image (right) of a tenebrionid beetle (left).

Left: The image shown above found its way to a "PR Newswire" display on the side of a building in New York's Times Square.

Insects are now much smaller than vertebrates, but they were not always so diminutive. In the Late Paleozoic Era (the earliest of three geologic eras of the Phanerozoic Eon, some 542 to 251 million years ago), millipedes longer than a human leg, cockroaches the size of house cats, and dragonflies with two-foot wingspans roamed our planet. Perhaps fortunately, these giants died out in the Triassic Period (the first period of the Mesozoic Era that extends from about 251 to 199 million years ago). The idea that the partial pressure of atmospheric oxygen (PO_2) limits the size of some types of animals is an important hypothesis. Using XOR beamline 1-ID-C at the APS, scientists have shown that in some insects, body size may be limited by the size of the tracheae. This evidence supports the hypothesis that the high oxygen content of the Late Paleozoic Era allowed giant insects to rule the Earth and skies.

Although the data are still sketchy, insect gigantism appears to correlate with high PO_2. Atmospheric oxygen is now steady at 21%, but for about 100 million years in the Late Paleozoic Era, oxygen levels rose as high as 35%, then plummeted to around 15% in the Triassic Period. The researchers in this study, from Arizona State University, Midwestern University, and Argonne, using the XOR 1-ID-C beamline, have gathered evidence that atmospheric PO_2 fostered the gigantic insects' success as well as their subsequent demise.

Insects deliver oxygen to their tissues differently from vertebrates, in which oxygen travels through the respiratory and circulatory systems. In insects, air enters through a line of tiny openings, called "spiracles," on the abdomen and thorax, then diffuses through the body through blind-ended tubes—the tracheae. Diffusion effectiveness is inversely related to the cross-sectional area of the tracheae and decreases with increasing distance down the tubes. Insects are sensitive to atmospheric oxygen levels: Small insects do better at hopping and flying in low-oxygen environments than do large insects, which fact may be related to the limitations of their respiratory system.

The researchers tested whether it is the tracheal tube system that limits insect size. They employed the phase-contrast-imaging technique developed at the APS, which uses synchrotron x-rays to produce highly detailed images (and even films) of live animals. The researchers analyzed tracheal volumes from 44 individual insects representing four species of darkling beetles (family *Tenebrionidae*), varying in body mass by a factor of 1,000.

In tenebrionid beetles, oxygen travels from thoracic or abdominal spiracles into the legs and head by crossing through exoskeletal orifices. The phase-contrast images (Fig. 1) show that tracheal-tube cross-sectional area through the orifice increases with insect body size. But, whereas in mammals, lung dimensions are proportional to body size, in these beetles the tracheal tube cross-sectional area increase relative to the cross-sectional area of the orifice is disproportionate: 18% in large insects versus 2% in small ones. If this pattern continued, the increasing cross-sectional area of the tracheae would limit the beetles' body size, because eventually there would not be enough space for other needed tissues. This relationship was not observed in the head orifice.

With the current tracheal tube system and at least 10% of the coxal orifice available for other tissues, the research team calculated the largest possible beetle at about 16 cm. Since the largest living beetle, *Titanus giganteus*, is approximately 17 cm long, the scientists suggest that it is the coxal orifice that limits beetle body size. Paleozoic insects could become giants because of the high atmospheric PO_2. With more oxygen, diffusion would be more efficient at greater distances down the tracheae, and the tracheae could evolve to be narrower and longer, permitting insects to reach greater sizes. Unfortunately, it is difficult to test this hypothesis on Late Paleozoic insects, because fossilized tracheae are rare and techniques for measuring them have not yet been developed. — *Dana Desonie*

See: Alexander Kaiser[1]*, C. Jaco Klok[2], John J. Socha[3], Wah-Keat Lee[3], Michael C. Quinlan[1], and Jon F. Harrison[2], "Increase in tracheal investment with beetle size supports hypothesis of oxygen limitation on insect gigantism," Proc. Natl. Acad. Sci. USA **104**(32), 13198 (August 7, 2007). DOI: 10.1073pnas.0611544104

Author affiliations: [1]Department of Basic Sciences, Midwestern University; [2]Section of Organismal, Integrative and Systems Biology, School of Life Sciences, Arizona State University; [3]X-ray Science Division, Advanced Photon Source, Argonne National Laboratory

Correspondence: *akaise@midwestern.edu

This work was supported by National Science Foundation Grants 0419704 (to J.F.H.) and IBN-0344963 (to M.C.Q.). Use of the Advanced Photon Source was supported by the U.S. Department of Energy, Office of Science, Office of Basic Energy Sciences, under Contract No. DE-AC02-06CH11357.

Note: This work is now on-going at beamline 32-ID-B,C • XOR • Materials science, life science • Phase-contrast imaging, ultra-small-angle x-ray scattering, radiography • 3.3-cm Undulator A • Accepting general users

It appears that copper is important for cooperation among cells—disrupting that cooperation could prevent tumors from growing new blood conduits, thereby halting the disease in its tracks

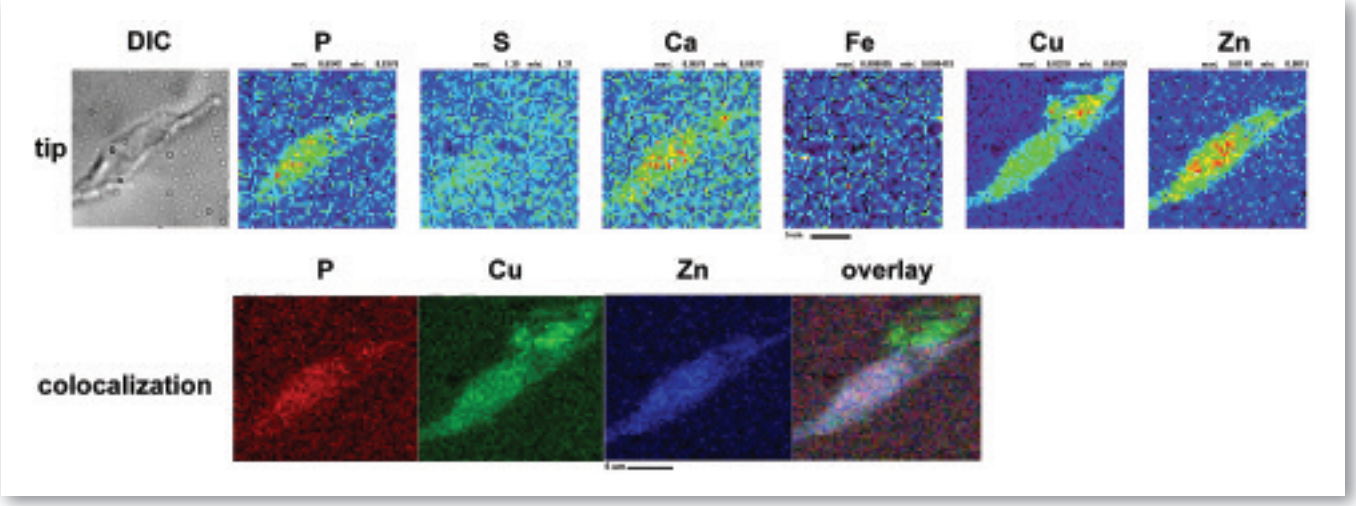

Fig. 1. Various metals such as phosphorus (P), sulfur (S), calcium (Ca), iron (Fe), copper (Cu), and zinc (Zn) light up in a growing endothelial cell's extension (top), but combine all the metals and only copper appears at the very tip of the growth (bottom, overlay, in green).

Cancer's Copper Wanderlust

Cancer kills when it causes cells to propagate out of control. While growing, tumors build new blood vessels to keep their burgeoning masses fed. Cancer researchers try to strangle growing tumors by cutting off their blood supply, and many take aim at the cancer proteins that do this. One way to trip up such proteins is to sequester the metals that the proteins require for functioning. Growing cancers are especially susceptible to having their copper removed, so researchers used XOR beamline 2-ID-E to "light up" copper and the other metals in young blood vessel cells. The team found that copper moved to the parts of the cells involved in the earliest stages of blood vessel formation. It appears that this copper is important for cooperation among the cells. Disrupting that cooperation could prevent tumors from growing new blood conduits, thereby halting the disease in its tracks.

To form a pipe through which blood can flow, tumors subvert endothelial cells, which normally become blood vessel walls. The cells protrude finger-like projections of themselves, reaching for other cells with which to interact. Fingers from multiple cells touch, forming a network. Additional cellular remodeling eventually morphs the endothelial cells into a seamless tube, the beginnings of a blood vessel. To find out which metals participate in vessel development, the team used cultured cells that mimic the early stages of vessel construction. After stimulating the cells to grow in culture dishes, the cells take about 8 h to form a tube-like network.

The research team, from The University of Chicago and Argonne, stimulated the cells to start forming their network, and then exposed them to the high-intensity x-ray beams at different time points. The rays caused metals such as phosphorus, calcium, zinc, and iron to luminesce at different wavelengths (Fig. 1). Before stimulation, the team found copper in the cells' middle; one hour later, the copper had traveled to the edges of the cells. A second hour passed and fingers extended, grabbing onto the surface matrix—here the copper was found in the tips. More copper filled up the fingers after 4 hours of vessel maturation. After the network had formed (at about 8 hours), the copper redistributed itself to its beginning positions. The team measured the amount of copper moving about and found 80% to 90% of the metal wandered to the tips at the height of its movement, at two hours. But the team didn't know whether the cell was using copper to generate the fingers, to grab onto the surface, or to make contact with other cells. To find out, the researchers added compounds that isolate copper. The compounds only interfered with cell-to-cell contact, suggesting that whatever proteins copper might work with are important in joining cells together.

The next question was, What happens in real cancerous tissue? The scientists took samples of breast cancer tissue and subjected the samples to APS x-rays. They found that in normal breast tissue, copper was spread all over the cell. In a cross section of a mature blood vessel, copper was equally distributed between endothelial cells in the vessel wall and the surrounding tissue in which the vessel sat, as expected from the cultured cells. In a vessel under construction, however, dots of copper appeared at the edges of cells involved in fabricating the walls. Zooming in at high resolution on these dots, it appeared that copper (and some zinc) might have been transported to the outside of the cells, suggesting that proteins involved in forming the vessel wall were at work. In a next round of experiments, the research team hopes to determine which proteins use the copper, establishing a roadmap to eventual development of new anti-cancer therapies. — *Mary Beckman*

See: Lydia Finney[1], Suneeta Mandava[1], Lyann Ursos[1], Wen Zhang[1], Diane Rodi[1], Stefan Vogt[2], Daniel Legnini[2], Jorg Maser[2], Francis Ikpatt[3], Olufunmilayo I. Olopade[3], and David Glesne[1]*, "X-ray fluorescence microscopy reveals large-scale relocalization and extracellular translocation of cellular copper during angiogenesis," Proc. Natl.. Acad. Sci. USA **104**, 2247 (February 13, 2007).
DOI: 10.1073pnas.0607238104
Author affiliations: [1]Biosciences Division, Argonne National Laboratory; [2]X-ray Science Division, Argonne National Laboratory; [3]Department of Medicine, Section of Hematology/ Oncology, The University of Chicago
Correspondence: *dglesne@anl.gov

This study, including use of the Advanced Photon Source, was supported by U.S. Department of Energy, Office of Science, Office of Basic Energy Sciences under Contract No. DE-AC-02-06CH11357. O.I.O. is a Doris Duke Distinguished Clinical Scientist.

2-ID-E • XOR • Life science, environmental science, materials science • Microfluorescence (hard x-ray) • 3.3-cm Undulator A • Accepting general users

A Nanoscopic View of How Bone Handles Stress

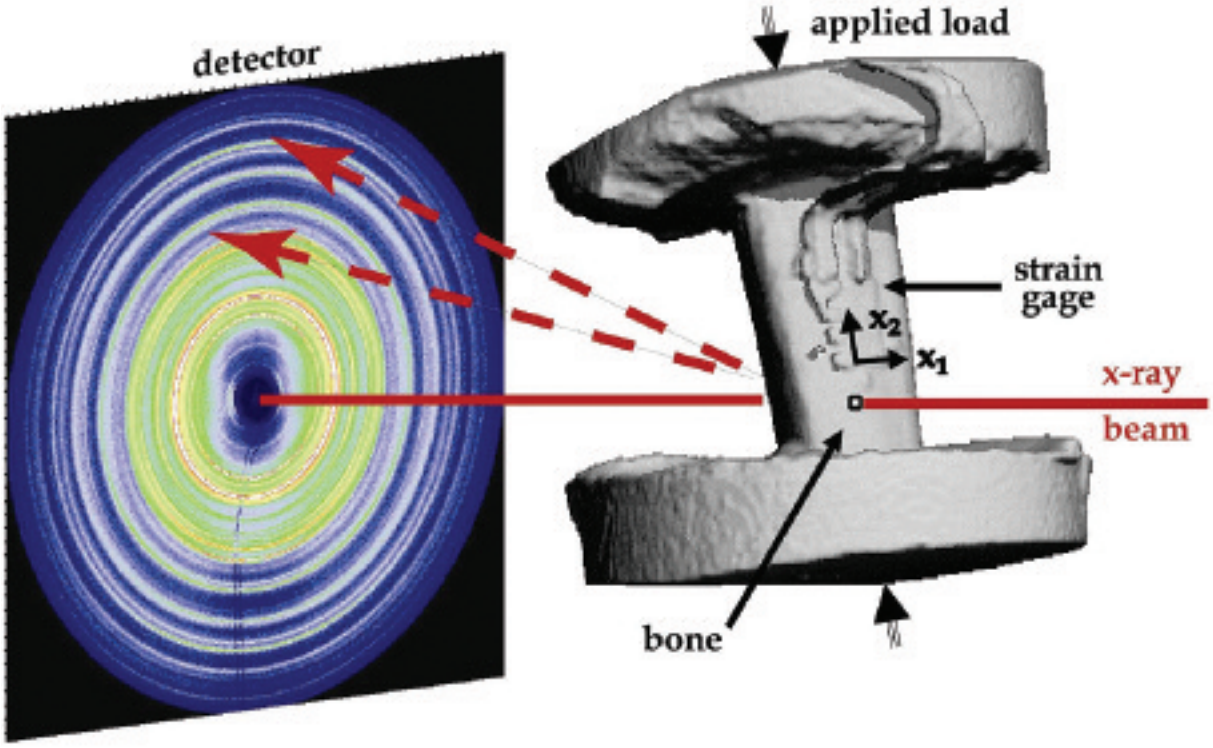

Fig. 1. Illustration of diffraction pattern collection for a bone sample. The x-ray beam (from right to left) shines through the specimen (right), and scattered x-rays produce rings on the area detector (left), with the higher intensities represented as brighter colors.

These results confirm some models for bone elasticity, reveal some new information about bone composition, and raise some new questions while providing a tool for finding the answers

Bone is a remarkably "smart" material that actively remodels itself in response to patterns of use. However, bone resilience is compromised in some disease states and in normal aging, particularly in postmenopausal women. Bone mineral density, measured by dual-energy x-ray absorptiometry, is the standard in the clinical assessment of fracture risk. But some older women with high bone mineral density experience pathologic fractures, whereas others with low bone density do not. Moreover, decreasing density is only one of several changes seen in osteoporotic bone. It is generally recognized that bone quality as well as bone quantity is important in determining an individual's risk of fracture, but bone quality is notoriously difficult to define, much less measure. Using the XOR 1-D-C beamline at APS, researchers explored nanoscale parameters of bone quality by measuring response to applied stress at the micromechanical level. Their results confirm some models for bone elasticity, reveal some new information about bone composition, and raise some new questions while providing a tool for finding the answers.

Bone is a nanoparticle-reinforced composite: a soft, yielding protein (primarily collagen) matrix reinforced by crystallites of carbonated apatite. The collagen matrix contributes a high degree of toughness, while the mineral phase provides stiffness. Bone has a complex hierarchical structure in which mineralized collagen fibrils form parallel, woven or lamellar arrays, depending on the type of bone. On the nanoscopic level, collagen molecules self-assemble into fibrils having a plied rope-like structure with a characteristic banding pattern that repeats about every 67 nm. This pattern, known as the D-period, produces peaks on small-angle x-ray scattering (SAXS). In wide-angle x-ray scattering (WAXS), the mineral crystallites embedded in and on the fibrils diffract the monochromatic x-rays and produce cones of increased intensity and concentric rings on area detectors (Fig. 1).

Force applied to the bone produces interpretable shifts in the x-ray scattering patterns for both phases (collagen and apatite), and these shifts can be converted into the longitudinal strain in each phase. The ratio of the longitudinal strain to the incrementally applied stress can then be used to calculate Young's modulus (sometimes called the modulus of elasticity), which is a measurement of stiffness expressed as gigapascals (GPa). The material studied was an intact 10-mm cross section of canine fibula fitted with a microstrain gauge to determine the overall Young's modulus of the specimen. The researchers in this study, from Northwestern University and Argonne, used the 1-ID-C beamline to collect data at five parallel positions along the cross section in order to detect any confounding effects of bending under load.

The overall Young's modulus was 25 GPa, which is consistent with the literature, in which the reported values for non-primate mammalian hind limb bones range from 18 to 32 GPa. For the collagen phase, Young's modulus was 18 GPa, six times the reported value of 3 GPa for the collagen of bovine tendon. For the carbonated apatite, Young's moduli were 38 GPa (00.4 WAXS reflection) and 44 GPa (22.2 WAXS reflection). By comparison, sintered hydroxyapatite (a purer form of apatite used for bone prostheses) has a much higher Young's modulus of 114 GPa.

These results are concordant with a model in which bone is not a simple, discontinuously reinforced composite but one organized as stiff rods of tightly bundled mineralized collagen fibrils glued together by surrounding non-collagen proteins. In this model, the tightly integrated mineral and collagen phases would not be expected to behave as they do in bulk.

As is often the case with well-designed research, this study raises new questions regarding the micromechanics of the matrix and reinforcing phases of normal versus osteoporotic or irradiated bone, while providing a methodology for exploring them. — *Carol Hart*

See: J.D. Almer[1], S.R. Stock[2]*, "Micromechanical Response of Mineral and Collagen Phases in Bone," J. Struct. Biol. **157**, 365 (2007). DOI: 10.1016/j.jsb.2006.09.001

Author affiliations: [1]Advanced Photon Source, Argonne National Laboratory, [2]Department of Molecular Pharmacology and Biological Chemistry, Northwestern University

Correspondence: *s-stock@northwestern.edu

Use of the Northwestern University MicroCT Facility's Scanco MicroCT-40 is acknowledged. Use of the Advanced Photon Source was supported by the U.S. Department of Energy, Office of Science, Office of Basic Energy Sciences, under Contract No. DE-AC02-06CH11357.

1-ID-C • XOR • Materials science, physics, chemistry • High-energy x-ray diffraction • 3.3-cm Undulator A • Accepting general users

Seeing What We Can't Hear

When sounds reach our ears, a membrane, a hair cell, and long projections called stereocilia work together to transmit a sound wave of a particular frequency to nerve cells. When the membrane vibrates at just the right frequency, the vibration travels through the hair cell to the sterocilia, which then cause the nerves to send a message to the brain. Mutations in one of the stereocilia proteins called espin cause deafness in people. Researchers used the XOR 12-ID-B,C,D beamline at the APS and beamline BL4-2 at the Stanford Synchrotron Radiation Laboratory to take a close look at how espin mutations affect the structure of the projections. The researchers found that healthy espin stiffens the architecture within the stereocilia, which allows the stereocilia to resonate at the right frequency and tickle the nerve cell. But mutations turned the architecture to various states of mush, which caused the stereocilia to flop and become unable to transmit the membrane vibrations correctly. The results suggest that stiffening up the stereocilia's internal architecture could help some deaf people hear. This research posits a conceptual connection between deafness and the organization of liquid crystals that are used in various types of video displays.

Inside healthy stereocilia, long, filamentous rods of the protein actin are linked together by espin, a protein that grabs two actin filaments like a person holding a broomstick in each hand. To find out how espin mutations affect this structure, the team of researchers from the University of Illinois at Urbana-Champaign and Northwestern University examined the ability of two espin mutants, which normally cause deafness in people, to reconstruct the actin-espin framework. They compared the mutants with a healthy human espin and a healthy rat espin. The mutants were progressively more damaged; the least-damaged mutant could grab one actin rod with normal strength and another filament weakly. The most-damaged mutant was essentially one-handed and could hold onto one actin rod at a time. Using the high-energy APS and Stanford Synchrotron Radiation Laboratory light sources, the team examined how well the mutants and normal espin built up the actin frameworks.

The normal espin packed the actin filaments (which were slightly helical) into tight hexagonal bundles (Fig. 1). In addition, the bundled rods were twisted slightly more than unbundled filaments, indicating that the filaments in the hexagon are under constant strain, adding to the stiffness of the overall structure. With the espin mutant, the hexagonal structure lost its definition. As the espin mutants were less able to grab onto the actin, the actin rods acquired more space between them and more easily slipped past each other. The more damaged the espin, the more espin was required to make a stable structure.

At concentrations approximating those found in people, the mutant bundles behaved like loose liquid crystals rather than tight hexagonal crystals. (In the liquid crystalline state, the bundles maintain their orientation order – that is, they point roughly along the same direction – but lose their positional order. These nematic liquid crystals are commonly used in watch displays and laptop displays.) Because the rods in a liquid crystal can slide past each other, the hairs bend and bounce. One of the mutants resulted in stereocilia that were a thousand times more floppy than the normal stereocilia. The lack of definition and stiffness affects the frequency at which the stereocilia resonate, preventing the hair cells from triggering the nerve cells. In addition, as the team added more espin to the actin, the switch from floppy to stiff occurred quite suddenly, suggesting that the mutant bundles could be fixed—along with hearing—if researchers could deliver healthy espin to damaged stereocilia. Although therapies that would allow such delivery are still in development, the results provide hope that one day people who are deaf due to a genetic mutation might be able to hear.

— Mary Beckman

See: Kirstin R. Purdy[1]*, James R. Bartles[2], and Gerard C.L. Wong[1], "Structural Polymorphism of the Actin-Espin System: A Prototypical System of Filaments and Linkers in Stereocilia," Phys. Rev. Lett. **98**, 058105 (February 2, 2007).
Author affiliations: [1]Department of Materials Science and Engineering, University of Illinois at Urbana-Champaign; [2]Department of Cell and Molecular Biology, Northwestern University, Feinberg School of Medicine
Correspondence: *krpurdy@gmail.com

This work was supported in part by the DOE DEFG02-91ER45439 through the Frederick Seitz Materials Research Laboratory, the NSF RPI-UIUC NSEC, and the NIH (No. DC004314 to J. R. B.). J. R. B. received support from the Hugh Knowles Center. Use of the APS was supported by the U.S. Department of Energy, Office of Science, Office of Basic Energy Sciences, under Contract No. DE-AC02-06CH11357.

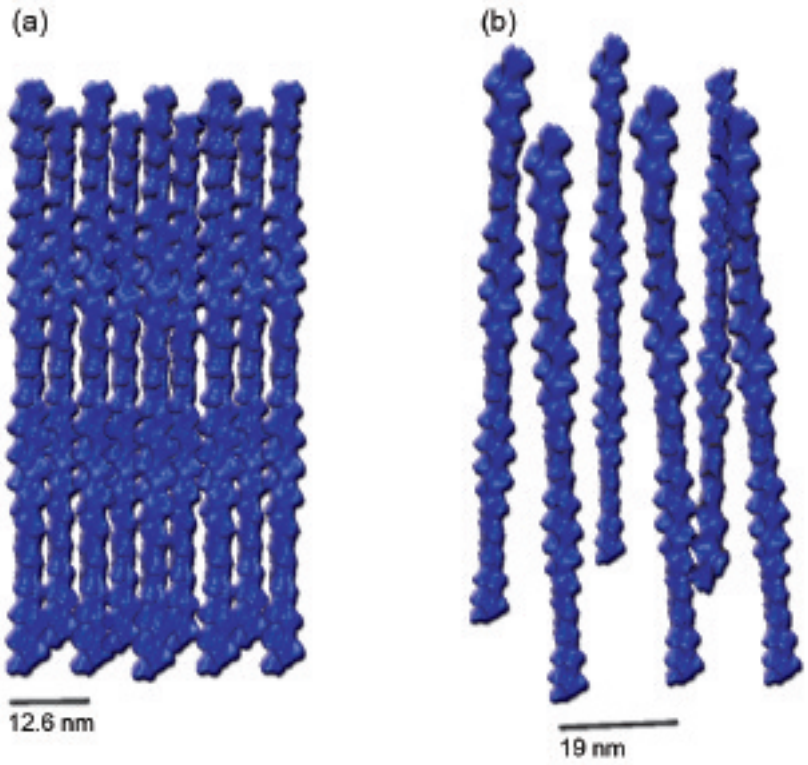

Fig. 1. Healthy espin forms tight, straight bundles (a) while mutant espin causes actin to form a liquid crystal-like structure (b).

12-ID-B,C,D • XOR/BESSRC • Chemistry, physics, materials science • Small-angle x-ray scattering, wide-angle x-ray scattering, grazing Incidence small-angle scattering • 3.3-cm Undulator A • Accepting general users

A "Copper Bullet" to Kill Cancer

A drug normally used to treat Alzheimer's disease may act as a "copper bullet," killing tumor cells by coating itself in copper ions, according to research derived in part from studies at the APS. Researchers from Wayne State University, the Henry Ford Hospital, the Illinois Institute of Technology, and Shandong University using Bio-CAT beamline 18-ID-D at the APS found that the drug clioquinol, when mixed with copper (Fig. 1), killed two types of prostate cancer cell in Petri dishes. The drug without copper also slowed the growth of prostate tumors implanted in mice by up to two-thirds, apparently by soaking up copper ions (charged atoms) present in the implanted tumor cells.

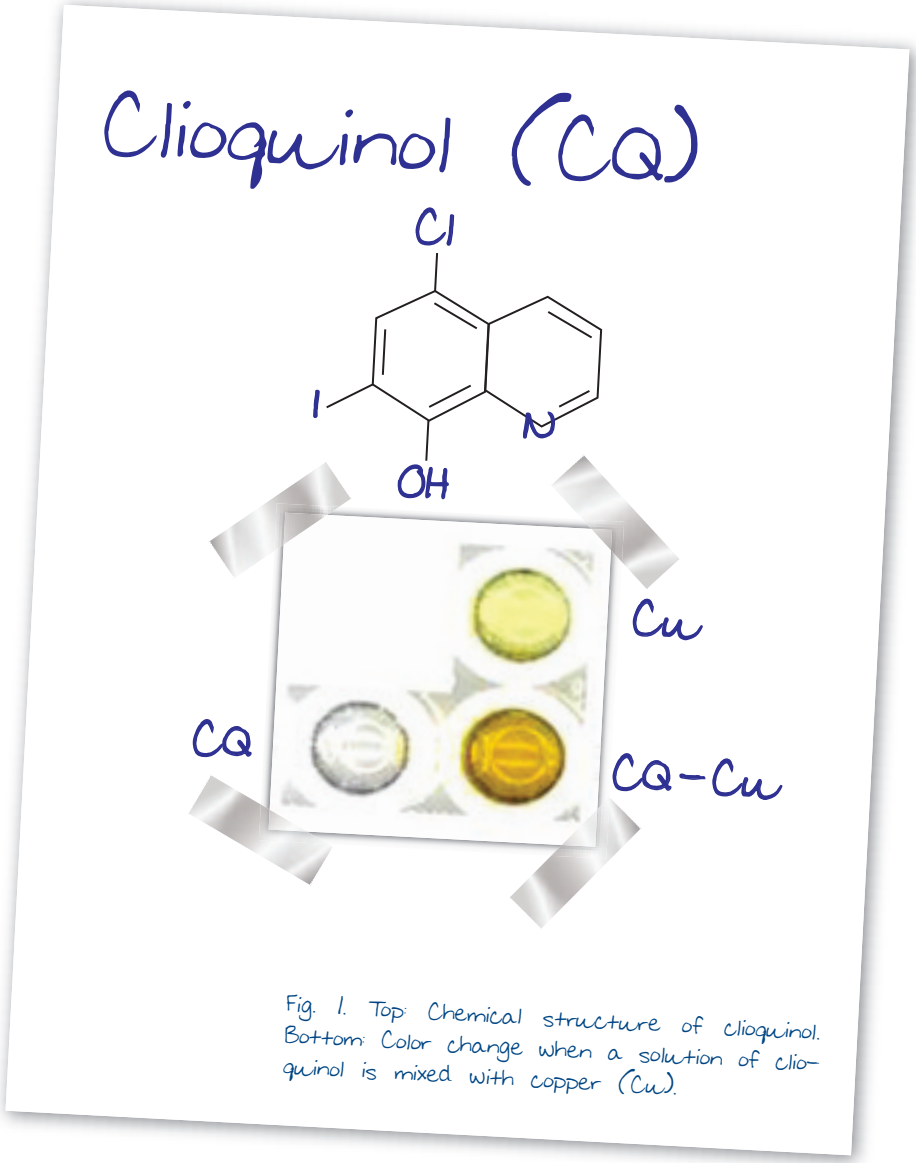

Fig. 1. Top: Chemical structure of clioquinol. Bottom: Color change when a solution of clioquinol is mixed with copper (Cu).

Prostate cancer struck approximately 219,000 U.S. men in 2007 and killed some 27,000 of them, according to National Cancer Institute estimates.

Many types of cancer typically show high levels of copper, including tumors of the prostate, breast, colon, lung, and brain. Traditional chemotherapy works by poisoning any rapidly growing cell, which includes healthy gut, blood, and hair follicles, resulting in hair loss, nausea, and other unpleasant side effects.

If only high concentrations of copper trigger clioquinol's harmful effects, these researchers noted, then the drug might selectively kill tumor cells, causing fewer side effects than other chemo-therapies. The researchers further noted that two clinical trials of the molecule as a treatment for Alzheimer's disease did not reveal any significant side effects.

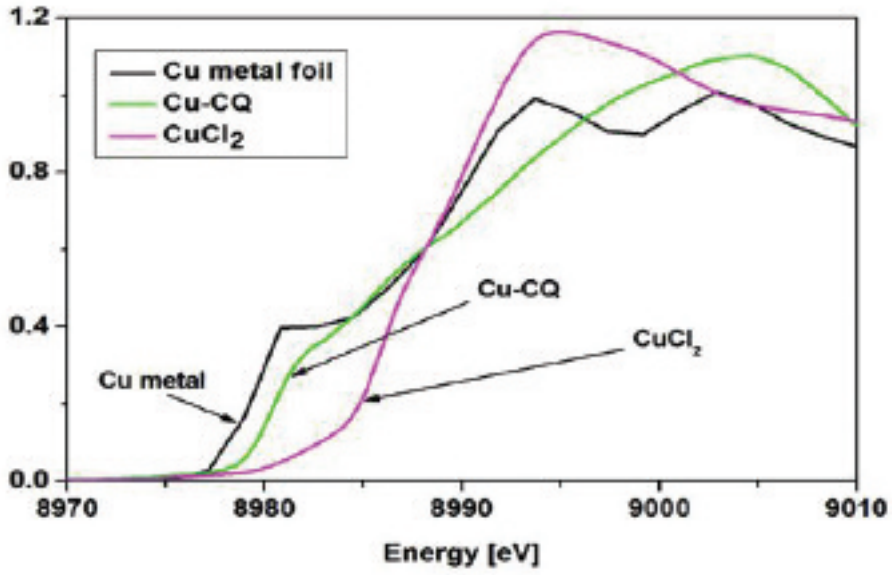

Fig. 2. The Alzheimer's drug clioquinol kills cancer cells in the presence of copper by inactivating a key cellular enzyme complex. Shown here are differences in x-ray absorption between copper foil (black line), copper chloride (purple), and copper complexed with clioquinol (green).

Intrigued by a study reporting that clioquinol shrank lymphoma tumors in rodents, the researchers suspected that copper could be the key, on the basis of previous work in which they observed that copper-containing compounds inhibited a protein "garbage disposal," called the proteasome, that keeps all cells running properly.

The first task was to confirm that clioquinol reacts with copper and forms a new complex. This was accomplished by x-ray absorption studies performed on the Bio-CAT beamline (Fig. 2). Compounds in hand, the group discovered that in two human prostate cell lines exposed to the clioquinol-copper "bullets," proteasome activity fell by up to 69%, which was followed by a loss of cell surface proteins that recognized the male hormone androgen, a known stimulator of prostate tumors. In effect, the molecule seemed to rob the deadly cells of a key signal that told them to go forth and multiply, all by way of the proteasome. As a result, the cells then began to self-destruct.

The compound by itself had similar effects on copper-rich human prostate cancer cells growing either in a Petri dish or in rodents. Researchers believe that copper ions promote the growth of new blood vessels that feed tumors, and the team observed that this growth (called angiogenesis) was reduced in the transplanted tumors exposed to clioquinol compared with untreated tumor transplants, suggesting that the molecule inhibited angiogenesis as well as the proteasome by soaking up the available copper.

— JR Minkel

See: Di Chen[1,2], Qiuzhi Cindy Cui[1,2], Huanjie Yang[1,2], Raul A. Barrea[4], Fazlul H. Sarkar[1,2], Shijie Sheng[1,2], Bing Yan[5], G. Prem Veer Reddy[1,2,3], and Q. Ping Dou[1,2]*, "Clioquinol, a Therapeutic Agent for Alzheimer's Disease, Has Proteasome-Inhibitory, Androgen Receptor-Suppressing, Apoptosis-Inducing, and Antitumor Activities in Human Prostate Cancer Cells and Xenografts," Cancer Res. **67**(4), 1636 (February 15, 2007).
DOI: 10.1158/0008-5472.CAN-06-354

Author affiliations: [1]Barbara Ann Karmanos Cancer Institute and [2]Department of Pathology, School of Medicine, Wayne State University; [3]Vattikuti Urology Institute, Henry Ford Hospital; [4]Biophysics Collaborative Access Team & Department of Biological, Chemical, and Physical Sciences, Illinois Institute of Technology; [5]School of Pharaceutical Sciences and Institute of Environmental Sciences, Shandong University
Correspondence: *doup@karmanos.org

This work was supported by Karmanos Cancer Institute of Wayne State University, Deparment of Defense Breast Cancer Research Program awards W8IX-04-1-0688 and DAMI7-03-I-0175, and National Cancer Institute grant CA112625 (Q.P. Dou); and by the National Cancer Institute/NIH Cancer Center Support grant (Karmanos Cancer Institute). The Biophysics Collaborative Access Team is an NIH-supported research center, RR08630. Use of the APS was supported by the U.S. Department of Energy, Office of Science, Office of Basic Energy Sciences, under Contract No. DE-AC02-06CH11357.

18-ID-D • Bio-CAT • Life science • Microfluorescence (hard x-ray), microdiffraction, small-angle x-ray scattering, time-resolved x-ray scattering, micro-x-ray absorption fine structure, fiber diffraction • 3.3-cm Undulator A • Accepting general users

Deconstructing Heart Muscle

The stars of muscle contraction—be it the flex of a bicep or the throb of the heart—are microscopic fibers spun from the proteins actin and myosin. To play their parts properly, these proteins need help from an additional, less well-understood molecule known as myosin-binding protein-C. Thanks to data collected at Bio-CAT beamline 18-ID-D at the APS, researchers from the University of Wisconsin Medical School and the Illinois Institute of Technology have gleaned insights into this protein's contribution to a smoothly beating heart.

Heart muscle fibers, like those of skeletal muscle, consist of alternating sets of parallel filaments. Thick filaments, which are bundles of myosin molecules, overlap at each end with thin filaments composed of small actin molecules. Connecting the filaments and driving muscle contraction are "cross bridges" that project from myosin. When the muscle is activated, the cross bridges repeatedly grasp, pull, and release adjacent actin, meshing the two sets of fibers together. The effect is akin to a person creeping up a chimney by pushing down with their arms and legs.

Cardiac myosin-binding protein-C (cMyBP-C) accounts for only 1-2% of heart muscle protein, but it plays a noticeable role. In mice bred to lack the protein, cardiac muscle contracts much more easily than that of normal mice, suggesting that the protein somehow acts as a brake on contraction. To figure out how this works, the researchers first extracted pieces of muscle from inside the hearts of the mice lacking cMyBP-C and soaked the muscle in solution to completely relax it. Next, they probed the muscle's molecular structure by measuring its x-ray diffraction pattern on beamline 18-ID-D. The diffraction pattern encoded two main properties: the spacing between actin and myosin filaments and the concentration of material along that spacing (Fig. 1). The researchers hypothesized that cMyBP-C works as a tether on cross bridges that happen to be tucked closer than others to their myosin filament at any given moment, preventing them from aiding contraction. In keeping with that idea, they discovered that the molecular mass in the heart muscle without cMyBP-C was less concentrated around myosin. Instead, the molecular mass was approximately 30% more spread out between filaments than in normal mouse heart muscle. The molecular mass was also about 40% more disordered than in normal muscle. The research team interprets the findings as evidence that more cross bridges than normal are projecting farther from the myosin filaments. This would explain earlier physiological studies, because such a change would allow more cross bridges to take part in contraction, resulting in quicker contractions and heightened resting tension in the muscles. — *JR Minkel*

See: Brett A. Colson[1]*, Tanya Bekyarova[2], Daniel P. Fitzsimons[1], Thomas C. Irving[2], and Richard L. Moss[1], "Radial Displacement of Myosin Cross-bridges in Mouse Myocardium due to Ablation of Myosin Binding Protein-C," J. Mol. Biol. **367**, 36 (2007). DOI: 0.1016/j.jmb.2006.12.063
Author affiliations: [1]Department of Physiology, University of Wisconsin Medical School; [2]CSRRI and Department of BCPS, Illinois Institute of Technology
Correspondence: *bacolson@wisc.edu

This work was supported by funding from the National Institutes of Health (R3782900) (to R.L.M.). Bio-CAT is a National Institutes of Health-supported Research Center (RR-08630). Use of the APS was supported by the U.S. Department of Energy, Office of Science, Office of Basic Energy Sciences, under Contract No. DE-AC02-06CH11357.

18-ID-D • **Bio-CAT** • Life science • Microfluorescence (hard x-ray), microdiffraction, small-angle x-ray scattering, time-resolved x-ray scattering, micro-x-ray absorption fine structure, fiber diffraction • 3.3-cm Undulator A • Accepting general users

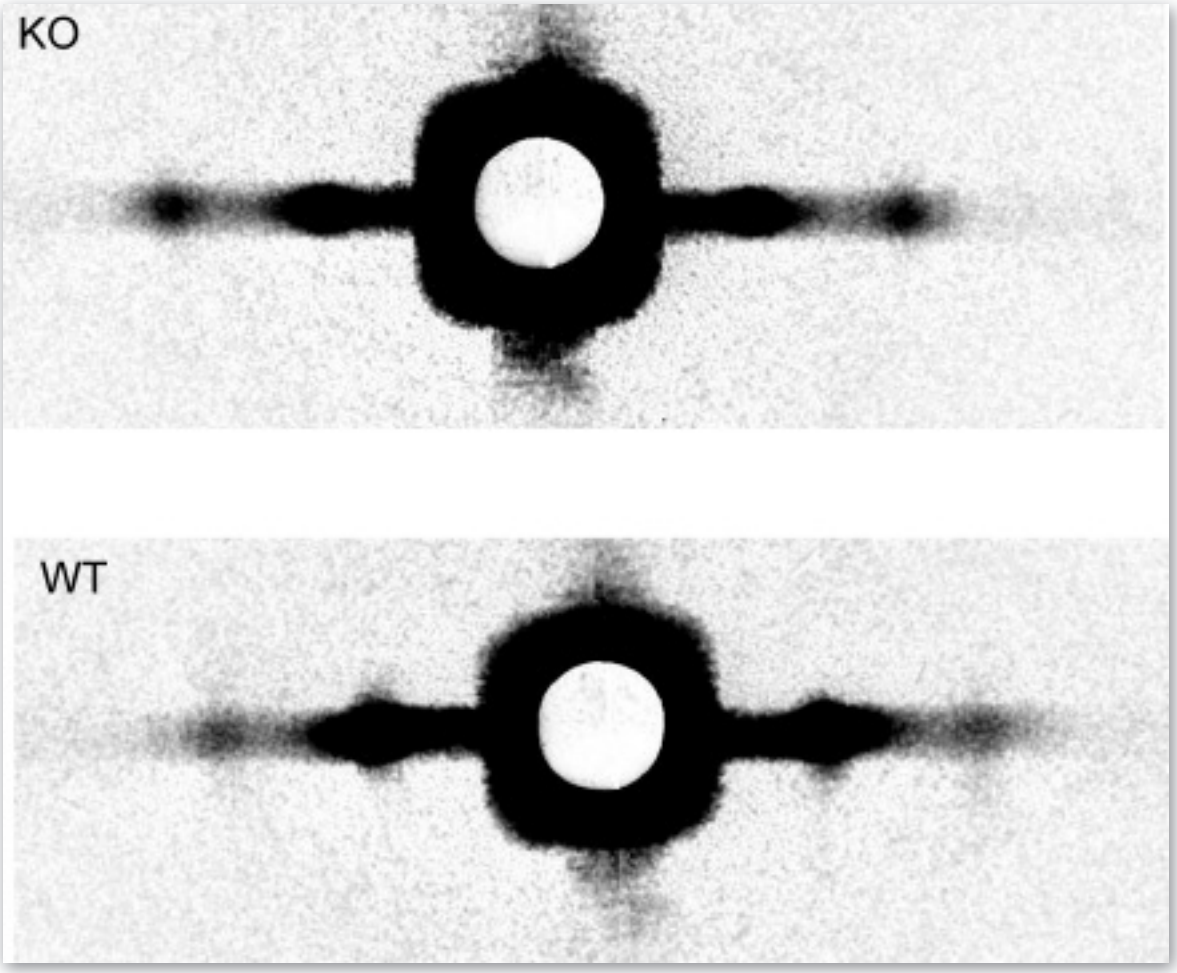

Fig. 1. X-ray diffraction patterns of normal mouse heart muscle (WT, bottom) and heart muscle from mice lacking cardiac myosin-binding protein-C (KO, top). Compared with WT muscle, the KO muscle matter is shifted toward its thin actin filaments (represented by the size of the outermost black dots in both images), as opposed to its thick myosin filaments (inner dots), implying that cardiac myosin-binding protein-C helps keep myosin filaments more tightly wound than they would be otherwise.

Muscle-Fiber Research Expands

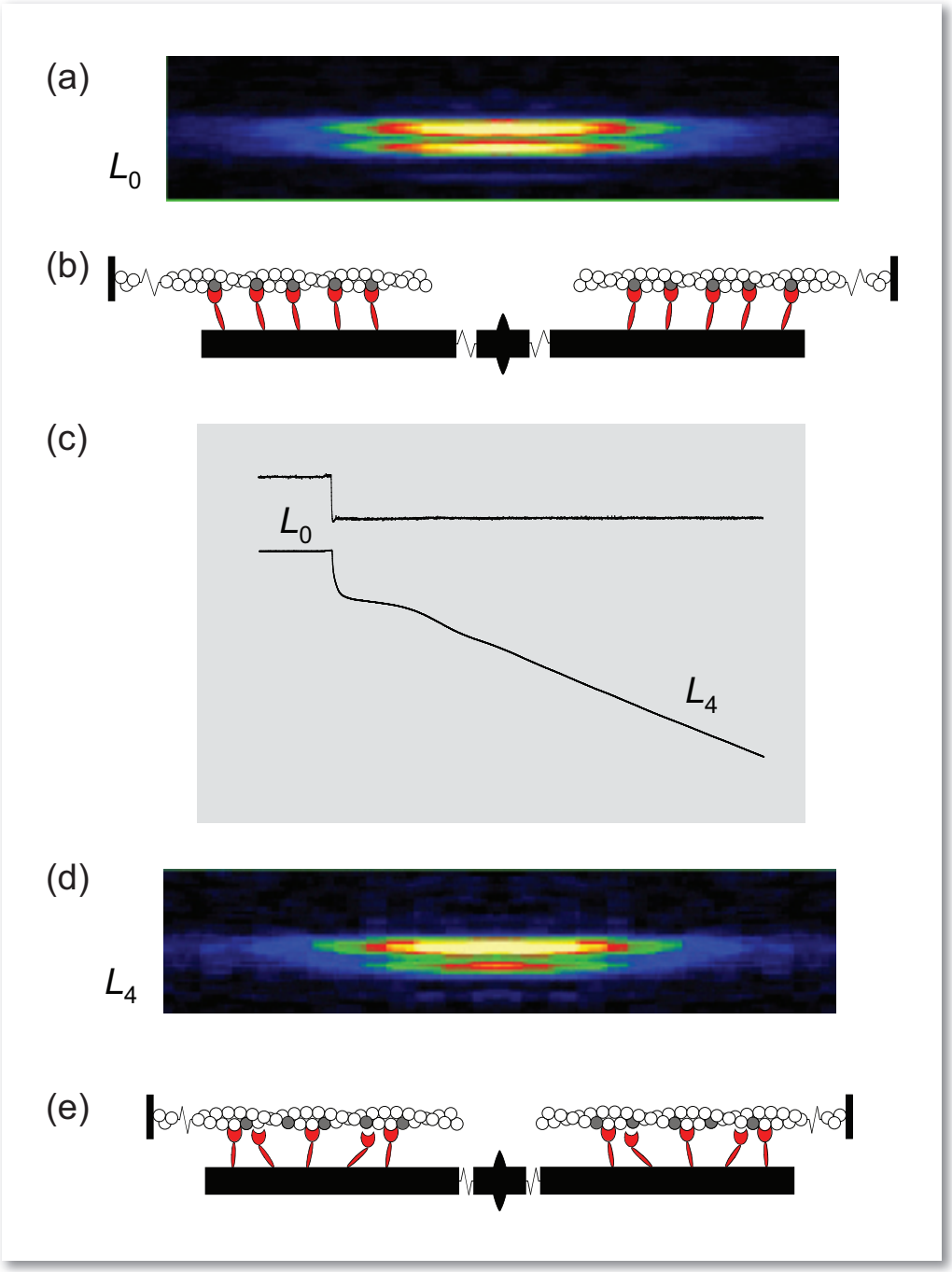

It has been known that muscle fibers shorten slowly under heavier loads and faster under lighter loads. Now, researchers from the Università degli Studi di Firenze, Università di Roma, Dexela Ltd., the Illinois institute of Technology, and King's College London, using the Bio-CAT 18-ID-D beamline at the APS have discovered the molecular basis of this fundamental property of muscle function. Their work was the cover article for the issue of *Cell* magazine in which it was published. Understanding exactly how muscle fibers work helps lay the groundwork for the development of new treatments for muscle disorders as well as enhancing the understanding of athletic performance.

The researchers gleaned these insights into muscle function by using the Bio-CAT beamline to study a key muscle protein called myosin. The group characterized the interaction of myosin with actin, another protein found in muscle. Actin and myosin are arranged within muscle fibers in alternating layers of filaments. The actin and myosin layers are connected by "myosin motors," which, during a muscle contraction, cause the layers to slide over each other in opposing directions, similar to the way oars dipped into water propel a row boat forward. The shortening of a muscle fiber is thought to correlate with the myosin and actin sliding over each other in this manner. When several fibers contract together, a muscle contraction takes place.

These researchers showed, for the first time, that muscle fibers not only shorten more slowly with a heavier load, but that the number of myosin motors attached to actin increases directly with increased load, while the size of their movement remains almost unchanged. This explanation more accurately depicts muscle performance than the previously accepted explanation.

The researchers conducted their experiments on single intact fibers, about 5 mm in length, dissected from frog muscle. Electrodes were used to deliver pulses of electric current to the muscle fibers that simulated what would take place in a real-life setting. In this way, the researchers were able to record the fiber contractions under various conditions. X-ray diffraction data were then collected from the fibers, which enabled the researchers to visualize and quantify the movement of attached myosin motors as load increased (Fig. 1).

Simultaneous mechanical measurements enabled the researchers to determine that the number of the attached myosin motors increased in proportion to the increase in load, while the force exerted by each of the myosin motors remained constant regardless of the load. This was in contrast to what had been previously thought—that the force of each myosin motor was higher when the load was higher. These researchers found that it was the increased number of connecting myosin motors that allows the muscle fiber to bear greater weight, not an increase in force within each myosin motor.

The researchers also found that detachment of a myosin motor from actin depended heavily on the motor's shape or conformation as a muscle progressed through a contraction. The change in shape allowed myosin motors to detach more quickly from actin while bearing lighter loads and remain attached while bearing heavier loads, a finding that gives a molecular explanation for the high efficiency of this motor. — *Emma Hitt*

< Fig. 1. The upper panel (a) shows the M3 x-ray reflection from an active single muscle fiber at constant length (*L*0) recorded at APS. The reflection is split into two peaks of roughly equal intensity by interference between the two arrays of myosin motors shown in red in the cartoon representation of the muscle sarcomere (b). When the load on the muscle fiber is decreased (c) it shortens, reaching a steady speed (at *L*4) that depends on the load. The M3 reflection recorded at *L*4 (d) has interference peaks of markedly different intensities (middle panel), and this signals motion of actin-attached myosin motors towards the midpoint of the sarcomere combined with some motor detachment (e).

See: Gabriella Piazzesi[1,2], Massimo Reconditi[1], Marco Linari[1], Leonardo Lucii[1], Pasquale Bianco[1,2], Elisabetta Brunello[1,2], Valérie Decostre[1], Alex Stewart[3], David B. Gore[4], Thomas C. Irving, Malcolm Irving[5]*, and Vincenzo Lombardi[1,2], "Skeletal Muscle Performance Determined by Modulation," **Cell** 131, 784 (November 16, 2007). DOI 10.1016/j.cell.2007.09.045

Author affiliations: [1]Laboratorio di Fisiologia, Dipartimento di Biologia Animale e Genetica, Università degli Studi di Firenze; [2]CRS SOFT-INFM-CNR, Università di Roma "La Sapienza"; [3]Dexela Ltd.; [4]Bio-CAT/Illinois Institute of Technology, Department of Biological, Chemical, & Physical Sciences; [5]Randall Division of Cell and Molecular Biophysics, King's College London
Correspondence: *malcolm.irving@kcl.ac.uk

Use of the Advanced Photon Source was supported by the U.S. Department of Energy, Office of Science, Office of Basic Energy Sciences, under Contract No. DE-AC02-06CH11357.

18-ID-D • Bio-CAT • Life science • Microfluorescence (hard x-ray), microdiffraction, small-angle x-ray scattering, time-resolved x-ray scattering, micro-x-ray absorption fine structure, fiber diffraction • 3.3-cm Undulator A • Accepting general users

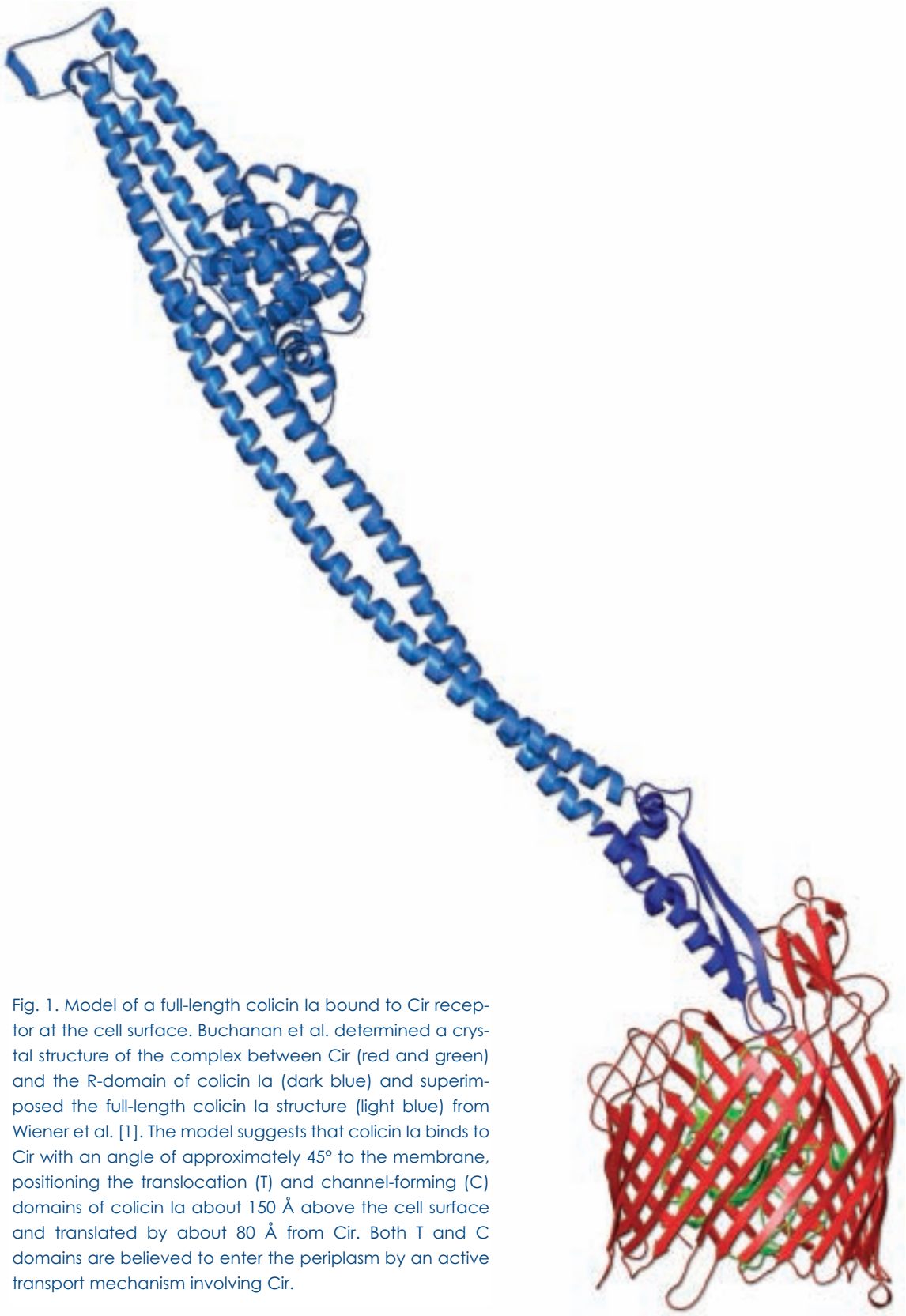

Fig. 1. Model of a full-length colicin Ia bound to Cir receptor at the cell surface. Buchanan et al. determined a crystal structure of the complex between Cir (red and green) and the R-domain of colicin Ia (dark blue) and superimposed the full-length colicin Ia structure (light blue) from Wiener et al. [1]. The model suggests that colicin Ia binds to Cir with an angle of approximately 45° to the membrane, positioning the translocation (T) and channel-forming (C) domains of colicin Ia about 150 Å above the cell surface and translated by about 80 Å from Cir. Both T and C domains are believed to enter the periplasm by an active transport mechanism involving Cir.

Germ Warfare: How Colicin Ia Breaches the *E. Coli* Cell Wall

Bacteria have many enemies—each other as well as their reluctant hosts—and many well-evolved offensive and defensive strategies. The gram-negative bacteria, which include *Escherichia coli* (*E. coli)*, among many others of medical significance, protect themselves with a castle-keep structure: two membranes and an intervening moat (the periplasm) enclose the bacterial cell in citadel-like isolation. As with stone-and-mortar castles, the increased fortifications create a dilemma for the bacterium as well as for its besiegers: obtaining necessary supplies becomes more difficult, requiring an active transport system across the outer membrane and periplasm into the cell. Modeling how proteins and other large molecules obtain entry to the gram-negative cell has relevance both for bioremediation applications and for the development of new and badly needed antibiotics and vaccines. By using the SER-CAT 22-ID-D beamline at the APS, researchers have solved crystal structures to successfully model the interactions of the colicin Ia protein with its target receptor on the outer membrane of *E. coli* cells.

The bacterial equivalent of the medieval portcullis is a family of barrel-shaped proteins embedded in the outer membrane that have a plug domain to limit entry to desirable molecules, such as vitamin B12 and chelated iron complexes. Colicins (*E. coli*-specific bacteriocins) are potent toxins secreted by *E. coli* to attack rival strains. A single colicin molecule, once it has breached the double walls, can destroy a sensitive *E. coli* cell, either by cleaving its DNA or (the strategy of colicin Ia) forming a voltage-gated ion channel that effectively blasts a hole through the cell. One such, colicin Ia, is decidedly undesirable. Colicin Ia is a large molecule (626 amino acids, 69 kilodaltons in mass) with three distinct domains that correspond to its one-two-three assault on its target. The receptor-binding (R) domain binds the target receptor, the N-terminal translocation (T) domain is required for penetrating the cell envelope, and the C-terminal channel-forming (C) domain delivers the death blow.

The work of the researchers from the National Institute of Diabetes & Digestive & Kidney Disorders and the National Cancer Institute, in collaboration with colleagues at the Albert Einstein College of Medicine, reveals the initial deployment of this sophisticated molecular weaponry (Fig. 1). Remarkably, the binding of colicin Ia to its target receptor, Cir, causes the receptor to undergo large conformational changes, stabilizing the receptor in a wide-open position, with the colicin Ia molecule positioned directly above it, poised to strike. This is the largest conformational change yet observed in a bacterial membrane receptor-protein interaction in this receptor family. Equally striking, the T and C domains are positioned far above the membrane at this first stage in their assault, and presumably must unfold at least partially to pass through the open receptor. How the colicin Ia molecule completes its penetration of the cell is not yet known, but further studies by the researchers suggests that both the Cir receptor and the TonB transport system are involved. — *Carol Hart*

Reference

[1] M. Wiener, D. Freymann, P. Ghosh, and R.M. Stroud, Nature **385**, 461 (1997)

See: Susan K. Buchanan[1]*, Petra Lukacik[1], Sylvestre Grizot[1], Rodolfo Ghirlando[1], Maruf M.U. Ali[1], Travis J. Barnard[1], Karen S. Jakes[2], Paul K. Kienker[2] and Lothar Esser[3], "Structure of colicin I receptor bound to the R-domain of colicin Ia: implications for protein import," EMBO J. **26**, 2594 (2007). DOI: 10.1038/sj.emboj.7601693
Author affiliations: [1]Laboratory of Molecular Biology, National Institute of Diabetes & Digestive & Kidney Diseases, National Institutes of Health; [2]Department of Physiology and Biophysics, Albert Einstein College of Medicine; [3]Laboratory of Cell Biology, National Cancer Institute, National Institutes of Health
Correspondence: *skbuchan@helix.nih.gov

This work was supported by the Intramural Research Program of the NIH, National Institute of Diabetes & Digestive & Kidney Diseases (S.K.B., P.L., S.G., R.G., M.A., T.J.B.) and the National Cancer Institute (L.E.). K.S.J. and P.K.K. acknowledge support from National Institutes of Health Grant GM31986. SER-CAT supporting institutions may be found at www.ser-cat.org/members.html. Use of the APS was supported by the U.S. Department of Energy, Office of Science, Office of Basic Energy Sciences, under Contract No. DE-AC02-06CH11357.

22-ID-D • **SER-CAT** • Life science • Macromolecular crystallography, multiwavelength anomalous dispersion • 3.3-cm Undulator A • Accepting general users

DNA for Fighting Infection

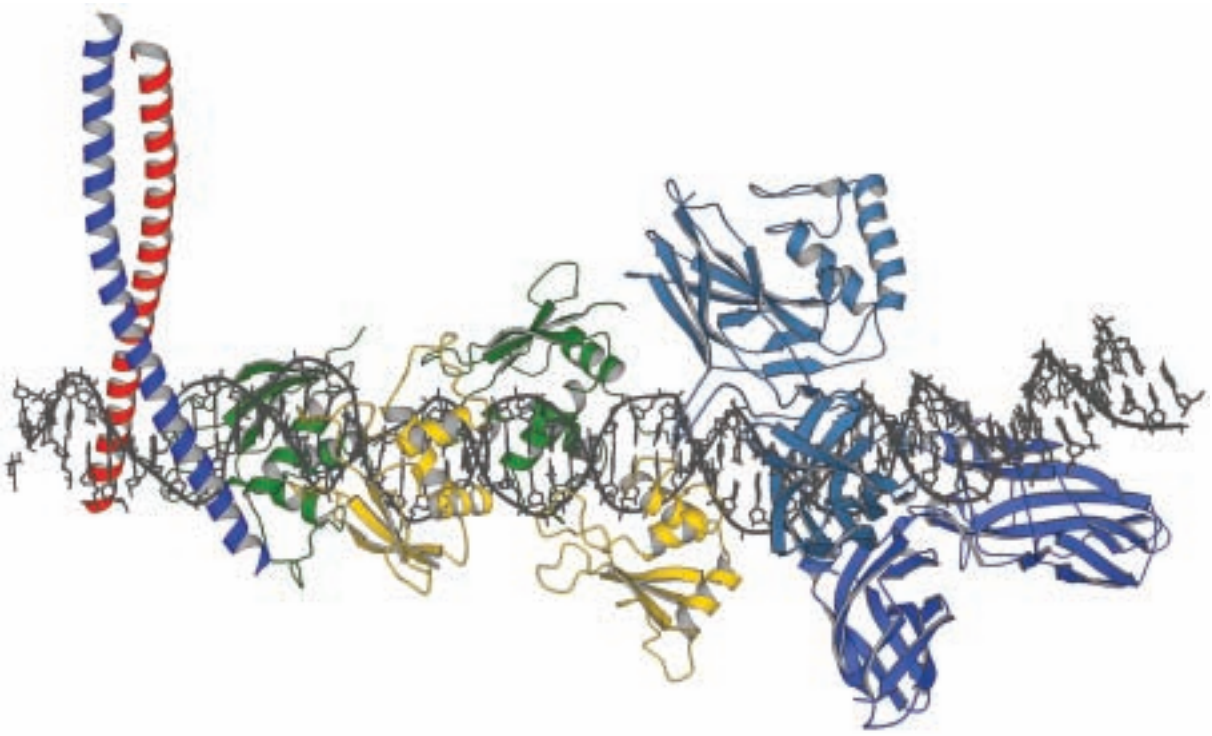

Fig. 1. Structure of the interferon-β enhanceosome: side view showing how the two DNA strands (gray) bend around enhanceosome domains (ribbons).

The result of this research is an elegantly complex molecular model, which makes it much easier to understand how synthesis of interferon-β is regulated

So much DNA, so little time to find and read the section of the genetic code that will keep cells functioning properly. The time factor is especially critical when a cell is faced with an intruder such as a virus ready to launch an assault. Virus reproductive cycles operate on the scale of minutes and hours, so there is no time to lose in marshalling a cell's defenses. In human cells, one response to viral entry involves synthesis of the protein interferon. How is the right DNA activated so that interferon production occurs at the right time and place? Researchers studied the complicated and intricate phenomenon and, utilizing the BioCARS beamline 14-BM-C at the APS and beamline 8.2.1 at the Advanced Light Source, produced a structure of half of the protein involved in the process. Combined with previous work on the other half of the assembly, the entire structure is now known in detail. The result is an elegantly complex molecular model, knowledge of which makes it much easier to understand how synthesis of interferon-β is regulated.

The activation of the interferon-β gene has been particularly well studied with respect to answering the "right time and place" question. The actual reading of the correct section of DNA depends on the presence of an enhancer sequence, which must be occupied by the appropriate protein factors for gene activation to be maintained. Some enhancers are "modular": their elements are spread out from each other at some distance from the gene that is to be activated. Other enhancers, such as the one that controls the interferon-β gene, are compact and located close to the beginning of the gene itself. The compact interferon-β enhancer is a stretch of DNA that binds protein to form an assemblage called an enhanceosome.

The research team from the Harvard Medical School and Harvard University focused on the interferon-β enhancer because it is known to be viral-induced and therefore important to the cell's immune response. Building the enhanceosome requires binding six different protein factors (two of them in multiple copies) to the enhancer DNA. The factors then recruit coactivators and chromatin remodeling proteins to the interferon-β promoter region. In the present study, the scientists were able to advance knowledge of how this all occurs by producing a crystal structure of the DNA-binding domains for four of the enhanceosome components (IRF-3, IRF-7, and NFKB p50 and p65) that were bound to one half of the enhancer DNA. They then combined this information with previous data collected for the other half of the enhancer and, by doing so, constructed a complete model for all the DNA-interacting parts of the enhanceosome (Fig. 1).

Several leaps in understanding can be gleaned from the details of the structure described by the research team. In total, eight protein subunits are needed to create a continuous binding surface for recognizing 50 base pairs of DNA. Although there is little direct interaction between the eight proteins, their association with the enhancer appears to be coordinated by binding-induced changes in DNA conformation and also by interaction of these eight protein subunits with additional components of the system. And the binding surface presented by this array of proteins appears to contact every DNA nucleotide pair on the enhancer. This last piece of information helps explain why the DNA sequence of the mammalian interferon-β enhancer has remained invariant over evolutionary time while the sequence of the gene itself has varied considerably.

Viral infection leads to synthesis of the proteins that bind to the enhancer and start the ball rolling for synthesis of interferon-β. The research team was able to show that all components of the enhanceosome system have to be present for interferon-β production to proceed. This all-or-none requirement is typical of many genetic switches; the principles embodied in the structure of interferon-β are likely to apply to many other gene-regulatory circuits. — *Mona Mort*

See: Daniel Panne[1], Tom Maniatis[2], and Stephen C. Harrison[1,*], "An Atomic Model of the Interferon-β Enhanceosome," Cell **129**, 1111 (June 15, 2007). DOI: 10.1016/j.cell.2007.05.019

Author affiliations: [1]The Jack and Eileen Connors Structural Biology Laboratory, Harvard Medical School, Department of Biological Chemistry and Molecular Pharmacology, Howard Hughes Medical Institute; [2]Harvard University, Department of Molecular and Cellular Biology
Correspondence: *harrison@crystal.harvard.edu

S.C.H. is an Investigator in the Howard Hughes Medical Institute. T.M. was supported by grant R01AI020642 from the National Institutes of Health. Use of the Advanced Photon Source was supported by DOE, Office of Basic Energy Sciences, under Contract No. DE-AC02-06CH11357.

14-BM-C • BioCARS • Life science • Macromolecular crystallography, fiber diffraction, biohazards at the BSL2/3 level, subatomic (<0.85 Å) resolution • Bending magnet • Accepting general users

Finding Ways to Fight Alzheimer's

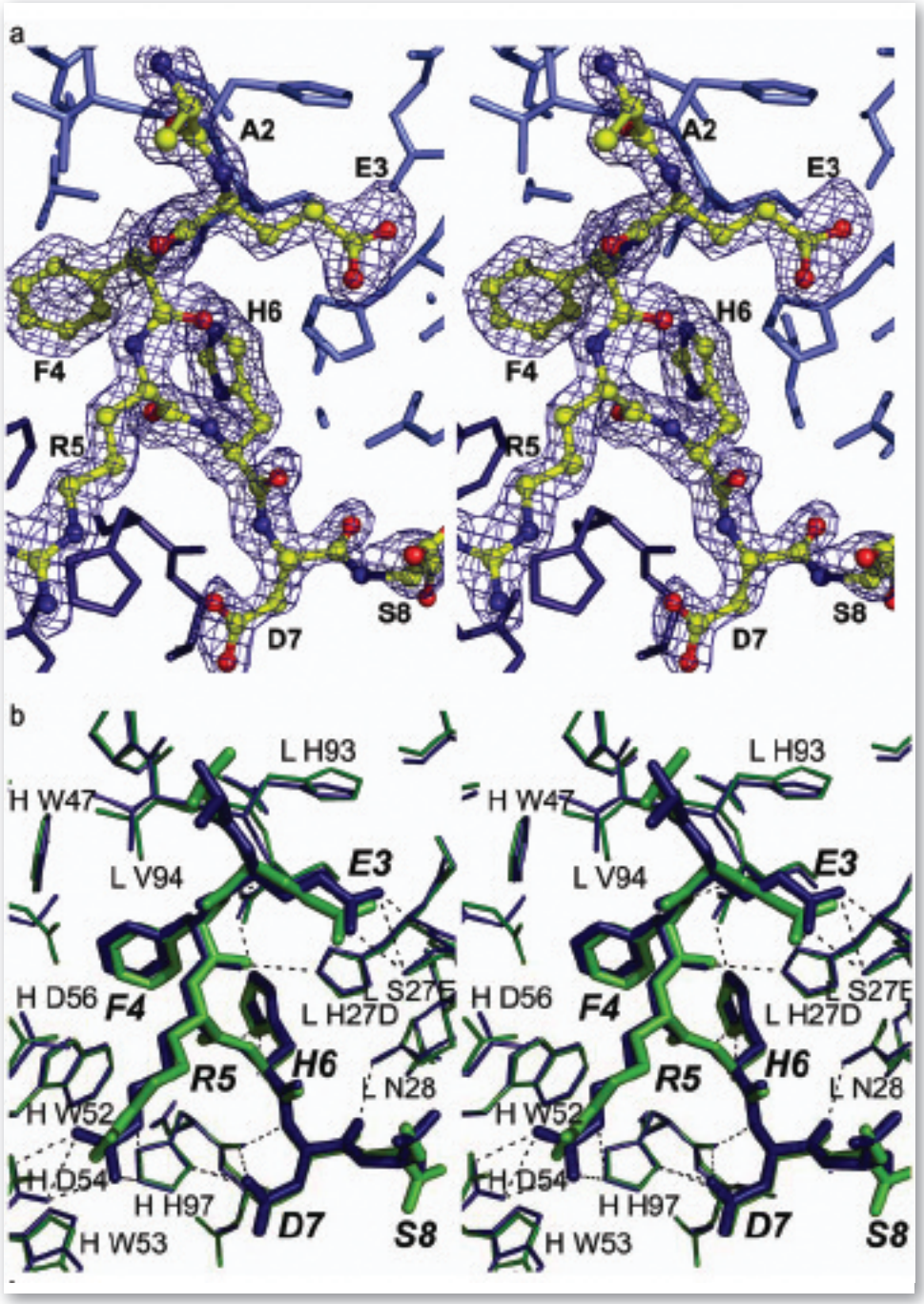

Fig. 1. Antibody binding to sections of amyloid-β: a, stereo view showing electron density for binding to PFA1; b, stereo view of overlay showing similarity in binding of PFA1 (blue) and PFA2 (green).

How and why do the brain and other parts of the nervous system lose function in patients afflicted with Alzheimer's disease? Searching for the answer to that question has been a top priority for biomedical researchers. The good news is that the biochemical mechanisms regulating progression of the disease are increasingly well understood. One well-known process is formation of soluble aggregates, or plaques, of a molecule called amyloid-β, which have been found in brain tissue samples of Alzheimer's patients. Slowing, or even preventing, aggregate formation is a major focus of therapeutic strategies. Recent efforts to treat and cure Alzheimer's disease have involved both active immunity—use of a vaccine to stimulate the body's own antibody production—and passive immunity, in which antibodies are produced in the laboratory and then administered directly to the patient. The advantages of passive immunity include greater control over the antibody response and a shorter time period to develop the therapy than would be involved in vaccine development, in which side effects are more difficult to anticipate. Important breakthroughs in using passive immunity have recently been made by a research team using the BioCARS 14-BM-C beamline at the APS. The team's work greatly advances knowledge about the use of passive immunization in treating Alzheimer's disease.

The scientists from Case Western Reserve University, the University of Tennessee, the University of Pittsburgh, the California Institute of Technology, and the University of Utah isolated and analyzed the structure of antibodies that bind amyloid molecules and thereby prevent them from forming plaques. The study built on previous work that had shown anti-amyloid-β monoclonal antibodies to be effective in binding amyloid-β aggregates, called the antigen because they are the molecule that the antibody will bind and disable. The anti-amyloid-β antibodies could bind amyloid-β both in the test tube and in non-human animal studies, showing promise for use in passive immunization. In fact, use of the antibodies is now well along in clinical trials in patients with Alzheimer's disease. Because of this, the detailed knowledge of the antibody-antigen binding system reported in the present study comes at a critical time.

The research team produced a wealth of new data that can be quickly and efficiently put to use in designing therapies to treat Alzheimer's disease. The most important results of the work lie in enhancing our understanding of how the antibodies react with amyloid-β. First, the group isolated two different types of antibody, called PFA1 and PFA2, which recognize the amyloid-β molecule in various stages of its assembly: monomers, protofibrils, and fibrils (Fig. 1). Knowing how the intermediate and final stages of the amyloid molecule will react with the antibody arms therapy designers with several ways to attack the problem. Second, the scientists produced a detailed structure of the antigen-binding area on the antibody when it is attached to a section of the amyloid-β molecule, thus allowing a very clear understanding of how the binding occurs. It is now possible to understand in fine detail the process that allows binding of amyloid-β to the antibody, thereby opening the door to finding ways to enhance that binding. Third, the team was also able to home in on sections of the amyloid molecule that appear to be particularly important in binding to the antibody and, therefore, important to the body's immune response. Focusing on these areas of the amyloid molecule will allow more efficient use of resources that are dedicated to developing passive immunization for treatment of Alzheimer's disease. Fourth, and perhaps most important for therapy development, the team showed that there was cross-reactivity of parts of the newly described antibodies with sections of other human proteins. This information will greatly aid predictions of side effects of the immunotherapy and allow fine-tuning of the specificity and affinity of the antibodies used to disable amyloid-β.

Thanks to the work done by these researchers in unveiling the details of binding antibodies to amyloid-β, using passive immunization to treat patients with Alzheimer's disease is now much easier to envision and further develop.

— *Mona Mort*

See: Anna S. Gardberg[1], Lezlee T. Dice[2], Susan Ou[3], Rebecca L. Rich[4], Elizabeth Helmbrecht[1], Jan Ko[3], Ronald Wetzel[5], David G. Myszka[4], Paul H. Patterson[3], and Chris Dealwis[1,6]*, "Molecular basis for passive immunotherapy of Alzheimer's disease," Proc. Natl. Acad. Sci. USA **104**, 15659 (October 2, 2007). DOI: 10.1073pnas.0705888104

Author affiliations: [1]Department of Biochemistry and Cellular and Molecular Biology, University of Tennessee; [2]Graduate School of Medicine, University of Tennessee; [3]Division of Biology, California Institute of Technology; [4]HSC Core Research Facilities, University of Utah; [5]Department of Structural Biology and Pittsburgh Institute for Neurodegenerative Diseases, University of Pittsburgh School of Medicine; and [6]Department of Pharmacology, Case School of Medicine

Correspondence: *chris.dealwis@case.edu

This work was supported by National Institutes of Health Grants NS46356 (to R.W., P.H.P., and C.D.) and R01 AG018416 (to R.W. and D.G.M.). Use of the Advanced Photon Source was supported by DOE, Office of Basic Energy Sciences, under Contract No. DE-AC02-06CH11357.

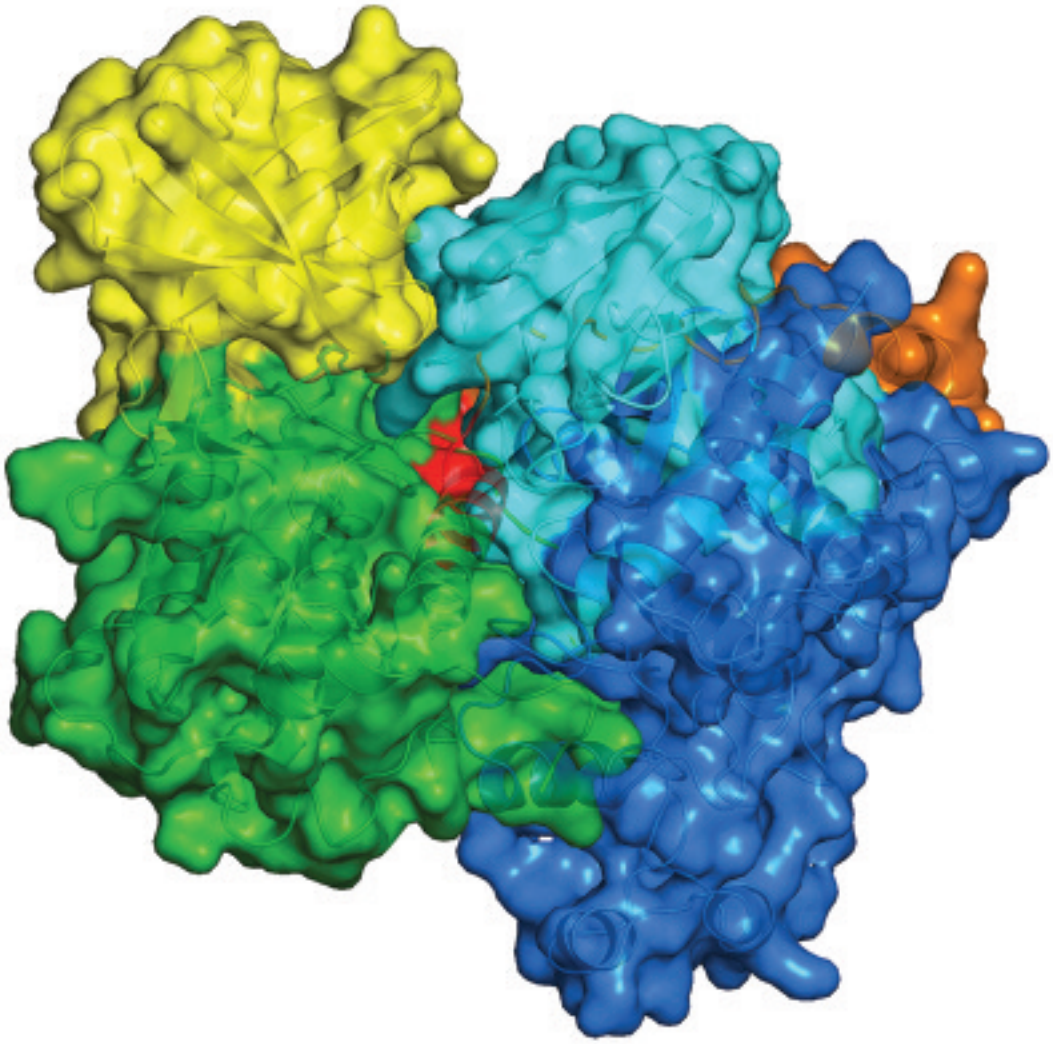

Fig. 1. Schematic illustration of two tightly bound cell signaling proteins, p38α (in cyan and blue) and MK2 (in yellow, green, red, and orange), which together initiate the inflammatory response of the immune system that contributes to arthritis. The proteins' backbones are shown with their secondary structure elements, arrows and bundles, and are overlaid on the molecules' overall shapes.

A Protein Embrace Could Spur New Arthritis Drugs

A high-resolution look at a pair of proteins locked in a tight embrace is giving researchers new leads in designing drugs to treat chronic inflammatory diseases such as rheumatoid arthritis. Scientists using the SGX-CAT 31-ID-D beamline at the APS determined the crystalline structure of two proteins that come together to play a key role in the cellular events that trigger the body's inflammatory response. Based on pre-existing biochemical data, they identified several locations where small-molecule drugs might be able to inhibit the function of these proteins, perhaps offering a way to ease the pain of arthritis and related ills.

Before a cell of the immune system can trigger the kind of inflammation that over time results in joint swelling and pain, it must undergo a series of internal biochemical reactions, referred to as signal transduction. Upon receiving some chemical cue from its surroundings, the cell kick starts a cascade of protein enzymes, each of which activates the next in the chain, culminating in the release of inflammation-promoting chemicals called cytokines. One of the first enzymes in this pathway is called p38α, which latches tightly onto its target, the enzyme MK2 (for MAPK-associated kinase 2), and activates it.

Cultured human cells lacking p38α are unable to secrete inflammatory cytokines. The Boehringer Ingelheim researchers wanted to zero in on the interaction between the pair, reasoning that if they could either disrupt the tight embrace or inhibit the function of either one of these enzymes, it would offer an effective, specific way of shutting down the pathway that leads to arthritis. To aid them in designing drugs for that purpose, they crystallized a mixture of the two proteins and solved the crystal's three-dimensional shape from x-ray diffraction measurements obtained on the SGX-CAT beamline (Fig. 1).

Consistent with the protein pair's known affinity for each other, the enzymes molded their surfaces together over a much larger area than is seen in most other protein-protein structures solved to date. Included in MK2's contact surface with p38α was a stretch of 31 amino acids (protein subunits) known to be crucial for the pair to bind to each other. Learning the shape of this so-called docking region gave the team new insight into the key features holding the proteins together and may help devise means of better inhibiting the biological function of the assembly.

Both enzymes are kinases, meaning they work by chemically affixing to their targets a cluster of phosphorus and oxygen atoms (a phosphoryl group). That is also how they themselves are activated. The researchers noted that the phosphorylation site of p38α was buried between the two proteins, suggesting that when a phosphoryl group is affixed to p38α, it wedges the proteins apart, but not enough to separate them completely.

Separation may come instead when MK2 is phosphorylated (by p38α). They noted that one of MK2's sites for accepting phosphoryl groups was likewise buried between the proteins, offering another avenue to wedge between the two proteins. Such sites offer targets for researchers to short-circuit signal transduction by designing small molecules that prevent phosphorylation. — *JR Minkel*

See: Andre White[1]*, Christopher A. Pargellis[2], Joey M. Studts[3], Brian G. Werneburg[2], and Bennett T. Farmer II[1], "Molecular basis of MAPK-activated protein kinase 2:p38 assembly," Proc. Natl. Acad. Sci. USA **104**(15), 6353 (April 10, 2007). DOI: 10.1073pnas.0701679104

Author affiliations: Departments of [1]Medicinal Chemistry, [2]Immunology and Inflammation, and [3]Biologics and Biomolecular Sciences, Boehringer Ingelheim Pharmaceuticals, Inc.

Correspondence:*andre.white@boehringer-ingelheim.com

Use of the SGX-CAT beamline at sector 31 of the Advanced Photon Source was provided by SGX Pharmaceuticals, Inc., who constructed and operate the facility. Use of the Advanced Photon Source was supported by the U.S. Department of Energy, Office of Science, Office of Basic Energy Sciences, under Contract No. DE-AC02-06CH11357.

31-ID-D • SGX-CAT • Life science • Macromolecular crystallography, single-crystal diffraction, fiber diffraction, single-wavelength anomalous dispersion • 3.3-cm Undulator A • Accepting general users

Another Step in the Ongoing Effort to Outsmart Bacteria

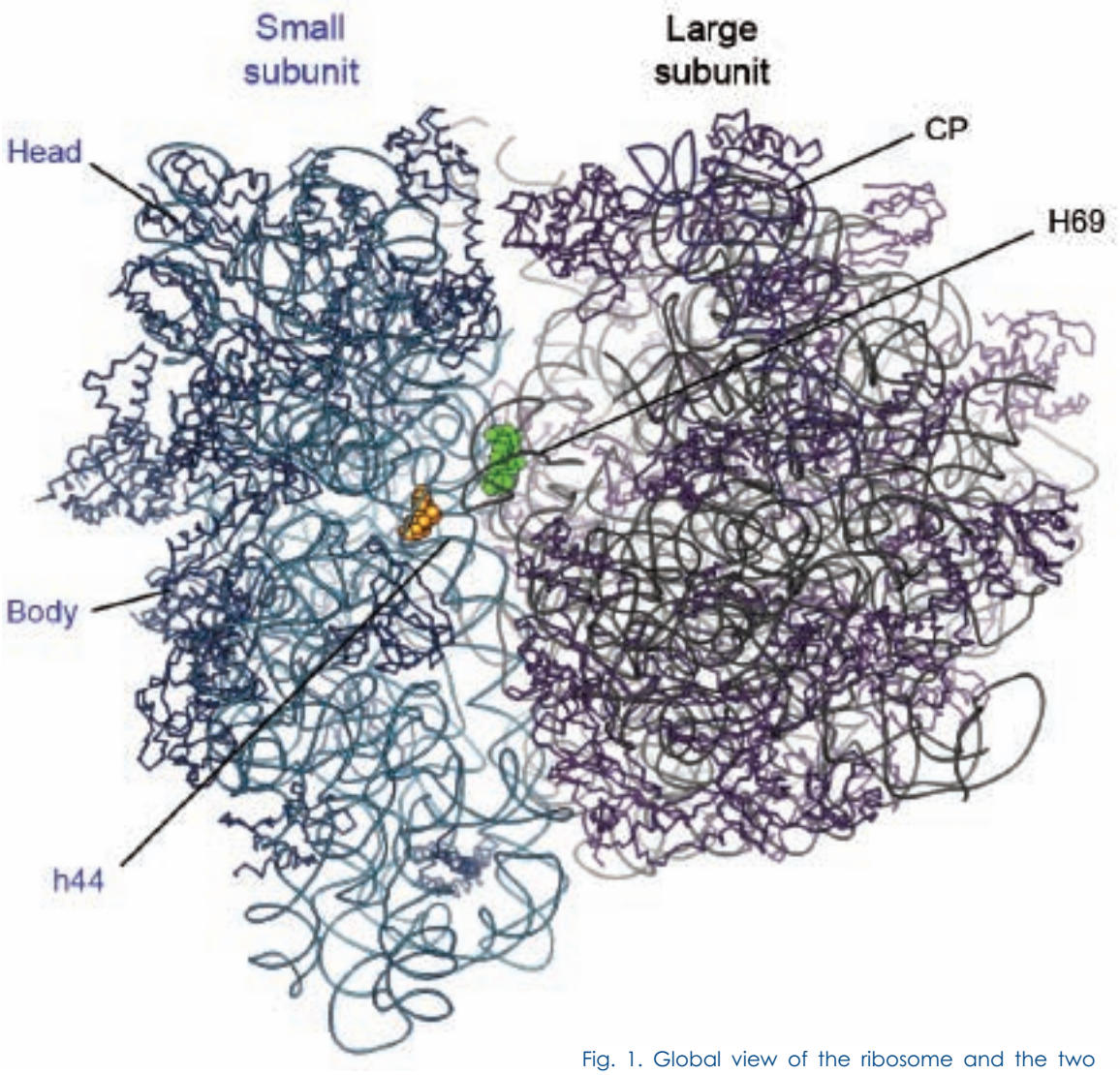

Fig. 1. Global view of the ribosome and the two binding sites for aminoglycosides. Gold and green, aminoglycosides bound to the small and large ribosomal subunits, respectively; light blue, 16S rRNA; gray, 23S rRNA; purple, 5S rRNA; dark blue and magenta, proteins of small and large subunits, respectively; CP, central protuberance.

Understanding the way in which antibiotics work aids in the development of new, powerful drugs needed to combat resistant strains of bacteria. A widely used class of antibiotics, called aminoglycosides, works by interfering with the translation of a bacterial cell's genetic code into proteins. Specifically, aminoglycoside antibiotics disrupt ribosomal function within bacteria. Ribosomes are essential cellular machines that serve as protein production factories within bacteria, and without their proper functioning, the bacteria die. Researchers set out to find out more about how antibiotics of this class disrupt ribosomal activity by employing the NE-CAT beamline 24-ID-C at the APS and the SIBYLS (12.3.1) and 8.3.1 beamlines at the Advanced Light Source (ALS) to derive structure-based information about ribsosomal function.

Aminoglycosides are known to interact with ribosomes and interfere with several aspects of ribosome function, including ribosome recycling. Ribosome recycling is the process of splitting the ribosome into its subunits (small and large) once the ribosome has stopped making proteins. Recycling is necessary for ongoing, healthy, fully functional protein manufacture. In bacteria, recycling is assisted by a protein called ribosome recycling factor (RRF). Until now, it was unclear how aminoglycosides interfere with RRF-assisted ribosome recycling.

To clarify the effects of aminoglycosides on the ribosome function in general and on RRF function in particular, the researchers from Lawrence Berkeley National Laboratory; the University of California, Berkeley; the University of California, San Francisco; the University of Pennsylvania School of Medicine; and Thomas Jefferson University crystallized ribosomes from *Escherichia coli* in complexes with the aminoglycoside antibiotics neomycin, paromomycin, and gentamicin, then obtained x-ray diffraction images of the ribosomes in complexes with the ligands by using diffraction at the APS and ALS beamlines (Fig. 1). The antibiotics were found to bind to RNA helix h44 in the small ribosomal subunit, which had previously been identified in other studies. The research team also found that the antibiotics bind to the RNA helix H69 in the large ribosomal subunit, which was previously unknown. The H69 region of the ribosome is located at the center of several key processes in the ribosome, including translocation and recycling, and is adjacent to the site of RRF binding to the ribosome.

Through additional x-ray crystallography studies of the structures of ribosomes from the bacterium *E. coli* in complex with RRF, the researchers found that RRF binding to the large ribosomal subunit caused helix H69 of the large subunit to swing away from the small subunit, thereby disrupting key intersubunit contacts and assisting ribosome recycling. However, when the antibiotics were added, the action of RRF was completely suppressed. Aminoglycosides would bind to the ribosome and prevent the conformational change in H69 caused by RRF. The researchers were able to see that aminoglycosides restored the contacts between the ribosomal subunits by binding to H69, thereby preventing RRF from proper separation of the subunits. These results provide a structural explanation for the ability of aminoglycosides to prevent ribosome recycling.

The researchers speculate that a mechanism of resistance to aminoglycoside antibiotics may involve destabilization of interactions of the H69 region in the large subunit with h44 in the small subunit, which would weaken the ability of aminoglycosides to bind to these regions. They also suggest that binding of aminoglycosides to H69 might affect other processes important in protein synthesis in addition to preventing proper ribosome recycling. By understanding more about the way in which aminoglycosides interact with bacterial ribosomes, researchers may be able to design more effective antibiotics and improve the antibiotics that are currently available. — *Emma Hitt*

See: Maria A. Borovinskaya[1], Raj D. Pai[2], Wen Zhang[3], Barbara S. Schuwirth[3], James M. Holton[1,4], Go Hirokawa[5], Hideko Kaji[6], Akira Kaji[5], and Jamie H. Doudna Cate[1–3]*, "Structural basis for aminoglycoside inhibition of bacterial ribosome recycling," Nat. Struct. Mol. Biol. **14**(8), 727 (August 2007). DOI: 10.1038/nsmb1271

Author affiliations: [1]Physical Biosciences Division, Lawrence Berkeley National Laboratory; [2]Department of Molecular and Cell Biology and [3]Department of Chemistry, University of California, Berkeley; [4]Department of Biochemistry and Biophysics, University of California, San Francisco; [5]Department of Microbiology, University of Pennsylvania School of Medicine; [6]Department of Biochemistry and Molecular Biology, Thomas Jefferson University

Correspondence: *jcate@lbl.gov

This work was supported by U.S. National Institutes of Health (NIH) grants GM65050 (J.H.D.C.) and GM60429 (A.K.), the Nippon Paint Fund (H.K.), NIH National Cancer Institute grant CA92584 (for the SIBYLS and 8.3.1 beamlines), NIH National Center for Research Resources grant RR-15301 (for beamline 24-IDC) and U.S. Department of Energy grants DE-AC03-76SF00098, KP110201, and LBNL LDRD 366851 (J.H.D.C.), DE-AC03 76SF00098 (for the SIBYLS and 8.3.1 beamlines) and DE-AC02-06CH11357 (for the Advanced Photon Source). Use of the APS was supported by the U.S. Department of Energy, Office of Science, Office of Basic Energy Sciences, under Contract No. DE-AC02-06CH11357.

24-ID-C • NE-CAT • Life science • Microfluorescence (hard x-ray), tomography, microdiffraction • 3.3-cm Undulator A • Accepting general users

Probing the Workings of Natural Killer T Cells

Natural killer T (NKT) cells are a subset of T lymphocytes, white blood cells that play a central role in cell-mediated immunity. NKT cells recognize only glycolipid antigens (carbohydrate-attached lipids that provide energy and serve as markers for cellular recognition), rather than peptide antigens that are bound to a CD1 antigen-presenting molecule. NKT cells are less well understood than conventional T lymphocytes. But because they combine features of adaptive and innate immunity, they may prove to be an important target for clinical interventions in a wide range of disorders. Using the IMCA-CAT 17-ID-B beamline at the APS, a team of researchers from Monash University and the University of Melbourne succeeded in demonstrating at an atomic level how the CD1d-antigen complex is recognized by the T cell receptor (TCR) of the NKT cell, providing new information that may further the development of immunotherapies for cancer, infection, allergy, and chronic inflammatory conditions.

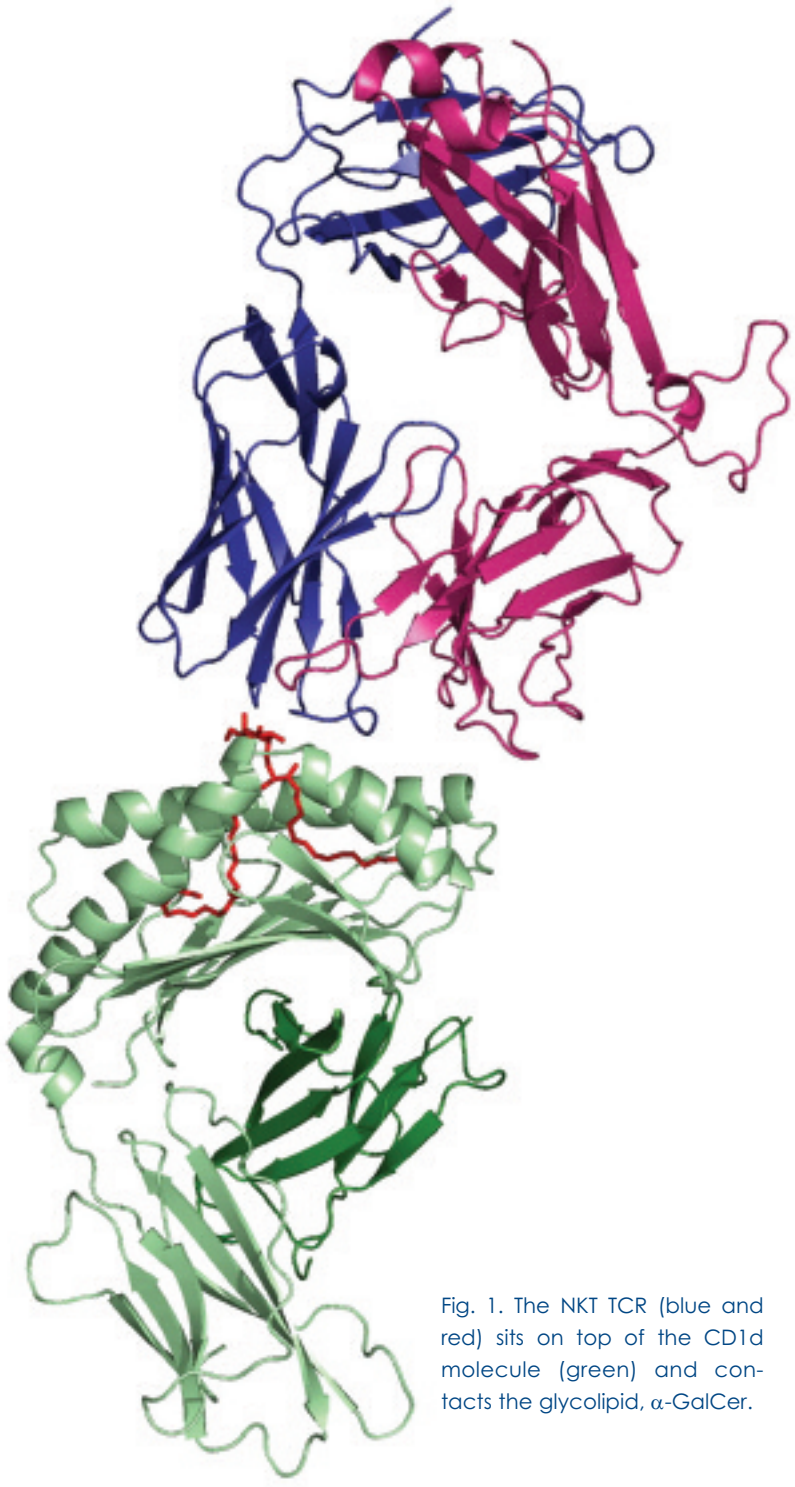

Fig. 1. The NKT TCR (blue and red) sits on top of the CD1d molecule (green) and contacts the glycolipid, α-GalCer.

This research provides new information that may further the development of immunotherapies for cancer, infection, allergy,and inflammatory conditions

The highly variable TCRs of conventional T cells are key to the adaptive immune response. They are specific to the individual: they will only recognize self (syngeneic) MHC molecules, which bind and present peptide antigens. NKT cells, in contrast, possess a semi-invariant TCR that is cross-reactive with CD1–antigen complexes from different individuals. In fact, if a sufficiently potent antigen is introduced, human NKT cells will react with murine CD1d-antigen complex, and murine NKT cells with human CD1d-antigen. NKT cells have immunoregulatory effects that can be either stimulatory or suppressive. Studies in mice suggest that NKT cells may mediate tolerance to organ transplants following immunosuppressive therapy. NKT cells are known to enhance the immune response to some types of cancer and many forms of infection, although they may also promote allergic and inflammatory responses in some settings. Given their limited degree of intraspecies variability, NKT cells represent a clinical target of great potential.

The antigen-binding cleft in the CD1 family contains two large hydrophobic pockets (A' and F') well suited to presenting lipid antigens to TCRs. Antigens capable of inducing a response in NKT cells include glycolipids derived from the cell walls of *Mycobacterium* species, a genus that comprises such age-old scourges as the pathogens responsible for leprosy and tuberculosis. In both mice and humans, the most potent known activator of the CD1d antigen-presenting molecule is a synthetic glycolipid called α-galactosylceramide (α-GalCer). Although this particular CD1d-antigen combination has been much studied, and α-GalCer has been investigated as a potential cancer therapy, the binding mechanisms of the complex formed by CD1d-α-GalCer-NKT TCR were previously unknown.

Structurally, CD1 molecules show substantial similarity to class I MHC molecules, which have a well-characterized mode of interacting with the TCRs of conventional T lymphocytes. In conventional T lymphocytes, the TCR assumes a roughly diagonal position relative to the long axis of the MHC-peptide-antigen complex, and it was therefore assumed that the NKT TCR would adopt a similar attitude in binding to the CD1d-lipid-antigen complex. Instead, the NKT TCR takes a position parallel to the long axis of the antigen-binding cleft at the extreme end of the complex, directly above the F' antigen-binding pocket of the CD1d (Fig. 1). This conformation has not been seen with any MHC–antigen–TCR complex.

The CD1-restricted NKT cells represent a little-understood but nonetheless important component of the immune system; its highly conserved, semi-invariant TCR affords greater possibilities for designing immunotherapeutic interventions than is possible with the polymorphic TCRs of conventional T lymphocytes. Understanding its binding conformation is an important guide to developing immunotherapies that might turn up its immunostimulatory activity in cancer and infection or turn down its activity in allergy and chronic inflammatory conditions. — *Carol Hart*

See: Natalie A. Borg[1], Kwok S. Wun[1], Lars Kjer-Nielsen[2], Matthew C.J. Wilce[1], Daniel G. Pellicci[2], Ruide Koh[1], Gurdyal S. Besra[3], Mandvi Bharadwaj[2], Dale I. Godfrey[2], James McCluskey[2], and Jamie Rossjohn[1]*, "CD1d-Lipid-Antigen Recognition by the Semi-Invariant NKT T-Cell Receptor," Nature **448**, 44 (5 July 2007).
DOI: 10.1038/nature05907
Author affiliations: [1]The Protein Crystallography Unit, ARC Centre of Excellence in Structural and Functional Microbial Genomics, Department of Biochemistry and Molecular Biology, School of Biomedical Sciences, Monash University; [2]Department of Microbiology & Immunology, University of Melbourne; [3]School of Biosciences, University of Birmingham
Correspondence: *jamie.rossjohn@med.monash.edu.au

The Australian Research Council (ARC), the National Health and Medical Research Council of Australia (NHMRC), the Cancer Council of Victoria, and a Monash Early Career Research grant (N.A.B.) supported this research. D.G.P. and D.I.G. receive support from an RO1 grant from the National Institutes of Health and the Association of International Cancer Research. G.S.B. acknowledges support in the form of a Personal Research Chair from J. Bardrick, as a former Lister Institute-Jenner Research Fellow, the Medical Research Council (UK) and the Wellcome Trust. N.A.B. is supported by an NHMRC Peter Doherty Fellowship, D.I.G. by an NHMRC Principal Research Fellowship, and M.C.J.W. by an NHMRC Senior Research Fellowship. J.R. is supported by an ARC Federation Fellowship. The Australian Synchrotron Research Program funded the travel to the APS. Use of the Advanced Photon Source was supported by the U.S. Department of Energy, Office of Science, Office of Basic Energy Sciences, under Contract No. DE-AC02-06CH11357.

17-ID-B • IMCA-CAT • Life science • Macromolecular crystallography, anomalous diffraction (MAD/SAD) • 3.3-cm Undulator A • Accepting general users

How a Cell Engulfs Particles

All living organisms consist of cells—sometimes one, but usually millions of them—each encased in a cell membrane. The cell membrane, in addition to simply enclosing the contents of the cell, is actually a dynamic, functional organelle that empowers the cell to carry out various functions. The cell membrane, for example, enables the movement, or motility, of the cell. The membrane also participates in a process called cytokinesis, whereby the cell splits in two during cell division. Another process is endocytosis, in which the cell membrane—in a manner reminiscent of the archaic video game Pac-Man—engulfs particles and draws them into the cell. One type of endocytosis is clathrin-mediated endocytosis (or CME), the process that all eukaryotic cells (from the Greek, freely translated as "truly nuclear": cells that are organized into complex structures by internal membranes and that have a membrane-bound nucleus) use to internalize nutrients, antigens, growth factors, pathogens, and recycling receptors. In CME, the cell can ingest relatively large particles by engulfing them with clathrin-coated pits that form in the membrane. Understanding how this process works is an important step toward a better understanding of intracellular transport, or how a particular protein is sent to the correct intracellular location.

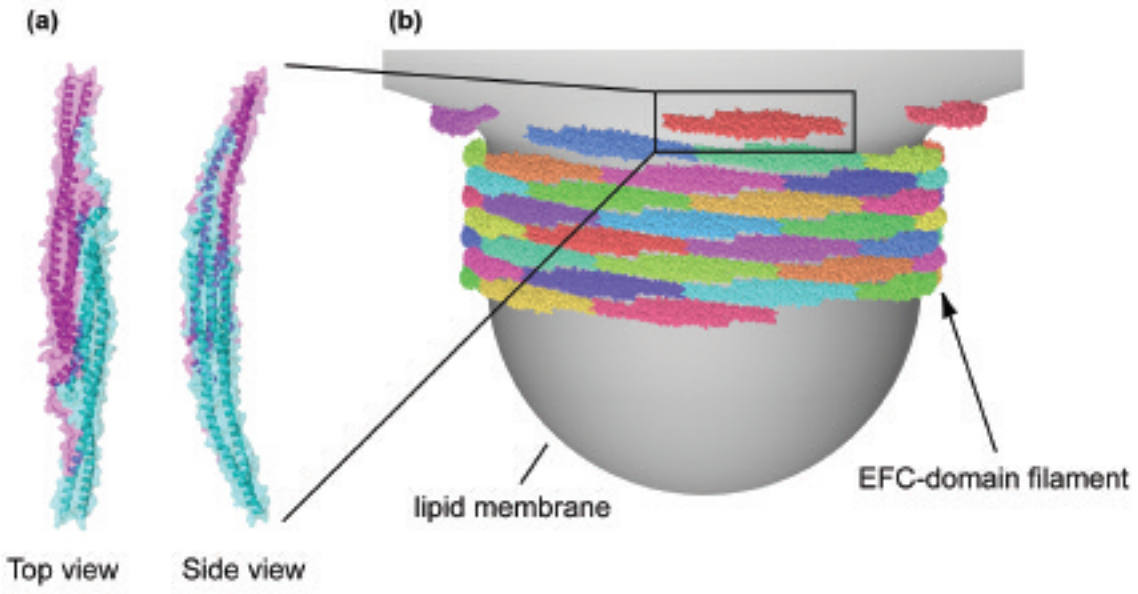

Fig. 1. (a) Ribbon and surface representations of the EFC-domain dimer with each monomer colored in cyan and magenta, respectively. (b) A model for membrane tubulation by the EFC domain. The EFC-domain dimers join end to end into a spiral filament, which wraps around the tubular membrane. EFC-domain dimers are highlighted in different colors.

To better understand the CME process, researchers from The Harima Institute; The University of Tokyo; PRESTO, JST; the National Institutes of Natural Sciences; and the University of Georgia focused on two proteins: FBP17 and CIP4. Specifically, the researchers resolved the structure of an area common to both proteins, called EFC. To do so, they enlisted the help of the SER-CAT 22-ID-D beamline at the APS. They also collected a high-resolution data set at the RIKEN Structural Genomics Beamline I (BL26B1) at SPring-8.

During endocytosis, the cell engulfs its particulate prey, and the membrane and its contents are drawn into the cell and then cut loose with a "scission" step once inside the cell. Several molecules are needed to assist with clathrin-mediated endocytosis, including a family of proteins referred to as the PCH proteins, which include FBP17 and CIP4. The PCH proteins allow the formation of a tubular shape, or tubulation, of the membrane, which sets off the process of endocytosis. The PCH proteins FBP17 and CIP4 both include an area called EFC, which has remained unchanged throughout evolution, highlighting the importance of its function in the long-term survival of the cell.

The researchers solved the structure of the EFC domain and were able to piece together a novel explanation for the way in which the EFC domain on FBP17 and CIP4 contributes to endocytosis: the EFC domain appeared to act as a point of contact between two FBP17 molecules, allowing them to pair together and form dimers. The same was true for CIP4 proteins. These protein dimers then assembled together to form strands or filaments by interacting end-to-end, a process that the researchers theorized actually drives the process of endocytosis. The spiral-like filaments appeared to wrap around the tubular membrane (Fig. 1). Thus, the filament formation allowed two key steps of endocytosis to take place—membrane tubulation and invagination, the formation of cavities that engulf particles.

Additional evidence for the role of the EFC domain in endocytosis was found when the researchers purposely disrupted filament formation and observed that neither tubulation nor invagination of the membrane took place. They also reported for the first time that FBP17 was present inside the clathrin-coated pits and may be involved late in the endocytosis process in the invagination and scission steps.

— Emma Hitt

See: Atsushi Shimada[1], Hideaki Niwa[1], Kazuya Tsujita[2,11], Shiro Suetsugu[2,3,4], Koji Nitta,[5] Kyoko Hanawa-Suetsugu[6], Ryogo Akasaka[6], Yuri Nishino[1], Mitsutoshi Toyama[6], Lirong Chen[7], Zhi-Jie Liu[7], Bi-Cheng Wang[7], Masaki Yamamoto[1], Takaho Terada[6], Atsuo Miyazawa[1], Akiko Tanaka[6], Sumio Sugano[8], Mikako Shirouzu[6], Kuniaki Nagayama[5], Tadaomi Takenawa[2]*, and Shigeyuki Yokoyama[1,6,9]**, "Curved EFC/F-BAR-Domain Dimers Are Joined End to End into a Filament for Membrane Invagination in Endocytosis," Cell **129**, 761 (May 18, 2007). DOI: 10.1016/j.cell.2007.03.040

Author affiliations: [1]RIKEN SPring-8 Center, Harima Institute; [2]Department of Biochemistry, Institute of Medical Science, The University of Tokyo; [3]PRESTO, JST; [4]Institute of Molecular and Cellular Biosciences, The University of Tokyo; [5]Okazaki Institute for Integrative Bioscience, National Institutes of Natural Sciences; [6]RIKEN Genomic Sciences Center; [7]Department of Biochemistry and Molecular Biology, University of Georgia; [8]Department of Medical Genome Sciences, Graduate School of Frontier Sciences, The University of Tokyo; [9]Department of Biophysics and Biochemistry, Graduate School of Science, The University of Tokyo

Correspondence: *takenawa@med.kobe-u.ac.jp, **yokoyama@biochem.s.u-tokyo.ac.jp

This work was supported by the RIKEN Structural Genomics/Proteomics Initiative, the National Project on Protein Structural and Functional Analyses, Ministry of Education, Culture, Sports, Science and Technology of Japan. This work was also supported by grants-in-aid for Scientific Research on Priority Areas from the Ministry of Education, Culture, Sports, and Technology of Japan and from the Japan Science and Technology Corporation. Use of the Advanced Photon Source was supported by the U.S. Department of Energy, Office of Science, Office of Basic Energy Sciences, under Contract No. DE-AC02-06CH11357.

A typical eukaryotic animal cell. Illustration courtesy of Lynn J. Fancher, Biology Department, College of DuPage. Used with permission of College of DuPage, Glen Ellyn, Illinois

22-ID-D • SER-CAT • Life science • Macromolecular crystallography, multiwavelength anomalous dispersion • 3.3-cm Undulator A • Accepting general users

How Algae Manufacture a Poison Pill

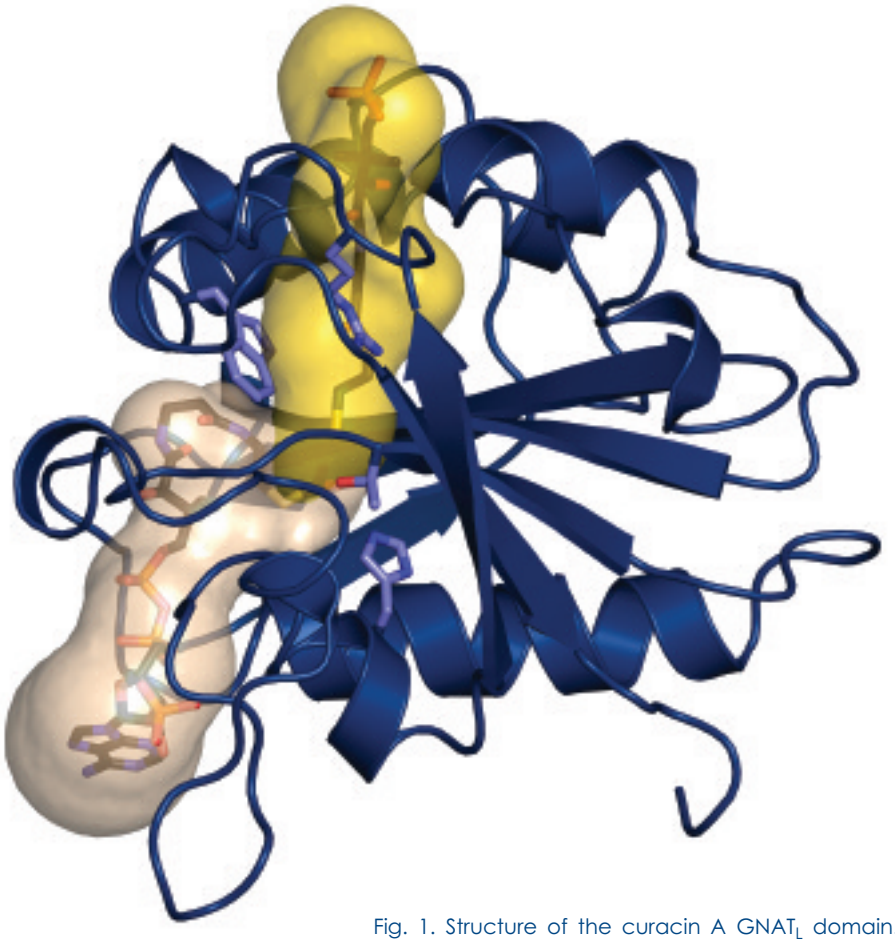

Fig. 1. Structure of the curacin A $GNAT_L$ domain. Computer modeling shows the configuration of carbon atoms (black) in acetyl-CoA (wheat) and the phosphopantetheine arm of ACPL (maize), along with important catalytic amino acids (blue).

New research reveals how blue-green algae from the Caribbean manufacture a curiously potent anticancer compound. A team of investigators using the GM/CA-CAT beamline 23-ID-D at the APS recently solved the three-dimensional crystal structure of one part of a sprawling cellular machine responsible for synthesizing curacin A, known for its ability to poison many common cancer cell types in the lab. The finding reveals a new and unexpected level of diversity in a well-known class of proteins.

First extracted from the marine cyanobacterium *Lyngbya majuscula* in the late 1990s, curacin A has proven too unstable and hard to process to be turned into a drug. But it opened new doors to biologists wishing to study the way that single-celled organisms assemble exotic compounds from common biochemical building blocks. The reactor that synthesizes curacin A is a conglomerate of different proteins, each of which catalyzes a different chemical reaction. Called a polyketide synthase (PKS), this protein-powered assembly line fuses together small building blocks one at a time into the larger curacin A molecule.

In the first step of the process, one of the protein modules attaches (or loads) the first building block to the larger PKS assembly line. The exact mechanism used by the loading module was unclear, however. To figure it out, a group of researchers from the University of Michigan at Ann Arbor; Purdue University; and the University of California, San Diego, crystallized the module and solved its structure using x-ray diffraction measurements collected on the GM/CA-CAT beamline.

The key piece of the loading module—a compact, dual-purpose enzyme called $GNAT_L$—has two openings on either side leading into tunnels that meet at a crooked junction in the middle of the enzyme (Fig. 1). The two tunnels seem to play distinct roles. The researchers found that a carrier molecule called malonyl-CoA was capable of threading into the tunnel facing away from the rest of the loading module, which latched onto the twisted malonyl segment. The first function of the $GNAT_L$ enzyme is to sever a molecule of carbon dioxide from malonyl-CoA, yielding acetyl-CoA. The researchers identified a pair of amino acids (protein building blocks) in the far tunnel near the site of the malonyl attachment that seemed likely to catalyze the removal of CO_2. When they chemically obstructed the amino acids, the enzyme produced far less carbon dioxide in the presence of malonyl-CoA, as predicted.

The enzyme's second task is to transfer the acetyl group to the rest of the PKS to be elongated into the larger curacin A chain. The researchers propose that after CO_2 removal, the second tunnel permits entry to a sort of protein dipstick (a "phosphopantetheine arm") projecting from a flexible part of the loading module called the acyl carrier protein (ACP_L) (Fig. 1). The tunnel catalyzes a reaction that swaps the acetyl group from CoA to the dipstick, allowing CoA to float off and the acetyl to be moved to an adjacent protein module.

For the researchers, the most unusual aspect of the process was $GNAT_L$'s ability to catalyze two very different reactions. The module is part of a large group of related GNAT enzymes, which play roles in everything from antibiotic resistance to hormone synthesis to gene activation, all through transfer of an acetyl group. The unprecedented dual-purpose enzyme that also removes CO_2 substantially broadens the chemical reaction inventory of this well-known protein superfamily. — *JR Minkel*

See: Liangcai Gu[1,2], Todd W. Geders[1,6], Bo Wang[4], William H. Gerwick[7], Kristina Håkansson[4], Janet L. Smith[1,3]**, and David H. Sherman[1,2,4,5]*, "GNAT-Like Strategy for Polyketide Chain Initiation," Science **318**, 970 (9 November 2007).
DOI: 10.1126/science.1148790
Author affiliations: [1]Life Sciences Institute, [2]Department of Medicinal Chemistry, [3]Department of Biological Chemistry, [4]Department of Chemistry, [5]Department of Microbiology and Immunology, University of Michigan; [6]Department of Biological Sciences, Purdue University; [7]Scripps Institution of Oceanography, University of California, San Diego
Correspondence: *davidhs@umich.edu,
**JanetSmith@umich.edu

This work was supported by NIH grants GM076477 (to D.H.S.) and DK42303 (to J.L.S.). L.G. is supported by an Eli Lilly graduate fellowship. The GM/CA Collaborative Access Team facility at the APS is supported by the NIH National Institute of General Medical Sciences and National Cancer Institute. Use of the Advanced Photon Source was supported by the U.S. Department of Energy, Office of Science, Office of Basic Energy Sciences, under Contract No. DE-AC02-06CH11357.

23-ID-D • GM/CA-CAT • Life science • Macromolecular crystallography, microdiffraction, anomalous diffraction (MAD/SAD), subatomic (<0.85 Å) resolution • 3.0-cm undulator • Accepting general users

The Fate of Vitamin B12

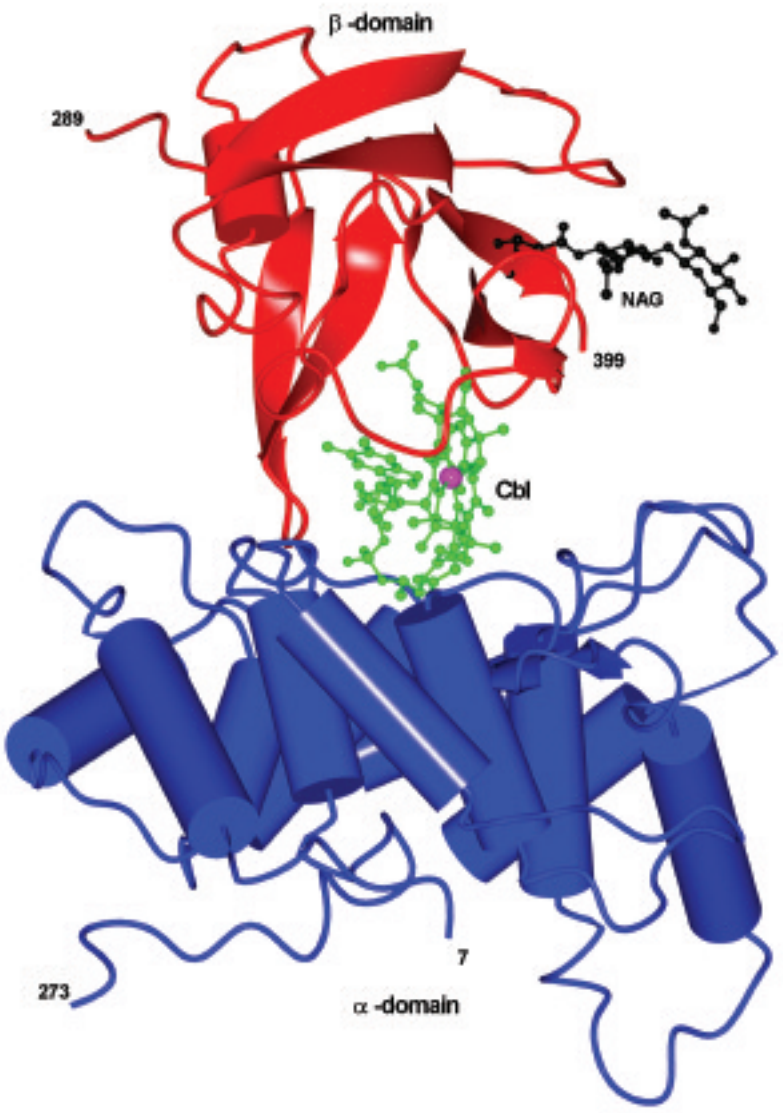

Fig. 1. Worms/tubes diagram of the IF-Cbl complex with α and β domains shown in blue and red, respectively. The cobalamin and sugar (N-acetyl-glucosamine; NAG) molecules are shown in ball and stick and in green and black colors, respectively. The cobalt atom is shown as a pink sphere.

Vitamin B12 (also known as cobalamin, or Cbl) is an essential vitamin for all mammals. But, unlike other water-soluble vitamins, cobalamin is stored in body tissues rather than being dispersed in urine. This can mask the effects of vitamin B12 deficiency in the diet for many years. Understanding the molecular processes that are involved in the delivery of Cbl to tissues in order to understand vitamin B12 deficiency clearly, and hopefully provide a target for new curative pharmaceuticals, was the goal of researchers using the NE-CAT 8-BM-B beamline at the APS. Their study provides important structural information that will facilitate those efforts.

Cobalamin delivery from food to tissues involves three successive transport proteins and their cellular receptors. The process begins when the food enters the digestive tract, where cobalamin is bound by a glycoprotein called haptocorrin (HC). After proteolysis of HC-Cbl complex in the small intestine, cobalamin is picked up by another glycoprotein called intrinsic factor (IF) that mediates the translocation of cobalamin into cells lining the ileum, the final section of the small intestine. Once IF has released cobalamin inside these cells, it is picked up by a protein called transcobalamin II (TC) that manages the final delivery into the circulation. The researchers using the NE-CAT facility at the APS determined the structure of the intrinsic factor-cobalamin complex at 2.6-Å resolution. The work reveals detailed information about the cobalamin binding site in IF. The identification of several important water molecules indicates their roles in Cbl binding, as well as the receptor binding site interactions at the N-terminal end of the protein. Comparison of the IF structure to that of TC reveals significant differences between them, though they perform a similar function. Determination of the IF structure enabled the team to investigate why rat IF and human IF are not interchangeable despite similarity at the amino acid sequence level. Recently, IF has generated interest as a possible drug discovery target that would allow uptake of small molecules linked either to Cbl or to a small peptide that would bind to the IF receptor.

The three-dimensional structure of IF is organized into two domains, an α-domain that is arranged as an $\alpha6/\alpha6$ helical barrel, and a β-domain that is made up of mostly β-sheet structures. The cobalamin binding site lies between these two domains (Fig. 1). The crystal structure also reveals a major sugar binding site at Asparagine 395, which can accommodate at least two sugar molecules that may be important for IF function (Fig. 1).

Comparison of the overall structure of IF to the structure of TC revealed differences in the length and orientation of various helices in the α-domain. Another important difference is that the β-side of the corrin ring of IF is empty even without any ordered water molecules with respect to TC. In IF the binding site and channel formation between the α and β domains are dominated by negatively charged residues that may play a role in the binding of Cbl at low pH. In addition, the binding site for cobalamin in IF is broad and open on both sides compared to that for TC; this may have important implications for binding and dissociation of the cobalamin to these two transport proteins.

This study also investigated the observation that rat IF cannot substitute for human IF in binding to its cellular receptor, though they share 80% sequence identity. The predicted receptor binding site of 37 amino acids varies at only six of these locations between the two proteins. In this study, using a homology model, substitution of these six amino acids from the rat sequence into the human IF did not change the predicted structure of the binding region at all but did change the charged nature of the site. This change in charge environment may interfere with proper binding of the rat IF to the human IF receptor and thus inhibit its ability to leave the digestive tract with its cargo. — *Sandy Field*

See: F.S. Mathews[1], M.M. Gordon[2], Z. Chen[1], K.R. Rajashankar[3], S.E. Ealick[3,4], D.H. Alpers[2], and N. Sukumar[3]*, "Crystal structure of human intrinsic factor: Cobalamin complex at 2.6-Å resolution," Proc. Natl. Acad. Sci. USA **104**(44) 17311 (October 30, 2007). DOI: 10.1073pnas.0703228104

Author affiliations: [1]Department of Biochemistry and Molecular Biophysics and [2]Division of Gastroenterology, Washington University School of Medicine; [3]Northeastern Collaborative Access Team, Argonne National Laboratory; [4]Department of Chemistry and Chemical Biology, Cornell University

Correspondence: *sukumar@aps.anl.gov

This work is supported by the NE-CAT facility at the Advanced Photon Source (Award RR-15301) from the National Center for Research Resources, National Institutes of Health; and Grants P01 DK-33487 (to D.H.A.) and GM20530 (to F.S.M.) from the National Institutes of Health. Use of the Advanced Photon Source was supported by the U.S. Department of Energy, Office of Science, Office of Basic Energy Sciences, under Contract No. DE-AC02-06CH11357.

Mechanisms of a Molecular Trash Disposal

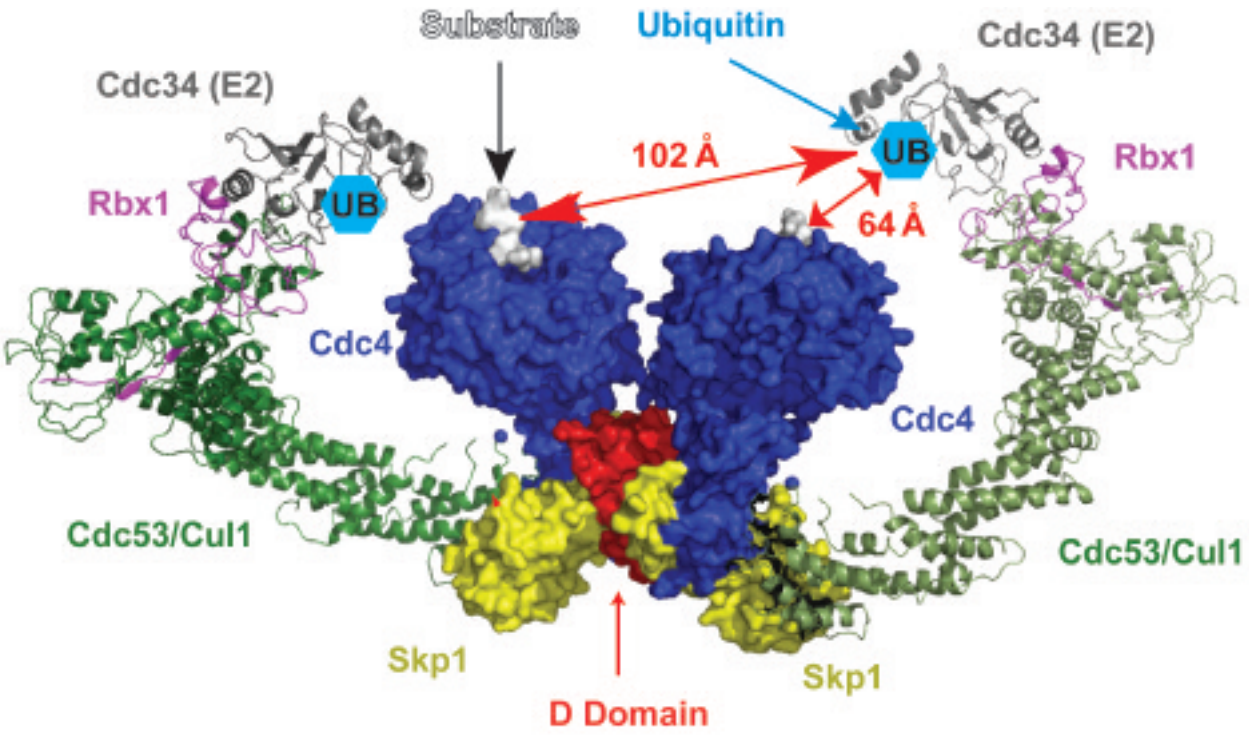

Fig. 1. X-ray and SAXS data reveal that the dimerization domain of Cdc4 (red) confers a coplanar configuration of the E3 ligase, which could accommodate a variety of substrates to E2 catalytic geometries. Distances from the substrate binding sites (white) to the catalytic site on the E2 enzyme (**UB** (ubiquitin) in light blue) are 64 Å and 102 Å for the intraprotomer and interprotomer distances, respectively. Proteins used in this study are displayed as space filling models: Cdc4 (dark blue), D-domain of Cdc4 (red), and Skp1 (yellow). Ribbon representations are models derived from previous crystal structures determined by Zheng et al. (Nature **416**, 703 (2002): Cdc53/Cul1 (green), Rbx1 (magenta), and Cdc34 (an E2 enzyme, gray).

14-BM-C • BioCARS • Life science • Macromolecular crystallography, fiber diffraction, biohazards at the BSL2/3 level, subatomic (<0.85 Å) resolution • Bending magnet • Accepting general users

18-ID-D • Bio-CAT • Life science • Macromolecular crystallography, microdiffraction, anomalous diffraction (MAD/SAD), subatomic (<0.85 Å) resolution • 3.3-cm Undulator A • Accepting general users

19-BM-D • SBC-CAT • Life science • Anomalous diffraction (MAD/SAD), ultra-low-temperature (15K) • Bending magnet • Accepting general users

The ubiquitin proteasome system (UPS) is part of the waste management system of a cell. Proteins that are destined to have limited life spans in the cell are identified and sorted for destruction. This is accomplished by labeling the proteins with the molecule ubiquitin, which is present in all eukaryotes. Once tagged, the proteins are degraded by a complex machine known as the proteasome. The UPS is not just a molecular wood chipper; it performs its function with specificity that is provided by the class of ubiquitination enzymes called E3 ligases. The E3 ligases identify proteins to be degraded through domains called F-boxes, but the mechanism of enzymatic transfer of ubiquitin to the doomed protein is still not completely understood and may be facilitated by the dimerization of another domain, known as the D-domain. In studies carried out at the NE-CAT 8-BM-B, BioCars 14-BM-C, BioCAT 18-ID-D, and SBC-CAT 19-BM-D beamlines, all at the APS, researchers solved the structures of two of these D-domains: one from the yeast protein Cdc4 (2.5 Å) and another from human β-TrCP (2.4 Å). This work provides new insights into the mechanism of the E3 ligases by revealing that D-domain dimerization plays a role in positioning different substrates for ubiquitination.

Using a combination of x-ray crystallography, mutational analysis, and small-angle x-ray scattering (SAXS) measurements, the researchers from the Samuel Lunenfeld Research Institute, the Cellgene Corporation, the University of Western Ontario, and the University of Toronto were able to reveal important new information regarding the role of the D-domain in the E3 ligase. Solution of the structures of the Cdc4 (Fig. 1) and β-TrCP D-domains reveals a common fold. Each fold is composed of three α helices that associate in a right-handed superhelical manner to form a parallel dimer. Of interest to the function of these proteins is that the sequences of the D-domains for Cdc4 and β-TrCP share only two conserved residues among the 16 amino acids involved in the dimerization interface. However, in both structures the dimerization interface is hydrophobic in nature, with variability between the two proteins imparting specificity of binding between different D-domains.

In order to learn more about how D-domain dimerization affects E3 ligase functions such as substrate recognition and ubiquitin conjugation, the team performed mutational analyses on the Cdc4 molecule. They found that dimerization of the D-domain is essential for the function of the full-length Cdc4 protein and showed that two residues were critical for dimer formation. However, although Cdc4 proteins that contained mutated D-domains did not dimerize, they were still able to bind substrates. Analysis of the catalytic activity of the ubiquitination reaction, however, revealed that the catalytic attachment of ubiquitin was impaired in these mutants. Therefore, it appears that dimerization of Cdc4 mediated through the D-domain is important for catalytic efficiency but not for substrate recognition.

SAXS analysis provided further insight into the importance of D-domain dimerization and its involvement in the catalytic efficiency of the ubiquitination reaction. Catalytic attachment of multiple ubiquitin molecules to lysine residues in a protein that may be spaced at different distances along the protein presents a situation that would be facilitated by an accommodating catalytic site. SAXS analysis of D-domain plus F-box domain constructs revealed that, although the distance between these domains is quite constrained, the configuration created by dimerization brings the substrate binding domain of the F-box into coplanar contact with the E2 catalytic enzyme. This allows for a wide variety of geometric configurations to fit within the catalytic domain, increasing catalytic efficiency. Together, this analysis of D-domain dimerization suggests that the flexibility of the system comes from dimerization imposed by the D-domain as shown in the crystal structure and the coplanar configuration created by dimerization that allows substrates of varying sizes and configurations to be available for polyubiquitination and subsequent disposal by the proteasome.

— Sandy Field

See: Xiaojing Tang[1], Stephen Orlicky[1], Zhenyuan Lin[1], Andrew Willems[1], Dante Neculai[1], Derek Ceccarelli[1], Frank Mercurio[2], Brian H. Shilton[3], Frank Sicheri[1,4]*, and Mike Tyers[1,4]**, "Suprafacial Orientation of the SCF^{Cdc4} Dimer Accommodates Multiple Geometries for Substrate Ubiquitination," Cell **129**, 1165 (June 15, 2007).
DOI 10.1016/j.cell.2007.04.042

Author affiliations: [1]Centre for Systems Biology, Samuel Lunenfeld Research Institute; [2]Cellgene Corporation; [3]Department of Biochemistry, University of Western Ontario; [4]Department of Molecular and Medical Genetics, University of Toronto

Correspondence: *sicheri@mshri.on.ca, **tyers@mshri.on.ca

This work was supported by grants to B.H.S., F.S., and M.T. from the Canadian Institutes of Health Research, the National Cancer Institute of Canada (NCIC), and the Natural Sciences and Engineering Research Council. Bio-CAT is National Institutes of Health-supported Research Center RR-08630. Use of the Advanced Photon Source was supported by the U.S. Department of Energy, Office of Science, Office of Basic Energy Sciences, under Contract No. DE-AC02-06CH11357.

Solution of the First Death Domain Complex Structure

Death is an important part of life for all organisms. This also turns out to be true for cells. For example, programmed cell death of particular cells in the embryo during development allows for the proper formation of body organs and structures. Cell death is also an important feature of the immune system, where cells that recognize autoimmune antigens or become infected with a virus are directed to self-destruct. One important biological function that involves programmed cell death is the cellular response to DNA damage. When DNA is damaged by harmful environmental factors, the cell can detect this and activate death domain (DD) proteins to mediate cellular destruction to prevent spread of the damage. In a recent study performed at the NE-CAT 24-ID-C beamline at the APS, researchers elucidated the crystal structure of the core of a particular DD complex. This new information about the complex could serve as a model for a common assembly mechanism of the DD protein superfamily, deepening our understanding of the molecular details of programmed cell death.

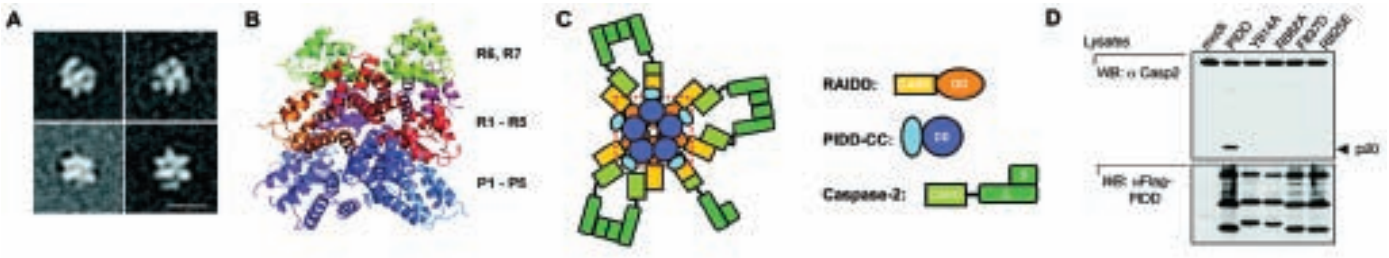

Fig. 1. The PIDDosome complex. A) Negative stain images of representative class averages, 50-170 particles per class. Scale bar = 10 nm. B) Side view of complex: 7 molecules of RAIDD DD (green and yellow, top; and red, purple, orange, magenta, pink, middle), 5 molecules of PIDD DD (different shades of blue, bottom). C) Model of PIDDosome activation of caspase-2. The death domain complex in the PIDDosome is in the red-dotted box; caspase-2 molecules are represented in proximity-induced dimer form. D) Mutational analysis of PIDDosome activation of caspase-2. Mutation of the PIDD death domains abolishes caspase-2 activation. Activated caspase-2 (p20 arrow) is only seen with non-mutated form (PIDD, lane 2).

When a cell has sustained too much damage to its DNA to function properly, signalling proteins within the cell begin a cascade of reactions that tell that cell to self-destruct. Activation of an enzyme called caspase-2 by the death domain complex PIDDosome is essential to this process. In their experimentation at 24-ID-C at the APS and the X4A beamline of the National Synchrotron Light Source, researchers from Cornell University, the University of Lausanne, and the Harvard Medical School elucidated the crystal structure of the core of the PIDDosome complex at resolutions of 3.2 Å and 4.0 Å, respectively, using single-wavelength anomalous diffraction of a mercury derivative. Their findings suggest that the complex, which is made up of seven molecules of one type of death domain protein, RAIDD DD (RIP-associated ICH-1 homologous protein with a death domain), and five molecules of another, PIDD DD (p53-induced protein with a death domain) may be a prototype for other complexes containing different stoichiometric combinations of DD proteins.

Orchestration of cellular signals involving activation of various enzymes involved in programmed cell death is

thought to occur through the creation of intracellular complexes that recruit and bind factors to bring them into proximity with each other to carry out their functions. A large superfamily of proteins, called death domain (DD) proteins, is critical to the formation of these complexes. Certain amino acid sequences have been identified that mediate the interactions of these proteins. They define subfamilies known as the DD subfamily, the death effector domain (DED) subfamily, the caspase recruitment domain (CARD) subfamily, and the pyrin domain (PYD) subfamily.

The structure of the PIDDosome core complex (Fig. 1) involves interactions between the DD domains of seven RAIDD and five PIDD molecules. This creates seven activation sites for the caspase-2 molecule, which binds to the CARD domain on the RAIDD protein. The recruited caspases are thought to be activated by their proximity to each other, and the PIDDosome complex brings them into the right orientation for this activation. RAIDD and PIDD also contain additional amino acid domains that can recruit other mediators of this process. An important finding of this work was that the DD domains involved in the formation of the complex are all required for proper caspase-2 activation. Mutations that disrupted any of the RAIDD DD and PIDD DD interactions also disrupted caspase-2 activation. Mapping of the interactions between the DD domains in the complex showed that although the structure was asymmetric, all of the DD domains were in similar biochemical environments, and their interactions could be grouped into three different types.

The authors hypothesize that the three DD interaction types may be sufficient to describe the interactions of all of the DD subfamily members and can account for the many different stoichiometries of similar complexes that have been observed in various organisms and biological systems.

— *Sandy Field*

See: Hyun Ho Park[1], Emmanuelle Logette[2], Stefan Raunser[3], Solange Cuenin[2], Thomas Walz[3], Jurg Tschopp[2], and Hao Wu[1]*, "Death Domain Assembly Mechanism Revealed by Crystal Structure of the Oligomeric PIDDosome Core Complex," Cell **128**, 533 (February 9, 2007).
DOI: 10.1016/j.cell.2007.01.019
Author affiliations: [1]Weill Medical College and Graduate School of Medical Sciences of Cornell University; [2]Department of Biochemistry, University of Lausanne; [3]Department of Cell Biology, Harvard Medical School
Correspondence: *haowu@med.cornell.edu

Use of the APS was supported by the U.S. Department of Energy, Office of Science, Office of Basic Energy Sciences, under Contract No. DE-AC02-06CH11357.

24-ID-C • NE-CAT • Life science • Macromolecular crystallography, anomalous diffraction (MAD/SAD) • 3.3-cm Undulator A • Accepting general users

Around the Experiment Hall

APS User Shares the "Israeli Nobel" for Chemistry

An Israeli structural biologist who is a frequent user of the Structural Biology Center beamlines at the APS (as well as beamlines at other light sources) shared the $100,000 Wolf Prize in Chemistry for discoveries leading to a unified picture of basic biological mechanisms.

Ada Yonath, of the Weizmann Institute of Science in Rehovot, Israel, and George Feher, of the University of California, San Diego, received the chemistry prize in the Israeli Knesset on May 13, 2007. The prizes were bestowed by the Wolf Foundation Council, which chooses what are considered to be Israel's equivalent to the Nobel Prize. Yonath is coauthor on 38 papers (to date) based on research carried out at the APS.

Yonath was awarded the prize for her work in understanding the production of proteins. "Her work paves the way to dealing with the crucial issue of drug activity and resistance mechanisms," the committee said. A member of the Israel Academy of Sciences and Humanities and the U.S. National Academy of Sciences, Yonath "was the first to discover the unified ribosomal mechanism leading to the production of proteins. She is the first and only person to determine, in an incredibly short period of time, the structures of over a dozen different complexes of antibiotics, to reveal the ribosome-antibiotics binding sites on the molecular level and to provide insight into antibiotics selectivity. Her work paves the way to dealing with the crucial issue of drug activity and resistance mechanisms, thus touching on a central problem in medicine," the international jury stated.

Ada Yonath

How a Powerful Molecular Motor Assembles Viruses

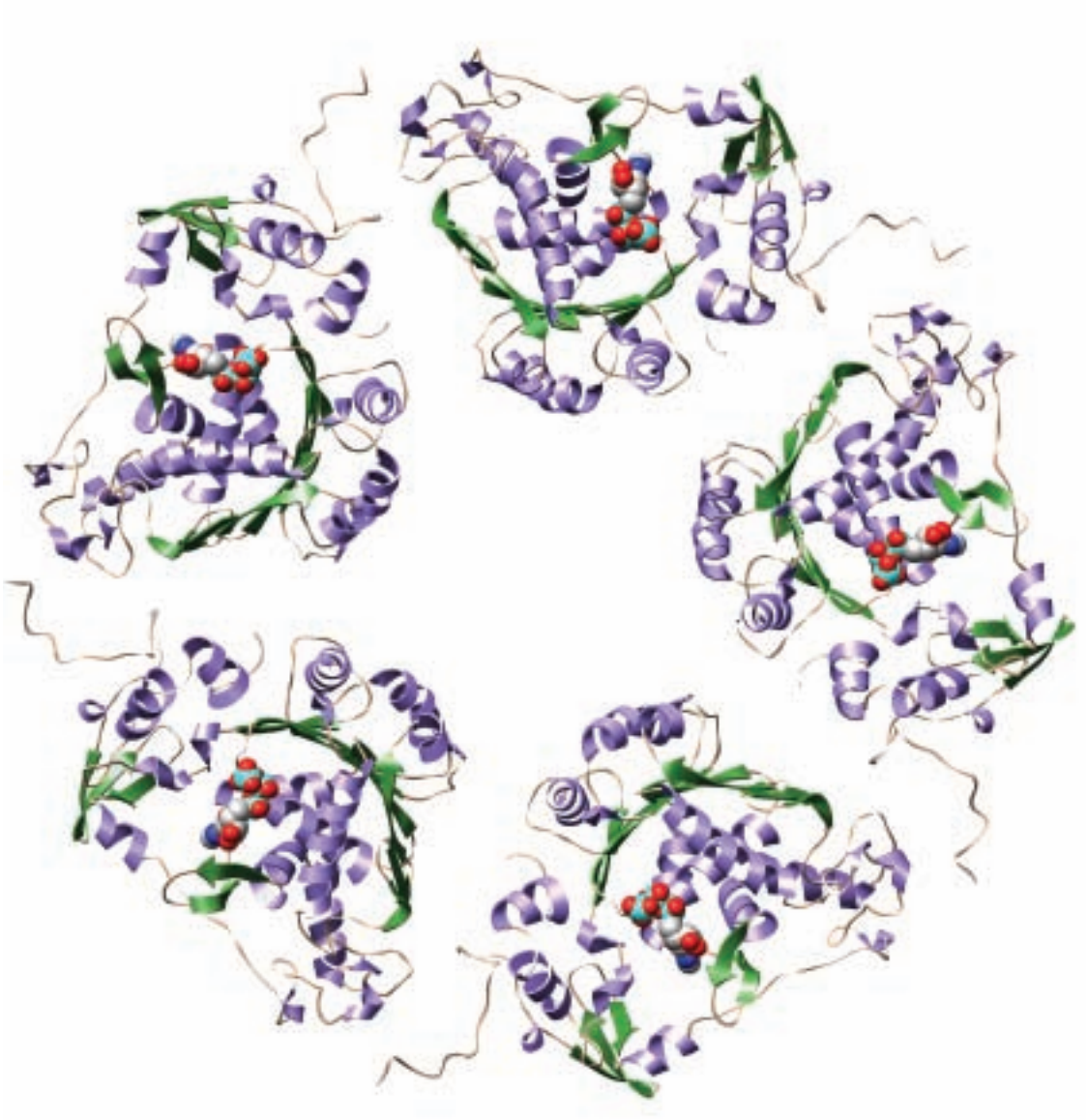

Fig. 1. The pentameric distribution of the gp17 ATPase in the T4 phage DNA packaging motor. The N-terminal ATPase domain of gp17 is shown distributed around a central hole through which the genomic DNA to phage T4 passes on its way into the phage capsid. The structure is shown as a ribbon presentation. The central six-stranded beta-sheet is in green, and the surrounding helices are in blue. The bound ATP molecule in the active center is shown as space-filling atoms with oxygen in red. This arrangement has in part been confirmed by recent three-dimensional electron microscopy studies that were not available at the time of the publication.

The T4 bacteriophage is a virus that targets *Escherichia coli* bacteria. T4 is also the laboratory rat of molecular biology, serving as a model system for studying gene transcription and protein synthesis. Importantly, some viruses infecting higher organisms (such as the herpes simplex virus in humans) are known to use a comparable nucleic acid packaging mechanism that has not yet been detailed. Understanding the structures of these highly efficient molecular motors may ultimately lead to applications in both antiviral drug design and nanotechnology. Now, the structure of the molecular motor that drives genome packaging in replicating T4 bacteriophages has been determined by a team of researchers using the BioCARS 14-BM-C and GM/CA-CAT 23-ID-B beamlines at the APS.

T4 is a large bacteriophage with an elongated icosahedral head, or capsid, enclosing its genes (coded as double-stranded DNA) and a helical contractile tail that attaches to the bacterial cell membrane using six leg-like tail fibers, then punches a hole in it. When the T4 phage injects its DNA into a host cell, it immediately hijacks the bacterial gene and protein synthesis machinery. In less than a half hour, the bacterial cell produces hundreds of copies of the viral genome, concatenated into a continuous chain of nucleotide pairs. Following the instructions of the viral genome, the enslaved cell also synthesizes the structural proteins that form the capsid and tail. The T4 genome is relatively large, with roughly 171,000 nucleotide base pairs. How that long, tangled skein of DNA gets properly trimmed and packaged into the empty capsids has long intrigued researchers.

Three proteins are involved in packing the viral DNA into the newly synthesized capsids: gene product (gp) 20, a 12-sided portal protein that connects to the empty capsid and holds the free end of the DNA molecule in place as packaging begins; and two proteins (gp16 and gp17) that form a terminase complex to power the DNA packaging via hydrolysis of adenosine triphosphate (ATP). Previous studies had established that the smaller protein, gp16, had no independent enzymatic activity but rather served to boost the efficiency of gp17. The focus of the research at the APS was, therefore, on visualizing the structure of gp17.

The wild-type protein resisted crystallization; however, the researchers, from Purdue University and The Catholic University of America, were able to crystallize a mutant variant. The structure of the ATP-binding and hydrolyzing N-domain (the ATPase motor) was mapped to a resolution of 1.8 Å, and the other structures in the protein were determined by molecular replacement. The ATPase domain has two spatially separated subdomains: one has a nucleotide-binding fold composed of six adjacent, parallel β strands (where the ATPase activity presumably resides); the other, smaller subdomain appears to be part of the nuclease component that cuts the concatenated DNA molecule when genome packaging is complete.

The researchers found that the structure of the ATPase subdomain is comparable to that of other ATPase motors in a range of organisms and tissues, from bacteria to bovine heart muscle mitochondria. It most closely resembles monomeric helicases, a class of motor proteins capable of binding to and moving along DNA strands. This similarity suggests the terminase complex pushes the DNA forward with an inchworm mechanism, in which two nucleotide binding folds alternately bind and release the DNA while ATP hydrolysis works a molecular hinge that pushes the DNA forward into the capsid. The number of gp17 proteins participating in the mechanism is unknown, but gp17 presumably forms a ring around the DNA, which has ten base pairs in each complete turn of the helix. Given that hydrolysis of a single ATP molecule provides sufficient energy to translocate two base pairs, the researchers proposed that a ring consisting of five gp17 monomers would provide optimal efficiency (see Fig. 1). — *Carol Hart*

See: Siyang Sun[1], Kiran Kondabagil[2], Petra M. Gentz[1], Michael G. Rossmann[1]*, and Venigalla B. Rao[2]**, "The Structure of the ATPase that Powers DNA Packaging into Bacteriophage T4 Procapsids," Mol. Cell **25**, 943 (23 March 2007). DOI: 10.1 016/j.molcel.2007.02.013

Author affiliations: [1]Department of Biological Sciences, Purdue University; [2]Department of Biology, The Catholic University of America

Correspondence: *mr@purdue.edu, **rao@cua.edu

This work was supported by National Science Foundation grants to M.G.R. (MCB-443899) and V.B.R. (MCB-423528). Use of the APS was supported by the U.S. Department of Energy, Office of Science, Office of Basic Energy Sciences, under Contract No. DE-AC02-06CH11357.

14-BM-C • BioCARS • Life science • Macromolecular crystallography, fiber diffraction, biohazards at the BSL2/3 level, subatomic (<0.85 Å) resolution • Bending magnet • Accepting general users

23-ID-B • GM/CA-CAT • Life science • Macromolecular crystallography, microdiffraction, anomalous diffraction (MAD/SAD), subatomic (<0.85 Å) resolution • 3.3-cm Undulator A • Accepting general users

A Conserved Mechanism for Identifying Breaks in DNA

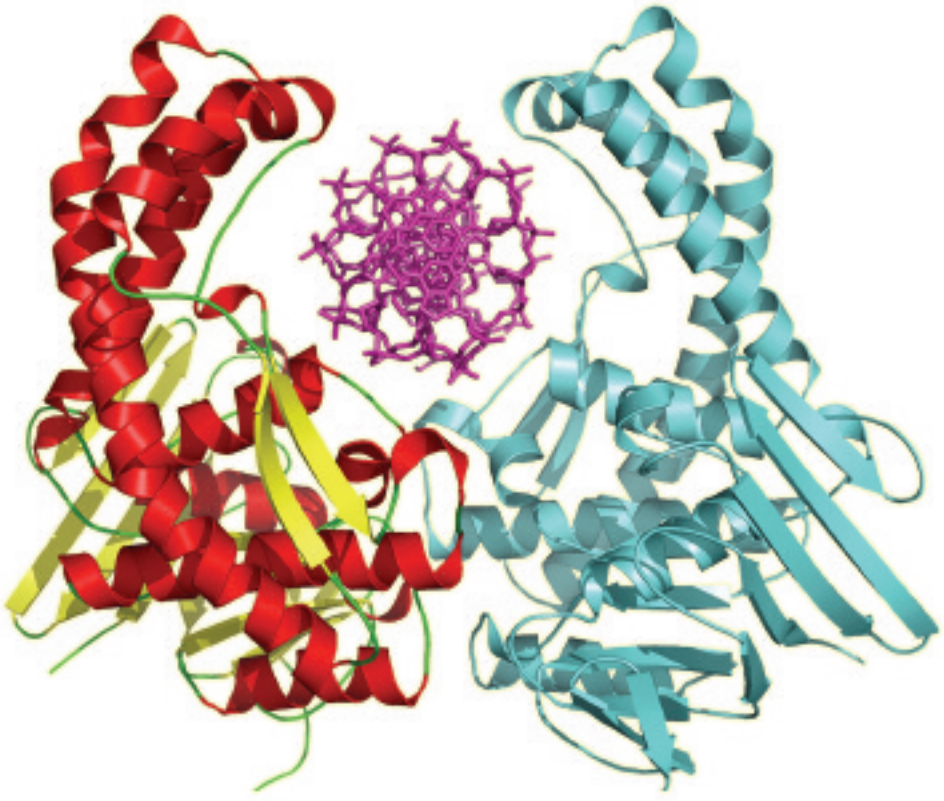

Fig. 1. Representation of the structure of the RecF dimer bound to DNA. Two RecF monomers are shown in the dimer predicted from the structural data and from modeling based on all known ABC ATPases known, including Rad50. One RecF monomer is shown in cyan only and one is shown with structural elements represented; α-helices are shown in red, β-strands in yellow, and loops are shown in green. DNA is shown in pink as it is predicted to lie in the "pocket" created by the RecF dimer (looking down the helix).

One of the most fundamental steps in the progression of any species is the replication of DNA that creates a copy of the genome for the new daughter cell. If DNA replication fails, the whole process can go awry. For this reason, the mechanisms that repair mistakes and breaks in DNA that are integral to the replication process have been evolutionarily conserved from bacteria to higher eukaryotic organisms. This conservation is reflected in genes that are conserved among species and can sometimes be seen in conserved protein structural elements. An elegant example of a conserved structure involved in DNA repair was solved by researchers using data collected at the SBC-CAT 19-ID-D beamline at the APS, who elucidated the structure of a bacterial DNA repair enzyme, RecF, at a resolution of 1.62 Å. The work revealed important structural conservation between the bacterial repair enzyme, RecF, and one from eukaryotic organisms called Rad50. Structural conservation of this type clearly indicates evolutionary preservation of RecF function. In addition, their study makes important findings regarding ATP-dependent dimerization of RecF and its mechanism of binding to DNA at the site of repair.

RecF belongs to a family of proteins that serve as recombination mediators (RMs), which are important for repair of single-stranded DNA (ssDNA) gaps. These proteins recognize the gap and recruit other repair enzymes to the site to fix the problem. Analysis of the amino acid sequence of RecF has revealed the presence of conserved motifs that identify a possible region responsible for DNA-dependent ATP binding. The first step in this study was to test the function of these regions. By using techniques of molecular biology to mutate these conserved amino acids, investigators from the St. Louis University School of Medicine and Portland State University were able to show that ATP binding is essential to RecF dimerization and DNA binding, providing important clues about the mechanism of action of this protein.

The next step was to solve the protein's three-dimensional structure, which revealed that the bacterial RecF protein contains two domains, both of which look like domains in the eukaryotic Rad50 protein. The first section of RecF is structurally similar to the ATPase domain of Rad50, and the second section is similar to the subdomain that is important for DNA recognition. This suggests that even though Rad50 binds double-stranded DNA (dsDNA) ends and RecF binds ssDNA breaks, they probably recognize and bind DNA in the same way.

Once they had solved the structure of RecF, the researchers were able to put their mutational analysis together with information from the structure to form a hypothesis about how DNA repair gets started. Here's how they think it might work. First, a DNA break occurs and is recognized by RecF. RecF bound to ATP can form a dimer with another ATP-bound RecF molecule, and the dimer binds to the DNA break (Fig. 1). This creates pockets for the two sides of the damaged DNA replication fork. Interestingly, the structure revealed that the inside of the RecF dimer pocket is positively charged, favoring binding of the negatively charged DNA molecule. The model predicts that one side of the dimer binds dsDNA, and the other side binds ssDNA. In Rad50, which recognizes blunt-ended dsDNA breaks, one side binds dsDNA, and the other side is free. Once the break is recognized, the RecF dimer recruits another protein, RecR, which binds RecF or DNA only when they are presented together. This suggests that RecF binding to the DNA break may change its conformation to create a binding site that can be recognized by RecR. In fact, it is predicted that four copies of RecR can bind to the RecF-DNA break complex to make what is called a tetrameric clamp. The resulting complex is a sort of molecular vice grip that holds the DNA break in place for enzymes to make the fix. — *Sandy Field*

See: Olga Koroleva[1], Nodar Makharashvili[1], Charmain T. Courcelle[2], Justin Courcelle[2], and Sergey Korolev[1]*, "Structural conservation of RecF and Rad50: implications for DNA recognition and RecF function," EMBO J. **26,** 867 (2007). DOI: 10.1038/sj.emboj.7601537

Author affiliations: [1]Edward A. Doisy Department of Biochemistry and Molecular Biology, Saint Louis University School of Medicine; [2]Department of Biology, Portland State University

Correspondence: *korolevs@slu.edu

These works were supported by the E.A. Doisy Trust Fund and SLU Medical School Start Up Fund and by NIH grant GM073837. J.C. and C.T.C. are supported by National Science Foundation Career Award MCB0551798. Use of the Argonne National Laboratory Structural Biology Center beamlines at the APS was supported by the US Department of Energy, Office of Biological and Environmental Research, under Contract No. W-31-109-ENG-38. Use of the APS was supported by the U.S. Department of Energy, Office of Science, Office of Basic Energy Sciences, under Contract No. DE-AC02-06CH11357.

19-ID-D • SBC-CAT • Life science • Anomalous diffraction (MAD/SAD), subatomic (<0.85 Å) resolution, ultra-low-temperature (15K) • 3.3-cm Undulator A • Accepting general users

Opening a Window of Vulnerability in HIV-1

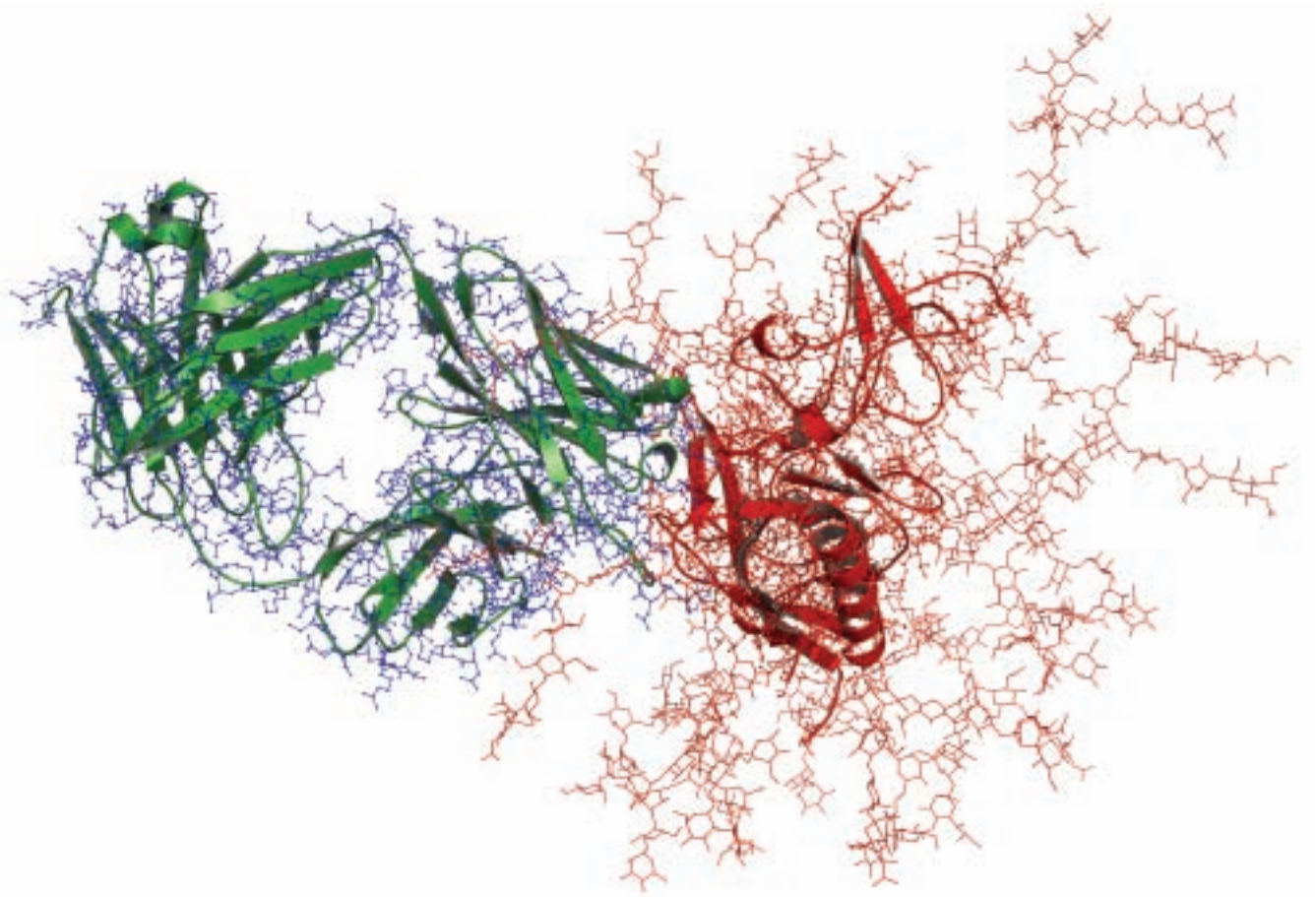

Fig. 1. Representation of the three-dimensional protein structure of the b12 neutralizing antibody in complex with gp120 from HIV-1. A ribbon diagram of the structure of b12 is shown in green with the amino acid side chains for b12 overlaid in blue. The gp120 structure is shown in red with amino acid side chains and glycans for gp120 overlaid, also in red.

HIV-1, the virus that causes the acquired immune deficiency syndrome, or AIDS, is a global health problem that has confounded vaccine researchers for many years. One of the things that makes HIV-1 so tricky is its remarkable ability to evade our immune system, in part by changing the three-dimensional appearance of its outer-envelope glycoprotein, gp120. This protein protrudes from the virus and binds to a host molecule called CD4 that makes it possible for the virus to gain entry into cells. This interaction is crucial to persistence of the infection and represents a good target for vaccine intervention. However, HIV-1 has eluded previous vaccination attempts because of its ability to mutate very quickly and change the way gp120 looks to the immune system, making it hard to track. Researchers used the SER-CAT 22-ID-D beamline at the APS to uncover new information that could represent a significant leap forward in HIV vaccine research.

In an attempt to identify a conserved feature of gp120 that might be used to generate a vaccine-stimulated immune response, the researchers from the National Institute of Allergy and Infectious Diseases, Scripps Research Institute, the Dana Farber Cancer Institute, and the National Cancer Institute used a clue from HIV-1-infected individuals who had shown some resistance to the virus. Scientists had found that some of these individuals were generating what were termed "broadly neutralizing" antibodies that presumably recognize an invariant part of the virus. One of these broadly neutralizing antibodies, called b12, appears to recognize an area of gp120 that is involved in the contact the virus makes with CD4. By using the 22-ID-D beamline, this research team achieved an important advance by solving the structure of the b12 antibody binding site to gp120 to a resolution of 2.3 Å. The structure reveals a vulnerable area where b12 can gain access to gp120 and prevent its interaction with host CD4 molecules.

The structure of the interaction between the neutralizing antibody, b12, and viral gp120 has been sought for some time, but the flexibility of the gp120 molecule made it difficult to capture the interaction in crystals of sufficient quality for this type of analysis. By using a trick to stabilize the interaction (trapping gp120 in the conformation it uses to bind CD4), the researchers were able to obtain a snapshot of the interaction (Fig. 1). The team credits APS high-brightness undulator x-ray beams for enabling this finding. The gp120-containing crystals were often quite small (needles with dimensions as small as 20 μM) and the cell constants were large (dimensions of up to 200 Å). Despite this, data were collected to at least 3-Å resolution for all of the 10 structures required to complete the analysis. Indeed, the analysis revealed important aspects of the interaction between b12 and gp120, showing that b12 binds gp120 in a region that is required for initial contact with CD4.

The implications of the work for vaccine research are significant. In general, vaccination is based on the principal of "teaching" or "priming" the immune system to recognize an invader by using a harmless form of the invader to generate an initial response. This gives the body a chance to identify the invader and generate both a memory of and a neutralizing response to it. When the body is challenged again with the real invader, it is ready with a full arsenal of memory cells to mount a full and rapid response. Previous attempts to use the whole gp120 protein as a vaccine have been foiled by the general variability of the molecule. The structural map of b12 binding to this conserved region of gp120 will allow vaccine researchers to design a structural analog of the vulnerable site to teach the immune system how to generate an effective neutralizing response. — *Sandy Field*

See: Tongqing Zhou[1], Ling Xu[1], Barna Dey[1], Ann J. Hessell[3], Donald Van Ryk[2], Shi-Hua Xiang[4], Xinzhen Yang[4], Mei-Yun Zhang[5], Michael B. Zwick[3], James Arthos[2], Dennis R. Burton[3], Dimiter S. Dimitrov[5], Joseph Sodroski[4], Richard Wyatt[1], Gary J. Nabel[1], and Peter D. Kwong[1]*, "Structural definition of a conserved neutralization epitope on HIV-1 gp120," Nature **445**, 732 (15 February 2007).
DOI: 10.1038/nature05580
Author affiliations: [1]Vaccine Research Center, and [2]Laboratory of Immunoregulation, National Institute of Allergy and Infectious Diseases, National Institutes of Health; [3]Departments of Immunology and Molecular Biology, Scripps Research Institute; [4]Department of Cancer Immunology and AIDS, Dana-Farber Cancer Institute, Harvard Medical School; [5]Center for Cancer Research, National Cancer Institute
Correspondence: *pdkwong@nih.gov

Support for this work was provided by the Intramural Research Program of the NIH, by the International AIDS Vaccine Initiative, by a grant from the Bill and Melinda Gates Foundation Grand Challenges in Global Heath Initiative, and by grants from the NIH. Use of the APS was supported by the U.S. Department of Energy, Office of Science, Office of Basic Energy Sciences, under Contract No. DE-AC02-06CH11357.

22-ID-D • SER-CAT • Life science • Macromolecular crystallography, multiwavelength anomalous dispersion • 3.3-cm Undulator A • Accepting general users

Exploring HIV Resistance

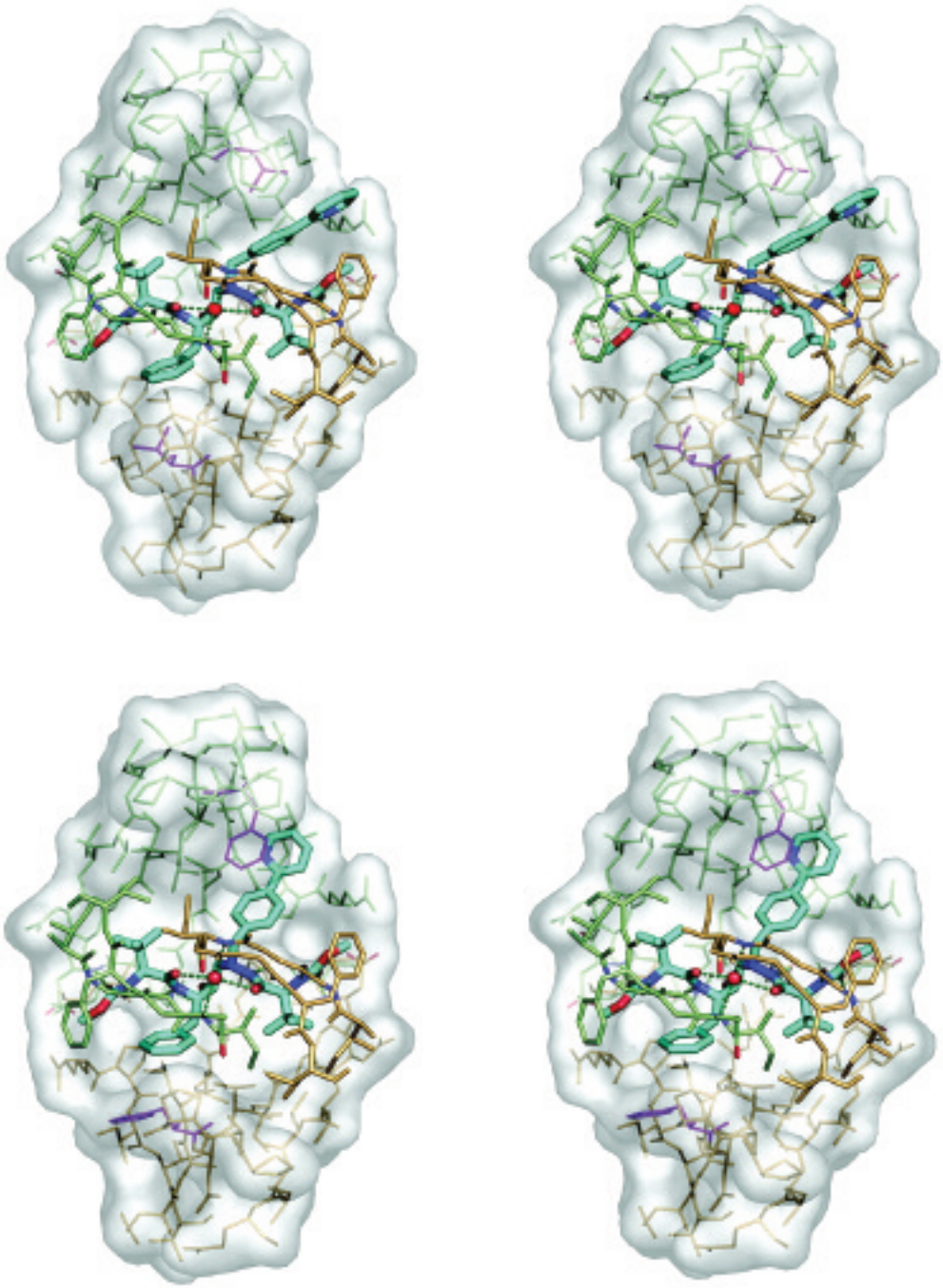

Fig. 1. Stereo illustration of the interactions between atazanavir and HIV-1 in the wild-type (top) and mutant (bottom) structures.

Since its appearance in the early 1980s, human immunodeficiency virus (HIV) infection and the often resulting acquired immunodeficiency syndrome (AIDS) have been responsible for the deaths of an estimated 25 million people. Fortunately, due to the discovery of powerful medicinal cocktails and heightened awareness, people can now live with AIDS for many years if the HIV virus is controlled. One enzyme essential for viral replication, HIV-1 protease, is the target of several drugs used to treat HIV, and these agents, the so-called HIV-1 protease inhibitors, were among the first treatments to prevent the progression of HIV to full-blown AIDS. When used in combination with other drugs, protease inhibitors extend the lives of many patients. Currently, eight protease inhibitors have been approved by the U.S. Food and Drug Administration for use in HIV-infected patients. One of the newest members of this class of drugs is called atazanavir, brand name Reyataz®, made by Bristol-Myers Squibb. Company researchers conducted experiments at the IMCA-CAT 17-ID-B beamline at the APS to find out more about how atazanavir interacts with mutant HIV-1 proteases at the atomic level. They were able to characterize the way in which atazanavir binds to HIV-1 protease with one common mutation, V82F, where the amino acid phenylalanine (F) is substituted for the usual amino acid valine (V) at residue 82. Their findings helped explain why this mutation is unlikely to result in atazanavir resistance by itself.

Despite their efficacy, all protease inhibitors must contend with the eventual emergence of HIV-1 strains that have some level of resistance to treatment. HIV-1 protease consists of amino acids, the building blocks of all proteins. Mutations occur when an amino acid is switched out for an incorrect amino acid. This can have the effect of decreasing how readily drug molecules can bind to, and thereby inhibit ,their target. Once present, a resistant strain can replicate without responding to treatment and place the patient at risk of increasing viral load.

The Bristol-Myers Squibb researchers used x-ray crystallography at the IMCA-CAT beamline to determine the structures of two HIV-1 proteases complexed with atazanavir (Fig. 1). One enzyme contained the customary sequence and was not resistant to protease inhibitors. The other enzyme was similar except it contained four mutations, one of which was V82F, that rendered it resistant to all approved HIV-1 protease inhibitors, atazanavir included.

They found that atazanavir could bind to both the non-resistant and resistant forms of the HIV-1 protease. However, in the cases of the V82F mutation, atazanavir was able to adopt an alternate binding mode. This observation is the likely explanation why the V82F substitution is not associated with clinical resistance to atazanavir unless several other mutations are also present. The analysis also showed atazanavir, which is nearly symmetrical in its chemical makeup, binds in two orientations.

In addition to providing a detailed view of how atazanavir binds to HIV-1 protease, these findings will also hopefully help in the development of future protease inhibitors and thereby offer further treatment options for AIDS patients who suffer from one of the most devastating epidemics to afflict humankind. — *Emma Hitt*

See: Herbert E. Klei[1]*, Kevin Kish[1], Pin-Fang M. Lin[5], Qi Guo[5,6], Jacques Friborg[5], Ronald E. Rose[5], Yaqun Zhang[2,3], Valentina Goldfarb[2], David R. Langley[4], Michael Wittekind[2,3], and Steven Sheriff[1], "X-ray Crystal Structures of Human Immunodeficiency Virus Type 1 Protease Mutants Complexed with Atazanavir," J. Virol. **81**, 9525 (September 2007). DOI: 10.1128/JVI.02503-05

Author affiliations: [1]Macromolecular Crystallography, [2]Macromolecular NMR, and [3]Gene Expression & Protein Biochemistry, Bristol-Myers Squibb Pharmaceutical Research Institute (Princeton, NJ); [4]Computer Assisted Drug Design and [5]Virology, Bristol-Myers Squibb Pharmaceutical Research Institute (Wallingford CT); and [6]Applied Genomics, Bristol-Myers Squibb Pharmaceutical Research Institute (Hopewell, NJ)

Correspondence: *herbert.klei@bms.com

IMCA is an association of pharmaceutical companies committed to the use of macromolecular crystallography in drug discovery and product development to which Bristol-Myers Squibb belongs. The Center for Synchrotron Radiation Research and Instrumentation at the Illinois Institute of Technology was contracted to construct and operate the beamlines, biochemistry laboratory, offices, and other resources within the facility. Use of the Advanced Photon Source was supported by the U.S. Department of Energy, Office of Science, Office of Basic Energy Sciences, under Contract No. DE-AC02-06CH11357.

17-ID-B • IMCA-CAT • Life science • Macromolecular crystallography, anomalous diffraction (MAD/SAD) • 3.3-cm Undulator A • Accepting general users

Architecture of a Vital Cellular Machine

Enzymes are essential molecules, working hard to catalyze and direct cellular reactions, and, incredibly, making it all look so easy and effortless. Yet the biochemical success of enzymes is usually dependent upon structure and timing that are anything but simple. The more we know about enzyme complexes, the more respect and awe we have for these wonder proteins. And this is especially true in the case of the newly discovered structure for a yeast enzyme, which, if awards could be given for awesome architecture in cells, would certainly take the grand prize. A research team from Yale University using SBC-CAT beamline 19-ID-D and NE-CAT beamline 24-ID-C at the APS and beamlines X25 at the National Synchrotron Light Source, A1 at the Cornell High Energy Synchrotron Source, and 8.2.1 and 8.2.2 at the Advanced Light Source, has discovered an important structure for a yeast enzyme involved in fatty acid synthesis. The research team's work constitutes immense progress in terms of our understanding of how fatty acid synthesis works and, when malfunctioning, can lead to disease.

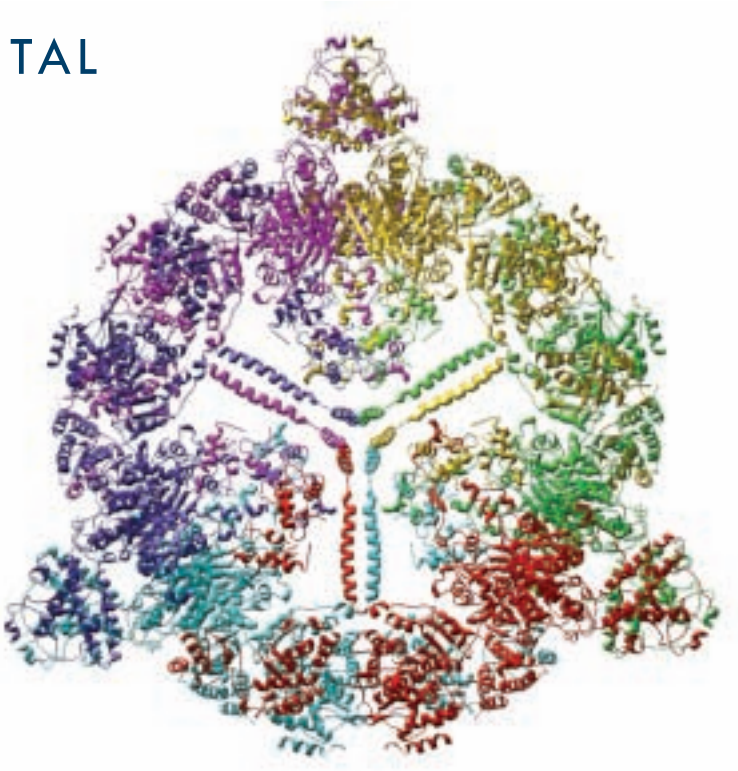

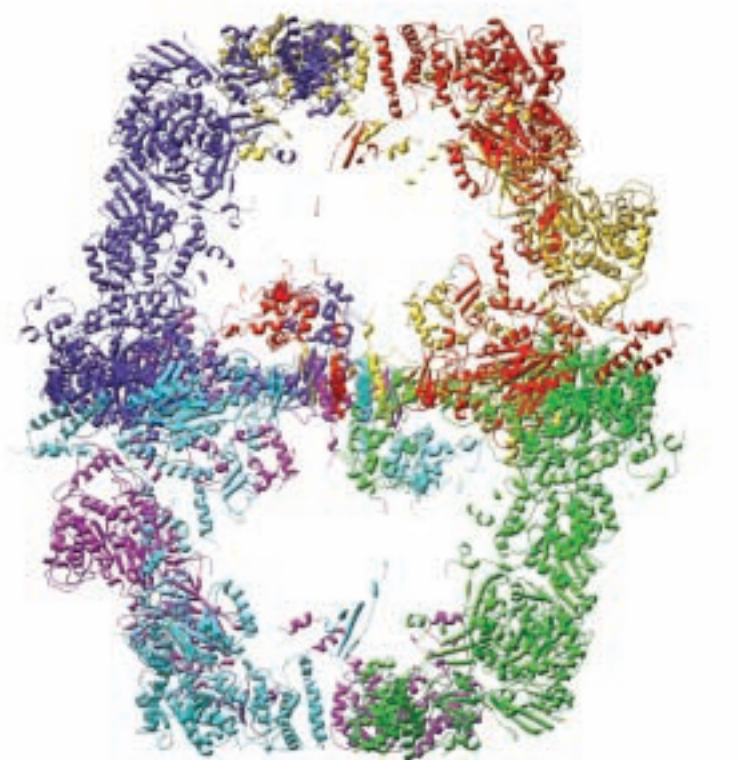

In yeast, in humans, and in most other living things, fatty acids are absolutely required for building cell membranes, for attaching to proteins to make sure that they function properly, and, in the case of saturated fatty acids, storing energy. If fatty acid synthesis works other than as it should, then many cellular functions are disrupted, possibly leading to cancer and obesity. By studying the enzyme responsible for making fatty acids in yeast, which is related to that in humans, the research team was able to glean extremely important information about the enzyme's structure and function, and it added to the wonders of the biochemical world by unveiling the extreme and breathtaking structural and functional complexity of this enzyme.

Serendipity played a role in providing the researchers with the opportunity to study the structure of the enzyme, known as yeast fatty acid synthase (FAS). While attempting to crystallize a different yeast (*Saccharomyces cerevisiae*) cellular component—a part of the protein production machinery called a ribosome—the team found that it had instead obtained FAS crystals. The researchers recognized that they had inadvertently been handed the chance to take a really close look at the structure of this extremely complicated enzyme. Previous research had revealed some structural features, but important links were still missing. So the group set to work and did not stop until it was able to characterize the entire enzyme structure and to model how FAS went about performing its all-important functions.

Fatty acid synthase is really a set of integrated multienzymes that starts from scratch to make 16-carbon and 18-carbon fatty acids, such as palmitic or stearic acid. There are eight functional domains, which catalyze all of the required reactions for fatty acid synthesis, including activation, priming, multiple cycles of elongation, and termination. Each of the eight domains is repeated six times for each enzyme complex, yielding an $\alpha_6\beta_6$ configuration and a total of 48 reaction sites (Fig. 1). The space within the enzyme complex is limited, so that the packaging of these reaction sites is a wonder of efficiency. And, FAS's fascinating nature became even more so when the research team discovered that a catalytic domain known as phosphopantetheinyl transferase (PPT), which is essential for activating fatty acid synthase, is actually located on the outside of the complex. The structure discovered by the research team revealed that once the complex is assembled, PPT is not able to reach the position required for activation. This observation led the team to conclude that activation of the FAS occurs before the final assembly of the complex, a finding that now explains previously inexplicable behavior for the FAS complex.

Certain aspects of the structure related to internal folding did appear to be unique to FAS and had not been previously discovered in other proteins. The research team continued to gather details that allowed it to elucidate exactly how the enzyme performs its remarkable task. The six reaction chambers produced by the six-fold repetition of subunits are isolated from each other. Within each chamber, six of the eight catalytic sites are in the wall and face an acyl carrier protein (ACP) that swings around to each of the six wall sites to deliver the intermediate molecules in the synthesis process. It is the ACP that needs to interact with the PPT, on the outside, to become active, and this occurs at some point before assembly of the complex is complete.

The beautiful architecture of an important enzyme—yeast FAS—and its important function are now known. Certain regions of the structure show promise for designing antibacterial and antifungal drugs. Future researchers concentrating on fatty acid synthesis and its malfunction will now be well armed with knowledge. — *Mona Mort*

< Fig. 1. Upper: Top view of the structural regions of the FAS particle displayed without the catalytic domains. Each subunit is a different color. Lower: Side view of the structural regions of the FAS particle displayed without the catalytic domains. Each subunit is a different color.

See: Ivan B. Lomakin[1], Yong Xiong[1]*, and Thomas A. Steitz[1,2,3]**, "The Crystal Structure of Yeast Fatty Acid Synthase, a Cellular Machine with Eight Active Sites Working Together," Cell **129**, 319 (April 20, 2007).
DOI: 10.1016/j.cell.2007.03.013
Author affiliations: [1]Department of Molecular Biophysics and Biochemistry, [2]Department of Chemistry, [3]Howard Hughes Medical Institute, Yale University
Correspondence: *yong.xiong@yale.edu,
**eatherton@csb.yale.edu

The x-ray- and neutron-scattering work was supported in part by the U.S. National Science Foundation with grant No. DMR-0453804 and by an award from the Research Corporation. The PLCCO single-crystal growth at the University of Tennessee is supported by the U.S. DOE BES under contract No. DE-FG02-05ER46202. ORNL is supported by the U.S. DOE grant No. DE-AC05-00OR22725 through UT/Battelle LLC. The part of the work done in Japan was supported by a Grant-in-Aid for Science provided by the Japan Society for the Promotion of Science. Use of the APS was supported by the U.S. Department of Energy, Office of Science, Office of Basic Energy Sciences, under Contract No. DE-AC02-06CH11357.

19-ID-D • SBC-CAT • Life science • Anomalous diffraction (MAD/SAD), subatomic (<0.85 Å) resolution, ultra-low-temperature (15K) • 3.3-cm Undulator A • Accepting general users

24-ID-C • NE-CAT • Life science • Macromolecular crystallography, anomalous diffraction (MAD/SAD) • 3.3-cm Undulator A • Accepting general users

Pushing the Pocket in Estrogen Receptors

Hormones are the cell's messengers—they are produced and outfitted for this role in one part of the body and sent on their way to target tissue. A hormone can arrive at the desired destination quickly and can have a profound impact on what happens next. Just how much of an impact the hormone actually has depends in part on how it is received in the target tissue, where elaborate receptor architecture regulates subsequent action. Receptors for steroid hormones, such as estrogen, have been well studied because of their potent effects, including links to cancer. Detailed knowledge of estrogen receptors (ERs) has been particularly important in designing drugs, such as tamoxifen and raloxifene, to fight breast and ovarian cancer. Until now, the steroid hormone receptors were thought to be somewhat rigid and inflexible when binding incoming messengers, thus limiting therapeutic strategies. But new research by scientists using two APS beamlines collected detailed and convincing data that show previously undetected structural flexibility and plasticity in the binding pocket of ERs. Drug designers will now have a much wider array of possibilities in choosing molecules to combat estrogen-regulated disease states, such as some cancers. The number of possible messengers has just gotten a lot bigger, making it ever more likely that the molecule chosen will get the right message through to the target tissue and in time to make a difference.

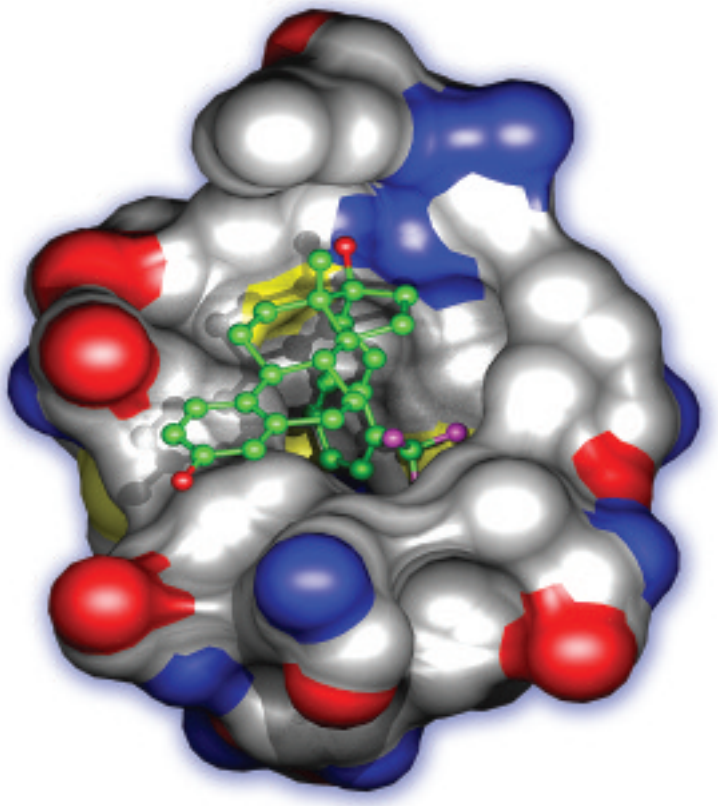

There are two types of estrogen receptors, ERα and ERβ, which are found in different tissues and have different biological roles. The researchers studied ERα, which operates in the nucleus and regulates the transcription of DNA, upon which a cascade of further reactions depends (Fig. 1). The ways in which ERα could bind incoming hormonal messengers had already been well characterized and served as the basis for design of existing ER drugs and therapeutics. The researchers in this study wondered whether the ER could be less rigid in binding molecules than what had been previously demonstrated. Are there other ways to regulate how this receptor behaves? The question was important not only to understanding the basic physiology of hormonal action but, perhaps even more critical, to gaining knowledge that could be used in designing drugs to fight disease.

The researchers, from The Scripps Research Institute, The University of Chicago, Argonne, and Northeastern University, used the SBC-CAT beamline 19-ID-D to screen the ER crystals, and the BioCARS beamline 14-BM-C, where the structure was obtained, to answer their questions. They studied crystal structure of the ERα bound to an estradiol derivative with a molecular complex known as ortho-trifluoromethylphenylvinyl (TFMPV-E2). The binding of this messenger complex produced a novel extended region that unequivocally "pushed the pocket" in terms of what the binding domain was able to accomplish. By binding this molecule, the ER demonstrated far more flexibility and plasticity than had ever been seen. Even better, where previous binding complexes, such as tamoxifen, behaved as estrogen receptor antagonists with bulky side groups, this new complex, TFMPV-E2, was neatly enclosed in the binding pocket and behaved in an opposite way, as an agonist. These structural and behavioral differences are good news indeed for pharmaceutical researchers, who may sometimes be in a frantic search for new ways to design therapies.

At least two general results arose from this work. First, given the great importance of steroid hormones in regulating what happens in the human body—and the past history of success in using drugs to regulate hormonal mechanisms gone awry—these new data open new paths to follow in seeking therapies not just for regulating ERs, but for steroid hormones in general. If both the binding molecule and the binding region can be treated as flexible instead of rigid, the number of approaches to regulating hormonal activity greatly increases. And, in terms of explaining previously unexplained differences, these data also show that the steroid hormone receptors actually are, at least in the case of ERα, like other members of the nuclear receptor superfamily, which show marked elasticity in the binding region.

Knowing as much as possible about the receiver of a message makes it a lot easier to choose the right messenger at the outset. Making the correct, disease-curing decisions about ERs, and perhaps all steroid hormone receptors is now much more likely. — *Mona Mort*

< Fig. 1. Structure of an estrogen receptor ligand-binding domain bound to a novel synthetic estrogen compound, TFMPV-estradiol. A portion of the ligand-binding pocket was rendered as a surface, with the ligand shown as ball and stick and colored green, with oxygen colored red, and fluorine colored pink. The trifluoro-phenyl group induces a novel extended binding pocket in the receptor.

See: Kendall W. Nettles[1]*, John B. Bruning[1], German Gil[1], Erin E. O'Neill[2], Jason Nowak[1], Alun Hughs[2], Younchang Kim[3], Eugene R. DeSombre[2], Robert Dilis[4], Robert N. Hanson[4], Andrzej Joachimiak[3], and Geoffrey L. Greene[2]**, "Structural plasticity in the oestrogen receptor ligand-binding domain," Embo Rep. **8**(6), 563 (2007).
DOI: 0.1038/nature05776

Author affiliations: [1]Department of Cancer Biology, The Scripps Research Institute; [2]Ben May Department for Cancer Research, The University of Chicago; [3]Midwest Center for Structural Genomics and Structural Biology Center, Argonne National Laboratory; [4]Department of Chemistry, Northeastern University
Correspondence:*knettles@scripps.edu,
**ggreene@uchicago.edu

This work was supported by the National Institutes of Health 1RO1 CA81049, R.N.H.); 5R01 CA89489 (G.L.G.), the Ludwig Fund for Cancer Research (G.L.G.) and the Department of Defense Breast Cancer Research Program (W81XWH-04-1-0791, G.L.G.); 17-99-1-09333 (R.N.H.) and 17-00-1-00384 (R.N.H.). Use of the BioCARS was supported by the National Institutes of Health, National Center for Research Resources, under grant number RR07707. Use of the APS was supported by the U.S. Department of Energy, Office of Science, Office of Basic Energy Sciences, under Contract No. DE-AC02-06CH11357.

14-BM-C • BioCARS • Life science • Macromolecular crystallography, fiber diffraction, biohazards at the BSL2/3 level, subatomic (<0.85 Å) resolution • Bending magnet • Accepting general users

19-ID-D • SBC-CAT • Life science • Anomalous diffraction (MAD/SAD), subatomic (<0.85 Å) resolution, ultra-low-temperature (15K) • 3.3-cm Undulator A • Accepting general users

Biological Springs from Cholesterol Ribbons?

Understanding the biological properties of cholesterol is a fundamental question that affects our health. One role of cholesterol is as a part of digestive bile in the gallbladder that aids in digestion of fats. However, in some cases, bile cholesterol becomes supersaturated and forms plate-like crystals of monohydrate cholesterol that seed the formation of cholesterol gallstones. The formation of these structures, while important to patients and their doctors, has also sparked the interest of lipid biophysicists for entirely different reasons. It turns out that bile cholesterol crystallization goes through a metastable helical ribbon intermediate. These helical ribbons of cholesterol are now being studied for their elastic properties. One such study, carried out at the SGX-CAT 31-ID-D beamline at the APS, casts light on the properties of cholesterol ribbons and could lead to new, bioengineered molecular devices.

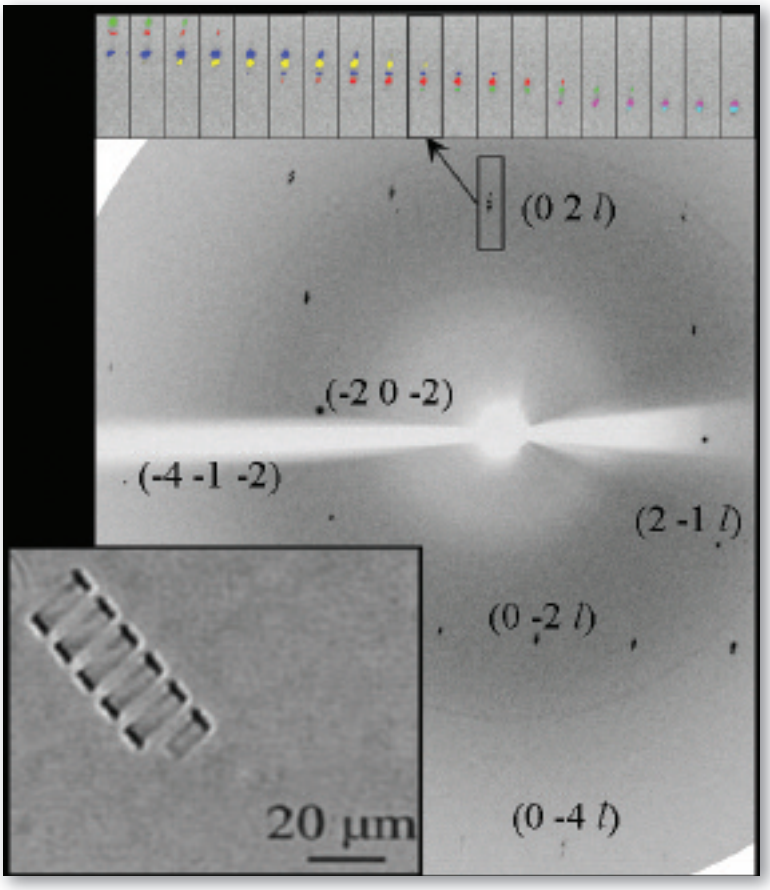

This study casts light on the properties of cholesterol ribbons and could lead to new, bioengineered molecular devices

The x-ray-scattering studies of helical ribbons formed in multicomponent solutions of cholesterol solubilized by various surfactants carried out at the SGX beamline by colleagues from the Massachusetts Institute of Technology reveal important information about the structure of these cholesterol intermediates, showing that they are formed from single crystals. This provides a sound basis for understanding the elastic properties of these helices.

Initial observations came from studies that looked at cholesterol structures in natural bile. The cholesterol in those solutions appeared to form helical ribbons with two well-defined pitch angles of 11° and 54°. In an effort to understand how these ribbons are formed, the researchers studied cholesterol in solution with various surfactants. The surfactants are detergent-like molecules that help keep fatty molecules like cholesterol in solution. The group studied 11° helical ribbons that exhibited Bragg reflections by x-ray-scattering (Fig. 1). The Bragg reflections they observed were unusually arced through multiple adjacent images, possibly due to the curvature of the ribbons, and the team developed its own software to analyze the data and determine the dimensions of the unit cell. Their analysis confirmed that the ribbons are single crystals formed from the chiral cholesterol molecules. Further analysis revealed that the dimensions of the unit cell were similar to those of cholesterol monohydrate but three times longer in the direction of the *c* axis, which is perpendicular to the ribbon plane.

The researchers hypothesize that the helical ribbons are the result of two features of the crystals. The dimensions of the ribbon strip are determined by the rate of crystal growth along different crystallographic axes. Cholesterol monomers add more quickly in one direction than in the other two directions perpendicular to the first, and so one direction grows more quickly, forming the length of the ribbons. Second, the chirality of the molecules in the crystal creates different surface tensions on each side of the crystal, causing it to bend. This bending occurs at the 11° angle relative to the ribbon edge, reflecting the underlying crystal structure. These helices have elastic properties just like a coiled spring. It is this property that authors hope to make use of in future work.

The elastic properties of the helical ribbons have offered a fortuitous surprise that may be useful in developing tools to make nanoscale measurements in biological systems. While this work had serendipitous roots in trying to understand a biomedical observation, the authors now speculate that the real value of these cholesterol ribbons may be in their biophysical properties as tiny springs. They plan to extend their work by developing ways to get homogeneously sized ribbons that could then be calibrated for their elastic constants. Once they know the strength of cholesterol springs of various radii and lengths, they can use light microscopy to measure forces. Another important problem is to develop means of functionalizing the ends of the springs so as to attach them to interesting biomolecules, with the objective of measuring the forces of various biological interactions. — *Sandy Field*

< Fig. 1. The lower left inset shows a typical helical ribbon of cholesterol. Above and behind this inset is a diffraction pattern of x-rays scattered by a flattened arc of another helical ribbon of larger radius. Such diffraction patterns demonstrate that each ribbon is a coiled crystalline strip. Detailed analysis of these patterns enables a determination of the unit cell of the cholesterol in the strip.

See: Boris Khaykovich[1], Chintan Hossain[2], Jennifer J. McManus[3], Aleksey Lomakin[3], David E. Moncton[1,2], and George B. Benedek[2,3,4]*, "Structure of cholesterol helical ribbons and self-assembling biological springs," PNAS **104**(23), 9656 (June 5, 2007).
DOI: 10.1073pnas.0702967104
Author affiliations: [1]Nuclear Reactor Laboratory, [2]Department of Physics, [3]Materials Processing Center, and [4]Center for Materials Science and Engineering, Massachusetts Institute of Technology
Correspondence: *benedek@mit.edu

This work is supported by the U.S. Department of Energy, Division of Materials Sciences and Engineering, Office of Basic Energy Sciences, under Award No. DE-FG02-04ER46149. Use of the SGX-CAT) beamline was provided by SGX Pharmaceuticals, Inc., who constructed and operates the facility. Use of the APS was supported by the U.S. Department of Energy, Office of Science, Office of Basic Energy Sciences, under Contract No. DE-AC02-06CH11357.

31-ID-D • SGX-CAT • Life science • Macromolecular crystallography, single-crystal diffraction, fiber diffraction, single-wavelength anomalous dispersion • 3.3-cm Undulator A • Accepting general users

Post-Perovskite and Seismic Anisotropy at the Core-Mantle Boundary

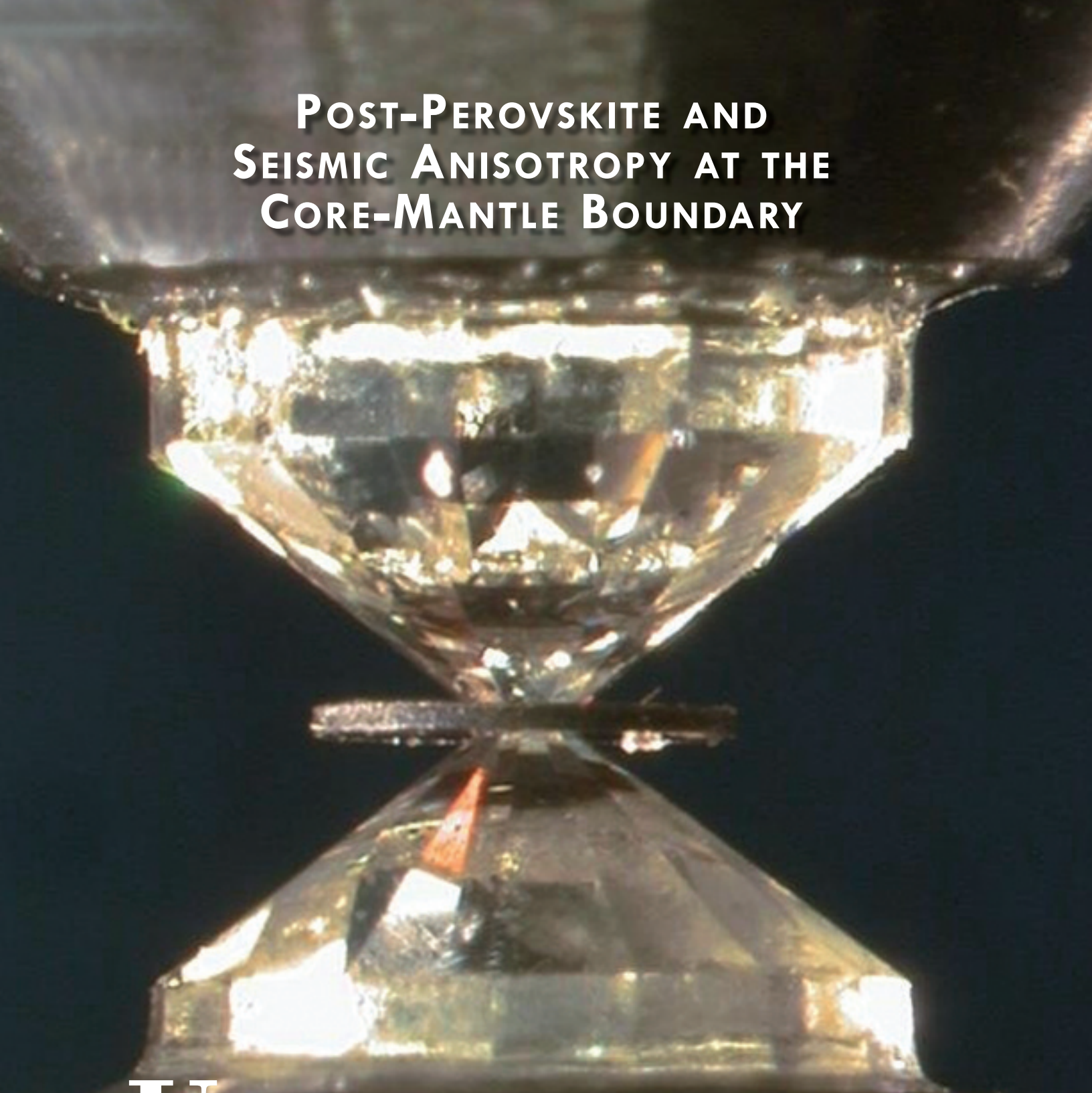

Understanding the physical and chemical composition of the Earth's interior, particularly a region as inaccessible as the core-mantle boundary (CMB), requires tremendous experimental ingenuity and advanced technology. By integrating data from ultrahigh-pressure experiments and geodynamic and mineral structure modeling, researchers from the Université de Sciences et Technologies de Lille; the University of California, Berkeley; Arizona State University; Princeton University; and the Carnegie Institution of Washington are making progress in understanding the unusual seismic properties of the lowermost mantle. Using HP-CAT beamline 16-ID-B at the APS, the researchers obtained detailed structural information on post-perovskite (pPv) that led them to conclude, within the scope of their model, that pPv does not explain the unusual seismic characteristics of the CMB.

Scientists have long theorized that the bulk of the lower mantle is composed of the magnesium silicate mineral perovskite. But perovskite cannot explain some of the more unusual characteristics of the D" (D double prime) layer, the 120-mile-thick region of the lowermost mantle. This includes one of the most important properties of the D" layer: its seismic anisotropy, by which the horizontal component of the shear (S) waves travels faster than the vertical component. In 2004, experimentalists discovered that under lowermost mantle conditions, perovskite changes to a high-pressure phase, which they named post-perovskite. The discovery of pPv allowed scientists to attribute many of the unusual characteristics of the region to its presence.

To learn more about the role of pPv at the D" layer, the researchers carrying out this study brought together their expertise in high-pressure deformation experiments and in the numerical modeling of the lower mantle. Princeton, Berkeley, and Lille scientists first compressed a powder of natural orthopyroxene in a diamond anvil cell and then converted it to pPv by laser heating (Fig. 1). By using angle dispersive radial x-ray diffraction at beamline 16-1D-B, the researchers monitored the plastic deformation and orientation of the pPv polycrystal to locate the planes of weakness.

To model lowermost mantle conditions, Arizona State University scientists calculated the deformation parameters (stresses, pressures, and temperatures) of mantle material as it flowed along the downward limb of a convection cell. Using this macroscale model, they located the depth of the perovskite/post-perovskite phase transformation and followed the flow of pPv minerals through the D" layer.

Once they had the deformation parameters, Berkeley scientists determined how an aggregate of pPv crystals would deform and orient under CMB conditions and calculated seismic velocities through the material in the horizontal and vertical directions. Their model shows that seismic anisotropy does not develop until just before the downwelling convective material reaches the CMB and begins to move horizontally. Although their calculations of seismic anisotropy vary depending on the location of the material in the D" layer and the elastic moduli used in the calculation, in general the vertically polarized S-wave components are faster than horizontally polarized S-wave components (Fig. 2), the opposite of observations of actual S-waves in the D" layer.

While pPv can explain other characteristics of the D" layer, the researchers think that, within the constraints of this study, something else must be causing the observed seismic anisotropy. The seismic patterns could indicate the presence of a different mineral in the D" layer, possibly magnesiowüstite. Alternatively, the deformation mechanisms seen in the experiment could differ from those active in the deep earth, or the elastic constants used in the models may not have been correct.

This study illustrates how the integration of information from ultrahigh-pressure experiments and microscale and macroscale modeling can yield insight into the structure and composition of the most mysterious portions of the earth.

— Dana Desonie

< Fig. 1. Diamonds in a diamond anvil cell. The sample is confined between the two diamond single crystals.

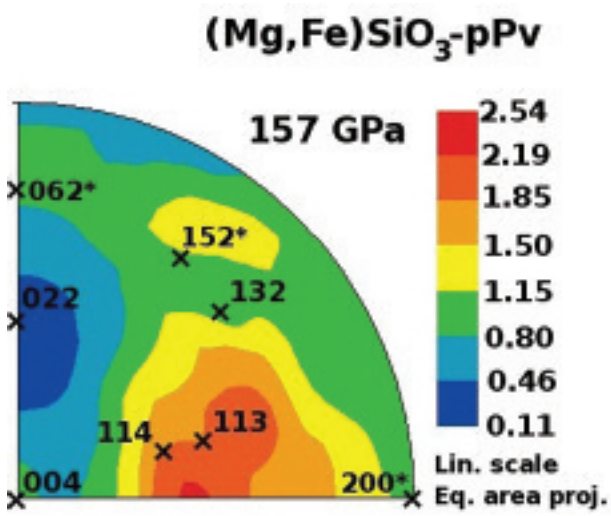

Fig. 2. Inverse pole figure of the compression direction illustrating lattice-preferred orientations measured in the post-perovskite sample at 157 GPa.

See: Sébastien Merkel[1,2]*, Allen K. McNamara[3], Atsushi Kubo[4], Sergio Speziale[1], Lowell Miyagi[1], Yue Meng[5], Thomas S. Duffy[4], and Hans-Rudolf Wenk[1], "Deformation of $(Mg,Fe)SiO_3$ Post-Perovskite and D" Anisotropy," Science **316**, 1729 (22 June 2007).

Author affiliations: [1]Department of Earth and Planetary Science, University of California, Berkeley; [2]Laboratoire de Structure et Propriétés de l'Etat Solide, Université des Sciences et Technologies de Lille; [3]School of Earth and Space Exploration, Arizona State University; [4]Department of Geosciences, Princeton University; [5]High-Pressure Collaborative Access Team, Carnegie Institution of Washington

Correspondence: *sebastien.merkel@univ-lille1.fr

This work was supported by NSF grants EAR-0510383 and EAR-0456356 (T.S.D., H.R.W., and A.K.M.) and the Carnegie/Department of Energy Alliance Center (T.S.D. and H.R.W.). Use of the HP-CAT facility was supported by the U.S. Department of Energy (DOE) Office of Basic Energy Sciences, DOE National Nuclear Security Administration, National Science Foundation, Department of Defense Tank-Automotive and Armaments Command, and the W. M. Keck Foundation. S.M. and S.S. also acknowledge support from the Miller Institute for Basic Research in Science. Use of the APS was supported by the U.S. Department of Energy, Office of Science, Office of Basic Energy Sciences, under Contract No. DE-AC02-06CH11357.

16-ID-B • HP-CAT • Materials science, geoscience • Microdiffraction, powder diffraction, single-crystal diffraction, high-pressure diamond anvil cell • 3.3-cm Undulator A • Accepting general users

Detecting a Spin Transition Zone in Earth's Lower Mantle

The model for the Earth's lower mantle has seen interesting adjustments over the last few years, as researchers have studied the properties of its main minerals: ferropericlase and silicate perovskite. It is generally believed that an iron in these minerals plays an important role in their properties, including sound velocities and transport properties. Researchers using the GSECARS beamline 13-ID-C,D at the APS have, for the first time, directly probed the spin states of iron in ferropericlase under pressures and temperatures representative of the lower mantle. They found a gradual spin transition across these pressures and temperatures, which suggests that ferropericlase at the deeper part of the lower mantle has a low-spin state, which refers to when, under extreme pressure, electrons with opposite spins pair up and thus lose their spin moments. The substantial effects of this spin transition on density and sound velocity suggest that classical models of the lower mantle need major adjustment.

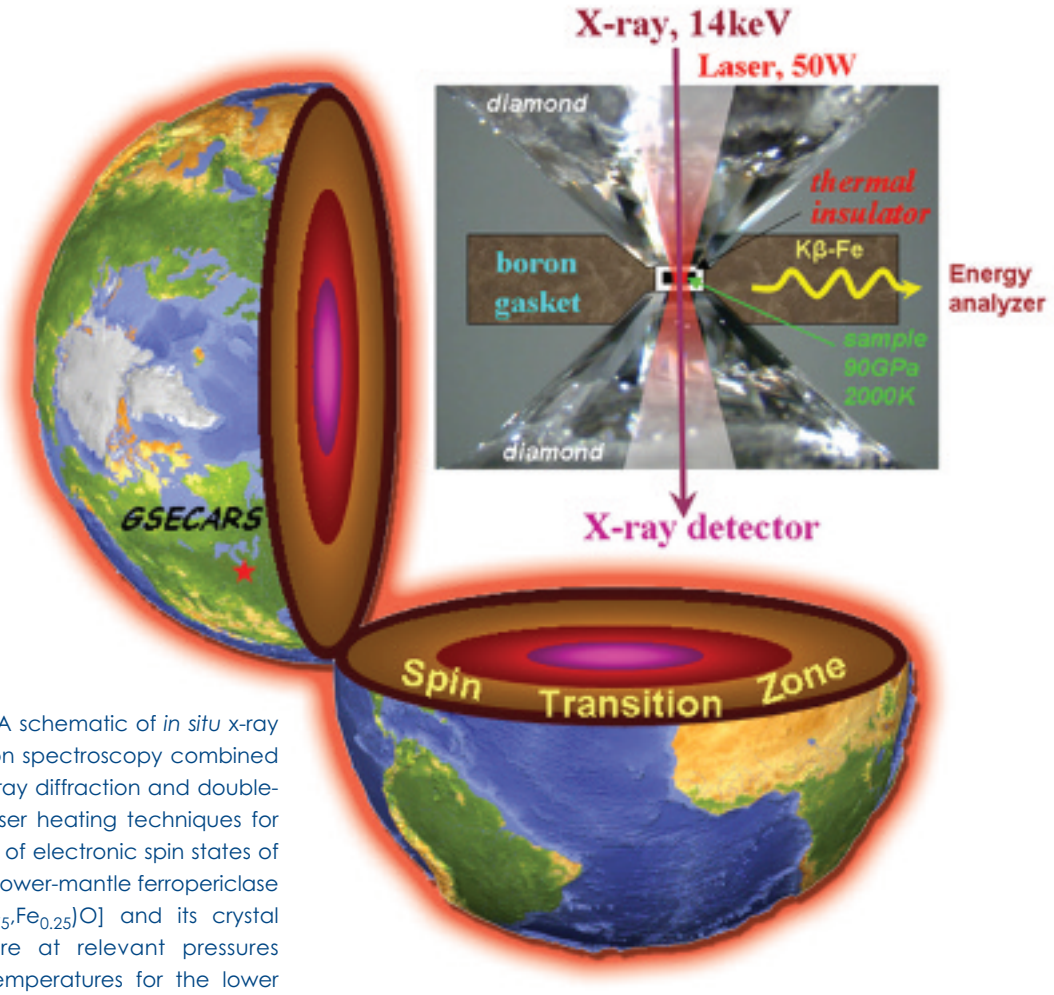

Fig. 1. A schematic of *in situ* x-ray emission spectroscopy combined with x-ray diffraction and double-side laser heating techniques for studies of electronic spin states of iron in lower-mantle ferropericlase [$(Mg_{0.75},Fe_{0.25})O$] and its crystal structure at relevant pressures and temperatures for the lower mantle of Earth.

The researchers, from Lawrence Livermore National Laboratory, the KFKI Research Institute for Particle and Nuclear Physics, the European Synchrotron Radiation Facility, Northwestern University, the Carnegie Institution of Washington, The University of Chicago, and Washington State University, studied the electron spin states and the crystal structure of ferropericlase by using x-ray emission spectroscopy (XES) and x-ray diffraction in a laser-heated diamond anvil cell at the 13-ID-C,D beamline. They examined the ferropericlase at up to 95 GPa and 2000K. To detect the spin transition zone of iron in the lower-mantle minerals, the scientists at GSECARS have built a benchmark system that employs the x-ray emission spectroscopy technique based on a Rowland circle spectrometer, combined with x-ray diffraction and double-sided laser-heating (Fig. 1). In this very challenging experiment, the team precisely aligned a small sample (usually sized down to 12 μm in thickness and 70 μm in diameter) with six optical axes: x-ray beam, emission spectrometer, downstream and upstream laser beams, and two optical paths for temperature measurements. The state-of-the-art system allowed the group to probe the electronic spin states of iron in the lower-mantle minerals *in situ* at high-pressure and high-temperature conditions generated in a sample chamber of the diamond anvil cell (Fig. 2).

Below 50 GPa and above 95 GPa, changes in temperature did not affect spin crossover. However, between 50 and 90 GPa, temperature had a strong effect on the spin state of iron in lower-mantle ferropericlase. The appearance of the low-spin state quickly reversed to mixed-spin states with high temperatures, which cannot be explained as the result of sluggish transitions. The researchers found that this pressure-temperature width is not as broad as theoretical models had predicted, which could be due to the model's use of approximations for the complex iron electronic structures.

When the data are applied to the Earth, this high-spin to low-spin crossover of iron should occur from the middle to the bottom of the lower mantle, approximately from 1000 km in depth and at a temperature of 1900K, to 2200 km and 2300K. Because this crossover is a continuous phenomenon over more than 1000 km, any physical effects, such as sound velocity or density, should be quite gradual. The gradualness of the change may explain why recent experiments have not revealed dramatic changes in iron partitioning between ferropericlase and perovskite at high temperatures.

Low-spin ferropericlase exhibits relatively high density, fast sound velocities, and lower radiative thermal conductivity. The spin crossover described here, therefore, would result in continuously enhanced density, sound velocities, and reduced radial thermal conductivity, though a reduction in sound velocities within the spin transition is recently reported. Spin transition may therefore account for some of the seismic wave heterogeneity in the lower mantle. The low-spin ferropericlase of the lowermost part of the mantle may also affect the thermal stability of the mantle upwellings.

These results imply that classical models for the lower mantle need to be revised and that the ratio of low-spin to high-spin states in the ferropericlase must be incorporated to construct more accurate models of density and sound velocities. In addition, the researchers point out that the lower mantle's dependence on an electronic transition such as this is unique, in that no other layers in the Earth's interior show such a dependence on an electronic structural transition.

— Karen Fox

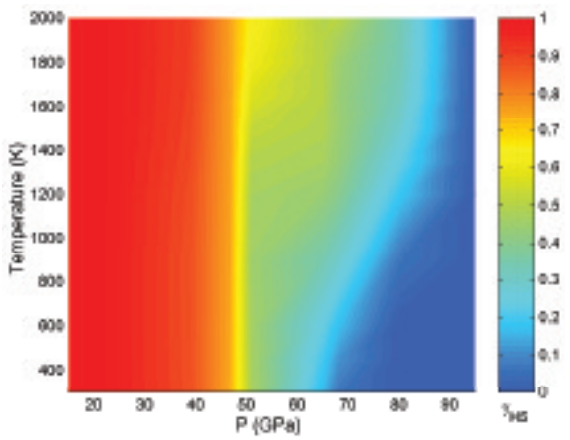

Fig. 2. Spin crossover of iron in the lower-mantle ferropericlase. The phase diagram is constructed from the interpolation and extrapolation of the derived fractions of the high-spin state in the sample. Colors in the vertical column on the right represent fractions of the high-spin iron in ferropericlase.

See: Jung-Fu Lin[1]*, György Vankó[2,3] Steven D. Jacobsen[4], Valentin Iota[1], Viktor V. Struzhkin[5], Vitali B. Prakapenka[6]**, Alexei Kuznetsov[6]***, Choong-Shik Yoo[1], "Spin Transition Zone in Earth's Lower Mantle," Science **317**, 1740 (21 September 2007). DOI: 10.1126/science.1144997

Author affiliations: [1]Lawrence Livermore National Laboratory; [2]KFKI Research Institute for Particle and Nuclear Physics; [3]European Synchrotron Radiation Facility; [4]Department of Earth and Planetary Sciences, Northwestern University; [5]Geophysical Laboratory, Carnegie Institution of Washington; [6]Consortium for Advanced Radiation Sources, The University of Chicago

Correspondence: *afu@llnl.gov, **prakapenka@cars.uchicago.edu, ***kuznetsov@cars.uchicago.edu

GSECARS is supported by NSF Earth Sciences (EAR-0622171) and DOE Geosciences (DE-FG02-94ER14466). This work at LLNL was performed under the auspices of the U.S. DOE by the University of California and LLNL under contract W-7405-Eng-48. J.-F.L. is also supported by the Lawrence Livermore Fellowship. S.D.J. acknowledges financial support from NSF/EAR 0721449, and V.V.S. acknowledges financial support from DOE. Use of the APS was supported by the U.S. Department of Energy, Office of Science, Office of Basic Energy Sciences, under Contract No. DE-AC02-06CH11357.

13-ID-C,D • GSECARS • Geoscience, environmental science • Microfluorescence (hard x-ray), x-ray absorption fine structure (XAFS), microdiffraction, micro-XAFS, high-pressure diamond anvil cell, high-pressure multianvil press, inelastic x-ray scattering • 3.3-cm Undulator A • Accepting general users

Reducing Uranium Waste

Waste uranium from power generation, the mining of raw feedstock, and past military-related activities is a growing environmental concern. Coping with this problem will only be possible with a new understanding of how uranium ions in the environment interact with soils and water, and how that affects their transport and fate. Researchers using the MR-CAT 10-ID-B beamline at the APS have turned to titration and x-ray absorption fine structure spectroscopy (EXAFS) analysis to help them determine what factors lead to the immobilization of uranium ions by reduction with sub-soil ferrous [iron(II)] ions. Fe(II) is produced by underground soil bacteria; it is found in clays, green rusts, and magnetite, and is adsorbed on minerals and bacteria. Their results hold promise for understanding how to protect the environment from uranium contamination and for designing methods to remediate water-rock systems.

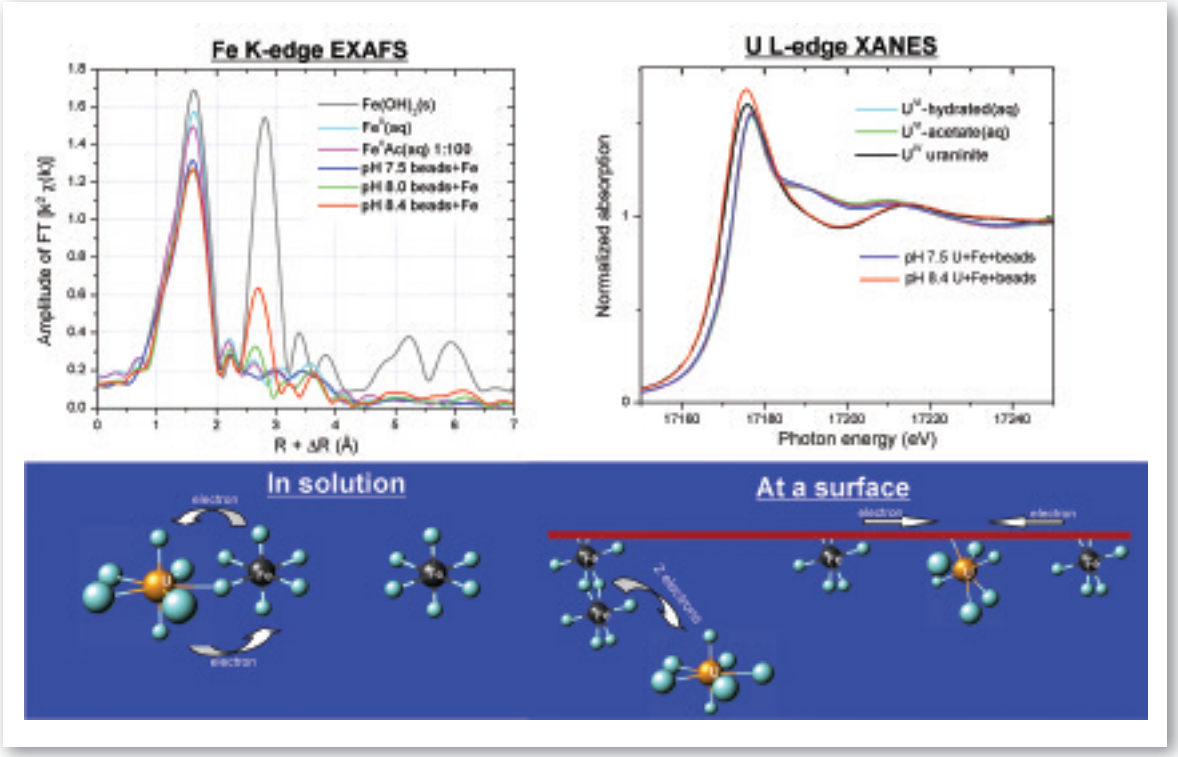

Fig. 1. X-ray absorption near edge structure and EXAFS reveal the differences in behavior of uranium ions in solution or on coated microspheres.

The results hold promise for understanding how to protect the environment from uranium contamination and for designing methods to remediate water-rock systems

Uranium in its common "VI" oxidation state, U(VI), can be reduced to a lower oxidation state U(IV) by Fe(II) ions. In the reduced state the uranium ions are not soluble in water and so can become immobilized below ground rather than leaching into water and being dispersed. The researchers have investigated how Fe(II) and U(VI) ions are absorbed onto the surface of microspheres of polystyrene. These microspheres, coated with acidic carboxyl groups, mimic the properties of soil particles and so can act as a model of the behavior of the iron and uranium ions below the surface.

The team used standard acid-base titrations (a method of quantitative/chemical analysis used to determine the concentration of a known reactant) to track the behavior of uranium ions when mixed with Fe(II) ions and the coated microspheres. They coupled these studies with Fe K-edge and U L-edge extended x-ray absorption fine structure (EXAFS) spectroscopy that allowed them to work out the bonding arrangements and the overall atomic environment of iron and uranium ions adsorbed on to the surface (Fig. 1). They found that iron ions mixed by themselves with the microspheres at mildly alkaline values of pH representative of groundwater systems; they had two distinct ways of adsorbing to the surface: either as single Fe(II) ions (pH 7.5) or as aggregates of Fe(II) species on the surface (pH 8.4). Uranium ions mixed alone with the microspheres stuck to the surface as isolated U(VI) ions at the same values of pH.

When the iron, uranium, and microspheres were all mixed together at pH 7.5, the Fe and U ions were co-adsorbed on the surface in the same manner as they are by themselves. After four months, the U(VI) was not reduced by either the adsorbed iron or any free-floating iron in the solution. This was in sharp contrast to the reaction at slightly more alkaline pH 8.4, where Fe(II) atoms aggregated and the U(VI) was completely and rapidly reduced to U(IV) in the form of nanoparticles. The U(IV) nanoparticles could be stored for at least four months in this immobile state provided they were not exposed to air. Air exposure rapidly reoxidized them to the U(VI) state.

These findings could explain why uranium ions appear to be more easily reduced by Fe(II) on a surface rather than free-flowing Fe(II) in solution: it is the ability of the U(VI) atom to rapidly receive two electrons for its reduction to U(IV).

The researchers suggest that a mechanism involving a two-electron transfer to the uranium ion would not occur readily in solution without the support of a surface. They propose that successful reduction from U(VI) to U(IV) requires a quick second electron transfer to a “dead-end” U(V)-Fe(III) intermediate, which returns to separate U(VI) and Fe(II) ions unless another electron is supplied in time.

Moreover, because the reduction takes place in two steps, they require the metal ions to stay close, which is less likely to happen in solution than on the microsphere surface. The presence of the iron oligomers at the higher pH also means there is a ready local supply of electrons for the second stage of reduction. — *David Bradley*

See: Maxim I. Boyanov[1,2]*, Edward J. O’Loughlin[1], Eric E. Roden[3], Jeremy B. Fein[2], and Kenneth M. Kemner[1], “Adsorption of Fe(II) and U(VI) to carboxyl-functionalized microspheres: The influence of speciation on uranyl reduction studied by titration and XAFS,” Geochim. Cosmochim. Acta **71**, 1898 (2007). DOI: 10.1016/j.gca.2007.01.025

Author affiliations: [1]Biosciences Division, Argonne National Laboratory; [2]Department of Civil Engineering and Geological Sciences, University of Notre Dame; [3]Department of Geology and Geophysics, University of Wisconsin-Madison

Correspondence: *mboyanov@nd.edu

Funding for this work was provided by the U.S. Department of Energy, Office of Science, Office of Biological and Environmental Research, Environmental Remediation Science Program (Contract No. DE-AC02-06CH11357), and the Environmental Molecular Science Institute at University of Notre Dame (funded by NSF Grant EAR-0221966). Work at the MR CAT beamline was supported by DOE under contract DE-FG02-94-ER45525 and the member institutions. Use of the Advanced Photon Source was supported by the U.S. Department of Energy, Office of Science, Office of Basic Energy Sciences, under Contract No. DE-AC02-06CH11357.

10-ID-B • MR-CAT • Materials science, environmental science, chemistry • Microfluorescence (hard x-ray), x-ray absorption fine structure (XAFS), diffraction anomalous fine structure, micro-XAFS • 3.3-cm undulator A • Accepting general users

The Structure of Alkali Borate Glasses at High Pressure

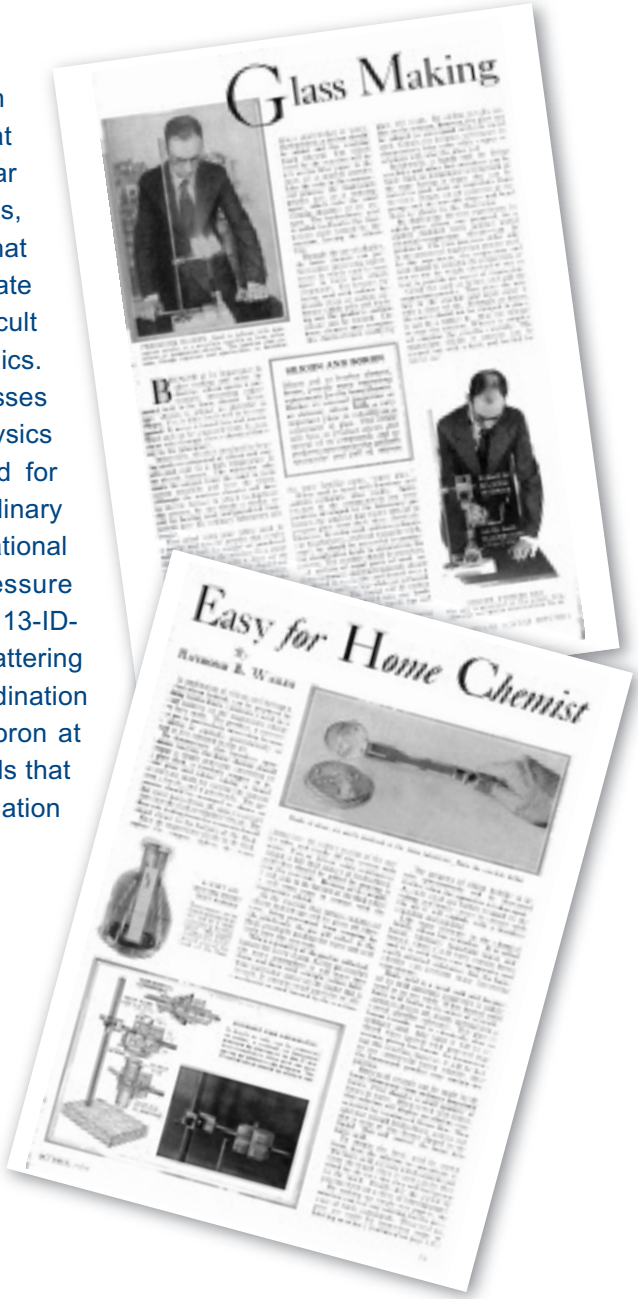

Making glass was simpler in 1934, as shown in the *Popular Science* article from that year, at right. Today, glass is studied at the molecular level so that it can be tailored for specific uses, and lessons learned along the way have ramifications that reach into the Earth. The macroscopic properties of alkali borate glasses—such as lithium borate—remain one of the most difficult and elusive problems in physics, glass science, and geophysics. Pressure-induced structural changes in the alkali borate glasses have strong implications for both condensed matter physics research and studies pertaining to the Earth's interior, and for practical and economically important applications from ordinary window glass to lab-quality glass. Researchers from Seoul National University and their colleagues from the High Pressure Collaborative Access Team employed GSECARS beamline 13-ID-C,D at the APS to carry out the first *in situ* inelastic x-ray scattering (IXS) study of alkali borate glasses, examining the coordination transformation from three-coordinated to four-coordinated boron at pressures up to 30 GPa. The data point to fabrication methods that can yield much improved glass and provide essential information about magmatic processes deep inside the Earth.

There had been no successful experiments that showed any hint of pressure-induced coordination transformation in alkali borate glasses. Previous attempts to utilize synchrotron x-ray scattering for the investigation of borates (and other low-*Z* glasses) under high pressure had run up against some limitations, including the extremely small sample environment and the equally small atomic scattering factors for low-*Z* elements. (Other non-synchrotron techniques have different but equally daunting problems. For instance, neutron scattering necessitates a large sample size that holds the useful pressure range to less than 10 GPa; vibrational spectroscopy and Brillouin scattering yield a small cross section and results that can lack clarity.) Building on advances in the optics, analyzers, and diamond-anvil cells used at synchrotron light sources, the researchers in this study have carried IXS over to the examination of complex alkali borates.

The researchers, from Seoul National University, The University of Chicago, the Carnegie Institution of Washington, and the High Pressure Collaborative Access Team at APS Sector 16, collected spectra from the glasses ($Li_2B_4O_7$) at beamline 13-ID-C,D. The power of a third-generation synchrotron radiation source such as the APS is needed to explore the structure and atomic environment around low-atomic-number elements, including boron, lithium, and oxygen. The researchers collected boron *K*-edge spectra at pressures from 0.1 MPa (1 atm) to 30 GPa, and lithium *K*-edge spectra up to 5 GPa.

The boron *K*-edge spectra (Fig. 1) showed that at 1 atm, most boron was surrounded by three nearby oxygen atoms (known as tri-coordinated boron). As pressure increased, the researchers found very little change before 5 GPa. Above

that, however, the tri-coordinated boron was no longer stable, and as the glass grew more dense, four oxygen atoms clustered around each boron atom. The percentage of four-coordinate boron changed gradually, but by 30 GPa, it accounted for more than 95% of the boron. After decompression from high pressure, the coordination transformation was reversible.

The researchers also reported the first lithium *K*-edge spectra at high pressure (Fig. 2). They found two weak features at 60 eV and 63 eV, suggesting 1-s core electron transition to valence band free orbitals. Much like the boron, the Li-IXS spectra show little change up to 5 GPa. More extensive theoretical and experimental Li *K*-edge studies are needed to obtain the systematic effect of composition and pressure on their local structures.

Geophysically, such information is crucial for understanding the Earth's interior, because the densification in the alkali borate will improve our understanding of the structures of silicate melts deep in the Earth. The transformation information can help determine melt properties, such as viscosity and density, which can affect processes that include magma dynamics and the Earth's evolution. For technological applications, the data suggest that glasses synthesized at high pressures should have much improved mechanical properties and chemical durability. — *Karen Fox*

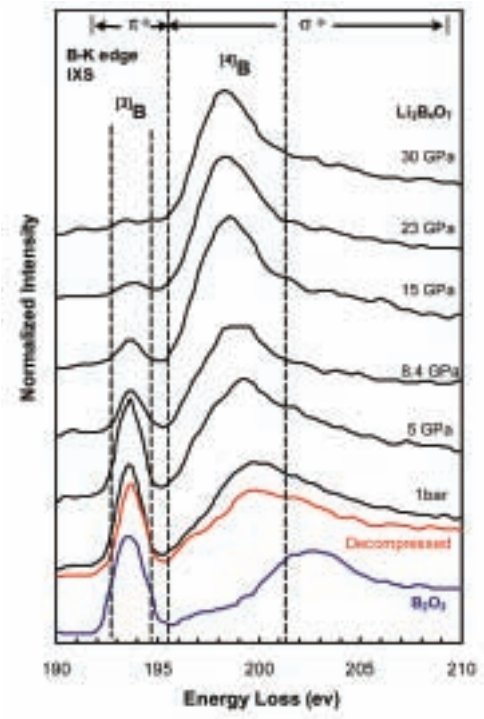

Fig. 1. Boron *K*-edge IXS spectra for $Li_2B_4O_7$ glass (black lines) and B_2O_3 glass (blue) at pressures ranging from 1bar to 30 GPa. The red line refers to IXS spectra for $Li_2B_4O_7$ glass decompressed to 1 atm from 30 GPa. The spectra are plotted as normalized scattered intensity vs. energy loss (incident energy–elastic energy).

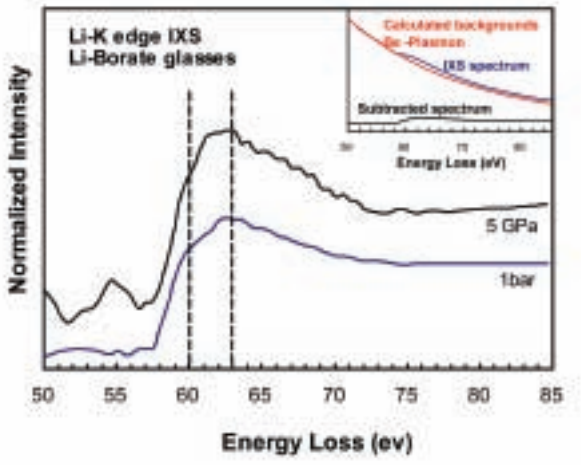

Fig. 2. Li *K*-edge IXS for Li-B_2O_3 glasses at 1 atm (blue line) and 5 GPa (black). The inset shows the background subtraction methods for IXS spectra at 5 GPa, where a significant contribution from Be Plasmon was subtracted. The contribution from Be plasmon was fitted using a complex linear function (red line) and then subtracted from the IXS spectra (blue, inset), yielding IXS spectra free from the Be plasmon effect (black).

See: Sung Keun Lee[1]*, Peter J. Eng[2,3], Ho-kwang Mao[4,5], Yue Meng[4,5], and Jinfu Shu[4], "Structure of Alkali Borate Glasses at High Pressure: B and Li *K*-Edge Inelastic X-ray Scattering Study," Phys. Rev. Lett. **98**, 105502 (9 March 2007). DOI: 10.1103/PhysRevLett.98.105502

Author affiliations: [1]School of Earth and Environmental Sciences, Seoul National University; [2]Consortium for Advanced Radiation Sources, The University of Chicago; [3]James Franck Institute, The University of Chicago; [4]Geophysical Laboratory, Carnegie Institution of Washington; [5]HP-CAT, Advanced Photon Source, Argonne National Laboratory

Correspondence: *sungklee@snu.ac.kr

GSECARS supported by DOE-BES Geosciences, NSF-Earth Sciences and the State of Illinois. HP-CAT supported by DOE-BES-Materials Science, DOE-NNSA, CDAC, NSF, DOD-TACOM, and the W.M. Keck Foundation. S.K. Lee was supported by funds from Korea Research Foundation (No. C00076). Use of the APS was supported by the U.S. Department of Energy, Office of Science, Office of Basic Energy Sciences, under Contract No. DE-AC02-06CH11357.

13-ID-C,D • GSECARS • Geoscience, environmental science • Microfluorescence (hard x-ray), x-ray absorption fine structure (XAFS), microdiffraction, micro-XAFS, high-pressure diamond anvil cell, high-pressure multianvil press, inelastic x-ray scattering • 3.3-cm Undulator A • Accepting general users

Seek and Destroy: Selectively Targeting Intracellular DNA

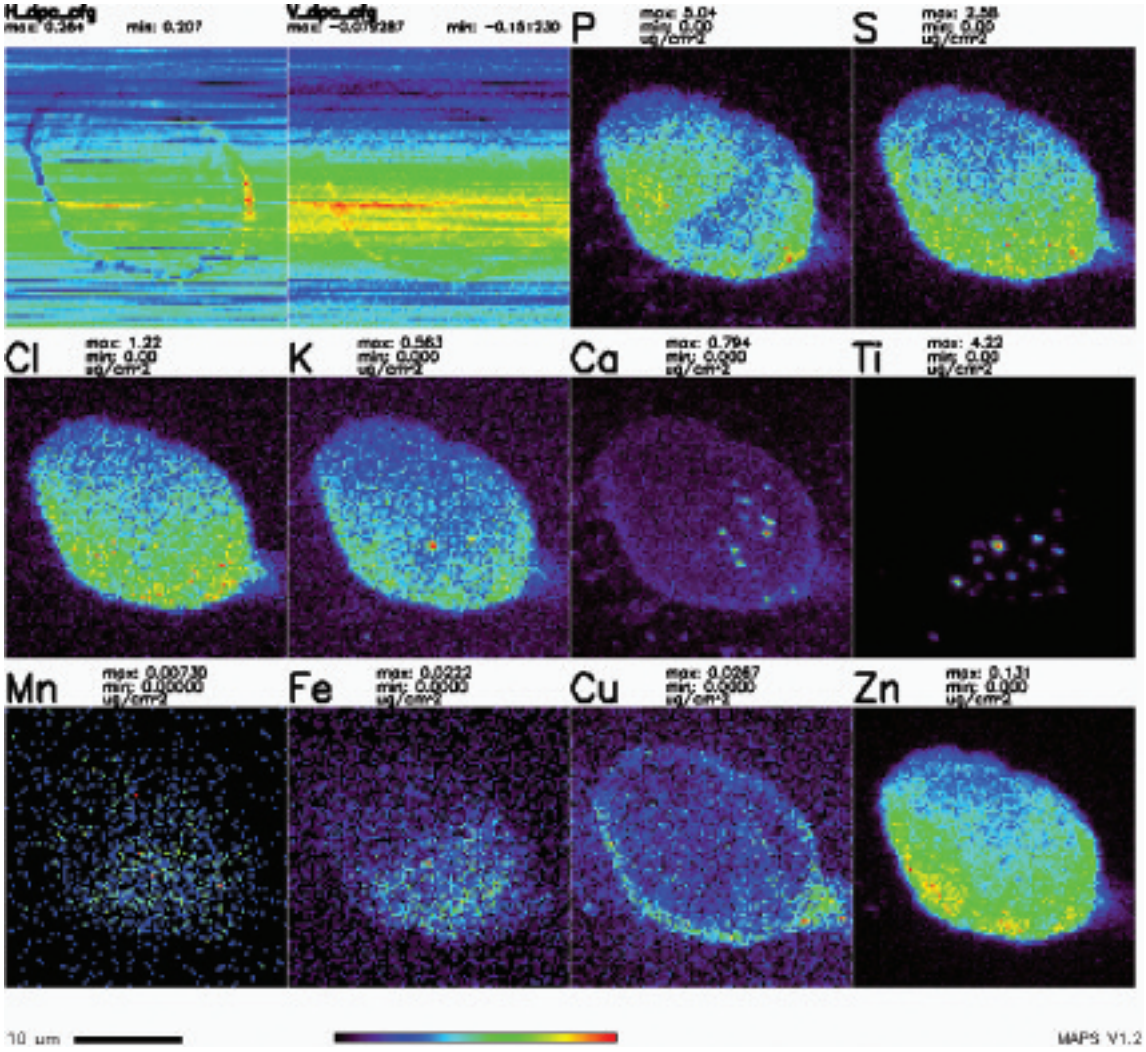

Fig. 1. X-ray fluorescence maps of the distribution of different elements present in a cell treated with TiO_2 nanoparticles. Titanium is not present in untreated cells, while all other elements shown are the natural content of cells. The presence of a titanium signal in this cell is evidence of nanoparticle uptake.

Much attention has focused on the promise and pitfalls of gene therapy to heal or repair defective genetic material by using a variety of vectors, including viruses. An alternative approach is to inactivate genomic DNA. In either case, a major obstacle has been the inability to penetrate the cell membrane and deliver a biological payload to the specific intracellular target. New discoveries in the realm of nanoconjugated materials consisting of biological and inorganic components are allowing researchers to fine-tune the delivery of nucleic acids and expand the practical applications of imaging, diagnosis, and therapeutic approaches to many diseases, including cancer. A limiting factor has been the shortcomings of optical microscopy in producing accurate images of hybrid nanoscale materials. But high-energy x-ray fluorescence microscopy (XFM) at XOR beamlines 2-ID-D and 2-ID-E at the APS allowed a team of researchers to directly map the destination and view the distribution and concentration of nanoconjugates, furthering efforts to utilize nanoconjugated materials as weapons against disease.

The targets of the nanoconjugates—which consisted of 3-nm to 5-nm particles of titanium dioxide (TiO_2) bound with a dopamine to 6-nm to 8-nm DNA oligonucleotides—were ribosomal 18S RNA, which is present in most mammalian cells, in the nucleolus inside the cell nucleus and in the mitochondria within the cell cytoplasm. The imaging technique relies on the ability of XFM to detect the K-α fluorescence spectra of the titanium, which acts as a photoreactive nanoscale semiconductor. Titanium nanoparticles free of oligonucleotides and therefore lacking in a specific target were used as a negative control and were found, as expected, to display little to no retention within the mitochondria and nucleoli, while composites containing DNA oligonucleotides specifically tailored to target nucleolic and mitochondrial cells showed an affinity to hybridize with the sequence-specific target within the cells.

The researchers, from Northwestern University, Argonne, Loyola University, and the University of Pennsylvania, transfected human breast cancer cell line MCF-7/WS8 with these nanoconjugates, which were coated with glycidyl isopropyl ether. They also transfected cell lines from human prostate (PC3) and rat adrenal tumor (PC12) to determine whether transfection was specific only to the human breast cell line. The cell lines were transfected via electroporation—which causes excitation of the titanium and helps the nanoconjugate penetrate the cell membrane—and also by natural uptake.

The team also subjected meticulously prepared, ultrathin sections of treated cells to conventional transmission electron microscopy (TEM) at the Northwestern University Cell Imaging Core Facility. Transmission electron microscopy analysis is a good way to measure details of materials to nearly the atomic level, but it has certain limitations; for example, it cannot be used to examine whole cells. Transmission electron microscopy images of the density of TiO_2 suggested the presence of the nanoconjugates within two spots of the nuclei. The XFM, which maps the elements of the periodic table between silicon and zinc (Fig. 1), also revealed a two-spot pattern of areas of denser concentration of TiO_2 in the three cancer cell lines: human breast, human prostate, and rat pheochromocytina cells. Cancer cells typically have two or more nucleoli; therefore, these results suggest that the nanoconjugate was able to reach the target. X-ray fluorescence microscopy and TEM images also detected titanium inside the mitochondria of the PC12 cells, though it was not possible to probe the human breast and prostate cells because the oligonucleotides used (ND2s) are specific only to the rat PC12 mitochondrial genomic sequence.

These results indicate that TiO_2-DNA nanoconjugates can be delivered and retained within the targeted material and thus lend themselves to imaging, diagnosis, and eventual treatment of sequence-specific intracellular targets within cancer cells.

— Elise LeQuire

See: Tatjana Paunesku[1,2], Stefan Vogt[3], Barry Lai[3], Jörg Maser[3], Nataša Stojićević[1], Kenneth T. Thurn[1], Clodia Osipo[4], Hong Liu[2], Daniel Legnini[3], Zhou Wang[5], Chung Lee[6], and Gayle E. Woloschak[1,2,7,8]*, "Intracellular Distribution of TiO_2-DNA Oligonucleotide Nanoconjugates Directed to Nucleolus and Mitochondria Indicates Sequence Specificity," Nano Lett. **7**(3), 596 (2007). DOI: 10.1021/nl0624723

Author affiliations: [1]Department of Radiation Oncology, Northwestern University; [2]Robert H. Lurie Comprehensive Cancer Center, Northwestern University; [3]X-ray Science Division, Advanced Photon Source, Argonne National Laboratory; [4]Cardinal Bernardin Cancer Center, Loyola University Medical Center; [5]Department of Urology, University of Pennsylvania Medical Center; [6]Department of Urology, Northwestern University; [7]Department of Radiology, Northwestern University; [8]Department of Cell and Molecular Biology, Northwestern University

Correspondence: *g-woloschak@northwestern.edu

This work was supported by NIH CA107467, EB002100, P50 CA89018, U54CA119341, and by DOE FG02-04 ER 63920. TiO_2 nanoparticles used for some of these studies were a gift from T. Rajh and M. Thurnauer (Chemistry Division, Argonne National Laboratory). Use of the APS was supported by the U.S. Department of Energy, Office of Science, Office of Basic Energy Sciences, under Contract No. DE-AC02-06CH11357.

2-ID-D • XOR • Life science, materials science, environmental science • Microfluorescence (hard x-ray), microdiffraction, micro-x-ray absorption fine structure • 3.3-cm Undulator A • Accepting general users

2-ID-E • XOR • Life science, environmental science, materials science • Microfluorescence (hard x-ray) • 3.3-cm Undulator A • Accepting general users

An Alternative Approach to Amorphization of Pure Copper

Amorphous metals have several useful properties, such as greater hardness and elasticity, when compared with their crystalline counterparts. Amorphous metallic alloys are thus used in, for example, golf club heads to maximize impact-energy transfer to the ball, but they have great potential for a wide range of engineering applications from aerospace to construction. It is relatively easy to make alloy materials in the amorphous state by simply rapidly cooling them from the liquid state. This process locks in the randomness found in the liquid and so produces a glassy, amorphous, solid structure. However, theoretical studies suggest that fabricating pure elemental amorphous metals is not achievable by the same method (without the introduction of impurities). This is due to the fact that the elemental metallic phase is regenerated rapidly because the viscosity of the elemental metallic liquid is simply too low. To lock in the glassy phase with a pure liquid metal, scientists would have to use cooling rates in excess of >10^{10}° C/s, which are unattainable with today's technology. In order to overcome the cooling rate issue and sidestep the need for adding impurities, researchers used ChemMatCARS beamline 15-ID-B,C,D at the APS to study an alternative approach to amorphization of pure copper metal.

Earlier investigators discovered that blasting a bulk metal with a beam of ion irradiation could, if there were impurities present in the metal, distort the crystalline structure somewhat. The ions, on colliding with the material, trigger a very short-lived cascade of structural damage among the metal atoms, resulting in localized pockets of glassiness. These pockets overlap if the ion irradiation level is high enough and if there is at least 10%–20% by atomic weight of impurities present in the metal. However, the need to add impurities to the metal means that the process is limited and precludes certain applications that would require highly pure amorphous metal. From this perspective, it is of fundamental interest to produce and characterize a pure amorphous elemental metal.

The researchers in this study, from Australian National University and the Australian Synchrotron Research Program, made elemental copper nanocrystals of approximately 2.5 nm diameter within a silica film on a layer of silicon. They then fired a beam of high-energy tin ions at the nanocrystals. The tin ions passed straight through the silica film containing the nanocrystals, but en route they disrupted the crystalline order enough to convert the nanocrystals into the glassy, amorphous state (Figs. 1 and 2). The researchers found that using this technique allowed them to minimize the effects of impurities, because the tin ions became embedded in the silicon substrate beneath, rather than lodging in, the metal.

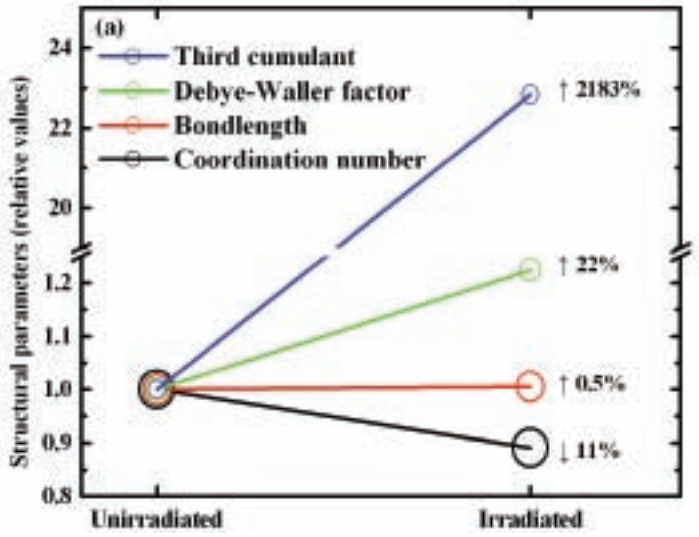

Fig. 1. The short-range atomic structure of the nanocrystals prior to and after irradiation is represented by the coordination number, bond length, Debye-Waller factor, and third cumulant of the bond length distribution function. Short-range atomic structure shifts from the crystalline to the amorphous in nanocrystals blasted with tin ions. Note that all values are relative to the unirradiated values, the latter normalized to unity. Prior to irradiation, the third cumulant was insignificant (close to zero), and upon irradiation the increase was very large (in percentage terms.

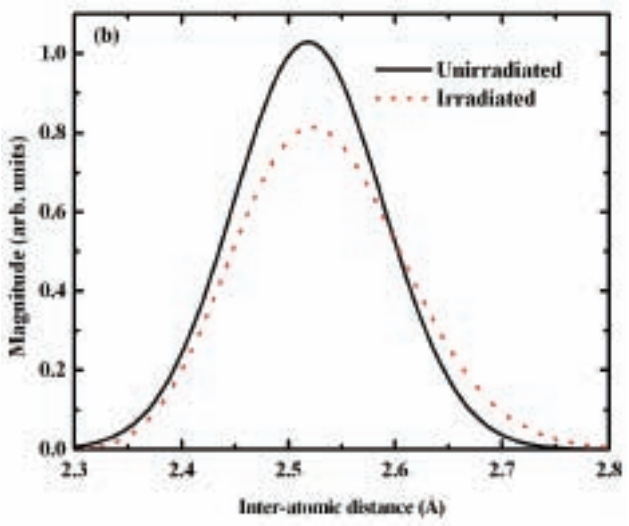

Fig. 2. Radial distribution functions (RDFs) for the unirradiated and irradiated nanocrystals. Bond lengths are stretched following ion irradiation.

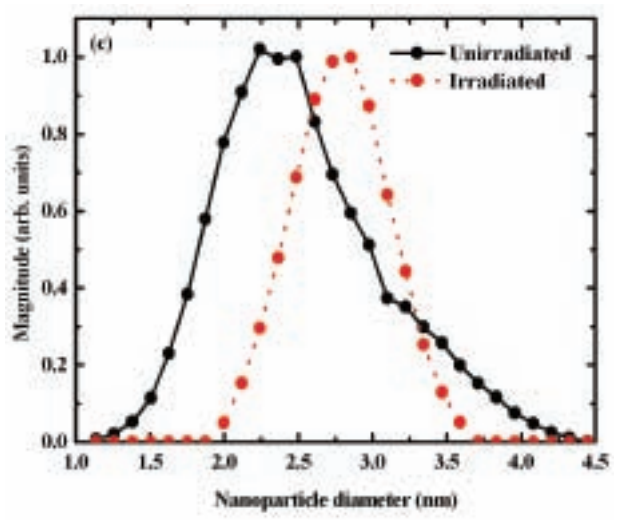

Fig. 3. Size distribution for unirradiated and irradiated nanocrystals. The average diameter is ~2.5 nm prior to irradiation and increases slightly upon irradiation.

This fundamental discovery means that the structurally governed properties of copper nanocrystals might be changed and so enable advanced technological applications. For instance, the very fact that these amorphized nanocrystals are supported on a semiconductor layer means the skills of the microelectronics industry might be brought to bear in fabricating novel structures for integration into devices.

Amorphous metallic nanoparticles embedded in such a dielectric matrix are expected to display nonlinear optical properties different from those of their nanocrystalline counterparts. They might be used in optical filters that block certain wavelengths of light above a certain intensity, for eye and equipment protection, or in optical switching devices and memory units for future optoelectronic computing systems.

The researchers attempted to study the structure of these copper nanocrystals using conventional x-ray diffraction methods, but they observed significantly broadened peaks with this approach because of the small size of the particles. This meant that they obtained very little detail. Instead, they turned to extended x-ray absorption fine structure (EXAFS) spectroscopy. This technique can resolve structural details at the atomic level in materials that lack a long-range order, a property exemplified by amorphous solids.

Unfortunately, the EXAFS technique does not provide information to accurately quantify changes in the distribution of nanocrystal sizes following ion irradiation. For this, the team exploited small-angle x-ray scattering (SAXS) at the APS. The SAXS study revealed that the volume-weighted average diameter of the nanocrystals increased slightly, as predicted, once the material was amorphized (Fig. 3).

The researchers point out that the overall appearance and size of the nanocrystals does not change significantly following ion irradiation, as revealed by electron microscopy. However, they did see dramatic changes in the short-range order between copper atoms as well as changes in the coordination around each atom (i.e., the number of nearest-neighbors changes). Such changes provide additional evidence of a shift from the crystalline to a glassy state.

— David Bradley

See: B. Johannessen[1], P. Kluth[1], D.J. Llewellyn[1], G.J. Foran[2], D.J. Cookson[2], and M.C. Ridgway[3], "Amorphization of embedded Cu nanocrystals by ion irradiation," Appl. Phys. Lett. **90**, 073119 (2007). DOI: 10.1063/1.2644413

Author affiliations: [1]Department of Electronic Materials Engineering, Research School of Physical Sciences and Engineering, Australian National University; [2]Australian Synchrotron Research Program, Australian Nuclear Science and Technology Organization; [3]Department of Electronic Materials Engineering, Research School of Physical Sciences and Engineering, Australian National University
Correspondence: *bej@anbf2.kek.jp

This work was supported by the Australian Synchrotron Research Program and the Australian Research Council. Use of the Advanced Photon Source was supported by the U.S. Department of Energy, Office of Science, Office of Basic Energy Sciences, under Contract No. DE-AC02-06CH11357.

15-ID-B,C,D • ChemMatCARS • Materials science, chemistry • Anomalous and resonant scattering (hard x-ray), liquid scattering, microdiffraction, single-crystal diffraction, small-angle x-ray scattering, surface diffraction, wide-angle x-ray scattering • 3.3-cm Undulator A • Accepting general users

Luminescence in Complex Nanowires

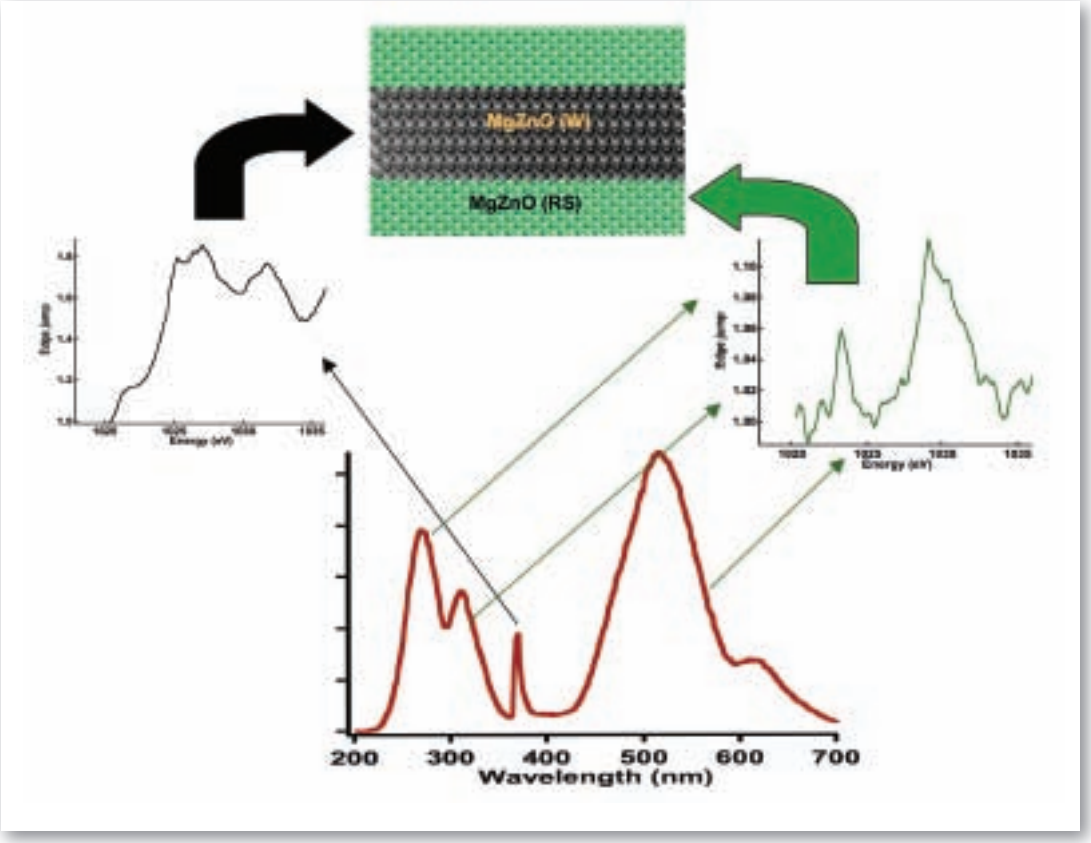

Fig. 1. Luminescence spectrum of a Type II nanowire (bottom). The Zn L XANES spectrum of the band gap (380 nm) peak is shown to the left, and that of the three broad defect levels is shown to the right. The data show that the band gap state originates in the wurtzite core and the defect levels arise in the shell (upper).

Zinc oxide thin films and nanostructures are proving to be versatile and useful in optical and electronic applications such as lasers, transistors, next-generation memory storage devices, and optical sensors and displays. But nanoengineers need a better understanding of the luminescence produced by the various structures that have been examined in the laboratory. Heterostructured nanowires span a wide range of band gaps, and the energy and intensity of the luminescent peaks have been determined to depend on the structural characteristics of different composites, as well as on the changing nature of the interface between the core and shell of the heterostructured nanowires. Researchers used time-resolved, x-ray-excited optical luminescence (XEOL) [1] at XOR beamline 4-ID-C at the APS to characterize the local chemical and structural environment that produces the luminescence peaks in heterostructural, one-dimensional nanowires. This work highlights the capacity of XEOL to determine the intensity of fluorescence emissions selectively, and to locate the precise site from which the luminescence emanates within these complex nanostructures.

Previous research had established a basic understanding of the structure of (Zn-Mg)O heteronanostructures. As the concentration of Mg increases from less than 37% to more than 62%, the structure changes from hexagonal to cubic, and the band gap increases from 3.3 to 7.8 eV. In the midrange, however, the structure is undefined. The potential to tune the energy band gaps in these materials makes such thin films and nanostructures very good candidates for optical devices in which intense, ultraviolet-visible luminescence is required.

The researchers in this study, from Argonne, Oak Ridge National Laboratory, and the University of Florida, examined two classes of heterostructures. Type I consisted of an alloy containing a low concentration of Mg in a hexagonal wurtzite core sheathed in a wurtzite shell with a higher proportion of Mg, while Type II consisted of a wurtzite core with little or no Mg and a cubic rock salt shell with a high concentration of Mg. The rods for both types, approximately 50 nm in diameter, were prepared on a silicon substrate at the University of Florida, producing randomly oriented structures.

X-ray absorption near-edge structure (XANES) measurements were used to pinpoint the specific origin of the luminescence in the two types. It was found that in both structures, the exciton state emanates from the wurtzite core. In Type I nanostructures, however, exciton peaks were found to be more than 750 times more intense than those of Type II. In addition, transmission electron spectroscopy indicated that in Type I structures, the interface and surface of the composite are smoother than in Type II, which suggests that the damping of luminescence from the wurtzite core in the latter may be a result of defects at the interface of the rock salt shell (Fig. 1). Measurements were obtained at room temperature and at ~40K.

Since the breakthrough discovery of ultraviolet lasing of ZnO nanowires at room temperature, researchers have sought to determine ways to increase the luminescence efficiency and thus pave the way for the creation of opto-electronic devices. The current results indicate that Type I structures, with their smooth interface leading to more intense luminescence, may be suitable for useful applications under real-world conditions. — *Elise LeQuire*

Reference

[1] *APS Science 2006*, ANL-06/23, 144 (Argonne National Laboratory, May 2007).

See: Richard A. Rosenberg[1]*, Gopal K. Shenoy[1], Matthew F. Chisholm[2], Li-Chia Tien[3], David Norton[3], and Steven Pearlon[3], "Getting to the Core of the Problem: Origin of the Luminescence from (Mg,Zn)0 Heterostructured Nanowires," Nano Lett. **7**(6) 1521 (2007). DOI: 10.1021/nl0702923
Author affiliations: [1]Argonne National Laboratory; [2]Oak Ridge National Laboratory; [3]Department of Materials Science and Engineering, University of Florida
Correspondence: *rar@aps.anl.gov

Work at Oak Ridge National Laboratory was sponsored by the U.S. DOE-BES, under contract managed and operated by UT-Battelle, LLC. The work at University of Florida (UF) was supported by the NSF (DMR 0400416, 0305228, Dr. L. Hess). The authors at UF acknowledge the Major Analytical Instrumentation Center, Department of Materials Science and Engineering, UF. Use of the APS was supported by the U.S. DOE-BES, under Contract No. DE-AC02-06CH11357.

4-ID-C • XOR • Physics, materials science • X-ray photoemission electron microscopy, x-ray photoemission spectroscopy, magnetic circular dichroism (soft x-ray), x-ray magnetic linear dichroism, magnetic x-ray scattering, anomalous and resonant scattering (soft x-ray) • Circularly polarized undulator • Accepting general users

Striking Nano Gold

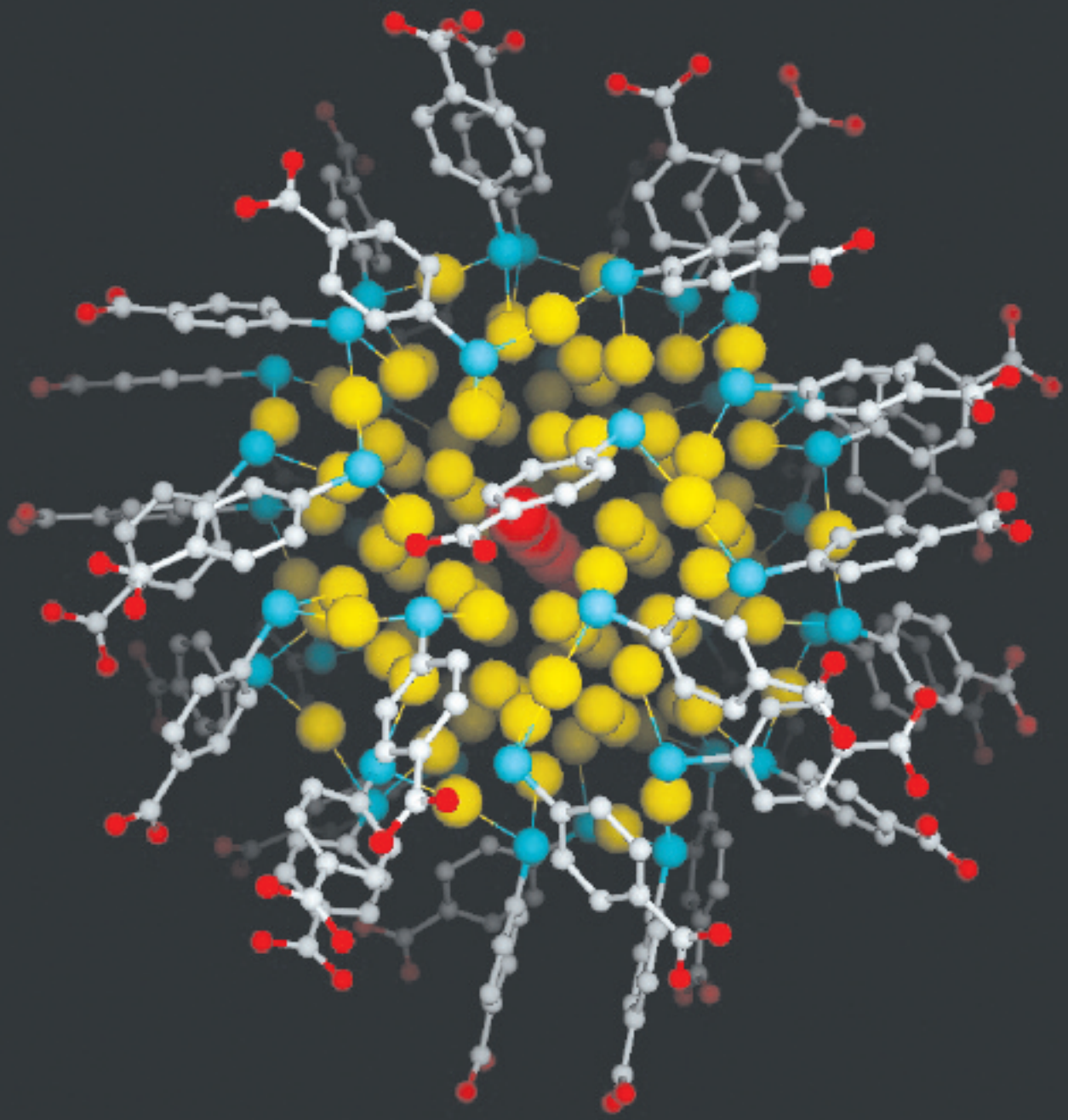

Fig. 1. X-ray crystal structure of the Au_{102}(p-MBA)44 nanoparticle.

The development of practical biomedical and electronic applications for monolayer-protected gold nanoparticles, an area of intense research activity, has been accelerated by scientists working at the GM/CA-CAT beamline 23-ID-B at the APS and beamlines at two other U.S. Department of Energy light sources. The group has succeeded in synthesizing and visualizing a pure crystal of gold nanoparticles coated with the thiol p-MBA (*p*-mercaptobenzoic acid). (Thiols, also called mercaptans, are organic compounds that contain a functional group composed of a sulfur atom and a hydrogen atom [—SH].) The achievement is noteworthy on several levels. First, the researchers developed a procedure for synthesizing stable clusters of a uniform size (precisely 102 gold [Au_{102}] and 44 p-MBA [p-MBA_{44}] atoms each). Second, they determined the structure of a monolayer-protected nanocluster to the atomic level (1.1-Å resolution) and in so doing addressed long-standing questions about how sulfur binds to gold. The work represents a major advance in synthesizing monolayer-protected clusters and determining the principles that guide self-assembly.

The structure of the crystallized gold-thiol cluster (Fig. 1) displays several intriguing and unexpected features. Previous studies suggested that stable clusters would have a "magic number" of gold atoms resulting from the closure of a geometric shell—forming, for example, icosahedral clusters of 55, 147, or 309 atoms when crystallized. Another view anticipated that the core would be amorphous or quasi-molten. In contrast, the $gold_{102}$ cluster has a well-ordered but chiral structure that was confirmed by screening 15 crystals derived from multiple nanoparticle preparations. It seems that electronic shell closing provides a better explanation for the uniform size of these clusters: in theory, each of the 44 sulfur atoms attracts a gold electron into a localized orbital, leaving 58 gold atoms—each contributing one valence electron—to form a filled shell.

The inner 49 atoms form a decahedron that is capped by two 20-atom poles arranged in C_5 symmetry, yielding a total of 89 atoms that display a five-fold symmetry. The cluster's chirality results from an asymmetric 13-atom band on the equator.

The gold-sulfur binding mode in such self-assembling nanoparticles had long been debated. One standard model had predicted that each sulfur atom would bind to two adjacent gold atoms. In the $gold_{102}$ crystal, however, the sulfur and gold atoms bind in a bridge conformation: each sulfur binds two gold atoms with one of the gold atoms binding two sulfurs, forming a staple-like motif. The cluster has a nucleus of gold atoms that do not contact sulfur, those in the next layer bind one sulfur, and those in the outer shell bind two sulfurs. The protective monolayer is further stabilized by interactions between the phenyl rings of the p-MBA molecules.

The Au_{102} cluster is notably more stable than other, larger clusters. The researchers, all from Stanford University, are currently engaged in extending their work by the synthesis, crystallization, and x-ray analysis of new gold nanoclusters with different sizes and protective monolayers.

In their initial exploration of the structure of the Au_{102} crystal, the researchers collected their atomic-resolution dataset by using the 23-ID-B beamline at around 1.4 Å. According to the researchers, experience and better-quality crystals enabled a 1.1-Å resolution data set at the Stanford Synchrotron Radiation Laboratory. Subsequent to publishing the *Science* paper, they have been collecting data at GM/CA-CAT at an ultra-high resolution of 0.75 Å in order to determine the role of the sulfhydryl proton in the sulfur-gold bond, work that is still under way. — *Carol Hart*

See: Pablo D. Jadzinsky[1,2], Guillermo Calero[1], Christopher J. Ackerson[1], David A. Bushnell[1], and Roger D. Kornberg[1]*, "Structure of a Thiol Monolayer-Protected Gold Nanoparticle at 1.1 Å Resolution," Science **318**, 430 (19 October 2007). DOI: 10.1126/science.1148624

Author affiliations: [1]Department of Structural Biology; [2]Department of Applied Physics, Stanford University School of Medicine

Correspondence: *kornberg@stanford.edu

GM/CA CAT at the APS is funded in whole or in part with federal funds from the National Cancer Institute (Y1-CO-1020) and the National Institute of General Medical Sciences (Y1-GM-1104). Portions of this research were carried out at the Stanford Synchrotron Radiation Laboratory (SSRL), a national user facility operated by Stanford University, on behalf of the U.S. Department of Energy (DOE), Office of Basic Energy Sciences. The SSRL Structural Molecular Biology Program is supported by DOE, Office of Biological and Environmental Research, and by NIH, National Center for Research Resources, Biomedical Technology Program, and the National Institute of General Medical Sciences. Portions of this research were conducted at the Advanced Light Source, a national user facility operated by Lawrence Berkeley National Laboratory, on behalf of the DOE, Office of Basic Energy Sciences. The Berkeley Center for Structural Biology is supported in part by DOE, Office of Biological and Environmental Research, and by NIH and the National Institute of General Medical Sciences. Use of the Advanced Photon Source was supported by DOE, Office of Basic Energy Sciences, under Contract No. DE-AC02-06CH11357.

23-ID-B • GM/CA-CAT • Life science • Macromolecular crystallography, microdiffraction, anomalous diffraction (MAD/SAD), subatomic (<0.85 Å) resolution • 3.3-cm Undulator A • Accepting general users

Suppression of Growth and Phase Transformation in Nanoscale Titania

Recent experiments carried out at the APS and Stanford Synchrotron Radiation Laboratory light sources show that an increase in the stability of nanocrystals is achieved through the introduction of small amounts of dopants. Researchers investigated yttrium-doped titanium oxide (TiO_2), or titania, to determine the effects of doping on nanoparticle physical size and phase stabilization. They uncovered new information concerning the retention of material properties by nanoparticles exposed to high temperatures that may be crucial to the future production of catalytic and photovoltaic materials. This is an important advance in the development of new materials with characteristics desirable for the production of both catalysts and photovoltaics. These materials may be crucial in many fields, particularly energy production and technology.

Titanium dioxide is a polymorph—a material that can exist in more than one crystal structure— that occurs naturally as anatase, brookite, and rutile. Using extended x-ray absorption fine structure (EXAFS) and wide-angle x-ray scattering (WAXS) experiments, the researchers from the University of California, Berkeley, and Lawrence Berkeley National Laboratory determined the heretofore unknown mechanism through which the thermal stability of titania is achieved. The group studied the doping effects using WAXS measurements on DND-CAT beamline 5-ID-B,C,D and XOR beamline 11-ID-C at the APS, and EXAFS measurements on beamlines 10-2 and 11-2 at the Stanford Synchrotron Radiation Laboratory. The group found a strong correlation between their results and predictions using molecular dynamics simulations. They also found that the introduction of yttrium, a doping material, into a titanium oxide nanoparticle produces both structural and phase transition effects. The yttrium-doped titania has a different free energy, resulting in extended phase stabilization in the anatase form of the nanoparticle.

Titanium-oxide nanoparticles, doped with a low concentration of yttrium ions, were annealed by heating in air at temperatures ranging from 572° to 1292° F (300° to 700° C) for 2 h. Subsequent x-ray diffraction indicated the sample consisted of an anatase-brookite mixture similar to undoped titanium oxide. The EXAFS measurements indicated yttrium is not distributed throughout the nanoparticles (Fig. 1); it combines with oxygen to form yttrium-oxide clusters that are confined to the titania nanoparticle surface. Approximately 15% of the surface oxygen is bound to the yttrium in single-atom, yttrium-oxide (Y-O) bonds. Because crystalline surface curvature is reduced (by coarsening) when the doped titania is heated, electrical interaction between the nanoparticle and yttrium-oxide cluster is reduced, thereby reducing the Y-O bond length.

Through the pair distribution function fit of the WAXS data (Fig. 1), the researchers observed that both the phase transformation (anatase-to-rutile) and particle coarsening are suppressed when yttrium is introduced into the titania nanocrystal. Surprisingly, there was a complete absence of the rutile phase in temperatures below 1112° F (600° C). This is in contrast to undoped anatase that typically begins transformation to rutile at approximately 572° F (300° C).

The inhibition of coarsening (thereby reducing particle growth) of the yttrium-doped titania was also detected. Yttrium-free anatase nanoparticles generally grow from 6 to 30 nm after undergoing 2 h of annealing at 977° F (525° C). Similarly, the researchers found the yttrium-doped sample grew slowly from 6 to 10 nm at 600° C.

Measurements performed on undoped titania nanoparticles found no parametric changes occurring as a result of increasing temperature within a limited coarsening range of 7 to 10 nm. However, the existence of surface yttrium-oxide clusters has a large impact on the internal nanoparticle structure. Relative to the undoped nanocrystals, the doped samples of both anatase and brookite exhibited unit cell volume increases.

These parametric changes were dependent on both phase and crystallographic orientation. For each given phase (anatase or brookite), different crystal faces experienced different cluster-particle interaction, with one face thermally favored over others. The effect of these surface interactions was a strong suppression of coarsening, with a resultant inhibition of particle growth.

Through measurements and data analyses, the researchers have shown that when low concentrations of surface-restricted ions are introduced to nanoparticles, both structural and material properties are affected. Specifically, with yttrium doping of titanium oxide, nanoparticle growth is suppressed, which results in the stabilization of phase over temperature ranges up to 700° C. Phase stabilization allows

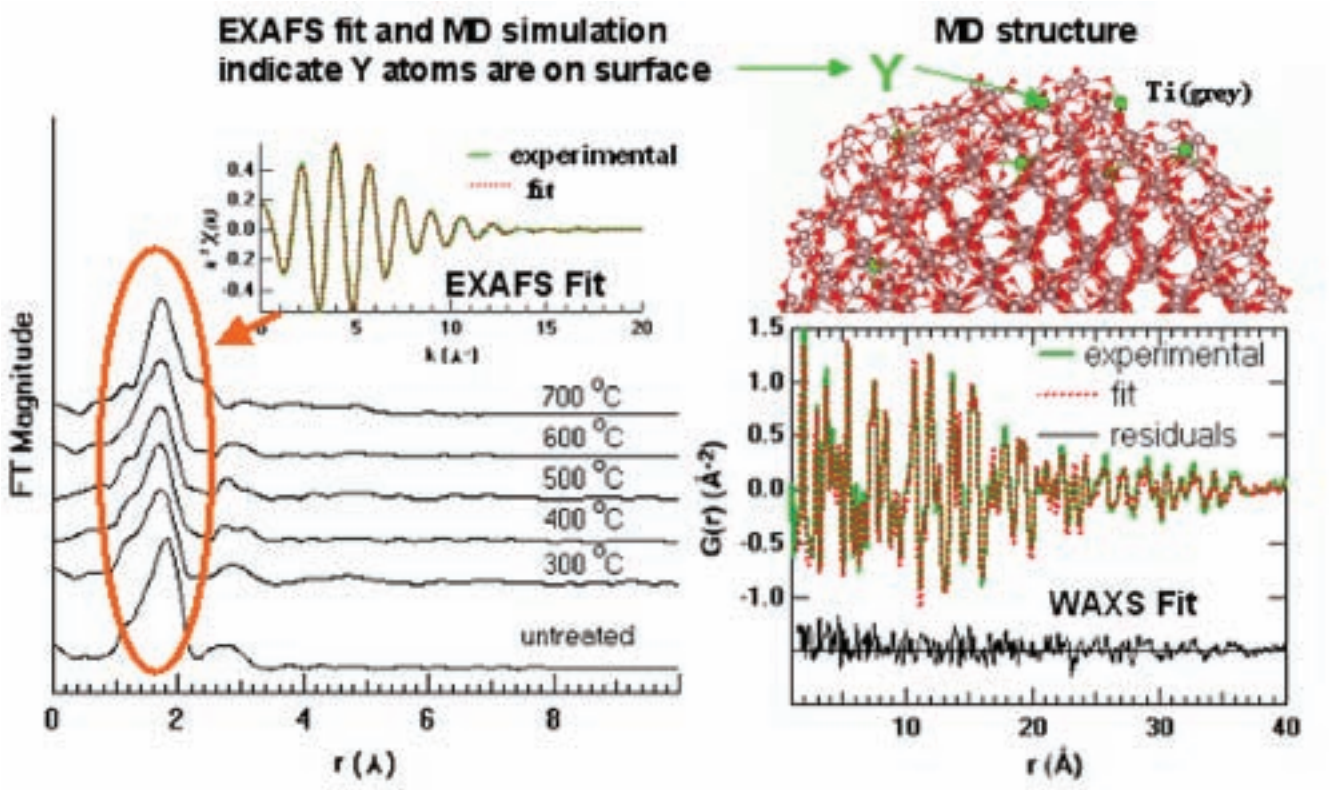

Fig. 1. Fourier transform magnitude of k3-weighted Y *K*-edge EXAFS spectra of yttrium-doped TiO_2 nanoparticles as a function of treatment temperature (left). Distribution of Y atoms (green) at the surface of a 4-nm anatase particle given by a molecular dynamics simulation (right top). The fit (dashed red) of a representative pair distance function (from WAXS measurements) of yttrium-doped TiO_2 nanoparticles (right bottom).

for longer retention of the material properties of nanoparticles under thermal heating conditions.

— Patricia E. Panatier and William Arthur Atkins

See: Bin Chen[1]*, Hengzhong Zhang[1], Benjamin Gilbert[2], and Jillian F. Banfield[1,2], "Mechanism of Inhibition of Nanoparticle Growth and Phase Transformation by Surface Impurities," Phys. Rev. Lett. **98**, 106103 (9 March 2007).
DOI: 10.1103/PhysRevLett.98.106103

Author affiliations: [1]Earth and Planetary Science, University of California, Berkeley; [2]Earth Science Division, Lawrence Berkeley National Laboratory
Correspondence: *binchen@berkeley.edu

Financial support for this work was provided by the U.S. Department of Energy (Grants No. DE-FG03-01ER15218 and DE-AC02-05CH11231) and the National Science Foundation (Grant No. EAR-0123967). Use of the Advanced Photon Source was supported by the U.S. Department of Energy, Office of Science, Office of Basic Energy Sciences, under Contract No. DE-AC02-06CH11357.

5-ID-B,C,D • DND-CAT • Materials science, polymer science • Powder diffraction, x-ray reflectivity, small-angle x-ray scattering, surface diffraction, wide-angle x-ray scattering, x-ray standing waves, x-ray optics development/techniques • 3.3-cm Undulator A • Accepting general users

11-ID-C • XOR/BESSRC • Materials science, geoscience, physics, chemistry • Diffuse x-ray scattering, high-energy x-ray diffraction, pair-distribution function • 2.3-cm undulator • Accepting general users

Solving the Riddle of Ferrihydrite's Elusive Structure

Ferrihydrite is a nanocrystalline iron hydroxide that occurs naturally at the interface of soil and water. Because of its large surface area and reactivity properties, it readily adsorbs heavy metals such as arsenic and is used to clean up mine wastewater and contaminated soils, and to purify drinking water. Despite its ubiquity and utility, its structure has remained a mystery. Researchers using the pair distribution function (PDF) obtained by Fourier transformation of total x-ray scattering at XOR beamlines 1-ID-C and 11-ID-B at the APS have recently refined the structural model and resolved the molecular formula of this intriguing material. The team, from SUNY Stony Brook, Argonne, and Temple University, was able to reveal a structural model not previously anticipated on the basis of data collected using conventional x-ray diffraction and transmission electron microscopy (TEM).

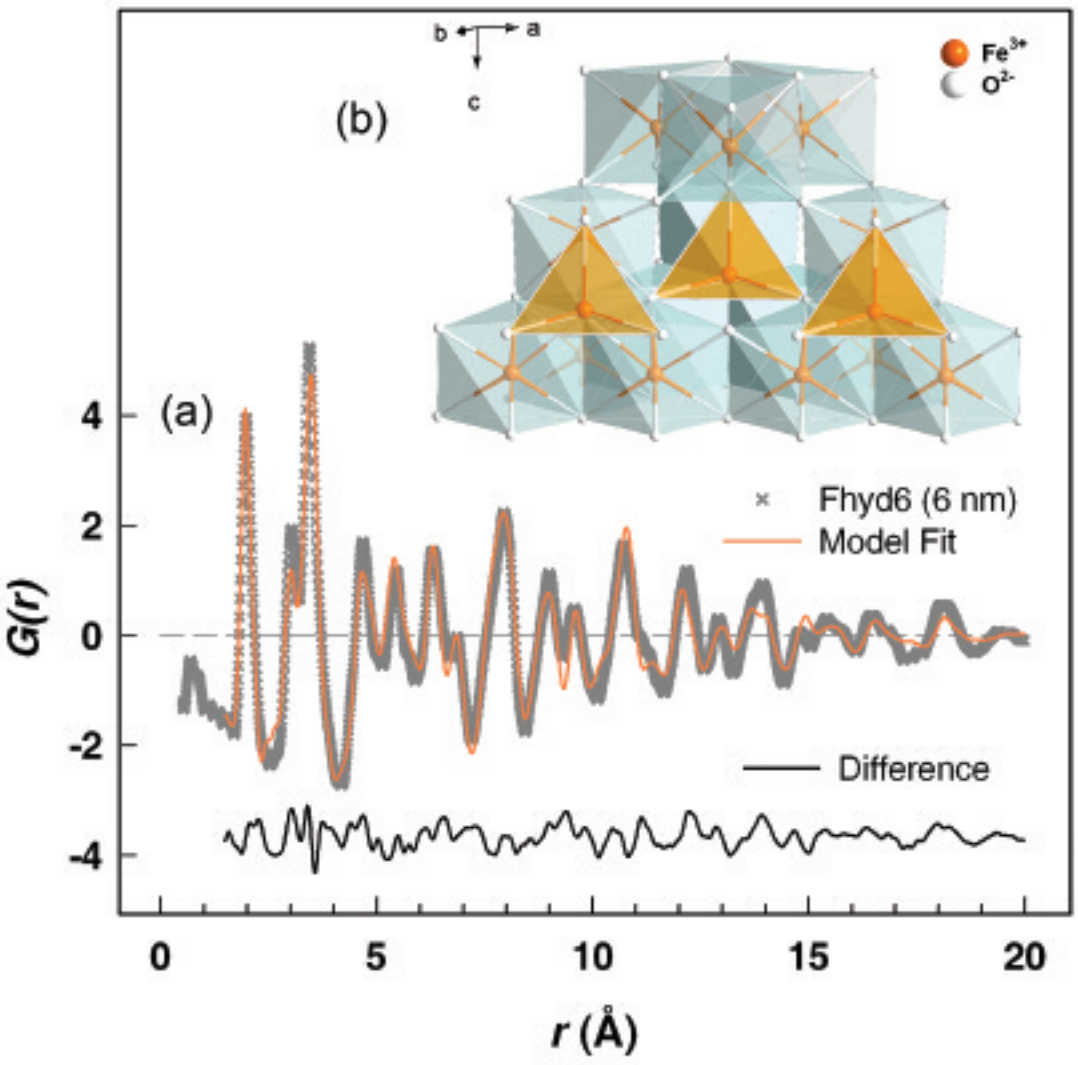

A key obstacle in determining the structure of this nanocrystalline material, which is considered a mineral in spite of the uncertainty surrounding its structure and composition, is its very small particle size, usually less than 10 nm. With well-ordered bulk materials, Bragg reflections occur as well-defined peaks, but with such small particles, the features in the diffraction patterns are broadened and have a significant diffuse component beneath the main peaks. At the nanoscale, PDF analysis of total scattering (with x-rays or neutrons)—combining weak Bragg peaks and broad, diffuse scattering—provides more detailed information about the three-dimensional structure of materials that lack long-range periodicity. The diffraction patterns characteristic of ferrihydrite may in fact be a result of internal disorder, stacking faults, and/or surface relaxation.

Traditional crystallographic methods such as diffraction and x-ray absorption spectroscopy are sufficient to measure long- or short-range order, respectively. The PDF method provides a comprehensive view of a structure because it reveals the short-, intermediate-, and long-range order. Recently published results by these researchers, who used high-energy x-ray total scattering combined with PDF analysis at XOR beamlines 1-ID-C and 11-ID-B, laid the groundwork for this revision of the structural model of ferrihydrite at the atomic scale, placing in doubt the accepted observation obtained from traditional crystallographic methods that ferrihydrite occurs in two distinct structural forms, 2-line and 6-line [1]. This study revealed that the structural motif for 2-, 3-, and 6-nm ferrihydrite is the same whether in powder form or dispersed in aqueous media.

In the current study, the team synthesized three preparations of ferrihydrite ranging from 2 nm to 6 nm and compared the real-space measurements of observed samples with potential structural models using the PDF method. They determined that the experimental PDFs conformed better to a single-phase model not previously proposed (Fig. 1, a and b). In addition, they calculated the ideal chemical formula for ferrihydrite as $Fe_{10}O_{14}(OH)_2$ with varying amounts of surface-adsorbed water, dependent on particle size.

A further impediment to resolving the structure of this and other nanoscale materials is the invasive nature of certain structure determination methods. A recent study using electron energy loss spectroscopy showed that increasing electron doses from TEM probes caused the ferric iron (Fe^{3+}) to be reduced to ferrous iron (Fe^{2+}) and to migrate from octahedral to tetrahedral sites in the structure. This suggests that investigations carried out with a focused electron beam may cause unwanted changes in a sample. In addition, the high-vacuum conditions necessary to perform TEM probes may also cause undetected structural changes.

Though this study solves the basic structural framework of ferrihydrite, it does not address the precise position of the hydrogen molecules. Further studies using neutron total scattering will one day provide an even more complete model and better understanding of the chemical, magnetic, and physical properties of this useful nanocrystalline material.

— Elise LeQuire

< Fig. 1. (a) The experimental PDF for 6-nm ferrihydrite (grey x) is overlain by the calculated model fit of the new ferrihydrite model (solid orange). The difference between the calculated and experimental results is shown below (solid black). (b) In ideal form, the basic structural motif for ferrihydrite has 20% tetrahedral and 80% octahedral iron.

Reference

[1] F.M. Michel, L. Ehm, G. Liu, W.Q. Han, S.M. Antao, P.J. Chupas, P.L. Lee, K. Knorr, H. Eulert, J. Kim, C.P. Grey, A.J. Celestian, J. Gillow, M.A.A. Schoonen, D.R. Strongin, and J.B. Parise, Chem. Mater. 19 (6) 1489 (2007). DOI: 10.1126/science.1142525

See: F. Marc Michel[1,2]*, Lars Ehm[1,2], Sytle M. Antao[3], Peter L. Lee[3], Peter J. Chupas[3], Gang Liu[1,4], Daniel R. Strongin[1,4], Martin A.A. Schoonen[1,2], Brian L. Phillips[1,2], and John B. Parise[1,2,5], "The Structure of Ferrihydrite, a Nanocrystalline Material," Science **316**, 1726 (22 June 2007).
DOI: 10.1126/science.1142535

Author affiliations: [1]Center for Environmental Molecular Science, SUNY Stony Brook; [2]Department of Geosciences, SUNY Stony Brook; [3]Advanced Photon Source, Argonne National Laboratory; [4]Department of Chemistry, Temple University; [5]Department of Chemistry, SUNY Stony Brook
Correspondence: *fmichel@ic.sunysb.edu

Support was provided by the Center for Environmental Molecular Science and the National Science Foundation Awards: CHE0221934, DMR-045244, and EAR-0510501, and also by the U.S. Dept. of Education through the GAANN Program Sponsor ID: P200A060248. Use of the APS was supported by the U.S. Department of Energy, Office of Science, Office of Basic Energy Sciences, under Contract No. DE-AC02-06CH11357.

1-ID-C • XOR • Materials science, physics, chemistry • High-energy x-ray diffraction • 3.3-cm Undulator A • Accepting general users

11-ID-B • XOR/BESSRC • Chemistry, environmental science, materials science • High-energy x-ray diffraction, pair distribution function • 3.3-cm Undulator A • Accepting general users

The EDL Interface Structure of Rutile Titanium Dioxide: A Key to New Applications?

When an oxide mineral, such as rutile titanium dioxide (TiO_2), comes into contact with an aqueous solution, an electrical double layer (EDL) develops that redistributes the water molecules and aqueous ions at the solid-electrolyte interface. While nearly all studies of EDL phenomena implicitly assume that the oxide surface structure itself remains unaffected, experiments conducted at several XOR beamlines at the APS using rutile TiO_2 indicate that structural changes do occur and extend unexpectedly far into the bulk crystal. The discoveries arising from these experiments detail key elements of the EDL that may be central to a fundamental understanding of ion adsorption, dissolution/precipitation rates and mechanisms, heterogeneous catalysis, and other EDL-related phenomena.

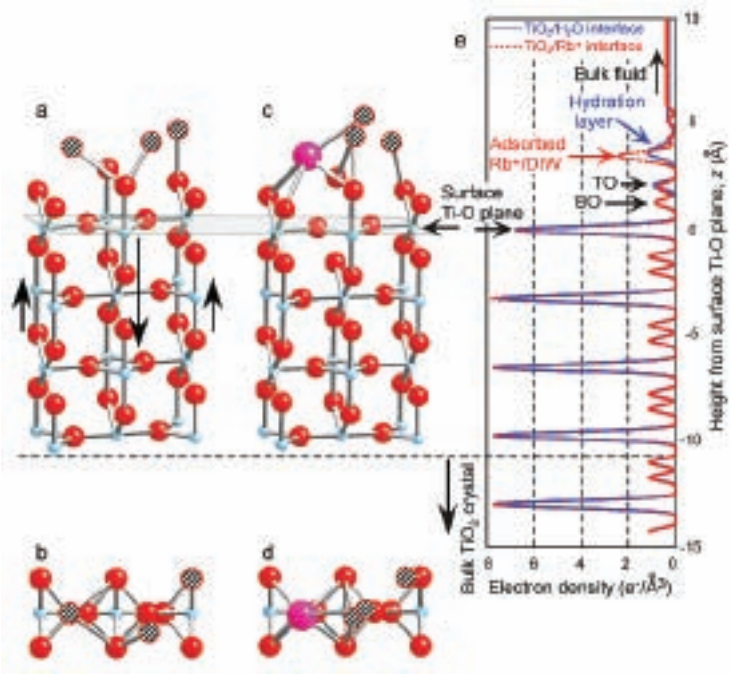

Fig. 1. A ball-and-stick model of the best-fit rutile (110)-aqueous solution interfaces. Perspective (a) and top (b) views of the interface in DIW. (c) Perspective and (d) top views of the interface in the RbCl solution. The small (cyan), medium (red), and large (pink) spheres represent Ti, O, and Rb^+, respectively, while the hatched circles represent H_2O. The arrows in (a) indicate the relaxation directions of the bulk Ti atoms in the vertical planes underneath BO (edges) and TO (center) rows. (e) Laterally averaged electron density profile for rutile (110) surface in DIW and the RbCl solution. The increase of the electron density above the TO site in 1 *m* Rb^+ indicates the specific adsorption of Rb^+ ions, displacing the water molecules that are specifically adsorbed in DIW.

These experiments detail key elements of the electronic double layer that may be central to a fundamental understanding of ion adsorption, dissolution/precipitation rates and mechanisms, heterogeneous catalysis, and other phenomena

The researchers, from Argonne, the University of Illinois at Chicago, Northwestern University, the Illinois State Water Survey, and Oak Ridge National Laboratory, made their discoveries using the crystal truncation rod (CTR) method, which is the interfacial analog of bulk x-ray crystallography, in that interfacial signals appear as continuously modulated rods (called "crystal truncation rods") of intensity extending from each Bragg peak. After a rutile TiO_2 crystal was mounted in ultra-filtered deionized water (DIW), a full set of CTR measurements was taken for the TiO_2-DIW interface. Then a 1-molal (m) RbCl + RbOH solution at pH 12 was exchanged into the sample cell, and another full set of CTR data was measured. The measurements were performed primarily at XOR beamline 1-BM-B,C at the APS, with preliminary work being done at XOR/BESSRC beamlines 11-ID-D, 12-BM-B, and 12-ID-B,C,D.

The rutile surface in both solutions was found to consist of a stoichiometric (1 × 1) surface unit mesh whose surface is terminated by bridging oxygen (BO) and terminal oxygen (TO) sites, with a mixture of water molecules and hydroxyl groups occupying the TO sites. An additional hydration layer was found above the TO site, with three distinct water adsorption sites, each having well-defined vertical and lateral locations. Rb^+ was seen to adsorb specifically at the tetradentate site between the TO and BO sites, replacing one of the adsorbed water molecules at the interface (Fig. 1). No further ordered water structure was observed above the hydration layer.

Ti atom displacements from their bulk lattice positions were found to be sensitive to solution composition. Displacements as large as 0.05 Å at the rutile (110)-DIW interface decayed in magnitude into the crystal, becoming ~0.01 Å at the fourth Ti layer below the surface. A systematic outward shift was observed for Ti atom locations below the BO rows, while systematic inward displacements were found for Ti atoms below the TO rows. The Ti displacements were mostly reduced when the oxide was in contact with the RbCl solution, there being no statistically significant displacements in the fourth-layer Ti atoms.

The distances of adsorbed Rb^+ ions to surface oxygens in the BO and TO sites were similar to the average bond length of hydrated Rb^+ in a bulk aqueous solution. This indicates that four of the hydrating water molecules are replaced by four surface oxygens when Rb^+ sorbs at the tetradentate site, to form an inner-sphere species. This observation provides definitive proof that "background electrolyte" ions compete directly with multivalent ions for sorption at inner-sphere sites, although the sorption affinities of the multivalent ions are much stronger, due to the increased cation charge. This competition for sorption at inner sphere sites provides a partial explanation for the often-observed ionic strength dependence of multivalent cation adsorption on metal oxide surfaces. — *Vic Comello*

See: Zhan Zhang[1]*, Paul Fenter[1], Neil C. Sturchio[2], Michael J. Bedzyk[1,3], Michael L. Machesky[4], and David J. Wesolowski[5], "Structure of rutile TiO_2 (110) in water and 1 molal Rb^+ at pH 12: Inter-relationship among surface charge, interfacial hydration structure, and substrate structural displacements," Surf. Sci. **601**, 1129 (2007).
DOI:10.1016/j.susc.2006.12.007
Author affiliations: [1]Argonne National Laboratory, [2]University of Illinois at Chicago, [3]Northwestern University, [4]Illinois State Water Survey, [5]Oak Ridge National Laboratory
Correspondence: *zhanzhang@anl.gov

The work was supported by the U.S. Department of Energy, Office of Science, Office of Basic Energy Sciences, Chemical Sciences, Geosciences, and Biosciences Division. Use of the APS was supported by the U.S. Department of Energy, Office of Science, Office of Basic Energy Sciences, under Contract No. DE-AC02-06CH11357.

1-BM-B,C • XOR • Physics, materials science, chemistry • Powder diffraction • Bending magnet • Operational

11-ID-D • XOR/BESSRC • Chemistry, geoscience, materials science • X-ray absorption fine structure (XAFS), general diffraction, time-resolved XAFS • 3.3-cm Undulator A • Accepting general users

12-BM-B • XOR/BESSRC • Materials science, geoscience, chemistry, polymer science, physics, environmental science • X-ray absorption fine structure (XAFS), fluorescence spectroscopy, powder diffraction, x-ray reflectivity, general diffraction • Bending magnet • Accepting general users

12-ID-B,C,D • XOR/BESSRC • Chemistry, physics, materials science • Small-angle x-ray scattering, wide-angle x-ray scattering, grazing Incidence small-angle scattering • 3.3-cm Undulator A • Accepting general users

Clarifying the Phase Transition in $SrTiO_3$

The antiferrodistortive structural phase transition in strontium titanate ($SrTiO_3$) is widely regarded as a prototype suitable for testing basic theories and concepts of phase transitions. For the most part, it is a second-order displacive phase transition governed by the softening of a zone boundary phonon mode (R_{25}), describing an antirotation of the oxygen octahedral, which results in a superlattice below the critical temperature $T_C \approx 105$K. Researchers using two APS beamlines combined x-ray thermal diffuse scattering (TDS) and the first-ever observation of a static coherent diffraction pattern (speckle pattern) within the anomalous critical scattering of $SrTiO_3$ to clarify several remaining issues concerning the phase transition. Their unified x-ray experiment studied both the critical phonon softening and anomalous critical scattering over a wide temperature range—from room temperature to the structural phase transition. The TDS experiment was performed at XOR/UNI 33-ID-D,E beamline at the APS, while the coherent diffraction images were obtained at the XOR 8-ID-E beamline, also at the APS.

Previous neutron experiments characterized the constituent R25 phonon frequency softening, but were unable to study critical softening behavior near the transition. The neutron results were also limited to a sparse data set above the transition. Analysis of the x-ray TDS line shape allowed the researchers, from Argonne, McGill University, and the University of Illinois at Urbana-Champaign, to establish mean-field and critical behavior of the dynamic lattice fluctuations of the system with a high degree of precision. The results of their TDS analysis agree well with the predictions of mean-field theory and available experimental data over a wide temperature range, and they confirm renormalization group predictions of critical behavior in the near-transition region.

The central peak critical scattering component has been previously observed in x-ray data at temperatures well above T_C and has been the subject of much debate, because this feature could represent a second critical length scale of the system, in principle, violating the scaling hypothesis central to many modern theories of phase transitions. The researchers' first-ever observation of a coherent speckle pattern within the central peak critical scattering shed new light on the nature and dynamics of this anomalous feature (Fig. 1). Speckle analysis led the researchers to the following conclusions regarding the central peak: (a) it is caused by Bragg diffraction from a remnant disordered state above T_C, (b) this disorder is static on all observed time scales and reproducible under thermal cycling, (c) the length scale of this disorder is comparable with the observed defect density, and (d) the criticality of this component is separate from the bulk phase transition. Accordingly, the researchers conclude that the anomalous central peak feature is a simple static mixture of high- and low-temperature structures pinned to defects within the scattering volume.

The researchers' method of complementing synchrotron x-ray TDS analysis with time-resolved observation of a coherent speckle pattern holds great potential for elucidating static and dynamic fluctuations in a wide range of critical systems of interest to materials studies. — *Vic Comello*

See: M. Holt[1]*, M. Sutton[2], P. Zschack[3], H. Hong[3], and T.-C. Chiang[3,4], "Dynamic Fluctuations and Static Speckle in Critical X-ray Scattering from $SrTiO_3$," Phys. Rev. Lett. **98**, 065501 (2007). DOI: 10.1103/PhysRevLett.98.065501

Author affiliations: [1]Center for Nanoscale Materials, Argonne National Laboratory; [2]Physics Department, McGill University; [3]Frederick Seitz Materials Research Laboratory, University of Illinois at Urbana-Champaign; [4]Department of Physics, University of Illinois at Urbana-Champaign
Correspondence: *mvholt@aps.anl.gov

H.H. and T.C.C.'s research was supported by DOE-BES under Contract No. DEFG02-91ER45439. The Petroleum Research Fund, administered by the American Chemical Society, and the NSF(Grant No. DMR-05-03323) provided partial equipment and personnel support. Use of the APS was supported by the U.S. Department of Energy, Office of Science, Office of Basic Energy Sciences, under Contract No. W-31-109-38.

33-ID-D,E • XOR/UNI • Materials science, physics, chemistry • Anomalous and resonant scattering (hard x-ray), diffuse x-ray scattering, x-ray reflectivity, surface diffraction, x-ray standing waves, general diffraction • 3.3-cm Undulator A • Accepting general users

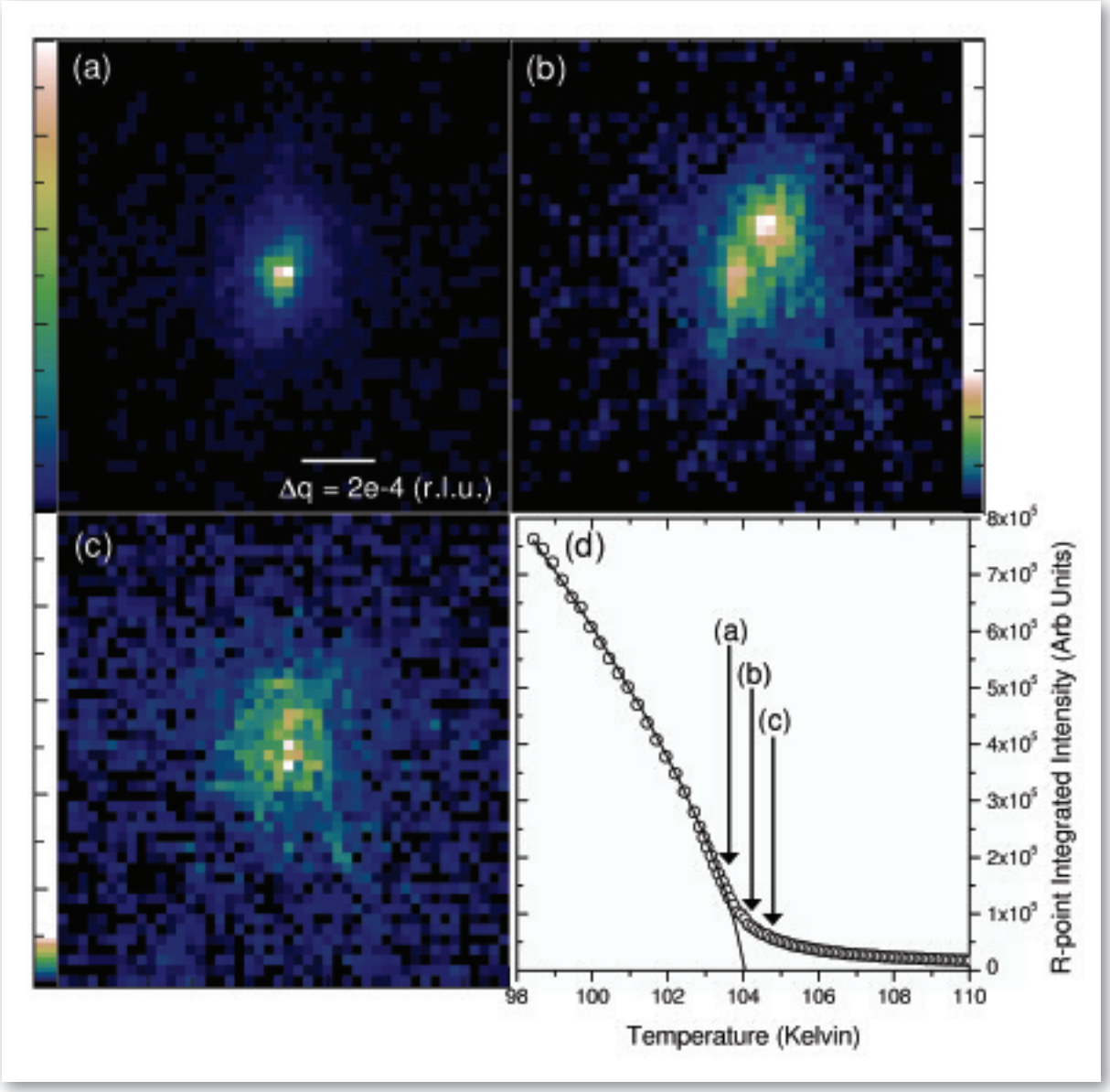

Fig. 1. The observation of a static speckle pattern within critical x-ray scattering from $SrTiO_3$ reveals the abrupt onset of anomalous static disorder (frames (a) through (c)) above the bulk phase transition temperature (shown for reference in frame (d)).

Phonon Density of States of Tin at High Pressures

Heretofore, scientists have not been able to determine experimentally the dynamics of atomic lattice vibrations for elemental tin (Sn) at high pressures. Now, researchers using XOR beamline 3-ID-B,C,D at the APS and the Nuclear Resonance Group beamline ID22N at the European Synchrotron Radiation Facility have obtained the first measurements of the quantized vibrational (phonon) density of states (DOS) in tin at high pressures—up to 64 GPa—by using nuclear resonant inelastic x-ray scattering (NRIXS). In condensed matter physics, DOS is the property that helps characterize and quantify the energy levels in a quantum physical system. The researchers also found a positive correlation between their experimental findings and their density functional theory calculations. Based on the results from the phonon DOS, the researchers can now derive several thermodynamic quantities that are important to a better understanding of tin and similar metals—and ultimately, of compounds—under high pressures.

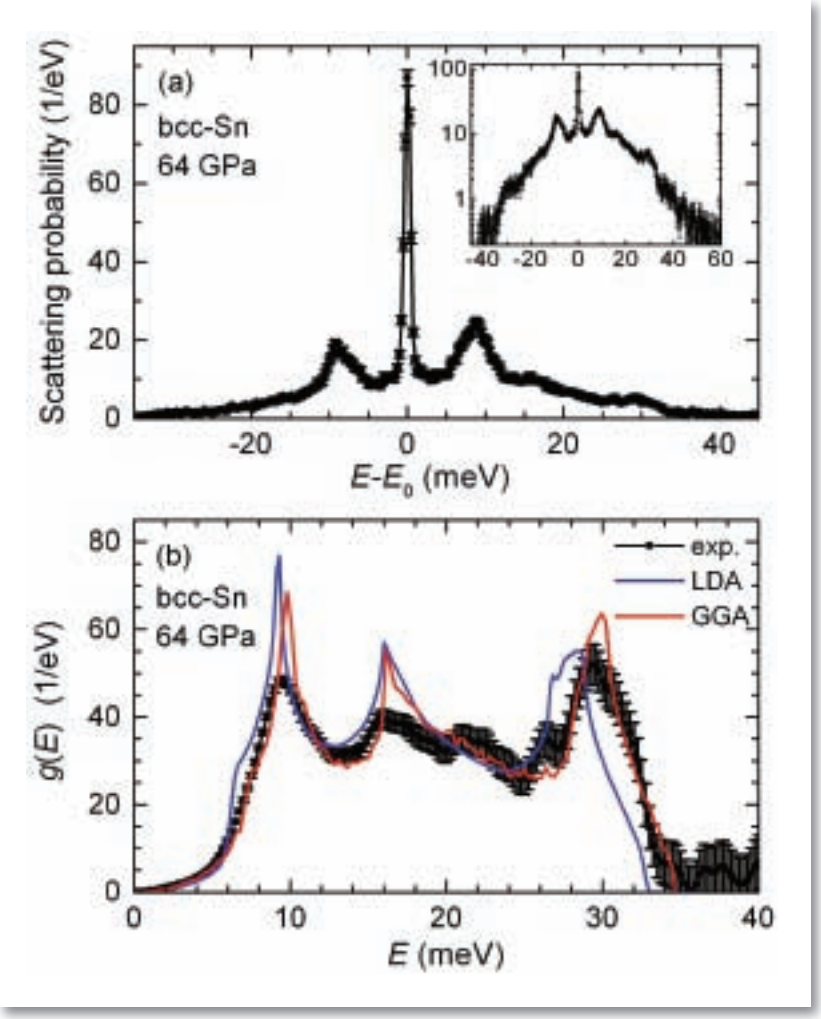

The NRIXS experiments performed by the researchers from the University of Nevada, Las Vegas; Los Alamos National Laboratory; East China Normal University; Wilbur Wright College; and Argonne used metallic tin enriched to 93% in the isotope of tin with nuclide symbol ^{119}Sn. Tin has several polymorphic modifications and phase transitions:

- Sn-I (gray tin or α-Sn): at ambient pressure, low-temperature phase is stable to 287K (14° C);
- Sn-II (white tin or β-Sn): at ambient pressure, the high-temperature phase is stable between 287K and the liquid phase at 505K (14 and 232° C, respectively);
- Phase transition of Sn-II to Sn-III: at ambient temperature at a pressure of 9.4 GPa;
- Sn-III: body-centered tetragonal,stable at ambient temperature between 9.4 and 45 ± 5 GPa;
- Phase transition of Sn-III to Sn-IV: at ambient temperature at about 45 ± 5 GPa; and
- Sn-IV: body-centered cubic, stable phase at ambient temperature between 45 ± 5 GPa up to at least 120 GPa.

At ambient conditions, the collaborators conducted their experiments with the Sn-II metal placed between two pieces of adhesive tape that was then placed between avalanche photodiode detectors (APDs). For measurements at ambient temperature and a pressure of 4.6 and 13.1 GPa, the metallic Sn was loaded into a beryllium gasket in a Paderborn-type diamond anvil cell (DAC). At pressures of 37 and 64 GPa, the research was performed using rhenium as the gasket material. A new gasket design made possible the use of this highly absorbent material.

A mixture of four parts methanol and one part ethanol was used to transmit the pressure, which was measured using spherical ruby crystals. Energy ranges of ± 60 meV for 0 and 4.6 GPa; and ± 70 meV for 13.1, 37, and 64 GPa were scanned in 0.25-meV increments.

At the highest pressure—64 GPa—multiphonon excitation contributions are effectively suppressed, making the extracted phonon DOS of Sn-IV very reliable. As expected, increasing pressure causes an increase in phonon energies. These experimental results (Fig. 1) provide a reliable comparison with the calculated (theoretical) results—for both the magnitude and energies of the spectra. Similar agreement between experimental and theoretical DOS was achieved at lower pressures.

< Fig. 1. (top) NRIXS signal after normalization of the body centered cubic (bcc) tin (the Sn-IV phase) at 64 GPa. The inset shows a logarithmic plot of the signal. E is the energy and E_0 is the Mössbauer resonance at 23.88 keV. (bottom) $g(E)$, the phonon DOS of tin at 64 GPa. The black graph represents the experimental result, whereas the blue graph shows the theoretical local density approximation (LDA) result and the red graph the theoretical generalized gradient approximation (GGA) from calculation.

From these results, elastic and thermodynamic quantities—such as Lamb-Mössbauer factor, mean force constant, vibrational contribution to the Helmholtz free energy, high- and low-temperature Debye temperatures, and Debye average phonon velocity—were obtained. These quantities are important for understanding the properties of tin, especially with regard to lattice dynamics and construction of the pressure-temperature phase diagram. The theoretical phonon DOS, which uses the generalized gradient approximation (GGA) calculation, produces these quantities in better agreement over the highest pressures—up to the maximum of 64 GPa—rather than at lower pressures, although agreement was good at these pressures, too.

By producing reliable phonon DOS of tin at high pressures, the researchers are providing accurate thermodynamic descriptions of tin and similar metals, as well as establishing consistency between historic theoretical models and recent experimental data. Such research in the prediction of bonding and interatomic forces in solids is important to the advancement of condensed matter physics. Because of this work, better theoretical models can be produced and ultimately, greater understanding is possible, which can lead to further technological advances. — *William Arthur Atkins*

See: Hubertus Giefers[1], Elizabeth A. Tanis[1], Sven P. Rudin[2], Carl Greeff[2], Xuezhi Ke[1,3], Changfeng Chen[1], Malcolm F. Nicol[1], Michael Pravica[1], Walter Pravica[4], Jiyong Zhao[5], Ahmet Alatas[5], Michael Lerche[5], Wolfgang Sturhahn[5], and Ercan Alp[5]*, "Phonon Density of States of Metallic Sn at High Pressure," Phys. Rev. Lett. **98**, 245502 (2007).
DOI: 10.1103/PhysRevLett.98.245502
Author affiliations: [1]Department of Physics and High Pressure Science and Engineering Center, University of Nevada, Las Vegas; [2]Los Alamos National Laboratory; [3]Department of Physics, East China Normal University; [4]Wilbur Wright College; [5]Advanced Photon Source, Argonne National Laboratory
Correspondence: *eea@aps.anl.gov

This work was supported by the U.S. Department of Energy Cooperative Agreement No. DEFC52-06NA26274 with the University of Nevada, Las Vegas. S. P. R. and C. G. are supported by the Department of Energy under Contract No. W-7405-Eng-36. Use of the APS was supported by the U.S. Department of Energy, Office of Science, Office of Basic Energy Sciences, under Contract No. DE-AC02-06CH11357.

3-ID-B,C,D • XOR • Physics, geoscience, life science, chemistry, materials science • Nuclear resonant scattering, high-pressure diamond anvil cell, inelastic x-ray scattering • 2.7-cm undulator • Accepting general users

Spotting Grown-in APBs Using Coherent X-ray Diffraction

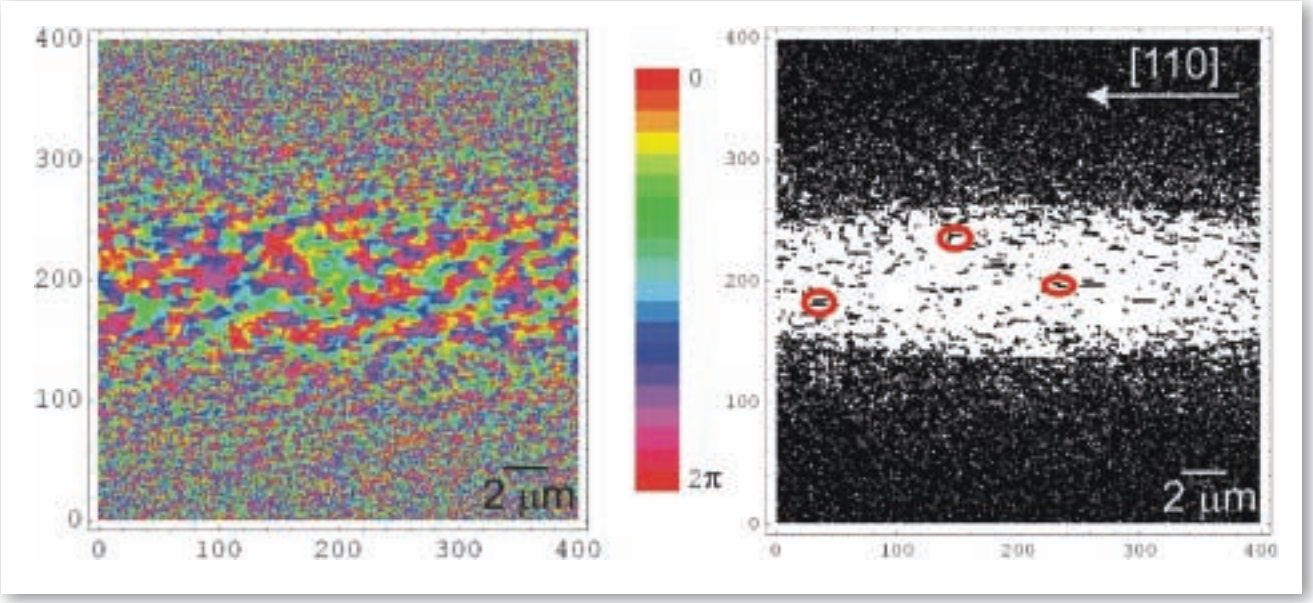

Fig. 1. Left: typical reconstructed phases showing a characteristic nonrandom patchwork structure in the region of the elliptic object support. Right: Derived phase jumps indicating APBs. Red ellipses designate examples of locally unique APB structures that were identified in all reconstruction runs.

Coherent x-ray diffraction measurements made at the APS offer an appealing alternative to transmission electron microscopy because delicate structures remain undisturbed, antiphase domains can be much larger, and x-rays can probe much thicker specimens

Coherent x-ray diffraction, used by itself, is one of the most promising methods for imaging the structure of large individual objects, such as those found in the life and materials sciences, and has been the focus of much recent experimentation. An advantage of the technique is its lack of reliance on x-ray lenses, which makes imaging resolution diffraction-limited, at least in principle. Researchers from Universität Wien and University College London, demonstrated the utility of the method by imaging grown-in antiphase boundaries (APBs) in the *B2*-ordered metal alloy $Fe_{65}Al_{35}$. The coherent x-ray diffraction measurements made at the XOR/UNI 34-ID-C,E undulator beamline at the APS offer an appealing alternative to transmission electron microscopy (TEM), because the necessary thinning procedures in TEM sample preparation would likely disturb delicate structures like APBs. Moreover, antiphase domains can be much larger than the sample thickness acceptable for TEM investigations. X-rays, by contrast, can probe much thicker specimens.

Intermetallic alloys often exhibit superstructures that are not perfectly established over a whole crystal, because the superstructures start to grow from different nucleation sites in a sample. That is why antiphase domains that are separated by APBs form. Because of this disorder, coherent x-ray scattering produces a so-called speckle pattern in the superstructure peaks that is an exact expression of the arrangement of scattering centers.

Imaging the APBs required that the researchers overcome two major difficulties. First, antiphase domains are usually established over a whole crystal, either in bulk or as a thin film. This means that the size of the sample volume is necessarily defined by the x-ray beam, making an exact knowledge of the beam profile mandatory. Second, APBs are purely phase objects, because adjacent antiphase domains consist of essentially the same kinds of atoms. As a result, the contrast between adjacent domains results simply from differing phase shifts among the photons scattered from each domain.

The (001) superstructure diffraction peak of the *B2*-ordered bulk $Fe_{65}Al_{35}$ sample was measured by using a direct illumination charge-coupled device (CCD) camera mounted on a goniometer arm. Inverting the fine structure within the peak was accomplished by means of iterative algorithms that Fourier transform between reciprocal and real space, with appropriate constraints being applied in each domain. Because the sample object was bigger than the x-ray beam footprint, it was essential to know the precise beam profile to define the real-space constraint that was used. The illumination function of the beam was measured by using an optical microscope with a fluorescent plate placed at the sample position. The optical microscope, which was connected to the CCD camera, also helped control further beam focusing with Kirkpatrick-Baez mirrors.

The researchers found phase jumps that they attributed to grown-in APBs. Although a unique long-range structure could not be derived, the iterative algorithms found phase structures that were locally unique (Fig. 1). These were identified in all the reconstruction runs by means of a cross-correlation analysis. The characteristic APB morphology that was obtained revealed nearly planar APB walls on {110} planes terminating at grown-in dislocations, a result that was confirmed by TEM results from the same sample.

— *Vic Comello*

See: Lorenz-M. Stadler[1†*], Ross Harder[2], Ian K. Robinson[2], Christian Rentenberger[1], H.-Peter Karnthaler[1], Bogdan Sepiol[1], and Gero Vogl[1], "Coherent X-ray Diffraction Imaging of Grown-in Antiphase Boundaries in $Fe_{65}Al_{35}$," Phys. Rev. B **76**, 014204 (2007). DOI: 10.1103/PhysRevB.76.014204

Author affiliations: [1]Fakultät für Physik, Universität Wien; [†]Present address: HASYLAB at DESY, Hamburg, Germany [2]London Centre for Nanotechnology and Department of Physics and Astronomy, University College London
Correspondence: *lorenz.stadler@desy.de

Two of the researchers (I.K.R. and R.H.) were supported by EPSRC Grant No. EP/D052939/1 and NSF Grant No. DMR 03-08660. APS beamline 34-ID-C was operated by the Materials Research Laboratory of the University of Illinois under DOE Contract No. DEFG02-91ER45439. The work was financially supported by the Austrian Federal Ministry for Education, Science, and Culture (Contract No. GZ45.529/2-VI/B/7a/2002), the Austrian Science Fund (Contract No. P17775-N02), and the EU Specific Targeted Research Project DYNASYNC (Contract No. NMP4-CT-2003-001516). Data were evaluated using the Schrödinger II(I) cluster of the Vienna University Computer Center. Use of the APS was supported by the U.S. Department of Energy, Office of Science, Office of Basic Energy Sciences, under Contract No. DE-AC02-06CH11357.

34-ID-C,E • XOR/UNI • Materials science, physics • Coherent x-ray scattering, microdiffraction • 3.3-cm Undulator A • Accepting general users

Flow Visualization Using Fast X-ray Phase-Contrast Imaging

Applications as diverse as arterial blood flow and polymer processing are pointing up the need for a new way of visualizing particle-laden liquid transport that is capable of making velocity measurements on tracer particles at high concentrations in a multiphase flow environment, even with particles that vary greatly in size. Such a method was recently developed by researchers using the XOR 7-ID-B,C,D and 32-ID-B,C beamlines at the APS, who demonstrated a particle tracking velocimetry technique based on x-ray phase-contrast imaging that is capable of measuring the velocities of tracer particles of varying size embedded in a flow field moving through an optically opaque vessel (Figs. 1 and 2). This unique technique can be easily extended to such vastly different applications as flow cytometry, DNA analysis, and flows in microfluidic devices that are fabricated on a sub-millimeter scale.

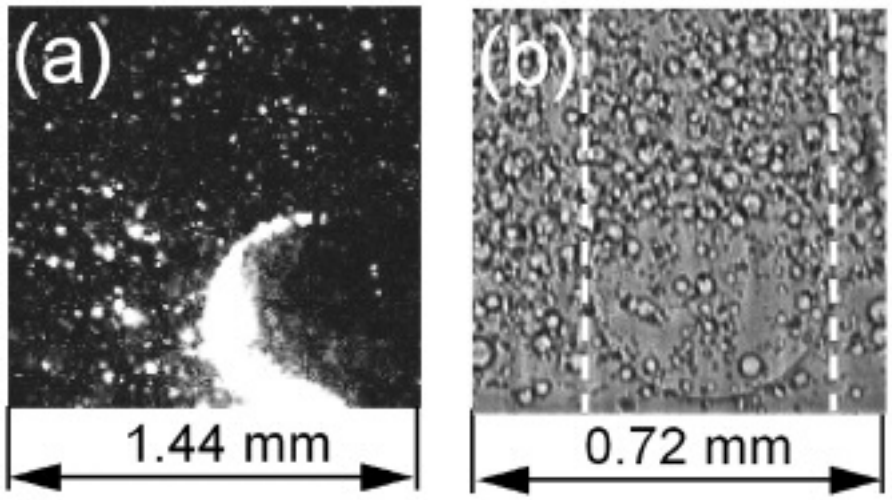

Fig. 1. Interaction flow of small fluid particles around a big particle between the vertical broken lines: a comparison between (a) visible light image and (b) x-ray phase-contrast image.

In the experiments, silver-coated hollow glass spheres with radii ranging from one to hundreds of micrometers were uniformly mixed in a working fluid of pure glycerin and injected into an opaque Teflon® tube having an inner diameter of 860 μm. A steady flow of 2 μL/min was developed using a syringe pump, and a test section area of 1.0 × 1.4 mm^2 defined by the size of the x-ray beam was located downstream from the tube inlet to ensure steady flow there. The transmitted and diffracted x-rays through the flow vessel were converted to visible light by a cerium-doped yttrium aluminum garnet scintillator crystal that was imaged onto a fast charge-coupled device camera.

The researchers from Argonne and Wayne State University collected and correlated 240 consecutive single-shot images taken every 125 ms and having an exposure time of 2.5 ms. Because of the line-of-sight nature of x-ray imaging, correlation can yield only the projected velocity distribution, which cannot in itself provide a statistically valid mean velocity at locations of interest in three-dimensional (3-D) space. To overcome this difficulty, the researchers developed a cross-correlation algorithm based on a direct single-particle tracking technique. The uniqueness of the tracer particles due to their size differences was used to obtain a unique correlation function.

In the case of small particles with a more uniform size distribution, the 3-D velocity distribution was reconstructed by simple single-projection tomography based on the particle density distribution, assuming the axisymmetry of both particle density and velocity in the cylindrical flow; the axisymmetry of the particle distribution was verified by counting the particles both radially and axially. The tomographic reconstruction yielded a 3-D velocity distribution that was in excellent agreement with an analytical solution for circular pipe flows, and the measurement was sensitive enough to show that the velocity of smaller particles was slightly higher than that of larger particles. Although the difference was small, the results agree well with theory and data by other researchers.

With this method, particle size diversity actually facilitates the exact measurement of the velocity field. In addition, x-ray phase contrast imaging provides a single-particle tracking capability that enables a tomographic reconstruction that yields the particle size dependence of the 3-D flow velocity field with unprecedented sensitivity. — *Vic Comello*

See: Kyoung-Su Im[1], K. Fezzaa[1], Y.J. Wang[1], X. Liu[1], Jin Wang[1]*, and M.-C. Lai[2], "Particle Tracking Velocimetry Using Fast X-ray Phase-contrast Imaging," Appl. Phys. Lett. **90**, 091919 (2007). DOI: 10.1063/1.2711372

Author affiliations: [1]Advanced Photon Source, Argonne National Laboratory; [2]Department of Mechanical Engineering, Wayne State University

Correspondence: *wangj@aps.anl.gov

This work and the use of the APS were supported by the U.S. Department of Energy, Office of Science, Office of Basic Energy Sciences, under Contract No. DE-AC02-06CH11357.

7-ID-B,C,D • XOR • Materials science, atomic physics, chemistry • Time-resolved x-ray scattering, radiography, time-resolved x-ray absorption fine structure • 3.3-cm Undulator A • Accepting general users

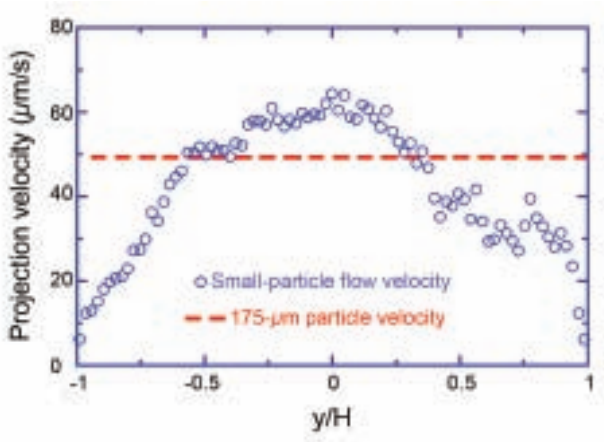

Fig 2. Projected velocity profile of the small particles in Fig. 1 with respect to that for a large particle, which is 175 μm in diameter

Around the Experiment Hall

Looking into the Solar Wind

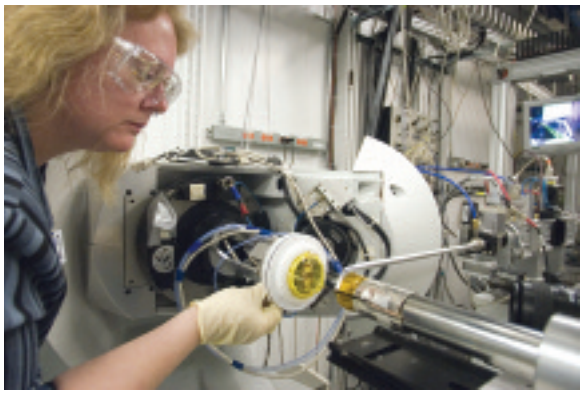

Kathy Kitts in the GSECARS research station, mounting one of the Genesis Probe samples (under the yellow plastic cover) prior to data taking.

What could have been a shattering let-down for NASA's Genesis Discovery Mission has become an opportunity for synchrotron light source science to shine. NASA's Genesis Discovery Mission was a space probe that went out beyond Earth's atmosphere to capture solar wind from our Sun. Kathy Kitts (Northern Illinois University), a Genesis Science Team member, explained the mission and the evolution of the studies she is carrying out at the University of Chicago's GeoSoilEnviroCARS Sector 13 beamline at the APS.

"As the Sun evaporates, the evaporation produces solar wind, and studying the composition of solar wind gives us the perfect resources for determining precisely what the Sun is made of," said Kitts. "These studies are important because they will give us a baseline for developing an understanding of how the solar system has evolved over time and how solar processes and solar wind mechanics behave. We can get a spectrum from the Sun, but we want the absolute details about the abundances of elements in the Sun. We know the Sun is made up of everything in our solar system—mostly hydrogen and helium—so if we know what the Sun is composed of, then we have a baseline for the composition of the solar system.

"The capture mechanisms used in the Genesis Discovery Mission were 10-cm hexagon wafers of sapphire, silicon, and germanium. When the probe encountered the solar wind, it deployed these wafers as detectors and collected a wide range of elements. With different detectors made of different materials, we can look for different things. So for instance, in the germanium wafer, one would not look for germanium because the signal would be undetectable.

"Unfortunately, when the probe came back to Earth exactly on time at exactly the right place, a component problem told the probe that it was falling up, not down, and so it did not deploy its parachute. When the probe impacted in the Utah desert, the hexagons shattered into tiny pieces, from about 2-cm by 1-cm down to microscopic. The shards we're examining at Sector 13 are aluminum on sapphire and silicon on sapphire. The APS and the GSECARS facility are the only ones at present that will enable studies of these tiny wafer fragments, thanks to the x-ray beam brightness. We are skimming the x-ray beam along the flat surface of the wafers at an angle of nearly zero degrees, using the grazing incidence x-ray diffraction technique. This way, we highlight the residue deposited on the top of the shards. When we very slightly change the angle of the sample relative to the x-ray beam, we can see the solar wind material that's trapped inside the detector shard. And straight up-and-down (at 90 degrees), we can see the background of the detector material itself. In this way, we can determine where the material from the solar wind is, how much of it there is, how deep it is, and what it is.

"There are other techniques and other collectors being studied, but we're looking at the transition metals—calcium through nickel and germanium. In that way, we can look at the sections of the Periodic Table that other techniques have not been able to do very well."

Progress on Multilayer Laue Lenses

A 16-nm line focus, a value unprecedented for hard x-rays, has been achieved with a multilayer Laue lens (MLL) that has parallel and planar interfaces, was tilted to an angle, and had a diffraction efficiency of 31% with 19.5-keV x-rays. A further optimized MLL structure, with layers that form wedges, has recently been fabricated. This structure was created by sputtering past a linear mask, forming a full linear zone-plate structure. The structure has 6,543 layers and a total deposited thickness of 40 μm. While wedged structures with planar interfaces are capable of focusing below 1 nm with efficiencies of ~ 50%, it was recently shown by means of a newly developed x-ray dynamical diffraction theory based on the Takagi-Taupin equations that still higher efficiencies are possible with parabolically or elliptically shaped interfaces. Such interfaces can possibly be achieved with a curved sputtering mask.

Multilayer Laue lenses are a new type of focusing optic for hard x-rays [1]. An unprecedented line focus of 16 nm with an efficiency of 31% has been achieved at a wavelength of λ = 0.064 nm (19.5 keV) for a partial MLL structure having an outermost zone width of 5 nm [2]. Alternating WSi_2 and Si layers corresponded to zones n = 66 through 1,653 of a structure with $\lambda f = 1.653 \times 10^{-13}$ m^2. The MLL comprised the outer 13.25 μm of the 16.53-μm radius that corresponds to one half of a full linear zone-plate. The optical depth, 15 μm, was chosen to optimize diffraction efficiency at λ near 0.06 nm. The synchrotron x-ray measurements were performed at the CNM/XOR beamline 26-ID-C at the APS. Supporting measurements were carried out at XOR beamlines 12-BM-B and 8-ID. Focal-width measurements were performed using a Pt analyzer produced by sectioning a 5-nm-thick Pt film. The intensity of the Pt fluorescence was measured, as was the scattering from the analyzer as the analyzer was scanned through the focus. Results are shown in Fig. 1. The focusing efficiency of the MLL was measured, by two different methods, to be 31%.

An MLL where every layer is grown at an individual tilt to produce zones at the correct local Bragg angle is expected to provide a record small focus with very high efficiency. Such an MLL has been dubbed a "wedged MLL" (wMLL), because each zone is in the shape of a wedge as shown schematically in Fig. 2. This MLL, with the correct wedge angle, has recently been demonstrated [3]. To form the wedge, a lateral film thickness gradient is grown using the profile-coating technique [4]. By occluding part of the sputtering flux by using a figured mask attached to the face of the sputtering gun, a film thickness gradient can be produced along the direction perpendicular to the translation of the substrate. Due to the extreme lateral gradient required, the profile of the mask takes the shape of a steep wedge. The layer thickness at a given point on the wMLL sample is controlled so that the ratio of layer thicknesses at the front and back faces are constant, thereby producing the proper Bragg angle for each layer. Growth of nonlinear gradients appears feasible by using a curved mask. A proof-of-concept wMLL sample, consisting of 1,588 alternating layers of WSi_2 and Si, has been reported [3]. More recently, a wMLL for a full linear zone-plate structure was successfully grown in a new rotary sputtering system. As indicated in Fig. 2, this structure consists of 6,543 layers for a total deposited thickness of 40 μm. This structure was for a 3-nm outermost zone, as corroborated with scanning electron microscopy. A newly developed Takagi-Taupin approach for dynamical x-ray diffraction [5] was used to simulate the expected performance of this new, full wMLL. The results are also shown in Fig. 2 in the form of a set of isophotes around the focus. The simulated full width at half maximum (FWHM) in the focal plane is 2.4 nm. Outermost zones thinner than 3 nm can be deposited by sputtering, and a thickness of 0.7 nm has been demonstrated at the APS [6]. A simulation [5] of a corresponding full wMLL is shown in Fig. 3 and demonstrates that a focus of 0.7 nm is feasible with the presently demonstrated wMLL technology.

The shape of the interfaces in the wMLL structure is planar. As found in simulations, parabolically or elliptically shaped interfaces can, in principle, result in a focus of only 0.21 nm with an efficiency of 68% [5]. However, the deposition technology for well-formed outermost zones of the requisite 0.25-nm thickness has yet to be demonstrated for amorphous multilayer structures.

The wMLLs detailed above have yet to be made into test lenses [7]; this work is ongoing. Experiments to produce a spot focus by using two lenses in a crossed geometry are planned. *Contact: Raymond Conley (rconley@aps.anl.gov), Hyon Chol Kang (kanghc@gist.ac.kr),Chian Liu (cliu@aps.anl.gov), Albert T. Macrander (macrander@aps.anl.gov), Jörg Maser (maser@aps.anl.gov), G. Brian Stephenson (stephenson@ anl.gov), Hanfei Yan (hyan@bnl.gov)*

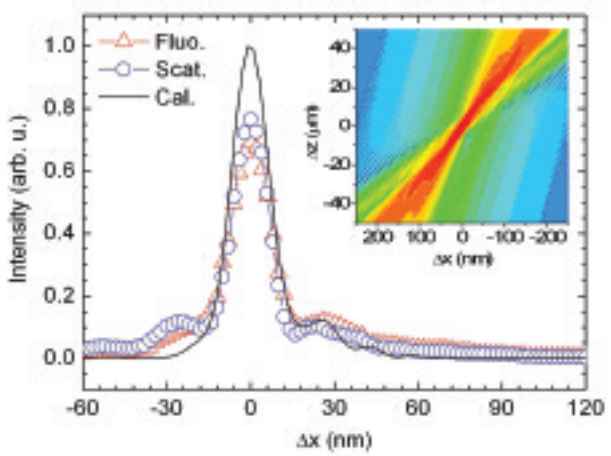

Fig. 1. Intensity distribution in the focal plane at λ = 0.064 nm from a 15-μm-deep section of a MLL positioned at a tilt of 0.10°. The data shown are fluorescence and scattering from a 5-nm Pt analyzer scanned through the line focus [2]. Also shown is the calculated result for this structure, with intensity scaled according to the measured and calculated integrated efficiencies. The widths are 17.6, 15.6, and 15.0 nm FWHM for the fluorescence measurements, scattering measurements, and calculation, respectively. The inset shows the isophote pattern near the focus, where coordinates z and x are parallel and transverse to the incident beam.

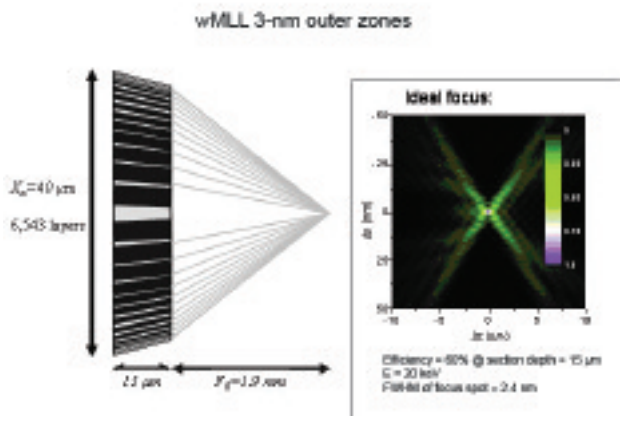

Fig. 2. Schematic for a full (i.e., double-sided) MLL with wedged layers made to satisfy a local Bragg condition [3]. The numeric values were recently achieved for a structure with a 3-nm outermost zone. The inset shows the results of simulations [5] for this structure.

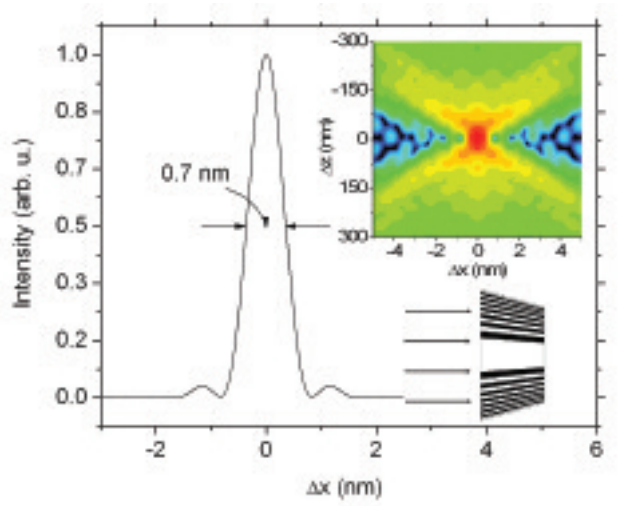

Fig. 3. Calculated results [5] for a full wMLL with an outermost zone width of 0.75 nm and a diameter of 80 μm. The width is 0.7-nm FWHM and the efficiency is 50% at λ = 0.064 nm. Insets show the isophote pattern near the focus and a schematic of the wedged multilayer structure.

References

[1] H.C. Kang, J. Maser, G.B. Stephenson, C. Liu, R. Conley, A.T. Macrander, and S. Vogt, Phys. Rev. Lett. **96**, 127401 (2006).

[2] H.C. Kang, H. Yan, R. Winarski, M.V. Holt, J. Maser, C. Liu, R. Conley, S. Vogt. A.T. Macrander, and G.B. Stephenson, Appl. Phys. Lett., in press.

[3] R. Conley, C. Liu, J. Qian, C.M. Kewish, A.T. Macrander, H. Yan, H.C. Kang, J. Maser, and G.B. Stephenson, Rev. Sci. Instrum., submitted.

[4] C. Liu, R. Conley, A.T. Macrander, and L. Assoufid, J. Vac. Sci. Tech. **21**, 1579 (2003).

[5] H. Yan, J. Maser, A. Macrander, Q. Shen, S. Vogt, G.B. Stephenson, and H.C. Kang, Phys. Rev. B. **76**, 115438 (2007).

[6] Y.S. Chu, C. Liu, D.C. Mancini, F. De Carlo, A.T. Macrander, B. Lai, and D. Shu, Rev. Sci. Instrum. **73**, 1485 (2002).

[7] H.C. Kang, G.B. Stephenson, C. Liu, R. Conley, R. Khachatryan, M. Wieczorek, A.T. Macrander, H. Yan, J. Maser, J. Hiller, and R. Koritala, Rev. Sci. Instrum. **78**, 046103 (2007).

This work and use of the Advanced Photon Source was supported by the U.S. Department of Energy, Office of Science, Office of Basic Energy Sciences, under Contract No. DE-AC02-06CH11357.

A New Gas-Loading System for Diamond Anvil Cells at GSECARS

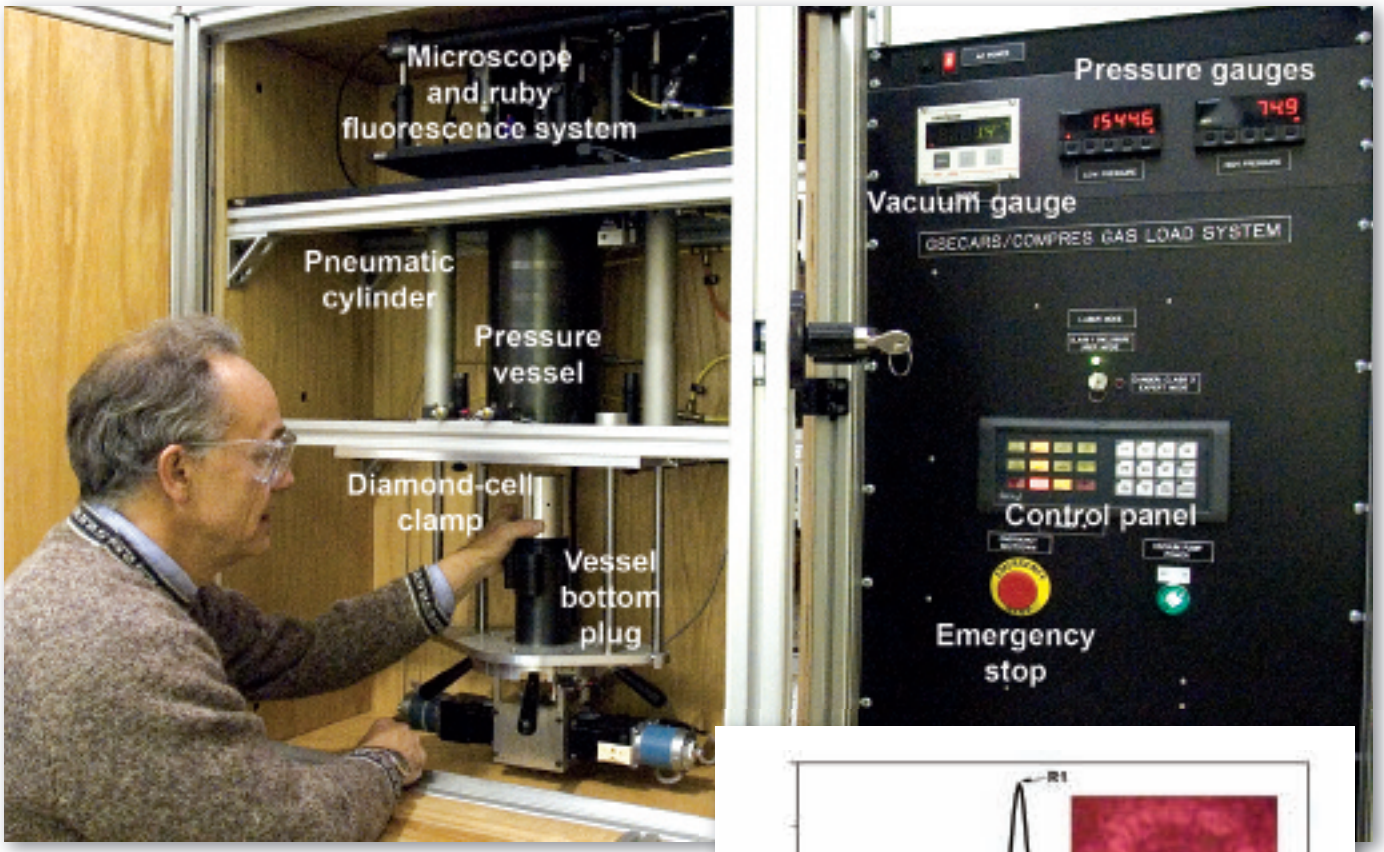

Fig. 1 (above). The gas-loading system at GSECARS. The vacuum pump, high-pressure valves, and compressor (not shown) are in a cabinet under the main system shown here.

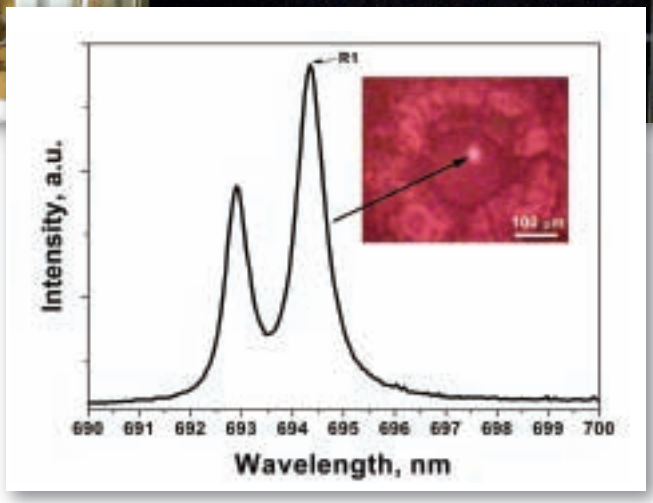

Fig. 2 (right). Photograph of a diamond anvil cell inside a pressure vessel. A ruby crystal is loaded in the cell and is fluorescing visibly. Inset: spectrum of the ruby fluorescence from the sample. The wavelength shift of the ruby fluorescence is used to measure the pressure in the diamond anvil cell as the stepper motors close the cell after pressurizing with gas.

The diamond anvil cell (DAC) is the most commonly used device for obtaining static high pressures above 3 GPa. Experiments in the DAC are frequently performed at the APS, in particular at GSECARS (Sector 13), HP-CAT (Sector 16), and at XOR sectors 1 and 3. In order to have the sample in the DAC be subject to a quasi-hydrostatic pressure it is necessary to surround the sample with a pressure medium that is relatively weak, is chemically inert to the sample, is optically and x-ray transparent, and does not produce a strong x-ray diffraction signal. The rare gases are the preferred pressure media for pressures above approximately 10 GPa; helium and neon are ideal because of their low x-ray scattering cross sections and low strength, which minimizes the lattice strain in the sample. However, it is necessary to load the gases into the DAC at a high gas pressure. If the gas pressure is 100-200 MPa, then the density is comparable to the liquid at room pressure. Such systems operate by loading a DAC into a pressure vessel, pressurizing the vessel, and then remotely sealing the DAC, trapping the high-pressure gas and the sample inside the gasket hole between the two diamonds. Because no gas-loading system was available at the APS, the COMPRES (an NSF-funded consortium for high-pressure research) and GSECARS designed and built one (Fig. 1).

Since the APS and GSECARS are national user facilities and have hundreds of high-pressure users from dozens of institutions, GSECARS wanted to build a system that could be safely operated by users with appropriate training. There are also many different DAC designs in use by the scientists who use APS and GSECARS beamlines. As a result, the following goals were developed when designing and building the system:

- The ability to load many kinds of DACs. A closure mechanism (motor-driven screws) closes a clamping device, which in turn clamps the DAC shut. By not turning the tightening screws on the DAC directly, it is simple to accommodate different DAC designs; in many cases, they just require different spacers, and in the worst case, a different clamp design.
- An optical access in order to view the cell while loading. This allows one to see when the diamonds contact the gasket as the cell is closed. It also allows an online ruby fluorescence system for directly measuring the pressure as the cell is closed (Fig. 2).
- A vacuum pump to clean the system before loading the gas.
- The ability to have no electrical parts except pressure transducers in the cabinet enclosing the high-pressure system. This allows flammable gas operation (e.g., hydrogen) in the future.
- Easy to operate safely, thanks to the use of air-driven valves, safety interlocks, and computer control.

The system received a detailed pressure safety review from the APS and Argonne, followed by approval to operate. At the time of writing, beamline staff at GSECARS had loaded more than 20 cells, with a nearly 100% success rate. Two types of cells have been loaded with He or Ne at pressures of about 25,000 psi. The ability to measure the pressure as the stepper motors are driven to close the cell clamp has proven to be invaluable. The operator simply rotates the stepper motors, closing the cell clamp, until the pressure measured with the ruby luminescence system begins to increase, and then continues to close it until a desired pressure is reached, typically 1-2 GPa. Once this pressure is reached, the pressure vessel (Fig. 3) is vented and the cell is removed. The screws on the diamond cell itself are then tightened, using an Allen wrench that passes through access holes in the top of the cell clamp.

A GSECARS user, Steve Jacobson from Northwestern University, collected data sets on single crystals of MgO loaded with the system. The data were excellent, showing a very smooth compression curve up to 110 GPa (1.2-million atmospheres).

It is expected that several additional cell types will be accommodated in the next few months. A new cell clamp to load panoramic DACs will be built, and GSECARS is currently accepting and prioritizing requests to build cell holders for other types of DACs. The system is being upgraded for rapid switching between He and Ne, and for convenient use of other gases. Finding a vendor who can supply copies of this system commercially is a priority, because at least six other laboratories have expressed an interest in obtaining one. *Contact: Mark Rivers (rivers@cars.uchicago.edu), Vitali Prakapenka (prakapenka@cars.uchicago.edu), Clayton Pullins (pullins@cars.uchicago.edu)*

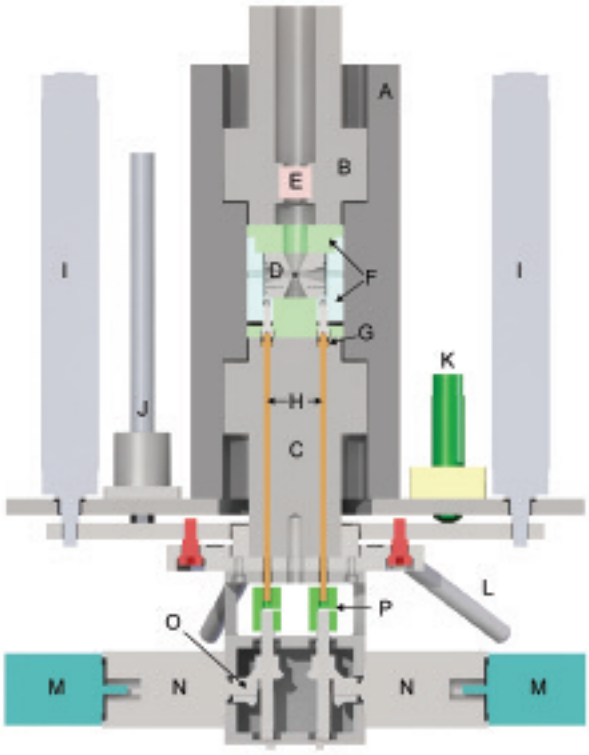

Fig. 3. Cross-section view of the pressure vessel. A) pressure vessel (outer diameter=16.5cm); B) top end plug; C) bottom end plug; D) diamond anvil cell; E) sapphire window; F) cell clamps; G) M6 screw; H) rotary feedthroughs; I) pneumatic lifter; J) guide bearing; K) damper; L) handle for rotating base assembly; M) stepper motor; N) gear reducer; O) 90° gear; P) coupling. The top and bottom end plugs are rotated 45° to seal using a clover-leaf closure. The base assembly (consisting of the bottom end plug, cell clamp with diamond anvil cell, stepper motors and gears) is raised pneumatically and then rotated 45° to seal the pressure vessel.

This research was partially supported by COMPRES, the Consortium for Materials Properties Research in Earth Sciences, under NSF Cooperative Agreement EAR 06-49658. It was also supported by GSECARS (Sector 13) and the APS. GeoSoilEnviroCARS is supported by the National Science Foundation-Earth Sciences (EAR-0622171) and Department of Energy-Geosciences (DE-FG02-94ER14466). Use of the Advanced Photon Source was supported by the U.S. Department of Energy, Office of Science, Office of Basic Energy Sciences, under Contract No. DE-AC02-06CH11357.

The X-ray Imaging Facility at XOR 32

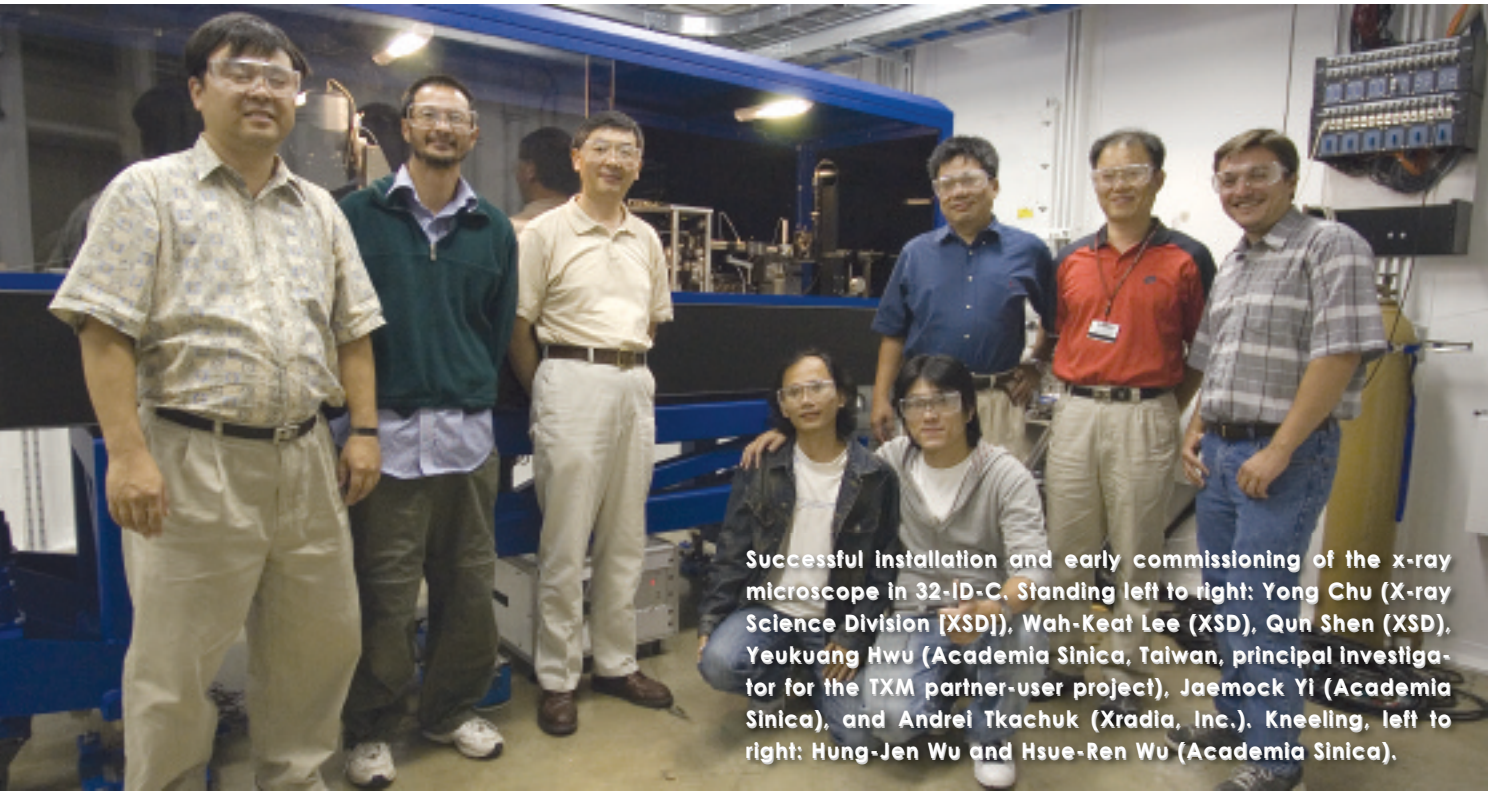

Successful installation and early commissioning of the x-ray microscope in 32-ID-C. Standing left to right: Yong Chu (X-ray Science Division [XSD]), Wah-Keat Lee (XSD), Qun Shen (XSD), Yeukuang Hwu (Academia Sinica, Taiwan, principal investigator for the TXM partner-user project), Jaemock Yi (Academia Sinica), and Andrei Tkachuk (Xradia, Inc.). Kneeling, left to right: Hung-Jen Wu and Hsue-Ren Wu (Academia Sinica).

The APS has completed a dedicated, full-field x-ray imaging facility at XOR beamline 32-ID-B,C. The facility began full operation and accepted general users in October 2007. The objective of the new facility, the first dedicated beamline for full-field imaging at the APS, is to satisfy rapidly growing needs for advanced x-ray imaging investigations in materials science and biology, and to promote research and development to advance the cutting-edge in x-ray imaging.

Planning for the facility dates back to 2004, when workshops were organized to evaluate emerging future scientific directions at the APS. At those workshops, one of the recommendations from the community was to establish a dedicated beamline for full-field x-ray imaging. This recommendation was fully endorsed by the APS Scientific Advisory Committee in early 2005. Following discussion among APS users and staff, a decision was made to reprogram the existing beamline 32-ID-B,C as the new full-field imaging facility by updating existing beamline components and optics, and by extending the beamline and constructing a new experiment hutch, 32-ID-C, at 70 m from the source to complement the existing 32-ID-B at 38 m from the source. Both are compatible with either a white undulator beam or a monochromatic undulator beam in the range of 8-35 keV provided by a pair of polished Si (111) flat crystals. A double-mirror system is used for harmonic rejection up to 18 keV.

The facility currently supports research programs in static and dynamic phase-contrast imaging, ultra-small-angle-scattering imaging, and transmission x-ray microscopy. For phase-contrast imaging, a special, local, low-β machine lattice may be employed to reduce the horizontal source size by >2, down to $\sigma = 210$ μm, leading to enhanced phase contrasts, especially for low-Z materials. This, coupled with the high x-ray flux offered by the APS undulator, allows high-definition phase-enhanced imaging with exposure times as short as 200 μs in the monochromatic mode, and down to ultrafast single-pulse temporal resolution of ~150 ps in the white-beam mode, with simultaneous spatial resolution in the 1- to 5-μm range. These unique capabilities open new research areas in synchrotron x-ray imaging applications, from ultrafast imaging of materials processing and transient fluid dynamics to real-time and sub-video-rate imaging of biological functions in live insects and small animals.

In order to satisfy the need for nanometer-scale imaging at the APS, an international partner-user collaboration on a hard x-ray transmission microscope (TXM) has been formed between Academia Sinica in Taiwan; Xradia, Inc., in the U.S.; and the APS. As a result, a new TXM has been designed and fabricated by Xradia and installed in 32-ID-C. This instrument exploits both absorption contrast and phase contrast via the Zernike method. It is equipped with several sets of Fresnel zone-plate objectives with 45-nm outermost zone width and is designed for operating in the 7- to 18-keV energy range. This instrument and all other instruments at 32-ID are available to general users through the APS General User Proposal System. *Contact: Qun Shen (qshen@aps.anl.gov)*
Wah-Keat Lee (wklee@aps.anl.gov)

Using Ultrasmall X-rays to Probe Ultrafast Laser-Induced Processes

X-rays are routinely used to characterize the static structures of complex materials, biomolecules, and surfaces to atomic resolution. However, all structures evolve in time, and the ability to see atoms move with sub-Å spatial resolution and 100-ps time resolution allows researchers to understand the initial response of complex systems to photoexcitation. In the most general terms, researchers can follow the structural response to electron motion induced by impulsive optical excitation. The relaxation to equilibrium contains detailed information about the system. The use of microfocused x-rays (~1–10 μm), in conjunction with ultrafast laser excitation, provides several advantages: access to multiple-wavelength excitation because of the extremely efficient use of laser power, the potential to use μm-sized rare samples, and a mitigation of sample damage. Tunable, monochromatic, polarized, microfocused x-rays synchronized with an ultrafast laser (to ~2-ps precision) enable the application of the powerful techniques of time-resolved x-ray absorption spectroscopy (both near-edge and extended) and time-resolved x-ray diffraction to study the electronic and structural response to photoexcitation. Research in atomic, molecular, optical [1], and condensed matter physics has been the mainstay at the XOR 7-ID-B,C,D beamline [2,3], but studies of chemical and biological systems are easily envisioned.

The new Ultrafast Laser Laboratory at Sector 7 was commissioned in October 2005. It features a regeneratively-amplified Ti:sapphire laser system (2.5-W average power, <50 fs, 1-5 kHz) in a 7.8-m × 3.7-m laser laboratory. This provides ample space for "laser-only" experiments, which can be performed during APS maintenance periods (~3 months/year). Such preliminary experiments are essential to commissioning complex apparatus (e.g., three-dimensional ion imaging detectors) prior to use during x-ray beam time.

An example of recent research using the time-resolved laser/x-ray facility is shown in Fig. 1 [1]. Here, microfocused, polarized x-rays probe the shape of the electron cloud of an atom that has been ionized via the strong electric field present in a tightly focused, intense laser beam (~2 × 10^{14} W/cm^2). The strong electric field of the laser rips out an electron from a krypton atom, leaving the electron cloud aligned with respect to the polarization axis of the laser. A direct experimental proof of this fundamental effect had been lacking so far. Using the time-resolved x-ray microprobe, the alignment was directly observed and the degree of alignment understood by taking into account spin-orbit coupling, a relativistic effect. Understanding the atomic response to strong laser fields is of significant fundamental and technological interest, since it forms the basis for compact, coherent sources of soft x-ray radiation.

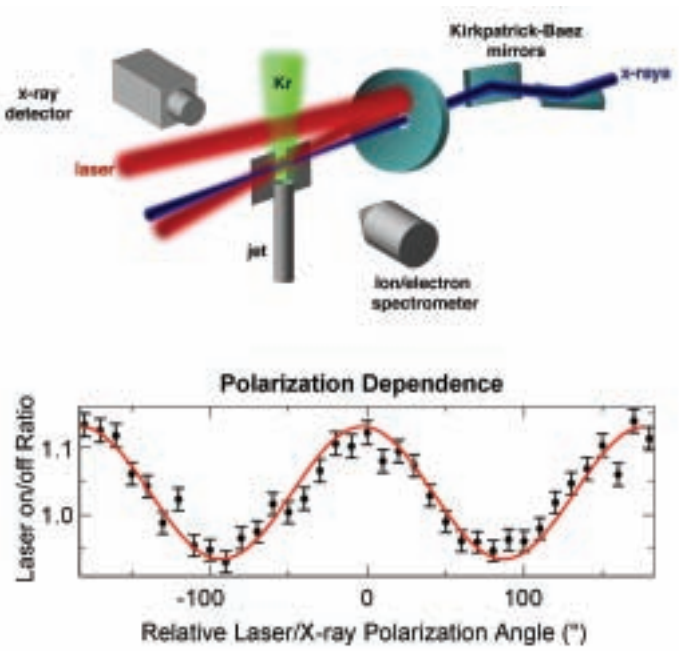

Fig 1. Top: Microfocused x-rays probe atoms in the focus of an intense ultrafast laser. Bottom: Intensity of the 1s → 4p resonance as a function of the angle between the polarization of the laser and x-rays. This intensity is a measure of the 4p orbital hole density and thus a measure of the alignment of the 4p electron shell.

Contact: Eric Landahl (elandahl@anl.gov), Jin Wang (wangj@aps.anl.gov)

References

[1] L. Young, D.A. Arms, E.M. Dufresne, R.W. Dunford, D.L. Ederer, C. Hohr, E.P. Kanter, B. Krassig, E.C. Landahl, E.R. Peterson, J. Rudati, R. Santra, and S.H. Southworth, Phys. Rev. Lett. **97**, 083601-1 (2006).

[2] S.H. Lee, A.L. Cavalieri, D.M. Fritz, M.C. Swan, R.S. Hegde, M. Reason, R.S. Goldman, and D.A. Reis, Phys. Rev. Lett. **95**, 246104 (2005).

[3] M.F. DeCamp, D.A. Reis, A. Cavalieri, P.H. Bucksbaum, R. Clarke, R. Merlin, E.M. Dufresne, D.A. Arms, A.M. Lindenberg, A.G. MacPhee, Z. Chang, B. Lings, J.S. Wark, and S. Fahy, Phys. Rev. Lett **91**, 165502 (2003).

The Nanoprobe at Sector 26

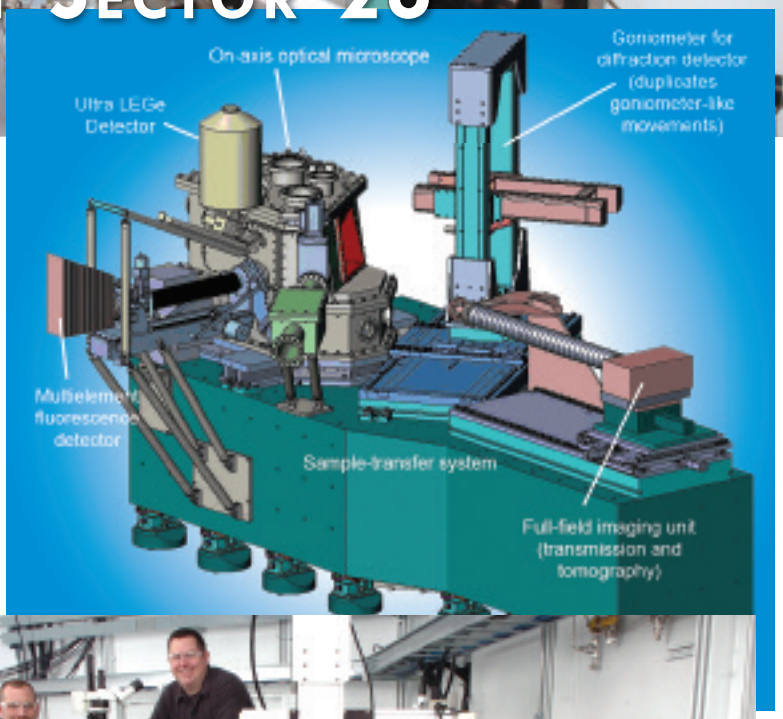

The hard x-ray nanoprobe at APS Sector 26 was constructed by and will be operated in a partnership between the Argonne Center for Nanoscale Materials (CNM) and the X-ray Operations and Research section of the APS X-ray Science Division. The instrument uses brilliant x-rays with photon energies from 3 to 30 keV to probe the properties of nanoscale materials with a spatial resolution of 30 nm. The system provides a combination of scanning-probe and full-field transmission imaging. Full-field imaging allows efficient three-dimensional visualization of complex systems and devices. Scanning-probe imaging provides sensitive, quantitative analysis of elemental composition, chemical states, crystallographic phase, and strain.

The nanoprobe instrument in the 26-ID-C endstation is shown in the photo above and rendering at right. A vacuum chamber contains the x-ray optics and specimen. Energy-dispersive detectors for x-ray fluorescence are mounted on the inboard side of the vacuum chamber (left in the photo). Different area detectors for detecting diffracted x-rays are mounted on a goniometer on the outboard side (right side of the photo). Transmitted x-rays used for full-field imaging propagate through a flight tube on the downstream side to an area detector downstream of the instrument chamber.. The technology for positioning of x-ray optics and specimen is based on laser Doppler interferometers and composite flexure stages. This approach allows positioning with an accuracy approaching 1 nm over a range of more than 5 mm.

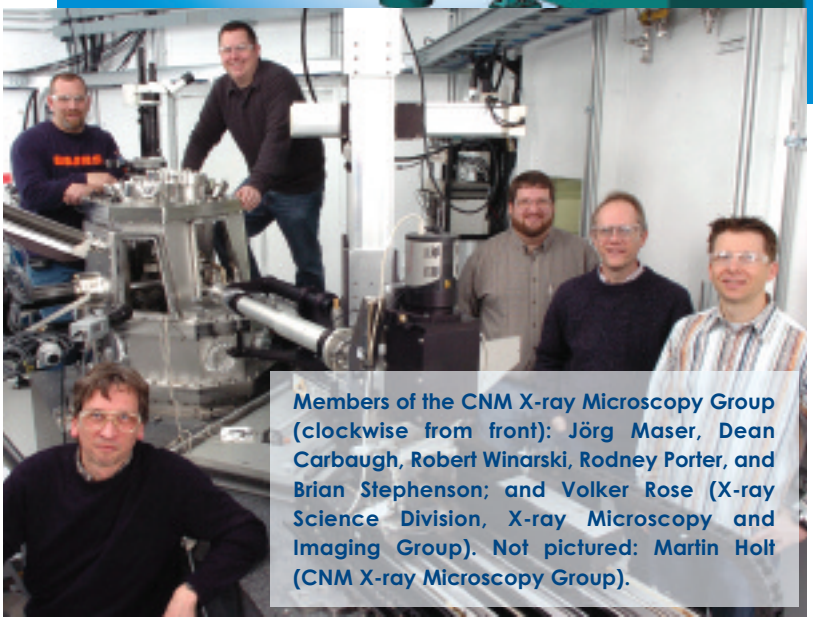

Members of the CNM X-ray Microscopy Group (clockwise from front): Jörg Maser, Dean Carbaugh, Robert Winarski, Rodney Porter, and Brian Stephenson; and Volker Rose (X-ray Science Division, X-ray Microscopy and Imaging Group). Not pictured: Martin Holt (CNM X-ray Microscopy Group).

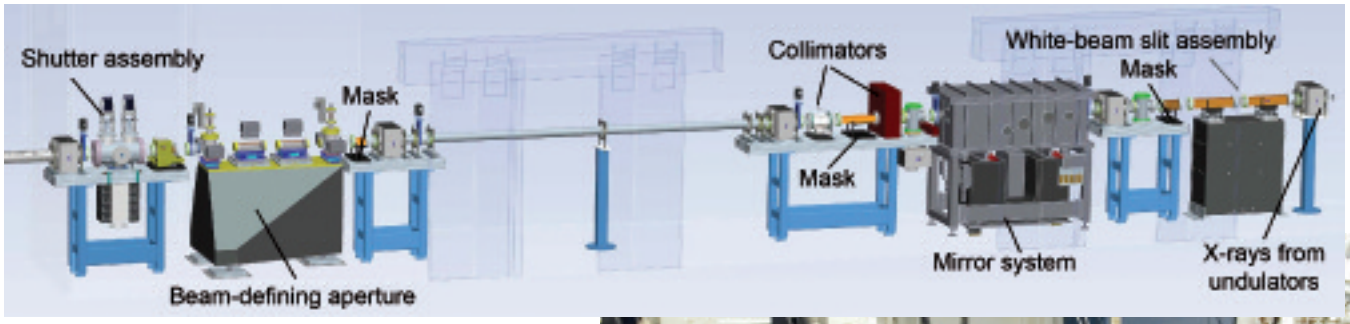

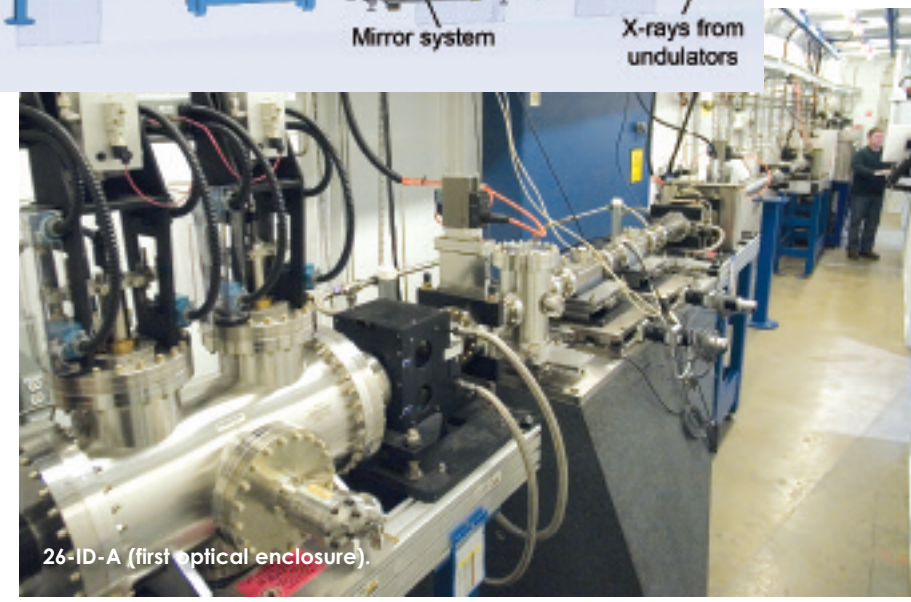
26-ID-A (first optical enclosure).

The first optical enclosure of the hard x-ray nanoprobe beamline, 26-ID-A (top photo at right, rendering above) contains the high-heat-load double-mirror system; a beam-defining aperture; and slits, masks, collimators, and beam shutters.

A cryogenically cooled double-crystal monochromator with submicroradian angular stability for high-resolution imaging, and a double multilayer monochromator for high-throughput imaging, are located in the second optical enclosure, 26-ID-B (lower photo at right, rendering below). A polarizer and a beam chopper will be installed in the near future. The polarizer employs a diamond phase retarder to obtain circularly polarized x-rays, which are used for magnetic studies. The chopper will allow extraction of individual APS pulses for time-resolved studies.

Contact: Jörg Maser (maser@anl.gov), Robert Winarski (winarski@aps.anl.gov), Martin Holt (mvholt@aps.anl.gov)


26-ID-B (second optical enclosure).

26-ID-C • CNM/XOR • Physics, materials science • Microfluorescence (hard x-ray), tomography, microdiffraction • 3.3-cm Undulator A • Operational • For more information on nanoprobe instrumentation and capabilities, visit: http://nano.anl.gov/research/nanoprobe.html

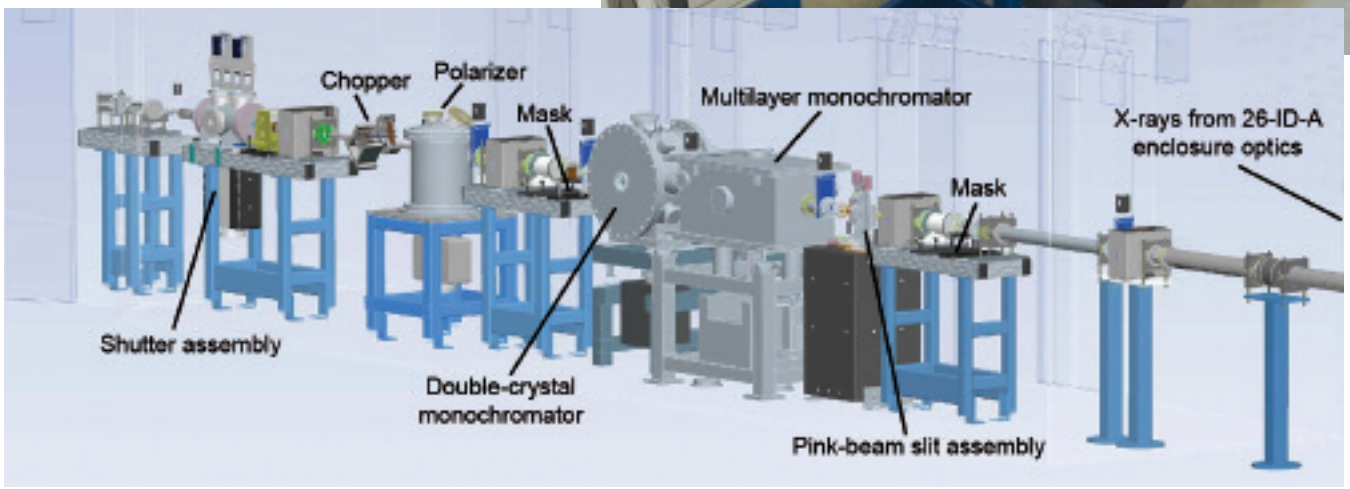

Mail-in MX for General Users at SGX-CAT

David Smith (left) and Stephen Wasserman (both of SGX Pharmaceuticals, Inc.) in the SGX-CAT control room at APS Sector 31.

Greyhounds of both the canine and vehicular varieties serve as apt metaphors for the SGX-CAT beamline at Sector 31 of the APS. Like the elegant greyhounds themselves, the SGX-CAT mail-in macromolecular crystallography (MX) program is designed for maximum speed and efficiency. And like the famed catch-phrase for the cross-continental U.S. bus company—Greyhound Lines, Inc.—the SGX-CAT byword for mail-in MX by both general users and strategic partners is, "Leave the driving to us." The beamline staff pride themselves on providing the best possible x-ray diffraction data to the user community.

The SGX-CAT facility was constructed and is operated by SGX Pharmaceuticals, Inc., of San Diego, California. From first operations, SGX-CAT has functioned as a 100% mail-in protein crystallography facility. This approach has resulted in the development of unique tools for automated sample handling, data collection, and information management. While total automation may prove elusive, SGX-CAT is currently at 90% hands-off sample handling and data collection. The last piece of the beamline's automation, a robot for changing sample carousels, is now in its final testing phase.

The automation focuses on three main components: sample placement, sample evaluation, and information management. SGX-CAT-developed software for automatic sample centering was brought on line in February 2005 and has to date been used for more than 30,000 crystals. Crystal-evaluation software, which has looked at more than 22,000 samples to date, is in general superior to humans for this task. Data collection throughput has been equally impres-

Continued on page 147

Mail-in Powder Diffraction for General Users at XOR 11-BM

One of the newest dedicated beamlines at the APS, bending magnet line 11-BM-B, aims to meet an emerging need in science—crystallographic structure determination of complex polycrystalline materials from powder diffraction—by providing high-resolution, high-energy, synchrotron powder diffraction data to researchers in materials science, chemistry, physics, geosciences, pharmaceutical studies, engineering, and other fields.

To meet requests from these communities and to facilitate access to researchers who have never used a synchrotron, the instrument has been opened for use via samples that are mailed to the APS. Mail-in users can have data collected at either room temperature or 100K. In the future, the instrument will be enhanced for a greater range of measurements. High-resolution synchrotron powder diffraction allows very precise measurements with optimal separation of peaks; this greatly simplifies the challenge of indexing new materials. Use of high-energy x-rays (30 keV, 0.4 Å) improves crystallographic accuracy by greatly reducing the impact of x-ray absorption effects and widens the range of accessible reflections.

Standing (left to right) in the 11-BM research station are Lynn Ribaud and Jun Wang (both beamline staff, X-ray Science Division Materials Characterization Group [XSD-MC]); software engineer Xuesong Jiao (APS Engineering Support [AES] Division Beamline Controls Group); Sytle Antao (beamline staff, XSD-MC); and Curt Preissner (AES Mechanical Engineering and Design Group), who, with Deming Shu (AES Mechanical and Interlock Systems) designed the robot sample changer and the unique detector system for 11-BM. Seated: Brian Toby, XSD-MC Group Leader.

The 11-BM-B beamline, which is funded by the U.S. Department of Energy's Office of Basic Energy Sciences (DOE-BES), is operated by the APS Materials Characterization Group, X-ray Operations and Research Section, X-ray Science Division, features a general-purpose diffractometer with a unique APS-designed 12-detector system increasing throughput 12-fold. Each detector has an individual analyzer crystal, with independent alignment control on two axes, so there is no degradation in data quality. A complete data set on a powder sample can be collected in an hour or less with an instrumental resolution under 2×10^{-4} $\Delta Q/Q$. Operation is further enhanced by a robotic sample exchange system that allows the beamline to accommodate >20 samples per day.

Users submit general-user proposals, specifying "rapid access" on the beam-time request. Upon acceptance, users enter sample identification data through a Web interface and send samples prepared on special mountings and Kapton capillaries provided by the beamline. Beamline staff make the measurements and return data via e-mail. Further information on 11-BM-B access can be found at: http://11bm.xor.aps.anl.gov.

A related education outreach effort, also intended to facilitate use of synchrotrons for crystallographic analysis of powder diffraction data, is a collection of pedagogical materials now available via the APS Web site. A series of lectures and tutorials related to crystallographic analysis of powder diffraction data can now be found at:

http://www.aps.anl.gov/Xray_Science_Division/Powder_Diffraction_Crystallography/

Presentations vary in content: Some are targeted for novices, while others are prepared for experts.

The beamline was funded by the U.S. DOE-BES in response to a proposal prepared by principal investigator (PI) John Mitchell and co-PIs James Jorgensen, Mark Beno, Robert Von Dreele, and Peter Lee (all with Argonne).

Contact: Brian Toby (brian.toby@anl.gov).

High-Pressure Synergy at the APS

A facility-wide approach to high-pressure (HP) synchrotron research is being fostered at the APS through the creation of the High-Pressure Synergetic Consortium (HPSynC, www.aps.anl.gov/Users/Scientific_Interest_Groups/HPSynC/), which is facilitated by scientists from the Geophysical Laboratory of the Carnegie Institution of Washington. An HPSynC team consisting of research scientists, engineers, and postdocs is engaged in high-pressure research, with staff support from the APS. To develop novel HP synchrotron techniques and make them available to user communities, HPSynC will develop experimental apparatus for specific beamline applications, as well as portable or fixed beamline optics and equipment to accommodate HP apparatus. HPSynC staff are seen as functioning in a manner similar to beamline scientists. But rather than concentrating on one beamline, they will conduct cutting-edge research and provide support on a range of instruments (such as high-P-T vessels, analytic probes, etc.) on many beamlines. In the process, they will bridge scientific disciplines and communities, including chemistry, physics, geoscience, planetary science, materials science, and general high-pressure science.

HPSynC has been focusing on four major areas.

Development of novel HP synchrotron techniques: The standard dedicated HP beamlines have been (and will continue to be) highly successful. They provide HP users with a home base, expert help, and fundamental techniques such as HP x-ray diffraction and some forms of spectroscopy. HPSynC, on the other hand, extends the same expert help to many cutting-edge techniques that cannot be included in the dedicated beamlines but are only available at specialized APS beamlines. HPSynC will tailor dozens of beamlines for the HP community, and is highly complementary to the existing dedicated beamlines.

Coordination of existing equipment and tools: A survey has been conducted by HPSynC and a detailed list of available equipment has been compiled, from sample preparation and characterization to various non-synchrotron probes (Raman, Brillouin, Mossbauer, and electron microscopy). For general HP users, HPSynC staff play an important role in facilitating access to this apparatus and providing the necessary training.

An advanced sample-preparation laboratory: HPSynC is establishing a world-leading sample-preparation laboratory that puts general users on equal footing with leading high-pressure-center scientists, who at present can prepare superior samples at their home bases and carry the high-pressure cells to synchrotron facilities. A dedicated high-pressure sample-preparation lab, located on the first floor of the main APS laboratory/office building, is equipped with tools and devices that can be accessed by any APS user.

Portable systems: A series of portable systems is dedicated to high-pressure researchers at various beamlines around APS. These systems are self-contained, with attached controls systems and software. Typically, they include a Kirkpatrick-Baez mirror system able to focus beam to a size of ~5 μm, a ruby-fluorescence system for on-line pressure measurements, a membrane control system for pressure control, and a laser heating system for heating samples *in situ* at high pressures.

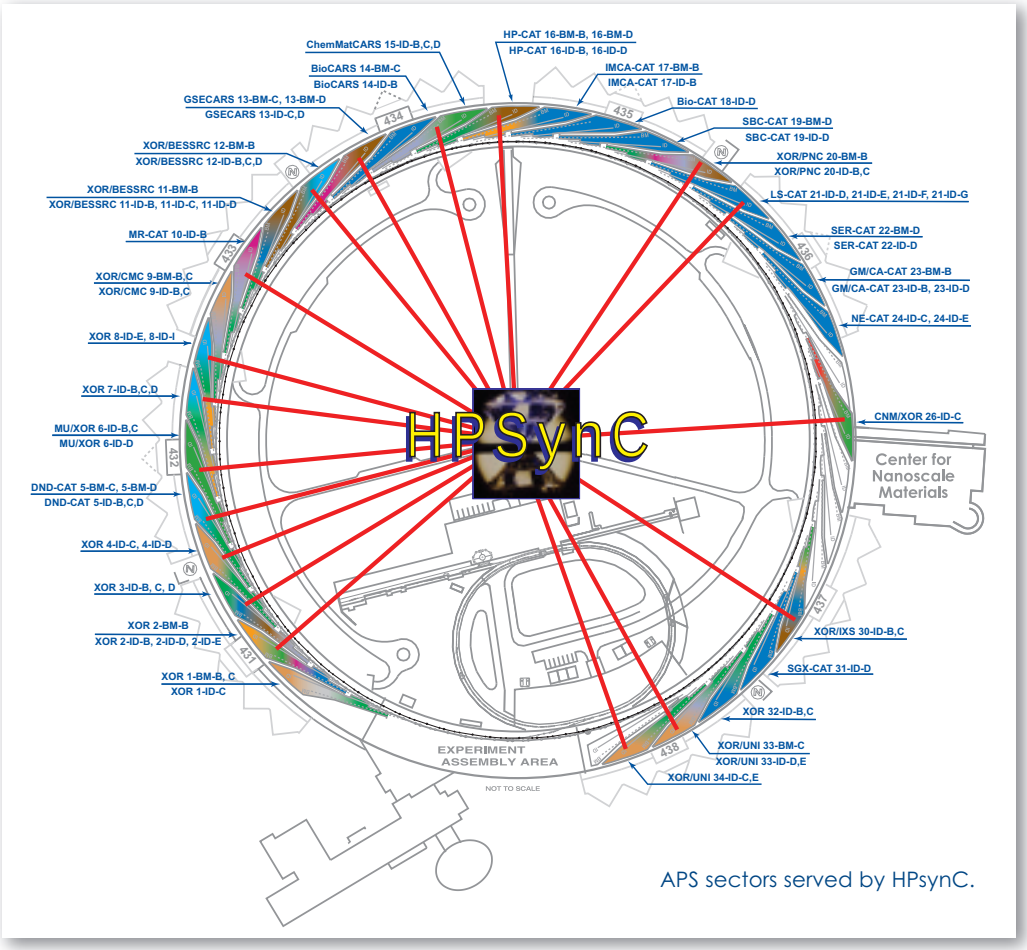

APS sectors served by HPsynC.

Contact: Ho-kwang Mao (h.mao@gl.ciw.edu), Guoyin Shen (gshen@ciw.edu)

"Mail-in MX" *continued from page 144*

sive, with an average of 4,000 data sets measured annually over the past three years. In a 2004 time study, SGX-CAT on average required approximately 13 min to screen each crystal. Most of this time was devoted to evaluation of the quality of diffraction, rather than to mounting the crystal and acquiring the diffraction images. This cycle time is now down to an average of four minutes per sample.

Information management, which is the glue that holds the SGX-CAT system together, is accomplished using an Oracle® database. A Web-based interface to the database is updated automatically every 15 minutes and tracks some 40 pieces of information about each crystalline sample from time of arrival at SGX-CAT to return of data (screening images from each crystal and raw data-collection images) to the user. The system links related samples and, based on the results of automated sample evaluation, identifies (highlighted on the display by a color code) superior samples as optimal candidates for data collection, helping the beamline staff to make correct decisions rapidly. All information about crystals is linked to the actual crystals through bar-codes on the samples (SGX-CAT supplies the bar codes), ensuring the highest accuracy in data entry and sample tracking.

Because its automation tools give users the greatest likelihood of success in data collection, SGX-CAT has developed a strong level of trust between beamline staff and users (both general users and strategic partners). The benefits of these tools, which were initially developed for proprietary use of SGX-CAT by the company, are now available to general users, who can access up to 25% of the beam time available at SGX-CAT.

Prospective general users wishing to avail themselves of the SGX-CAT mail-in crystallography program must first submit a proposal to the APS..

A PDF file detailing the SGX-CAT "Express Crystallography General User Program" can be downloaded from http://www.sgxcat.com. *Contact: Laura Morisco (lmorisco@sgxpharma.com)*

NOTE: Other sectors accepting mail-in samples (CAT members only) are 17-BM-B, 17-ID-B, 22-BM-D, and 22-ID-D.

Around the Experiment Hall

An R&D 100 Award for a New Mammography System

< Photostimulated luminescence image of part of a Huettner phantom recorded on a 2% Eu^{2+}-doped FCZ glass-ceramic plate (1 mm in thickness) annealed at 285° C for 20 min.

A 2007 R&D 100 Award was given to the Ultra-High-Resolution Mammography System (UHRMS), which equips doctors with a low-cost, high-quality alternative to digital radiography (currently the most popular mammographic technology at leading hospitals). The new mammography system was developed thanks in part to research carried out at the XOR 2-BM-B beamline at the APS. The developers/researchers are Jacqueline Anne Johnson (now at The University of Tennnessee Space Institute), SUNY Stony Brook Research Assistant Professor Anthony R. Lubinsky, and University of Paderborn (Germany) Scientific Employee Stefan Schweizer.

The Ultra-High-Resolution Mammography System represents a form of computed radiographic technology that replaces traditional x-ray film with a glass-ceramic imaging plate made of fluorochlorozirconate (FCZ), which then can be scanned, with the resulting data fed into a computer and digitized. The UHRMS offers several notable improvements over common x-ray films and scintillating screens, including reusability, wide dynamic range, and direct digitization.

As noted in their 2007 paper published in the Journal of the American Chemical Society, the researchers used beamline 2-BM-B to characterize the new fluorochlorozirconate image plates. They further note that, "The materials show the potential for superior resolution to existing polycrystalline x-ray imaging systems, and they provide high x-ray conversion efficiency." The group has obtained a $2 M National Institutes of Health grant to develop the system to its full potential.

Contact: Jacqueline A. Johnson (jjohnson@utsi.edu)

See: Jacqueline A. Johnson, Stefan Schweizer, and Anthony R. Lubinsky, "A Glass-Ceramic Plate for Mammography," J. Am. Ceram. Soc. **90**(3), 693 (2007). DOI: 10.1111/j.1551-2916.2007.01488

Use of the Advanced Photon Source was supported by the U.S. Department of Energy, Office of Science, Office of Basic Energy Sciences, under Contract No. DE-AC02-06CH11357.

A Year of New Opportunities for APS Users

The year 2007 brought significant new opportunities for APS users in many areas: more research shifts, more beamlines, more world-class capabilities, more options for access, and more tools available for new users.

The number of 8-h shifts available to general users increased from 9,692 in 2006 to 11,280 in 2007 as six new beamlines joined the General User Program (GUP) and beamlines transitioning to the APS provided additional general-user shifts. Noteworthy are increased opportunities for macromolecular crystallography. Figure 1 summarizes the shifts (excluding those reserved for rapid access) and beamlines available by type (macromolecular crystallography and all other science) since the centralized GUP began in 2003.

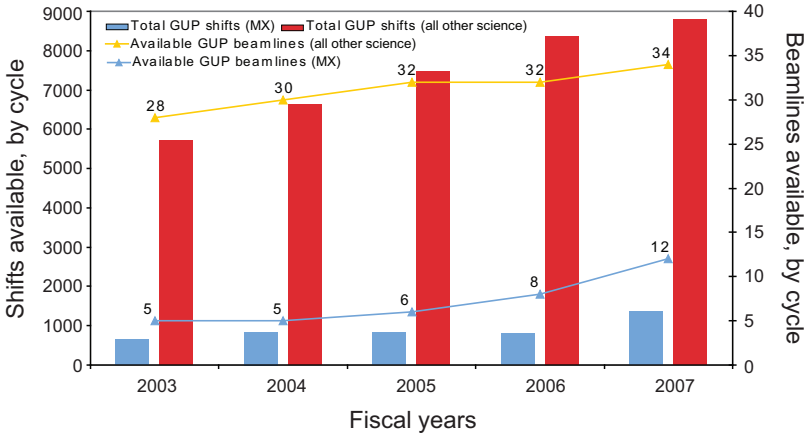

Fig.1. Available APS user shifts (excluding rapid access) and beamlines by type, fiscal years 2003-2007.

Beamline 30-ID-B,C became operational, providing cutting-edge inelastic x-ray scattering capabilities with two specialized spectrometers: HERIX for high-resolution (about 1.5 meV) inelastic x-ray scattering and MERIX for medium resolution (90-200 meV), inelastic x-ray scattering. High-resolution, high-throughput automated powder diffraction capabilities are now available on beamline 11-BM-B, which currently operates in a mail-in mode for general users (see page 145). Microfocusing capabilities are now in place at several of the macromolecular crystallography beamlines: 23-ID-B and 23-ID-D (operated by GM/CA-CAT) and 24-ID-E (operated by NE-CAT).

New access modes include remote access (actual manipulation of the beamline remotely) for SER-CAT members, and mail-in crystallography for IMCA-CAT members at 17-BM and 17-ID-B, SER-CAT members at 22-BM-D and 22-ID-D, and SGX-CAT members at 31-ID-D. Beamline 31-ID-D also offers this capability through the GUP.

In addition, a new proposal type was added to the GUP system: project proposals. Approved project proposals are guaranteed time each run for two years. In contrast, for regular proposals, requests for time must be submitted each cycle and compete each run on the basis of score. Candidate project proposals are evaluated by the appropriate proposal review panel (PRP); they then receive additional scrutiny by a subcommittee of the Scientific Advisory Committee (SAC). The SAC subcommittee uses the following criteria to determine whether a proposal should be granted project status: (1) PRP rating, (2) supplemental information provided by the principal investigator on the proposal, and (3) input from the management of the requested beamline(s). Final decisions on project status are made by APS management.

Demand for beam time continued to rise, as did oversubscription. The oversubscription rate (number of beam time requests submitted divided by the number allocated) rose in 2007 to 180% from 160% in 2006. See Fig. 2.

The APS Web site was redesigned, with new tools for first-time and returning users. Chief among them is an updated beamline directory with comprehensive information about each beamline (http://beam.aps.anl.gov/pls/apsweb/beamline_display_pkg.beamline_dir) as well as an interactive map that enables searches for appropriate beamlines by technique, discipline, status (i.e., construction, commissioning, operational, accepting general users), and instrument (http://www.aps.anl.gov/Beamlines/). Both of these tools are located under the “Beamlines” tab on the APS home page.

For the 11th straight year, the number of unique users (individuals coming to the APS one or more times to conduct experiments) rose—to 3,412 in 2007 from 3,274 in 2006—with the number of user visits continuing to rise as well. The graphs and figures on the facing page show pertinent data about user community (and publication) growth since 1997.

Contact: Susan Strasser (strasser@aps.anl.gov)

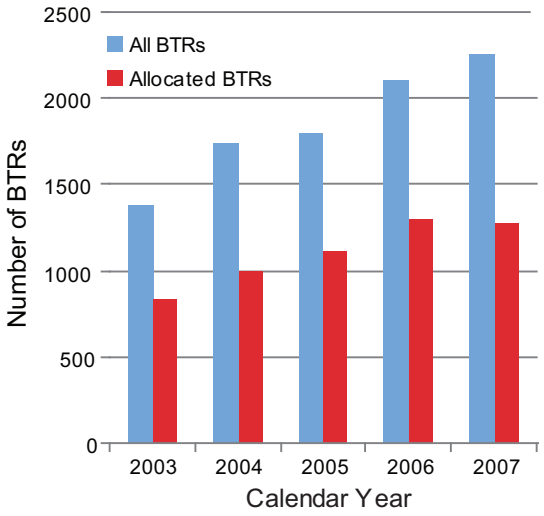

Fig. 2. Total number of GUP beam time requests (BTRs) vs. BTRs receiving time (excluding rapid-access), by calendar year.

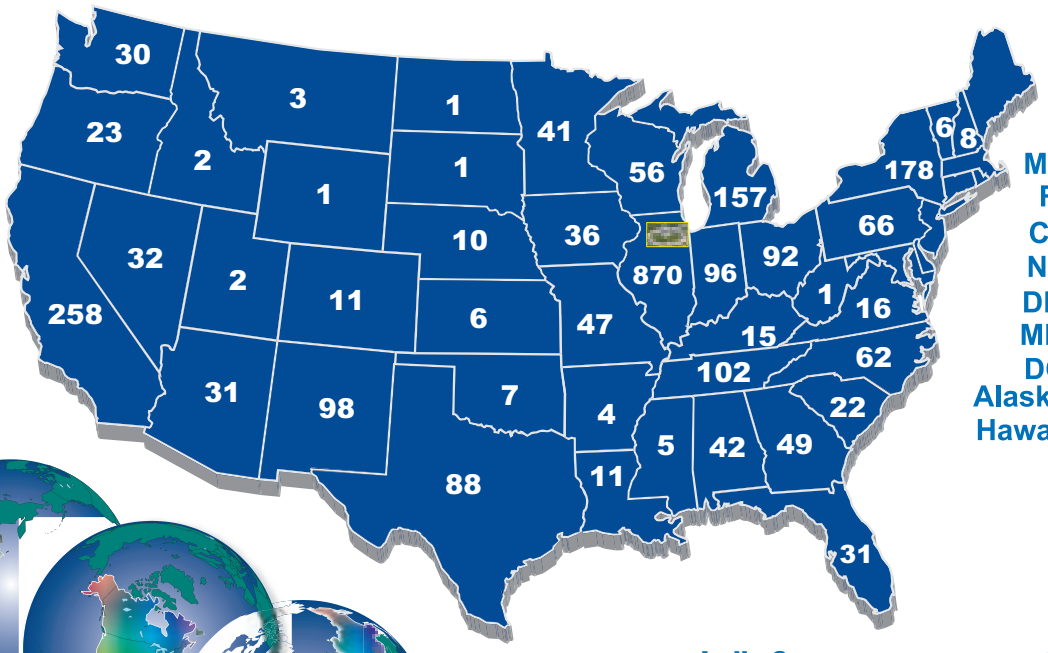

MA 149
RI 3
CT 36
NJ 37
DE 14
MD 104
DC 25
Alaska 5
Hawaii 4

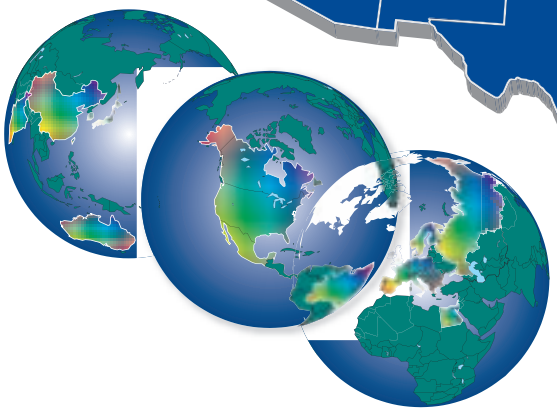

Australia 134
Belgium 4
Brazil 6
Bulgaria 1
Canada 116
China 15
Denmark 19
France 20
Germany 29

India 3
Israel 14
Italy 10
Japan 14
S. Korea 25
Malaysia 1
Mexico 3
Netherlands 3
New Zealand 4

Poland 1
Russia 3
Singapore 4
Spain 9
Sweden 4
Switzerland 6
Taiwan 6
UK 28

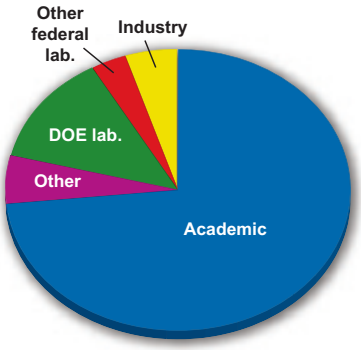

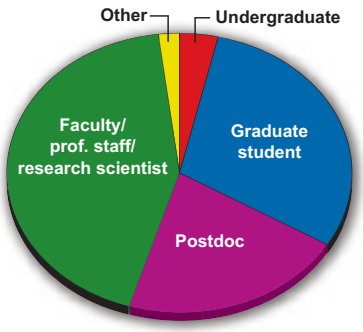

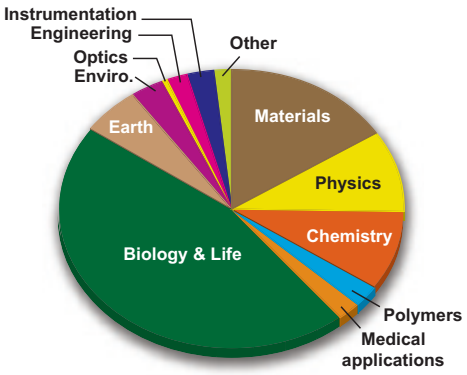

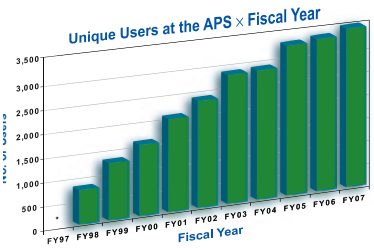

One-time user visits to the APS, by fiscal year (*N/A)

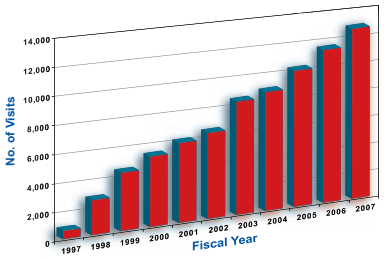

Total user visits to the APS, by fiscal year

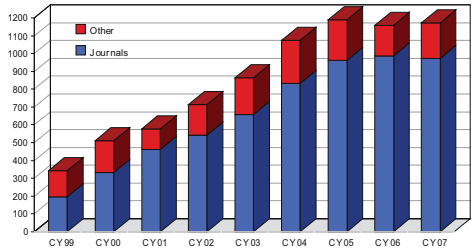

APS publications CY99-CY07 (as of 4.4.08)

A searchable database of all APS publications can be accessed at
http://beam.aps.anl.gov/pls/apsweb/pub_v2_0006.review_start_page

Users Week 2007 Draws Record Crowd

It seems to be said every year, but the 2007 Argonne Basic Energy Sciences Facilities User Week was the best yet. More than 740 people attended all or part of the activities, which ranged from scientifically exciting to socially entertaining. For the first time, this year's events included full participation from all four of Argonne's DOE-Basic Energy Sciences user facilities: the APS, the Center for Nanoscale Materials (CNM), the Electron Microscopy Center (EMC), and the Intense Pulsed Neutron Source (IPNS). Included in the week were 2 plenary sessions (the second segued into talks and classes geared toward users of the newly operational CNM), 5 targeted science sessions (including student talks), 2 poster sessions, 11 workshops, vendor exhibits, and social events, including a conference banquet at the Adler Planetarium in Chicago.

Presentation of the 2007 Compton Award. Left to right: Gene Ice (APSUO Chair), Tim Graber (APSUO Vice-Chair), winners Andrzej Joachimiak and Gerold Rosenbaum, and Murray Gibson (APS Director).

The 11 workshops were sponsored by two or more of the four user facilities and focused on research that could benefit from instruments and techniques available at more than one. The CNM organized six half-day, hands-on training sessions on electron beam lithography and focused ion beams for nanofabrication. The workshop titles included "Intermediate Energy Science at the APS," "Time-resolved X-ray and Neutron Scattering," "Kinetics and Dynamics in Soft Condensed Matter," "Drug Discovery at the APS," "Frontiers of Structure Analysis Using Powders," "Hard X-ray Nanoprobe," "X-ray Nanotomography, Synthesis and Self-assembly of Nanomaterials," and "Nanoelectronics." Further information about the workshops can be found at www.aps.anl.gov/Users/Meeting/2007/Workshops/index.htm.

During the meeting, the eighth Arthur H. Compton Award was presented to Andrzej Joachimiak and Gerold Rosenbaum (see following story).

Contact: Susan Strasser (strasser@aps.anl.gov)

2007 Arthur H. Compton Award

The 2007 APS and APS Users Organization (APSUO) Arthur H. Compton Award presented to Andrzej Joachimiak and Gerold Rosenbaum cites their "pioneering advances and leadership in establishing the APS as a premier location worldwide for protein crystallography research." The award consists of a plaque and a monetary award of $5,000.

Gerold—known to most as "Gerd"—Rosenbaum was recognized for his pioneering demonstration in 1970 that synchrotron radiation could be a source for biological x-ray diffraction, and for his innovative beamline designs, including 19-ID, 19-BM, and 22-ID at the APS, that have set a world standard for biological diffraction. Rosenbaum has spent a lifetime tackling the myriad technical challenges posed by synchrotron macromolecular crystallography; the optics he has designed to meet those challenges now permit the solution of immensely difficult structures. Currently, Rosenbaum is a senior beamline scientist at SER-CAT, operated by the University of Georgia, where he holds an appointment with the Department of Biochemistry and Molecular Biology. He is also associated with the Structural Biology Center (SBC) at Argonne.

Andrzej Joachimiak was recognized for his talents as a prolific crystallographer and innovator working with difficult structures, and for his foresight and pragmatism as the director of two highly productive and influential organizations: the SBC and the Midwest Center for Structural Genomics (MCSG), both within the Biosciences Division at Argonne.

As director of SBC, Joachimiak is responsible for the operation of the world's most productive synchrotron beamline, APS 19-ID. As of April 14, 2007, this beamline—designed by Rosenbaum—had submitted 1,100 protein structures to the Protein Data Bank, roughly 400 more than any other beamline in the world. Under his leadership, the SBC has been consistently lauded within the structural biology community for the outstanding care taken to make the beamlines operate to the tightest specifications and for the tremendous user support provided to crystallographers. The MCSG, which Joachimiak initiated, is the most productive among several centers in the Protein Structure Initiative funded by the National Institutes of Health and, with the help of synchrotron-based data, is establishing structural genomics as an important force in modern biology.

The selection of these two eminent individuals recognizes the international stature of protein crystallography conducted at the APS, the importance of this field of research, and the major roles played by Joachimiak and Rosenbaum in the development of this field.

From the 2007 Users Meeting program book

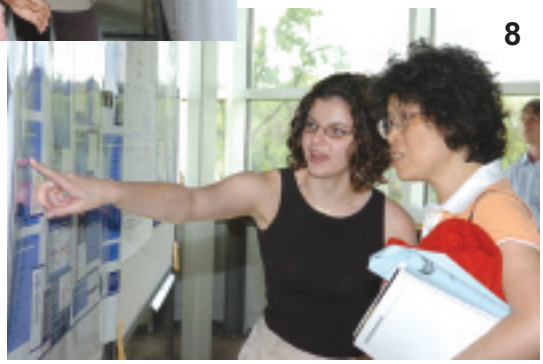

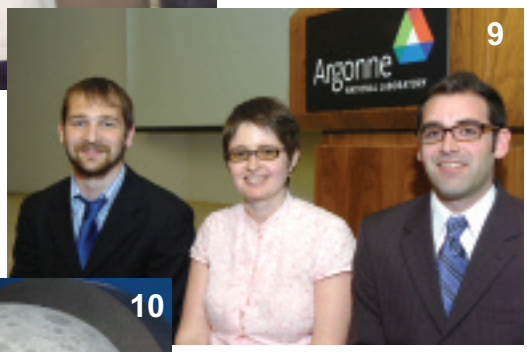

1: Rene Carder (Chief of Staff, Office of the Director, Argonne), welcomed attendees. 2: U.S. Representative Judy Biggert (R-IL-13th) gave the current congressional perspective, while (3) Pedro Montano (Director, Scientific User Facilities Division, U.S. Department of Energy [DOE], Office of Basic Energy Sciences) did likewise for DOE. 4. Eric Isaacs, Director of the CNM, gave an update on the just-opened facility. 5-8: Scenes from the poster sessions. 9: Poster abstracts by Michael Gramlich (left, University of Missouri), Nataliya Yufa (The University of Chicago), and James Wilson (Northwestern University) were selected to be presented as talks at the meeting. 10-11: Scenes at the Adler Planetarium during the banquet.

SESS 2007: Training the Next Generation of Synchrotron Environmental Scientists

Practitioners of the environmental sciences have traditionally been under-represented as users of x-ray spectromicroscopy tools. In a first step toward rectifying that situation, a two-week School for Environmental Sciences with Synchrotrons (SESS) was held at the APS on October 10-22, 2007. The APS is the only synchrotron radiation facility in the U.S. with a beamline that specializes in x-ray spectromicroscopy experiments in the intermediate energy (1-4 keV) range. The aim of the school was to introduce young scientists to the capabilities of the APS, under the tutelage of established environmental scientists. The hope is that initiatives such as this will encourage the next generation of environmental scientists to begin their own research projects at the APS and other synchrotron facilities.

Workshop attendees were given training on the scanning x-ray microscope at XOR beamline 2-ID-B. This instrument is one of the few in the world where spectral and spatial information can be obtained on chemical speciation of phosphorus, sulfur, and chlorine in specimens by x-ray near-edge absorption spectroscopy in combination with fluorescence mapping. These elements are of great interest to environmental scientists because of their prevalence and importance in systems such as soils, marine sediments, and bio-geo-chemical interfaces.

Four environmental researchers with synchrotron radiation science experience brought teams of graduate students and postdoctoral fellows to the school. The groups learned about the principles of x-ray spectromicroscopy and carried out hands-on work on the 2-ID-B scanning x-ray microscope. The younger scientists brought their own samples, assuring that the experiments were relevant to their work. John Coates's group, from the Department of Plant and Microbial Biology at the University of California, Berkeley, studied the fate of sulfur during reduction/reoxidation of humic substances and organic soil components, with the goal of comparing reduction pathways. Dean Hesterberg's group from the Department of Soil Science at North Carolina State University in Raleigh analyzed molecular mechanisms of phosphate retention and dissolution in organic matter and clay-organic systems. A group led by Johannes Lehmann from the College of Agriculture and Life Sciences at Cornell University aimed to understand mechanisms of stabilization of organic carbon in soil, namely the interactions between mineral and black carbon surfaces and microbial metabolites. Satish Myneni and his team from the Department of Geosciences at Princeton University studied phosphorus distribution and speciation in soil bacteria.

Juergen Thieme explains operation of the scanning x-ray microscope at 2-ID-B to (from left) Amanda Zelasko, Jieling Kizewski, and Yu-Ting Liu, all of North Carolina State University.

Concurrent with their experiments, the teams each gave seminars on their research to the APS community, contributing substantially to the breadth of the program. By the end of the school, all four groups planned to submit proposals for new experiments and to continue their research at the APS. In sum, the school introduced young scientists to the powerful capabilities of x-ray spectromicroscopy, gave them confidence to pursue their research programs, and broadened understanding of environmental research at the APS. The organizers, Juergen Thieme (Institute for X-ray Physics, University of Goettingen) and Ian McNulty (APS, Argonne), look forward to the next SESS school in 2008, and to introducing a new group of students to the exciting prospects for environmental x-ray spectromicroscopy.

Contact: Juergen Thieme (jthieme@gwdg.de), Ian McNulty (mcnulty@aps.anl.gov)

Reference

J. Thieme, I. McNulty, D. Paterson, and S. Vogt, Environ. Sci. Technol. 41, 6885 (2007).

Fast Charcterization of IDs

Insertion devices (IDs) at the APS are characterized and fine-tuned against their design specifications at the Magnetic Measurement Laboratory (MML) before installation in the storage ring. The MML is operated by the Magnetic Devices Group of the Accelerator Systems Division. A stretched coil system is used to measure the ID magnetic field integrals. Due to radiation damage, specific IDs must be pulled out of the storage ring during each scheduled accelerator maintenance period and retuned to their original design specifications. Because of time constraints set by the maintenance period, an efficient system was needed that achieves the highest accuracy possible to reduce characterization time.

The product of this necessity is the APS ID field integral measurement system (IFIMS). The IFIMS has been in use for three years and was recently upgraded. It has significantly reduced the turnaround time for characterization of IDs at the APS, from three weeks to one week.

The system consists of a long coil supported by two sets of stages, each with four axes of motion. A LabVIEW-based software control system has been developed to coordinate the stage motion control, position feedback, measurement data acquisition, and real-time data analysis. Figure 1 shows the schematic layout of the system. The system can be accessed via a wired or wireless Internet connection from anywhere, anytime, through the APS virtual private network. The motion status of the system, along with the lab environment, can be monitored through three sets of network cameras mounted in the lab.

Fig. 1. System control and data acquisition schematic layout.

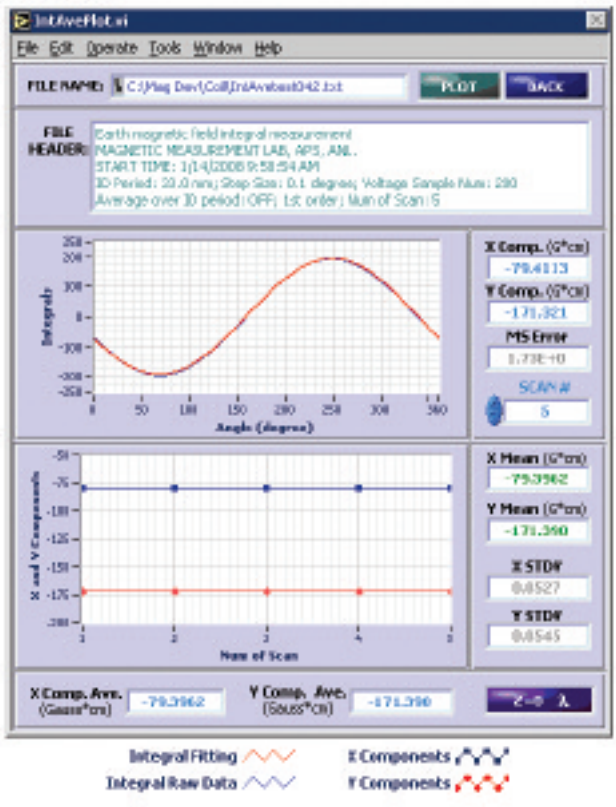

Fig. 2. Earth magnetic field integral measurements.

The system has the following operation modes. Rotation coil: First field integral (horizontal and vertical) measurements, second field integral (horizontal and vertical) measurements, and multipole components of first field integral measurements. Translation coil: multipole components of first field integral measurements. Stretched wire: first field integral (horizontal and vertical) measurements, second field integral (horizontal and vertical) measurements. The system also provides a user-friendly graphical user interface. The way to characterize a magnetic field integral measurement system is to measure the Earth magnetic-field integral. A typical Earth magnetic-field integral measurement is shown in Fig. 2.

With state-of-the-art field programmable gate array technology and linear ball bearing stages, the system is capable of synchronized measurements of position (0.005°/0.5 μm in resolution), time (25 ns), and voltage (16 bits). The system achieves the measurement accuracy of 0.06 Gauss centimeter (G-cm) in a field integral measurement of the Earth's magnetic field, which is more than 15 times better than current similar state-of-the-art systems reported elsewhere.

Contact: Joseph Z. Xu (jzxu@aps.anl.gov), Isaac Vasserman (isaac@aps.anl.gov)

XSD Beamline Technical Support

The members of the Beamline Technical Support (BTS) Group in the X-ray Science Division (*APS Science 2004*, ANL-05/04, pg. 145 [May 2005, Argonne National Laboratory]) expanded their mission of facilitating user experimentation at the APS through loans of acquired x-ray detectors and associated equipment via the Detector Pool, and the development of home-grown detectors.

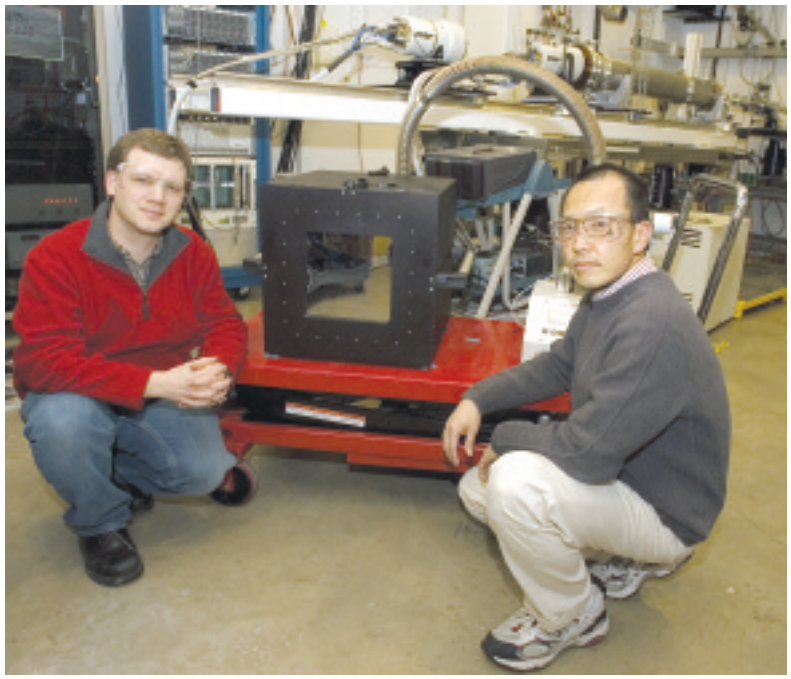

Tim Madden (left) and John Lee of the BTS Group, with the small-angle x-ray scattering detector in the 12-ID research station. The detector, which was designed and fabricated by BTS specifically for 12-ID, has four fiber-optic coupled CCDs, for a total active area of (170 mm)^2.

The Detector Pool

Approximately 260 loan transactions were made, to about 70% of the APS operational beamlines in 2007, with an average duration of 13 days per loan.

The Detector Pool expanded its inventory through the purchase of a 4-element silicon drift detector for spectroscopy applications (acquired from SII NanoTechnology USA, Inc.), a Sarnoff Corporation 10-ms readout charge-coupled device (CCD) camera for microscopy/tomography, and a Pilatus 100K silicon pixel array detector from the Swiss Light Source, PSI. The pool also purchased an amorphous silicon flat-panel detector that had been on lease from GE HealthCare since 2005.

Detector Pool staff also collaborated with beamline personnel at APS in the development of new techniques, such as rapid three-dimensional x-ray diffraction at high energies using the a-Si detector and time-resolved EXAFS using the Pilatus 100K.

Detector Development

The BTS Group designed and manufactured a high-sensitivity CCD camera for small-angle scattering at beamline 12-ID. The camera uses four Kodak KAF-4320E CCDs, each coupled to a 1:1.74 fiber-optic taper; the four tapers are tiled such that the detector sensitive area is (170 mm)^2. A Gd_2S_2O:Tb phosphor provides x-ray conversion. The camera is capable of operating up to 5 frames/s in 4 × 4 binned mode, where the effective pixel size is (168 μm)^2. The CCDs are operated under vacuum at -50° C to minimize dark current. The system electronic read noise is about 20 electrons. The detector was delivered to 12-ID in October 2007 for commissioning during run 2008-01. Future plans in this area include the design and manufacture of an in-vacuum version of the 4-element CCD detector (also at 12-ID) and the delivery to the APS Detector Pool of the single-element prototype camera built as part of this project.

Collaboration with the Advanced Light Source (ALS) on the development of high-frame-rate CCD detectors continued apace. The BTS Group designed and manufactured printed circuit board electronics for the project, including the clock drivers for the CCD and the FPGA-based data handling modules. The ALS designed and manufactured the almost-column-parallel CCD; with 96 outputs, this CCD is capable of being read at 200 frames/s. Integration of the first prototype camera (i.e., the ALS front end with the APS back end) is planned for spring 2008.

Efforts in the development of radio-frequency electronics for single-element avalanche photodiode (APD) detectors resulted in the delivery of seven units to the APS Detector Pool. The output signal from these custom-packaged detectors is typically 10-ns long, allowing for single-photon counting rates on the order of several tens of MHz. A multiphoton counting technique using these detectors has also been developed in collaboration with personnel from beamline 7-ID.

The BTS Group APD effort has moved on to the development of APD arrays in collaboration with Voxtel, Inc., under the auspices of the U.S. Department of Energy Small Business Innovation Research program. Voxtel made a presentation at the APS in November 2007 to discuss the possible parameters for the proposed detectors and to seek guidance from APS scientists on desired specifications.

With the aim of bringing integrated circuit design capabilities to the APS, the BTS Group strengthened its collaboration with Northern Illinois University on application-specific integrated circuits (ASIC). Another promising path being explored is collaboration with Cornell University on analog pixel-array detectors and with the ASIC Development Group in the Electrical Engineering Department of the Fermilab Particle Physics Division on the development of custom silicon x-ray sensors and integrated electronics.

Contact: Patricia Fernandez (fernandz@aps.anl.gov)

APS Light Source Operations, CY 2007

In 2007, the APS operated with exceptional reliability and availability, continuing the stellar performance of the previous years. No changes were made in fill patterns in '07, and the APS operated in its three standard patterns (in order of most time spent using the fill pattern): 24 singlets, 324 singlets, and hybrid fill. The APS storage ring was operated using the standard and "reduced horizontal beamsize" (RHB) lattices. Accelerator R&D concentrated on short-pulse production using pulsed crab cavities and exploration of options for the APS upgrade, as discussed elsewhere in this report.

Beam Availability & MTBF

In calendar year (CY) 2007, the APS scheduled 4,840 h for user operations and delivered 4,770 h, for an x-ray availability of 98.57% for the year, slightly higher than CY 2006. The mean time between faults (MTBF) was 101.5 h, 10% higher than CY 2006. Injector availability remained high at 98.2%, providing reliable beam for top-up. Table 1 shows detailed statistics for CY 2007.

The APS is continuing a period of mature, stable operation, characterized by unparalleled reliability. Indeed, the last run of 2007 was the thirteenth consecutive run for which the MTBF exceeded 48 h. The lowest MTBF during that thirteen-run period was 55.9 h, which is already very good. However, the median value was even more impressive at 89.1 h. The lowest availability during the same period was 96.9%, with a median of 98.3%.

Fill Patterns

The APS ring has the flexibility to support different fill patterns and lattices to serve special needs. The fill patterns used in CY 2007 (Table 1) were the same as those used in CY 2006. The standard average beam current for all operating modes is 100 mA.

- *24 uniformly-spaced bunches in top-up mode, used 61.5% of the time.* This is the most common fill pattern, also called 24 singlets, and features 24 equally-populated bunches separated by 154 ns. The bunch length is 40 ps rms. This bunch pattern is a good compromise between the needs of timing users, who benefit from the bunch separation, and flux-hungry users, who require 100 mA but do not have requirements for the bunch distribution. Bunch purity is very important in this mode. The particle accumulator ring (PAR), one of the injector systems, has a bunch cleaning system that has been operating since 2005 (see "The Particle Accumulator Ring Gets Cleaner," *APS Science 2005*, ANL-05/29, pg. 178 [May 2006, Argonne National Laboratory]), and keeps the bunch purity to a level of a few parts in 10^7. Top-up at a 2-min interval is needed for this pattern due to the relatively short beam lifetime (about 6 h). High-current machine studies have shown that up to 164 mA can be stored stably in the 24-singlets mode. Higher-order mode dampers installed during 2005 have raised instability thresholds in this mode to above 164 mA.
- *324 uniformly spaced bunches in non-top-up mode, used 20.7% of the time.* Non-top-up operation, whereby the storage ring is refilled to 100 mA twice every 24 h, is mainly used to allow for injector maintenance and improvement, operator training, and injector beam time for parasitic injector study. The beam lifetime in the 324-bunch mode is such that the beam decays to about 83 mA after 12 h. With smaller bunch currents compared with 24 singlets, the bunch length in the 324-bunch mode is 25 ps rms. High-current studies have shown stable operation up to 200 mA in this bunch pattern. In contrast with the 24-singlet case, there are no accelerator component heating issues in this mode, a result of the much smaller bunch current.
- *1 + 8 × 7 hybrid pattern in top-up mode with 16 mA in the isolated bunch, used 17.8% of the time*. In this pattern, a single 16-mA bunch is injected on one side of the ring. The remaining 84 mA of stored beam current resides in 8 groups of 7 bunches on the other side of the

Continued on page 156

Table 1. Availability statistics for CY 2006 (totals) and CY 2007 (by run).

	CY2006	CY2007			
	Totals	Run07-1	Run07-2	Run07-3	Totals
Scheduled hours (h)	4986.1	1535	1728	1577	4840
Available for users (h)	4875.2	1514.8	1692.7	1563.1	4770.6
Beam availability (%)	97.98	98.7	98.0	99.1	98.57
Total downtime (h)	110.9	20.2	35.3	13.9	69.4
Average current (mA)	100.1	101.2	99.7	98.6	9.8
Number of faults	52	13	19	15	47
Mean time between faults (h)	92.3	116.5	89.1	104.2	101.5
Mean time to recovery (h)	2.13	1.56	1.86	0.93	1.48
Injector availability (%)	98.2	99.3	98.7	98.2	98.7

"Operations" continued from page 155

Table 2. Parameters at RHB sectors vs. standard sectors.

Type	Horiz. Beta (m)	Horiz. Eta (m).	Horiz. Size (μm)	Horiz. Diverg. (μrad)	Vert. Beta (m)	Vert. Size (μm)	Vert. Diverg. (μrad)
Normal	19.5	0.170	286	12.0	2.9	9.0	3.1
RHB	3.2	0.078	120	29.6	5.4	12.3	2.3

ring. This arrangement results in symmetrical, beam-free regions with a duration of 1.59 μsec on either side of the intense bunch. The bunch length of the 16-mA bunch is 65 ps rms and that of the remaining bunches is 32 ps rms. Top-up is essential for the hybrid pattern. Because of the short lifetime of the intense bunch, the top-up interval is 1 min when using this pattern. Roughly three out of four top-up injections go toward maintaining the current in the intense bunch.

The RHB Lattice

The standard symmetric low-emittance lattice introduced in CY 2003 was utilized for almost all user operations during CY 2007. In 2006, for the first time, the APS delivered beam to users in the so-called RHB (non-symmetric) lattice. In 2007, the APS had two periods using this lattice (runs 07-02 and 07-03), where the rms horizontal beam size at beamline 32-ID is reduced from 280 × μm to 120 μm, at the expense of a <10% increase in horizontal emittance, which is more or less transparent to other users while offering better beam on selected sectors. This was accomplished by reducing the horizontal beta function and dispersion at those insertion devices by adjusting quadrupoles in the surrounding sectors. Table 2 gives a comparison of the parameters at the RHB sectors to those in standard sectors, assuming nominal 1% coupling. This lattice was used in 24-singlets mode for 13.5% of the total time. Other periods of operation with this lattice are planned for CY 2008.

The benefits of the RHB lattice were demonstrated by the APS X-ray Science Division X-ray Microscopy and Imaging Group using in-line phase-contrast imaging studies (see "X-ray Imaging & Optics Development," *APS Science 2002*, ANL-03/15, pg. 93 [May 2003, Argonne National Laboratory] and "Operations," *APS Science 2006*, ANL-06/23, pg. 160 [May 2007, Argonne National Laboratory]).

Booster Parameters Online

A set of booster parameters is now online and borrows from the development last year of the storage ring parameter pages. From the APS home page (http://www.aps.anl.gov) one can follow the "Facility" pull-down menu to find the "Booster Parameters." This link gives access to a set of Web pages that form a living document that is periodically updated to correspond to operational and/or hardware changes. Detailed information is provided on the main beam parameters, lattice, operation modes, and hardware such as magnets and power supplies. Plans are afoot to expand these pages in the future to include the PAR and linac and any other data requested by users.

Contact: Michael Borland (borland@aps.anl.gov)

Around the APS

Distinguished Achievements in Accelerator Science

Michael Borland, Operations Analysis Group Leader in the APS Accelerator Systems Division, was one of four Argonne employees to be presented with a Distinguished Performance Award for 2007. Borland was recognized for his work in "the development and implementation of software for accelerator research that is recognized internationally and that represents groundbreaking achievements in the field of computational accelerator physics," according to Efim Gluskin, Accelerator Systems Division Director. The University of Chicago Distinguished Performance Awards, which recognize outstanding scientific or technical achievements or a distinguished record of achievement by select Argonne employees, are presented by the UChicago Argonne, LLC Board of Governors.

Borland's best-known work is **elegant** (**ele**ctron **g**eneration **an**d **t**racking) (see *APS Science 2005*, ANL-05/29, p. 174 [May 2006, Argonne National Laboratory]), an accelerator simulation code that provides physicists with a flexible tool to design and understand linear accelerators and storage rings. **elegant** was used to develop the present APS storage ring lattice that is producing an electron beam with the record low emittance and reduced horizontal beam size that are vital to providing users with a reliable supply of x-ray beams. **elegant** is in use at light sources worldwide.

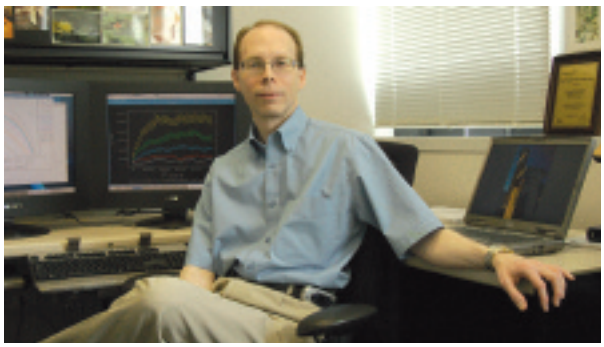

Michael Borland

Testing the APS Storage Ring RF Cavity Dual-Coupler

It has long been anticipated that the APS could need additional space for straight sections, driven by applications ranging from bunch-by-bunch feedback kickers, a higher harmonic cavity, and transfer lines for a major APS upgrade. Without sacrificing x-ray beamlines, the available straight-section space will come from the locations where radio-frequency (rf) cavities are located. In order to reduce the number of cavities, more power must be delivered to the cavities; to accomplish this, additional cavity power couplers are needed. As part of a feasibility study, the Accelerator Systems Division Radio Frequency Group tested an rf cavity configuration equipped with a dual-coupler to determine if the number of cavities in the storage ring could be reduced while maintaining 100-mA current.

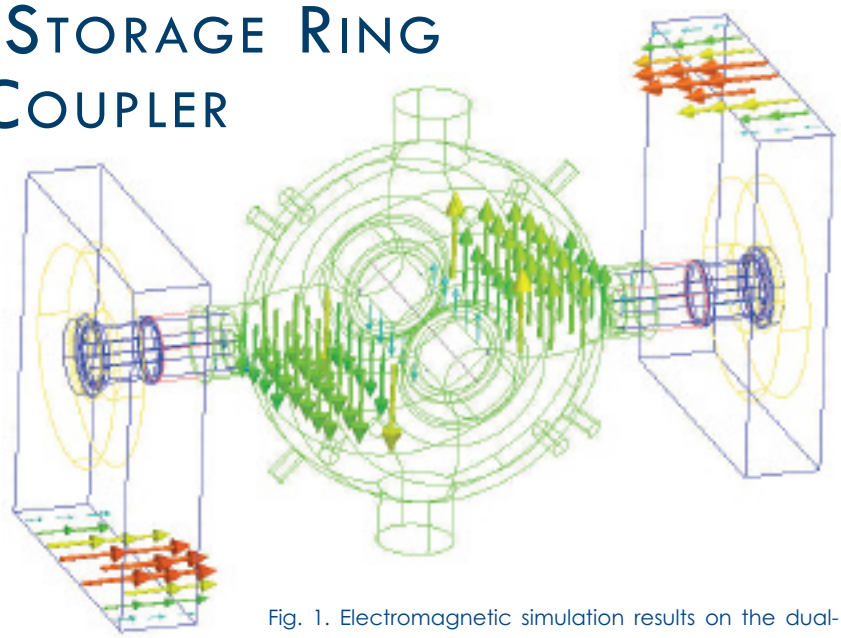

Fig. 1. Electromagnetic simulation results on the dual-coupler/ cavity assembly indicating vector plots of the cavity magnetic fields and properly phased electric fields in the input waveguide feeding each coupler.

An electromagnetic simulation model of the two-coupler-cavity configuration was developed and utilized to successfully predict the optimum match setting of each coupler to achieve the best total return loss from the cavity. Figure 1 shows the simulation model, indicating the orientation and intensity of the electric and magnetic fields in the waveguide and cavity, respectively. The simulation results predicted that the cavity would develop a peak gap voltage of 1.45 MV with 183-kW forward power into the cavity.

The dual-coupler test was designed to determine the capability of the existing APS 350-MHz single-cell storage ring rf cavity design and related components to operate reliably at a total power level of 200 kW in continuous-wave (cw) mode. The test utilized two separate input couplers on the cavity, thereby enhancing reliability by keeping the power handled by each coupler at the nominal value of 100 kW [1]. The APS 350-MHz rf test stand was utilized to perform the test. A photo of the test cavity assembly is shown in Fig. 2.

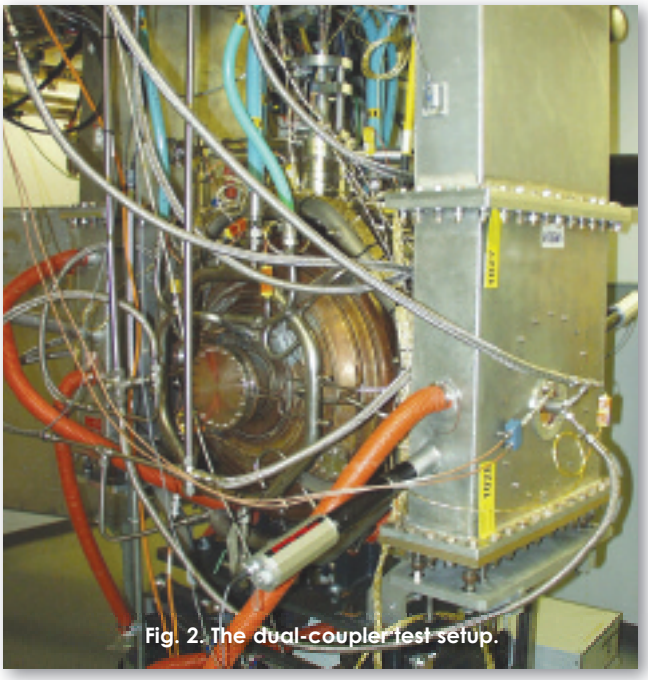

Fig. 2. The dual-coupler test setup.

Radio-frequency power is supplied to the cavity by a WR2300 waveguide system, which includes a 3dB/90º hybrid to produce two equal-power feeds, each of which drives a separate input coupler on the cavity. Two manual waveguide phase shifters are used in the half-power feed to coupler #1 to optimize the relative phase of the two power feeds at the cavity in order to achieve maximum power transfer.

By utilizing normal rf conditioning, a total cavity rf input power of 200 kW was achieved and maintained with no damage to the cavity, power couplers, or related components. Normal vacuum behavior was noted during the conditioning process, and the cavity vacuum base pressure became very quiet and unresponsive to power increases over approximately 170 kW. Cooling-water flow was increased slightly to the cavity and tuner piston to keep the cavity center copper and tuner piston return water temperatures below 92º C and 42º C, respectively. All other cavity system temperatures were within normal range.

Based on operating data recorded during the test, a dual-coupler configuration would allow operation of the existing APS single-cell cavity design beyond the original and current operating power of 100 kW, providing the option of reducing the number of cavities in the storage ring to create additional straight sections in Zone F, thereby accommodating new science drivers, while maintaining 100-mA operational capability. *Contact: Ali Nassiri (nassiri@aps.anl.gov), Douglas Horan (horan@aps.anl.gov)*

Reference

[1] D. Horan, D. Bromberek, D. Meyer, and G. Waldschmidt, Proc. of PAC2007, (Albuquerque, NM, 2007), pg. 2227.

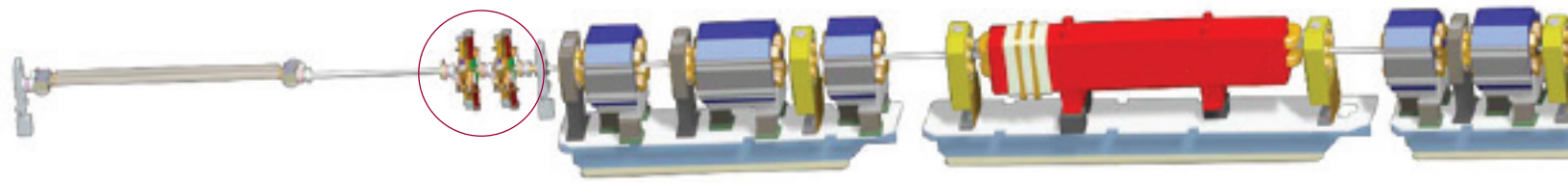

Fig. 1. Two-sector implementation of room-temperature deflecting cavities (circled).

The APS Short-Pulse X-ray Project

For over a decade, researchers have used the APS to study structural changes on the atomic length scale and on time scales of 100 ps and longer by employing pump-probe techniques. In order that the APS remain a leader in ultrafast science, it is important that the time domain from 1 to 100 ps be covered to bridge the gap between the capabilities at current storage rings and future hard x-ray free-electron lasers (FELs). Exciting scientific problems on this time scale include, but are not limited to, thin-film and nanoscale materials on the time scales of thermal relaxation and transport; picosecond x-ray spectroscopy measurements on low-density samples; time-resolved structural studies of molecular electronic excited states and reaction intermediate structures; and ultrafast scattering from solid-state physics, including inverse-Peirls, diffuse scattering, anharmonic decay, softening diffuse scattering, softening volume collapse, and insulator-metal and other ultrafast solid-phase transitions. These important scientific problems have motivated APS to pursue the development of high-flux picosecond beamlines through advanced accelerator techniques.

APS accelerator physicists and engineers have explored options for generating short x-ray pulses via Zholents' scheme [1], which uses radio-frequency (rf) deflecting cavities to impart a transverse momentum chirp to the electron beam. This allows the creation of an angle-chirped x-ray pulse and thus short pulses by slitting or using compression optics. In 2006, a team began designing pulsed room-temperature copper deflecting cavities, with the goal of later pursuing a superconducting system (see "Short Pulses on a Fast Track," *APS Science 2006*, ANL-06/23, p. 164). For the warm system, a configuration consisting of two pairs of 3-cell rf cavities installed in two consecutive straight sections was chosen (Fig. 1). With a 4-MV deflecting voltage, an x-ray pulse length of under 2 ps full width half maximum (FWHM) with 1% transmission relative to the nominal intensity through a 0.5-mm by 0.5-mm slit, 26.5 m from the insertion device (the configuration for APS beamline 7-ID) is predicted. The warm system is limited to operation in "hybrid" mode (see "Operations," page 155) and to a maximum rate of 1 kHz by rf heating of copper structures. The cold system could operate continuous-wave in all operating modes.

The Room-Temperature Cavity

A baseline rf and electrical engineering design of the deflecting cavity has been completed. The cavity consists of three cells [Figs. 2(a) and (b)] operated at 2815 MHz (eight times the storage ring rf frequency). Power is symmetrically coupled to the structure through two high-power waveguides connected to the end cell. For damping of long-range wakefields, each cell is loaded by waveguides. The waveguides are designed so the fields of the working mode do not propagate into the broadband loads, but lower- and higher-order modes are heavily loaded.

Single Particle Beam Dynamics

Single particle beam dynamics, tolerances, and performance were modeled in detail [2]. These studies allow minimizing vertical emittance growth, which is a primary concern. For a 1-kHz repetition rate, the equilibrium vertical emittance is about 27 pm (starting from 13 pm), compared to 25 pm used in normal operations. Emittance growth negatively impacts the x-ray pulse duration. A point of reduced returns is reached at about 4 MV (Fig. 3). The x-ray pulse duration is affected by the intrinsic divergence of the photon beam. Using 25 keV instead of 10 keV, a 3.3-m U18 device instead of a 2.4-m U33, and increasing the beta function from 3 m to 6 m reduces the predicted pulse duration below 1-ps FWHM.

The Zholents scheme relies on cancellation of the strong perturbation of the upstream cavities by the downstream cavities. Hence, some of the tolerances are quite challenging: ± 0.07º for static intercavity phase errors and ± 0.12% for static intercavity voltage errors.

Beam Stability & Intensity Limits

An important criterion for the APS short-pulse project is to have little or no impact on beam stability or intensity limits. Preliminary studies found no issues with maintaining present APS orbit stability. Regarding intensity limits, compatibility with all operating modes was evaluated. The reduction in the single-bunch limit (now 20 mA) was specified to be under 5%, which was used to determine the cavity iris dimension via wakefield calculation and tracking [3]. The design margin for multibunch collective instability thresholds was 100% (equivalent to 204-mA operation). This was used to determine the required damping of parasitic higher- and lower-order rf cavity modes to ensure that the instability growth rate is less than the radiation damping rate [4].

Highly Stable RF Distribution

The deflecting cavity fields must maintain a stable phase to ±10° at 2815 MHz relative to electron beam arrival time. An additional important requirement is that an rf reference (88 MHz) provided to the beamline laser have a phase stability of ±0.9° (at 2815 MHz) relative to the deflecting-cavity field. To meet these requirements, a fiber-optic link with active phase stabilization is being developed to transport a 351.9-MHz phase reference signal to the short-pulse x-ray sector low-level rf system. A detailed concept was developed for a

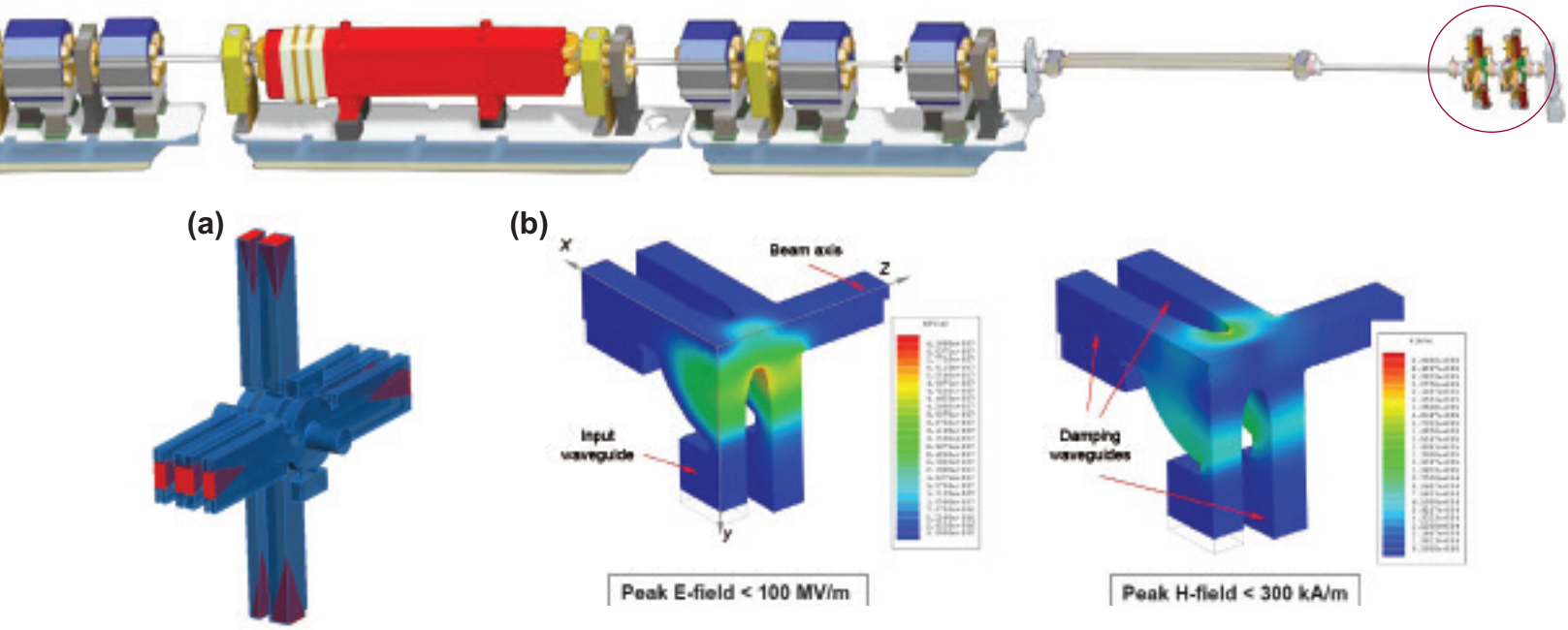

Fig. 2. (a) Three-cell deflecting cavity with end-cell input coupler. (b) Surface electric (l.) and magnetic (r.) fields in 1/8 of the 3-cell standing-wave deflecting structure. Peak surface electric field is <100 MV/m and peak magnetic field is <300 kA/m. Fields are scaled for a 2-MV vertical kick with ~2.8 MW of rf power.

phase-stabilized fiber optic link, which is an outgrowth of previous developments for linear colliders and x-ray free-electron lasers. A future energy recovery linac upgrade to the APS would likely require a similar system.

Future Plans

Although the design of a room-temperature pulsed system is essentially complete, plans to install this have been shelved due to high cost for limited scientific benefit. Instead, superconducting rf (SCRF) technology is being explored as an alternative with greater scientific potential. A cold system provides greater operational flexibility by allowing cw operation in more general filling modes; this is an attractive feature for specific time-resolved experiments. The objective is to initiate a three-year R&D program to conduct feasibility design studies of multi-cell SCRF deflecting cavities. A prototype SCRF cavity cell has already been designed and built in collaboration with researchers at Thomas Jefferson National Laboratory, and will soon be characterized.

As in the pulsed case, it is challenging to effectively damp long-range wakefields in the cavity. In recent years, the KEK B Factory in Japan has successfully developed and implemented a 500-MHz SCRF deflecting cavity in order to raise the luminosity of colliding beams. For mode damping, KEK used a coxal beam-pipe transmission line. Because space is at a premium in the APS, alternative compact designs that rely on waveguide damping will be investigated.

Tolerances for the SCRF system have already been investigated, and are similar to those for the room-temperature system. Work will thus continue on development of precision rf phase distribution and control. Related issues, such as bunch-to-bunch charge uniformity and fill pattern effects will be investigated. As in the case of the room-temperature system, single-bunch intensity limits and multi-bunch instabilities will be evaluated in an iterative fashion to arrive at a final cavity design and configuration. Use of SCRF may well require lengthening several straight sections to make room for the cavity cryostats. The impact of this on storage ring operation will be thoroughly investigated in simulation and machine studies. *Contacts: SPX project: Ali Nassiri (nassiri@aps.anl.gov), Michael Borland (borland@aps.anl.gov), Katherine Harkay (harkay@aps.anl.gov). Stable rf distribution: Frank Lenkszus (frl@aps.anl.gov)*

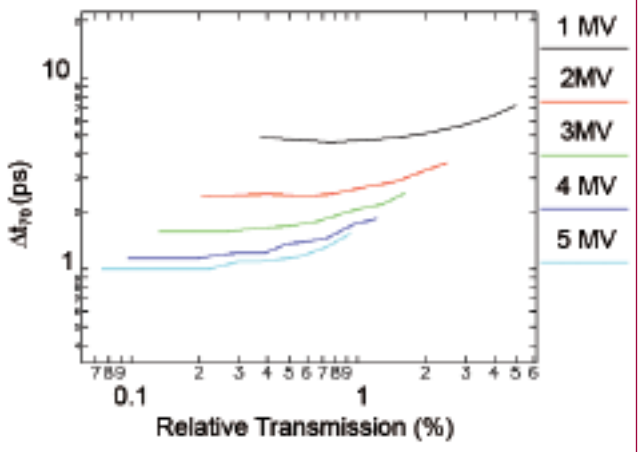

Fig. 3. Duration of the sliced x-ray pulse as a function of relative transmission through the slits. In this case, a 0.5-mm horizontal slit at 26.5 m from the source is included, as this slit is normally present for beamline 7-ID.

References

[1] A. Zholents, P. Heimann, M. Zolotorev, and J. Byrd, NIM A **425**(1-2), 385 (1999).

[2] M. Borland, L. Emery, V. Sajaev, Proc. of PAC 2007, Albuquerque, NM, pg. 3429 (2007).

[3] Y.-C. Chae, G. Waldschmidt, and V. Dolgashev, Proc. of PAC 2007, pg. 4339 (2007).

[4] L. Emery, Proc. of PAC 2007, Albuquerque, NM, pg. 348 (2007).

Status of Energy-Recovery Linac R&D

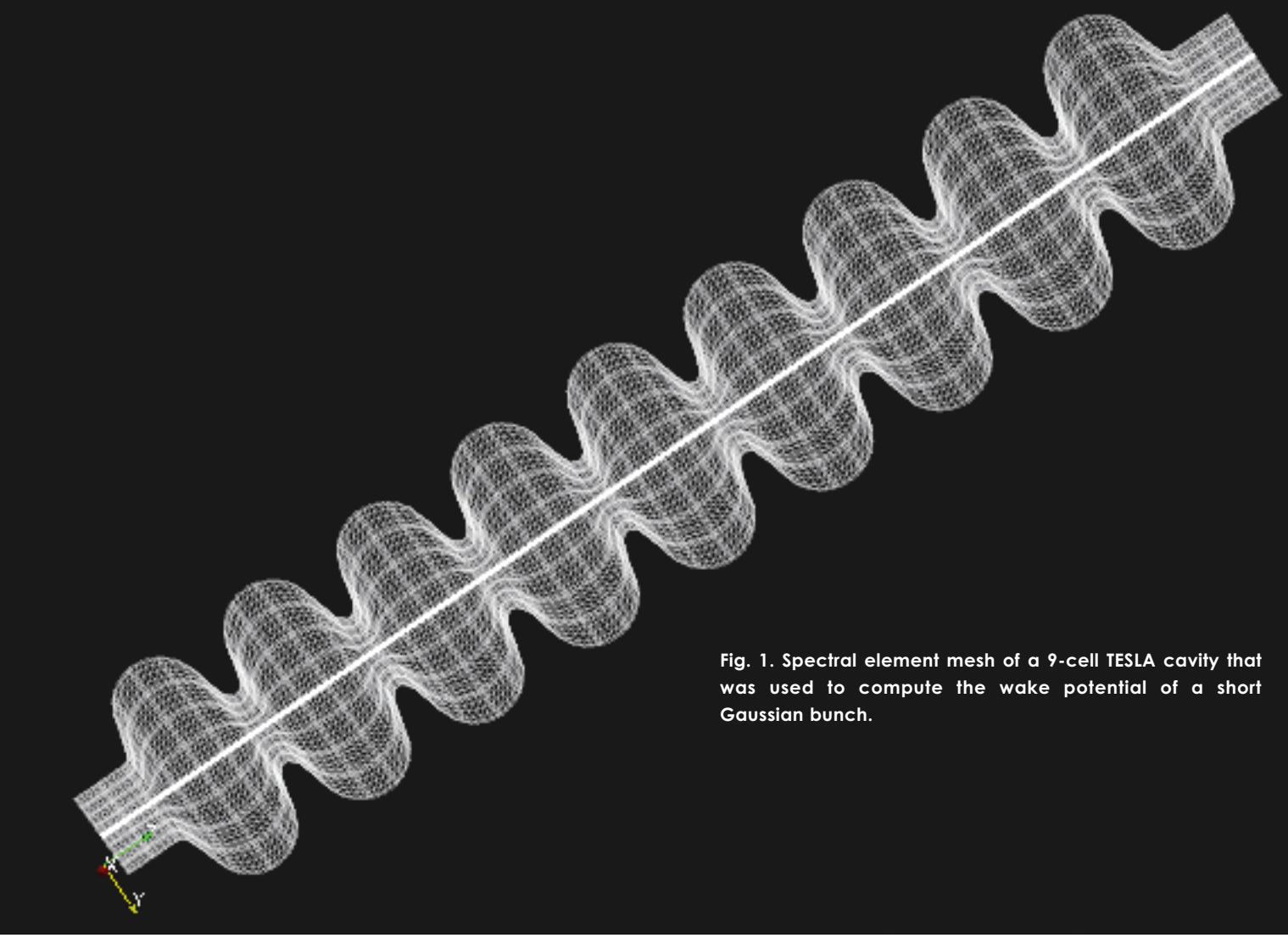

Fig. 1. Spectral element mesh of a 9-cell TESLA cavity that was used to compute the wake potential of a short Gaussian bunch.

For several years, APS accelerator physicists have explored a number of options for upgrades, both minor and major, to the light source. Higher brightness and coherence are always in mind when one speaks of an upgrade, but there are other considerations as well, including bunch duration, flux, the number of straight sections, and the length of straight sections. The two concepts of greatest interest for a major APS upgrade are a replacement storage ring and an energy-recovery linac (ERL [1]). In 2006, the APS, in consultation with users, reached the conclusion that of these, only an ERL promises a revolutionary improvement in x-ray brightness and transverse coherence. In 2007, the R&D necessary to eventually build an ERL at APS was mapped out and work began to address the physics and technical issues.

Progress on Beam Dynamics

Beam dynamics in ERLs is quite different from that in storage rings, in that the beam never comes to equilibrium in an ERL as it does in a ring. Indeed, this is why an ERL promises such high brightness. Because good ERL performance demands excellent gun performance, several studies were begun related to the gun and its performance requirements. Predictions of ERL performance assume very small "normalized" emittances from the injector, on the order of 0.1 μm for a 20-pC bunch with 2-ps bunch duration [2]. This has some support in simulations performed at Cornell [3] and KEK [4], but it is prudent to ascertain what the impact of larger emittance would be. This was analyzed [5] under the assumption of the same undulator in the ERL as is used today, namely, a 2.4-m-long U33 device. For the 25-mA "high-coherence" mode, an emittance of 1.6 μm, about equal to the present state of the art, is required to break even with the present-day APS in terms of brightness, while giving a roughly four-fold increase in coherent fraction. An order-of-magnitude increase in brightness requires an emittance of 0.2 μm, about an order of magnitude less than what can presently be achieved. The

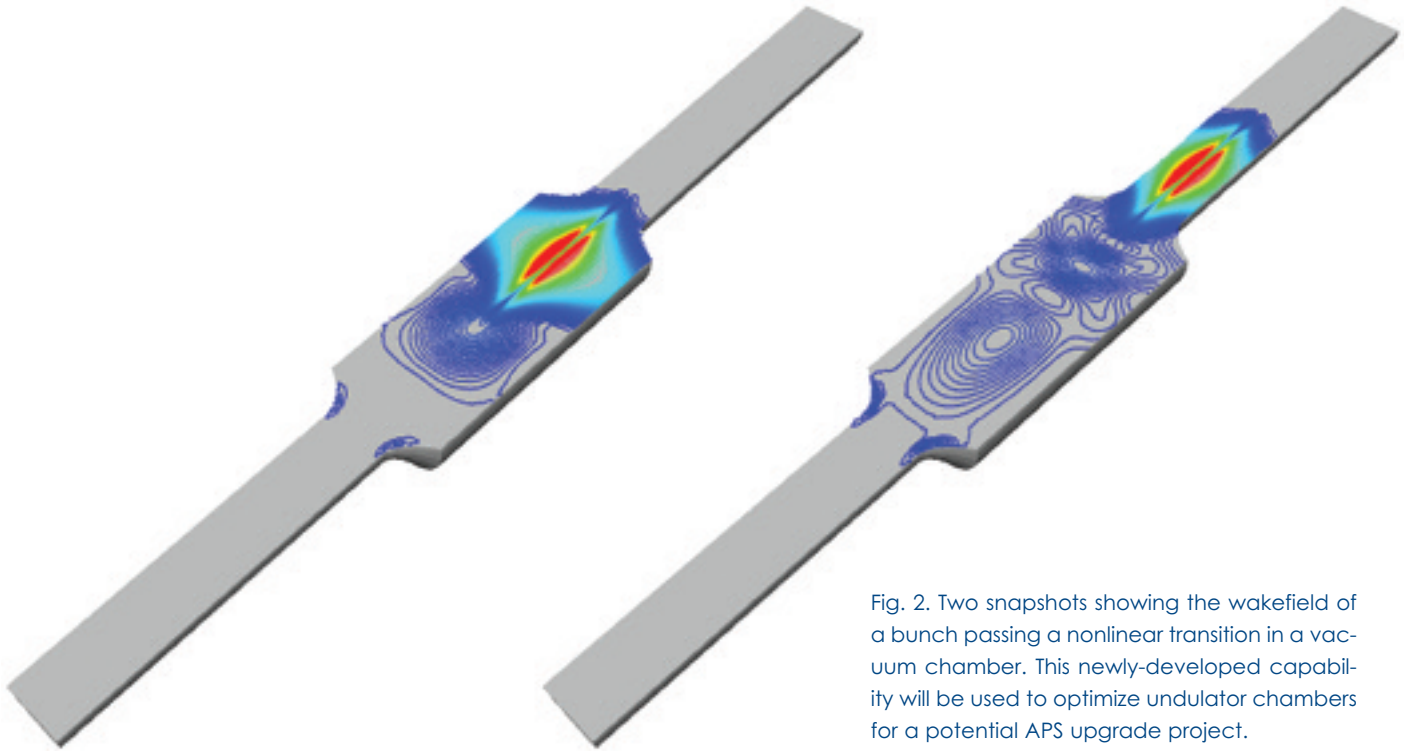

Fig. 2. Two snapshots showing the wakefield of a bunch passing a nonlinear transition in a vacuum chamber. This newly-developed capability will be used to optimize undulator chambers for a potential APS upgrade project.

bunch length, which influences brightness of high harmonics by influencing the energy spread of the beam at the end of the linac, can actually be increased considerably from the nominal 2 ps rms. Even with 4 ps rms, the brightness is only reduced by a factor of two. This is welcome news because it is easier to achieve smaller emittance with a longer bunch.

Also initiated was a program of injector optimization studies [6,7] using parallel genetic optimization software originally developed at the APS for storage ring applications. Initial results show emittances of 0.1 μm at the entrance of the linac merger. An ellipsoidal beam shape, which should be practical, gives better results than the traditional "beer-can" shape. Work is under way to include the merger system and also decrease the required gun voltage.

Because the APS operates at 7 GeV, it is perhaps natural to think of the ERL as operating at the same energy. However, higher energy is more expensive, and it is not a foregone conclusion that the performance is better if carefully optimized undulators are used. For one thing, certain emittance-corrupting mechanisms are dramatically less severe at lower energy. The optimum beam energy, undulator gap, and undulator period for a series of target photon wavelengths were determined, including details about how the beam properties are affected by the energy. The conclusion [8] was that for hybrid permanent magnet undulators, the optimum energy is above 7 GeV for photon energies above 3 keV.

Beam loss is a particular concern in ERLs because of the continuously available beam from the injector. One of the primary mechanisms for beam loss for low-emittance beams is particle-on-particle scattering, known as Touschek scattering. Like other beam-loss mechanisms in ERLs, the loss probability for an individual particle is very small, which introduces challenges for simulation. The program **elegant** [9] was extended to allow Monte Carlo simulation of Touschek scattering and prediction of beam-loss rates and locations [10]. A study of beam loss in the APS ERL design is ongoing using this software.

Plans for Improving Cavity Q

The wall-plug power requirement for high-current light source ERLs is on the order of tens of megawatts. Design, implementation, and operation of a large cryoplant are all very challenging, not to mention the high operational cost [11]. It is therefore necessary to improve existing processing techniques and, in parallel, to explore the suitability of other superconducting (SC) materials to obtain and retain a very high cavity quality factor (Q_0). Improving cavity Q_0 by a factor of two will result in many-megawatts reduction of wall-plug power. The goal for the intrinsic quality factor of a multi-cell cavity is between 5×10^{10} and 1×10^{11} operating at a cryogenic temperature of 2K. Recently, several new ideas and approaches to improving Q_0 have been proposed:

Godeke [12] has studied the suitability of Nb_3Sn to improve the SC radio-frequency (rf) cavity quality factor at 4.2K. Nb_3Sn is promising for rf cavity applications, due to the material's superior intrinsic properties compared to Nb. Further research is required to investigate its applicability to large-scale SC rf cavity production.

Gurevich [13] has shown that the magnetic field at which rf breakdown occurs in SC cavities can be significantly increased by a multilayer coating consisting of alternating insulating layers and thin SC layers of thickness smaller than the London penetration depth. This may delay the onset of the drop in Q that occurs as the field is raised, thus helping to maintain a high Q at operating field levels.

Continued on page 162

"Linac R&D" *continued from page 161*

Atomic layer deposition (ALD) can be used to grow multiple, epitaxial (polycrystalline or amorphous), monolayer coatings of a variety of materials on a variety of substrates with a fast deposition rate [14]. These facts indicate that this research should readily transfer to growing films on complex rf cavity structures to improve the surface intrinsic quality factor, Q_0. The APS is working with the Argonne Materials Science Division to explore ALD on bulk Nb cavities.

Intrinsic Emittance in Cathodes

The highest-brightness electron sources available today are based on warm rf gun technology using laser-driven photocathodes. Such guns can produce pulsed 1-nC bunches with 1-2 μm normalized emittance and 1-ps to 2-ps duration. In comparison, an ERL source demands a CW beam with an emittance (~0.1 μm) that is an order of magnitude smaller than the best pulsed sources presently available, albeit at much lower charge per bunch (~20 pC). While it is debatable whether DC or rf technology is best for such a source, we can confidently assume that cathode development will be required for ultra-low emittance. However, the critical physics near the cathode surface is incompletely understood. Even if one could achieve perfect emittance compensation, the fundamental material properties of the cathode would determine the lower bound on the achievable emittance of the electron source. There is no fundamental new physics related to electron emission, but there is a gap in our ability to combine all of the relevant phenomena into a complete and useful physical model [15]. For this reason we developed a plan for a fundamental, systematic study of cathode materials and intrinsic emission properties.

A major goal of the cathode test-and-development effort will be to systematically measure the properties of candidate cathodes suitable for an ERL and to formulate proper control for cathode fabrication. Of particular interest is the systematic experimental characterization of the intrinsic emittance in a controlled environment. These data will be benchmarked against existing emission models and used to develop improved models. The key technique for measuring the momentum distribution of the emitted electrons is angle-resolved photoemission spectroscopy (ARPES). Specification has begun for the hardware required to upgrade the existing surface analysis laboratory [16] to add ARPES capability for wavelengths down to UV. The study of the cathode lifetime and evolution of the intrinsic emittance under operating conditions will be carried out in the injector test stand [17].

Another major goal is to understand in detail the physics trade-offs among intrinsic emittance, quantum efficiency (QE), and drive laser power in a realistic electron injector environment. Boundaries on maximum intrinsic emittance, minimum QE, and drive laser requirements for the ERL source are being established. Also in process is analysis of the literature to identify potential cathode candidates for further study. While the initial emphasis is on photocathodes, field emission and other sources have not been ruled out. These efforts are complementary to similar R&D efforts elsewhere, and productive collaborations are being established.

To preserve the beam emittance produced at the cathode, a homogeneous ellipsoidal beam is best, due to the linear space-charge force throughout the electron beam. To this end, laser pulse shaping that can produce an ellipsoidal beam distribution is being studied. Preliminary experimental results are encouraging and are continuing. The final ingredient is numerical study of injector design and optimization, as described above.

Analysis of Wakefield Effects

The ERL will accelerate and transport very short bunched beams, on the order of a few ps rms. The dynamics of short-pulsed beam will require advanced computational methods for time-domain electromagnetic fields. With existing software, it would take about 10,000 days to compute the wake potential of an undulator chamber using a 100-fs probe beam. In order to resolve this computational bottleneck, development of a higher-order code was initiated in collaboration with the Argonne Mathematics and Computer Science Division. The new code uses the Spectral Element Discontinuous Galerkin method for performing a high-order solution of Maxwell's equations. The code will be used to investigate the energy spread induced in the beam from passing through the 7-GeV superconducting linear accelerators as shown in Fig. 1. It will also be used to evaluate and optimize undulator chamber shapes to minimize the transverse wakefield. An example of a computation for an undulator chamber is shown in Fig. 2.

Contact: Michael Borland (borland@aps.anl.gov),
Yong-chul Chae (chae@aps.anl.gov),
Katherine Harkay (harkay@aps.anl.gov),
Ali Nassiri (nassiri@aps.anl.gov)

References

[1] M. Tigner, Nuovo Cimento **37**, 1228 (1965).

[2] G. Hoffstaetter, Presentation at FLS2006, http://fls2006.desy.de.

[3] I. Bazarov et al., Phys. Rev. ST Accel. Beams **8**, 034202 (2005).

[4] R. Hajima et al., NIM A **557**, 103 (2006).

[5] M. Borland et al., Proc. AccApp'07, 196 (2007).

[6] H. Shang et al., OAG-TN-2007-028 (2007).

[7] Y. Sun et al., unpublished.

[8] M. Borland, Proc. PAC 2007, 1121 (2007), www.jacow.org.

[9] M. Borland, APS LS-287, September 2000.

[10] A. Xiao, unpublished code.

[11] A. Nassiri, Proceedings of ERL07, to be published.

[12] A. Godeke, LBNL-62140, December 2006.

[13] A. Gurevich, SRF Material Workshop, FNAL, May 2007.

[14] M. Pellin, SRF Material Workshop, FNAL, May 2007.

[15] K.-J. Kim (ed.), ANL Theory Institute on Production of Bright Electron Beams, ANL/APS/LS-305 (2004).

[16] Rosenberg 2007: Courtesy R. Rosenberg.

[17] J.W. Lewellen et al., Proc. 2003 PAC, 2038 (2003).

An X-ray FEL Oscillator

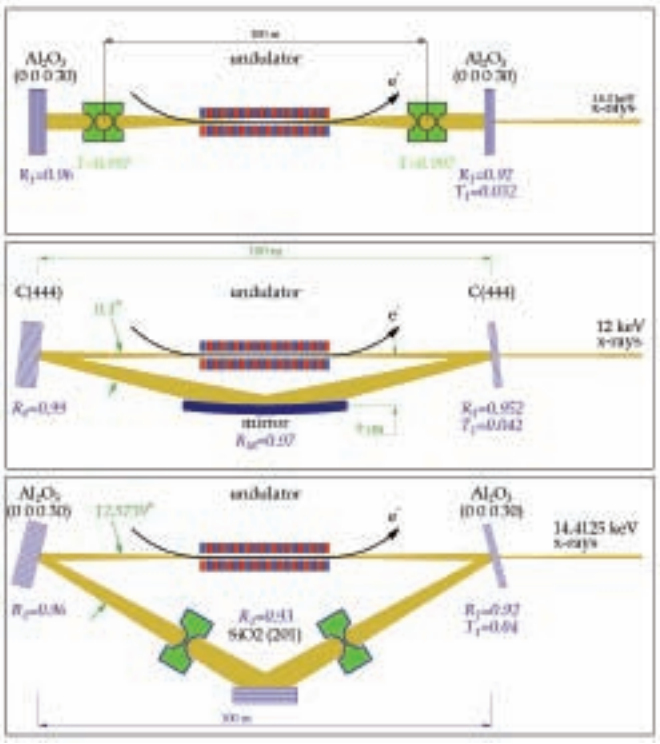

Fig. 1. Schemes for an x-ray resonator.

Currently, the main direction for development of a free-electron laser (FEL) in the hard x-ray region is based on self-amplified spontaneous emission (SASE), in which initial noise is amplified by a factor of a million or more in a single pass. However, the high-quality electron beams anticipated for energy-recovery linacs (ERLs), such as the one being discussed as an option for the future APS upgrade, can be used to drive an x-ray free-electron laser oscillator (X-FELO) for photons with an energy of 10 keV or higher. In an X-FELO, the radiation intensity builds up to saturation via repeated amplification in an optical cavity consisting of high-reflectivity Bragg mirrors. The optical characteristics of an X-FELO are unique and complementary to that of the SASE: The pulse intensity is lower by two or three orders of magnitude, but its spectrum is narrower by more than three orders of magnitude. The pulse repetition rate is at least 1 MHz, higher by at least two orders of magnitude than that of the state-of-the-art high-gain FEL facility planned at DESY. An X-FELO is therefore expected to open new scientific opportunities in various areas, including a drastic improvement in experiments involving inelastic scattering and nuclear resonance scattering, x-ray imaging, and accurate determination of the Fermi surface in bulk materials via time-resolved ARPES (angle-resolved photoemission electron spectroscopy).

The principles of an FEL oscillator are well known: An electron pulse enters an undulator and generates an x-ray pulse, which is reflected back into the undulator entrance by two Bragg mirrors and meets the next electron bunch for another trip down the undulator, the process to be repeated indefinitely. The electron beam after the undulator is transported out of the optical cavity and then either dumped or routed back to an ERL. The intensity of the x-ray pulse trapped in the optical cavity continues to increase if the gain due to the FEL interaction is larger than the loss in the mirror. As the optical intensity builds exponentially, the gain starts to decrease, and the system eventually reaches a steady state when the gain-per-pass becomes equal to the loss. Part of the loss will constitute the FEL output.

Many FEL oscillators for spectral ranges from infrared to ultraviolet are currently in operation around the world. The challenges presented by an FEL oscillator for hard x-rays are the availability of electron beams with suitable qualities, and high-reflectivity mirrors at normal incidence. In 1983, it was pointed out that crystals can be used as x-ray mirrors. However, no serious study of the concept has been reported to date except for two papers on regenerative amplifiers using electron beams appropriate for high-gain systems. Presented here is the case for an X-FELO with electron beams, as considered in recent ERL-based x-ray facility proposals such as the APS upgrade.

Diamond and sapphire are good candidates for high-reflectivity crystals in normal incidence. The reflectivity and transmissivity of sapphire as a function of the photon energy for normal incidence on the (0 0 0 30) plane were computed for two thicknesses: 0.07 mm and 0.2 mm. The thinner crystal can be used for out-coupling X-FELO radiation. The peak reflectivities are about 90% for the thinner crystal and greater than 95% for the thicker crystal, leading to a combined reflectivity greater than 85%. An optical cavity for an X-FELO must also provide focusing to control the intracavity mode shape. A simple way to accomplish this would be to curve the crystals. But even a very gentle curve can destroy the high reflectivity required for the optical cavity. A promising possibility is the compound refractive lens developed recently for use in synchrotron radiation beamlines. Another option is the curved grazing-incidence mirrors. Three examples of an optical resonator concept by Y. Shvyd'ko are shown in Fig. 1. The third scheme is particularly suitable for nuclear resonance scattering experiments. In all these cases, about 4% of the intracavity power is transmitted to useful output power.

Parameters specifying electron beam qualities are those in the proposed Cornell ERL: normalized transverse emittance 0.82 $\times 10^{-7}$ m-r, rms energy spread of 0.7 MeV, rms bunch length of 2 ps, and bunch charge between 19 and 60 pC. These values are assumed to be the same for a 7-GeV ERL under consideration for the APS upgrade. Table 1 shows the performance of an X-FELO for a few cases. For all cases except one, the bunch charge is taken to be 19 pC. The initial gain G_0 was computed by an analytic formula and also by simulation using the steady-state version of the GENESIS code; the two values were in fair agreement. The saturated intracavity peak power P_{sat} was computed by steady-state GENESIS. Assuming 4% output coupling, the output of the X-FELO will be a sequence of coherent x-ray pulses, each of which contains about 10^9 photons.

Continued on page 164

"X-ray FEL" continued from page 163

Time-dependent study of the mode evolution in the optical resonator has been performed by S. Reiche at the University of California, Los Angeles (UCLA). He modified the GENESIS code to add propagation and reflection in the optical cavity. To reduce the central processing unit time, a short window of 25 fs was chosen. It proved to be sufficient to track a single-frequency component for all radiation wave fronts because other components are outside the crystal bandpass. Even with this simplification, simulation of a single pass took about two hours with a computer cluster at UCLA. A full tracking from initial spontaneous emission to final saturation took about one month. Figure 2 shows the evolution of the power as a function of the pass number. Approximately 100 passes are needed for an exponential growth to emerge from the initial randomness.

The bandwidth of an X-FELO will be narrow because the bandwidth of the crystal reflectors is narrow: less than 10 meV. If the temporal profile of the coherent optical pulse is the same as that of the Gaussian electron beam with 2-ps rms pulse length, the full width half maximum bandwidth of the X-FELO output is approximately 0.4 meV. The optical pulse will probably be shorter than the electron beam, perhaps as much as an order of magnitude. In that case, the bandwidth will be around 4 meV.

The FEL interaction causes the energy spread of the electron beam to increase. In fact, GENESIS calculations indicate an increase in the rms energy spread from 0.02% to 0.05%. It is then necessary to check whether the ERL return pass can accommodate the increased energy spread. The answer is affirmative, according to the calculation by M. Borland, indicating that the fractional loss of particles is well below the 1×10^{-4} level with increased energy spread.

The length of the undulator studied for the cases discussed here is about 60 m. Thus, the length of the optical cavity will be about 100 m. If a single optical pulse is stored in the optical cavity, then the repetition rate is about 0.7 MHz. The low repetition rate is useful for some time-resolved experiments. The X-FELO can be operated with multiple x-ray pulses stored in the cavity, with the higher repetition rate of the FEL output. The maximum repetition rate is determined by the thermal loading that can be handled by the crystals. The average power incident on the 100-μm-radius hot spot receiving the coherent x-rays is about 14 W for 0.7-MHz operation. A preliminary study indicates that such a loading will not present a problem. It appears, therefore, that operation at higher repetition rate, perhaps 10 MHz, is feasible.

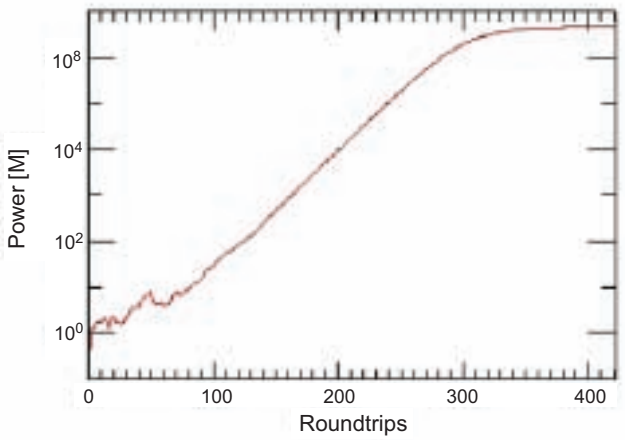

Fig. 2. Evolution of intracavity peak power for the case corresponding to the first row in Table I.

Our study of X-FELO reported here is based on a straight undulator. Higher gain may be possible with an optical klystron configuration that employs two undulators separated by a dispersive section. If two undulators are oriented at right angles to each other, then the polarization of the X-FELO can be switched between two linear polarization at right angles or between two circular polarizations of opposite helicity. The switching can be fast and is accomplished by modulating a part of the dispersion magnet. This is an FEL oscillator version of the cross undulator scheme proposed in 1983 and experimentally demonstrated recently.

A summary of the expected performance of an X-FELO is as follows:

- Wavelength: 1 Å or shorter, ε_γ = 12.4 keV or higher
- Full transverse and temporal coherence
- $\Delta\varepsilon_\gamma$ = 4 meV
- Not tunable
- Variable polarization between two opposite circular polarizations or between two orthogonal linear polarizations.
- 10^9 photons (~ 1 μJ) /pulse
- Peak spectral brightness ~ LCLS
- Average spectral brightness 10^{27} ($\rightarrow 10^{29}$) photons/(mm-mr)^2(0.1% BW) (assuming 1-MHz to 100-MHz operation). This is higher by a factor of 10^5 to 10^7 than other future light sources considered so far, ERL-based or high-gain FEL-based.

Contact: Kwang-Je Kim (kwangje@aps.anl.gov)

Table 1. Performance of X-FELO. Here λ is the x-wavelength, E is the electron energy, K is the undulator deflection parameter, λ_U is the undulator period length, N_U is the number of undulator periods, G_0 is the initial gain, R_T is the round-trip reflectivity, and P_{sat} is the intracavity power at saturation.

λ(Å)	E(GeV)	Q(pC)	K	λ_U(cm)	N_U	G_0(%)	R_T(%)	P_{sat}(MW)
1	7	19	1.414	1.88	3000	28	90	19
1	7	40	1.414	1.88	3000	66	83	21
0.84	7.55	19	1.414	1.88	3000	28	90	20
0.84	10	19	2	2.2	2800	45	83	18

A New Beam Position Monitor System for the LCLS

The Linac Coherent Light Source (LCLS) will be the world's first hard-x-ray free-electron laser (FEL) when it becomes operational in 2009. The FEL will produce x-ray radiation over the 1.5-Å to 15-Å wavelength range. To produce x-rays in this regime, the electron and photon beams within the 131-m-long undulator must be collinear to within less than 10% of the transverse beam size (≈ 37 μm rms) over a minimum distance that is comparable to the FEL amplitude gain length (≈ 10 m) in order to achieve saturation. To establish and maintain the electron beam trajectory, a high-resolution and stable beam position monitor (BPM) system has been designed.

The LCLS undulator hall will house 33 undulators, with the BPMs located in the drift spaces between each undulator and at the upstream end of the first undulator, for a total of 34 BPMs. There are also two BPMs placed in the linac-to-undulator (LTU) transport line. The BPMs are critical for beam-based alignment studies and routine operations.

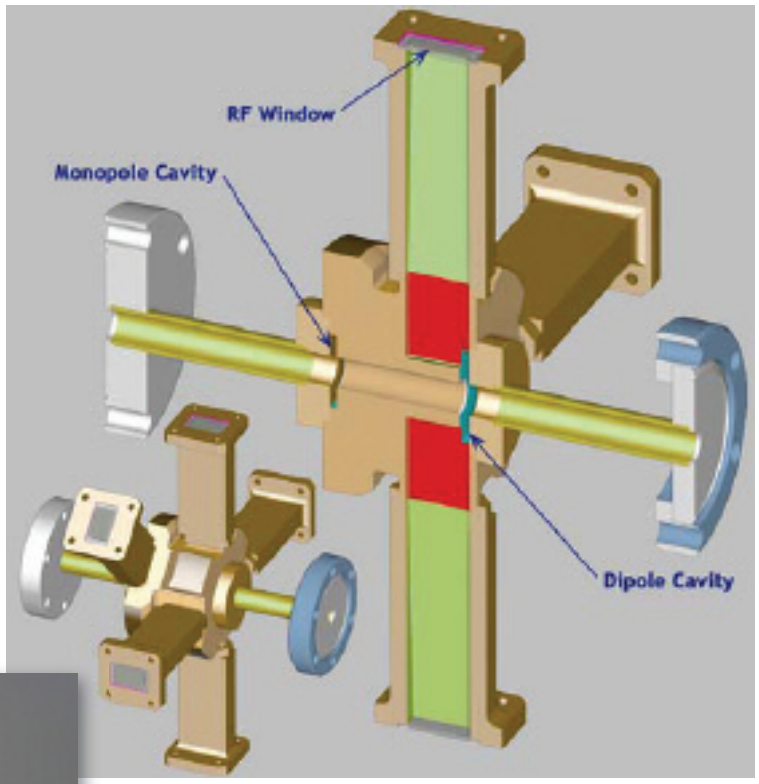

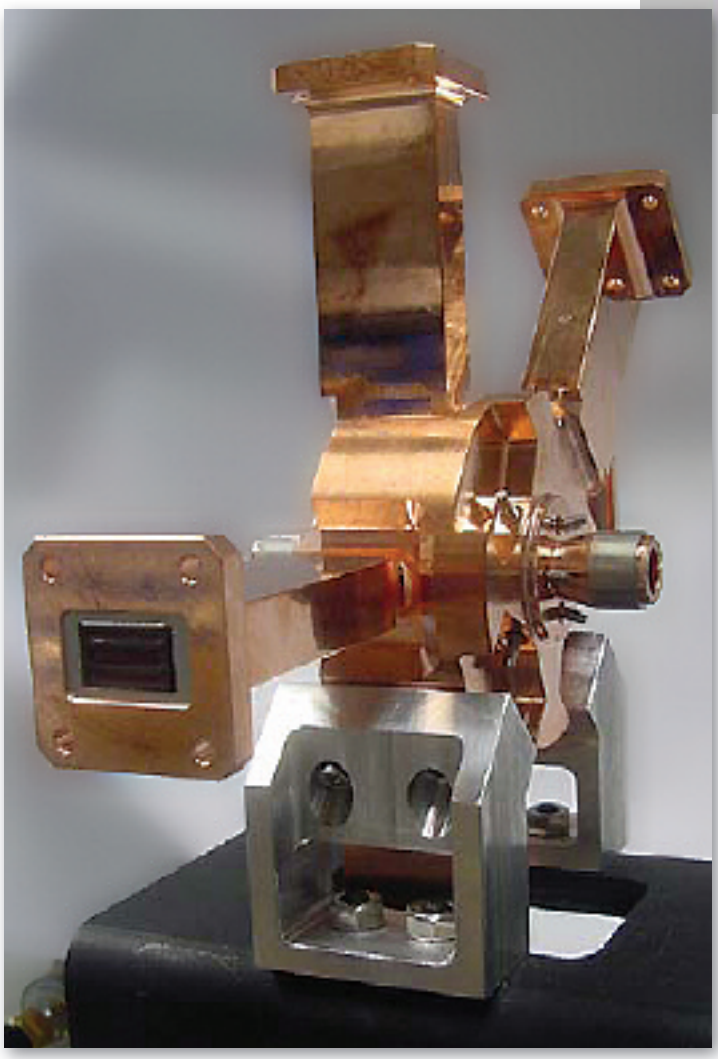

Fig. 1. X-band cavity beam position monitor: computer-aided design cutaway (above) and actual device (below left).

The two-cavity BPM design in Fig. 1 illustrates the cross section of the detector. The beam passes through the reference monopole cavity, shown on the left, which excites a signal proportional to the beam intensity. The dipole cavity shown at the far right of the figure produces a signal that is dependent on the relative beam displacement. Horizontal and vertical position signals are generated from the two polarizations of the dipole mode in this cavity. The polarized fields are coupled to four iris slots equally spaced around the cavity, each leading to a radio-frequency waveguide with a vacuum window. The iris couplers are precisely electrical-discharge machined into the solid copper block to ensure repeatable and accurate coupling. The two cavities are designed to operate at the same frequency, and a small amount of tuning is provided for adjustment after brazing. To ensure that the cavities are within tuning range, machining tolerances as tight as 15 μm are required on the cavity diameters.

The receiver topology used is a single-stage three-channel heterodyne receiver. The cavity BPM X-band signals are first amplified in a low noise amplification stage, and then downconverted to a 25-MHz to

Continued on page 168

In Pursuit of Bunch Purity

X-ray nuclear resonance experiments that make use of the time structure of the stored electron bunches in a synchrotron light source require high contrast between the radio-frequency (rf) "buckets" that contain electrons and those that are supposed to be empty.

This contrast is referred to as the bunch purity. The ratio of charge in the filled buckets to charge in the unfilled buckets should be at least 10^9. Bunch purity monitoring of the longitudinal electron distribution in the storage ring is an indispensible tool for quality assurance.

Three performance parameters can be used to characterize a bunch purity monitor:

- Impurity detection limit: the lower limit of detectable bunch impurity. This is determined by the dark counts of the detector and noise of the electronics.
- Next-bucket detection limit: the detection limit for the first bucket following a filled bucket. This is determined by the time resolution of the detector and electronics.
- Integration time: the time required to meet the specified measurement precision. This is determined by the maximum count rate or bandwidth of the detector and electronics.

The APS has used an avalanche photodiode (APD) bunch purity measurement system since 1999. A stainless steel foil intercepts the x-ray beam from a bending magnet source. The fluorescence x-ray photons from this foil are detected by an APD detector and preamplifier. Pulses from the preamplifier are then transported to a constant-fraction discriminator (CFD), which produces a digital pulse corresponding to the arrival of a photon at the APD. Further processing electronics builds up a histogram of pulse arrival times. The processing electronics had a detection limit of better than 10^{-8} for long integration times and a next-bucket detection limit around 10^{-5}.

A new system has been developed by the APS Engineering Support Division Controls Group. The new system has a long-range detection limit of around 3×10^{-12} with a next-bucket detection limit of 10^{-8} across a 2.68-ns bucket spacing. The electronics is based on a field-programmable gate array (FPGA) chip. This fully digital implementation imposes no dead time on the detection of pulses from the CFD, yet is much less expensive than the electronics it replaced. Sampling logic in the FPGA provides measurement of the arrival time of the signal from the CFD to a resolution of better than 200 ps even though the FPGA is operating with a much slower 352-MHz clock (2.8 ns per cycle). This performance is achieved by the novel approach of using polyphase clocks within the FPGA. When the sampling logic detects a pulse from the CFD, further logic in the FPGA updates two histograms in parallel. Each histogram has 7,778 bins, sufficient to account for six channels within each rf bucket in the storage ring. The counters are 32 bits wide, allowing for counts up to 4.3×10^9. Counting range beyond this 32-bit limit is handled by 64-bit counters in a single-chip microcontroller that reads out the histograms and makes the values available as Experimental Physics and Industrial Control System (EPICS) process variables to the facility control system. The two histograms have separate readout and reset controls, allowing simultaneous acquisition of both short- and long-term statistics.

Results of a long-term acquisition during one week of storage ring top-up operation using the new electronics are shown in Fig. 1. The "wing" around the main bunch comes from the bunch compression process in the APS particle accumulator ring (PAR), where an rf cavity with a wavelength 1/12 the ring circumference (RF12) is used to make a shorter rf bucket and compress the bunch. Electrons in Satellite 3 and -3 are from the tails of the original bunch extending far from the center and captured by RF12. Electrons in the other "wing" buckets are from the longitudinal halo collected in the PAR fundamental rf (RF1) bucket. The total width of the halo is determined by the RF1 bucket size. The counts around satellite bucket number 36 are due to occasional incomplete extractions from the PAR. In special circumstances, a few electrons remain in the PAR after the main bunch has been extracted and leave the PAR in the next turn. These electrons in a satellite bunch (if more than 10^{-9} of those in the main bunch) may generate spurious signals for user experiments; their population is monitored closely during user runs. Notice that nearly 2×10^{11} counts have been recorded for the filled bucket and that many of the unfilled buckets have produced no counts at all. This indicates that it is very likely (97% confidence) that there are at most two electrons in these buckets. Such resolution is far in excess of both the old APS electronics and the published results from any other synchrotron light source.

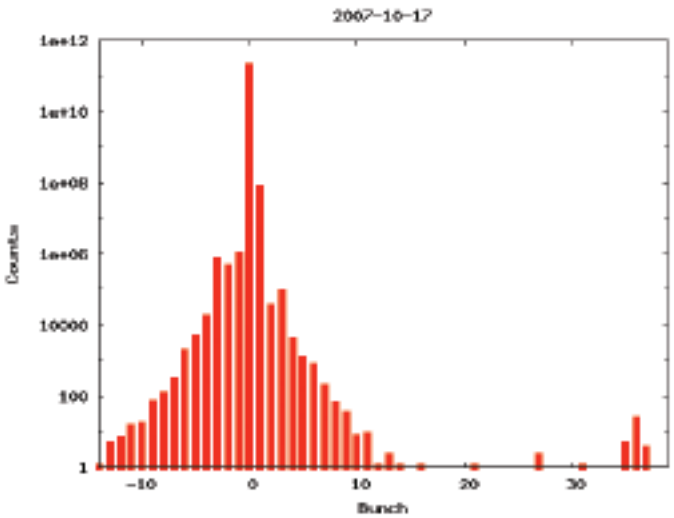

Fig. 1. Long-term acquisition results showing charge leakage into the +36 bucket.

Contact: Eric Norum (norume@aps.anl.gov), Bingxin Yang (bxyang@aps.anl.gov)

Impedance and Collective Effects

One of the main challenges in maintaining high single-bunch intensity in either the 24-bunch or the hybrid operating mode is characterizing and mitigating intensity-dependent collective instabilities in the storage ring. Such collective effects can arise when the electron beam excites electromagnetic fields as it traverses the vacuum chamber, and these fields act back on and perturb the beam. The integral of the field behind the beam is the wake potential, which represents the impact of chamber structure on the beam; its Fourier transform is called the coupling impedance, which can be used as a versatile tool for beam instability analysis.

The first impedance database (DB1) was completed by the Accelerator Systems Division Accelerator Physics Group in 2003 (see "Impedance and Collective Effects," *APS Science 2003*, ANL-04/07, pg. 142 [May 2004, Argonne National Laboratory] and *APS Science 2002*, ANL-03/15, pg. 114 [May 2003, Argonne National Laboratory]). DB1 was a collection of wake potentials excited by the beam passing through all the mechanical components in the storage ring [1]. Because of the reciprocity between duration in time and bandwidth in frequency, the shorter the electron bunch, the broader the impedance. Broadband impedance is needed to investigate fine density modulation in the beam, but limited computer resources available at the time restricted DB1 to computations based on a 5-mm-long electron bunch. Despite this limitation, modeling the storage ring with DB1 and the particle tracking code **elegant** reproduced various instabilities observed in the ring, including anomalous bunch lengthening and energy spread growth with single-bunch current, horizontal bunch centroid relaxation oscillations, and vertical beam size blow-up [2,3,4].

Importantly and for the first time, the single-bunch injection accumulation limit was reproduced by DB1, and stored beam loss during injection was found to significantly contribute to this limit. However, the prediction accuracy was only about 60%; the impedance had to be scaled by about +35% for good agreement between modeling and experiment. The ad hoc scaling was necessary, as it turned out, in order to make up for the missing high-frequency impedance. Until the broader impedance model was available, the scaled DB1 was used as a working impedance model for practical application to the storage ring. One example was predicting the single-bunch current limit in the future ring. The result in Fig. 1 shows that a 30% increase in the impedance will reduce the single-bunch limit by a factor of two, from 20 mA to 10 mA. We also found that one 5-mm-gap insertion device (ID) chamber is equivalent to four 8-mm-gap chambers, and increases the ring impedance by 6%. These results guide the plans for the design and installation of new ID chambers or radio-frequency cavities [5].

Improved accuracy for state-of-the-art modeling of the APS storage ring required an impedance computation up to 100 GHz or greater, which could be obtained by computing the wake potential excited by the 1-mm or shorter bunched beam. The computational requirements were estimated to be

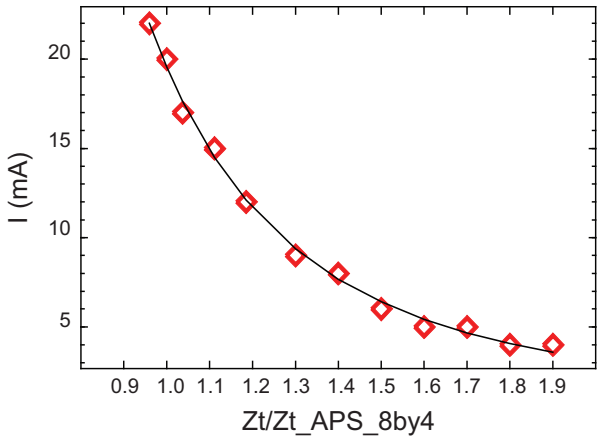

Fig. 1. The current limit of a single bunch (vertical axis) can be reduced as the transverse impedance of the ring increases. The horizontal axis is the transverse impedance normalized to the transverse impedance of the present APS storage ring. The symbols give the simulation results and the line is a polynomial fit.

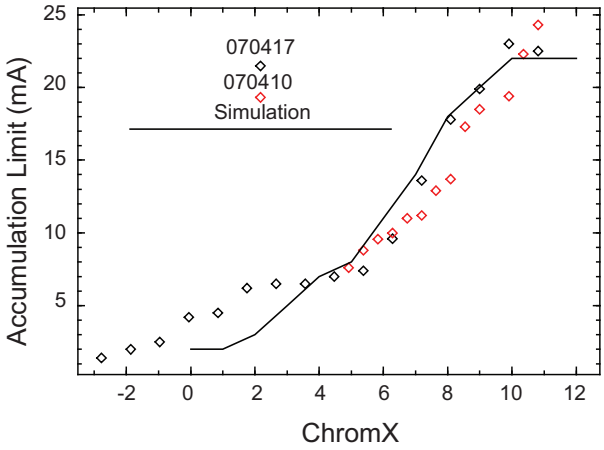

Fig. 2. Modeling the single-bunch accumulation limit in the APS storage ring as a function of chromaticity agrees very well with measurements. The wake potentials were computed for a 1-mm bunch with the code GdfidL on the APEX cluster.

300 GB of memory and a speed of 10 Gflop. A new APEX Linux cluster was purchased, equipped with 60 cores of processing units and 240 GB of memory. Efficient use of the cluster prompted the purchase of the parallelized software GdfidL, a state-of-the-art, three-dimensional electromag-

Continued on page 168

"Impedance" *continued from page 167*

netic code. The second impedance database (DB2) was thereby completed in 2007 [6,7,8]. With the broader impedance available from DB2, simulations tracking sub-million particles by the parallelized **elegant** program resulted in excellent agreement between accelerator modeling and actual operation without introducing any ad hoc modification to the impedance. The prediction accuracy of DB2 for the dependence of collective effects on the ring lattice is shown in Fig. 2, where the single-bunch limit is modeled as a function of the chromaticity set by the sextupole magnets. The simulation results agree very well with observations. Furthermore, analysis of the phase-space data of Fig. 2 showed that the resistivity of the ID chamber was a critical horizontal impedance source limiting injection efficiency. This was not clearly understood using DB1. Thus, the broadband impedance from DB2 not only reproduced the ring performance accurately, but also enhanced understanding of the intricate role of each impedance source.

The impedance database project started with a modest goal: to provide accelerator scientists with a simulation tool that could be used to analyze data acquired during machine studies. Over the last four years, the improvements made in wake potential computation, particle tracking, and parallelization of software, as well as the purchase of a powerful computer with large memory, pushed the capability to model the accelerator in operation as closely as possible. This has greatly enhanced confidence in predicting future machine performance. The intelligent convergence of scientific modeling and accelerator control software can perhaps be used to optimize the performance of the storage ring in real time.

Contact Yong-chul Chae (chae@aps.anl.gov)

References

[1] Y.-C. Chae, Proc. of PAC2003 (Portland, OR, 2003), pg. 3017.

[2] Y.-C. Chae, K. Harkay, and X. Sun, Proc. of PAC2003 (Portland, OR, 2003), pg. 3008.

[3] Y.-C. Chae, K. Harkay, and X. Sun, Proc. of PAC2003 (Portland, OR, 2003), pg. 3011.

[4] Y.-C. Chae, K. Harkay, and X. Sun, Proc. of PAC2003 (Portland, OR, 2003), pg. 3014.

[5] Y. Chae, G. Waldschmidt, and V. Dolgashev, Proc. of PAC2007 (Albuquerque, NM, 2007), pg. 4339.

[6] Y. Chae, "The Impedance Database Computation and Prediction of Single Bunch Instabilities," invited talk presented at PAC2007 (Albuquerque, NM, 2007), pg. 1996.

[7] Y. Chae, Y. Wang, and A. Xiao, Proc. of PAC2007 (Albuquerque, NM, 2007), pg. 4330.

[8] Y. Chae, Y. Wang, Proc. of PAC2007 (Albuquerque, NM, 2007), pg. 4336.

"Beam Position Monitor" *continued from page 165*

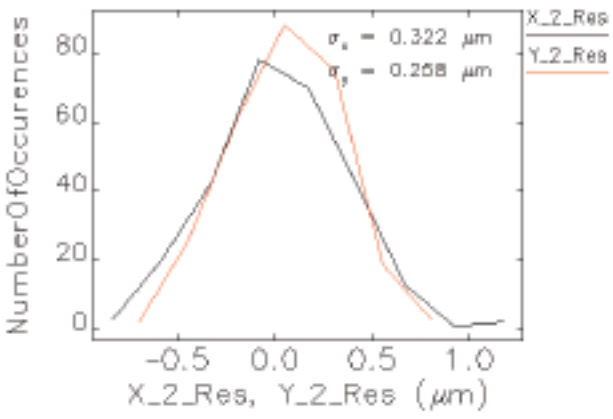

Fig. 2. LCLS cavity BPM single-shot resolution.

50-MHz intermediate frequency in the accelerator tunnel by mixing with a local oscillator (LO). The LO is a phase-locked dielectric resonator oscillator featuring low phase noise that can be locked to the Stanford Linear Accelerator Center (SLAC) 119-MHz timing reference.

Argonne and SLAC have collaborated closely on testing the LCLS cavity BPM system. The first phase of testing required the installation of a single-cavity BPM in the injector test stand at Argonne. In this phase, the overall design concept was tested with beam and validated for the LCLS application.

The second phase of beam testing required the manufacture of three BPM assemblies and supporting electronics. These units were installed in tandem inside the APS undulator test line hall for detailed studies using beam derived from the APS photocathode electron gun. The BPMs were first calibrated individually using a precision translation stage. On a pulse-to-pulse basis, data from the first and third BPMs were fit to a straight line. Deviations of the second BPM's readback from this line then provided a direct measure of the device resolution. This procedure was necessary because the BPM resolution is significantly smaller than the shot-to-shot beam motion. Shown in Fig. 2 is a histogram of the resulting residuals, indicating typical system performance that falls well within the 1-μm rms requirement for single-shot resolution.

Argonne is currently in the production phase on this project. Installation and commissioning will begin later in 2008. This technology holds potential for application to the proposed energy-recovery linac upgrade to the APS, providing enhanced source stability.

This work was carried out by members of the Accelerator Systems Division Diagnostics and RF groups in collaboration with the APS Engineering Support Division Controls and Mechanical Engineering groups and Stanford Linear Accelerator Center scientists.

Contact: Glenn Decker (decker@aps.anl.gov)

Heat Transfer Optimization for High-Heat-Load/Flux Components

Fig.1. Liquid nitrogen-cooled silicon crystal holder assembly for the 20-ID-A monochromator.

Many APS components require high levels of internal-flow, forced-convection heat transfer to minimize surface temperatures, thermal gradients, and thermally-induced stress on beam-interacting surfaces. Wire-coil inserts fabricated and optimized by the Mechanical Engineering and Design Group in the APS Engineering Support Division are mechanically fitted inside component cooling passages. They are routinely used in APS front end and beamline high-heat-load/flux components to significantly enhance convection heat transfer—up to 400% compared to plain open passages. This has the additional benefit of greatly reducing coolant flow requirements for these components. This use of wire-coil inserts is ideally suited for synchrotron components because component lengths tend to be short, and consequently, sustained pressure losses are generally modest. Figure 1 shows wire-coil inserts being fitted prior to final insertion into a liquid-nitrogen-cooled silicon crystal holder assembly, which was later installed in the 20-ID-A monochromator.

Wire-coil inserts, which are physically similar to a common spring, can be described by three characteristic dimensions: the wire diameter (**e**), the cooling passage diameter (**D**), and the wire coil pitch (**p**), where the pitch is the linear distance between successive coil turns along the coil length. The outer dimension of the wire-coil insert is made slightly smaller than the cooling passage diameter to provide a tight mechanical slip-fit into the cooling passage. Using several cooling passage sizes, five different wire sizes, and a range of pitch values, an experimental investigation conducted at the APS has determined the average heat-transfer coefficient and resulting pressure loss as a function of water flow rate for 65 different wire-coil inserts. Data from this study have been non-dimensionalized and generalized to yield relationships that can be used to determine the heat-transfer performance and resulting pressure loss for any given wire coil insert. Through data reduction, the wire-coil insert characteristic dimensions have also been optimized to yield the highest heat-transfer enhancement while minimizing coolant flow requirements.

The heat-transfer performance for any given wire-coil insert can be determined using a non-dimensional expression that relates the Nusselt number ($\mathbf{Nu_D}$) to the Reynolds number ($\mathbf{Re_D}$), Prandtl number (**Pr**), and ratios of the wire-coil insert characteristic dimensions. Similarly, the pressure loss performance for any given wire-coil insert can be determined using a non-dimensional expression that relates the Fanning friction factor ($\mathbf{f_D}$) to the Reynolds number and ratios of the wire-coil insert characteristic dimensions. These expressions can be used in the transition/turbulent flow regimes for single-phase fluids including water, liquid nitrogen, or any other fulid with a similar Prandtl number.

Figure 2 shows the heat transfer performance data from all 65 wire-coil inserts generalized into one relationship that can predict the performance of any given insert within the data set. A similar relationship has been developed that can predict the pressure loss performance for any given wire-coil insert within the data set.

These generalized expressions for wire-coil inserts can be used by scientists and engineers during the component design process to evaluate required heat transfer performance and associated pressure loss, aiding in the establishment of operating parameters and cooling passage flow distribution schemes. Analysts will also find these expressions useful for component modeling in the evaluation of component temperature and thermally induced stress distributions resulting from beam interaction.

Contact: Jeff T. Collins (collins@aps.anl.gov), William R. O'Brien (wrobrien@mail.uri.edu)

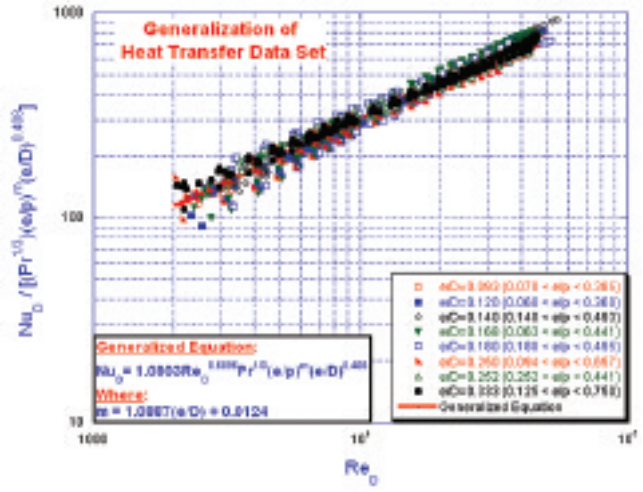

Fig. 2. Generalized heat-transfer performance for wire-coil inserts.

Delivering Power

Mark Gibson (AES Safety Interlocks Group) with one of the new 80-kW UPSs on the storage ring mezzanine, prior to commissioning.

When storms thunder through the Chicago area or some other occurrence interrupts power delivery, the APS can be subjected to a variety of power quality issues that can cause the stored electron beam to dump. When the APS was being designed, this was recognized as a potential source of extended down time. So uninterruptable power supplies (UPSs) were installed to feed power to critical equipment in order to minimize the effects of such disturbances. The primary function of UPSs is to provide battery backup when electrical power fails or drops to an unacceptable voltage level. The APS Engineering Support Division Safety Interlocks Group is in the final stage of replacing the original 18-kW single-phase and individual low-kilowatt UPSs with new 100% redundant units.

Uninterruptable power supplies provide a level of line filtering that protects the downstream equipment from damage due to powerline transients caused by lightning strikes and normal switching operations. The UPSs installed at the APS are "on-line" units that use double-conversion technology and are designed to ride through disturbances of 7 min or until the generators are started, typically 10 s.

Three groups of UPSs will be installed at the APS: central, storage ring, and controls. The central UPSs feed power to all of the Building 401 networking equipment, servers, and APS management databases. The central UPSs are 80-kW, 3-phase units that replaced three 18-kW, single-phase units and provide 100% redundancy; if one of the two UPSs fails, the other can support the full load intended for both. Five 40-kW, 3-phase UPSs were installed around the storage ring to replace more than 75 individual 2-kW (or less) units. These provide power to the beamline personnel protection systems, insertion device control systems, access control interlock systems, and control systems racks. These units are not redundant. The controls UPSs are being installed and will feed power to all accelerator networking equipment and servers. As with the central UPSs, these two 3-phase, 80-kW UPSs will replace three 18-kW single-phase units and provide 100% redundancy.

Contact: Greg Markovich (gmm@aps.anl.gov)

The APS Front End Equipment Protection System (FEEPS) designed and maintained by the APS Engineering Support Division Safety Interlocks Group has three primary functions. The first is to prevent damage to the components in the front ends that join storage ring radiation sources to beamlines. A front-end component may be damaged when it is unable to dissipate the power absorbed during control of the synchrotron beam, or when a component is not designed to withstand the synchrotron radiation that is present. The second function is to prevent the propagation of a vacuum loss along the front end, into the storage ring, or into a beamline. Propagation of a vacuum loss could result in longer down time and may increase the amount of maintenance needed to bring the front end back to operational status. The third function is to provide control of certain front-end components and to provide information to the EPICS for data logging and trending.

Over the past several years, changes have been made to the FEEPS in order to improve maintainability and reliability and to aid in troubleshooting. These improvements have included replacing the problematic Love controllers with analog modules, adding a personnel protection system test key that allows the front-end shutters to be operated during the maintenance periods, improving the way faults are handled so that troubleshooting is more intuitive, reducing the number of versions of PLC code from 20 to 2, and reducing the number of Experimental Physics and Industrial Control System (EPICS) displays for each front end from 11 status displays to 1 main display and an engineering display. A test cart was also built with a touch screen to allow for troubleshooting when the network is unavailable.

In the 18 months prior to the upgrade, there were 8 controller failures that caused storage ring down time. In the 18 months since the upgrade, there has been one analog module problem that resulted in down time.

Contact: Phil McNamara (mcnamara@aps.anl.gov)

Lessons Learned from "Near-Miss" Events

We all understand the concept of the "near miss" event, such as a car sliding on ice and into a ditch instead of an oncoming truck. Such near misses offer us safety lessons without causing injury in the process, and while we would rather never experience them, lessons can be learned. A near-miss incident that occurred at the APS in 2007 provided several lessons, not least of which was the willingness of a user's home institution to work with the APS rapidly and proactively on a plan to prevent future incidents. This cooperation can serve as a model for facility-institution safety initiatives.

A student from a Chicago-area university was granted beam time for an experiment related to his dissertation topic. He and a fellow student set up their equipment in the evening, after beamline personnel had departed for the day. The student had to remove a piece of equipment left by the previous users and attempted to remove the equipment's electrical plug from a 208-VAC outlet. The plug first had to be rotated counterclockwise to disengage the prongs. The student thought he had fully turned the plug and disengaged it, but he was unable to withdraw it from the receptacle. He pulled harder on the plug, and the cable and plug housing came off in his hand; the base portion of the plug containing the prongs remained in the receptacle. He showed his fellow student what had happened, and that student advised him not to touch the plug base and to notify the beamline staff. After the other student left, the first student decided that he could remove the base from the receptacle. He noticed there was a slight gap between the base and the receptacle face, found a thin needle-nosed pliers that could fit into the gap, and used the pliers to pry the base out of the receptacle.

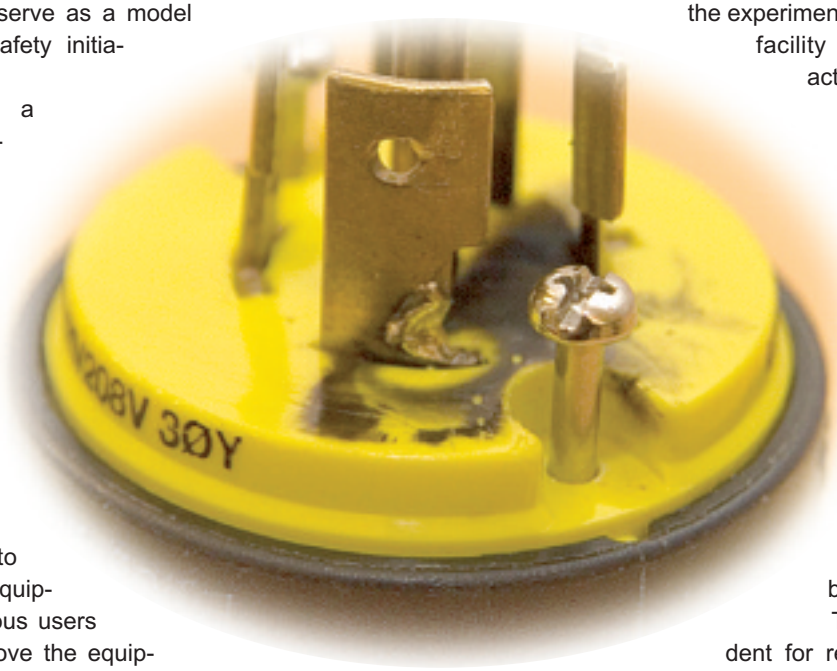

The student was aware the circuit was energized but felt he could be careful to not cause a short. But the pliers' tip contacted an energized prong at the same time the pliers' body was touching the grounded plate surrounding the receptacle, causing a short-to-ground and a small arc flash that melted part of the prong (photograph above). The circuit breaker did not open because the melting copper acted as a fuse and terminated the short circuit. The student continued to pry around the plug until it came loose and he could remove it from the receptacle. He noted that one side of one prong had been damaged by the short circuit, set the plug base aside, continued with his set-up, and then, the next day, told beamline staff what had occurred.

This event resulted in a formal report being made to the Department of Energy and various corrective actions being taken. The student was prohibited from completing the experiment and was asked to leave the facility pending final corrective action. A letter was sent to the university asking that corrective action be taken by the university. The APS also mandated that the involved student, his faculty advisor, and all other students of that faculty advisor who were APS users had to retake all required user training before they would be given permission to use a beamline.

The university's vice-president for research immediately recognized the importance of the event, and the potentially (and, fortunately, avoided) catastrophic consequences, and requested assistance from APS management in developing a presentation to the university's APS users. Attending the presentation, or viewing a videotape made of it, was then required by the university before university management would approve any further experiments at APS by university personnel or students. The university presentation emphasized lessons learned from the event:

- Immediately notify APS staff of abnormal conditions, even if beamline personnel are not present.
- Having a "can do" attitude and following safety rules are not mutually exclusive.
- Just being careful is not a justification for performing an inherently unsafe action.
- Do not continue a course of action when told it is unsafe.
- Following safety rules is not optional.

Perhaps the most important lesson learned is this: A proactive, cooperative response by both the facility and the user institution assures that everything possible is being done to guard against future occurrences.

Contact: Thomas Barkalow (barkalow@aps.anl.gov)

Typical APS Machine Operations Parameters

Linac

Output energy	325 MeV
Maximum energy	450 MeV
Output beam charge	1–3 nC
Normalized emittance	10–20 mm-mrad
Frequency	2.856 GHz
Modulator pulse rep rate	30 Hz
Gun rep rate (1–6 pulses, 33.3 ms apart every 0.5 s)	2–12 Hz
Beam pulse length	8–30 ns
Bunch length	1–10 ps FWHM

Particle Accumulator Ring

Nominal energy	325 MeV
Maximum energy	450 MeV
Circumference	30.66 m
Cycle time	500 ms
Fundamental radio frequency (RF1)	9.77 MHz
12th harmonic rf frequency (RF12)	117.3 MHz
RMS bunch length (after compression)	0.34 ns

Injector Synchrotron (Booster)

Nominal extraction energy	7.0 GeV
Injection energy	325 MeV
Circumference	368.0 m
Lattice structure	10 FODO cells/ quadrant
Ramping rep rate	2 Hz
Natural emittance	65 nm-rad-92 nm-rad
Radio frequency	351.930 MHz

Storage Ring System

Nominal energy	7.0 GeV
Circumference	1,104 m
Number of sectors	40
Length available for insertion device	5.0 m
Nominal circulating current, multibunch	100 mA
Natural emittance	2.5 nm-rad
RMS momentum spread	0.096%
Effective emittance	3.1 nm-rad
Vertical emittance	0.040 nm-rad
Coupling	1.5%
Revolution frequency	271.554 kHz
Radio frequency	351.930 MHz
Number of bunches	24 to 1296
Time between bunches	153 to 2.8 ns
RMS bunch length	25 ps to 40 ps
RMS bunch length of 16 mA in hybrid mode	65 ps

APS Source Parameters

Undulator A

Period: 3.30 cm
Length: 2.4 m
K_{max}: 2.74 (effective; at minimum gap)
Minimum gap: 10.5 mm
Tuning range: 3.0–13.0 keV (1st harmonic)
3.0–45.0 keV (1st-5th harmonic)
On-axis brightness:
5.0×10^{19} ph/s/mrad^2/mm^2/0.1%bw at 7 keV
Source size and divergence at 8.0 keV:
Σ_x: 275 μm Σ_y: 9 μm
$\Sigma_{x'}$: 12.6 μrad $\Sigma_{y'}$: 6.4 μrad

2.30-cm Undulator (sectors 1, 11, 14)

Period: 2.30 cm
Length: 2.4 m
K_{max}: 1.19 (effective; at minimum gap)
Minimum gap: 10.5 mm
Tuning range: 11.8–20.0 keV (1st harmonic)
11.8–70.0 keV (1st-5th harmonic, non-contiguous)
On-axis brightness:
8.7×10^{19} ph/s/mrad^2/mm^2/0.1%bw at 12 keV
Source size and divergence at 12.0 keV:
Σ_x: 275 μm Σ_y: 9 μm
$\Sigma_{x'}$: 12.2 μrad $\Sigma_{y'}$: 5.5 μrad

2.70-cm Undulator (sectors 3 & 14)

Period: 2.70 cm
Length: 2.4 m
K_{max}: 1.78 (effective; at minimum gap)
Minimum gap: 10.5 mm
Tuning range: 6.7–16.0 keV (1st harmonic)
6.7–60.0 keV (1st-5th harmonic, non-contiguous)
On-axis brightness:
7.0×10^{19} ph/s/mrad^2/mm^2/0.1%bw at 8.5 keV
Source size and divergence at 8.0 keV:
Σ_x: 275 μm Σ_y: 9 μm
$\Sigma_{x'}$: 12.6 μrad $\Sigma_{y'}$: 6.4 μrad

APS Source Parameters

3.00-cm Undulator (sectors 21, 23, 30)

Period: 3.00 cm
Length: 2.1 m in sectors 21 and 23, 2.4 m in sector 30
K_{max}: 2.20 (effective; at minimum gap)
Minimum gap: 10.5 mm
Tuning range: 4.6–14.5 keV (1st harmonic)
4.6–50.0 keV (1st-5th harmonic)
On-axis brightness:
5.9×10^{19} ph/s/mrad^2/mm^2/0.1%bw at 8 keV
Source size and divergence at 8.0 keV:
Σ_x: 275 μm Σ_y: 9 μm
$\Sigma_{x'}$: 12.6 μrad $\Sigma_{y'}$: 6.4 μrad

3.50-cm SmCo Undulator (sector 4)

Period: 3.50 cm
Length: 2.4 m
K_{max}: 3.08 (effective; at minimum gap)
Minimum gap: 9.5 mm
Tuning range: 2.3–12.5 keV (1st harmonic)
2.3–42.0 keV (1st-5th harmonic)
On-axis brightness:
4.5×10^{19} ph/s/mrad^2/mm^2/0.1%bw at 7 keV
Source size and divergence at 8.0 keV:
Σ_x: 275 μm Σ_y: 9 μm
$\Sigma_{x'}$: 12.6 μrad $\Sigma_{y'}$: 6.4 μrad

5.50-cm Undulator (sector 2)

Period: 5.50 cm
Length: 2.4 m
K_{max}: 4.97 (effective; at minimum gap)
Minimum gap: 14.0 mm
Tuning range: 0.6–7.0 keV (1st harmonic)
0.6–25.0 keV (1st-5th harmonic)
On-axis brightness:
2.0×10^{19} ph/s/mrad^2/mm^2/0.1%bw at 4 keV
Source size and divergence at 4.0 keV:
Σ_x: 275 μm Σ_y: 9 μm
$\Sigma_{x'}$: 13.9 μrad $\Sigma_{y'}$: 8.6 μrad

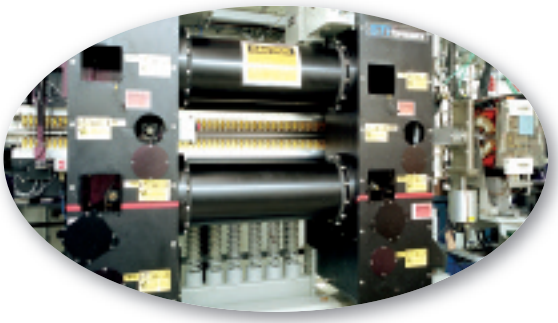

APS Source Parameters

Circularly Polarized Undulator (sector 4)

Period: 12.8 cm
Length: 2.1 m
Circular mode:
K_{max}: 2.65 (effective; for both horizontal and vertical fields at maximum currents of 1.2 kA horizontal and 0.34 kA vertical)
B_{max}: 0.26 T (peak fields)
Tuning range: 0.5–3.0 keV (1st harmonic)
On-axis circular brightness:
3.6×10^{18} ph/s/mrad^2/mm^2/0.1%bw at 1.8 keV
Linear mode:
K_{max}: 2.80 (effective; for both horizontal and vertical fields at maximum currents 1.4 kA horizontal and 0.40 kA vertical)
B_{max}: 0.29 T (peak fields)
Tuning range: 0.8–3.0 keV (1st harmonic)
0.8–10.0 keV (1st–5th harmonic)
On-axis linear brightness:
2.7×10^{18} ph/s/mrad^2/mm^2/0.1%bw at 2.1 keV
Switching frequency: 0-5 Hz
Switching rise time: 20 ms
Source size and divergence at 1.5 keV:
Σ_x: 275 μm Σ_y: 9 μm
$\Sigma_{x'}$: 18.0 μrad $\Sigma_{y'}$: 14.3 μrad

APS Bending Magnet

Critical energy: 19.51 keV
Energy range: 1–100 keV
On-axis brightness:
6.5×10^{15} ph/s/mrad^2/mm^2/0.1%bw at 16 keV
On-axis angular flux density:
9.6×10^{13} ph/s/mrad^2/0.1%bw at 16 keV
On-axis horizontal angular flux density:
1.6×10^{13} ph/s/mradh/0.1%bw at 6 keV
Source size and divergence at the critical energy:
Σ_x: 92 μm Σ_y: 26 μm
$\Sigma_{x'}$: 6 mrad $\Sigma_{y'}$: 47 μrad

APS Beamline Directory*

*As of 3.27.08. Source: http://beam.aps.anl.gov/pls/apsweb/beamline_display_pkg.beamline_dir

KEY: CPU = Circularly Polarized Undulator; CU: Canted undulator; GU: General Users

Beamline	Operator	Disciplines	Techniques	Source	Status
1-BM-B,C	XOR	Physics, materials science, chemistry	Powder diffraction	Bending magnet	Operational
1-ID-C	XOR	Materials science, physics, chemistry	High-energy x-ray diffraction	3.3-cm Undulator A	Operational/ GU
2-BM-B	XOR	Physics, life science	Phase-contrast imaging, tomography microdiffraction, general diffraction	Bending magnet	Operational/ GU
2-ID-B	XOR	Materials science, environmental, science, physics	Coherent x-ray scattering (soft x-ray), microfluorescence (soft x-ray)	5.5-cm undulator	Operational/ GU
2-ID-D	XOR	Life science, materials science, environmental science	Microfluorescence (hard x-ray), microdiffraction, micro-XAFS	3.3-cm Undulator A	Operational/ GU
2-ID-E	XOR	Life science, environmental science, materials science	Microfluorescence (hard x-ray)	3.3-cm Undulator A	Operational/ GU
3-ID-B,C,D	XOR	Physics, geoscience, life science, chemistry, materials science	Nuclear resonant scattering, high-pressure diamond anvil cell, inelastic x-ray scattering	2.7-cm undulator	Operational/s GU
4-ID-C	XOR	Physics, materials science	X-ray photoemission electron microscopy, x-ray photoemission spectroscopy, magnetic circular dichroism (soft x-ray), x-ray magnetic linear dichroism, magnetic x-ray scattering, anomalous and resonant scattering (soft x-ray)	CPU	Operational/ GU
4-ID-D	XOR	Physics, materials science	Anomalous and resonant scattering (hard x-ray), magnetic x-ray scattering, magnetic circular dichroism (hard x-ray)	3.5-cm undulator	Operational/ GU
5-BM-C	DND-CAT	Materials science, polymer science	Tomography, powder diffraction	Bending magnet	Operational/ GU
5-BM-D	DND-CAT	Materials science, polymer science	X-ray absorption fine structure (XAFS), high-energy x-ray diffraction	Bending magnet	Operational/ GU
5-ID-B,C,D	DND-CAT	Materials science, polymer science	Powder diffraction, x-ray reflectivity, small-angle x-ray scattering, surface diffraction, wide-angle x-ray scattering, x-ray standing waves, x-ray optics development/techniques	3.3-cm Undulator A	Operational/ GU
6-ID-B,C	MU/XOR	Physics, materials science	Anomalous and resonant scattering (hard x-ray), liquid scattering, magnetic x-ray scattering, powder diffraction, general diffraction, grazing-incidence diffraction, surface diffraction (UHV)	3.3-cm Undulator A	Operational/ GU
6-ID-D	MU/XOR	Physics, materials science	High-energy x-ray diffraction, magnetic x-ray scattering, powder diffraction, pair distribution function	3.3-cm Undulator A	Operational/ GU
7-ID-B,C,D	XOR	Materials science, atomic physics, chemistry	Time-resolved x-ray scattering, radiography, time-resolved XAFS	3.3-cm Undulator A	Operational/ GU

Beamline	Operator	Disciplines	Techniques	Source	Status
8-ID-E	XOR	Materials science, polymer science, physics	Intensity fluctuation spectroscopy, x-ray reflectivity, x-ray photon correlation spectroscopy, grazing-incidence small-angle scattering	3.3-cm Undulator A	Operational/ GU
8-ID-I	XOR	Polymer science, materials science, physics	Intensity fluctuation spectroscopy, coherent x-ray scattering, small-angle x-ray scattering, x-ray photon correlation spectroscopy	3.3-cm Undulator A	Operational/ GU
9-BM-B,C	XOR/CMC	Materials science, chemistry	XAFS	Bending magnet	Operational/ GU
9-ID-B,C	XOR/CMC	Physics, materials science	Liquid scattering, inelastic x-ray scattering, resonant inelastic x-ray scattering	3.3-cm Undulator A	Operational/ GU
10-ID-B	MR-CAT	Materials science, environmental science, chemistry	Microfluorescence (hard x-ray), XAFS, diffraction anomalous fine structure, micro-XAFS	3.3-cm Undulator A	Operational/ GU
11-BM-B	XOR/BESSRC	Chemistry, materials science, physics, geoscience, life science	Powder diffraction	Bending magnet	Operational
11-ID-B	XOR/BESSRC	Chemistry, environmental science, materials science	High-energy x-ray diffraction, pair-distribution function	3.3-cm Undulator A	Operational/ GU
11-ID-C	XOR/BESSRC	Materials science, geoscience, physics, chemistry	Diffuse x-ray scattering high-energy x-ray diffraction, pair-distribution function	2.3-cm Undulator	Operational GU
11-ID-D	XOR/BESSRC	Chemistry, geoscience, materials science	XAFS, general diffraction ,time-resolved XAFS	3.3-cm Undulator A	Operational/ GU
12-BM-B	XOR/BESSRC	Materials science, geoscience, chemistry, polymer science, physics, environmental science	XAFS, fluorescence spectroscopy, powder diffraction, x-ray reflectivity, general diffraction	Bending Magnet	Operational/ GU
12-ID-B,C,D	XOR/BESSRC	Chemistry, physics, materials science	Small-angle x-ray scattering, wide-angle x-ray scattering, grazing-incidence small-angle scattering	3.3-cm Undulator A	Operational/ GU
13-BM-C	GSECARS	Geoscience, environmental science	Single-crystal diffraction, surface diffraction, high-pressure diamond anvil cell	Bending magnet	Operational/ GU
13-BM-D	GSECARS	Geoscience, environmental science	Tomography, XAFS, high-pressure diamond anvil cell, high-pressure multianvil press	Bending magnet	Operational/ GU
13-ID-C,D	GSECARS	Geoscience, environmental science	Microfluorescence (hard x-ray), XAFS, microdiffraction, micro-XAFS, high-pressure diamond anvil cell, high-pressure multianvil press, inelastic x-ray scattering	3.3-cm Undulator A	Operational/ GU
14-BM-C	BioCARS	Life science	Macromolecular crystallography, fiber diffraction, biohazards at the BSL2/3 level, subatomic (<0.85 Å) resolution	Bending magnet	Operational/ GU

Continued on page 176

KEY: CPU = Circularly Polarized Undulator; CU: Canted undulator; GU: General Users

Beamline	Operator	Disciplines	Techniques	Source	Status
14-ID-B	BioCARS	Life science	Macromolecular crystallography, time-resolved x-ray scattering, Laue crystallography, anomalous diffraction (MAD/SAD), biohazards at the BSL2/3 level	2.7-cm Undulator	Operational/ GU
15-ID-B,C,D	ChemMatCARS	Materials science, chemistry	Anomalous and resonant scattering (hard x-ray), liquid scattering, microdiffraction, single-crystal diffraction, small-angle x-ray scattering, surface diffraction wide-angle x-ray scattering	3.3-cm Undulator A	Operational/ GU
16-BM-B	HP-CAT	Materials science, geoscience	Powder diffraction, single-crystal diffraction	Bending Magnet	Operational/ GU
16-BM-D	HP-CAT	Materials science, geoscience	Powder diffraction, single-crystal diffraction	Bending magnet	Operational/ GU
16-ID-B	HP-CAT	Materials science, geoscience	Microdiffraction, powder diffraction, single-crystal diffraction high-pressure diamond anvil cell	3.3-cm Undulator A	Operational/ GU
16-ID-D	HP-CAT	Materials science, geoscience, physics	Nuclear resonant scattering, inelastic x-ray scattering, x-ray Raman scattering, x-ray emission spectroscopy	3.3-cm Undulator A	Operational/ GU
17-BM-B	IMCA-CAT	Life science	Macromolecular crystallography, anomalous diffraction (multiwavelength anomalous dispersion [MAD]/single-wavelength anomalous dispersion [SAD])	Bending magnet	Operational/ GU
17-ID-B	IMCA-CAT	Life science	Macromolecular crystallography, anomalous diffraction (MAD/SAD)	3.3-cm Undulator A	Operational/ GU
18-ID-D	Bio-CAT	Life science	Microfluorescence (hard x-ray), microdiffraction, small-angle x-ray scattering, time-resolved x-ray scattering, micro-XAFS, fiber diffraction	3.3-cm Undulator A	Operational/ GU
19-BM-D	SBC-CAT	Life science	Anomalous diffraction (MAD/SAD), ultra-low-temperature (15K)	Bending magnet	Operational/ GU
19-ID-D	SBC-CAT	Life science	Anomalous diffraction (MAD/SAD), subatomic (<0.85 Å) resolution, ultra-low-temperature (15K)	3.3-cm Undulator A	Operational/ GU
20-BM-B	XOR/PNC	Materials science, environmental science, chemistry, geoscience	Microfluorescence (hard x-ray), XAFS, micro-XAFS	Bending magnet	Operational/ GU
20-ID-B,C	XOR/PNC	Materials science, environmental science, chemistry, geoscience	Microfluorescence (hard x-ray), XAFS, surface diffraction, micro-XAFS, x-ray Raman scattering, time-resolved XAFS	3.3-cm Undulator A	Operational/ GU
21-ID-D	LS-CAT	Life science	Macromolecular crystallography, MAD, MAD phasing, SAD	U33S undulator	Operational

Beamline	Operator	Disciplines	Techniques	Source	Status
21-ID-F	LS-CAT	Life science	Macromolecular crystallography single-wavelength anomalous dispersion	3.0-cm Undulator	Operational/ GU
21-ID-G	LS-CAT	Life science	Macromolecular crystallography, single-wavelength anomalous dispersion	3.0-cm undulator	Operational/
22-BM-D	SER-CAT	Life science	Macromolecular crystallography	Bending magnet	Operational/ GU
22-ID-D	SER-CAT	Life science	Macromolecular crystallography, multiwavelength anomalous dispersion	3.3-cm Undulator A	Operational/ GU
23-BM-B	GM/CA-CAT	Life science	Macromolecular crystallography multiwavelength anomalous dispersion	Bending magnet	Operational
23-ID-B	GM/CA-CAT	Life science	Macromolecular crystallography, microdiffraction, anomalous diffraction (MAD/SAD), subatomic (<0.85 Å) resolution	3.3-cm Undulator A	Operational/ GU
23-ID-D	GM/CA-CAT	Life science	Macromolecular crystallography, microdiffraction, anomalous diffraction (MAD/SAD), subatomic (<0.85 Å) resolution	3.0-cm undulator	Operational/ GU
24-ID-C	NE-CAT	Life science	Macromolecular crystallography, anomalous diffraction (MAD/SAD)	3.3-cm Undulator A	Operational/ GU
24-ID-E	NE-CAT	Life science	Macromolecular crystallography, microbeam	3.3-cm Undulator A	Operational/ GU
26-ID-C	CNM/XOR	Physics, materials science	Microfluorescence (hard x-ray), tomography, microdiffraction	3.3-cm Undulator A	Operational/ GU
30-ID-B,C	XOR/IXS	Physics, materials science, geoscience, life science	Inelastic x-ray scattering	3.0-cm undulator	Operational/ GU
31-ID-D	SGX-CAT	Life science	Macromolecular crystallography, single-crystal diffraction, fiber diffraction, single-wavelength anomalous dispersion	3.3-cm Undulator A	Operational/ GU
32-ID-B,C	XOR	Materials science, life science	Phase-contrast imaging, ultra-small-angle x-ray scattering, radiography	3.3-cm Undulator A	Operational/ GU
33-BM-C	XOR/UNI	Materials science, physics, chemistry	Anomalous and resonant scattering (hard x-ray), diffuse x-ray scattering, powder diffraction, x-ray reflectivity, general diffraction, grazing incidence diffraction	Bending magnet	Operational/ GU
33-ID-D,E	XOR/UNI	Materials science, physics, chemistry	Anomalous and resonant scattering (hard x-ray), diffuse x-ray scattering, x-ray reflectivity, surface diffraction, x-ray standing waves, general diffraction	3.3-cm Undulator A	Operational/ GU
34-ID-C,E	XOR/UNI	Materials science, physics	Coherent x-ray scattering, microdiffraction	3.3-cm Undulator A	Operational/ GU

Active Partner User Proposals Approved for Beam Time*

Investigators	Partner User Proposal Title (PUP number)	Beamline	Beam Time Award
R. Garrett	Australian Synchrotron Research Program-XOR Partnership Proposal (PUP-15)	1,3,4	Negotiated each run
L. Soderholm, P. Burns, J. Neuefeind, M. Beno, S. Skanthakumar	Short-range Order in Solution: Development of a Dedicated Beamline for Pair-distribution Functions (PDF) studies at the APS (PUP-52)	11-ID-B	20% beginning 2005-3 through 2008-2
E. Stern, E.D. Crozier, S. Heald, G. Seidler, D. Brewe, J. Cross	Novel X-ray Spectroscopies and Microscopies for the Determination of Structure with Atomic Resolution (extension of PUP-24) (PUP-55)	20-ID	Various allocations for different programs
L. Chen, K. Attenkofer, G. Jennings, D. Tiede	Developing Laser Initiated Time-resolved X-ray Facility at 11-ID-D for Photochemical Research using XAS and WAXS (PUP-56)	11-ID-D	20% beginning 2006-2 through 2007-3
A. Allen, L.E. Levine	Advanced USAXS Studies for Solution-Mediated Nanoscale Processing, Nanostructural Materials Imaging, and High-Spatial-Resolved Gradient Microstructure Characterization (PUP-59)	32-ID	10% beginning 2007-1 through 2008-3
E. D. Crozier, T.-K. Sham	Pacific Northwest Consortium Synchrotron Radiation Facility XOR Bending Magnet Partnership Proposal (PUP-60)	20-BM	10% beginning 2007-1 through 2009-3
B. Ocko, K. Blasie, T. Gog, I. Kuzmenko	Partner User Proposal: Liquid Surface Scattering (LSS) at Sector 9 (PUP-61)	9-ID	15% beginning 2007-1 through 2009-3
J. Hill, Y.-J. Kim, T. Gog, D. Casa	Partner User Proposal: Inelastic X-ray Scattering (IXS) at Sector 9 (PUP-62)	9-ID	15% beginning 2007-1 through 2009-3
Y. Hwu, T.-K. Lee, J.H. Je, G. Margaritondo, K.S. Liang	Short Proposal for Limited Scope Partnership User at the Advanced Photon Source Phase-Contrast Hard X-ray Microscopy for Biological and *In Situ* Materials Science Applications at Sub 6-nm Spatial Resolution (PUP-64)	32-ID	20% of the beam time on 32-ID for 2007-2 through 2010-1
E.D. Crozier, T.-K. Sham	Renewal Proposal for PUP-21, Pacific Northwest Consortium Synchrotron Radiation Facility-XOR Insertion Device Partnership User Proposal (PUP-65)	20-ID	10% for 2007-1, 20% for 2007-2, and 15% for 2007-3 through 2009-3
Z. Islam, J. Lang, D. Haskel, Y. Matsuda, H. Nojiri, B. Gaulin, Z. Mao, I. Fisher, P. Canfield	A Portable High-field (30-45 Tesla) Pulsed-magnet Setup for Novel Scattering and Spectroscopic Studies of Materials in Extreme Conditions (PUP67)	4-ID-D	18 shifts/cycles for two years (108 shifts total) beginning with 2007-3 through 2009-2
L. Young, S. Southworth, E. Kanter, B. Kraessig, R. Dunford, R. Santra, D. Arms, E. Dufresne, E. Lindahl, J. Ye, D. Yost	High-Repetition Rate Ultrafast Laser/X-ray Techniques (PUP-71)	7-ID	~15% of the time on 7-ID/cycle for three years beginning with 2007-3 through 2010-2
K. Nugent, A. Peele, L. Tilley, G. Williams, M. Pfeifer, M.-T. Tang, T.-K. Lee, I. McNulty, Q. Shen	Short Proposal for Limited-Scope Partnership User at the Advanced Photon Source Dedicated Fresnel Coherent Diffractive Imaging Facility at 2-ID-B (PUP-74)	2-ID-B	Thirty-six shifts/cycle for three years begining with 2008-2 through 2011-1

* As of 4.9.08

Source: http://www.aps.anl.gov/Users/Scientific_Access/Partner_User_Information/Results/index.html

Abstracts for these proposals are at the URL above.

Completed Partner User Proposals:
http://www.aps.anl.gov/Users/Scientific_Access/Partner_User_Information/Results/completed.html

Partner user call for proposals:
www.aps.anl.gov/Users/Scientific_Access/Partner_User_Information/Call_For_Proposals/index.html

Partner user procedure: www.aps.anl.gov/Users/General_Reference/Policy_Procedures/Partner_Users/access_procedures.htm

Partner user policy: www.aps.anl.gov/Users/General_Reference/Policy_Procedures/Partner_Users/access_policy.htm

Partner users are individuals or groups whose work involves a greater degree of collaboration with the APS than is generally expected of general users.

Collaborative access teams are the most comprehensive type of partner users.

Another type is a collaborative development team, an external partner group that drives the development of a beamline that will be ultimately operated by the APS. Typically, a partner user requires access to more than 10% of the beam time on a beamline or sector for two years or more. (Source: www.aps.anl.gov/Users/Scientific_Access/Partner_User_Information/index.html)

APS Organization Chart

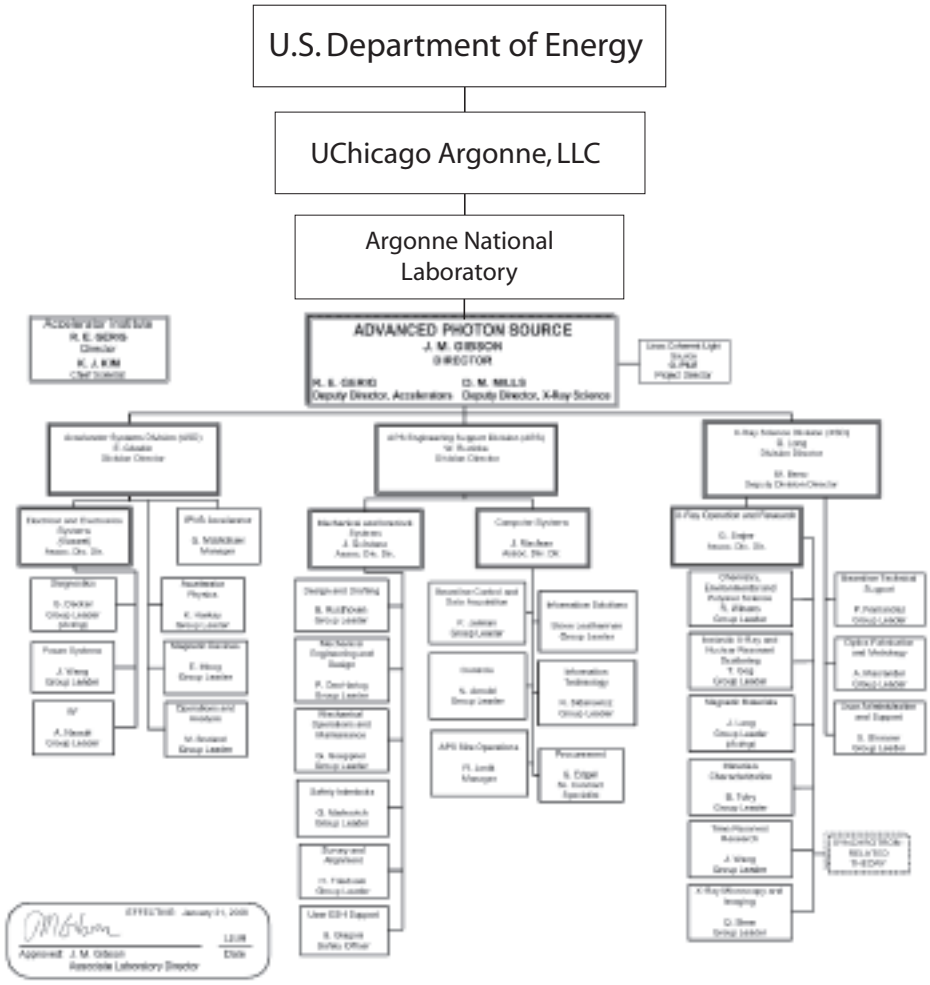

APS Staffing and Funding (FY 2002-FY 2007)

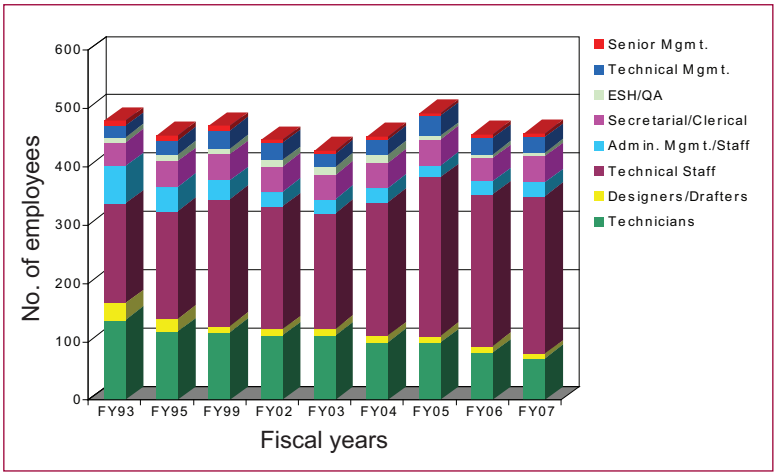

APS staffing levels, FY93-FY07

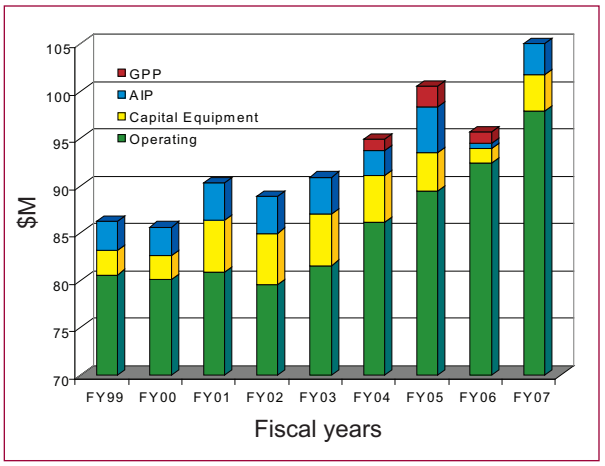

APS funding levels, FY99-FY07

Acknowledgments

***APS Science* Editorial Board:**

Cele Abad-Zapatero (University of Illinois at Chicago), Mark A. Beno (ANL-XSD), Bruce A. Bunker (University of Notre Dame), Rodney E. Gerig (ANL-SUF), J. Murray Gibson (ANL-SUF), Efim Gluskin (ANL-ASD), Timothy J. Graber (The University of Chicago), Gabrielle G. Long (ANL-XSD), Dennis M. Mills, (ANL-SUF), William G. Ruzicka (ANL-AES), George Srajer (ANL-XSD)

The research highlights in this report were written in whole or in part by:

William Arthur Atkins (waarc@grics.net)
Jim Barlow (jebarlow@uoregon.edu)
David Bradley (david@sciencebase.com)
Vic Comello (ANL-TSD, vcomello@anl.gov)
Dana Desonie (desonie@cox.net)
Sandy Field (sfield@fieldscientific.com)
Karen Fox (kfox@nasw.org)
Carol Hart (chart@nasw.org)
Emma Hitt (emma@emmasciencewriter.com)
Elise LeQuire (cygnete@mindspring.com)
JR Minkel (jrminkel@gmail.com)
Mona A. Mort (mamort@nasw.org)
Luis Nasser (luis.nasser@gmail.com)
Patricia E. Panatier (pep2@optonline.net)
Mark Wolverton (exetermw@earthlink.net)

Mechanical editing: Floyd Carse Bennett, Jr. (ANL-TSD), Catherine E. Eyberger (ANL-AES), and Mary L. Fitzpatrick (ANL-TSD)
Photography: Wes P. Agresta and George J. Joch (both ANL-TSD)
Rights, permissions, and contracts: Jessie L. Skwarek (ANL-SUF)
Project coordination, photography, cover design: Richard B. Fenner (ANL-SUF)

Our thanks to the corresponding authors who assisted in the preparation of the research highlights, to the users and APS personnel who wrote articles for the report, and our apologies to anyone inadvertently left off this list. To all: your contributions are appreciated.

APS Publications - Calendar Year 2007

APS Publications - Calendar year 2007

The APS publications database can be found at http://beam.aps.anl.gov/pls/apsweb/pub_v2_0006.review_start_page

C. Adriano, R. Lora-Serrano, C. Giles, F. de Bergevin, J.C. Lang, G. Srajer, C. Mazzoli, L. Paolasini, P.G. Pagliuso, "Magnetic structure of Sm[subscript 2]Ir[subscript 8] determined by x-ray resonant magnetic scattering," Phys. Rev. B 76, 104515-1-104515-8 (2007). DOI: 10.1103/PhysRevB.76.104515

Johnson Agniswamy, Bin Fang, Irene T. Weber, "Plasticity of S2-S4 specificity pockets of executioner caspase-7 revealed by structural and kinetic analysis," FEBS J. 274 (18), 4752-4765 (2007). DOI: 10.1111/j.1742-4658.2007.05994.x

Sarvesh K. Agrawal, Naomi Sanabria-DeLong, Pete R. Jemian, Gregory N. Tew, Surita R. Bhatia, "Micro- to Nanoscale Structure of Biocompatible PLA-PEO-PLA Hydrogels," Langmuir 23 (9), 5039-5044 (2007). DOI: 10.1021/la063390x

Riaz Akhtar, "Micromechanical behaviour of bone," Masters, Manchester University, 2007.

Riyadh Al-Raoush, "Microstructure characterization of granular materials," Physica A 377 (2), 545-558 (2007). DOI: 10.1016/j.physa.2006.11.090

Rebecca A. Alderden, Howard R. Mellor, Szabolcs Modok, Matthew D. Hall, Stephen R. Sutton, Matthew G. Newville, Richard Callaghan, Trevor W. Hambley, "Elemental Tomography of Cancer-Cell Spheroids Reveals Incomplete Uptake of Both Platinum(II) and Platinum(IV) Complexes," J. Am. Chem. Soc. 129 (44), 13400-13401 (2007). DOI: 10.1021/ja076281t

Andrew J. Allen, Jeffrey J. Thomas, Hamlin M. Jennings, "Composition and density of nanoscale calcium–silicate–hydrate in cement," Nat. Mater. 6 (4), 311-316 (2007). DOI: 10.1038/nmat1871

Pierre Aller, Mark A. Rould, Matthew Hogg, Susan S. Wallace, Sylvie Doublie´, "A structural rationale for stalling of a replicative DNA polymerase at the most common oxidative thymine lesion, thymine glycol," Proc. Natl. Acad. Sci. USA 104 (3), 814-818 (2007). DOI: 10.1073pnas.0606648104

John S. Allingham, Lisa R. Sproul, Ivan Rayment, Susan P. Gilbert, "Vik1 Modulates Microtubule-Kar3 Interactions through a Motor Domain that Lacks an Active Site," Cell 128, 1161-1172 (2007). DOI: 10.1016/j.cell.2006.12.046

J.D. Almer, S.R. Stock, "Micromechanical response of mineral and collagen phases in bone," J. Struct. Biol. 157 (2), 365-370 (2007). DOI: 10.1016/j.jsb.2006.09.001

Benjamin J. Anderson, Charles F. Zukoski, "Nanoparticle Stability in Polymer Melts As Determined by Particle Second Virial Measurement," Macromolecules 40 (14), 5133-5140 (2007). DOI: 10.1021/ma0624346

David R. Anderson, Marvin J. Meyers, William F. Vernier, Matthew W. Mahoney, Ravi G. Kurumbail, Nicole Caspers, Gennadiy I. Poda, John F. Schindler, David B. Reitz, Robert J. Mourey, "Pyrrolopyridine Inhibitors of Mitogen-Activated Protein Kinase-Activated Protein Kinase 2 (MK-2)," J. Med. Chem. 50 (11), 2647-2654 (2007). DOI: 10.1021/jm0611004

Travis M. Anderson, Steven G. Thoma, Francois Bonhomme, Mark A. Rodriguez, Hyunsoo Park, John B. Parise, Todd M. Alam, James P. Larentzos, May Nyman, "Lithium Polyniobates. A Lindqvist-Supported Lithium-Water Adamantane Cluster and Conversion of Hexaniobate to a Discrete Keggin Complex," Cryst. Growth Des. 7 (4), 719-723 (2007). DOI: 10.1021/cg0606904

M. Angst, R.P. Hermann, W. Schweika, J.-W. Kim, P. Khalifah, H.J. Xiang, M.-H. Whangbo, D.-H. Kim, B.C. Sales, D. Mandrus, "Incommensurate Charge Order Phase in Fe[subscript 2]OBO[subscript 3] due to Geometrical Frustration," Phys. Rev. Lett. 99 (25), 256402-1-256402-4 (2007). DOI: 10.1103/PhysRevLett.99.256402

L.L. Araujo, P. Kluth, G.de M. Azevedo, M.C. Ridgway, "Short-range thermal and structural properties of Ge nanocrystals," Nucl. Instrum. Methods B 257 (1-2), 56-59 (2007). DOI: 10.1016/j.nimb.2006.12.115

D.A. Arena, E. Vescovo, C.-C. Kao, Y. Guan, W.E. Bailey, "Combined time-resolved x-ray magnetic circular dichroism and ferromagnetic resonance studies of magnetic alloys and multilayers (invited)," J. Appl. Phys. 101, 09C109-1-09C109-6 (2007). DOI: 10.1063/1.2712294

B.D. Arhatari, F. De Carlo, A.G. Peele, "Direct quantitative tomographic reconstruction for weakly absorbing homogeneous phase objects," Rev. Sci. Instrum. 78, 053701-1-053701-5 (2007). DOI: 10.1063/1.2735583

L. Armelao, F. Heigl, A. Jurgensen, R.I.R. Blyth, T. Regier, X.-T. Zhou, T.K. Sham, "X-ray Excited Optical Luminescence Studies of ZnO and Eu-Doped ZnO Nanostructures," J. Phys. Chem. C 111 (28), 10194-10200 (2007). DOI: 10.1021/jp071379f

Manish Arora, Brendan J. Kennedy, Chris G. Ryan, Ross A. Boadle, D. Murray Walker, Cathy L. Harland, Barry Lai, Zhonghou Cai, Stefan Vogt, Hans Zoellner, Sheena W.Y. Chan, "The application of synchrotron radiation induced X-ray emission in the measurement of zinc and lead in Wistar rat ameloblasts," Arch. Oral Biol. 52 (10), 938-944 (2007). DOI: 10.1016/j.archoralbio.2007.04.003

Emily B. Askew, Robert T. Gampe, Jr., Thomas B. Stanley, Jonathan L. Faggart, Elizabeth M. Wilson, "Modulation of Androgen Receptor Activation Function 2 by Testosterone and Dihydrotestosterone," J. Biol. Chem. 282 (35), 25801-25816 (2007). DOI: 10.1074/jbc.M703268200

Shane Atwell, Kris Conners, Spencer Emtage, Tarun Gheyi, Hal Lewis, Frances Lu, Rich Romero, Xun Zhao, "Structure of the Human CFTR NBD1 Domain as a Homodimer: Insights and Applications," Pediatr. Pulmonol. Suppl. 42 (S30), 73-428 (2007). DOI: 10.2210/pdb2pze/pdb

C.C. Aydınera, D.W. Brown, A. Misra, N.A. Mara, Y.-C. Wang, J.J. Wall, J. Almer, "Residual strain and texture in free-standing nanoscale Cu-Nb multilayers," J. Appl. Phys. 102, 083514-1-083514-10 (2007). DOI: http:/10.1063/1.2794862

Santanu Bag, Pantelis N. Trikalitis, Peter J. Chupas, Gerasimos S. Armatas, Mercouri G. Kanatzidis, "Porous Semiconducting Gels and Aerogels from Chalcogenide Clusters," Science 317 (5837), 490-493 (2007). DOI: 10.1126/science.1142535

Alaji Bah, Zhiwei Chen, Leslie A. Bush-Pelc, F. Scott Mathews, Enrico Di Cera, "Crystal structures of murine thrombin in complex with the extracellular fragments of murine protease-activated receptors PAR3 and PAR4," Proc. Natl. Acad. Sci. USA 104 (28), 11603-11608 (2007). DOI: 10.1073/pnas.0704409104

J.L. Bailey, J.W. Morgan, D. Capatina, H.-D. Nuhn, "An Instrument Design for the Accurate Determination of the Electron Beam Location in the Linac Coherent Light Source Undulator," Proc. of the 22nd Particle Accelerator Conference (PAC07), IEEE, (2007), 4324 - 4326.

S. Bailey, W.K. Eliason, T.A. Steitz, "Structure of hexameric DnaB helicase and its complex with a domain of DnaG primase," Science 318, 459-463 (2007). DOI: 10.1126/science.1147353

Yu Bai, "Electrostatic underpinnings of nucleic acid structure and folding," Ph.D., Stanford University, 2007.

V.S.K. Balagurusamy, Reinhard Streitel, Oleg G. Shpyrko, P.S. Pershan, Mati Meron, Binhua Lin, "X-ray reflectivity studies of atomic-level surface-segregation in a liquid eutectic alloy of AuSn," Phys. Rev. B 75, 104209-1-104209-7 (2007). DOI: 10.1103/PhysRevB.75.104209

M. Balasubramanian, C.S. Johnson, J.O. Cross, G.T. Seidler, T.T. Fister, E.A. Stern, C. Hamner, S.O. Mariager, "Fine structure and chemical shifts in nonresonant inelastic x-ray scattering from Li-intercalated graphite," Appl. Phys. Lett. 91, 031904-1-031904-3 (2007). DOI: 10.1063/1.2752755

O.M. Barabash, R.I. Barabash, G.E. Ice, S.A. David, Z. Feng, J. Horton, "X-ray MicroBeam Characterization of the Near Surface Nanostructured Layer in Ti after Friction Stir Processing," Rev. Adv. Mater. Sci. 15 (1), 49-55 (2007).

R.I. Barabash, G.E. Ice, C. Roder, J. Budai, W. Liu, S. Figge, S. Einfeldt, D. Hommel, R.F. Davis, "Characterization of growth defects in thin GaN layers with X-ray microbeam," Phys. Status Solidi. b. 244 (5), 1735-1742 (2007). DOI: 10.1002/pssb.200675113

D. J. Barber, H.-R. Wenk, J. Gomez-Barreiro, E. Rybacki, G. Dresen, "Basal slip and texture development in calcite: new results from torsion experiments," Phys. Chem. Miner. 34 (2), 73-84 (2007). DOI: 10.1007/s00269-006-0129-3

S.R. Bare, N. Yang, S.D. Kelly, G.E. Mickelson, F.S. Modica, "Design and operation of a high pressure reaction cell for in situ X-ray absorption spectroscopy," Catal. Today 126 (1-2), 18-26 (2007). DOI: 10.1016/j.cattod.2006.10.007

Cyril Barinka, Miroslava Rovensk, Petra Mlochova, Klra Hlouchova, Anna Plechanovova, Pavel Majer, Takashi Tsukamoto, Barbara S. Slusher, Jan Konvalinka, Jacek Lubkowski, "Structural Insight into the Pharmacophore Pocket of Human Glutamate Carboxypeptidase II," J. Med. Chem. 50 (14), 3267-3273 (2007). DOI: 10.1021/jm070133w

Cyril Barinka, Jana Starkova, Jan Konvalinka, Jacek Lubkowski, "A high-resolution structure of ligand-free human glutamate carboxypeptidase II," Acta Crystallogr. F 63, 150-153 (2007). DOI: 10.1107/S174430910700379X

Travis J. Barnard, Nathalie Dautin, Petra Lukacik, Harris D. Bernstein, Susan K. Buchanan, "Autotransporter structure reveals intra-barrel cleavage followed by conformational changes," Nat. Struct. Mol. Biol. 14 (12), 1214-1220 (2007). DOI: 10.1038/nsmb1322

Travis J. Barnard, Nathalie Dautin, Petra Lukacik, Harris D. Bernstein, Susan K. Buchanan, "Autotransporter structure reveals intro-barrel cleavage followed by conformational changes," Nat. Struct. Mol. Biol. 14, 1214-1220 (2007). DOI: 10.1038/nsmb1322

Rajiv Basu, Jui-Ching Lin, Chang-Yong Kim, Matthew J. Schmitz, Nathan L. Yoder, Joshua A. Kellar, Michael J. Bedzyk, Mark C. Hersam, "Structural Characterization of 4-Bromostyrene Self-Assembled Monolayers on Si(111)," Langmuir 23 (4), 1905-1911 (2007). DOI: 10.1021/la062759f

Dolly Batra, Sonke Seifert, Millicent A. Firestone, "The Effect of Cation Structure on the Mesophase Architecture of Self-Assembled and Polymerized Imidazolium-Based Ionic Liquids," Macromol. Chem. Phys. 208 (13), 1416-1427 (2007). DOI: 10.1002/macp.200700174

D. Batra, S. Seifert, L.M. Varela, A.C.Y. Liu, M.A. Firestone, "Solvent-Mediated Plasmon Tuning in a Gold-Nanoparticle-Poly(Ionic Liquid) Composite," Adv. Funct. Mater. 17 (8), 1279-1287 (2007). DOI: 10.1002/adfm.200600797

Richard H.G. Baxter, Chung-I Chang, Yogarany Chelliah, Stephanie Blandin, Elena A. Levashina, Johann Deisenhofer, "Structural basis for conserved complement factor-like function in the antimalarial protein TEP1," Proc. Natl. Acad. Sci. USA 104 (28), 11615-11620 (2007). DOI: 10.1073/pnas.0704967104

Timothy H. Bayburt, Andrew J. Leitz, Guifu Xie, Daniel D. Oprian, Stephen G. Sligar, "Transducin Activation by Nanoscale Lipid Bilayers Containing One and Two Rhodopsins," J. Biol. Chem. 282 (20), 14875-14881 (2007). DOI: 10.1074/jbc.M701433200

N. Bedford, C. Dablemont, G. Viau, P. Chupas, V. Petkov, "3-D Structure of Nanosized Catalysts by High-Energy X-ray Diffraction and Reverse Monte Carlo Simulations: Study of Ru," J. Phys. Chem. C 111 (49), 18214-18219 (2007). DOI: 10.1021/jp0752062

J.J. Bellizzi, III, P.K. Sorger, S.C. Harrison, "Crystal structure of the yeast inner kinetochore subunit Cep3p," Struct. Fold. Des. 15, 1422-1430 (2007). DOI: 10.1016/j.str.2007.09.008

Angelica M. Bello, Ewa Poduch, Masahiro Fujihashi, Merhnaz Amani, Yan Li, Ian Crandall, Raymond Hui, Ping I. Lee, Kevin C. Kain, Emil F. Pai, Lakshmi P. Kotra, "A Potent, Covalent Inhibitor of Orotidine 5[prime]-Monophosphate Decarboxylase with Antimalarial Activity," J. Med. Chem. 50 (5), 915-921 (2007). DOI: 10.1021/jm060827p

Georgiy A. Belogurov, Marina N. Vassylyeva, Vladimir Svetlov, Sergiy Klyuyev, Nick V. Grishin, Dmitry G. Vassylyev, Irina Artsimovitch, "Structural Basis for Converting a General Transcription Factor into an Operon-Specific Virulence Regulator," Mol. Cell 26 (1), 117-129 (2007). DOI: 10.1016/j.molcel.2007.02.021

Brad C. Bennett, Hai Xu, Richard F. Simmerman, Richard E. Lee, Chris G. Dealwis, "Crystal Structure of the Anthrax Drug Target, Bacillus anthracis Dihydrofolate Reductase," J. Med. Chem. 50 (18), 4374-4381 (2007). DOI: 10.1021/jm070319v

C. Benson, Y. Jaski, J. Maser, T. Powers, O. Schmidt, E. Rossi, "White Beam Slits and Pink Beam Slits for the Hard X-ray Nanoprobe Beamline at the Advanced Photon Source," Proc. of the Ninth International Conference on Synchrotron Radiation Instrumentation, 879, AIP, (2007), 1061 - 1064.

Asim K. Bera, Lena S. Polovnikova, Juliatek Roestamadji, Theodore S. Widlanski, George L. Kenyon, Michael J. McLeish, Miriam S. Hasson, "Mechanism-Based Inactivation of Benzoylformate Decarboxylase, A Thiamin Diphosphate-Dependent Enzyme," J. Am. Chem. Soc. 129 (14), 4120-4121 (2007). DOI: 10.1021/ja068636z

U. Bergmann, D. Nordlund, Ph. Wernet, M. Odelius, L.G.M. Pettersson, A. Nilsson, "Isotope effects in liquid water probed by x-ray Raman spectroscopy," Phys. Rev. B 76, 024202-1-024202-6 (2007). DOI: 10.1103/PhysRevB.76.024202

W.J. Berg, B.X. Yang, L.L. Erwin, S.E. Shoaf, "LCLS-S1 Optical Transition Radition Monitor," Proc. of the 22nd Particle Accelerator Conference (PAC07), IEEE, (2007), 4396 - 4398.

Andrea J. Berman, Satwik Kamtekar, Jessica L. Goodman, Jose M. Lazaro, Miguel de Vega, Luis Blanco, Margarita Salas, Thomas A. Steitz, "Structures of phi29 DNA polymerase complexed with substrate: the mechanism of translocation in B-family polymerases," EMBO J. 26, 3494-3505 (2007). DOI: 10.1038/sj.emboj.7601780

S.A. Bernal, E. Rodriguez, R.M. de Gutierrez, V. Rose, F. Puertes, S. Delvasto, "Carbonation behavior of mortar produced by alkali-activation of a granular blast furnace slag," The 23rd International Conference on Solid Waste Technology and Management, Iraj Zandi, Ronald L. Mersky, Wen K. Shieh, eds., 23, The Journal of Solid Waste Technology and Management, (2007), 945 - 956.

S. Bernardini, M. Ishii, E. Whittaker, B. Hamilton, J.W. Freeland, N.R.J. Poolton, S. De Gendt, "Nanoscale imaging and X-ray spectroscopy of electrically active defects in ultra thin dielectrics on silicon," Microelectronic Eng. 84 (9-10), 2286-2289 (2007). DOI: 10.1016/j.mee.2007.04.054

Massimo F. Bertino, Raghuveer R. Gadipalli, Lane A. Martin, Lauren E. Rich, Alexey Yamilov, Brian R. Heckman, Nicholas Leventis, Suchi Guha, John Katsoudas, Ralu Divan, Derrick C. Mancini, "Quantum dots by ultraviolet and x-ray lithography," Nanotechnology 18, 315603-1-315603-6 (2007). DOI: 10.1088/0957-4484/18/31/315603

F.L. Beyer, C.R. Ziegler, K. Sill, T. Emrick, N.M. Benetatos, K.I. Winey, "Directed Assembly of Quantum Dots in a Diblock Copolymer Matrix," ARL-TR-4204, (2007).

S. Bhowmik, G.P. Horsman, J.T. Bolin, L.D. Eltis, "The molecular basis for inhibition of BphD, a C-C bond hydrolase involved in polychlorinated biphenyls degradation; large 3-substituents prevent tautomerization," J. Biol. Chem. 282 (50), 36377-36385 (2007). DOI: 10.1074/jbc.M707035200

Marianna Biadene, Isabelle Hazemann, Alexandra Cousido, Steve Ginell, Andrzej Joachimiak, George M. Sheldrick, Alberto Podjarny, Thomas R. Schneiderd, "The atomic resolution structure of human aldose reductase reveals that rearrangement of a bound ligand allows the opening of the safety-belt loop," Acta Crystallogr. D 63 (6), 665-672 (2007). DOI: 10.1107/S0907444907011997

Christopher M. Bianchetti, Li Yi, Stephen W. Ragsdale, George N. Phillips, Jr., "Comparison of Apo- and Heme-bound Crystal Structures of a Truncated Human Heme Oxygenase-2," J. Biol. Chem. 282 (52), 37624-37631 (2007). DOI: 10.1074/jbc.M707396200

S.G. Biedron, J.W. Lewellen, S.V. Milton, N.S. Gopalsami, J. Schneider, L. Skubal, Y. Li, M. Virgo, G. P. Gallerano, A. Doria, E. Giovenale, G. Messina, I. P. Spassovsky, "Compact, High-Power Electron Beam Based Terahertz Sources," P. IEEE 95, 1666-1678 (2007).

Christian Biertumpfel, Wei Yang, Dietrich Suck, "Crystal structure of T4 endonuclease VII resolving a Holliday junction," Nature 449 (7162), 616-620 (2007). DOI: 10.1038/nature06152

Eduard Bitto, Craig A. Bingman, Gary E. Wesenberg, Jason G. McCoy, George N. Phillips, Jr., "Structure of aspartoacylase, the brain enzyme impaired in Canavan disease," Proc. Natl. Acad. Sci. USA 104 (2), 456-461 (2007). DOI: 10.1073/pnas.0607817104

Jimmy A. Blair, Daniel Rauh, Charles Kung, Cai-Hong Yun, Qi-Wen Fan, Haridas Rode, Chao Zhang, Michael J. Eck, William A. Weiss, Kevan M. Shokat, "Structure-guided development of affinity probes for tyrosine kinases using chemical genetics," Nat. Chem. Biol. 3 (4), 229-238 (2007). DOI: 10.1038/nchembio866

Gina Boanca, Aaron Sand, Toshihiro Okada, Hideyuki Suzuki, Hidehiko Kumagai, Keiichi Fukuyama, Joseph J. Barycki, "Autoprocessing of Helicobacter pylori [gamma]-Glutamyltranspeptidase Leads to the Formation of a Threonine-Threonine Catalytic Dyad," J. Biol. Chem. 282 (1), 534-541 (2007). DOI: 10.1074/jbc.M607694200

T. Boehmer, T.U. Schwartz, "Purification, crystallization and preliminary X-ray analysis of a Nup107-Nup133 heterodimeric nucleoporin complex," Acta Crystallogr. F 63 (9), 816-818 (2007). DOI: 10.1107/S1744309107040523

David J. Boerema, "Total chemical synthesis of ribonuclease A and designed analogues with enhanced catalytic activity," Ph.D., University of Chicago, 2007.

Luis Bollmann, Vikrant N. Urade, Hugh W. Hillhouse, "Controlling Interfacial Curvature in Nanoporous Silica Films Formed by Evaporation-Induced Self-Assembly from Nonionic Surfactants. I. Evolution of Nanoscale Structures in Coating Solutions," Langmuir 23 (8), 4257-4267 (2007). DOI: 10.1021/la0626407

Dominika Borek, Stephan L. Ginell, Marcin Cymborowski, Wladek Minor, Zbyszek Otwinowskia, "The many faces of radiation-induced changes," J. Synchrotron Rad. 14 (1), 24-33 (2007). DOI: 10.1107/S0909049506046589

Natalie A. Borg, Kwok S. Wun, Lars Kjer-Nielsen, Matthew C.J. Wilce, Daniel G. Pellicci, Ruide Koh, Gurdyal S. Besra, Mandvi Bharadwaj, Dale I. Godfrey, James McCluskey, Jamie Rossjohn, "CD1d–lipid-antigen recognition by the semi-invariant NKT T-cell receptor," Nature 448, 44-49 (2007). DOI: 10.1038/nature05907

M. Borland, J. Carwardine, Y. Chae, L. Emery, P. Den Hartog, K. Harkay, A. Lumpkin, A. Nassiri, V. Sajaev, N. Sereno, G. Waldschmidt, B. Yang, V. Dolgashev, "Planned Use of Pulsed Crab Cavities for Short X-ray Pulse Generation at the Advanced Photon Source," Proc. of the 22nd Particle Accelerator Conference (PAC07), IEEE, (2007), 1127 - 1129.

M. Borland, G. Decker, A. Nassiri, Y.-e Sun, M. White, "Potential Performance and Challenges of an Energy Recovery Linac Upgrade tothe Advanced Photon Source," Nucl. Instrum. Methods A 582 (1), 54-56 (2007).

M. Borland, G. Decker, A. Nassiri, Y.-e Sun, M. White, "Potential and Challenges of Upgrading the Advanced Photon Source to an Energy Recovery Linac," Proc. of AccApp'07, American Nuclear Society (2007), 196 - 203.

M. Borland, G. Decker, A. Nassiri, M. White, "Configuration, Optics, and Performance of a 7-GeV Energy Recovery Linac Upgrade for the Advanced Photon Source," Proc. of the 22nd Particle Accelerator Conference (PAC07), IEEE, (2007), 1121 - 1123.

M. Borland, L. Emery, "Evaluation of the Possibility of Using Damping Wigglers in the Advanced Photon Source," Proc. of the 22nd Particle Accelerator Conference (PAC07), IEEE, (2007), 1124 - 1126.

M. Borland, L. Emery, V. Sajaev, "Beam Dynamics, Performance, and Tolerances for Pulsed Crab Cavities at the Advanced Photon Source for Short X-ray Pulse Generation," Proc. of the 22nd Particle Accelerator Conference (PAC07), IEEE, (2007), 3429 - 3431.

Maria A. Borovinskaya, Raj D. Pai, Wen Zhang, Barbara S. Schuwirth, James M. Holton, Go Hirokawa, Hideko Kaji, Akira Kaji, Jamie H. Doudna Cate, "Structural basis for aminoglycoside inhibition of bacterial ribosome recycling," Nat. Struct. Mol. Biol. 14, 727-732 (2007). DOI: 10.1038/nsmb1271

M. Jack Borrok, Laura L. Kiessling, Katrina T. Forest, "Conformational changes of glucose/galactose-binding protein illuminated by open, unliganded, and ultra-high-resolution ligand-bound structures," Protein Sci. 16 (6), 1032-1041 (2007). DOI: 10.1110/ps.062707807

Sergei P. Boudko, Richard J. Kuhn, Michael G. Rossmann, "The Coiled-coil Domain Structure of the Sin Nombre Virus Nucleocapsid Protein," J. Mol. Biol. 366 (5), 1538-1544 (2007). DOI: 10.1016/j.jmb.2006.12.046

S. Boutet, I.K. Robinson, "Precrystallization clusters of holoferritin and apoferritin at low temperature," Phys. Rev. E 75, 021913-1-021913-12 (2007). DOI: 10.1103/PhysRevE.75.021913

Matthew B. Boxer, Hisashi Yamamoto, "'Super Silyl' Group for Diastereoselective Sequential Reactions: Access to Complex Chiral Architecture in One Pot," J. Am. Chem. Soc. 129 (10), 2762-2763 (2007). DOI: 10.1021/ja0693542

Maxim I. Boyanov, Edward J. O'Loughlin, Eric E. Roden, Jeremy B. Fein, Kenneth M. Kemner, "Adsorption of Fe(II) and U(VI) to carboxyl-functionalized microspheres: The influence of speciation on uranyl reduction studied by titration and XAFS," Geochim. Cosmochim. Acta 71 (8), 1898-1912 (2007). DOI: http://www.sciencedirect.com/science?_ob=ArticleURL&_udi=B6V66-4N0HJHD-1&_user=1722207&_rdoc=1&_fmt=&_orig=search&_sort=d&view=c&_acct=C000053990&_version=1&_urlVersion=0&_userid=1722207&md5=14a598857cfa53ee84c05774a3117b49

Christina M. Bradley, Sarah Jones, Ying Huang, Youichi Suzuki, Mamuka Kvaratskhelia, Allison B. Hickman, Robert Craigie, Fred Dyda, "Structural Basis for Dimerization of LAP2[alpha], a Component of the Nuclear Lamina," Structure 15 (6), 643-653 (2007). DOI: 10.1016/j.str.2007.04.007

B. Brajuskovic, J. Collins, P. Den Hartog, L. Morrison, G. Waldschmidt, "Thermomechanical Design of Normal-Conducting Deflecting Cavities at the Advanced Photon Source for Short X-ray Pulse Generation," Proc. of the 22nd Particle Accelerator Conference (PAC07), IEEE, (2007), 3827 - 3829.

J.A. Brandes, E. Ingall, D. Paterson, "Characterization of minerals and organic phosphorus species in marine sediments using soft X-ray fluorescence spectromicroscopy," Mar. Chem. 103 (3-4), 250-265 (2007). DOI: 10.1016/j.marchem.2006.09.004

G.L. Brennecka, D.A. Payne, P. Sarin, J.-M. Zuo, W.M. Kriven, H. Hellwig, "Phase Transformations in the High-Temperature Form of Pure and TiO[subscript 2]-Stabilized Ta[subscript 2]O[subscript 5]," J. Am. Ceram. Soc. 90 (9), 2947-2953 (2007). DOI: 10.1111/j.1551-2916.2007.01790.x

K.L. Brinker, "Studies of Structural Dynamics in Polymer Blends Using Rheology and Small-Angle X-Ray Scattering Techniques," Ph.D., Northwestern University, 2007.

Kristin L. Brinker, Simon G.J. Mochrie, Wesley R. Burghardt, "Equilibrium Dynamics of a Polymer Bicontinuous Microemulsion," Macromolecules 40 (14), 5150-5160 (2007). DOI: 10.1021/ma0704820

Peter R. Brotherhood, Richard A.-S. Wu, Peter Turner, Maxwell J. Crossley, "Cavity effect amplification in the recognition of dicarboxylic acids by initial ditopic H-bond formation followed by kinetic trapping," Chem. Comm. 3, 225-227 (2007). DOI: 10.1039/b614575b

M.D. Brown, B.M. Law, L. Marchand, L.B. Lurio, I. Kuzmenko, T. Gog, W.A. Hamilton, "X-ray and ellipsometric study of strong critical adsorption," Phys. Rev. E 75, 061606-1-061606-7 (2007). DOI: 10.1103/PhysRevE.75.061606

Michael I. Bruce, Paul A. Humphrey, Martyn Jevric, Brian W. Skelton, Allan H. White, "Preparation, structure and some chemistry of FcCCCCCCRu(dppe)Cp," J. Organomet. Chem. 692 (12), 2564-2574 (2007). DOI: 10.1016/j.jorganchem.2007.02.043

John B. Bruning, Michael J. Chalmers, Swati Prasad, Scott A. Busby, Theodore M. Kamenecka, Yuanjun He, Kendall W. Nettles, Patrick R. Griffin,

"Partial Agonists Activate PPAR[gamma] Using a Helix 12 Independent Mechanism," Structure 15 (10), 1258-1271 (2007). DOI: 10.1016/j.str.2007.07.014

M.L. Brusseau, S. Peng, G. Schnaar, A. Murao, "Measuring air-water interfacial areas with x-ray microtomography and interfacial partitioning tracer tests," Environ. Sci. Technol. 41 (6), 1956-1961 (2007). DOI: 10/1021/es061474m

Susan K. Buchanan, Petra Lukacik, Sylvestre Grizot, Rodolfo Ghirlando, Maruf M.U. Ali, Travis J. Barnard, Karen S. Jakes, Paul K. Kienker, Lothar Esser, "Structure of colicin I receptor bound to the R-domain of colicin Ia: implications for protein import," EMBO J. 26 (10), 2594-2604 (2007). DOI: 10.1038/sj.emboj.7601693

P.S. Budnik, R.A. Gordon, E.D. Crozier, "The Pd/Fe Interface in the Epitaxial System Pd/Fe/GaAs(001)- 4 x 6," AIP Conference Proceedings, B. Hedman, P. Pianetta, eds., 882, American Institute of Physics, (2007), 398 - 400.

Greg Buhrman, Glenna Wink, Carla Mattos, "Transformation Efficiency of RasQ61 Mutants Linked to Structural Features of the Switch Regions in the Presence of Raf," Structure 15, 1618-1629 (2007). DOI: 10.1016/j.str.2007.10.011

T. Buonassisi, M. Heuer, A.A. Istratov, M.D. Pickett, M.A. Marcus, B. Lai, Z. Cai, S.M. Heald, E.R. Weber, "Transition metal co-precipitation mechanisms in silicon," Acta Mater. 55 (18), 6119-6126 (2007). DOI: 10.1016/j.actamat.2007.07.030

E. Sethe Burgie, James B. Thoden, Hazel M. Holden, "Molecular architecture of DesV from Streptomyces venezuelae: A PLP-dependent transaminase involved in the biosynthesis of the unusual sugar desosamine," Protein Sci. 16 (5), 887-896 (2007). DOI: 10.1110/ps.062711007

William D. Burgos, John M. Senko, Brian A. Dempsey, Eric E. Roden, James J. Stone, Ken M. Kemner, Shelly D. Kelly, "Soil Humic Acid Decreases Biological Uranium(VI) Reduction by Shewanella putrefaciens CN32," Environ. Eng. Sci. 24 (6), 755-761 (2007). DOI: 10.1089/ees.2006.0009

Leslie A. Bush-Pelc, Francesca Marino, Zhiwei Chen, Agustin O. Pineda, F. Scott Mathews, Enrico Di Cera, "Important Role of the Cys-191-Cys-220 Disulfide Bond in Thrombin Function and Allostery," J. Biol. Chem. 282 (37), 27165-27170 (2007). DOI: 10.1074/jbc.M703202200

R. Callens, C. L'abbe, J. Meersschaut, I. Serdons, W. Sturhahn, T.S. Toellner, "Determination of the magnetic spin direction from the nuclear forward-scattering line intensities," J. Synchrotron Rad. 14 (4), 366-371 (2007). DOI: 10.1107/S0909049507023229

A.J. Campbell, C.T. Seagle, D.L. Heinz, G. Shen, V. Prakapenka, "Partial melting in the iron–sulfur system at high pressure: A synchrotron X-ray diffraction study," Phys. Earth Planet. In. 162 (1-2), 119-128 (2007). DOI: 10.1016/j.pepi.2007.04.001

Elizabeth A. Campbell, Roger Greenwell, Jennifer R. Anthony, Sheng Wang, Lionel Lim, Kalyan Das, Heidi J. Sofia, Timothy J. Donohue, Seth A. Darst, "A Conserved Structural Module Regulates Transcriptional Responses to Diverse Stress Signals in Bacteria," Mol. Cell 27 (5), 793-805 (2007). DOI: 10.1016/j.molcel.2007.07.009

P.A. Candela, C.D. Crummett, D.J. Earnest, M.R. Frank, A.G. Wylie, "Low-pressure decomposition of chrysotile as a function of time and temperature," Am. Mineral. 92, 1704-1713 (2007). DOI: 10.2138/am.2007.2559

Ahmet E. Cansizoglu, Brittany J. Lee, Zi Chao Zhang, Beatriz M.A. Fontoura, Yuh Min Chook, "Structure-based design of a pathway-specific nuclear import inhibitor," Nat. Struct. Mol. Biol. 14 (5), 452-454 (2007). DOI: 10.1038/nsmb1229

A.D. Capili, C.D. Lima, "Structure and analysis of a complex between SUMO and Ubc9 illustrates features of a conserved E2-Ubl interaction," J. Mol. Biol. 369 (3), 608-618 (2007). DOI: 10.1016/j.jmb.2007.04.006

Raanan Carmieli, Todd M. Larsen, George H. Reed, Samir Zein, Frank Neese, Daniella Goldfarb, "The Catalytic Mn [superscript 2+] Sites in the Enolase-Inhibitor Complex: Crystallography, Single-Crystal EPR, and DFT Calculations," J. Am. Chem. Soc. 129, 4240-4252 (2007). DOI: 10.1021/ja066124e

Christopher J. Carrell, Robert C. Bruckner, David Venci, Gouhua Zhao, Marilyn Schuman Jorns, F. Scott Mathews, "NikD, an Unusual Amino Acid Oxidase Essential for Nikkomycin Biosynthesis: Structures of Closed and Open Forms at 1.15 and 1.90 Å Resolution," Structure 15 (8), 928-941 (2007). DOI: 10.1016/j.str.2007.06.010

Christopher J. Carrell, John K. Ma, William E. Antholine, Jonathan P. Hosler, F. Scott Mathews, Victor L. Davidson, "Generation of Novel Copper Sites by Mutation of the Axial Ligand of Amicyanin. Atomic Resolution Structures and Spectroscopic Properties," Biochemistry-US 46 (7), 1900-1912 (2007). DOI: 10.1021/bi0619674 S0006-2960(06)01967-2

J. Carwardine, N. Arnold., F. Lenkszus, C. Saunders, B. Banerjee, B. Chase, E. Gottschalk, P. Joireman, P. Kasley, S. Lackey, P. McBride, V. Pavlicek, J. Patrick, M. Votava, S. Wolbers, K. Furukawa, S. Michizono, R.S. Larsen, R. Downing, "The ILC Control System Design," Proc. of the 22nd Particle Accelerator Conference (PAC07), IEEE, (2007), 868 - 872.

Jeffrey G. Catalano, Paul Fenter, Changyong Park, "Interfacial water structure on the (0 1 2) surface of hematite: Ordering and reactivity in comparison with corundum," Geochim. Cosmochim. Acta 71 (22), 5313-5324 (2007). DOI: 10.1016/j.gca.2007.09.019

J.G. Catalano, Z. Zhang, C. Park, P. Fenter, M.J. Bedzyk, "Bridging arsenate surface complexes on the hematite (012) surface," Geochim. Cosmochim. Acta 71 (8), 1883-1897 (2007). DOI: 10.1016/j.gca.2007.01.015

Kevin A. Cavicchi, Thomas P. Russell, "Solvent Annealed Thin Films of Asymmetric Polyisoprene-Polylactide Diblock Copolymers," Macromolecules 40 (4), 1181-1186 (2007). DOI: 10.1021/ma061163w

Derek F.J. Ceccarelli, Ivan M. Blasutig, Marilyn Goudreault, Zhiqin Li, Julie Ruston, Tony Pawson, Frank Sicheri, "Non-canonical Interaction of Phosphoinositides with Pleckstrin Homology Domains of Tiam1 and ArhGAP9," J. Biol. Chem. 282 (18), 13864-13874 (2007). DOI: 10.1074/jbc.M700505200

A.J. Celestian, J.B. Parise, R.I. Smith, B.H. Toby, A. Clearfield, "Role of the Hydroxyl-Water Hydrogen-Bond Network in Structural Transitions and Selectivity toward Cesium in Cs[subscript 0.38](D[subscript 1.08]H[subscript 0.54])SiTi[subscript 2]O[subscript 7] . (D[subscript 0.86]H[subscript 0.14)[subscript 2]O Crystalline Silicotitanate," Inorg. Chem. 46 (4), 1081-1089 (2007). DOI: 10.1021/ic0611387

M. Cetinkol, P.L. Lee, A.P. Wilkinson, "Preparation and characterization of In(I)-[beta"]-alumina," MRS Bull. 42 (4), 713-719 (2007). DOI: 10.1016/j.materresbull.2006.07.015

Y.-C. Chae, G. Waldschmidt, V. Dolgashev, "The Wakefield Effects of Pulsed Crab Cavities at the Advanced Photon Source for Short X-ray Pulse Generation," Proc. of the 22nd Particle Accelerator Conference (PAC07), IEEE, (2007), 4339 - 4341.

Y.-C. Chae, Y. Wang, "Impedance Database II for the Advanced Photon Source Storage Ring," Proc. of the 22nd Particle Accelerator Conference (PAC07), IEEE, (2007), 4336 - 4338.

Y.-C. Chae, Y. Wang, A. Xiao, "Single-Bunch Instability Estimates for the 1-nm APS Storage Ring Upgrade with a Smaller Vacuum Chamber," Proc. of the 22nd Particle Accelerator Conference (PAC07), IEEE, (2007), 4330 - 4332.

J. Chakhalian, J.W. Freeland, H.-U. Habermeier, G. Cristiani, G. Khaliullin, M. van Veenendaal, B. Keimer, "Orbital Reconstruction and Covalent Bonding at an Oxide Interface," Science 318, 1114-1117 (2007). DOI: 10.1126/science.1149338

K.-C. Chang, A. Menzel, V. Komanicky, H. You, "Electrosorbed carbon monoxide monolayers on Pt(1 1 1)," Electrochim. Acta 52 (18), 5749-5758 (2007). DOI: 10.1016/j.electacta.2007.01.070

Kinlin L. Chao, Lavanya Muthukumar, Osnat Herzberg, "Structure of Human Hyaluronidase-1, a Hyaluronan Hydrolyzing Enzyme Involved in Tumor Growth and Angiogenesis," Biochemistry-US 46 (23), 6911-6920 (2007). DOI: 10.1021/bi700382g

Karena W. Chapman, Peter J. Chupas, Charles A. Kurtz, Darren R. Locke, John B. Parise, Joseph A. Hriljac, "Hydrostatic low-range pressure applications of the Paris–Edinburgh cell utilizing polymer gaskets for diffuse X-ray scattering measurements," J. Appl. Crystallogr. 40 (1), 196-198 (2007). DOI: 10.1107/S0021889806047923

Mark A. Chappell, Kirk G. Scheckel, "Pyromorphite formation and stability after quick lime neutralisation in the presence of soil and clay sorbents," Environ. Chem. 4 (2), 109-113 (2007). DOI: 10.1071/EN06081

Joon Chatterjee, Sumeet Jain, Frank S. Bates, "Comprehensive Phase Behavior of Poly(isoprene-b-styrene-b-ethylene oxide) Triblock Copolymers," Macromolecules 40 (8), 2882-2896 (2007). DOI: 10.1021/ma062249s

S. Chattopadhyay, S.D. Kelly, T. Shibata, R. Viswanatha, M. Balasubramanian, S. Stoupin, C.U. Segre, D.D. Sarma, "EXAFS Studies of Nanocrystals of Zn[subscript 1−x]Mn[subscript x]O: A Dilute Magnetic Semiconductor Oxide System," X-Ray Absorption Fine Structure - XAFS13, Britt Hedman, Piero Pianetta, eds., 882, AIP, (2007), 809 - 811. DOI: 10.1063/1.2644672

Baoyu Chen, Michaeleen Doucleff, David E. Wemmer, Sacha De Carlo, Hector H. Huang, Eva Nogales, Timothy R. Hoover, Elena Kondrashkina, Liang Guo, B. Tracy Nixon, "ATP Ground- and Transition-States of Bacterial Enhancer Binding AAA+ ATPases Support Complex Formation with Their Target Protein, [sigma]54," Structure 15 (4), 429-440 (2007). DOI: 10.1016/j.str.2007.02.007

Bin Chen, Hengzhong Zhang, Benjamin Gilbert, Jillian F. Banfield, "Mechanism of Inhibition of Nanoparticle Growth and Phase Transformation by Surface Impurities," Phys. Rev. Lett. 98, 106103-1-106103-4 (2007). DOI: 10.1103/PhysRevLett.98.106103

Di Chen, Qiuzhi Cindy Cui, Huanjie Yang, Raul A. Barrea, Fazlul H. Sarkar, Shijie Sheng, Bing Yan, G. Prem Veer Reddy, Q. Ping Dou, "Clioquinol, a Therapeutic Agent for Alzheimer's Disease, Has Proteasome-Inhibitory, Androgen Receptor–Suppressing, Apoptosis-Inducing, and Antitumor Activities in Human Prostate Cancer Cells and Xenografts," Cancer Res. 67 (4), 1636-1644 (2007). DOI: 10.1158/0008-5472.CAN-06-3546

Lin X. Chen, Dijia Liu, Erik C. Wasinger, Xiaoyi Zhang, Klaus Attenkofer, Guy Jennings, "Ultrafast structural dynamics of photoactive metal complexes in solar hydrogen generation," Solar Hydrogen and Nanotechnology II, Jinghua Guo, eds., 6650, SPIE (2007), 66500I-1 - 66500I-10. DOI: 10.1117/12.745507

L.X. Chen, G.B. Shaw, E.C. Wasinger, X. Zhang, K. Attenkofer, G. Jennings, "Molecular Structural Dynamics of Photoactive Transition Metal Complexes in Solar Energy Conversion Studied by Ultrafast Optical Spectroscopy and LITR-XAS," AIP Proceedings, B. Hedman, P. Pianetta, eds., 882, AIP, (2007), 844 - 848.

Lin X. Chen, Xiaoyi Zhang, Erik C. Wasinger, Klaus Attenkofer, Guy Jennings, Ana Z. Muresan, Jonathan S. Lindsey, "Tracking Electrons and Atoms in a Photoexcited Metalloporphyrin by X-ray Transient Absorption Spectroscopy," J. Am. Chem. Soc. 129, 9616-9618 (2007). DOI: 10.1021/ja072979v

Peng Chen, "Probing the Mechanism of Bacterial Metalloregulation and Virulence Regulation," Masters, University of Chicago, 2007.

X. Chen, T.D. Kim, C.V. Carman, L.Z. Mi, G. Song, T.A. Springer, "Structural plasticity in Ig superfamily domain 4 of ICAM-1 mediates cell surface dimerization," Proc. Natl. Acad. Sci. USA 104 (39), 15358-15363 (2007). DOI: 10.1073/pnas.0707406104

Vadim Cherezov, Daniel M. Rosenbaum, Michael A. Hanson, Soren G.F. Rasmussen, Foon Sun Thian, Tong Sun Kobilka, Hee-Jung Choi, Peter Kuhn, William I. Weis, Brian K. Kobilka, Raymond C. Stevens, "High-Resolution Crystal Structure of an Engineered Human [beta subscript 2]-Adrenergic G Protein–Coupled Receptor," Science 318, 1258-1265 (2007). DOI: 10.1126/science.1150577

Gary N. Chesnut, Nenad Velisavljevic, Lilliana Sanchez, "Static High Pressure X-Ray Diffraction of TI-6AL-4V," Shock Compression of Condensed Matter, M. Elert, M.D. Furnish, R. Chau, N. Holmes, J. Nguyen, eds., 955, AIP, (2007), 27 - 30. DOI: 10.1063/1.2833031

Mariya K. Chhatriwala, Laurie Betts, David K. Worthylake, John Sondek, "The DH and PH Domains of Trio Coordinately Engage Rho GRPases for their Efficient Activation," J. Mol. Biol. 368 (5), 1307-1320 (2007). DOI: 10.1016/j.jmb.2007.02.060

P. Chien, R.A. Grant, R.T. Sauer, T.A. Baker, "Structure and Substrate Specificity of an SspB Ortholog: Design Implications for AAA+ Adaptors," Structure 15, 1265-1305 (2007). DOI: 10.1016/j.str.2007.08.008

Unmesh Chinte, Binal Shah, Yu-Sheng Chen, A. Alan Pinkerton, Constance A. Schall, B. Leif Hanson, "Cryogenic (<20 K) helium cooling mitigates radiation damage to protein crystals," Acta Crystallogr. D D63 (4), 486-492 (2007). DOI: 10.1107/S0907444907005264

Catalin Chiritescu, David G. Cahill, Ngoc Nguyen, David Johnson, Arun Bodapati, Pawel Keblinski, Paul Zschack, "Ultralow Thermal Conductivity in Disordered, Layered WSe[subscript 2] Crystals," Science 315 (5810), 351-353 (2007). DOI: 10.1126/science.1136494

Malcolm H. Chisholm, Judith C. Gallucci, Hongfeng Yin, "18-Membered cyclic esters derived from glycolide and lactide: preparations, structures and coordination to sodium ions," Dalton T. 42, 4811-4821 (2007). DOI: 10.1039/b709081a

Y. Choi, J.S. Jiang, Y. Ding, R.A. Rosenberg, J.E. Pearson, S.D. Bader, A. Zambano, M. Murakami, I. Takeuchi, Z.L. Wang, J.P. Liu, "Role of diffused Co atoms in improving effective exchange coupling in Sm-Co/Fe spring magnets," Phys. Rev. B 75, 104432-1-104432-6 (2007). DOI: 10.1103/PhysRevB.75.104432

Y. Choi, J.S. Jiang, J.E. Pearson, S.D. Bader, J.J. Kavich, J.W. Freeland, J.P. Liu, "Controlled interface profile in Sm–Co/Fe exchange-spring magnets," Appl. Phys. Lett. 91, 072509-1-072509-3 (2007). DOI: 10.1063/1.2769755

Y. Choi, J.S. Jiang, J.E. Pearson, S.D. Bader, J.P. Liu, "Origin of recoil hysteresis loops in Sm–Co/Fe exchange-spring magnets," Appl. Phys. Lett. 91, 022502-1-022502-3 (2007). DOI: 10.1063/1.2752534

Y. Choi, Y.Z. Yoo, O. Chmaissem, A. Ullah, S. Kolesnik, C.W. Kimball, D. Haskel, J.S. Jiang, S.D. Bader, "Ferromagnetic Mn moments at SrRuO[subscript 3]/SrMnO[subscript 3] interfaces," Appl. Phys. Lett. 91, 022503-1-022503-3 (2007). DOI: 10.1063/1.2753100

Maria Chondroudi, Mahalingam Balasubramanian, Ulrich Welp, Wai-K. Kwok, Mercouri G. Kanatzidis, "Mixed Valency in Yb[subscript 7]Co[subscript 4]InGe[subscript 12]: A Novel Intermetallic Compound Stabilized in Liquid Indium," Chem. Mater. 19 (19), 4769-4775 (2007). DOI: 10.1021/cm071687q

Renee Chosed, Diana R. Tomchick, Chad A. Brautigam, Sohini Mukherjee, Veera S. Negi, Mischa Machius, Kim Orth, "Structural Analysis of Xanthomonas XopD Provides Insights into Substrate Specificity of Ubiquitin-like Protein Proteases," J. Biol. Chem. 282 (9), 6773-6782 (2007). DOI: 10.1074/jbc.M608730200

Jill E. Chrencik, Alexei Brooun, Michael I. Recht, George Nicola, Leila K. Davis, Ruben Abagyan, Hans Widmer, Elena B. Pasquale, Peter Kuhn, "Three-dimensional Structure of the EphB2 Receptor in Complex with an Antagonistic Peptide Reveals a Novel Mode of Inhibition," J. Biol. Chem. 282 (50), 36505-36513 (2007). DOI: 10.1074/jbc.M706340200

Peter J. Chupas, Karena W. Chapman, Guy Jennings, Peter L. Lee, Clare P. Grey, "Watching Nanoparticles Grow: The Mechanism and Kinetics for the Formation of TiO[subscript 2]-Supported Platinum Nanoparticles," J. Am. Chem. Soc. 129 (45), 13822-13824 (2007). DOI: 10.1021/ja076437p

Peter J. Chupas, Karena W. Chapman, Peter L. Lee, "Applications of an amorphous silicon-based area detector for high resolution, high sensitivity and fast time-resolved pair distribution function measurements," J. Appl. Crystallogr. 40 (3), 463-470 (2007). DOI: 10.1107/S0021889807007856

C.N. Cionca, D.A. Walko, Y. Yacoby, C. Dorin, J. Mirecki Millunchick, R. Clarke, "Interfacial structure, bonding and composition of InAs and GaSb thin films determined using coherent Bragg rod analysis," Phys. Rev. B 75, 115306-1-115306-7 (2007). DOI: 10.1103/PhysRevB.75.115306

Sara E. Cnudde, Mary Prorok, Qiuyun Dai, Francis J. Castellino, James H. Geiger, "The Crystal Structures of the Calcium-Bound con-G and con-T[K7[gamma]] Dimeric Peptides Demonstrate a Metal-Dependent Helix-Forming Motif," J. Am. Chem. Soc. 129 (6), 1586-1593 (2007). DOI: 10.1021/ja065722q

Eric N. Coker, William A. Steen, James E. Miller, "Zeolite-templated Pt/C electrocatalysts," Micropor. Mesopor. Mat. 104 (1-3), 236-247 (2007). DOI: 10.1016/j.micromeso.2007.02.044

Eric N. Coker, William A. Steen, Jeffrey T. Miller, A. Jeremy Kropf, James E. Miller, "Nanostructured Pt/C electrocatalysts with high platinum dispersions through zeolite-templating," Micropor. Mesopor. Mat. 101 (3), 440-444 (2007). DOI: 10.1016/j.micromeso.2006.12.022

Eric N. Coker, William A. Steen, Jeffrey T. Miller, A. Jeremy Kropf, James E. Miller, "The preparation and characterization of novel Pt/C electrocatalysts with controlled porosity and cluster size," J. Mater. Chem. 17 (31), 3330-3340 (2007). DOI: 10.1039/b703916f

Brian A. Collins, Yuncheng Zhong, Yong S. Chu, Liang He, Frank Tsui, "Anomalous x-ray diffraction study of disorders in epitaxial films of the Heusler alloy Co[subscript 2]MnGe," J. Vac. Sci. Technol. B 25 (3), 999-1003 (2007). DOI: 10.1116/1.2720857

Brett A. Colson, Tanya Bekyarova, Daniel P. Fitzsimonsk, Thomas C. Irving, Richard L. Moss, "Radial Displacement of Myosin Cross-bridges in Mouse Myocardium due to Ablation of Myosin Binding Protein-C," J. Mol. Biol. 367 (1), 36-41 (2007). DOI: 10.1016/j.jmb.2006.12.063

Roxana M. Coman, Arthur Robbins, Maureen M. Goodenow, Robert McKenna, Ben M. Dunn, "Expression, purification and preliminary X-ray crystallographic studies of the human immunodeficiency virus 1 subtype C protease," Acta Crystallogr. F 63, 320-323 (2007). DOI: 10.1107/S174430910701161X

Carlos Contreras-Martel, Adelio Matamala, Carola Bruna, German Poo-Caamano, Daniel Almonacid, Maximiliano Figueroa, Jose Martinez-Oyanedel, Marta Bunster, "The structure at 2 Å resolution of Phycocyanin from Gracilaria chilensis and the energy transfer network in a PC–PC complex," Biophys. Chem. 125 (2-3), 388-396 (2007). DOI: 10.1016/j.bpc.2006.09.014

David R. Cooper, Tomasz Boczek, Katarzyna Grelewska, Malgorzata Pinkowska, Malgorzata Sikorska, Michal Zawadzki, Zygmunt Derewenda, "Protein Crystallization by surface entropy reduction: optimization of the SER strategy," Acta Crystallogr. D 63 (5), 636-645 (2007). DOI: 10.1107/S907444907010931

Julio F. Cordero-Morales, Vishwanath Jogini, Anthony Lewis, Valeria Vasquez, D. Marien Cortes, Benoit Roux, Eduardo Perozo, "Molecular driving forces determining potassium channel slow inactivation," Nat. Struct. Mol. Biol. 14 (11), 1062-1069 (2007). DOI: 10.1038/nsmb1309

Julien Cotelesage, "Structural and functional studies of Phosphoenolpyruvate carboxykinase," Masters, University of Saskatchewan, 2007.

Julien J.H. Cotelesage, Jennifer Puttick, Hughes Goldie, Babak Rajabi, Brian Novakovski, Louis T.J. Delbaere, "How does an enzyme recognize CO[subscript 2]?," Int. J. Biochem. Cell B. 39 (6), 1204-1210 (2007). DOI: 10.1016/j.biocel.2007.03.015

N.P. Coussens, J.C. Mowers, C. McDonald, G. Nunez, S. Ramaswamy, "Crystal structure of the Nod1 caspase activation and recruitment domain," Biochem. Biophys. Res. Commun. 353 (1), 1-5 (2007). DOI: 10.1016/j.bbrc.2006.11.122

Jean-Francois Couture, Evys Collazo, Patricia A. Ortiz-Tello, Joseph S. Brunzelle, Raymond C. Trievel, "Specificity and mechanism of JMJD2A, a trimethyllysine-specific histone demethylase," Nat. Struct. Mol. Biol. 14 (8), 689-695 (2007). DOI: 10.1038/nsmb1273

Brett A. Cromer, Michael A. Gorman, Guido Hansen, Julian J. Adams, Marjorie Coggan, Philip G. Board, Michael W. Parker, "Expression, purification, crystallization and preliminary X-ray diffraction analysis of chloride intracellular channel 2 (CLIC2)," Acta Crystallogr. F 63 (11), 961-963 (2007). DOI: 10.1107/S1744309107049159

Brett A. Cromer, Michael A. Gorman, Guido Hansen, Julian J. Adams, Marjorie Coggan, Dene R. Littler, Louise J. Brown, Michele Mazzanti, Samuel N. Breit, Paul M.G. Curmi, Angela F. Dulhunty, Philip G. Board, Michael W. Parker, "Structure of the Janus Protein Human CLIC2," J. Mol. Biol. 374 (3), 719-731 (2007). DOI: 10.1016/j.jmb.2007.09.041

Jonathan Crowhurst, Alexander Goncharov, Babak Sadigh, Joseph Zaug, Yue Meng, Vitali Prakapenka, "Synthesis and Characterization of Nitrides of Iridium and Palladium," Materials Research at High Pressure, M.R. Manaa, A.F. Goncharov, R.J. Hemley, R. Bini, eds., 987, AIP (2007), online.

B. Roldan Cuenya, A. Naitabdi, J. Croy, W. Sturhahn, J.Y. Zhao, E.E. Alp, R. Meyer, D. Sudfeld, E. Schuster, W. Keune, "Atomic vibrations in iron nanoclusters: Nuclear resonant inelastic x-ray scattering and molecular dynamics simulations," Phys. Rev. B 76, 195422-1-195422-5 (2007). DOI: 10.1103/PhysRevB.76.195422

M.E. Cuff, H. Li, S. Moy, J. Watson, A. Cipriani, A. Joachimiak, "Crystal structure of an acetyltransferase protein from Vibrio cholerae strain N16961," Proteins 69 (2), 422-427 (2007). DOI: 10.1002/prot.21417

Yan Cui, Stefan Vogt, Neal Olson, Andrew G. Glass, Thomas E. Rohan, "Levels of Zinc, Selenium, Calcium, and Iron in Benign Breast Tissue and Risk of Subsequent Breast Cancer," Cancer Epidem. Biomar. 16 (8), 1682-1685 (2007). DOI: 10.1158/1055-9965.EPI-07-0187

Nicholas C. Cunningham, Wei Qiu, Kevin M. Hope, Hanns-Peter Liermann, Yogesh K. Vohra, "Symmetry lowering under high pressure: Structural evidence for f-shell delocalization in heavy rare earth metal terbium," Phys. Rev. B 76, 212101-1-212101-4 (2007). DOI: 10.1103/PhysRevB.76.212101

Leslie Cuthbertson, Matthew S. Kimber, Chris Whitfield, "Substrate binding by a bacterial ABC transporter involved in polysaccharide export," Proc. Natl. Acad. Sci. USA 104 (49), 19529-19534 (2007). DOI: 10.1073/pnas.0705709104

J. Alejandro D'Aquino, Judith R. Lattimer, Andrew Denninger, Katharine E. D'Aquino, Dagmar Ringe, "Role of the N-Terminal Helix in the Metal Ion-Induced Activation of the Diphtheria Toxin Repressor DtxR," Biochemistry-US 46 (42), 11761-11770 (2007). DOI: 10.1021/bi7007883

Harry A. Dailey, Chia-Kuei Wu, Peter Horanyi, Amy E. Medlock, Wided Najahi-Missaoui, Amy E. Burden, Tamara A. Dailey, John Rose, "Altered Orientation of Active Site Residues in Variants of Human Ferrochelatase. Evidence for a Hydrogen Bond Network Involved in Catalysis," Biochemistry-US 46 (27), 7973-7979 (2007). DOI: 10.1021/bi700151fS0006-2960(70)00151-4

Shaodong Dai, Rosmarie Friemann, Dominique A. Glauser, Florence Bourquin, Wanda Manieri, Peter Schurmann, Hans Eklund, "Structural snapshots along the reaction pathway of ferredoxin–thioredoxin reductase," Nature 448, 92-96 (2007). DOI: 10.1038/nature05937

Michael J. Daly, Elena K. Gaidamakova, Vera Y. Matrosova, Alexander Vasilenko, Min Zhai, Richard D. Leapman, Barry Lai, Bruce Ravel, Shu-Mei W. Li, Kenneth M. Kemner, James K. Fredrickson, "Protein Oxidation Implicated as the Primary Determinant of Bacterial Radioresistance," PLoS Biol. 5 (4), 0769-0779 (2007). DOI: :10.1371/journal.pbio.0050092

Stephen M. Danauskas, Maria K. Ratajczak, Yuji Ishitsuka, Jeffrey Gebhardt, David Schultz, Mati Meron, Binhua Lin, Ka Yee C. Lee, "Monitoring x-ray beam damage on lipid films by an integrated Brewster angle microscope/x-ray diffractometer," Rev. Sci. Instrum. 78, 103705-1-103705-9 (2007). DOI: 10.1063/1.2796147

L.R. Danielson, K. Righter, S. Sutton, M. Newville, L. Le, "The Oxidation State of Tungsten in Iron Bearing and Iron Free Silicate Glasses: Results from W L-Edge XANES Measurements," Lunar and Planetary Science XXXVIII, LPI, (2007), 2113.

Gregory Darnell, Joseph P.R.O. Orgel, Reinhard Pahl, Stephen C. Meredith, "Flanking Polyproline Sequences Inhibit [beta]-Sheet Structure in Polyglutamine Segments by Inducing PPII-like Helix Structure," J. Mol. Biol. 374 (3), 688-704 (2007). DOI: 10.1016/j.jmb.2007.09.023

Amaresh Das, Zheng-Qing Fu, Wolfram Tempel, Zhi-Jie Liu, Jessie Chang, Lirong Chen, Doowon Lee, Weihong Zhou, Hao Xu, Neil Shaw, John P. Rose, Lars G. Ljungdahl, Bi-Cheng Wang, "Characterization of a corrinoid protein involved in the C1 metabolism of strict anaerobic bacterium Moorella Thermoacetica," Proteins 67 (1), 167-176 (2007). DOI: 10.1002/prot.21094

Kalyan Das, StefanG. Sarafianos, Arthur D. Clark Jr., Paul L. Boyer, Stephen H. Hughes, Eddy Arnold, "Crystal Structures of Clinically Relevant Lys103Asn/Tyr181Cys Double Mutant HIV-1 Reverse Transcriptase in Complexes with ATP and Non-nucleoside Inhibitor HBY 097," J. Mol. Biol. 365 (1), 77-89 (2007). DOI: 10.1016/j.jmb.2006.08.097

Chen Davidovich, Anat Bashan, Tamar Auerbach-Nevo, Rachel D. Yaggie, Richard R. Gontarek, Ada Yonath, "Induced-fit tightens pleuromutilins binding to ribosomes and remote interactions enable their selectivity," Proc. Natl. Acad. Sci. USA 104 (11), 4291-4296 (2007). DOI: 10.1073pnas.0700041104

Melissa L. Davis, James B. Thoden, Hazel M. Holden, "The X-ray Structure of dTDP-4-Keto-6-deoxy-D-glucose-3,4-ketoisomerase," J. Biol. Chem. 282 (26), 19227-19236 (2007). DOI: 10.1074/jbc.M702529200

M.R. Daymond, M.L. Young, J.D. Almer, D.C. Dunand, "Strain and texture evolution during mechanical loading of a crack tip in martensitic shape-memory NiTi," Acta Mater. 55 (11), 3929-3942 (2007). DOI: 10.1016/j.actamat.2007.03.013

Martin D. de Jonge, Chanh Q. Tran, Christopher T. Chantler, Zwi Barnea, Bipin B. Dhal, David Paterson, Elliot P. Kanter, Stephen H. Southworth, Linda Young, Mark A. Beno, Jennifer A. Linton, Guy Jennings, "Measurement of the x-ray mass attenuation coefficient and determination of the imaginary component of the atomic form factor of tin over the energy range of 29–60 keV," Phys. Rev. A 75, 032702-1-032702-14 (2007). DOI: 10.1103/PhysRevA.75.032702

M.D. de Jonge, S. Vogt, D. Legnini, I. McNulty, C. Rau, D. Paterson, B. Hornberger, C. Holzner, C. Jacobsen, "A method for phase reconstruction from measurements obtained using a configured detector with a scanning transmission x-ray microscope," Nucl. Instrum. Methods A 582 (1), 218-220 (2007). DOI: 10.1016/j.nima.2007.08.111

Erik W. Debler, Gunnar F. Kaufmann, Robert N. Kirchdoerfer, Jenny M. Mee, Kim D. Janda, Ian A. Wilson, "Crystal structures of a quorum-quenching antibody," J. Mol. Biol. 368 (5), 1392-1402 (2007). DOI: 10.1016/j.jmb.2007.02.081

G. Decker, P. Den Hartog, O. Singh, G. Rosenbaum, "Progress Toward a Hard X-ray Insertion Device Beam Position Monitor at the Advanced Photon Source," Proc. of the 22nd Particle Accelerator Conference (PAC07), IEEE, (2007), 4342 - 4344.

Olga Degtyareva, Eduardo R. Hernandez, Jorge Serrano, Maddury Somayazulu, Ho-kwang Mao, Eugene Gregoryanz, Russell J. Hemley, "Vibrational dynamics and stability of the high-pressure chain and ring phases in S and Se," J. Chem. Phys. 126, 084503-1-084503-11 (2007). DOI: 10.1063/1.2433944

Olga Degtyareva, Miguel Martinez Canales, Aitor Bergara, Xiao-Jia Chen, Yang Song, Viktor V. Struzhkin, Ho-kwang Mao, Russell J. Hemley, "Crystal structure of SiH[subscript 4] at high pressure," Phys. Rev. B 76, 064123-1-064123-4 (2007). DOI: 10.1103/PhysRevB.76.064123

R. Dejus, I. Vasserman, "Phasing of Two Undulators with Different K Values at the Advanced Photon Source," Proc. of the 22nd Particle Accelerator Conference (PAC07), IEEE, (2007), 1130 - 1132.

Ranjit K. Deka, Chad A. Brautigam, Farol L. Tomson, Sarah B. Lumpkins, Diana R. Tomchick, Mischa Machius, Michael V. Norgard, "Crystal Structure of the Tp34 (TP0971) Lipoprotein of Treponema pallidum: IMPLICATIONS OF ITS METAL-BOUND STATE AND AFFINITY FOR HUMAN LACTOFERRIN," J. Biol. Chem. 282 (8), 5944-5958 (2007). DOI: 10.1074/jbc.M610215200

Shahab Derakhshan, Abdeljalil Assoud, Katja M. Kleinke, Trupti Khaire, Ahmad S. Masadeh, Simon J.L. Billinge, Holger Kleinke, "Square net distortion engineering in the ternary variants of titanium antimonide, Ti[subscript 2-delta]M[subscript delta]Sb (M=Zr Hf)," Intermetallics 15 (8), 1071-1077 (2007). DOI: 10.1016/j.intermet.2006.12.011

Darrell Desveaux, Alex U. Singer, Ai-Jiuan Wu, Brian C. McNulty, Laura Musselwhite, Zachary Nimchuk, John Sondek, Jeffery L. Dangl, "Type III Effector Activation via Nucleotide Binding, Phosphorylation, and Host Target Interaction," PLoS Pathogens 3 (3), 0456-0469 (2007). DOI: 10.1371/journal.ppat.0030048

Sanghamitra Dey, Zhiqin Hu, Xiao Lan Xu, James C. Sacchettini, Gregory A. Grant, "The Effect of Hinge Mutations on Effector Binding and Domain Rotation in Escherichia coli D-3-Phosphoglycerate Dehydrogenase," J. Biol. Chem. 282 (25), 18418-18426 (2007). DOI: 10.1074/jbc.M701174200

N. DiMonte, "The P0 Feedback Control System Blurs the Line between IOC and FPGA," Proc. of the 22nd Particle Accelerator Conference (PAC07), IEEE, (2007), 431 - 433.

Yang Ding, Rajeev Ahuja, Jinfu Shu, Paul Chow, Wei Luo, Ho-kwang Mao, "Structural Phase Transition of Vanadium at 69 GPa," Phys. Rev. Lett. 98, 085502-1-085502-4 (2007). DOI: 10.1103/PhysRevLett.98.085502

W. Dmowski, T. Egami, "Observation of structural anisotropy in metallic glasses induced by mechanical deformation," J. Mater. Res. 22 (2), 412-418 (2007). DOI: 10.15557/JMR.2007.0043

W. Dmowski, T. Egami, K. Swider-Lyons, W.-F. Yan, S. Dai, S. Overbury, "Local atomic structure in disordered and nanocrystalline catalytic materials," Z. Kristallogr. 222, 617-624 (2007). DOI: 10.1524/zkri.2007.222.11.617

Ninh Doan, Peter G.W. Gettins, "Human[alpha subscript 2]-macroglobulin is composed of multiple domains, as predicted by homology with complement component C3," Biochem. J. 407, 23-30 (2007). DOI: 10.1042/BJ20070764

Tabbetha A. Dobbins, Edward L. Bruster, Ejiroghene U. Oteri, Jan Ilavsky, "Ultrasmall-angle X-ray scattering (USAXS) studies of morphological trends in high energy milled NaAlH[subscript 4] powders," J. Alloy Comp. 446, 248-254 (2007). DOI: 10.1016/j.jallcom.2007.02.161

V. Dolgashev, M. Borland, G. Waldschmidt, "RF Design of Normal Conducting Deflecting Structures for the Advanced Photon Source," Proc. of the 22nd Particle Accelerator Conference (PAC07), IEEE, (2007), 2427 - 2429.

D. Eric Dollins, Joshua J. Warren, Robert M. Immormino, Daniel T. Gewirth, "Structures of GRP94-Nucleotide Complexes Reveal Mechanistic Differences between the hsp90 Chaperones," Mol. Cell 28, 41-56 (2007). DOI: 10.1016/j.molcel.2007.08.024

G. Dong, M. Medkova, P. Novick, K.M. Reinisch, "A Catalytic Coiled Coil: Structural Insights into the Activation of the Rab GTPase Sec4p by Sec2p," Mol. Cell 25 (3), 455-462 (2007).

J.C. Dooling, F.R. Brumwell, L.I. Donley, K.C. Harkay, R.L. Kustom, M.K. Lien, G.E. McMichael, M.E. Middendorf, A. Nassiri, S. Wang, "Observations of Rising Tune During the Injection Instability of IPNS RCS Proton Bunch," Proc. of the 22nd Particle Accelerator Conference (PAC07), IEEE, (2007), 4345 - 4347.

D.B. Drazkowski, "Characterization of the Thermodynamics and Deformation Behavior of Styrene-Butadiene-Styrene Grafted with Polyhedral Oligomeric Silsesquioxanes," Ph.D., Michigan State University, 2007.

Daniel B. Drazkowski, Andre Lee, Timothy S. Haddad, "Morphology and Phase Transitions in Styrene-Butadiene-Styrene Triblock Copolymer Grafted with Isobutyl-Substituted Polyhedral Oligomeric Silsesquioxanes," Macromolecules 40 (8), 2798-2805 (2007). DOI: 10.1021/ma062393d

T. Droubay, K.M. Rosso, S.M. Heald, D.E. McCready, C.M. Wang, S.A. Chambers, "Structure, magnetism, and conductivity in epitaxial Ti-doped [alpha]-Fe[subscript 2]O[subscript 3] hematite: Experiment and density functional theory calculations," Phys. Rev. B 75, 104412-1-104412-7 (2007). DOI: 10.1103/PhysRevB.75.104412

L. Dubrovinsky, N. Dubrovinskaia, O. Narygina, I. Kantor, A. Kuznetzov, V.B. Prakapenka, L. Vitos, B. Johansson, A.S. Mikhaylushkin, S.I. Simak, I.A. Abrikosov, "Body-Centered Cubic Iron-Nickel Alloy in Earth's Core," Science 316 (5833), 1880-1883 (2007). DOI: 10.1126/science.1142105

David M. Duda, Robert C.A.M. van Waardenburg, Laura A. Borg, Sierra McGarity, Amanda Nourse, M.Brett Waddell, Mary-Ann Bjornsti, Brenda A. Schulman, "Structure of a SUMO-binding-motif Mimic Bound to Smt3p-Ubc9p: Conservation of a Non-covalent Ubiquitin-like Protein-E2 Complex as a Platform for Selective Interactions within a SUMO Pathway," J. Mol. Biol. 369 (3), 619-630 (2007). DOI: 10.1016/j.jmb.2007.04.007

Martine C. Duff, Douglas B. Hunter, Patterson Nuessle, David R. Black, Harold Burdette, Joseph Woicik, Arnold Burger, Michael Groza, "Synchrotron X-ray Based Characterization of CdZnTe Crystals," J. Electro. Mater. 36 (8), 1092-1097 (2007). DOI: 10.1007/s11664-007-0181-x

Eric M. Dufresne, B.W. Adams, E.C. Landahl, "A study of laser-generated strain fields with X-ray microdiffraction," Nucl. Instrum. Methods A 582 (1), 205-207 (2007). DOI: 10.1016/j.nima.2007.08.138

Eric M. Dufresne, Dohn A. Arms, Eric C. Landahl, Donald A. Walko, "Impact of Pressure Regulation of Cryogenic Fluids and EPICS EPID Feedback on the Monochromatic Beam Position Stability of the 7ID Beamline at the Advanced Photon Source," SYNCHROTRON RADIATION INSTRUMENTATION: Ninth International Conference on Synchrotron Radiation Instrumentation, Jae-Young Choi, Seungyu Rah, eds., 879, American Institue of Physics, (2007), 950 - 953. DOI: 10.1063/1.2436219

Eric M. Dufresne, Dohn A. Arms, Eric C. Landahl, Donald A. Walko, "The Impact of Pressure Regulation of Cryogenics Fluids and EPICS PID Feedback on the Monochromatic Beam Position Stability," SYNCHROTRON RADIATION INSTRUMENTATION: Ninth International Conference on Synchrotron Radiation Instrumentation, Jae-Young Choi, Seungyu Rah, eds., 879, Springer, (2007), 950 - 953.

Eric M. Dufresne, Ali Khounsary, "Observation of a tilted Gaussian beam on the 7ID beamline of the Advanced Photon Source," Nucl. Instrum. Methods A 582 (1), 63-65 (2007). DOI: 10.1016/j.nima.2007.08.063

Eric M. Dufresne, Eric C. Landahl, Bernhard Adams, David Fritz, Sooheyong Lee, David Reis, "Studies of Ultrafast fs-laser Generated Strain Fields with Coherent X-rays," SYNCHROTRON RADIATION INSTRUMENTATION: Ninth International Conference on Synchrotron Radiation Instrumentation, Jae-Young Choi, Seungyu Rah, eds., 879, Springer, (2007), 1210 - 1213.

Thomas Durek, Vladimir Yu. Torbeev, Stephen B.H. Kent, "Convergent chemical synthesis and high-resolution x-ray structure of human lysozyme," Proc. Natl. Acad. Sci. USA 104 (12), 4846-4851 (2007). DOI: 10.1073/pnas.0610630104

Michael P. Dwyer, Kamil Paruch, Carmen Alvarez, Ronald J. Doll, Kerry Keertikar, Jose Duca, Thierry O. Fischmann, Alan Hruza, Vincent Madison, Emma Lees, David Parry, Wolfgang Seghezzi, Nicole Sgambellone, Frances Shanahan, Derek Wiswell, Timothy J. Guzi, "Versatile templates for the development of novel kinase inhibitors: Discovery of novel CDK inhibitors," Bioorg. Med. Chem. Lett. 17 (22), 6216-6219 (2007). DOI: 10.1016/j.bmcl.2007.09.018

Kevin D. Dykstra, Liangqin Guo, Elizabeth T. Birzin, Wanda Chan, Yi Tien Yang, Edward C. Hayes, Carolyn A. DaSilva, Lee-Yuh Pai, Ralph T. Mosley, Bryan Kraker, Paula M.D. Fitzgerald, Frank DiNinno, Susan P. Rohrer, James M. Schaeffer, Milton L. Hammonda, "Estrogen receptor ligands. Part 16: 2-Aryl indoles as highly subtype selective ligands for ER[alpha]," Bioorg. Med. Chem. Lett. 17 (8), 2322-2328 (2007). DOI: 10.1016/j.bmcl.2007.01.054

L. D'Souza, L. Jiao, J.R. Regalbuto, J.T. Miller, A.J. Kropf, "Preparation of silica- and carbon-supported cobalt by electrostatic adsorption of Co(III) hexaammines," J. Catal. 248 (2), 165-174 (2007). DOI: 10.1016/j.jcat.2007.03.010

Richard T. Eastman, John White, Oliver Hucke, Kohei Yokoyama, Christophe L.M.J. Verlinde, Michael A. Hast, Lorena S. Beese, Michael H . Gelb, Pradipsinh K. Rathod, Wesley C. Van Voorhis, "Resistance mutations at the lipid substrate binding site of Plasmodium falciparum protein farnesyltransferase," Mol. Biochem. Parasit. 152 (1), 66-71 (2007). DOI: 10.1016/j.molbiopara.2006.11.012

D.S. Ebel, M.L. Rivers, "Meteorite 3-D synchrotron microtomography: Methods and applications," Metorit. Planet Sci. 42 (9), 1627-1646 (2007).

Michael J. Eddins, Ranjani Varadan, David Fushman, Cecile M. Pickart, Cynthia Wolberger, "Crystal Structure and Solution NMR Studies of Lys48-linked Tetraubiquitin at Neutral pH," J. Mol. Biol. 367 (1), 204-211 (2007). DOI: 10.1016/j.jmb.2006.12.065

L. Ehm, S.M. Antao, J. Chen, D.R. Locke, F.M. Michel, C.D. Martin, .T. Yu, P.L. Lee, P.J. Chupas, S.D. Shastri, Q. Guo, J.B. Parise, "Studies of

Local and Intermediate Range Structure in Crystalline and morphous Materials at High Pressure Using High-Energy X-Ray," Powder Diffr. 22, 108-112 (2007). DOI: 10.1154/1.2737456

J.W. Elmer, T.A. Palmer, E.D. Specht, "Direct observations of sigma phase formation in duplex stainless steels using in-situ synchrotron X-ray diffraction," Metall. Mater. Trans. A 38 (3), 464-475 (2007). DOI: 10.1007/s11661-006-9076-3

J.W. Elmer, T.A. Palmer, E.D. Specht, "In situ observations of sigma phase dissolution in 2205 duplex stainless steel using synchrotron X-ray diffraction," Mat. Sci. Eng. A 459 (1-2), 151-155 (2007). DOI: 10.1016/j.msea.2007.01.071

L. Emery, "Coupled-Bunch Instability Study of Multi-cell Deflecting Mode Cavities for the Advanced Photon Source," Proc. of the 22nd Particle Accelerator Conference (PAC07), IEEE, (2007), 4348 - 4350.

E.D. Emmons, "Vibrational Spectroscopy of Polymers at High Pressure," Ph.D., University of Nevada Reno, 2007.

D. Enlow, A. Rawal, M. Kanapathipillai, K. Schmidt-Rohr, S. Mallapragada, C.-T. Lo, P. Thiyagarajan, M. Akinc, "Synthesis and characterization of self-assembled block copolymer templated calcium phosphate nanocomposite gels," J. Mater. Chem. 17 (16), 1570-1578 (2007). DOI: 10.1039/b613760a

Robert L. Eoff, Karen C. Angel, Martin Egli, F. Peter Guengerich, "Molecular Basis of Selectivity of Nucleoside Triphosphate Incorporation Opposite O[superscript 6]-Benzylguanine by Sulfolobus solfataricus DNA Polymerase Dpo4: STEADY-STATE AND PRE-STEADY-STATE KINETICS AND X-RAY CRYSTALLOGRAPHY OF CORRECT AND INCORRECT PAIRING," J. Biol. Chem. 282 (18), 13573-13584 (2007). DOI: 10.1074/jbc.M700656200

Robert L. Eoff, Adriana Irimia, Karen C. Angel, Martin Egli, F. Peter Guengerich, "Hydrogen Bonding of 7,8-Dihydro-8-oxodeoxyguanosine with a Charged Residue in the Little Finger Domain Determines Miscoding Events in Sulfolobus solfataricus DNA Polymerase Dpo4," J. Biol. Chem. 282 (27), 19831-19843 (2007). DOI: 10.1074/jbc.M702290200

Deniz Erdemir, Soma Chattopadhyay, Liang Guo, Jan Ilavsky, Heinz Amenitsch, Carlo U. Segre, Allan S. Myerson, "Relationship between Self-Association of Glycine Molecules in Supersaturated Solutions and Solid State Outcome," Phys. Rev. Lett. 99, 115702-1-115702-4 (2007). DOI: 10.1103/PhysRevLett.99.115702

K.S. Erdmann, Y. Mao, H.J. McCrea, R. Zoncu, S. Lee, S. Paradise, J. Modregger, D. Biemesderfer, D. Toomre, P. De Camilli, "A role of the lowe syndrome protein OCRL in early steps of the endocytic pathway," Dev. Cell 13 (3), 377-390 (2007). DOI: 10.1016/j.devcel.2007.08.004

D. Errandonea, "Landau theory applied to phase transitions in calcium orthotungstate and isostructural compounds," EPL Journal 77 (5), 56001-p1-56001-p5 (2007). DOI: 10.1209/0295-5075/77/56001

B.E. Etschmann, C.G. Ryan, S. Vogt, J. Maser, J. Brugger, C.L. Harland, D. Legnini, "Selective x-ray Bragg spectrometry: optimizing fluorescence microprobe sensitivity for precious metals," X-ray Spectrom. 36 (2), 111-121 (2007). DOI: 10.1002/xrs.937

K.A. Evans, J. Mavrogenes, M. Newville, "The effect of CO[subscript 2] on the speciation of bromine in low-temperature geological solutions: an XANES study," J. Synchrotron Rad. 14 (2), 219-226 (2007). DOI: 10.1107/S0909049507001112

William J. Evans, Choong-Shik Yoo, Geun Woo Lee, Hyunchae Cynn, Magnus J. Lipp, Ken Visbeck, "Dynamic diamond anvil cell (dDAC): A novel device for studying the dynamic-pressure properties of materials," Rev. Sci. Instrum. 78, 073904-1-073904-6 (2007). DOI: 10.1063/1.2751409

Artem G. Evdokimov, Matthew Pokross, Richard L. Walter, Marlene Mekel, Bobby L. Barnett, Jack Amburgey, William L. Seibel, Shari J. Soper, Jane F. Djung, Neil Fairweather, Conrad Diven, Vinit Rastogi, Leo Grinius, Charles Klanke, Richard Siehnel, Tracy Twinem, Ryan Andrews, Alan Curnow, "Serendipitous Discovery of Novel Bacterial Methionine Aminopeptidase Inhibitors," Proteins 66 (3), 538-546 (2007). DOI: 10.1002/prot.21207

Obidimma C. Ezezika, Sandra Haddad, Todd J. Clark, Ellen L. Neidle, Cory Momany, "Distinct Effector-binding Sites Enable Synergistic Transcriptional Activation by BenM, a LysR-type Regulator," J. Mol. Biol. 367 (3), 616-629 (2007). DOI: 10.1016/j.jmb.2006.09.090

Obidimma C. Ezezika, Sandra Haddad, Ellen L. Neidle, Cory Momany, "Oligomerization of BenM, a LysR-type transcriptional regulator: structural basis for the aggregation of proteins in this family," Acta Crystallogr. F 63, 361-368 (2007). DOI: 10.1107/S1744309107019185

L. Fan, D. Paterson, I. McNulty, M.M.J. Treacy, J.M. Gibson, "Fluctuation X-ray microscopy: a novel approach for the structural study of disordered materials," J. Microsc-Oxford 225 (1), 41-48 (2007). DOI: 10.1111/j.1365-2818.2007.01714.x

L. Fan, D. Paterson, I. McNulty, M.M.J. Treacy, D. Kumar, P. Du, U. Wiesner, J.M. Gibson, "Characterization of medium-range order in self-assembled organic-inorganic hybrid by fluctuation x-ray microscopy," Mater. Res. Soc. Symp. Proc., R. Kalyanaraman, U. Valbusa, Z. Zhang, eds., 960E, Materials Research Society, (2007), 0960-N09-09.

Alan S. Fanning, Ming F. Lye, James M. Anderson, Arnon Lavie, "Domain Swapping within PDZ2 Is Responsible for Dimerization of ZO Proteins," J. Biol. Chem. 282 (52), 37710-37716 (2007). DOI: 10.1074/jbc.M707255200

Quan Fan, Peter J. Chupas, M. Stanley Whittingham, "Characterization of Amorphous and Crystalline Tin-Cobalt Anodes," Electrochem. Solid St. 10 (12), A274-A278 (2007). DOI: 10.1149/1.2789418

Gerrie P. Farman, Edward J. Allen, David Gore, Thomas C. Irving, Pieter P. de Tombe, "Interfilament Spacing Is Preserved during Sarcomere Length Isometric Contractions in Rat Cardiac Trabeculae," Biophys. J. 92 (9), L73-L75 (2007). DOI: 10.1529/biophysj.107.104257

Stephan Fath, Joseph D. Mancias, Xiping Bi, Jonathan Goldberg, "Structure and organization of coat proteins in the COPII cage," Cell 129 (7), 1325-1336 (2007). DOI: 10.1016/j.cell.2007.05.036

Y. Fei, A. Ricolleau, M. Frank, K. Mibe, G. Shen, V. Prakapenka, "Toward an internally consistent pressure scale," Proc. Natl. Acad. Sci. USA 104 (22), 9182-9186 (2007). DOI: 10.1073/pnas.0609013104

Y. Fei, L. Zhang, A. Corgne, H. Watson, A. Ricolleau, Y. Meng, V. Prakapenka, "Spin transition and equations of state of (Mg, Fe)O solid solutions," Geophys. Res. Lett. 34, L17307-L17311 (2007). DOI: 10.1029/2007GL030712

R. Felici, N.M. Jeutter, V. Mussi, F. Buatier de Mongeot, C. Boragno, U. Valbusa, A. Toma, Y.W. Zhang, C. Rau, I. K. Robinson, "In situ study of the dewetting behavior of Ni-films on oxidized Si(0 0 1) by GISAXS," Surf. Sci. 601 (18), 4526-4530 (2007). DOI: 10.1016/j.susc.2007.04.210

Gustavo Fenalti, Ruby H.P. Law, Ashley M. Buckle, Christopher Langendorf, Kellie Tuck, Carlos J. Rosado, Noel G. Faux, Khalid Mahmood, Christiane S. Hampe, J. Paul Banga, Matthew Wilce, Jason Schmidberger, Jamie Rossjohn, Ossama El-Kabbani, Robert N. Pike, A. Ian Smith, Ian R. Mackay, Merrill J. Rowley, James C. Whisstock, "GABA production by glutamic acid decarboxylase is regulated by a dynamic catalytic loop," Nat. Struct. Mol. Biol. 14 (4), 280-286 (2007). DOI: 10.1038/nsmb1228

G. Feng, B. Deriy, J. Wang, "A Linear MOSFET Regulator for Improving Performance of the Booster Ramping Power Supplies at the APS," Proc. of the 22nd Particle Accelerator Conference (PAC07), IEEE, (2007), 434 - 436.

Yejun Feng, R. Jaramillo, G. Srajer, J.C. Lang, Z. Islam, M.S. Somayazulu, O.G. Shpyrko, J.J. Pluth, H.-k. Mao, E.D. Isaacs, G. Aeppli, T.F. Rosenbaum, "Pressure-Tuned Spin and Charge Ordering in an Itinerant Antiferromagnet," Phys. Rev. Lett. 99, 137201-1-137207-4 (2007). DOI: 10.1103/PhysRevLett.99.137201

Richard B. Fenner, Rodney E. Gerig, J. Murray Gibson, Efim Gluskin, Gabrielle G. Long, Dennis M. Mills, William G. Ruzicka, "The Advanced Photon Source looks to the future," Nucl. Instrum. Methods A 582 (1), 5-10 (2007). DOI: 10.1016/j.nima.2007.08.051

P. Fenter, Z. Zhang, C. Park, N. C. Sturchio, X. M. Hu, S. R. Higgins, "Structure and Reactivity of the Dolomite (104)-Water Interface: New Insights into the Dolomite Problem," Geochim. Cosmochim. Acta 71 (3), 566-579 (2007). DOI: 10.1016/j.gca.2006.10.006

Marcos Fernandez-Garcia, Carolina Belver, Jonathan C. Hanson, Xianqin Wang, Jose A. Rodriguez, "Anatase-TiO[subscript 2] Nanomaterials: Analysis of Key Parameters Controlling Crystallization," J. Am. Chem. Soc. 129 (44), 13604-13612 (2007). DOI: 10.1021/ja074064m

Daniel J. Ferraro, Eric N. Brown, Chi-Li Yu, Rebecca E. Parales, David T. Gibson, S. Ramaswamy, "Structural investigations of the ferredoxin and terminal oxygenase components of the biphenyl 2,3-dioxygenase from Sphingobium yanoikuyae B1," BMC Struct. Biol. 7 (10), 1-14 (2007). DOI: 10.1186/1472-6807-7-10

Francois Ferron, Grzegorz Rebowski, Sung Haeng Lee, Roberto Dominguez, "Structural basis for the recruitment of profilin–actin complexes during filament elongation by Ena/VASP," EMBO J. 26 (21), 4597-4606 (2007). DOI: 10.1038/sj.emboj.7601874

Larry W. Finger, Martin Kroeker, Brian H. Toby, "DRAWxtl, an open-source computer program to produce crystal structure drawings," J. Appl. Crystallogr. 40 (1), 188-192 (2007). DOI: 10.1107/S0021889806051557

Lydia Finney, Suneeta Mandava, Lyann Ursos, Wen Zhang, Diane Rodi, Stefan Vogt, Daniel Legnini, Jorg Maser, Francis Ikpatt, Olufunmilayo I. Olopade, David Glesne, "X-ray fluorescence microscopy reveals large-scale relocalization and extracellular translocation of cellular copper during angiogenesis," Proc. Natl. Acad. Sci. USA 104 (7), 2247-2252 (2007). DOI: 10.1073/pnas.0607238104

Bradley Finnigan, Phil Casey, David Cookson, Peter Halley, Kevin Jack, Rowan Truss, Darren Martin, "Impact of controlled particle size nanofillers on the mechanical properties of segmented polyurethane nanocomposites," Int. J. Nanotech. 4 (5), 496-515 (2007). DOI: 10.1504/IJNT.2007.014747

R.F. Fischetti, D.W. Yoder, S. Xu, S. Stepanov, O. Makarov, R. Benn, S. Corcoran, W. Diete, M. Schwoerer-Boehing, R. Signorato, L. Schroeder, L. Berman, P.J. Viccaro, J.L. Smith, "Optical Performance of the GM/CA-CAT Canted Undulator Beamlines for Protein Crystallography," American Instutte of Physics, J.-Y. Choi, S. Rah, eds., Synchrotron Radiation Instrumentation (2007), 754 - 757.

S. Zoe Fisher, Chingkuang Tu, Deepa Bhatt, Lakshmanan Govindasamy, Mavis Agbandje-McKenna, Robert McKenna, David N. Silverman, "Speeding Up Proton Transfer in a Fast Enzyme: Kinetic and Crystallographic Studies on the Effect of Hydrophobic Amino Acid Substitutions in the Active Site of Human Carbonic Anhydrase II," Biochemistry-US 46 (12), 3803-3813 (2007). DOI: 10.1021/bi602620k

T.T. Fister, G.T. Seidler, J.O. Cross, J.J. Rehr, J.A. Soininen, "Measurement of the Full XAFS Spectrum of MgO Using Nonresonant Inelastic X-ray Scattering," AIP Conference Proceedings, B. Hedman, P. Pianetta, eds., 882, American Institute of Physics, (2007), 156 - 158.

T.T. Fister, G.T. Seidler, J.J. Rehr, J.J. Kas, W.T. Elam, J.O. Cross, K.P. Nagle, "Deconvolving instrumental and intrinsic broadening in core-shell x-ray spectroscopies," Phys. Rev. B 75, 174106-1-174106-10 (2007). DOI: 10.1103/PhysRevB.75.174106

John F. Flanagan, Bartlomiej J. Blus, Daesung Kim, Katrina L. Clines, Fraydoon Rastinejad, Sepideh Khorasanizadeh, "Molecular Implications of Evolutionary Differences in CHD Double Chromodomains," J. Mol. Biol. 369 (2), 334-342 (2007). DOI: 10.1016/j.jmb.2007.03.024

Christopher D. Fleming, Carol C. Edwards, Stephen D. Kirby, Donald M. Maxwell, Philip M. Potter, Douglas M. Cerasoli, Matthew R. Redinbo, "Crystal Structures of Human Carboxylesterase 1 in Covalent Complexes with the Chemical Warfare Agents Soman and Tabun," Biochemistry-US 46 (17), 5063-5071 (2007). DOI: 10.1021/bi700246n

R.P. Fliller, D.A. Edwards, H. Edwards, T.W. Koeth, K.C. Harkay, K.-J. Kim, "Transverse to Longitudinal Emittance Exchange Beamline at the A0 Photoinjector," Proc. of the 22nd Particle Accelerator Conference (PAC07), IEEE, (2007), 3702 - 3704.

P. Fons, D. Brewe, E. Stern, A.V. Kolobov, T. Fukaya, M. Suzuki, T. Uruga, N. Kawamura, M. Takagaki, H. Ohsawa, H. Tanida, J. Tominaga, "Sub-nanosecond laser-induced structural changes in the phase change material Ge2Sb2Te5 measured by an optical pump/x-ray probe technique," EPCOS 2007, M. Wuttig, N. Yamada, T. Ohata, T. Kubo, eds., 2007, European Symposium on Phase Change and Ovonic Science, (2007), 10-1 - 10-7.

Farhad Forouhar, J.L. Ross Anderson, Christopher G. Mowat, Sergey M. Vorobiev, Arif Hussain, Mariam Abashidze, Chiara Bruckmann, Sarah J. Thackray, Jayaraman Seetharaman, Todd Tucker, Rong Xiao, Li-Chung Ma, Li Zhao, Thomas B. Acton, Gaetano T. Montelione, Stephen K. Chapman, Liang Tong, "Molecular insights into substrate recognition and catalysis by tryptophan 2,3-dioxygenase," Proc. Natl. Acad. Sci. USA 104 (2), 473-478 (2007). DOI: 10.1073/pnas.0610007104

Jeffrey A. Fortner, A. Jeremy Kropf, James L. Jerden, James C. Cunnane, "Chemical Effects at the Reaction Front in Corroding Spent Nuclear Fuel," Scientific Basis for Nuclear Waste Management XXX, D. Dunn, C. Poinssot, B. Begg, eds., 985, MRS (2007), online.

J.W. Freeland, J. Chakhalian, H.-U. Habermeier, G. Cristiani, B. Keimer, "On magnetic interlayer coupling and proximity effect in a La[subscript 0.67]Ca[subscript 0.33]MnO[subscript 3] (10 nm)/YBa[subscript 2]Cu[subscript 3]O[subscript 7] (10 nm) superlattice," Appl. Phys. Lett. 90, 242502-1-242502-3 (2007). DOI: 10.1063/1.2747678

J.W. Freeland, J.J. Kavich, K.E. Gray, L. Ozyuzer, H. Zheng, J.F. Mitchell, M.P. Warusawithana, P. Ryan, X. Zhai, R.H. Kodama, J.N. Eckstein, "Suppressed magnetization at the surfaces and interfaces of ferromagnetic metallic manganites," J. Phys. Condens. Matter 19 (31), 315210-1-315210-13 (2007). DOI: 10.1088/0953-8984/19/31/315210

John N. Freskos, Yvette M. Fobian, Timothy E. Benson, Michael J. Bienkowski, David L. Brown, Thomas L. Emmons, Robert Heintz, Alice Laborde, Joseph J. McDonald, Brent V. Mischke, John M. Molyneaux, Joseph B. Moon, Patrick B. Mullins, D. Bryan Prince, Donna J. Paddock, Alfredo G. Tomasselli, Gregory Winterrowd, "Design of potent inhibitors of human [beta]-secretase. Part 1," Bioorg. Med. Chem. Lett. 17 (1), 73-77 (2007). DOI: 10.1016/j.bmcl.2006.09.092

John N. Freskos, Yvette M. Fobian, Timothy E. Benson, Joseph B. Moon, Michael J. Bienkowski, David L. Brown, Thomas L. Emmons, Robert Heintz, Alice Laborde, Joseph J. McDonald, Brent V. Mischke, John M. Molyneaux, Patrick B. Mullins, D. Bryan Prince, Donna J. Paddock, Alfredo G. Tomasselli, Greg Winterrowd, "Design of potent inhibitors of human [beta]-secretase. Part 2," Bioorg. Med. Chem. Lett. 17 (1), 78-81 (2007). DOI: 10.1016/j.bmcl.2006.09.091

John L. Fulton, John C. Linehan, Tom Autrey, Mahalingam Balasubramanian, Yongsheng Chen, Nathaniel K. Szymczak, "When is a Nanoparticle a Cluster? An Operando EXAFS Study of Amine Borane Dehydrocoupling by Rh[subscript 4-6] Clusters," J. Am. Chem. Soc. 129 (39), 11936-11949 (2007). DOI: 10.1021/ja073331l

Zheng-Qing Fu, John Chrzas, George M. Sheldrick, John Rose, Bi-Cheng Wang, "A parallel program using SHELXD for quick heavy-atom partial structural solution on high-performance computers," J. Appl. Crystallogr. 40 (2), 387-390 (2007). DOI: 10.1107/S0021889807003998

J.-F. Gaillard, "Probing Environmental Particles and Colloids with X-Rays," Environmental Particles and Colloids: Behaviour, Structure, and Characterisation, K.J. Wilkinson, J.R. Lead, eds., Wiley, 2007, 613 - 666.

Jean-Francois Gaillard, Cheng Chen, Susa H. Stonedahl, Boris L.T. Lau, Denis T. Keane, Aaron I. Packman, "Imaging of colloidal deposits in granular porous media by X-ray difference micro-tomography," Geophys. Res. Lett. 34, L18404 (2007). DOI: 10.1029/2007GL030514

Andrey Galkin, Liudmila Kulakova, Eugene Melamud, Ling Li, Chun Wu, Patrick Mariano, Debra Dunaway-Mariano, Theodore E. Nash, Osnat Herzberg, "Characterization, Kinetics, and Crystal Structures of Fructose-1,6-bisphosphate Aldolase from the Human Parasite, Giardia lamblia," J. Biol. Chem. 282 (7), 4859-4867 (2007). DOI: 10.1074/jbc.M609534200

Kelly A. Gangwer, Darren J. Mushrush, Devin L. Stauff, Ben Spiller, Mark S. McClain, Timothy L. Cover, D. Borden Lacy, "Crystal structure of the Helicobacter pylori vacuolating toxin p55 domain," Proc. Natl. Acad. Sci. USA 104 (41), 16293-16298 (2007). DOI: 10.1073/pnas.0707447104

Jianhua Gan, Yan Wu, Ponraj Prabakaran, Yijun Gu, Yue Li, Michelle Andrykovitch, Hehua Liu, Yunchen Gong, Honggao Yan, Xinhua Ji, "Structural and Biochemical Analyses of Shikimate Dehydrogenase AroE from Aquifex aeloicus: Implications for the Catalytic Mechanism," Biochemistry-US 46 (33), 9513-9522 (2007). DOI: 10.1021/bi602601eS0006-2960(60)02601-9

Robert G. Garces, Wanda Gillon, Emil F. Pai, "Atomic model of human Rcd-1 reveals an armadillo-like-repeat protein with in vitro nucleic acid binding properties," Protein Sci. 16 (2), 176-188 (2007). DOI: 10.1110/ps.062600507

Consuelo Garcia-Rodriguez, Raphael Levy, Joseph W. Arndt, Charles M. Forsyth, Ali Razai, Jianlong Lou, Isin Geren, Raymond C. Stevens, James D. Marks, "Molecular evolution of antibody cross-reactivity for two subtypes of type A botulinum neurotoxin," Nature Biotechnol. 25 (1), 107-116 (2007). DOI: 10.1038/nbt1269

Anna S. Gardberg, Lezlee T. Dice, Susan Ou, Rebecca L. Rich, Elizabeth Helmbrecht, Jan Ko, Ronald Wetzel, David G. Myszka, Paul H. Patterson, Chris Dealwis, "Molecular basis for passive immunotherapy of Alzheimer's disease," Proc. Natl. Acad. Sci. USA 104 (40), 15659-15664 (2007). DOI: 10.1073/pnas.0705888104

Graeme S. Garvey, Christopher J. Rocco, Jorge C. Escalante-Semerena, Ivan Rayment, "The three-dimensional crystal structure of the PrpF protein of Shewanella oneidensis complexed with trans-aconitate: Insights into its biological function," Protein Sci. 16, 1274-1284 (2007). DOI: 10.1110/ps.072801907

Milen Gateshki, Qing Chen, Lian-Mao Peng, Peter Chupas, Valeri Petkov, "Structure of nanosized materials by high-energy X-ray diffraction: study of titanate nanotubes," Z. Kristallogr. 222, 612-616 (2007). DOI: 10.1524/zkri.2007.222.11.612

Milen Gateshki, Markus Niederberger, Atul S. Deshpande, Yang Ren, Valeri Petkov, "Atomic-scale structure of nanocrystalline CeO[subscript 2]–ZrO[subscript 2] oxides by total x-ray diffraction and pair distribution function analysis," J. Phys. Condens. Matter 19 (15), 156205-1-156205-12 (2007). DOI: 10.1088/0953-8984/19/15/156205

Milen Gateshki, Shu Yin, Yang Ren, Valeri Petkov, "Titania Polymorphs by Soft Chemistry: Is There a Common Structural Pattern?," Chem. Mater. 19 (10), 2512-2518 (2007). DOI: 10.1021/cm0630587

Joseph Gawronski-Salerno, Douglas M. Freymann, "Structure of the GMPPNP-stabilized NG domain complex of the SRP GTPases Ffh and FtsY," J. Struct. Biol. 158 (1), 122-128 (2007). DOI: 10.1016/j.jsb.2006.10.025

Todd W. Geders, Liangcai Gu, Jonathan C. Mowers, Haichuan Liu, William H. Gerwick, Kristina Hakansson, David H. Sherman, Janet L. Smith, "Crystal Structure of the ECH[subscript 2] Catalytic Domain of CurF from Lyngbya majuscula: Insights into a Decarboxylase Involved in Polyketide Chain [beta]-Branching," J. Biol. Chem. 282 (49), 35954-35963 (2007). DOI: 10.1074/jbc.M703921200

Cory Gerdts, "Creating Functional Reaction Networks Using Plug-Based Microfluidics with Applications in Protein Crystallization," Ph.D., University of Chicago, 2007.

Arun K. Ghosh, Kai Xi, Valerie Grum-Tokars, Xiaoming Xu, Kiira Ratia, Wentao Fu, Katherine V. Houser, Susan C. Baker, Michael E. Johnson, Andrew D. Mesecar, "Structure-based design, synthesis, and biological evaluation of peptidomimetic SARS-CoV 3CLpro inhibitors," Bioorg. Med. Chem. Lett. 17 (21), 5876-5880 (2007). DOI: 10.1016/j.bmcl.2007.08.031

Mahua Ghosh, Gregor Meiss, Alfred M. Pingoud, Robert E. London, Lars C. Pedersen, "The Nuclease A-Inhibitor Complex Is Characterized by a Novel Metal Ion Bridge," J. Biol. Chem. 282 (8), 5682-5690 (2007). DOI: 10.1074/jbc.M605986200

J. Murray Gibson, "Understanding the limits of pair-distribution functions for nanoscale correlation function measurement," J. Phys. Condens. Matter 19, 455217-455222 (2007). DOI: 10.1088/0953-8984/19/45/455217

Hubertus Giefers, Felix Porsch, "Shear induced phase transition in PbO under high pressure," Physica B 400 (1-2), 53-58 (2007). DOI: 10.1016/j.physb.2007.06.033

Hubertus Giefers, Elizabeth A. Tanis, Sven P. Rudin, Carl Greeff, Xuezhi Ke, Changfeng Chen, Malcolm F. Nicol, Michael Pravica, Walter Pravica, Jiyong Zhao, Ahmet Alatas, Michael Lerche, Wolfgang Sturhahn, Ercan Alp, "Phonon Density of States of Metallic Sn at High Pressure," Phys. Rev. Lett. 98, 245502-1-245502-4 (2007). DOI: 10.1103/PhysRevLett.98.245502

Gerald Giester, Uwe Kolitsch, Peter Leverett, Peter Turner, Peter A. Williams, "The crystal structures of lavendulan, sampleite, and a new polymorph of sampleite," Eur. J. Mineral. 19 (1), 75-93 (2007). DOI: 10.1127/0935-1221/2007/0019-0075

M. Ginder-Vogel, W.-M. Wu, S. Kelly, C.S. Criddle, J. Carley, P. Jardine, K.M. Kemner, S. Fendorf, "Micro-scale heterogeneity in biogeochemical uranium cycling," X-Ray Absorption Fine Structure - XAFS13, Britt Hedman, Piero Pianetta, eds., 882, American Institue of Physics, (2007), 190 - 192. DOI: 10.1063/1.2644470

R. Giulian, P. Kluth, B. Johannessen, L.L. Araujo, D.J. Llewellyn, D.J. Cookson, M.C. Ridgway, "Synthesis and characterization of ion-implanted Pt nanocrystals in SiO[subscript 2]," Nucl. Instrum. Methods B 257 (1-2), 33-36 (2007). DOI: 10.1016/j.nimb.2006.12.139

S. Glasauer, S. Langley, M. Boyanov, B. Lai, K. Kemner, T.J. Beveridge, "Mixed-Valence Cytoplasmic Iron Granules Are Linked to Anaerobic Respiration," Appl. Environ. Microb. 73 (3), 993-996 (2007). DOI: 10.1128/AEM.01492-06

Michael H. Godsey, George Minasov, Ludmilla Shuvalova, Joseph S. Brunzelle, Ivan I. Vorontsov, Frank R. Collart, Wayne F. Anderson, "The 2.2 Å resolution crystal structure of Bacillus cereus Nif3-family protein YqfO reveals a conserved dimetal-binding motif and a regulatory domain," Protein Sci. 16, 1285-1293 (2007). DOI: 10.1110/ps.062674007

T. Gog, D.M. Casa, I. Kuzmenko, R.J. Krakora, T.B. Bolin, "Windowless transition between atmospheric pressure and high vacuum via differential pumping for synchrotron radiation applications," J. Synchrotron Rad. 14 (4), 339-344 (2007). DOI: 10.1107/S0909049507016317

Leticia Gomez-Gil, Pravindra Kumar, Diane Barriault, Jeffrey T. Bolin, Michel Sylvestre, Lindsay D. Eltis, "Characterization of biphenyl dioxygenase of Pandoraea pnomenusa B-356 as a potent polychlorinated biphenyl-degrading enzyme," J. Bacteriol. 189 (15), 5705-5715 (2007). DOI: 10.1128/JB.01476-06

Alexander F. Goncharov, Jonathan Crowhurst, "Proton delocalization under extreme conditions of high pressure and temperature," Phase Transit. 80 (10-12), 1051-1072 (2007). DOI: 10.1080/01411590701473101

Alexander F. Goncharov, Chrystele Sanloup, Nir Goldman, Jonathan C. Crowhurst, Lawrence E. Fried, Nicola Guignot, Mohamed Mezouar, Yue Meng, "Probing of Structure Factor of Water to 57 GPa and 1500 K," Materials Research at High Pressure, M.R. Manaa, A.F. Goncharov, R.J. Hemley, R. Bini, eds., 987, AIP (2007), online.

A.F. Goncharov, S. Singeikin, J.C. Crowhurst, M. Ahart, D. Lakshtanov, V. Prakapenka, J. Bass, P. Beck, S.N. Tkachev, J.M. Zaug, Y. Fei, "Cubic boron nitride as a primary calibrant for a high temperature pressure scale," High Pressure Res. 27 (4), 409-417 (2007). DOI: 10.1080/08957950701659726

Lilian Gonzlez-Segura, John F. Witte, Ronald W. McClard, Thomas D. Hurley, "Ternary Complex Formation and Induced Asymmetry in Orotate Phosphoribosyltransferase," Biochemistry-US 46 (49), 14075-14086 (2007). DOI: 10.1021/bi701023z

R. Gordon, E.D. Crozier, D.-T. Jiang, J. Shoults, B. Barg, P.S. Budnik, "Characteristics of the MBE1 End-Station at PNC/XOR," AIP Conference Proceedings, B. Hedman, P. Pianetta, eds., 882, American Institute of Physics, (2007), 887 - 889.

Markus Grafe, Balwant Singh, Mahalingam Balasubramanian, "Surface speciation of Cd(II) and Pb(II) on kaolinite by XAFS spectroscopy," J. Colloid Interf. Sci. 315 (1), 21-32 (2007). DOI: 10.1016/j.jcis.2007.05.022

Matthew J. Graneto, Ravi G. Kurumbail, Michael L. Vazquez, Huey-Sheng Shieh, Jennifer L. Pawlitz, Jennifer M. Williams, William C. Stallings, Lifeng Geng, Ashok S. Naraian, Francis J. Koszyk, Michael A. Stealey, Xiangdong D. Xu, Richard M. Weier, Gunnar J. Hanson, Robert J. Mourey, Robert P. Compton, Stephen J. Mnich, Gary D. Anderson, Joseph B. Monahan, Rajesh Devraj, "Synthesis, Crystal Structure, and Activity of Pyrazole-Based Inhibitors of p38 Kinase," J. Med. Chem. 50 (23), 5712-5719 (2007). DOI: 10.1021/jm0611915

Henk Granzier, Michael Radke, Joseph Royal, Yiming Wu, Thomas C. Irving, Michael Gotthardt, Siegfried Labeit, "Functional genomics of chicken, mouse, and human titin supports splice diversity as an important mechanism for regulating biomechanics of striated muscle," Am. J. Physiol.-Lung C 293, R557-R567 (2007). DOI: 10.1152/ajpregu.00001.2007

Eugene Gregoryanz, Alexander F. Goncharov, Chrystele Sanloup, Maddury Somayazulu, Ho-kwang Mao, Russell J. Hemley, "High P-T transformations of nitrogen to 170 GPa," J. Chem. Phys. 126, 184505-1-184505-5 (2007). DOI: 10.1063/1.2723069

A.E. Grelick, A. Cours, N.P. DiMonte, A. Nassiri, T.L. Smith, G. Waldschmidt, "The Advanced Photon Source Pulsed Deflecting Cavity RF System," Proc. of the 22nd Particle Accelerator Conference (PAC07), IEEE, (2007), 2224 - 2226.

Alexei Grigoriev, Dal-Hyun Do, Paul G. Evans, Bernhard Adams, Eric Landahl, Eric M. Dufresne, "Synchronizing fast electrically driven phenomena with synchrotron x-ray probes," Rev. Sci. Instrum. 78, 023105-1-023105-4 (2007). DOI: 10.1063/1.2668989

Andrew P. Grosvenor, Ronald G. Cavell, Arthur Mar, "Next-nearest neighbour contributions to P 2p[subscript 3/2] X-ray photoelectron binding energy shifts of mixed transition-metal phosphides M[subscript 1−x]M′[subscript x]P with the MnP-type structure," J. Solid State Chem. 180 (10), 2702-2712 (2007). DOI: 10.1016/j.jssc.2007.07.027

M. Groves, E.A. Stern, G. Seidler, M. Balasubramanian, "Solving a Historical Puzzle," AIP Conference Proceedings, B. Hedman, P. Pianetta, eds., 882, American Institute of Physics, (2007), 165 - 167.

P. Gryko, M. Liang, R. Harder, I.K. Robinson, "Observation of interference effects in coherent diffraction of nanocrystals under X-ray standing-wave illumination," J. Synchrotron Rad. 14 (6), 471-476 (2007). DOI: 10.1107/S0909049507040228

Guilherme Gualda, "Crystal and bubble populations in the early-erupted Bishop rhyolitic magma : microscopy, X-ray tomography and microanalysis of pumice clasts," Ph.D., The University of Chicago, 2007.

Rong Guan, Han Dai, Diana R. Tomchick, Irina Dulubova, Mischa Machius, Thomas C. Sudhof, Josep Rizo, "Crystal Structure of the RIM1[alpha] C[subscript 2]B Domain at 1.7 Å Resolution," Biochemistry-US 46 (31), 8988-8998 (2007). DOI: 10.1021/bi700698a

Y. Guan, W.E. Bailey, E. Vescovo, C.-C. Kao, D.A. Arena, "Phase and amplitude of element-specific moment precession in Ni[subscript 81]Fe[subscript 19]," J. Magn. Magn. Mater. 312 (2), 374-378 (2007). DOI: 10.1016/j.jmmm.2006.10.1111

G. Guilherme, A.T. Anderson Jr. , "Magnetite scavenging and the buoyancy of bubbles in magmas. Part 1: Discovery of a pre-eruptive bubble in Bishop rhyolite," Contrib. Mineral. Petr. 153 (6), 733-742 (2007). DOI: 10.1007/s00410-006-0173-5

Liangcai Gu, Todd W. Geders, Bo Wang, William H. Gerwick, Kristina Hakansson, Janet L. Smith, David H. Sherman, "GNAT-Like Strategy for Polyketide Chain Initiation," Science 318, 970-974 (2007). DOI: 10.1126/science.1148790

H. Guo, J.N. Wilking, D. Liang, T.G. Mason, J.L. Harden, R.L. Leheny, "Slow, nondiffusive dynamics in concentrated nanoemulsions," Phys. Rev. E 75, 041401-1-041401-8 (2007). DOI: 10.1103/PhysRevE.75.041401

W. Guo, M. Borland, K.C. Harkay, C.-x. Wang, B. Yang, "A Kilohertz Picosecond X-Ray Pulse Generation Scheme," Proc. of the 22nd Particle Accelerator Conference (PAC07), IEEE, (2007), 1133 - 1135.

W. Guo, B. Yang, C.-x. Wang, K. Harkay, M. Borland, "Generating Picosecond X-ray Pulses in Synchrotron Light Sources Using Dipole Kickers," Phys. Rev. Spec. Top., Accel. Beams 10, 020701-1-020701-6 (2007). DOI: 10.1103/PhysRevSTAB.10.020701

C. Gutt, M. Sprung, R. Fendt, A. Madsen, S.K. Sinha, M. Tolan, "Partially Wetting Thin Liquid Films: Structure and Dynamics Studied with Coherent X Rays," Phys. Rev. Lett. 99 (9), 096104-1-096104-4 (2007). DOI: 10.1103/PhysRevLett.99.096104

Aleta Hagman, "Studies of Nanoparticle Marker Motion in Ultra Thin Polymer Films With X-ray Standing Waves," Ph.D., Northwestern, 2007.

Andrei S. Halavaty, Keith Moffat, "N- and C-Terminal Flanking Regions Modulate Light-Induced Signal Transduction in the LOV2 Domain of the Blue Light Sensor Phototropin 1 from Avena sativa," Biochemistry-US 46 (49), 14001-14009 (2007). DOI: 10.1021/bi701543e

Branwen M. Hall, "Functional Evolution of the Cro Protein Family of Transcription Factors," Ph.D., University of Arizona, 2007.

J.J. Hamlin, S. Deemyad, J.S. Schilling, M.K. Jacobsen, R.S. Kumar, A.L. Cornelius, G. Cao, J.J. Neumeier, "ac susceptibility studies of the weak itinerant ferromagnet SrRuO[subscript 3] under high pressure to 34 GPa," Phys. Rev. B 76, 014432-1-014432-7 (2007). DOI: 10.1103/PhysRevB.76.014432

Michal Hammel, Daniel Nmeek, J. Andrew Keightley, George J. Thomas, Jr., Brian V. Geisbrecht, "The Staphylococcus aureus extracellular adherence protein (Eap) adopts an elongated but structured conformation in solution," Protein Sci. 16 (12), 2605-2617 (2007). DOI: 10.1110/ps.073170807

Michal Hammel, Georgia Sfyroera, Serapion Pyrpassopoulos, Daniel Ricklin, Kasra X. Ramyar, Mihai Pop, Zhongmin Jin, John D. Lambris, Brian V. Geisbrecht, "Characterization of Ehp, a secreted complement inhibitory protein from staphylococcus aureus," J. Biol. Chem. 282 (41), 30051-30061 (2007). DOI: 10.1074/jbc.M704247200

Michal Hammel, Georgia Sfyroera, Daniel Ricklin, Paola Magotti, John D. Lambris, Brian V. Geisbrecht, "A structural basis for complement inhibition by Staphylococcus aureus," Nat. Immunol. 8 (4), 430-437 (2007). DOI: 10.1038/ni1450

N. Handa, S. Kishishita, S. Morita, R. Akasaka, Z. Jin, J. Chrzas, L. Chen, Z.-J. Liu, B.-C. Wang, S. Sugano, A. Tanaka, T. Terada, M. Shirouzu, S. Yokoyama, "Structure of the human Tim44 C-terminal domain in complex with pentaethylene glycol: ligand-bound form," Acta Crystallogr. D 63 (12), 1225-1234 (2007). DOI: 10.1107/S0907444907051463

Tracey Hanley, David Sutton, Inna Karatchevtseva, David Cookson, Robert Burford, Robert Knott, "Effects of selected process parameters on the morphology of poly(ethylene terephthalate) preforms and bottles," J. Appl. Polym. Sci. 106 (1), 238-247 (2007). DOI: 10.1002/app.26472

S.-W. Han, H.-S. Kang, B.-Z. Jiang, S.-Y. Seo, H.-W. Park, H.-C. Ri, "Structural and magnetic properties of ZnMnTe semiconductor," J. Magn. Magn. Mater. 310 (2-3), 2114-2116 (2007). DOI: 10.1016/j.jmmm.2006.10.788

X.F. Han, M. Grimsditch, J. Meersschaut, A. Hoffmann, Y. Ji, J. Sort, J. Nogues, R. Divan, J.E. Pearson, D.J. Keavney, "Magnetic Instability Regions in Patterned Structures: Influence of Element Shape on Magnetization Reversal Dynamics," Phys. Rev. Lett. 98 (14), 147202-1-147202-4 (2007). DOI: 10.1103/PhysRevLett.98.147202

Bing Hao, Stephanie Oehlmann, Mathew E. Sowa, J. Wade Harper, Nikola P. Pavletich, "Structure of a Fbw7-Skp1-Cyclin E Complex: Multisite-Phosphorylated Substrate Recognition by SCF Ubiquitin Ligases," Mol. Cell 26 (1), 131-143 (2007). DOI: 10.1016/j.molcel.2007.02.022

R. Harder, M. A. Pfeifer, G. J. Williams, I. A. Vartaniants, I. K. Robinson, "Orientation variation of surface strain," Phys. Rev. B 76 (11), 115425-1-115425-4 (2007). DOI: 10.1103/PhysRevB.76.115425

K. Harkay, Y.-C. Chae, L. Emery, A. Nassiri, G. Waldschmidt, L.H. Morrison, "200-mA Studies in the APS Storage Ring," Proc. of the 22nd Particle Accelerator Conference (PAC07), IEEE, (2007), 4354 - 4356.

K. Harkay, V. Sajaev, B.X. Yang, "Transverse Multibunch Bursting Instability in the APS Storage Ring," Proc. of the 22nd Particle Accelerator Conference (PAC07), IEEE, (2007), 4360 - 4362.

D. Haskel, Y.B. Lee, B.N. Harmon, Z. Islam, J.C. Lang, G. Srajer, Ya. Mudryk, K.A. Gschneidner, Jr., V.K. Pecharsky, "Role of Ge in Bridging Ferromagnetism in the Giant Magnetocaloric Gd[subscript 5]Ge[subscript 1-x]Si[subscript x])[subscript 4] Alloys," Phys. Rev. Lett. 98, 247205-1-247205-4 (2007). DOI: 10.1103/PhysRevLett.98.247205

D. Haskel, Y.C. Tseng, J.C. Lang, S. Sinogeikin, "Instrument for x-ray magnetic circular dichroism measurements at high pressures," Rev. Sci. Instrum. 78, 083904-1-083904-5 (2007). DOI: 10.1063/1.2773800

J. Hass, R. Feng, J.E. Millan-Otoya, X. Li, M. Sprinkle, P.N. First, W.A. de Heer, E.H. Conrad, "Structural properties of the multilayer graphene/4H-SiC(0001) system as determined by surface x-ray diffraction," Phys. Rev. B 75, 214109-1-214109-8 (2007). DOI: 10.1103/PhysRevB.75.214109

S.M. Heald, J.O. Cross, D.L. Brewe, R.A. Gordon, "The PNC/XOR X-ray microprobe station at APS Sector-20," Nucl. Instrum. Methods A 582 (1), 215-217 (2007). DOI: 10.1016/j.nima.2007.08.109

S.M. Heald, J.M. Zachara, B.-H. Jeon, J.P. McKinley, R. Kukkadapu, D. Moore, "XAFS Study of the Chemical and Structural States of Technetium in Fe(III) Oxide Co-precipitates," AIP Conference Proceedings, B. Hedman, P. Pianetta, eds., 882, American Institute of Physics, (2007), 173 - 175.

John Healy, Graham H. Edward, Robert B. Knott, "Residual orientation in micro-injection molded parts," J. Appl. Crystallogr. 40, s393-s396 (2007). DOI: 10.1107/S0021889807005080

Peter Hedstrom, Ulrich Lienert, Jon Almer, Magnus Oden, "Stepwise transformation behavior of the strain-induced martensitic transformation in a metastable stainless steel," Scripta Mater. 56 (3), 213-216 (2007). DOI: 10.1016/j.scriptamat.2006.10.009

F. Heigl, A. Jurgensen, X.-T. Zhou, S. Lam, M. Murphy, J.Y.P. Ko, T.K. Sham, R.A. Rosenberg, R. Gordon, D. Brewe, T. Regier, L. Armelao, "Dynamic View on Nanostructures: A Technique for Time Resolved Optical Luminescence Using Synchrotron Light Pulses at SRC, APS, and CLS," AIP Conference Proceedings, Jae-Young Choi, ed.., 879, American Institute of Physics, (2007), 1202 - 1205.

F. Heigl, A. Jurgensen, X.-T. Zhou, M. Murphy, J.Y.P. Ko, S. Lam, T.K. Sham, T. Regier, R.I.R. Blyth, I. Coulthard, L. Zuin, Y.-F. Hu, L. Armelao, R.A. Gordon, D. Brewe, "Time Resolved Studies of ZnO(Eu) Nanostructure Luminescence Using Short Synchrotron Radiation Pulses," AIP Conference Proceedings, B. Hedman, P. Pianetta, eds., 882, American Institute of Physics, (2007), 864 - 866.

F. Heigl, X.H.J Sun, S. Lam, T.K. Sham, R. Gordon, D. Brewe, R. Rosenberg, G. Shenoy, M. Yablonskikh, J. MacNaughton, A. Moewes, "Optical XAFS of ZnO Nanowires at the Zn K-Edge and Related Phenomena," AIP Conference Proceedings, B. Hedman, P. Pianetta, eds., 882, American Institute of Physics, (2007), 734 - 736.

L. He, B.A. Collins, F. Tsui, Y. Zhong, S. Vogt, Y.S. Chu, "Epitaxial growth of (FeCo)[subscript x]Ge[subscript 1−x](001)," J. Vac. Sci. Technol. B 25 (4), 1217-1220 (2007). DOI: 10.1116/1.2748409

R.J. Hemley, V.V. Struzhkin, R.E. Cohen, "Theory and Practice – Measuring High-Pressure Electronic and Magnetic Properties," Treatise on Geophysics, G. Schubert, eds., Elsevier, 2007, 293 - 337. DOI: 10.1016/B978-044452748-6.00039-0

J. Nathan Henderson, Hui-wang Ai, Robert E. Campbell, S. James Remington, "Structural basis for reversible photobleaching of a green fluorescent protein homologue," Proc. Natl. Acad. Sci. USA 104 (16), 6672-6677 (2007). DOI: 10.1073/pnas.0700059104

Nathan Henderson, "Crystallographic and spectroscopic studies of photoswitching in fluorescent proteins," Ph.D., University of Oregon, 2007.

Bastian Henke, Stefan Schweizer, Jacqueline A. Johnson, Denis T. Keane, "Zr and Ba edge phenomena in the scintillation intensity of fluorozirconate-based glass-ceramic X-ray detectors," J. Synchrotron Rad. 14 (3), 252-256 (2007). DOI: 10.1107/S0909049507007959

L. Hennet, I. Pozdnyakova, V. Cristiglio, S. Krishnan, A. Bytchkov, F. Albergamo, G.J. Cuello, J.-F. Brun, H.E. Fischer, D. Zanghi, S. Brassamin, M.-L. Saboungi, D.L. Price, "Structure and dynamics of levitated liquid aluminates," J. Non-Cryst. Solids 353 (18-21), 1705-1712 (2007). DOI: 10.1016/j.jnoncrysol.2007.01.040

Jungseok Heo, You-Moon Jeon, Chad A. Mirkin, "Reversible Interconversion of Homochiral Triangular Macrocycles and Helical Coordination Polymers," J. Am. Chem. Soc. 129 (25), 7712-7713 (2007). DOI: 10.1021/ja0716812

Aitor Hierro, Adriana L. Rojas, Raul Rojas, Namita Murthy, Gregory Effantin, Andrey V. Kajava, Alasdair C. Steven, Juan S. Bonifacino, James H. Hurley, "Functional architecture of the retromer cargo-recognition complex," Nature 449, 1063-1067 (2007). DOI: 10.1038/nature06216

Steven R. Higgins, Xiaoming Hu, Paul Fenter, "Quantitative Lateral Force Microscopy Study of the Dolomite (104)-Water Interface," Langmuir 23 (17), 8909-8915 (2007). DOI: 10.1021/la700467q

M. Highland, B.C. Gundrum, Yee Kan Koh, R.S. Averback, David G. Cahill, V.C. Elarde, J.J. Coleman, D.A. Walko, E.C. Landahl, "Ballistic-phonon heat conduction at the nanoscale as revealed by time-resolved x-ray diffraction and time-domain thermoreflectance," Phys. Rev. A 76, 075337-1-075337-7 (2007). DOI: 10.1103/PhysRevB.76.075337

N. Hilairet, B. Reynard, Y. Wang, I. Daniel, S. Merkel, N. Nishiyama, S. Petitgirard, "High-Pressure Creep of Serpentine, Interseismic Deformation, and Initiation of Subduction," Science 318, 1910-1913 (2007). DOI: 10.1126/science

J.P. Hill, D.S. Coburn, Y.-J. Kim, T. Gog, D.M. Casa, C.N. Kodituwakku, H. Sinn, "A 2m inelastic X-ray scattering spectrometer at CMC-XOR, Advanced Photon Source," J. Synchrotron Rad. 14 (4), 361-365 (2007). DOI: 10.1107/S0909049507018006

C.E. Ho, A. Lee, K.N. Subramanian, W. Liu, "Early stage of material movements in eutectic SnPb solder joint undergoing current stressing at 150 °C," Appl. Phys. Lett. 91 (2), 021906-1-021906-3 (2007). DOI: 10.1063/1.2756292

Matthew Hogg, Pierre Aller, William Konigsberg, Susan S. Wallace, Sylvie Doublie, "Structural and Biochemical Investigation of the Role in Proofreading of a [beta] Hairpin Loop Found in the Exonuclease Domain of a Replicative DNA Polymerase of the B Family," J. Biol. Chem. 282 (2), 1432-1444 (2007). DOI: 10.1074/jbc.M605675200

C. Hohr, E.R. Peterson, N. Rohringer, J. Rudati, D.A. Arms, E.M. Dufresne, R.W. Dunford, D.L. Ederer, E.P. Kanter, B. Krassig, E.C. Landahl , R. Santra, S.H. Southworth, L. Young, "Alignment dynamics in a laser-produced plasma," Phys. Rev. A 75, 011403-1-011403-4 (2007). DOI: 10.1103/PhysRevA.75.011403

Marc A. Holbert, Timothy Sikorski, Juliana Carten, Danielle Snowflack, Santosh Hodawadekar, Ronen Marmorstein, "The Human Monocytic Leukemia Zinc Finger Histone Acetyltransferase Domain Contains DNA-binding Activity Implicated in Chromatin Targeting," J. Biol. Chem. 282 (50), 36603-36613 (2007). DOI: 10.1074/jbc.M705812200

M. Holt, M. Sutton, P. Zschack, H. Hong, T.-C. Chiang, "Dynamic Fluctuations and Static Speckle in Critical X-Ray Scattering from SrTiO(subscript 3)," Phys. Rev. Lett. 98 (6), 065501-1-065501-4 (2007). DOI: 10.1103/PhysRevLett.98.065501

H. Hong, L. Basile, P. Czoschke, A. Gray, T.-C. Chiang, "Self-organization of Pb islands on Si(111) caused by quantum size effects," Appl. Phys. Lett. 90, 051911-1-051911-3 (2007). DOI: 10.1063/1.2435615

H. Hong, T.-C. Chiang, "A six-circle diffractometer system for synchrotron X-ray studies of surfaces and thin film growth by molecular beam epitaxy," Nucl. Instrum. Methods A 572 (2), 942-947 (2007). DOI: 10.1016/j.nima.2006.11.056

Xinguo Hong, Guoyin Shen, VitaliB. Prakapenka, Matt Newville, MarkL. Rivers, StephenR. Sutton, "Intermediate states of GeO[subscript 2] glass under pressures up to 35 GPa," Phys. Rev. B 75, 104201-1-104201-5 (2007). DOI: 10.1103/PhysRevB.75.104201

X. Hong, G. Shen, V.B. Prakapenka, M.L. Rivers, S.R. Sutton, "Density measurements of noncrystalline materials at high pressure," Rev. Sci. Instrum. 78, 103905-1-103905-6 (2007). DOI: 10.1063/1.2795662

Kevin G. Honnell, Nenad Velisavljevic, Chris D. Adams, Paulo A. Rigg, Gary N. Chesnut, Robert M. Aikin, Jr., Jonathan C. Boettger, "Equation of State for TI-BETA-21S," Compression of Condensed Matter, M. Elert, M.D. Furnish, R. Chau, N. Holmes, J. Nguyen, eds., 955, AIP, (2007), 55 - 58. DOI: 10.1063/1.2833146

D. Horan, D. Bromberek, D. Meyer, G. Waldschmidt, "High-Power Tests of a Single-Cell Copper Accelerating Cavity Driven by Two Input Couplers," Proc. of the 22nd Particle Accelerator Conference (PAC07), IEEE, (2007), 2227 - 2229.

W. Seth Horne, Joshua L. Price, James L. Keck, Samuel H. Gellman, "Helix Bundle Quaternary Structure from [alpha/beta]-Peptide Foldamers," J. Am. Chem. Soc. 129 (14), 4178-4180 (2007). DOI: 10.1021/ja070396f

Geoff P. Horsman, Shiva Bhowmik, Stephen Y.K. Seah, Pravindra Kumar, Jeffrey T. Bolin, Lindsay D. Eltis, "The Tautomeric Half-reaction of BphD, a C-C Bond Hydrolase Kinetic and Structural Evidence Supporting a Key Role for Histidine 265 of the Catalytic triad," J. Biol. Chem. 282 (27), 19894-19904 (2007). DOI: 10.1074/jbc.M702237200

Aaron A. Hoskins, Mariya Morar, T. Joseph Kappock, Irimpan I. Mathews, Judith B. Zaugg, Timothy E. Barder, Paul Peng, Akimitsu Okamoto, Steven E. Ealick, JoAnne Stubbe, "N[superscript 5]-CAIR Mutase: Role of a CO[subsript 2] Binding Site and Substrate Movement in Catalysis," Biochemistry-US 46 (10), 2842-2855 (2007). DOI: 10.1021/bi602436g

P.Y. Hou, A.P. Paulikas, B.W. Veal, J.L. Smialek, "Thermally grown Al2O3 on a H2-annealed Fe3Al alloy: Stress evolution and film adhesion," Acta Mater. 55, 5601-5613 (2007). DOI: 10.1016/j.actamat.2007.06.018

X. Hou, M. Chen, Liqing Chen, Ed. J. Meehan, J. Xie, J. Huang, "X-ray sequence and crystal structure of luffaculin 1, a novel type 1 ribosome-inactivating protein," BMC Struct. Biol. 7, 29-38 (2007). DOI: 10.1186/1472-6807-7-29

Xiao-Min Hou, Ming-Huang Chen, Peng Qi, Li-Qing Chen, Edward J. Meehan, Ming-Dong Huang, "Crystallization and preliminary crystallographic analysis of B-Trichosanthin, an isoform of trichosanthin from the tuber root of trichosanthe kirilowii," Chin. J. Struct. Chem. 26 (11), 1303-1307 (2007).

Xiaowei Hou, Rujuan Liu, Stuart Ross, Eric J. Smart, Haining Zhu, Weimin Gong, "Crystallographic Studies of Human MitoNEET," J. Biol. Chem. 282 (46), 33242-33246 (2007). DOI: 10.1074/jbc.C700172200

D. Hovis, L. Hu, A. Reddy, A.H. Heuer, A.P. Paulikas, B.W. Veal, "In-situ studies of the TGO growth stresses and the martensitic transformation in the B2 phase in commercial Pt-modified NiAl and NiCoCrAlY bond coat alloys," Int. J. Mater. Res. 2007/12, 1209-1213 (2007). DOI: 10.3139/146.101586

Chih-chin Huang, Son N. Lam, Priyamvada Acharya, Min Tang, Shi-Hua Xiang, Syed Shahzad-ul Hussan, Robyn L. Stanfield, James Robinson, Joseph Sodroski, Ian A. Wilson, Richard Wyatt, Carole A. Bewley, Peter D. Kwong, "Structures of the CCR5 N Terminus and of a Tyrosine-Sulfated Antibody with HIV-1 gp120 and CD4," Science 317 (5846), 1930-1934 (2007). DOI: 10.1126/science.1145373

Danny T. Huang, Harold W. Hunt, Min Zhuang, Melanie D. Ohi, James M. Holton, Brenda A. Schulman, "Basis for a ubiquitin-like protein thioester switch toggling E1-E2 affinity," Nature 445, 394-398 (2007). DOI: 10.1038/nature05490

E.-W. Huang, R. Barabash, B. Clausen, Y. Wang, R. Yang, L. Li, H. Choo, P.K. Liaw, "Neutron Diffraction Study on Plastic behavior of a Nickel-Based Alloy Under the Monotonic-Tension and the Low-Cyclic-Fatigue Experiments," Plasticity 2007, A.S. Khan, B. Farrokh, eds., NEAT PRESS, (2007), 148 - 150.

Kexin Huang, Ian Ferrin-O'Connell, Wei Zhang, Gordon A. Leonard, Erin K. O'Shea, Florante A. Quiocho, "Structure of the Pho85-Pho80 CDK-Cyclin Complex of the Phosphate-Responsive Signal Transduction Pathway," Mol. Cell 28 (4), 614-623 (2007). DOI: 10.1016/j.molcel.2007.09.013

X.R. Huang, D.R. Black, A.T. Macrander, J. Maj, Y. Chen, M. Dudley, "High-geometrical-resolution imaging of dislocations in SiC using monochromatic synchrotron topography," Appl. Phys. Lett. 91, 231903-1-231903-3 (2007). DOI: 10.1063/1.2814032

X.R. Huang, R.W. Peng, Z. Wang, F. Gao, S.S. Jiang, "Charge-oscillation-induced light transmission through subwavelength slits and holes," Phys. Rev. A 76 (3), 035802-1-035802-4 (2007). DOI: 10.1103/PhysRevA.76.035802

Yuxiang Huang, Alena Fedarovich, Stephen Tomlinson, Christopher Davies, "Crystal structure of CD59: implications for molecular recognition of the complement proteins C8 and C9 in the membrane-attack complex," Acta Crystallogr. D 63, 714-721 (2007). DOI: 10.1107/S0907444907015557

Z. Huang, K.-J. Kim, "Review of X-ray Free-Electron Laser Theory," Phys. Rev. Spec. Top., Accel. Beams 10, 034801-1-034801-26 (2007). DOI: 10.1103/PhysRevSTAB.10.034801

Paul A. Hubbard, Dominique Padovani, Tetyana Labunska, Sarah A. Mahlstedt, Ruma Banerjee, Catherine L. Drennan, "Crystal Structure and Mutagenesis of the Metallochaperone MeaB: Insight into the Causes of Methylmalonic Aciduria," J. Biol. Chem. 282 (43), 31308-31316 (2007). DOI: 10.1074/jbc.M704850200

Gang Hu, Alexander B. Taylor, Lee McAlister-Henn, P. John Hart, "Crystal structure of the yeast nicotinamidase Pnc1p," Arch. Biochem. Biophys. 461 (1), 66-75 (2007). DOI: 10.1016/j.abb.2007.01.037

Anthony S. Humphreys, Aleksandra Filipovska, Susan J. Berners-Price, George A. Koutsantonis, Brian W. Skelton, Allan H. White, "Gold(I) chloride adducts of 1,3-bis(di-2-pyridylphosphino)propane: synthesis, structural studies and antitumour activity," Dalton T. 43, 4943-4950 (2007). DOI: 10.1039/b705008a

Xia Huo, Dan Su, Aojin Wang, Yujia Zhai, Jianxing Xu, Xuemei Li, Mark Bartlam, Fei Sun, Zihe Rao, "Preliminary molecular characterization and crystallization of mitochondrial respiratory complex II from porcine heart," FASEB J. 274 (6), 1524-1529 (2007). DOI: 10.1111/j.1742-4658.2007.05698.x

Nick D. Hutson, Brian C. Attwood, Kirk G. Scheckel, "XAS and XPS Characterization of Mercury Binding on Brominated Activated Carbon," Environ. Sci. Technol. 41 (5), 1747-1762 (2007). DOI: 10.1021/es062121q

H.E. Huxley, "Structural Behavior of Myosin Crossbridges during muscle contraction," Regulatory Mechanisms of striated Muscle Contration Series, Ebashi, Setsuro; Ohtsuki, Iwao, eds., Springer, 2007, 315 - 326.

Xiaozhen Hu, Huanchen Wang, Hengming Ke, Brian Kuhlman, "High-resolution design of a protein loop," Proc. Natl. Acad. Sci. USA 104 (45), 17668-17673 (2007). DOI: 10.1073/pnas.0707977104

Trevor Huyton, Cynthia Wolberger, "The crystal structure of the tumor suppressor protein pp32 (Anp32a): Structural insights into Anp32 family of proteins," Protein Sci. 16 (7), 1308-1315 (2007). DOI: 10.1110/ps.072803507

Trevor Huyton, Jian-Guo Zhang, Cindy S. Luo, Mei-Zhen Lou, Douglas J. Hilton, Nicos A. Nicola, Thomas P.J. Garrett, "An unusual cytokine:Ig-domain interaction revealed in the crystal structure of leukemia inhibitory factor (LIF) in complex with the LIF receptor," Proc. Natl. Acad. Sci. USA 104 (31), 12737-12742 (2007). DOI: 10.1073/pnas.0705577104

C. Höhr, E. Peterson, R.W. Dunford, E.P. Kanter, L. Young, E. Landahl, D.A. Walko, "A Simple Short-range Point-focusing Spatial Filter for Time-resolved X-ray Fluorescence," Proceedings of the Ninth International Conference on Synchrotron Radiation Instrumentation, Jae-Young Choi, Seungyu Rah, eds., 879, Springer, (2007), 1226 - 1229.

G.E. Ice, R.I. Barabash, "Chapter 79 White Beam Microdiffraction and Dislocations Gradients," Dislocations in Solids, F.R.N. Nabarro, J.P. Hirth, eds., Elsevier, 2007, 499 - 601. DOI: 10.1016/S1572-4859(07)80011-8

Hakim Iddir, Vladimir Komanicky, Serdar Ogut, Hoydoo You, Peter Zapol, "Shape of Platinum Nanoparticles Supported on SrTiO[subscript 3]: Experiment and Theory," J. Phys. Chem. C 111 (40), 14782-14789 (2007). DOI: 10.1021/jp073041r

Mari Ikuta, Maria Kornienko, Noel Byrne, John C. Reid, Shinji Mizuarai, Hidehito Kotani, Sanjeev K. Munshi, "Crystal structures of the N-terminal kinase domain of human RSK1 bound to three different ligands: Implications for the design of RSK1 specific inhibitors," Protein Sci. 16, 2626-2635 (2007). DOI: 10.1110/ps.073123707

J. Ilavsky, D. Shu, P.R. Jemian, G.G. Long, "Versatile Collimating Crystal Stage for a Bonse-Hart USAXS Instrument," AIP Conference Proceedings, Synchrotron Radiation Instrumentation: Ninth International Conference, Jae-young Choi and Seungya Rah, eds., CP879, AIP (2007), 1833 - 1836. DOI: 10.1063/1.2436427

Hookang Im, Marika Manolopoulou, Enrico Malito, Yuequan Shen, Ji Zhao, Marie Neant-Fery, Ching-Yu Sun, Stephen C. Meredith, Sangram S. Sisodia, Malcolm A. Leissring, Wei-Jen Tang, "Structure of Substrate-free Human Insulin-degrading Enzyme (IDE) and Biophysical Analysis of ATP-induced Conformational Switch of IDE," J. Biol. Chem. 282 (35), 25453-25463 (2007). DOI: 10.1074/jbc.M701590200

Kyoung-Su Im, K. Fezzaa, Y.J. Wang, X. Liu, Jin Wang, M.-C. Lai, "Particle tracking velocimetry using fast x-ray phase-contrast imaging," Appl. Phys. Lett. 90, 091919-1-091919-3 (2007). DOI: 10.1063/1.2711372

C.A. Impellitteri, O. Evans, B. Ravel, "Speciation of organotins in polyvinyl chloride pipe via X-ray absorption spectroscopy and in leachates using GC-PFPD after derivitisation," J. Environ. Monitor. 9, 358-365 (2007). DOI: 10.1039/b617711e

F. Inam, M.T. Shatnawi, D. Tafen, S.J.L. Billinge, P. Chen, D.A. Drabold, "An intermediate phase in Ge[subscript x]Se[subscript 1-x] glasses: experiment and simulation," J. Phys. Condens. Matter 19 (45), 455206-1-455206-10 (2007). DOI: 10.1088/0953-8984/19/45/455206

Junji Inukai, Dianxue Cao, Andrzej Wieckowski, Kee-Chul Chang, Andreas Menzel, Vladimir Komanicky, Hoydoo You, "In Situ Synchrotron X-ray Spectroscopy of Ruthenium Nanoparticles Modified with Selenium for an Oxygen Reduction Reaction," J. Phys. Chem. C 111 (45), 16889-16894 (2007). DOI: 10.1021/jp072581l

V. Iota, J. Park Klepeis, C. Yoo, J. C. Lang, D. Haskel, G. Srajer, "Electronic structure and magnetism in compressed 3d transition metals," Appl. Phys. Lett. 90, 042505-1-042505-3 (2007). DOI: 10.1063/1.2434184

Adriana Irimia, Robert L. Eoff, Pradeep S. Pallan, F. Peter Guengerich, Martin Egli, "Structure and Activity of Y-class DNA Polymerase DPO4 from Sulfolobus solfataricus with Templates Containing the Hydrophobic Thymine Analog 2,4-Difluorotoluene," J. Biol. Chem. 282 (50), 36421-36433 (2007). DOI: 10.1074/jbc.M707267200

Valentin Itoa, Choong-Shik Yoo, Jae-Hyun Klepeis, Zsolt Jenei, William Evans, Hyunchae Cynn, "Six-fold coordinated carbon dioxide VI," Nat. Mater. 6 (1), 34-38 (2007). DOI: 10.1038/nmat1800

Dmitri Ivanov, Oleg V. Tsodikov, Jeremy Kasanov, Tom Ellenberger, Gerhard Wagner, Tucker Collins, "Domain-swapped dimerization of the HIV-1 capsid C-terminal domain," Proc. Natl. Acad. Sci. USA 104 (11), 4353-4358 (2007). DOI: 10.1073/pnas.0609477104

Jaby Jacob, Robin S. Dothager, P. Thiyagarajan, Tobin R. Sosnick, "Fully Reduced Ribonuclease A Does not Expand at High Denaturant Concentration or Temperature," J. Mol. Biol. 367 (3), 609-615 (2007). DOI: 10.1016/j.jmb.2007.01.012

M.K. Jacobsen, R.S. Kumar, A.L. Cornelius, S.V. Sinogeiken, M.F. Nico, "High Pressure X-Ray Diffraction Studies of Bi[subscript 2-x]Sb[subscript x]Te[subscript 3] (x=0,1,2)," Shock Compression of Condensed Matter, M. Elert, M.D. Furnish, R. Chau, N. Holmes, J. Nguyen, eds., 955, AIP (2007), 171 - 174.

Pablo D. Jadzinsky, Guillermo Calero, Christopher J. Ackerson, David A. Bushnell, Roger D. Kornberg, "Structure of a Thiol Monolayer-Protected Gold Nanoparticle at 1.1 Å Resolution," Science 318, 430-433 (2007). DOI: 10.1126/science.1148624

B. Jakobsen, U. Lienert, J. Almer, W. Pantleon, H.F. Poulsen, "Properties and Dynamics of Bulk Subgrains Probed In-Situ Using a Novel X-Ray Diffraction Method," Mater. Sci. Forum 550, 613-618 (2007).

B. Jakobsen, H. F. Poulsen, U. Lienert, X. Huang, W. Pantleon, "Investigation of the deformation structure in an aluminium magnesium alloy by high angular resolution three-dimensional X-ray diffraction," Scripta Mater. 56 (9), 769-772 (2007). DOI: 10.1016/j.scriptamat.2007.01.022

B. Jakobsen, H.F. Poulsen, U. Lienert, W. Pantleon, "Direct determination of elastic strains and dislocation densities in individual subgrains in deformation structures," Acta Mater. 55 (10), 3421-3430 (2007). DOI: 10.1016/j.actamat.2007.01.049

R. Jaramillo, T.F. Rosenbaum, E.D. Isaacs, OG. Shpyrko, P.G. Evans, G. Aeppli, Z. Cai, "Microscopic and Macroscopic Signatures of Antiferromagnetic Domain Walls," Phys. Rev. Lett. 98 (11), 117206-1-117206-4 (2007). DOI: 10.1103/PhysRevLett.98.117206

Y. Jaski, D. Cookson, "Design and Application of CVD Diamond Windows for X-Rays at the Advanced Photon Source," Proc. of the Ninth International Conference on Synchrotron Radiation Instrumentation, 879, AIP, (2007), 1053 - 1056.

Henrik Jensen, Martin Bremholm, Rudi P. Nielsen, Karsten D. Joensen, Jan S. Pedersen, Henrik Birkedal, Yu-Sheng Chen, Jon Almer, Erik G. Sogaard, Steen B. Iversen, Bo B. Iversen, "In Situ High-Energy Synchrotron Radiation Study of Sol–Gel Nanoparticle Formation in Supercritical Fluids," Angew. Chem. Int. Ed. 119 (7), 1131-1134 (2007). DOI: 10.1002/ange.200603386

S. Jeudy, T.U. Schwartz, "Crystal structure of nucleoporin Nic96 reveals a novel, intricate helical domain architecture," J. Biol. Chem. 282 (48), 34904-34912 (2007). DOI: 10.1074/jbc.M705479200

Da Jia, "Crystallographic and Biochemical Studies of Mammalian de novo DNA Methyltransferases Dnmt3," Ph.D., Emery University, 2007.

Da Jia, Renata Z. Jurkowska, Xing Zhang, Albert Jeltsch, Xiaodong Cheng, "Structure of Dnmt3a bound to Dnmt3L suggests a model for de novo DNA methylation," Nature 449, 248-251 (2007). DOI: 10.1038/nature06146

D.T. Jiang, D. Shu, W. Sheng, "Canadian Light Source Front Ends Development," SYNCHROTRON RADIATION INSTRUMENTATION: Ninth International Conference on Synchrotron Radiation Instrumentation, Jae-Young Choi, Seungyu Rah, eds., 879, Amer. Inst. Physics (2007), 1022 - 1025. DOI: 10.1063/1.2436236

Zhang Jiang, Hyunjung Kim, X. Jiao, H. Lee, Y.-J. Lee, Y. Byun, S. Song, D. Eom, C. Li, M.H. Rafailovich, L.B. Lurio, S.K. Sinha, "Evidence for Viscoelastic Effects in Surface Capillary Waves of Molten Polymer Films," Phys. Rev. Lett. 98 (22), 227801-1-227801-4 (2007). DOI: 10.1103/PhysRevLett.98.227801

Zhang Jiang, Hyunjung Kim, Heeju Lee, Young Joo Lee, Xuesong Jiao, Chunhua Li, Laurence B. Lurio, Xuesong Hu, Jyotsana Lal, Suresh Narayanan, Alec Sandy, Miriam Rafailovich, Sunil K. Sinha, "Structure and dynamics of thin polymer films using synchrotron X-ray scattering," J. Appl. Crystallogr. 40 (1), s18-s22 (2007). DOI: 10.1107/S0021889807007996

J. Jin, X. Ma, C.-Y. Kim, D.E. Ellis, M.J. Bedzyk, "Adsorption of V on a Hematite (0001) Surface and its Oxidation: Submonolayer Coverage," Surf. Sci. 601 (14), 3082-3098 (2007). DOI: 10.1016/j.susc.2007.05.028

J. Jin, X. Ma, C.-Y. Kim, D.E. Ellis, M.J. Bedzyk, "Adsorption of V on a Hematite (0001) Surface and its Oxidation: Monolayer Coverage," Surf. Sci. 601 (19), 4571-4581 (2007). DOI: 10.1016/j.susc.2007.07.010

Tengchuan Jin, Feng Guo, Sunghee Kim, Andrew Howard, Yu-Zhu Zhang, "X-ray crystal structure of TNF ligand family member TL1A at 2.1 [angstrom]," Biochem. Biophys. Res. Commun. 364 (1), 1-6 (2007). DOI: 10.1016/j.bbrc.2007.09.097

X. Jin, R. Townley, L. Shapiro, "Structural Insight into AMPK Regulation: ADP Comes into Play," Structure 15, 1285-1295 (2007). DOI: 10.1016/j.str.2007.07.017

B. Johannessen, P. Kluth, R. Giulian, L.L. Araujo, D.J. Llewellyn, G.J. Foran, D.J. Cookson, M.C. Ridgway, "Modification of embedded Cu nanoparticles: Ion irradiation at room temperature," Nucl. Instrum. Methods B 257 (1-2), 37-41 (2007). DOI: 10.1016/j.nimb.2006.12.122

B. Johannessen, P. Kluth, D.J. Llewellyn, G.J. Foran, D.J. Cookson, M.C. Ridgway, "Amorphization of embedded Cu nanocrystals by ion irradiation," Appl. Phys. Lett. 90, 073119-1-073119-3 (2007). DOI: 10.1063/1.2644413

B. Johannessen, P. Kluth, D.J. Llewellyn, G.J. Foran, D.J. Cookson, M.C. Ridgway, "Ion-irradiation-induced amorphization of Cu nanoparticles embedded in SiO[subscript 2]," Phys. Rev. B 76, 184203-1-184203-11 (2007). DOI: 10.1103/PhysRevB.76.184203

Bryan J. Johnson, Jordi Cohen, Richard W. Welford, Arwen R. Pearson, Klaus Schulten, Judith P. Klinman, Carrie M. Wilmot, "Exploring Molecular Oxygen Pathways in Hansenula polymorpha Copper-containing Amine Oxidase," J. Biol. Chem. 282 (24), 17767-17776 (2007). DOI: 10.1074/jbc.M701308200

Erik C.B. Johnson, Enrico Malito, Yuequan Shen, Brad Pentelute, Dan Rich, Jan Florian, Wei-Jen Tang, Stephen B.H. Kent, "Insights from Atomic-Resolution X-Ray Structures of Chemically Synthesized HIV-1 Protease in Complex with Inhibitors," J. Mol. Biol. 373 (3), 573-586 (2007). DOI: 10.1016/j.jmb.2007.07.054

Jacqueline A. Johnson, Sungkyun Park, Sujoy Roy, Sunil K. Sinha, Ali Erdemir, Osman L. Eryilmaz, John B. Woodford, "Complementary neutron and x-ray reflectivity studies of 'near-frictionless' carbon films," J. Appl. Phys. 101, 103538-1-103538-6 (2007). DOI: 10.1063/1.2735678

Jacqueline A. Johnson, Stefan Schweizer, Anthony R. Lubinsky, "A Glass-Ceramic Plate for Mammography," J. Am. Ceram. Soc. 90 (3), 693-698 (2007). DOI: 10.1111/j.1551-2916.2007.01488.x

J.L. Jones, S.M. Motahari, M. Varlioglu, U. Lienert, J.V. Bernier, M. Hoffman, E. Ustundag, "Crack tip process zone domain switching in a soft lead zirconate titante ceramic," Acta Mater. 55 (16), 5538-5548 (2007). DOI: 10.1016/j.actamat.2007.06.012

Jeremiah S. Joseph, Kumar Singh Saikatendu, Vanitha Subramanian, Benjamin W. Neuman, Michael J. Buchmeier, Raymond C. Stevens, Peter Kuhn, "Crystal Structure of a Monomeric Form of Severe Acute Respiratory Syndrome Coronavirus Endonuclease nsp15 Suggests a Role for Hexamerization as an Allosteric Switch," J. Virol. 81 (12), 6700-6708 (2007). DOI: 10.1128/JVI.02817-06

Kevin Jude, "Crystallography at Ultrahigh and Infralow Resolution: Studies of Carbonic Anhydrase and Ribonuclease P," Ph.D., University of Pennsylvania, 2007.

Young-Shin Jun, Sanjit K. Ghose, Thomas P. Trainor, Peter J. Eng, Scot T. Martin, "Structure of the Hydrated (1014) Surface of Rhodochrosite (MnCO[subscript 3])," Environ. Sci. Technol. 41 (11), 3918-3925 (2007). DOI: 10.1021/es062171v

A.C. Jupe, A.P. Wilkinson, K. Luke, G.P. Funkhouser, "Slurry Consistency and In-situ Synchrotron X-ray Diffraction during the Early Hydration of Portland Cements with Calcium Chloride," J. Am. Ceram. Soc. 90 (8), 2595-2602 (2007). DOI: 10.1111/j.1551-2916.2007.01806.x

Ryan S. Justice, David H. Wang, Loon-Seng Tana, Dale W. Schaefer, "Simplified tube form factor for analysis of small-angle scattering data from carbon nanotube filled systems," J. Appl. Crystallogr. 40, s88-s92 (2007). DOI: 10.1107/S0021889807004153

Alexander Kaiser, C. Jaco Klok, John J. Socha, Wah-Keat Lee, Michael C. Quinlan, Jon F. Harrison, "Increase in tracheal investment with beetle size supports hypothesis of oxygen limitation on insect gigantism," Proc. Natl. Acad. Sci. USA 104 (32), 13198-13203 (2007). DOI: 10.1073/pnas.0611544104

Sachin Kale, Palaniappa Arjunan, William Furey, Frank Jordan, "A Dynamic Loop at the Active Center of the Escherichia coli Pyruvate Dehydrogenase Complex E1 Component Modulates Substrate Utilization and Chemical Communication with the E2 Component," J. Biol. Chem. 282 (38), 28106-28116 (2007). DOI: 10.1074/jbc,M704326200

A.R. Kampf, J.J. Pluth, Y.-S. Chen, "The crystal structure of meurigite," Am. Mineral. 92 (8-9), 1518-1524 (2007). DOI: 10.2138/am.2007.2486

S. Kamtekar, M.J. Hohn, H.S. Park, M. Schnitzbauer, A. Sauerwald, D. Soll, T.A. Steitz, "Toward understanding phosphoseryl-tRNA[superscript Cys] formation: the crystal structure of Methanococcus maripaludis phosphoseryl-tRNA synthetase," Proc. Natl. Acad. Sci. USA 104 (8), 2620-2625 (2007). DOI: 10.1073/pnas.0611504104

Hye Jung Kang, Pengcheng Dai, Branton J. Campbell, Peter J. Chupas, Stephan Rosenkranz, Peter L. Lee, Qingzhen Huang, Shiliang Li, Seiki Komiya, Yoichi Ando, "Microscopic annealing process and its impact on superconductivity in T'-structure electron-doped copper oxides," Nat. Mater. 6 (3), 224-229 (2007). DOI: 10.1038/nmat1847

Hyon Chol Kang, G. Brian Stephenson, Chian Liu, Ray Conley, Ruben Khachatryan, Michael Wieczorek, Albert T. Macrander, Hanfei Yan, Jörg Maser, Jon Hiller, Rachel Koritala, "Sectioning of multilayers to make a multilayer Laue lens," Rev. Sci. Instrum. 78, 046103-1-046103-3 (2007). DOI: 10.1063/1.2713439

S.-H. Kang, P. Kempgens, S. Greenbaum, A.J. Kropf, K. Amine, M.M. Thackeray, "Interpreting the structural and electrochemical complexity of 0.5Li[subscript 2]MnO[subscript 3]·0.5LiMO[subscript 2] electrodes for lithium batteries (M = Mn[subscript 0.5–x]Ni[subscript 0.5–x]Co[subscript 2x], 0 [less then or equal to] x [less then or equal to] 0.5)," J. Mater. Chem. 17 (20), 2069-2077 (2007). DOI: 10.1039/b618715c

S.-W. Kang, Q. Li, B.D. Chapman, R. Pindak, J.O. Cross, L. Li, M. Nakata, S. Kumar, "Micro-focus x-ray diffraction study of the columnar phase of porphyrin-based mesogens," Chem. Mater. 19 (23), 5657-5663 (2007). DOI: 10.1021/cm702063a

Shin-Woong Kang, Quan Li, Brandon D. Chapman, Ron Pindak, Julie O. Cross, Langfang Li, Michi Nakata, Satyendra Kumar, "Microfocus X-ray Diffraction Study of the Columnar Phase of Porphyrin-Based Mesogens," Chem. Mater. 19 (23), 5657-5663 (2007). DOI: 10.1021/cm702063a

You-Na Kang, Anh Tran, Robert H. White, Steven E. Ealick, "A Novel Function for the NTN Hydrolase Fold Demonstrated by the Structure of an Archeal Inosine Monophosphate Cyclohydrolase," Biochemistry-US 46 (17), 5050-5062 (2007). DOI: 10.1021/bi061637j

You-Na Kang, Anh Tran, Robert H. White, Steven E. Ealick, "A Novel Function for the N-Terminal Nucleophile Hydrolase Fold Demonstrated by the Structure of an Archaeal Inosine Monophosphate Cyclohydrolase," Biochemistry-US 46 (17), 5050-5062 (2007). DOI: 10.1021/bi061637j

J.M. Karner, J.J. Papike, S.R. Sutton, C.K. Shearer, G. McKay, L. Le, P. Burger, "Valence state partitioning of Cr between pyroxene-melt: Effects of pyroxene and melt composition and direct determination of Cr valence states by XANES. Application to Martian basalt QUE 94201 composition," Am. Mineral. 92 (11-12), 2002-2005 (2007). DOI: 10.2138/am.2007.2724

J.J. Kavich, M.P. Warusawithana, J.W. Freeland, P. Ryan, X. Zhai, R.H. Kodama, J.N. Eckstein, "Nanoscale suppression of magnetization at atomically assembled manganite interfaces: XMCD and XRMS measurements," Phys. Rev. B 76, 014410-1-014410-8 (2007). DOI: 10.1103/PhysRevB.76.014410

A. Kavner, D. Walker, S. Sutton, M. Newville, "Externally-driven charge transfer in silicates at high pressure and temperature: A XANES study," Earth Planet Sci. Lett. 256 (3-4), 314-327 (2007). DOI: 10.1016/j.epsl.2006.12.020

Jennifer M. Kavran, Sarath Gundllapalli, Patrick O'Donoghue, Markus Englert, Dieter Soll, Thomas A. Steitz, "Structure of pyrrolysyl-tRNA synthetase, an archaeal enzyme for genetic code innovation," Proc. Natl. Acad. Sci. USA 104 (27), 11268-11273 (2007). DOI: 10.1073/pnas.0704769104

Jennifer M. Kavran, Thomas A. Steitz, "Structure of the Base of the L7/L12 Stalk of the Haloarcula marismortui Large Ribosomal Subunit: Analysis of L11 Movements," J. Mol. Biol. 371 (4), 1047-1059 (2007). DOI: 10.1016/j.jmb.2007.05.091

A. Kazimirov, A.A. Sirenko, D.H. Bilderback, Z.-H. Cai, B. Lai, "Microbeam High Angular Resolution Diffraction Applied to Optoelectronic Devices," Synchrotron Radiation Instrumentation: Ninth International Conference on Synchrotron Radiation Instrumentation, Jae-Young Choi, Seungyu Rah, eds., 879, American Institute of Physics, (2007), 1395 - 1398. DOI: 10.1063/1.2436325

D.J. Keavney, D.B. Buchholz, Q. Ma, R.P.H. Chang, "Where does the spin reside in ferromagnetic Cu-doped ZnO?," Appl. Phys. Lett. 91, 012501-1-012501-3 (2007). DOI: 10.1063/1.2751587

S. R. Kelemen, M. Afeworki, M.L. Gorbaty, M. Sansone, P.J. Kwiatek, C.C. Walters, H. Freund, M. Siskin, A.E. Bence, D.J. Curry, M. Solum, R.J. Pugmire, M. Vandenbroucke, M. Leblond, F. Behar, "Direct Characterization of Kerogen by X-ray and Solid-State [superscript 13]C Nuclear Magnetic Resonance Methods," Energ. Fuel 21 (3), 1548-1561 (2007). DOI: 10.1021/ef060321h

Laura-Lee Clancy Kelley, Bret D. Dillard, Wolfram Tempel, Lirong Chen, Neil Shaw, Doowon Lee, M. Gary Newton, Frank J. Sugar, Francis E. Jenney, Jr., Han Seung Lee, Claudia Shah, Farris L. Poole III, Michael W.W. Adams, Jane S. Richardson, David C. Richardson, Zhi-Jie Liu, Bi-Cheng Wang, John Rose, "Structure of the hypothetical protein PF0899 from Pyrococcus furiosus at 1.85 Å resolution," Acta Crystallogr. F 63 (7), 549-552 (2007). DOI: 10.1107/S1744309107024049

Richard F. Kelley, Won Suk Shin, Boris Rybtchinski, Louise E. Sinks, Michael R. Wasielewski, "Photoinitiated Charge Transport in Supramolecular Assemblies of a 1,7,N,N-Tetrakis(zinc porphyrin)-perylene-3,4:9,10-bis(dicarboximide)," J. Am. Chem. Soc. 129 (11), 3173-3181 (2007). DOI: 10.1021/ja0664741

Shelly D. Kelly, Kenneth M. Kemner, Scott C. Brooks, "X-ray absorption spectroscopy identifies calcium-uranyl-carbonate complexes at environmental concentrations," Geochim. Cosmochim. Acta 71 (4), 821-834 (2007). DOI: 10.1016/j.gca.2006.10.013

Shelly D. Kelly, Peng Lu, Trudy Bolin, Soma Chattopadhyay, Matthew G. Newville, Tomohiro Shibata, Chen Zhu, "Chapter 3 Molecular Structure of Lead(II) Coprecipitated with Iron(III) Oxyhydroxide," Adsorption of Metals by Geomedia II: Variables, Mechanisms, and Model Applications, Mark O. Barnett and Douglas B. Kent, eds., Elsevier, 2007, 67 - 93. DOI: 10.1016/S1571-9197(07)07003-6

Shelly D. Kelly, Bruce Ravel, "EXAFS Analysis with Self-consistent Atomic Potentials," X-Ray Adsorption Fine Structure - XAFS13:13th International Conference, Britt Hedman, Piero Pianetta, eds., 882, Amer. Inst. Physics (2007), 135 - 137. DOI: 10.1063/1.2644452

K.M. Kemner, S.D. Kelly, "Synchrotron-based Techniques for Monitoring Metal Tranformations," Manual of Environmental Microbiology, C. Hurst, R. Crawford, J. Garland, D. Lipson, A. Mills, L. Stetzenbach, eds., Blackwell Publishing, 2007, 1183 - 1194.

Ken Kemner, Ed O'Loughlin, Shelly Kelly, Bruce Ravel, Maxim Boyanov, Deirdre Sholto-Douglas, Barry Lai, Russ Cook, Everett Carpenter, Vince Harris, Ken Nealson, "XAFS and X-Ray and Electron Microscopy Investigations of Radionuclide Transformations at the Mineral-Microbe Interface," XAFS13: 13th International Conference, Britt Hedman, Piero Pianetta, eds., 882, American Institute of Physics, (2007), 250 - 252. DOI: 10.1063/1.2644491

Michael Kemp, Brian Bae, John Paul Yu, Maloy Ghosh, Michael Leffak, Satish K. Nair, "Structure and Function of the c-myc DNA-unwinding Element-binding Protein DUE-B," J. Biol. Chem. 282 (14), 10441-10448 (2007). DOI: 10.1074/jbc.M609632200

Amy Kendall, Wen Bian, Justin Junn, Ian McCullough, David Gore, Gerald Stubbs, "Radial density distribution and symmetry of a Potexvirus, narcissus mosaic virus," Virology 357 (2), 158-164 (2007). DOI: 10.1016/j.virol.2006.07.051

Amy Kendall, Michele McDonald, Gerald Stubbs, "Precise determination of the helical repeat of tobacco mosaic virus," Virology 369 (1), 226-227 (2007). DOI: 10.1016/j.virol.2007.08.013

William P. Kennedy, Jamila R. Momand, Y. Whitney Yin, "Mechanism for De Novo RNA Synthesis and Initiating Nucleotide Specificity by T7 RNA Polymerase," J. Mol. Biol. 370 (2), 256-268 (2007). DOI: 10.1016/j.jmb.2007.03.041

M.S. Kent, H. Yim, J.K. Murton, D.Y. Sasaki, B.D. Polizzotti, M.B. Charati, K.L. Kiick, I. Kuzmenko, S. Satija, "Synthetic Polypeptide Adsorption to Cu-IDA Containing Lipid Films: A Model for Protein-Membrane Interactions," Langmuir 24 (3), 932-942 (2007). DOI: 10.1021/la700940x

Iain D. Kerr, Sivashankar Livakolundu, Zhenmei Li, Jeffrey C. Buchsbaum, Luke A. Knox, Richard Kriwacki, Stephen W. White, "Crystallographic and NMR Analyses of UvsW and UvsW.1 from Bacteriophage T4," J. Biol. Chem. 282 (47), 34392-34400 (2007). DOI: 10.1074/jbc.M705900200

Wei Ke, Christopher R. Bethel, Jodi M. Thomson, Robert A. Bonomo, Focco van den Akker, "Crystal Structure of KPC-2: Insights into Carbapenemase Activity in Class A [beta]-Lactamases," Biochem. J. 46, 5732-5740 (2007). DOI: 10.1021/bi700300u

Jason Key, Marco Hefti, Erin B. Purcell, Keith Moffat, "Structure of the Redox Sensor Domain of Azotobacter vinelandii NifL at Atomic Resolution: Signaling, Dimerization, and Mechanism," Biochemistry-US 46 (12), 3614-3623 (2007). DOI: 10.1021/bi0620407

Jason Key, Vukica Srajer, Reinhard Pahl, Keith Moffat, "Time-Resolved Crystallographic Studies of the Heme Domain of the Oxygen Sensor FixL: Structural Dynamics of Ligand Rebinding and Their Relation to Signal Transduction," Biochemistry-US 46 (16), 4706-4715 (2007). DOI: 10.1021/bi700043c

D.R. Khanal, T. Buonassisi, M.A. Marcus, A.A. Istratov, E.R. Weber, "Physical mechanisms of in situ surface gettering of metals in ribbon silicon for solar cells," Appl. Phys. Lett. 90, 102110-1-102110-3 (2007). DOI: 10.1063/1.2711523

V. Khanna, B.J. Kim, A. Hexemer, T.E. Mates, E.J. Kramer, X. Li, J. Wang, S.F. Hahn, "Chain Architecture Effects on the Diffusion of Cylinder-Forming Block Copolymers," Macromolecules 40 (7), 2443-2452 (2007). DOI: 10.1021/ma061703p

Boris Khaykovich, Chintan Hossain, Jennifer J. McManus, Aleksey Lomakin, David E. Moncton, George B. Benedek, "Structure of cholesterol helical ribbons and self-assembling biological springs," Proc. Natl. Acad. Sci. USA 104 (23), 9656-9660 (2007). DOI: 10.1073/pnas.0702967104

Ali Khounsary, Eric M. Dufresne, Cameron M. Kewish, Jun Qian, Lahsen Assoufid, Ray Conley, "Fabrication and evaluation of variable focus X-ray lenses," Nucl. Instrum. Methods A 582 (1), 117-119 (2007). DOI: 10.1016/j.nima.2007.08.075

Choel Kim, Cecilia Y. Cheng, S. Adrian Saldanha, Susan S. Taylor, "PKA-I Holoenzyme Structure Reveals a Mechanism for cAMP-Dependent Activation," Cell 130, 1032-1043 (2007). DOI: 10.1016/j.cell.2007.07.018

Chang-Yong Kim, Anthony A. Escuadro, Peter C. Stair, Michael J. Bedzyk, "Atomic-Scale View of Redox-Induced Reversible Changes to a Metal-Oxide Catalytic Surface: VO[subscript x]/[alpha]r-Fe[subscript 2]O[subscript 3](0001)," J. Phys. Chem. C 111 (5), 1874-1877 (2007). DOI: 10.1021/jp067862s

Chinkyo Kim, Rui Feng, Edward H. Conrad, Paul F. Miceli, "Nanoclustering of vacancies in thin metal films revealed by x-ray diffuse scattering," Appl. Phys. Lett. 91, 093131-1-093131-3 (2007). DOI: 10.1063/1.2779097

Eunja Kim, Ravhi Kumar, Philippe F. Weck, Andrew L. Cornelius, Malcolm Nicol, Sven C. Vogel, Jianzhong Zhang, Monika Hartl, Ashley C. Stowe, Luke Daemen, Yusheng Zhao, "Pressure-Driven Phase Transitions in NaBH[subscript 4]: Theory and Experiments," J. Phys. Chem. B 111 (50), 13873-13876 (2007). DOI: 10.1021/jp709840w

H. J. Kim, E. S. Bozin, S. M. Haile, G. J. Snyder, S. J. L. Billinge, "Nanoscale [alpha]-structural domains in the phonon-glass thermoelectric material [beta]-Zn[subscript 4]Sb[subscript 3]," Phys. Rev. B 75, 134103-1-134103-4 (2007). DOI: 10.1103/PhysRevB.75.134103

J.W. Kim, A. Kreyssig, P. Ryan, E. Mun, P.C. Canfield, A.I. Goldman, "X-ray resonant magnetic scattering study of spontaneous ferrimagnetism," Appl. Phys. Lett. 90, 202501-1-202501-3 (2007). DOI: 10.1063/1.2739403

J. Kim, H. You, S. Ducharme, S. Adenwalla, "The effect of interlayer interactions on the ferroelectric–paraelectric phase transition in multilayered thin films of vinylidene fluoride–trifluoroethylene copolymers," J. Phys. Condens. Matter 19 (8), 086206-1-086206-21 (2007). DOI: 10.1088/0953-8984/19/8/086206

K.-J. Kim, "Transverse-Transverse and Transverse-Longitudinal Phase-Space Converters for Tailoring Beam Phase Spaces," Proc. of the 22nd Particle Accelerator Conference (PAC07), IEEE, (2007), 775 - 779.

K.-J. Kim, V. Kumar, "Electron Beam Requirements for a Three-Dimensional Smith-Purcell Backward Wave Oscillator for Intense Terahertz Radiation," Phys. Rev. Spec. Top., Accel. Beams 10, 080702 (2007).

Young-Il Kim, Katharine Page, Ram Seshadri, "Synchrotron x-ray study of polycrystalline wurtzite Zn[sub1-x]Mg[subx]O(0 [less than or equal to] x [lessthan or equal to] 0.15): Evolution of crystal structure and polarization," Appl. Phys. Lett. 90 (10), 101904-1-101904-3 (2007). DOI: 10.1063/1.2711289

Pil-Sook G. Kim, Yongfeng Hu, Marie-C. Brandys, Tara J. Burchell, Richard J. Puddephatt, Tsun K. Sham, "X-ray-Excited Optical Luminescence (XEOL) and X-ray Absorption Fine Structures (XAFS) Studies of Gold(I) Complexes with Diphosphine and Bipyridine Ligands," Inorg. Chem. 46 (3), 949-957 (2007). DOI: 10.1021/ic0609352

S.H. Kim, C.L. Doose, "Development of a Model Superconducting Helical Undulator for the ILC Positron Source," Proc. of the 22nd Particle Accelerator Conference (PAC07), IEEE, (2007), 1136 - 1138.

Seokhee Kim, Juliana C. Malinverni, Piotr Sliz, Thomas J. Silhavy, Stephen C. Harrison, Daniel Kahne, "Structure and Function of an Essential Component of the Outer Membrane Protein Assembly Machine," Science 317, 961-964 (2007). DOI: 10.1126/science.1143993

Y.-J. Kim, J.P. Hill, S. Wakimoto, R.J. Birgeneau, F.C. Chou, N. Motoyama, K.M. Kojima, S. Uchida, D. Casa, T. Gog, "Observations on the resonant inelastic x-ray scattering cross section in copper oxide compounds," Phys. Rev. B 76, 155116-1-155116-7 (2007). DOI: 10.1103/PhysRevB.76.155116

Young-Il Kim, Katharine Page, Andi M. Limarga, David R. Clarke, Ram Seshadri, "Evolution of local structures in polycrystalline Zn1−xMgxO (0<=x<=0.15) studied by Raman spectroscopy and synchrotron x-ray pair-distribution-function analysis," Phys. Rev. B 76, 115204-1-115204-10 (2007). DOI: 10.1103/PhysRevB.76.115204

N.M. Kirby, D.J. Cookson, C.E. Buckley, E. Bovell, T. St. Pierre, "Iron K-Edge Anomalous Small Angle Xray Scattering at 15-ID-D at the Advanced Photon Source," J. Appl. Crystallogr. 40 (s1), s402-S407 (2007).

Melissa L. Kistler, Anish Bhatt, Guang Liu, Diego Casa, Tianbo Liu, "A Complete Macroion-'Blackberry' Assembly-Macroion Transition with Continuously Adjustable Assembly Sizes in {Mo[subscript 132]} Water/Acetone Systems," J. Am. Chem. Soc. 129 (20), 6453-6560 (2007). DOI: 10.1021/ja0685809

K. Kitts, S. Sutton, M. Newville, "Abundance and Charge State of Implanted Solar Wind Transition Metals in Individual Apollo 16 and 17 Lunar Soil Plagioclase Grains Determined In Situ Using Synchrotron X-ray Fluorescence," Lunar and Planetary Science XXXVIII, LPI, (2007), 1106.

K. Kitts, S. Sutton, M. Newville, "A New In Situ Method of Determining Relative Abundances and Charge States of Implanted Transition Metals in Individual Grains Using Synchrotron X-Ray Fluorescence," Lunar and Planetary Science XXXVIII, LPI, (2007), 1128.

Herbert E. Klei, Kevin Kish, Pin-Fang M. Lin, Qi Guo, Jacques Friborg, Ronald E. Rose, Yaqun Zhang, Valentina Goldfarb, David R. Langley, Michael Wittekind, Steven Sheriff, "X-Ray Crystal Structures of Human Immunodeficiency Virus Type 1 Protease Mutants Complexed with Atazanavir," J. Virol. 81 (17), 9525-9535 (2007). DOI: 10.1128/JVI.02503-05

P. Kluth, B. Johannessen, R. Giulian, C.S. Schnohr, G.J. Foran, D.J. Cookson, A.P. Byrne, M.C. Ridgway, "Ion irradiation effects on metallic nanocrystals," Radiat. Eff. Defect S. 162 (7&8), 501-513 (2007). DOI: 10.1080/10420150701472221

I. Koch, K. McPherson, P. Smith, L. Easton, K.G. Doe, K.J. Reimer, "Arsenic bioaccessibility and speciation in clams and seaweed from a contaminated marine environment," Mar. Pollut. Bull. 54 (5), 586-594 (2007). DOI: 10.1016/j.marpolbul.2006.12.004

Akiko Koide, Ryan N. Gilbreth, Kaori Esaki, Valentina Tereshko, Shohei Koide, "High-affinity single-domain binding proteins with a binary-code interface," Proc. Natl. Acad. Sci. USA 104 (16), 6632-6637 (2007). DOI: 10.1073/pnas.0700149104

Akiko Koide, Valentina Tereshko, Serdar Uysal, Katrina Margalef, Anthony A. Kossiakoff, Shohei Koide, "Exploring the Capacity of Minimalist Protein Interfaces: Interface Energetics and Affinity Maturation to Picomolar K[subscript D] of a Single-domain Antibody with a Flat Paratope," J. Mol. Biol. 373 (4), 941-953 (2007). DOI: 10.1016/j.jmb.2007.08.027

Mustafa Koksal, "Structural Studies on extradiol dioxygenases: strategies for improved bioremediation of PCBs," Ph.D., Purdue University, 2007.

Mustafa Koksal, "Structural Studies on Extradiol Dioxygenases: Strategies for Improved Bioremediation of PCBs," Masters, Purdue University, 2007.

Derrick J. Kolling, Joseph S. Brunzelle, SanMoon Lhee, Antony R. Crofts, Satish K. Nair, "Atomic Resolution Structures of Rieske Iron-Sulfur Protein: Role of Hydrogen Bonds in Tuning the Redox Potential of Iron-Sulfur Clusters," Structure 15 (1), 29-38 (2007). DOI: 10.1016/j.str.2006.11.012

R. Prakash Kolli, Zugang Mao, David N. Seidman, Denis T. Keane, "Identification of a Ni[subscript 0.5](Al[subscript 0.5−x]Mn[subscript x]) B2 phase at the heterophase interfaces of Cu-rich precipitates in an [alpha]-Fe matrix," Appl. Phys. Lett. 91, 241903-1-241903-3 (2007). DOI: 10.1063/1.2820378

Takashi Komesu, G.D. Waddill, S.-W. Yu, J.G. Tobin, "Spin dependent electron transmission through ferromagnetic thin films," Phys. Lett. A. 368 (1-2), 129-133 (2007). DOI: 10.1016/j.physleta.2007.03.070

Vasilis G. Komvokis, Eleni F. Iliopoulou, Iacovos A. Vasalos, Kostas S. Triantafyllidis, Christopher L. Marshall, "Development of optimized Cu–ZSM-5 deNOx catalytic materials both for HC-SCR applications and as FCC catalytic additives," Appl. Catal. A-Gen. 325 (2), 345-352 (2007). DOI: 10.1016/j.apcata.2007.02.035

Fathima Kona, Xingjue Xu, Philip Martin, Petr Kuzmic, Domenico L. Gatti, "Structural and Mechanistic Changes along an Engineered Path from Metallo to Nonmetallo 3-Deoxy-D-manno-octulosonate 8-Phosphate Synthases," Biochemistry-US 46 (15), 4532-4544 (2007). DOI: 10.1021/bi6024879

G.K.-W. Kong, J.J. Adams, R. Cappai, M.W. Parker, "Structure of Alzheimer's disease amyloid precursor protein copper-binding domain at atomic resolution," Acta Crystallogr. F 63 (10), 819-824 (2007). DOI: 10.1107/S1744309107041139

Geoffrey K.-W. Kong, Julian J. Adams, Hugh H. Harris, John F. Boas, Cyril C. Curtain, Denise Galatis, Colin L. Masters, Kevin J. Barnham, William J. McKinstry, Roberto Cappai, Michael W. Parker, "Structural Studies of the Alzheimer's Amyloid Precursor Protein Copper-binding Domain Reveal How it Binds Copper Ions," J. Mol. Biol. 367 (1), 148-161 (2007). DOI: 10.1016/j.jmb.2006.12.04

Olga Koroleva, Nodar Makharashvili, Charmain T. Courcelle, Justin Courcelle, Sergey Korolev, "Structural conservation of RecF and Rad50: implications for DNA recognition and RecF function," EMBO J. 26 (3), 867-877 (2007). DOI: 10.1038/sj.emboj.7601537

Nicole M. Koropatkin, David W. Koppenaal, Himadri B. Pakrasi, Thomas J. Smith, "The Structure of a Cyanobacterial Bicarbonate Transport Protein, CmpA," J. Biol. Chem. 282 (4), 2606-2614 (2007). DOI: 10.1074/jbc.M610222200

I. Koshelev, R. Huang, T. Graber, M. Meron, J.L. Muir, W. Lavender, K. Battaile, A.M. Mulichak, L.J. Keefe, "Upgrade of IMCA-CAT Bending Magnet Beamline 17-BM for Macromolecular Crystallography at the Advanced Photon Source," AIP Conference Proceedings, J.Y. Choi, S. Rah, eds., 879, Amer. Inst. Physics, (2007), 840 - 843. DOI: 10.1063/1.2436191

I.K. Koshelev, A.P. Paulikas, M. Beno, G. Jennings, J. Linton, M. Grimsditch, S. Uran, B.W. Veal, "Chromium-oxide Growth on Fe–Cr–Ni Alloy Studied with Grazing-emission X-ray Fluorescence," Oxid. Met. 68, 37-51 (2007). DOI: 10.1007/s11085-007-9053-2

Michael S. Kostelansky, Karim C. Lounes, Li Fang Ping, Sarah K. Dickerson, Oleg V. Gorkun, Susan T. Lord, "Probing the (gamma)2 Calcium-Binding Site: Studies with (gamma)D298,301A Fibrinogen Reveal Changes in the (gamma)294-301 Loop that Alter the Integrity of the "a" Polymerization Site," Biochemistry-US 46 (17), 5114-5123 (2007). DOI: 10.1021/bi602607a

Michael S. Kostelansky, Cayetana Schluter, Yuen Yi C. Tam, Sangho Lee, Rodolpho Ghirlando, Bridgette Beach, Elizabeth Conibear, James H. Hurley, "Molecular architecture and functional model of the complete yeast ESCRT-I heterotetramer," Cell 129, 485-498 (2007). DOI: 10.1016/j.cell.2007.03.016

Y.Y. Kostogorova-Beller, J.E. Shield, M. J. Kramer, "Order-disorder transformations in Sm–Co and Sm–Co–ZrC systems with 2-17 stoichiometry," J. Appl. Phys. 101, 09K521-1-09K521-2 (2007). DOI: 10.1063/1.2712525

Michael Kothe, Darcy Kohls, Simon Low, Rocco Coli, Alan C. Cheng, Suzanne L. Jacques, Theresa L. Johnson, Cristina Lewis, Christine Loh, Jim Nonomiya, Alissa L. Sheils, Kimberly A. Verdries, Thomas A. Wynn, Cyrille Kuhn, Yuan-Hua Ding, "Structure of the Catalytic Domain of Human Polo-like Kinase 1," Biochem. J. 46, 5960-5971 (2007). DOI: 10.1021/bi602474j

Andrey Y. Kovalevsky, Alexander A. Chumanevich, Fengling Liu, John M. Louis, Irene T. Weber, "Caught in the Act: The 1.5 Å Resolution Crystal Structures of the HIV-1 Protease and the I54V Mutant Reveal a Tetrahedral Reaction Intermediate," Biochemistry-US 46 (51), 14854-14864 (2007). DOI: 10.1021/bi700822g

Rumiana Koynova, Robert C. MacDonald, "Natural lipid extracts and biomembrane-mimicking lipid compositions are disposed to form nonlamellar phases, and they release DNA from lipoplexes most efficiently," BBA-Biomembranes 1768 (10), 2373-2382 (2007). DOI: 10.1016/j.bbamem.2007.04.026

Rumina Koynova, Yury S. Tarahovsky, Li Wang, Robert C. MacDonald, "Lipoplex formulation of superior efficacy exhibits high surface activity and fusogenicity, and readily releases DNA," BBA-Biomembranes 1768 (2), 375-386 (2007). DOI: 10.1016/j.bbamem.2006.10.016

Rumiana Koynova, Li Wang, Robert C. MacDonald, "Synergy in Lipofection by Cationic Lipid Mixtures: Superior Activity at the Gel-Liquid Crystalline Phase Transition," J. Phys. Chem. B 111 (27), 7786-7795 (2007). DOI: 10.1021/jp071286y

M.J. Kramer, "A strategy for rapid analysis of the variations in the reduced distribution function of liquid metals and metallic glasses," J. Appl. Crystallogr. 40 (1), 77-86 (2007). DOI: 10.1107/S0021889806042944

M.J. Kramer, R.T. Ott, D.J. Sordelet, "Anisotropic atomic structure in a homogeneously deformed metallic glass," J. Mater. Res. 22 (2), 382-388 (2007). DOI: 10.1557/JMR.2007.0044

V.V. Krishnamurthy, J. C. Lang, D. Haskel, D.J. Keavney, G. Srajer, J.L. Robertson, B.C. Sales, D. G. Mandrus, D.J. Singh, D.I. Bilc, "Ferrimagnetism in EuFe[subscript 4]Sb[subscript 12] due to the Interplay of f-Electron Moments and a Nearly Ferromagnetic Host," Phys. Rev. Lett. 98, 126403-1-126403-4 (2007). DOI: 10.1103/PhysRevLett.98.126403

Vengadesan Krishnan, Yuanyuan Xu, Kevin Macon, John E. Volanakis, Sthanam V.L. Narayana, "The Crystal Structure of C2a, the Catalytic Fragment of Classical Pathway C3 and C5 Convertase of Human Complement," J. Mol. Biol. 367 (1), 224-233 (2007). DOI: 10.1016/j.jmb.2006.12.039

Vengadesan Krishnan, Yuanyuan Xu, Kevin Macon, John E. Volanakis, Sthanam V.L. Narayana, "The Crystal Structure of C2a, the Catalytic Fragment of Classical Pathway C3 and C5 Convertase of Human Complement," J. Mol. Biol. 367 (1), 224-233 (2007). DOI: 10.1016/j.jmb.2006.12.039

Sergei O. Kucheyev, Milos Toth, Theodore F. Baumann, Alex V. Hamza, Jan Ilavsky, W. Ralph Knowles, Cheng K. Saw, Bradley L. Thiel, Vasiliki Tileli, Tonyvan Buuren, Y. Morris Wang, Trevor M. Willey, "Structure of Low-Density Nanoporous Dielectrics Revealed by Low-Vacuum Electron Microscopy and Small-Angle X-ray Scattering," Langmuir 23 (2), 353-356 (2007). DOI: 10.1021/la0619729

Mukesh Kumar, Hariharan Jayaram, Rodrigo Vasquez-Del Carpio, Xiaofang Jiang, Zenobia F. Taraporewala, Raymond H. Jacobson, John T. Patton, B.V. Venkataram Prasad, "Crystallographic and Biochemical Analysis of Rotavirus NSP2 with Nucleotides Reveals a Nucleoside Diphosphate Kinase-Like Activity," J. Virol. 81 (22), 12272-12284 (2007). DOI: 10.1128/JVI.00984-07

Ravhi S. Kumar, Andrew L. Cornelius, Malcolm F. Nicol, "Structure of nanocrystalline ZnO up to 85GPa," Curr. Appl. Phys. 7 (2), 135-138 (2007). DOI: 10.1016/j.cap.2006.02.009

Ravhi S. Kumar, Andrew L. Cornelius, Malcolm F. Nicol, "Equation of state of nanocrystalline BaTiO[subscript 3] up to 52 GPa at room temperature," Phys. Status Solidi. b. 244 (1), 290-294 (2007). DOI: 10.1002/pssb.200672572

Ravhi S. Kumar, Andrew L. Cornelius, Michael G. Pravica, Malcolm F. Nicol, Michael Y. Hu, Paul C. Chow, "Bonding changes in single wall carbon nanotubes (SWCNT) on Ti and TiH[subscript 2] addition probed by X-ray Raman scattering," Diam. Relat. Mater. 16 (4-7), 1136-1139 (2007). DOI: 10.1016/j.diamond.2006.12.047

Ravhi S. Kumar, Andrew L. Cornelius, Maddury Somayazulu, Daniel Errandonea, Malcolm F. Nicol, Jason Gardner, "High pressure structure of Tb[subscript 2]Ti[subscript 2]O[subscript 7] pyrochlore at cryogenic temperatures," Phys. Status Solidi. b. 244 (1), 266-269 (2007). DOI: 10.1002/pssb.200672558

Ravhi S. Kumar, Eunja Kim, Oliver Tschauner, Andrew L. Cornelius, "Pressure-induced structural phase transition in NaAlH[subsrcipt 4]," Phys. Rev. B 75, 174110-1-174110-7 (2007). DOI: 10.1103/PhysRevB.75.174110

Ravhi S. Kumar, Michael G. Pravica, Andrew L. Cornelius, Malcolm F. Nicol, Michael Y. Hu, Paul C. Chow, "X-ray Raman scattering studies on C[subscript 60] fullerenes and multi-walled carbon nanotubes under pressure," Diam. Relat. Mater. 16 (4-7), 1250-1253 (2007). DOI: 10.1016/j.diamond.2006.11.103

Sandeep Kumar, Tracy M. Davis, Harikrishnan Ramanan, R. Lee Penn, Michael Tsapatsis, "Aggregative Growth of Silicalite-1," J. Phys. Chem. B 111 (13), 3398-3403 (2007). DOI: 10.1021/jp0677445

Mayfair C. Kung, Robert J. Davis, Harold H. Kung, "Understanding Au-Catalyzed Low-Temperature CO Oxidation," J. Phys. Chem. C 111 (32), 11767-11775 (2007). DOI: 10.1021/jp072102i

Bradley P. Ladewig, Robert B. Knott, Anita J. Hill, James D. Riches, John W. White, Darren J. Martin, Joao C. Diniz da Costa, Gao Qing Lu, "Physical and Electrochemical Characterization of Nanocomposite Membranes of Nafion and Functionalized Silicon Oxide," Chem. Mater. 19, 2372-2381 (2007). DOI: 10.1021/cm0628698

Bradley P. Ladewig, Robert B. Knott, Darren J. Martin, Joao C. Diniz da Costa, Gao Qing Lu, "Nafion-MPMDMS nanocomposite membranes with low methanol permeability," Electrochem. Commun. 9 (4), 781-786 (2007). DOI: 10.1016/j.elecom.2006.11.015

B. Lai, S. Vogt, J. Maser, "Beamline Design for a BioNanoprobe: Stability and Coherence," AIP Conference Proceedings, J.Y. Choi, S. Rah, eds., 879, Amer. Inst. Physics, (2007), 1313 - 1316. DOI: 10.1063/1.2436305

D.L. Lakshtanov, S.V. Sinogeikin, K.D. Litasov, V.B. Prakapenka, H. Hellwig, J. Wang, C. Sanches-Valle, J. Perrillat, B. Chen, M. Somayazulu, J. Li, E. Ohtani, J.D. Bass, "The post-stishovite phase transition in hydrous alumina-bearing SiO[subscript 2] in the lower mantle of the earth," Proc. Natl. Acad. Sci. USA 104 (34), 13588-13590 (2007). DOI: 10.1073/pnas.0706113104

S. Lam, F. Heigl, P.-S.G. Kim, T.K. Sham, R.A. Gordon, D. Brewe, T. Regier, I. Coulthard, R.I.R. Blyth, "X-ray Excited Optical Luminescence from (Ru(bipy)[subscript3])[superscript 2+] and (Ru(phen)[subscript3])[superscript 2+] in the Energy and Time Domains," AIP Conference Proceedings, B. Hedman, P. Pianetta, eds., 882, American Institute of Physics, (2007), 687 - 689.

Fei Lan, Robert E. Collins, Rossella DeCegli, Roman Alpatov, John R. Horton, Xiaobing Shi, Or Gozani, Xiaodong Cheng, Yang Shi, "Recognition of unmethylated histone H3 lysine 4 links BHC80 to LSD1-mediated gene repression," Nature 448, 718-722 (2007). DOI: 10.1038/nature06034

Alexander C. Langheinrich, Agata Michniewicz, Daniel G. Sedding, Barry Lai, Steven M. Jorgensen, Rainer M. Bohle, Erik L. Ritman, "Quantitative X-Ray Imaging of Intraplaque Hemorrhage in Aortas of ApoE[superscript -/-]/LDL[superscript -/-] Double Knockout Mice," Invest. Radiol. 42 (5), 263-273 (2007).

P.J. LaRiviere, P. Vargas, M. Newville, S.R. Sutton, "Reduced-Scan Schemes for X-Ray Fluorescence Computed Tomography," IEEE T. Nucl. Sci. 54 (5), 1535-1542 (2007). DOI: 10.1109/TNS.2007.906167

Nicole LaRonde-LeBlanc, Arti N. Santhanam, Alyson R. Baker, Alexander Wlodawer, Nancy H. Colburn, "Structural Basis for Inhibition of Translation by the Tumor Suppressor Pdcd4," Mol. Cell Biol. 27 (1), 147-156 (2007). DOI: 10.1128/MCB.00867-06

B.C. Larson, A. El-Azab, W. Yang, J.Z. Tischler, W.J. Liu, G.E. Ice, "Experimental characterization of the mesoscale dislocation density tensor," Philos. Mag. 87 (8-9), 1327-1347 (2007). DOI: 10.1080/14786430600943930

Heather N. Larson, "Structural Studies of Intersubunit Communication in Mitochondrial Aldehyde Dehydrogenase," Ph.D., Indiana University, 2007.

Heather N. Larson, Jianzhong Zhou, Zhiqiang Chen, Jonathan S. Stamler, Henry Weiner, Thomas D. Hurley, "Structural and Functional Consequences of Coenzyme Binding to the Inactive Asian Variant of Mitochondrial Aldehyde Dehydrogenase," J. Biol. Chem. 282 (17), 12940-12950 (2007). DOI: 10.1074/jbc.M607959200

Kristi Lazar, "Non-Amyloid Protein Aggregates," Masters, University of Chicago, 2007.

Amy Lazicki, "Experimental and theoretical investigation of the properties of low-z lithium-containing compounds at high pressure," Ph.D., University of California, Davis, 2007.

A. Lee, W. Liu, C.E. Ho, K.N. Subramanian, "Synchrotron x-ray microscopy studies on electromigration of a two-phase material," J. Appl. Phys. 102, 053507-1-053507-5 (2007). DOI: 10.1063/1.2777122

Byeongdu Lee, Chieh-Tsung Lo, Soenke Seifert, Nancy L. Dietz Rago, Randall E. Winans, Pappannan Thiyagarajan, "Anomalous Small-Angle X-ray Scattering Characterization of Bulk Block Copolymer/Nanoparticle Composites," Macromolecules 40 (12), 4235-4243 (2007). DOI: 10.1021/ma062916h

Byeongdu Lee, Insun Park, Haewoong Park, Chieh-Tsung Lo, Taihyun Chang, Randall E. Winans, "Electron density map using multiple scattering in grazing-incidence small angle x-ray scattering," J. Appl. Crystallogr. 40 (3), 496-504 (2007). DOI: 10.1107/S0021889807011399

Dong Ryeol Lee, John W. Freeland, Yongseong Choi, George Srajer, Vitali Metlushko, Bojan Ilic, "X-ray resonant magnetic scattering study of magnetization reversals in a nanoscale spin-valve array," Phys. Rev. B 76, 144425-1-144425-5 (2007). DOI: 10.1103/PhysRevB.76.144425

Mihwa Lee, Camilla W. Chan, Stephen C. Graham, Richard I. Christopherson, J. Mitchell Guss, Megan J. Maher, "Structures of Ligand-free and Inhibitor Complexes of Dihydroorotase from Escherichia coli: Implications for Loop Movement in Inhibitor Design," J. Mol. Biol. 370 (5), 812-825 (2007). DOI: 10.1016/j.jmb.2007.05.019

Sung Keun Lee, Peter J. Eng, Ho-kwang Mao, Yue Meng, Jinfu Shu, "Structure of Alkali Borate Glasses at High Pressure: B and Li K-Edge Inelastic X-Ray Scattering Study," Phys. Rev. Lett. 98, 105502-1-105502-4 (2007). DOI: 10.1103/PhysRevLett.98.105502

Sung Haeng Lee, Frederic Kerff, David Chereau, Francois Ferron, Alexandra Klug, Roberto Dominguez, "Structural Basis for the Actin-Binding Function of Missing-in-Metastasis," Structure 15 (2), 145-155 (2007). DOI: 10.1016/j.str.2006.12.005

S.Y. Lee, C.P. Kim, J.D. Almer, U. Lienert, E. Ustundag, W.L. Johnson, "Pseudo-binary phase diagram for Zr-based in situ [beta] phase composites," J. Mater. Res. 22 (2), 538-543 (2007). DOI: 10.1557/JMR.2007.0066

Sang Soo Lee, Kathryn L. Nagy, Paul Fenter, "Distribution of barium and fulvic acid at the mica–solution interface using in-situ X-ray reflectivity," Geochim. Cosmochim. Acta 71 (23), 5763-5781 (2007). DOI: 10.1016/j.gca.2007.05.031

Y.-R. Lee, A. Gray, J. Tischler, P. Czoschke, H. Hong, S.-L. Chang, T.-C. Chiang, "Quantum Oscillations and Beats in X-Ray Diffraction during Film Growth," Phys. Rev. Lett. 99, 156103-1-156103-4 (2007). DOI: 10.1103/PhysRevLett.99.156103

Y. Lee, B.N. Harmon, A.I. Goldman, J.C. Lang, "Temperature dependent x-ray magnetic circular dichroism in Er[subscript 2]Fe[subscript 17]," J. Appl. Phys. 101, 09G525-1-09G525-3 (2007). DOI: 10.1063/1.2713428

C. Leighton, M. Manno, A. Cady, J.W. Freeland, L. Wang, K. Umemoto, R.M. Wentzcovitch, T.Y. Chen, C.L. Chien, P.L. Kuhns, M.J. R. Hoch, A.P. Reyes, W.G. Moulton, E.D. Dahlberg, J. Checkelsky, J. Eckert, "Composition controlled spin polarization in Co[subscript 1-x]Fe[subscript x]S[subscript 2] alloys," J. Phys. Condens. Matter 19 (31), 315219-1-315219-22 (2007). DOI: 10.1088/0953-8984/19/31/315219

M.F. Lengke, B. Ravel, M.E. Fleet, G. Wanger, R.A. Gordon, G. Southam, "Precipitation of gold by the reaction of aqueous gold(III) chloride with cyanobacteria at 25 - 80 C - Studied by X-ray absorption spectroscopy," Can. J. Chem. 85, 651-659 (2007). DOI: 10.1139/V07-024

Dmitry V. Lesnyak, Jerzy Osipiuk, Tatiana Skarina, Petr V. Sergiev, Alexey A. Bogdanov, Aled Edwards, Alexei Savchenko, Andrzej Joachimiak, Olga A. Dontsova, "Methyltransferase That Modifies Guanine 966 of the 16 S rRNA: FUNCTIONAL IDENTIFICATION AND TERTIARY STRUCTURE," J. Biol. Chem. 282 (8), 5880-5887 (2007). DOI: 10.1074/jbc.M608214200

Bogdan M. Leu, Nathan J. Silvernail, Marek Z. Zgierski, Graeme R.A. Wyllie, Mary K. Ellison, W. Robert Scheidt, Jiyong Zhao, Wolfgang Sturhahn, E. Ercan Alp, J. Timothy Sage, "Quantitative Vibrational Dynamics of Iron in Carbonyl Porphyrins," Biophys. J. 92, 3764-3783 (2007). DOI: 10.1529/biophysj.106.093773

Elena J. Levin, Dmitry A. Kondrashov, Gary E. Wesenberg, George N. Phillips, Jr., "Ensemble Refinement of Protein Crystal Structures: Validation and Application," Structure 15 (9), 1040-1052 (2007). DOI: 10.1016/j.str.2007.06.019

E.J. Levin, D.A. Kondrashov, G.E. Wesenberg, G.N. Phillips, "Ensemble refinement of protein crystal structures: validation and application," Struct. Fold. Des. 15, 1040-1052 (2007). DOI: 10.1016/j.str.2007.06.019

L.E. Levine, G.G. Long, J. Ilavsky, R.A. Gerhardt, R. Ou, C.A. Parker, "Self-assembly of carbon black into nanowires that form a conductive three dimensional micronetwork," Appl. Phys. Lett. 90, 014101-1-014101-3 (2007). DOI: 10.1063/1.242501

Bo Liang, Song Xue, Rebecca M. Terns, Michael P. Terns, Hong Li, "Substrate RNA positioning in the archaeal H/ACA ribonucleoprotein complex," Nat. Struct. Mol. Biol. 14 (12), 1189-1195 (2007). DOI: 10.1038/nsmb1336

B. Li, R.C. Liebermann, "Indoor seismology by probing the Earth's interior by using sound velocity measurements at high pressures and temperatures," Proc. Natl. Acad. Sci. USA 104 (22), 9145-9150 (2007). DOI: 10.1073/pnas.0608609104

Raquel L. Lieberman, Brandon A. Wustman, Pedro Huertas, Allan C. Powe Jr, Corey W. Pine, Richie Khanna, Michael G. Schlossmacher, Dagmar Ringe, Gregory A. Petsko, "Structure of acid [beta]-glucosidase with pharmacological chaperone provides insight into Gaucher disease," Nat. Chem. Biol. 3 (2), 101-107 (2007). DOI: 10.1038/nchembio850

Kirsten Liebert, John R. Horton, Sanjay Chahar, Marcella Orwick, Xiaodong Cheng, Albert Jeltsch, "Two Alternative Conformations of S-Adenosyl-L-homocysteine Bound to Escherichia coli DNA Adenine Methyltransferase and the Implication of Conformational Changes in Regulating the Catalytic Cycle," J. Biol. Chem. 282 (31), 22848-22855 (2007). DOI: 10.1074/jbc.M700926200

U. Lienert, J. Almer, B. Jakobsen, W. Pantleon, H.F. Poulsen, D. Hennessy, C. Xiao, R.M. Suter, "3-Dimensional Characterization of Polycrystalline Bulk Materials Using High-Energy Synchrotron Radiation," Mater. Sci. Forum 539-543, 2353-2358 (2007).

H.P. Liermann, A.K. Singh, M. Somayazulu, S.K. Saxena, "Compression behavior of NbC under nonhydrostatic conditions to 57 GPa," Int. J. Refract. Met. H. 25 (5-6), 386-391 (2007). DOI: 10.1016/j.ijrmhm.2006.12.002

Daniel Lietha, Xinming Cai, Derek F. Ceccarelli, Yiquin Li, Michael D. Schaller, Michael J. Eck, "Structural basis for the autoinhibition of focal adhesion kinase," Cell 129 (8), 1177-1187 (2007). DOI: 10.1016/j.cell.2007.05.041

Feng Li, Pradeep S. Pallan, Martin A. Maier, Kallanthottathil G. Rajeev, Steven L. Mathieu, Christoph Kreutz, Yupeng Fan, Joyodita Sanghvi, Ronald Micura, Eriks Rozners, Muthiah Manoharan, Martin Egli, "Crystal structure, stability and in vitro RNAi activity of oligoribonucleotides containing the ribo-difluorotoluyl nucleotide: insights into substrate requirements by the human RISC Ago2 enzyme," Nucleic Acids Res. 35 (19), 6424-6438 (2007). DOI: 10.1093/nar/gkm664

Jun Li, Mischa Machius, Jacinta L. Chuang, R. Max Wynn, David T. Chuang, "The Two Active Sites in Human Branched-chain [alpha]-Keto Acid Dehydrogenase Operate Independently without an Obligatory Alternating-site Mechanism," J. Biol. Chem. 282 (16), 11904-11913 (2007). DOI: 10.1074/jbc.M610843200

R. Lill, E. Norum, L. Morrison, N. Sereno, G. Waldschmidt, D. Walters, S. Smith, T. Straumann, "Design and Performance of the LCLS Cavity BPM System," Proc. of the 22nd Particle Accelerator Conference (PAC07), IEEE, (2007), 4366 - 4368.

Santiago Lima, Roman Khristoforov, Cory Momany, Robert S. Phillips, "Crystal Structure of Homo sapiens Kynureninase," Biochemistry-US 46 (10), 2735-2744 (2007). DOI: 10.1021/bi0616697

Eun Jeong Lim, Sowmya Sampath, Jerry Coll-Rodriguez, Jack Schmidt, Kallol Ray, David W. Rodgers, "Swapping the Substrate Specificities of the Neuropeptidases Neurolysin and Thimet Oligopeptidase," J. Biol. Chem. 282 (13), 9722-9732 (2007). DOI: 10.1074/jbc.M609897200

Binhua Lin, David G. Schultz, Xiao-Min Lin, Dongxu Li, Jeff Gebhardt, Mati Meron, P.J. Viccaro, "Langmuir monolayers of gold nanoparticles," Thin Solid Films 515 (14), 5669-5673 (2007). DOI: 10.1016/j.tsf.2006.12.023

Jung-Fu Lin, Hiroshi Fukui, David Prendergast, Takuo Okuchi, Yong Q. Cai, Nozomu Hiraoka, Choong-Shik Yoo, Andrea Trave, Peter Eng, Michael Y. Hu, Paul Chow, "Electronic bonding transition in compressed SiO[subscript 2] glass," Phys. Rev. B 75 (1), 012201-1-012201-4 (2007). DOI: 10.1103/PhysRevB.75.012201

Jung-Fu Lin, Steven D. Jacobsen, Wolfgang Sturhahn, Jennifer M. Jackson, Jiyong Zhao, Choong-Shik Yoo, "Correction to 'Sound velocities of ferropericlase in the Earth's lower mantle'," Geophys. Res. Lett. 34, L09301 (2007). DOI: 10.1029/2007GL029880

Jung-Fu Lin, Viktor V. Struzhkin, Alexander G. Gavriliuk, Igor Lyubutin, "Comment on 'Spin crossover in (Mg,Fe)O: A Mossbauer effect study with an alternative interpretation of x-ray emission spectroscopy data'," Phys. Rev. B 75, 177102-1-177102-4 (2007). DOI: 10.1103/PhysRevB.75.177102

J.-F. Lin, G. Vanko, S.D. Jacobsen, V. Iota, V.V. Struzhkin, V.B. Prakapenka, A. Kuznetsov, C.-S. Yoo, "Spin transition zone in Earth's lower mantle," Science 317, 1740-1743 (2007). DOI: 10.11/science.1144997

Jan Lipfert, "Small-Angle X-ray Scattering of RNA, Proteins, and Membrane Protein-Detergent Complexes," Ph.D., Stanford University, 2007.

Jan Lipfert, Vincent B. Chu, Yu Bai, Daniel Herschlag, Sebastian Doniach, "Low-resolution Models for Nucleic Acids from Small-Angle X-ray Scattering," J. Appl. Crystallogr. 40 (1), 229-234 (2007). DOI: 10.1107/S0021889807001707

Jan Lipfert, Linda Columbus, Vincent B. Chu, Sebastian Doniach, "Analysis of Small-Angle X-ray Scattering Data of Protein-Detergent Complexes by Singular Value Decompositon," J. Appl. Crystallogr. 40 (1), 235-239 (2007). DOI: 10.1107/S0021889807005791

Jan Lipfert, Linda Columbus, Vincent B. Chu, Scott A. Lesley, S. Doniach, "Size and Shape of Detergent Micelles Determined by Small-Angle X-ray Scattering," J. Phys. Chem. B 111 (43), 12427-12438 (2007). DOI: 10.1021/jp073016l

J. Lipfert, R. Das, V.B. Chu, M. Kudaravalli, N. Boyd, D. Herschlag, S. Doniach, "Structural Transitions and Thermodynamics of a Glycine-Dependent Riboswitch from Vibrio cholerae," J. Mol. Biol. 365 (5), 1393-1406 (2007). DOI: 10.1016/j.jmb.2006.10.022

J. Lipfert, S. Doniach, "Small-angle x-ray scattering from RNA, proteins and protein complexes," Annu. Rev. Bioph. Biom. 36, 307-327 (2007). DOI: 10.1146/annurev.biophys.36.040306.132655

M.J. Lipp, J. Park Klepeis, B.J. Baer, H. Cynn, W.J. Evans, V. Iota, C.-S. Yoo, "Transformation of molecular nitrogen to nonmolecular phases at megabar pressures by direct laser heating," Phys. Rev. B 76, 014113-1-014113-5 (2007). DOI: 10.1103/PhysRevB.76.014113

Qing' An Li, K.E. Gray, H. Zheng, H. Claus, S. Rosenkranz, S. Nyborg Ancona, R. Osborn, J.F. Mitchell, Y. Chen, J.W. Lynn, "Reentrant Orbital Order and the True Ground State of LaSr[subscript 2]Mn[subscript 2]O[subscript 7]," Phys. Rev. Lett. 98, 167201-1-167201-4 (2007). DOI: 10.1103/PhysRevLett.98.167201

Qianzhi Li, Mark R. Nance, Rima Kulikauskas, Kevin Nyberg, Richard Fehon, P. Andrew Karplus, Anthony Bretscher, John J.G. Tesmer, "Self-masking in an Intact ERM-merlin Protein: An Active Role for the Central [alpha]-Helical Domain," J. Mol. Biol. 365 (5), 1446-1459 (2007). DOI: 10.1016/j.jmb.2006.10.075

Dongxiang Liu, Navid Madani, Ying Li, Rong Cao, Won-Tak Choi, Sameer P. Kawatkar, Mi Youn Lim, Santosh Kumar, Chang-Zhi Dong, Jun Wang, Julie D. Russell, Caroline R. Lefebure, Jing An, Scott Wilson, Yi-Gui Gao, Luke A. Pallansch, Joseph G. Sodroski, Ziwei Huang, "Crystal Structure and Structural Mechanism of a Novel Anti-Human Immunodeficiency Virus and D-Amino Acid-Containing Chemokine," J. Virol. 81 (20), 11489-11498 (2007). DOI: 10.1128/JVI.02845-06

Dali Liu, Edwin Pozharski, Bryan W. Lepore, Mengmeng Fu, Richard B. Silverman, Gregory A. Petsko, Dagmar Ringe, "Inactivation of Escherichia

coli L-Aspartate Aminotransferase by (S)-4-Amino-4,5-dihydro-2-thiophenecarboxylic Acid Reveals 'A Tale of Two Mechanisms'," Biochemistry-US 46 (37), 10517-10527 (2007). DOI: 10.1021/bi700663n

Dali Liu, Pei W. Thomas, Jessica Momb, Quyen Q. Hoang, Gregory A. Petsko, Dagmar Ringe, Walter Fast, "Structure and Specificity of a Quorum-Quenching Lactonase (AiiB) from Agrobacterium tumefaciens," Biochemistry-US 46 (42), 11789-11799 (2007). DOI: 10.1021/bi7012849

Di-Jia Liu, Junbing Yang, David J. Gosztola, "Investigation of Aligned Carbon Nanotubes as a Novel Catalytic Electrodes for PEM Fuel Cells," ECS Transactions 5 (1), 147-154 (2007). DOI: 10.1149/1.2728997

Fengling Liu, "Kinetic and Crystallographic Studies of Drug-Resistant Mutants of HIV-1 Protease: Insights into the Drug Resistance Mechanisms," Ph.D., Georgia State University, 2007.

Heli Liu, Xiaoyan Chen, Pamela J. Focia, Xiaolin He, "Structural basis for stem cell factor–KIT signaling and activation of class III receptor tyrosine kinases," EMBO J. 26 (3), 891-901 (2007). DOI: 10.1038/sj.emboj.7601545

Ping Liu, Hosam E. Ewis, Phang C. Tai, Chung-Dar Lu, Irene T. Weber, "Crystal Structure of the Geobacillus stearothermophilus Carboxylesterase Est55 and Its Activation of Prodrug CPT-11," J. Mol. Biol. 367 (4), 212-223 (2007). DOI: 10.1016/j.jmb.2006.12.067

Tong Liu, Arati Ramesh, Zhen Ma, Sarah K. Ward, Limei Zhang, Graham N. George, Adel M. Talaat, James C. Sacchettini, David P. Giedroc, "CsoR is a novel Mycobacterium tuberculosis copper-sensing transcriptional regulator," Nat. Chem. Biol. 3 (1), 60-68 (2007). DOI: 10.1038/nchembio844

W. Liu, W. Gai, K.-J. Kim, "Systematic Study of Undulator Based ILC Positron Source: Production and Capture," Proc. of the 22nd Particle Accelerator Conference (PAC07), IEEE, (2007), 2918 - 2920.

Xin Liu, Ronen Marmorstein, "Structure of the retinoblastoma protein bound to adenovirus E1A reveals the molecular basis for viral oncoprotein inactivation of a tumor suppressor," Gene Dev. 27, 2711-2716 (2007). DOI: 10.1101/gad.1590607

Yongjian Liu, Jeff Terry, Silvia S. Jurisson, "Pertechnetate immobilization in aqueous media with hydrogen sulfide under anaerobic and aerobic environments," Radiochim. Acta 95, 717-725 (2007). DOI: 10.1524/ract.2007.95.12.717

Weikai Li, Sol Schulman, Dana Boyd, Karl Erlandson, Jon Beckwith, Tom A. Rapoport, "The Plug Domain of the SecY Protein Stabilizes the Closed State of the Translocation Channel and Maintains a Membrane Seal," Mol. Cell 26 (4), 511-521 (2007). DOI: 10.1016/j.molcel.2007.05.002

Xintian Li, Hunjoong Lee, Jin Wu, Esther Breslow, "Contributions of the interdomain loop, amino terminus, and subunit interface to the ligand-facilitated dimerization of neurophysin: Crystal structures and mutation studies of bovine neurophysin-I," Protein Sci. 16 (1), 52-68 (2007). DOI: 10.1110/ps.062444807

X. Li, S. Narayanan, M. Sprung, A. R. Sandy, D. R. Lee, J. Wang, "Developing a Dedicated GISAXS Beamline at the APS," AIP Conference Proceedings, Jae-Young Choi, Seungyu Rah, eds., 879, American Institute of Physics, (2007), 1387 - 1390.

Y. Li, X. Chang, "Generation of Ellipsoidal Beam through 3-D Pulse Shaping of a Photoinjector Drive Laser," Proc. of the 2006 Linear Accelerator Conference (Linac06), SNS (2007), 776 - 778.

Y. Li, R. Crowell, "Shortening of a Laser Pulse with a Self-modulated Phase at the Focus of a Lens," Opt. Lett. 32 (1), 93-95 (2007).

Ying Li, Dongxiang Liu, Rong Cao, Santosh Kumar, Changzhi Dong, Jing An, Scott R. Wilson, Yi-Gui Gao, Ziwei Huang, "Crystal Structure of Chemically Synthesized vMIP-II," Proteins 67 (1), 243-246 (2007). DOI: 10.1002/prot.21172

Yongdong Li, Graham Parry, Liqing Chen, Jennifer A. Callahan, David E. Shaw, Edward J. Meehan, Andrew P. Mazar, Mingdong Huang, "An Anti-urokinase Plasminogen Activator Receptor (uPAR) Antibody: Crystal Structure and Binding Epitope," J. Mol. Biol. 365 (4), 1117-1129 (2007). DOI: 10.1016/j.jmb.2006.10.059

Yong-Fu Li, Steven Poole, Fatima Rasulova, Annette L. McVeigh, Stephen J. Savarino, Di Xia, "A Receptor-binding Site as Revealed by the Crystal Structure of CfaE, the Colonization Factor Antigen I Fimbrial Adhesin of Enterotoxigenic Escherichia coli," J. Biol. Chem. 282 (33), 23970-23980 (2007). DOI: 10.1074/jbc.M700921200

Chieh-Tsung Lo, Byeongdu Lee, Nancy L. Dietz Rago, Randall E. Winans, P. Thiyagarajan, "Strategy for Better Ordering in Diblock Copolymer Based Nanocomposites," Macromol. Rapid Commun. 28 (16), 1607-1612 (2007). DOI: 10.1002/marc.200700412

Chieh-Tsung Lo, Byeongdu Lee, Vilas G. Pol, Nancy L. Dietz Rago, Soenke Seifert, Randall E. Winans, P. Thiyagarajan, "Effect of Molecular Properties of Block Copolymers and Nanoparticles on the Morphology of Self-Assembled Bulk Nanocomposites," Macromolecules 40 (23), 8302-8310 (2007). DOI: 10.1021/ma070835v

Chieh-Tsung Lo, Byeongdu Lee, Randall E. Winans, P. Thiyagarajan, "Phase Behavior of Nanoparticle/Diblock Copolymer Complex in a Selective Solvent," Macromolecules 40 (3), 641-647 (2007). DOI: 10.1021/ma061950t

C.S. Lo, K.S. Tanwar, A.M. Clark, T.P. Trainor, "Density functional theory study of the clean and hydrated hematite ($11\bar{0}2$) surfaces," Phys. Rev. B 75, 075425-1-075425-15 (2007). DOI: 10.1103/PhysRevB.75.209901

Ivan B. Lomakin, Yong Xiong, Thomas A. Steitz, "The Crystal Structure of Yeast Fatty Acid Synthase, a Cellular Machine with Eight Active Sites Working Together," Cell 129, 319-332 (2007). DOI: 10.1016/j.cell.2007.03.013

Ivan Lonardelli, Hans-Rudolf Wenk, Y. Ren, "Preferred orientation and elastic anisotropy in shales," Geophysics 72 (2), D33-D40 (2007). DOI: 10.1190/1.2435966 Additional Information

Antonella Longo, Gerald P. Guanga, Robert B. Rose, "Structural Basis for Induced Fit Mechanisms in DNA Recognition by the Pdx1 Homeodomain," Biochem. J. 46 (11), 2948-2957 (2007). DOI: 10.0121/bi0609691

Amparo Lopez-Rubio, Aung Htoon, Elliot P. Gilbert, "Influence of Extrusion and Digestion on the Nanostructure of High-Amylose Maize Starch," Biomacromolecules 8 (5), 1564-1572 (2007). DOI: 10.1021/bm061124s

J. Lopez-Solano, P. Rodriguez-Hernandez, S. Radescu, A. Mujica, A. Munoz, D. Errandonea, F.J. Manjon, J. Pellicer-Porres, N. Garro, A. Segura, Ch. Ferrer-Roca, R.S. Kumar, O. Tschauner, G. Aquilanti, "Crystal stability and pressure-induced phase transitions in scheelite AWO[subscript 4] (A = Ca, Sr, Ba, Pb, Eu) binary oxides. I: A review of recent ab initio calculations, ADXRD, XANES, and Raman studies," Phys. Status Solidi. b. 244 (1), 325-330 (2007). DOI: 10.1002/pssb.200672559

Graciela L. Lorca, Alexandra Ezersky, Vladimir V. Lunin, John R. Walker, Svetlana Altamentova, Elena Evdokimova, Masoud Vedadi, Alexey Bochkarev, Alexei Savchenko, "Glyoxylate and Pyruvate Are Antagonistic Effectors of the Escherichia coli Ic1R Transcriptional Regulator," J. Biol. Chem. 282 (22), 16476-16491 (2007). DOI: 10.1074/jbc.M610838200

Lioudmila V. Loukachevitch, Martin Egli, "Crystallization and preliminary X-ray analysis of Escherichia coli RNase HI–dsRNA complexes," Acta Crystallogr. F 63 (2), 84-88 (2007). DOI: 10.1107/S1744309106055461

Leslie L. Lovelace, Lydia M. Gibson, Lukasz Lebioda, "Cooperative Inhibition of Human Thymidylate Synthase by Mixtures of Active Site Binding and Allosteric Inhibitors," Biochemistry-US 46 (10), 2823-2830 (2007). DOI: 10.1021/bi061309j

Matthew S. Lucas, A. Papandrew, B. Fultz, Michael Y. Hu, "Partial phonon densities of states of [superscript 57]Fe in Fe-Cr: Analysis by a local-order cluster expansion," Phys. Rev. B 75, 054307-1-054307-8 (2007). DOI: 10.1103/PhysRevB.75.054307

Scott A. Lujan, Laura M. Guogas, Heather Ragonese, Steven W. Matson, Matthew R. Redinbo, "Disrupting antibiotic resistance propagation by inhibiting the conjugative DNA relaxase," Proc. Natl. Acad. Sci. USA 104 (30), 12282-12287 (2007). DOI: 10.1073/pnas.0702760104

Jun Lu, Wuyi Meng, Florence Poy, Sankar Maiti, Bruce L. Goode, Michael J. Eck, "Structure of the FH2 domain of Daam1: Implications for formin regulation of actin assembly," J. Mol. Biol. 369, 1258-1269 (2007). DOI: 10.1016/j.jmb.2007.04.002

Randall Lukasiewicz, Bradley Nolen, Joseph A. Adams, Gourisankar Ghosh, "The RGG Domain of Npl3p Recruits Sky1p Through Docking Interactions," J. Mol. Biol. 367 (1), 249-261 (2007). DOI: 10.1016/j.jmb.2006.12.031

Zigmund Luka, Svetlana Pakhomova, Lioudmila V. Loukachevitch, Martin Egli, Marcia E. Newcomer, Conrad Wagner, "5-Methyltetrahydrofolate Is Bound in Intersubunit Areas of Rat Liver Folate-binding Protein Glycine N- Methyltransferase," J. Biol. Chem. 282 (6), 4069-4075 (2007). DOI: 10.1074/jbcM610384200

A.H. Lumpkin, W.J. Berg, N.S. Sereno, D.W. Rule, C.-Y. Yao, "Near-Field Imaging of Optical Diffraction Radiation Generated by a 7-GeV Electron Beam," Phys. Rev. Spec. Top., Accel. Beams 10, 022802-1-022802-8 (2007). DOI: 10.1103/PhysRevSTAB.10.022802

A.H. Lumpkin, P. Evtushenko, A.P. Freyberger, C.Y. Liu, "Feasibility of Near-field ODR Imaging of Multi-GeV Electron Beams at CEBAF," Proc. of the 22nd Particle Accelerator Conference (PAC07), IEEE, (2007), 4381 - 4383.

A.H. Lumpkin, V.E. Scarpine, G.R. Tassotto, "Initial Far-Field OTR Images Generated by 120-GeV Protons at FNAL," Proc. of the 22nd Particle Accelerator Conference (PAC07), IEEE, (2007), 4378 - 4380.

A.H. Lumpkin, B.X. Yang, W.J. Berg, D.W. Rule, N.S. Sereno, C.-Y. Yao, "Far-Field OTR/ODR Images Produced by 7-GeV Electron Beams at APS," Proc. of the 22nd Particle Accelerator Conference (PAC07), IEEE, (2007), 4372 - 4374.

Wei Luo, Rajeev Ahuja, Yang Ding, Ho-kwang Mao, "Unusual lattice dynamics of vanadium under high pressure," Proc. Natl. Acad. Sci. USA 104 (42), 16428-16431 (2007). DOI: 10.1073/pnas.0707377104

L. Lurio, N. Mulders, M. Paetkau, P.R. Jemian, S. Narayanan, A. Sandy, "Windows for small-angle X-ray scattering cryostats," J. Synchrotron Rad. 14 (6), 527-531 (2007). DOI: 10.1107/S0909049507042409

Nathaniel A. Lynd, Marc A. Hillmyer, "Effects of Polydispersity on the Order-Disorder Transition in Block Copolymer Melts," Macromolecules 40 (22), 8050-8055 (2007). DOI: 10.1021/ma070962r

J.W. Lynn, D.N. Argyriou, Y. Ren, Y. Chen, Y.M. Mukovskii, D.A. Shulyatev, "Order and dynamics of intrinsic nanoscale inhomogeneities in manganites," Phys. Rev. B 76 (1), 014437-1-014437-8 (2007). DOI: 10.1103/PhysRevB.76.014437

Kevin P. Madauss, Eugene T. Grygielko, Su-Jun Deng, Anthony C. Sulpizio, Thomas B. Stanley, Charlene Wu, Steve A. Short, Scott K. Thompson, Eugene L. Stewart, Nicholas J. Laping, Shawn P. Williams, Jeffrey D. Bray, "A Structural and in vitro Characterization of Asoprisnil: A Selective Progesterone Receptor Modulator," Mol. Endocrinol. 21 (5), 1066-1081 (2007). DOI: 10.1210/me.2006-0524

D. Ma, A.D. Stoica, L. Yang, X.L. Wang, Z.P. Lu, J. Neuefeind, M.J. Kramer, J.W. Richardson, Th. Proffen, "Nearest-neighbor coordination and chemical ordering in multicomponent bulk metallic glasses," Appl. Phys. Lett. 90 (21), 211908-1-211908-3 (2007). DOI: 10.1063/1.2742315

Mahesh K. Mahanthappa, Lisa S. Lim, Marc A. Hillmyer, Frank S. Bates, "Control of Mechanical Behavior in Polyolefin Composites: Integration of Glassy, Rubbery, and Semicrystalline Components," Macromolecules 40 (5), 1585-1593 (2007). DOI: 10.1021/ma0617421

Michel C. Maillard, Roy K. Hom, Timothy E. Benson, Joseph B. Moon, Shumeye Mamo, Michael Bienkowski, Alfredo G. Tomasselli, Danielle D. Woods, D. Bryan Prince, Donna J. Paddock, Thomas L. Emmons, John A. Tucker, Michael S. Dappen, Louis Brogley, Eugene D. Thorsett, Nancy Jewett, Sukanto Sinha, Varghese John, "Design, Synthesis, and Crystal Structure of Hydroxyethyl Secondary Amine-Based Peptidomimetic Inhibitors of Human [beta]-Secretase," J. Med. Chem. 50 (4), 776-781 (2007). DOI: 10.1021/jm061242y

John K. Ma, Yongting Wang, Christopher J. Carrell, F. Scott Mathews, Victor L. Davidson, "A Single Methionine Residue Dictates the Kinetic Mechanism of Interprotein Electron Transfer from Methylamine Dehydrogenase to Amicyanin," Biochemistry-US 46 (39), 11137-11146 (2007). DOI: 10.1021/bi7012307

Koki Makabe, Shude Yan, Valentina Tereshko, Grzegorz Gawlak, Shohei Koide, "[Beta]-strand Flipping and Slipping Triggered by Turn Replacement Reveal the Opportunistic Nature of [Beta]-strand Pairing," J. Am. Chem. Soc. 129 (47), 14661-14669 (2007). DOI: 10.1021/ja074252cS0002-7863(07)04252-7

Kira S. Makarova, Marina V. Omelchenko, Elena K. Gaidamakova, Vera Y. Matrosova, Alexander Vasilenko, Min Zhai, Alla Lapidus, Alex Copeland, Edwin Kim, Miriam Land, Konstantinos Mavrommatis, Samuel Pitluck, Paul M. Richardson, Chris Detter, Thomas Brettin, Elizabeth Saunders, Barry Lai, Bruce Ravel, Kenneth M. Kemner, Yuri I. Wolf, Alexander Sorokin, Anna V. Gerasimova, Mikhail S. Gelfand, James K. Fredrickson, Eugene V. Koonin, Michael J. Daly, "Deinococcus geothermalis: The Pool of Extreme Radiation Resistance Genes Shrinks," PLoS One 2 (9), e955 (2007). DOI: 10.1371/journal.pone.0000955

M. Manghnani, X. Hong, M. Newville, J. Balogh, "Structural Investigation of Fe-Ni-S and Fe-Ni-Si Melts by High-temperature Fluorescence XAFS Measurements," Proceedings 13th International Conference on X-Ray Absorption Fine Structure, 882, AIP - American Institute of Physics (2007), 466 - 468. DOI: 10.1063/1.2644560

F.J. Manjon, D. Errandonea, J. Lopez-Solano, P. Rodriguez-Hernandez, S. Radescu, A. Mujica, A. Munoz, N. Garro, J. Pellicer-Porres, A. Segura, Ch. Ferrer-Roca, R.S. Kumar, O. Tschauner, G. Aquilanti, "Crystal stability and pressure-induced phase transitions in scheelite AWO[subscript 4] (A = Ca, Sr, Ba, Pb, Eu) binary oxides. II: Towards a systematic understanding," Phys. Status Solidi. b. 244 (1), 295-302 (2007). DOI: 10.1002/pssb.200672588

Bruce A. Manning, Jon R. Kiser, Hancheol Kwon, Sushil Raj Kanel, "Spectroscopic Investigation of Cr(III)- and Cr(VI)-Treated Nanoscale Zerovalent Iron," Environ. Sci. Technol. 41 (2), 586-592 (2007). DOI: 10.1021/es061721m

Ben J. Mans, Eric Calvo, Jose M.C. Ribeiro, John F. Andersen, "The Crystal Structure of D7r4, a Salivary Biogenic Amine-binding Protein from the Malaria Mosquito Anopheles gambiae," J. Biol. Chem. 282 (50), 36626-36633 (2007). DOI: 10.1074/jbc.M706410200

Ho-kwang Mao, Russell J. Hemley, "The high-pressure dimension in earth and planetary science," Proc. Natl. Acad. Sci. USA 104 (22), 9114-9115 (2007). DOI: 10.1073/pnas.0703653104

H.-K. Mao, W.L. Mao, "Theory and Practice – Diamond-Anvil Cells and Probes for High P–T Mineral Physics Studies," Treatise on Geophysics, G. Schubert, eds., Elsevier, 2007, 231 - 267. DOI: 10.1016/B978-044452748-6.00037-7

Wendy L. Mao, Carolyn A. Koh, E. Dendy Sloan, "Clathrate Hydrates Under Pressure," Phys. Today 60 (10), 42-47 (2007). DOI: 10.1063/1.2800096

Laura L. Marcotte, Amanda B. Wass, David W. Gohara, Harsh B. Pathak, Jamie J. Arnold, David J. Filman, Craig E. Cameron, James M. Hogle, "Crystal Structure of Poliovirus 3CD Protein: Virally Encoded Protease and Precursor to the RNA-Dependent RNA Polymerase," J. Virol. 81 (7), 3583-3596 (2007). DOI: 10.1128/JVI.02306-06

Anthony W. Maresso, Ruiying Wu, Justin W. Kern, Rongguang Zhang, Dorota Janik, Dominique M. Missiakas, Mark-Eugene Duban, Andrzej Joachimiak, Olaf Schneewind, "Activation of Inhibitors by Sortase Triggers Irreversible Modification of the Active Site," J. Biol. Chem. 282 (32), 23129-23139 (2007). DOI: 10.1074/jbc.M701857200

Joseph P. Marino, Jr., Paul W. Fisher, Glenn A. Hofmann, Robert B. Kirkpatrick, Cheryl A. Janson, Randall K. Johnson, Chun Ma, Michael Mattern, Thomas D. Meek, M. Dominic Ryan, Christina Schulz, Ward W. Smith, David G. Tew, Thaddeus A. Tomazek, Jr., Daniel F. Veber, Wenfang C. Xiong, Yuuichi Yamamoto, Keizo Yamashita, Guang Yang, Scott K. Thompson, "Highly Potent Inhibitors of Methionine Aminopeptidase-2 Based on a 1,2,4-Triazole Pharmacophore," J. Med. Chem. 50 (16), 3777-3785 (2007). DOI: 10.1021/jm061182w

Francesca Marino, Zhi-Wei Chen, Can E. Ergenekan, Leslie A. Bush-Pelc, F. Scott Mathews, Enrico Di Cera, "Structural Basis of Na[superscript +] Activation Mimicry in Murine Thrombin," J. Biol. Chem. 282 (22), 16355-16361 (2007). DOI: 10.1074/jbc.M701323200

L. W. Marschand, X. Jiao, M. Sprung, D. Kubik, B. Tieman, L. B. Lurio, A. R. Sandy, "Adaptation of a Commercial Optical CMOS Image Sensor for Direct-Detection Fast X-ray Imaging," AIP Conference Proceedings, Jae-Young Choi, Seungyu Rah, eds., 879, American Institute of Physics, (2007), 1172 - 1175.

C.D. Martin, "Structure and Elasticity of NaMgF3 and CaIrO3 at High Pressures and Temperatures—the Perovskite and Post-Perovskite Structure Model of MgSiO3 Investigated with Rietveld Structure Refinement and Ultrasonic Interferometry," Ph.D., State University of NY - Stony Brook, 2007.

Charles David Martin, "Structure and Elasticity of NaMgF3 and CaIrO3 at High Pressures and Temperatures-the Perovskite and Post-Perovskite Structure Model of MgSiO3 Investigated with Rietveld Structure Refinement and Ultrasonic Interferometry," Ph.D., State University of New York, 2007.

C.D. Martin, K.W. Chapman, P.J. Chupas, V. Prakapenka, P.L. Lee, S.D. Shastri, J.B. Parise, "Compression, thermal expansion, structure, and instability of CaIrO[subscript 3], the structure model of MgSiO[subscript 3] post-perovskite," Am. Mineral. 92 (7), 1048-1053 (2007). DOI: 10.2138/am.2007.2473

C. David Martin, Peter J. Chupas, Karena W. Chapman, John B. Parise, "Local versus average structure: a study of neighborite (NaMgF[subscript 3]) utilizing the pair distribution function method for structure determination," J. Appl. Crystallogr. 40 (3), 441-448 (2007). DOI: 10.1107/S0021889807014148

Maria M. Martinez-Inesta, Raul F. Lobo, "Investigation of the Structure of Platinum Clusters Supported in Zeolite Beta Using the Pair Distribution Function," J. Phys. Chem. C 111 (24), 8573-8579 (2007). DOI: 10.1021/jp061728q

R.R. Martin, S.J. Naftel, A.J. Nelson, A.B. Feilen, A. Narvaez, "Metal distributions in the cementum rings of human teeth: possible depositional chronologies and diagenesis," J. Archaeol. Sci. 34 (6), 936-945 (2007). DOI: 10.1016/j.jas.2006.09.018

R.R. Martin, S.J. Naftel, A.J. Nelson, W.D. Sapp III, "Comparison of the distributions of bromine, lead and zinc in tooth and bone from an ancient Peruvian burial site by X-ray fluorescence," Can. J. Chem. 85, 831-836 (2007). DOI: 10.1139/V07-100

A.S. Masadeh, E.S. Bozin, C.L. Farrow, G. Paglia, P. Juhas, A. Karkamkar, M.G. Kanatzidis, S.J. L. Billinge, "Quantitative size-dependent structure and strain determination of CdSe nanoparticles using atomic pair distribution function analysis," Phys. Rev. B 76 (11), 115413-1-115413-11 (2007). DOI: 10.1103/PhysRevB.76.115413

F.S. Mathews, M.M. Gordon, Z. Chen, K.R. Rajashankar, S.E. Ealick, D.H. Alpers, N. Sukumar, "Crystal structure of human intrinsic factor: Cobalamin complex at 2.6-Å resolution," Proc. Natl. Acad. Sci. USA 104 (44), 17311-17316 (2007). DOI: 10.1073/pnas.0703228104

Aleksi Mattila, Jean-Pascal Rueff, James Badro, Gyorgy Vanko, Abhay Shukla, "Metal-Ligand Interplay in Strongly Correlated Oxides: A Parametrized Phase Diagram for Pressure-Induced Spin Transitions," Phys. Rev. Lett. 98, 196404-1-196404-4 (2007). DOI: 10.1103/PhysRevLett.98.196404

Artur Matysik, "Structural and functional characterization of Corynactis Californica derived fluorescent proteins in comparison to DsRed," Masters, Jagiellonian University, 2007.

Relindis Y. Mawo, Sheikh Mustakim, Victor G. Young Jr., Mark R. Hoffmann, Irina P. Smoliakova, "Endo-Effect-Driven Regioselectivity in the Cyclopalladation of (S)-2-tert-Butyl-4-phenyl-2-oxazoline," Organometallics 26 (7), 1801-1810 (2007). DOI: 10.1021/om061132p

Xiaolei Ma, Nazish Sayed, Annie Beuve, Focco van den Akker, "NO and CO differentially activate soluble guanylyl cyclase via a heme pivot-bend mechanism," EMBO J. 26 (2), 578-588 (2007). DOI: 10.1038/sj.emboj.7601521

Robert A. Mayanovic, Alan J. Anderson, William A. Bassett, I-Ming Chou, "On the formation and structure of rare-earth element complexes in aqueous solutions under hydrothermal conditions with new data on gadolinium aqua and chloro complexes," Chem. Geol. 239 (3-4), 266-283 (2007). DOI: 10.1016/j.chemgeo.2006.10.004

Robert A. Mayanovic, Alan J. Anderson, William A. Bassett, I-Ming Chou, "Synchrotron x-ray spectroscopy of Eu/HNO[subscript 3] aqueous solutions at high temperatures and pressures and Nb-bearing silicate melt phases coexisting with hydrothermal fluids using a modified hydrothermal diamond anvil cell and rail assembly," Rev. Sci. Instrum. 78, 053904-1-053904-9 (2007). DOI: 10.1063/1.2737748

M. May, S. Mehboob, D.C. Mulhearn, Z. Wang, H. Yu, G.R. Thatcher, B.D. Santarsiero, M.E. Johnson, A.D. Mesecar, "Structural and Functional Analysis of Two Glutamate Racemase Isozymes from Bacillus anthracis and Implications for Inhibitor Design," J. Mol. Biol. 371 (5), 1219-1237 (2007). DOI: 10.1016/j.jmb.2007.05.093

Jason G. McCoy, Eduard Bitto, Craig A. Bingman, Gary E. Wesenberg, Ryan M. Bannen, Dmitry A. Kondrashov, George N. Phillips,Jr., "Structure and Dynamics of UDP-Glucose Pyrophosphorylase from Arabidopsis thaliana with Bound UDP-Glucose and UTP," J. Mol. Biol. 366 (3), 830-841 (2007). DOI: 10.1016/j.jmb.2006.11.059

Heather M. McDonald, Pamela S. Pruett, Champion Deivanayagam, Irina I. Protasevich, W. Michael Carson, Lawrence J. DeLucas, Wayne J. Brouillette, Christie G. Brouillette, "Structural adaptation of an interacting non-native C-terminal helical extension revealed in the crystal structure of NAD[superscript +] synthetase from Bacillus anthracis," Acta Crystallogr. D 63 (8), 891-905 (2007). DOI: 10.1107/S0907444907029769

James P. McKinley, John M. Zachara, Jiamin Wan, David E. McCready, Steven M. Heald, "Geochemical Controls on Contaminant Uranium in Vadose Hanford Formation Sediments at the 200 Area and 300 Area, Hanford Site, Washington," Vadose Zone J. 6 (4), 1004-1017 (2007). DOI: 10.2136/vzj2006.0184

S.E. McLain, A.K. Soper, J.J. Molaison, C.J. Benmore, M.R. Dolgos, J.L. Yarger, J.F.C. Turner, "On the structure of liquid antimony pentafluoride," J. Mol. Liq. 131-132, 239-245 (2007). DOI: 10.1016/j.molliq.2006.08.042

Rob Meijers, Roland Puettmann-Holgado, Georgios Skiniotis, Jin-huan Liu, Thomas Walz, Jia-huai Wang, Dietmar Schmucker, "Structural basis of Dscam isoform specificity," Nature 449, 487-491 (2007). DOI: 10.1038/nature06147

Q. Mei, C.J. Benmore, J.K.R. Weber, "Structure of Liquid SiO[subscript 2]: A Measurement by High-Energy X-Ray Diffraction," Phys. Rev. Lett. 98, 057802-1-057802-4 (2007). DOI: 10.1103/PhysRevLett.98.057802

Q. Mei, R.T. Hart, C.J. Benmore, S. Amin, K. Leinenweber, J.L. Yarger, "The structure of densified As[subscript 2]O[subscript 3] glasses," J. Non-Cryst. Solids 353 (18-21), 1755-1758 (2007). DOI: 10.1016/j.jnoncrysol.2007.01.044

M.I. Mendelev, D.K. Rehbein, R.T. Ott, M.J. Kramer, D.J. Sordelet, "Computer simulation and experimental study of elastic properties of amorphous Cu-Zr alloys," J. Appl. Phys. 102 (9), 093518-1-093518-8 (2007). DOI: 10.1063/1.2805655

M.I. Mendelev, D.J. Sordelet, M.J. Kramer, "Using atomistic computer simulations to analyze x-ray diffraction data from metallic glasses," J. Appl. Phys. 102, 043501-1-043501-7 (2007). DOI: 10.1063/1.2769157

A. Menzel, K.-C. Chang, V. Komanicky, Y.V. Tolmachev, A.V. Tkachuk, Y.S. Chu, H. You, "High-density electrosorbed carbon monoxide monolayers on Pt(111) under atmospheric pressure," Phys. Rev. B 75 (3), 035426-1- 035426-11 (2007). DOI: 10.1103/PhysRevB.75.035426

Sebastien Merkel, Allen K. McNamara, Atsushi Kubo, Sergio Speziale, Lowell Miyagi, Yue Meng, Thomas S. Duffy, Hans-Rudolf Wenk, "Deformation of (Mg,Fe)SiO[subscript 3] Post-Perovskite and D' Anisotropy," Science 316 (5832), 1729-1732 (2007). DOI: 10.1126/science.1140609

Audrey H. Metz, Thomas Hollis, Brandt F. Eichman, "DNA damage recognition and repair by 3-methyladenine DNA glycosylase I (TAG)," EMBO J. 26 (9), 2411-2420 (2007). DOI: 10.1038/sj.emboj.7601649

F. Marc Michel, Lars Ehm, Sytle M. Antao, Peter L. Lee, Peter J. Chupas, Gang Liu, Daniel R. Strongin, Martin A.A. Schoonen, Brian L. Phillips, John B. Parise, "The Structure of Ferrihydrite, a Nanocrystalline Material," Science 316 (5832), 1726-1729 (2007). DOI: 10.1126/science.1142525

F. M. Michel, L. Ehm, G. Liu, W. Q. Han, S. M. Antao, P. J. Chupas, P. L. Lee, K. Knorr, H. Eulert, J. Kim, C. P. Grey, A. J. Celestian, J. Gillow, M. A. A. Schoonen, D. R. Strongin, J. B. Parise, "Similarities in 2- and 6-Line Ferrihydrite Based on Pair Distribution Function Analysis of X-ray Total Scattering," Chem. Mater. 19 (6), 1489-1496 (2007). DOI: 10.1021/cm062585n

M.E. Middendorf, F.R. Brumwell, J.C. Dooling, D. Horan, R.L. Kustom, M.K. Lien, G.E. McMichael, M.R. Moser, A. Nassiri, S. Wang, "The IPNS Second Harmonic RF Upgrade," Proc. of the 22nd Particle Accelerator Conference (PAC07), IEEE, (2007), 2233 - 2235.

P.E. Mijnarends, S. Kaprzyk, B. Barbiellini, Yinwan Li, J.F. Mitchell, P.A. Montano, A. Bansil, "Magnetic momentum density, Fermi surface, and directional magnetic Compton profiles in LaSr[subscript 2]Mn[subscript 2]O[subscript 7] and La[subscript 1.2]Sr[subscript 1.8]Mn[subscript 2]O[subscript 7]," Phys. Rev. B 75 (1), 014428-1-014428-8 (2007). DOI: 10.1103/PhysRevB.75.014428

Sara L. Milam, Nathan I. Nicely, Brett Feeney, Carla Mattos, Clark A. Clay, "Rapid Folding and Unfolding of Apaf-1 CARD," J. Mol. Biol. 369 (1), 290-304 (2007). DOI: 10.1016/j.jmb.2007.02.105

Michael J. Miley, Agnieszka K. Zielinska, Jeffrey E. Keenan, Stacie M. Bratton, Anna Radominska-Pandya, Matthew R. Redinbo, "Crystal Structure of the Cofactor-Binding Domain of the Human Phase II Drug-Metabolism Enzyme UDP-Glucuronosyltransferase 2B7," J. Mol. Biol. 369 (2), 498-511 (2007). DOI: 10.1016/j.jmb.2007.03.066

Paul J. Milham, Timothy E. Payne, Barry Lai, Rachael L. Trautman, Zhonghou Cai, Paul Holford, Anthony M. Haigh, Jann P. Conroy, "Can synchrotron micro-X-ray fluorescence spectroscopy be used to map the distribution of cadmium in soil particles?," Aust. J. Soil Res. 45 (8), 624-628 (2007). DOI: 10.1071/SR06179

Darcie J. Miller, Ludmilla Shuvalova, Elena Evdokimova, Alexei Savchenko, Alexander F. Yakunin, Wayne F. Anderson, "Structural and biochemical characterization of a novel Mn[superscript 2+]-dependent phosphodiesterase encoded by the yfcE gene," Protein Sci. 16, 1338-1348 (2007). DOI: 10.1110/ps.072764907

Lisa M. Miller, Qi Wang, Randy J. Smith, Hui Zhong, Donald Elliott, John Warren, "A new sample substrate for imaging and correlating organic and trace metal composition in biological cells and tissues," Anal. Bioanal. Chem. 387 (5), 1705-1715 (2007). DOI: 10.1007/s00216-006-0879-2

Peter J. Miller, Yael Pazy, Brian Conti, David Riddle, Ettore Appella, Edward J. Collins, "Single MHC Mutation Eliminates Enthalpy Associated with T Cell Receptor Binding," J. Mol. Biol. 373 (2), 315-327 (2007). DOI: 10.1016/j.jmb.2007.07.028

J.H. Min, N.P. Pavletich, "Recognition of DNA damage by the Rad4 nucleotide excision repair protein," Nature 449, 570-575 (2007). DOI: 10.1038/nature06155

M. Min, Y.H. Chin, P.F. Fischer, Y.-C. Chae, K.-J. Kim, "Fourier Spectral Simulation for Wake Field in Conducting Cavities," Proc. of the 22nd Particle Accelerator Conference (PAC07), IEEE, (2007), 3432 - 3434.

M. Min, P.F. Fischer, Y.-C. Chae, "Spectral-Element Discontinuous Galerkin Simulations for Wake Potential Calculations: NEKCEM," Proc. of the 22nd Particle Accelerator Conference (PAC07), IEEE, (2007), 3435 - 3437.

Kalam A. Mir, Allison Rutter, Iris Koch, Paula Smith, Ken J. Reimer, John S. Poland, "Extraction and speciation of arsenic in plants grown on arsenic contaminated soils," Talanta 72 (4), 1507-1518 (2007). DOI: 10.1016/j.talanta.2007.01.068

Bhoopesh Mishra, Jeremy B. Fein, Maxim I. Boyanov, Shelly D. Kelly, Kenneth M. Kemner, Bruce A. Bunker, "Comparison of Cd Binding Mechanisms by Gram-Positive, Gram-Negative and Consortia of Bacteria Using XAFS," X-Ray Absorption Fine Structure - XAFS13, Britt Hedman, Piero Pianetta, eds., 882, AIP, (2007), 343 - 345. DOI: 10.1063/1.2644520

Bhoopesh Mishra, Elizabeth A. Haack, Igor F. Vasconcelos, Patricia A. Maurice, Bruce A. Bunker, "XAFS Determination of Pb and Cd Speciation with Siderophores and the Metal/Siderophore/Kaolinite System," X-Ray Absorption Fine Structure - XAFS13, Britt Hedman, Piero Pianetta, eds., 882, AIP, (2007), 196 - 198. DOI: 10.1063/1.2644472

Natalia Mitin, Laurie Betts, Marielle E. Yohe, Channing J. Der, John Sondek, Kent L. Rossman, "Release of autoinhibition of ASEF by APC leads to CDC42 activation and tumor suppression," Nat. Struct. Mol. Biol. 14 (9), 814-823 (2007). DOI: 10.1038/nsmb1290

E. Miura, G.E. Ice, E.D. Specht, J.W.L. Pang, H. Kato, K. Hisatsune, A. Inoue, "X-ray Study of Pd[subscript 40]Cu[subscript 30]Ni[subscript 10]P[subscript 20] Bulk Metallic Glass Brazing Filler For Ti-6Al-7Nb Alloy," THERMEC 2006, 5th International Conference, T. Chandra, K. Tsuzaki, M. Militzer, C. Ravindran, eds., 539-543, Materials Science Forum (2007), 1983 - 1987.

E. Miura, H. Kato, T. Ogata, N. Nishiyama, E.D. Specht, T. Shiraishi, A. Inoue, K. Hisatsune, "Mechanical Property and Corrosion Resistance Evaluations of Ti-6Al-7Nb Alloy Brazed with Bulk Metallic Glasses," Mater. Trans. 48 (8), 2235-2243 (2007). DOI: 10.2320/matertrans.MER2007612

Igor Mochalkin, Sandra Lightle, Yaqi Zhu, Jeffrey F. Ohren, Cindy Spessard, Nickolay Y. Chirgadze, Craig Banotai, Michael Melnick, Laura McDowell, "Characterization of substrate binding and catalysis in the potential antibacterial target N-acetylglucosamine-1-phosphate uridyltransferase (GlmU)," Protein Sci. 16, 2657-2666 (2007). DOI: 10.1110/ps.073135107

Eric B. Mock, Charles F. Zukoski, "Determination of Static Microstructure of Dilute and Concentrated Suspensions of Anisotropic Particles by Ultra-Small-Angle X-ray Scattering," Langmuir 23, 8760-8771 (2007). DOI: 10.1021/la062784l

Andreas Moglich, Keith Moffat, "Structural Basis for Light-dependent Signaling in the Dimeric LOV Domain of the Photosensor YtvA," J. Mol. Biol. 373 (1), 112-126 (2007). DOI: 10.1016/j.jmb.2007.07.039

Andrea F. Moon, Miguel Garcia-Diaz, Katarzyna Bebenek, Bryan J. Davis, Xuejun Zhong, Dale A Ramsden, Thomas A. Kunkel, Lars C. Pedersen, "Structural insight into the substrate specificity of DNA Polymerase [mu]," Nat. Struct. Mol. Biol. 14 (1), 45-53 (2007). DOI: 10.1038/nsmb1180

M. Morar, R.H. White, S.E. Ealick, "Structure of 2-Amino-3,7-dideoxy-D-threo-hept-6-ulosonic Acid Synthase, a Catalyst in a Novel Pathway for the Biosynthesis of Aromatic Amino Acids," Biochemistry-US 46 (37), 10562-10571 (2007). DOI: 10.1021/bi700934v

J.R. Morris, M. Xu, Y.Y. Ye, D.J. Sordelet, M.J. Kramer, "Theoretical and experimental studies of devitrification pathways in the Zr[subscript 2]Cu[subscript 1-x]Pd[subscript x] metallic glass system," Acta Mater. 55 (17), 5901-5909 (2007). DOI: 10.1016/j.actamat.2007.07.021

Amy L. Morrow, Kristin Williams, Aaron Sand, Gina Boanca, Joseph J. Barycki, "Characterization of Helicobacter pylori [gamma]-Glutamyltranspeptidase Reveals the Molecular Basis for Substrate Specificity and a Critical Role for the Tyrosine 433-Containing Loop in Catalysis," Biochemistry-US 46 (46), 13407-13414 (2007). DOI: 10.1021/bi701599e

D.J. Morré, S.M. Heald, J. Coleman, J. Orczyk, Z. Jiang, D.M. Morré, "Structural observations of time dependent oscillatory behavior of Cu[superscript II]Cl[subscript 2] solutions measured via extended X-ray absorption fine structure," J. Inorg. Biochem. 101 (4), 715-726 (2007). DOI: 10.1016/j.jinorgbio.2006.12.010

Tinoush Moulaei, Istvan Botos, Natasza E. Ziolkowska, Heidi R. Bokesch, Lauren R. Krumpe, Tawnya C. McKee, Barry R. O'Keefe, Zbigniew Dauter, Alexander Wlodawer, "Atomic-resolution crystal structure of the antiviral lectin scytovirin," Protein Sci. 16, 2756-2760 (2007). DOI: 10.1110/ps.073157507

Aaron Moulin, Jason H. Bell, R.F. Pratt, Dagmar Ringe, "Inhibition of Chymotrypsin by a Complex of Ortho-Vanadate and Benzohydroxamic Acid: Structure of the Inert Complex and Its Mechanistic Interpretation," Biochemistry-US 46 (20), 5982-5990 (2007). DOI: 10.1021/bi6025209

Kent W. Mouw, Phoebe A. Rice, "Shaping the Borrelia burgdorferi genome: crystal structure and binding properties of the DNA-bending protein Hbb," Mol. Microbiol. 63 (5), 1319-1330 (2007). DOI: 10.1111/j.1365-2958.2007.05586.x

T. Mukherjee, K.M. McCulloch, S.E. Ealick, T.P. Begley, "Gene identification and structural characterization of the PLP degradative protein 3-hydroxy-2-methylpyridine-4, 5-dicarboxylate decarboxylase from Mesorhizobium loti MAFF303099.," Biochemistry-US 46 (51), 13606-13615 (2007). DOI: 10.1021/bi701439j

Tathagata Mukherjee, Kathryn M. McCulloch, Steven E. Ealick, Tadhg P. Begley, "Gene Identification and Structural Characterization of the Pyridoxal 5'-Phosphate Degradative Protein 3-Hydroxy-2-methylpyridine-4,5-dicarboxylate Decarboxylase from Mesorhizobium loti MAFF303099," Biochemistry-US 46 (47), 13606-13615 (2007). DOI: 10.1021/bi701439j

Petra Munih, Aaron Moulin, Carin C. Stamper, Brian Bennett, Dagmar Ringe, Gregory A. Petsko, Richard C. Holz, "X-ray crystallographic characterization of the Co(II)-substituted Tris-bound form of the aminopeptidase from Aeromonas proteolytica," J. Inorg. Biochem. 101 (8), 1099-1107 (2007). DOI: 10.1016/j.jinorgbio.2007.03.010

M.T. Murakami, J. Rios-Steiner, S.E. Weaver, A. Tulinsky, J.H. Geiger, R.K. Arni, "Intermolecular Interactions and Characterization of the Novel Factor Xa Exosite Involved in Macromolecular Recognition and Inhibition: Crystal Structure of Human Gla-domainless Factor Xa Complexed with the Anticoagulant Protein NAPc2 from the Hematophagous Nematode Ancylostoma caninum," J. Mol. Biol. 366 (2), 602-610 (2007). DOI: 10.1016/j.jmb.2006.11.040

Conal E. Murray, M. Sankarapandian, S.M. Polvino, I.C. Noyan, B. Lai, Z. Cai, "Submicron mapping of strained silicon-on-insulator features induced by shallow-trench-isolation structures," Appl. Phys. Lett. 90, 171919-1-171919-3 (2007). DOI: 10.1063/1.2732180

S.J. Naftel, R.R. Martin, S.M. Macfie, F. Courchesne, V. Seguin, "An Investigation of Metals at the Soil/Root Interface using Synchrotron Radiation Analysis," Can. J. Anal. Sci. Spect. 52, 18-24 (2007).

Vivek V. Nagarkar, Bipin Singh, Liang Guo, David Gore, Thomas C. Irving, "Cost-effective EMCCD-based detector for time-resolved biological SAXS applications," Nucl. Instrum. Methods A 576 (1), 38-42 (2007). DOI: 10.1016/j.nima.2007.01.116

Vivek V. Nagarkar, Bipin Singh, Liang Guo, David Gore, Thomas C. Irving, "EMCCD-Based Detector for Time-Resolved X-Ray Diffraction and Scattering Studies of Biological Specimens," 2006 IEEE Nuclear Science Symposium Conference, N19-6, IEEE (2007), 740 - 743. DOI: 10.1109/NSSMIC.2006.355960

Pravin A. Nair, Jayakrishnan Nandakumar, Paul Smith, Mark Odell, Christopher D. Lima, Stewart Shuman, "Structural basis for nick recognition by a minimal pluripotent DNA ligase," Nat. Struct. Mol. Biol. 14 (8), 770-778 (2007). DOI: 10.1038/nsmb1266

Michi Nakata, Giuliano Zanchetta, Brandon D. Chapman, Christopher D. Jones, Julie O. Cross, Ronald Pindak, Tommaso Bellini, Noel A. Clark, "End-to-End Stacking and Liquid Crystal Condensation of 6-to 20-Base Pair DNA Duplexes," Science 318, 1276-1279 (2007). DOI: 10.1126/science.1143826

Hyun-Joo Nam, Michael Douglas Lane, Eric Padron, Brittney Gurda, Robert McKenna, Erik Kohlbrenner, George Aslanidi, Barry Byrne, Nicholas Muzyczka, Sergei Zolotukhin, Mavis Agbandje-McKenna, "Structure of Adeno-Associated Virus Serotype 8, a Gene Therapy Vector," J. Virol. 81 (22), 12260-12271 (2007). DOI: 10.1128/JVI.01304-07

Jayakrishnan Nandakumar, Pravin A. Nair, Stewart Shuman, "Last Stop on the Road to Repair: Structure of E. coli DNA Ligase Bound to Nicked DNA-Adenylate," Mol. Cell 26 (2), 257-271 (2007). DOI: 10.1016/j.molcel.2007.02.026

Suresh Narayanan, Dong Ryeol Lee, Aleta Hagman, Xuefa Li, Jin Wang, "Particle Dynamics in Polymer-Metal Nanocomposite Thin Films on

Nanometer-Length Scales," Phys. Rev. Lett. 98, 185506-1-185506-4 (2007). DOI: 10.1103/PhysRevLett.98.185506

S. Narayanan, A. R. Sandy, M. Sprung, J. Sullivan, C. Preissner, D. Shu, "Initial Characterization and Design of an UHV-Compatible Artificial Channel-Cut Monochromator," AIP Conference Proceedings, Jae-Young Choi, Seungyu Rah, eds., 879, American Institute of Physics, (2007), 911 - 914.

Kendall W. Nettles, John B. Bruning, German Gil, Erin E. O'Neill, Jason Nowak, Alun Hughs, Younchang Kim, Eugene R. DeSombre, Robert Dilis, Robert N. Hanson, Andrzej Joachimiak, Geoffrey L. Greene, "Structural plasticity in the oestrogen receptor ligand-binding domain," EMBO reports 8 (6), 563-568 (2007). DOI: 10.1038/sj.embor.7400963

S. M. Neville, B. A. Leita, D. A. Offermann, M. B. Duriska, B. Moubaraki, K. W. Chapman, G. J. Halder, K. S. Murray, "Spin-Crossover Studies on a Series of 1D Chain and Dinuclear Iron(II) Triazine-Dipyridylamine Compounds," Eur. J. Inorg. Chem. 2007 (8), 1073-1085 (2007). DOI: 10.1002/ejic.200790012

Ngoc T. Nguyen, Brandon Howe, Juliana R. Hash, Nicholas Liebrecht, Paul Zschack, David C. Johnson, "Synthesis of a Family of {[(VSe[subscript 2])[subscript n]][subscript 1.06](TaSe[subscript 2])[subscript m]}[subscript z] Compounds," Chem. Mater. 19, 1923-1930 (2007). DOI: 10.1021/cm062509k

Guy Tran Van Nhieu, Tina Izard, "Vinculin binding in its closed conformation by a helix addition mechanism," EMBO J. 26, 4588-4596 (2007). DOI: 10.1038/sj.emboj.7601863

Karin Nienhaus, James E. Knapp, Pasquale Palladino, William E. Royer, Jr., G. Ulrich Nienhaus, "Ligand Migration and Binding in the Dimeric Hemoglobin of Scapharca inaequivalvis," Biochemistry-US 46 (49), 14018-14031 (2007). DOI: 10.1021/bi7016798

T. Nimalasuriya, J.J. Curry, C.J. Sansonetti, E.J. Ridderhof, S.D. Shastri, A.J. Flikweert, W.W. Stoffels, M. Haverlag, J.J.A.M. van der Mullen, "X-ray induced fluorescence measurement of segregation in a DyI[subscript 3]–Hg metal-halide lamp," J. Phys. D 40 (9), 2831-2838 (2007). DOI: 10.1088/0022-3727/40/9/025

N. Nishiyama, Y. Wang, M.L. Rivers, S.R. Sutton, D. Cookson, "Rheology of [epsilon]-iron up to 19 GPa and 600 K in the D-DIA," Geophys. Res. Lett. 34, L233304-L233308 (2007). DOI: 10.1029/2007GL031431

N. Nishiyama, T. Yagi, S. Ono, H. Gotou, T. Harada, T. Kikegawa, "Effect of incorporation of iron and aluminum on the thermoelastic properties of magnesium silicate perovskite," Phys. Chem. Miner. 34 (3), 131-143 (2007). DOI: 10.1007/s00269-006-0134-6

Zhongwei Niu, Michael A. Bruckman, Siqi Li, L. Andrew Lee, Byeongdu Lee, Sai Venkatesh Pingali, P. Thiyagarajan, Qian Wang, "Assembly of Tobacco Mosaic Virus into Fibrous and Macroscopic Bundled Arrays Mediated by Surface Aniline Polymerization," Langmuir 23 (12), 6719-6724 (2007). DOI: 10.1021/la070096b

B. Nocek, E. Evdokimova, M. Proudfoot, M. Kudritska, L.L. Grochowski, R.H. White, A. Savchenko, A.F. Yakunin, A. Edwards, A. Joachimiak, "Structure of an Amide Bond Forming F[subscript 420]:[gamma]-glutamyl Ligase from Archaeoglobus Fulgidus - A Member of a New Family of Non-ribosomal Peptide Synthases," J. Mol. Biol. 372 (2), 456-469 (2007). DOI: 10.1016/j.jmb.2007.06.063

Bryan H. Norman, Timothy I. Richardson, Jeffrey A. Dodge, Lance A. Pfeifer, Gregory L. Durst, Yong Wang, Jim D. Durbin, Venkatesh Krishnan, Sean R. Dinn, Shengquan Liu, John E. Reilly, Kendal T. Ryter, "Benzopyrans as selective estrogen receptor [beta] agonists (SERBAs). Part 4: Functionalization of the benzopyran A-ring," Bioorg. Med. Chem. Lett. 17 (18), 5082-5085 (2007). DOI: 10.1016/j.bmcl.2007.07.009

W.E. Norum, B. Yang, "A Novel FPGA-Based Bunch Purity Monitor System at the APS Storage Ring," Proc. of the 22nd Particle Accelerator Conference (PAC07), IEEE, (2007), 4384 - 4386.

Marcin Nowotny, Sergei A. Gaidamakov, Rodolfo Ghirlando, Susana M. Cerritelli, Robert J. Crouch, Wei Yang, "Structure of Human RNase H1 Complexed with an RNA/DNA Hybrid: Insight into HIV Reverse Transcription," Mol. Cell 28 (2), 264-276 (2007). DOI: 10.1016/j.molcel.2007.08.015

May Nyman, James P. Larentzos, Edward J. Maginn, Margaret E. Welk, David Ingersoll, Hyunsoo Park, John B. Parise, Ivor Bull, Francois Bonhomme, "Experimental and Theoretical Methods to Investigate Extraframework Species in a Layered Material of Dodecaniobate Anions," Inorg. Chem. 46 (6), 2067-2079 (2007). DOI: 10.1021/ic061454l

H. Ohfuji, N. Sata, H. Kobayashi, Y. Ohishi, K. Hirose, T. Irifune, "A new high-pressure and high-temperature polymorph of FeS," Phys. Chem. Miner. 34 (5), 335-343 (2007). DOI: 10.1007/s00269-007-0151-0

Jeffrey F. Ohren, "Structural and Functional studies of Aspartate ? -Semialdehyde Dehydrogenase, Aspartate Kinase and Creatine Kinase," Masters, University of Toledo, 2007.

A. Olczak, M.L. Glowka, M. Szczesio, J. Bojarsk, W.L. Duax, B.M. Burkhart, Z. Wawrzak, "Nonstoichiometric complex of gramicidin D with KI at 0.80 [angstrom] resolution," Acta Crystallogr. D D63, 319-327 (2007). DOI: 10.1107/S0907444906053649

Bradley D. Olsen, Xuefa Li, Jin Wang, Rachel A. Segalman, "Thin Film Structure of Symmetric Rod-Coil Block Copolymers," Macromolecules 40 (9), 3287-3295 (2007). DOI: 10.1021/ma062402i

Steen K.T. Ooi, Chen Qiu, Emily Bernstein, Keqin Li, Da Jia, Zhe Yang, Hediye Erdjument-Bromage, Paul Tempst, Shau-Ping Lin, C. David Allis, Xiaodong Cheng, Timothy H. Bestor, "DNMT3L connects unmethylated lysine 4 of histone H3 to de novo methylation of DNA," Nature 448, 714-717 (2007). DOI: 10.1038/nature05987

Eric A. Ortlund, Jamie T. Bridgham, Matthew R. Redinbo, Joseph W. Thornton, "Crystal Structure of an Ancient Protein: Evolution by Conformational Epistasis," Science 317 (5844), 1544-1548 (2007). DOI: 101126/science.1142819

Sri Oruganti, Yanming Zhang, Hongzhi Li, Howard Robinson, Michael P. Terns, Rebecca M. Terns, Wei Yang, Hong Li, "Alternative conformations of the archaeal Nop56/58-fibrillarin complex imply flexibility in box C/D RNPs," J. Mol. Biol. 371 (5), 1141-1150 (2007). DOI: 10.1016/j.jmb.2007.06.029

Kanji Oshima, Yasunori Takezawa, Yasunobu Sugimot, Takakazu Kobayashi, Thomas C. Irving, Katsuzo Wakabayashi, "Axial Dispositions and Conformations of Myosin Crossbridges Along Thick Filaments in Relaxed and Contracting States of Vertebrate Striated Muscles by X-ray Fiber Diffraction," J. Mol. Biol. 367 (1), 275-301 (2007). DOI: 10.1016/j.jmb.2006.12.036

T.A. O'Brien, F. Bridges, L. Downward, J.F. Mitchell, H. Zheng, "Evidence for magnetic dimerons in the anisotropic bilayer system La[subscript 1.2]Sr[subscript 1.8]Mn[subscript 2]O[subscript 7]: An EXAFS study," Phys. Rev. B 75, 064417-1-064417-8 (2007). DOI: 10.1103/PhysRevB.75.064417

Jodi L. O'Donnell, Xiaobing Zuo, Andrew J. Goshe, Lev Sarkisov, Randall Q. Snurr, Joseph T. Hupp, David M. Tiede, "Solution-Phase Structural Characterization of Supramolecular Assemblies by Molecular Diffraction," J. Am. Chem. Soc. 129 (6), 1578-1585 (2007). DOI: 10.1021/ja0659065

Hugh O'Neill, William T. Heller, Katherine E. Helton, Volker S. Urban, Elias Greenbaum, "Small-Angle X-ray Scattering Study of Photosystem I-Detergent Complexes: Implications for Membrane Protein Crystallization," J. Phys. Chem. B 111 (16), 4211-4219 (2007). DOI: 10.1021/jp067463x

M.A. Paesler, D.A. Baker, G. Lucovsky, A.E. Edwards, P.C. Taylor, "EXAFS study of local order in the amorphous chalcogenide semiconductor Ge[subscript 2]Sb[subscript 2]Te[subscript 5]," J. Phys. Chem. Solids 68 (5-6), 873-877 (2007). DOI: 10.1016/j.jpcs.2007.03.041

Katharine Page, Christina S. Schade, Jinping Zhang, Peter J. Chupas, Karena W. Chapman, Thomas Proffen, Anthony K. Cheetham, Ram Seshadri, "Preparation and characterization of Pd2Sn nanoparticles," MRS Bull. 42 (12), 1969-1975 (2007). DOI: 10.1016/j.materres-bull.2007.05.010

Daniel Panne, Tom Maniatis, Stephen C. Harrison, "An Atomic Model of the Interferon-[beta] Enhanceosome," Cell 129, 1111-1123 (2007). DOI: 10.1016/j.cell.2007.05.019

A. Parikh, W. Yarbrough, M. Mason, S. Sridhar, P.R. Chidambaram, Z. Cai, "Characterization of structure and morphology of an advanced p-channel field effect transistor under uniaxial stress by synchrotron x-ray diffraction," Appl. Phys. Lett. 90, 172117-1-172117-3 (2007). DOI: 10.1063/1.2734480

Changyong Park, Paul A. Fenter, "Phasing of Resonant Anomalous X-ray Reflectivity Spectra and Direct Fourier Synthesis of Element-Specific Partial Structures at Buried Interfaces," J. Appl. Crystallogr. 40 (2), 290-301 (2007). DOI: 10.1107/S0021889806053131

H. Park, "Synthesis and Structural Studies of New Microporous Framework Materials," Ph.D., The State University of New York at Stony Brook, 2007.

H. Park, J.F. Britten, U. Mueller, J.Y. Lee, J. Li, J.B. Parise, "Synthesis, Structure Determination, and Hydrogen Sorption Studies of New Metal-Organic Frameworks Using Triazole and Naphthalenedicarboxylic Acid," Chem. Mater. 19 (6), 1302-1308 (2007). DOI: 10.1021/cm0623918

Ho Bum Park, Chul Ho Jung, Young Moo Lee, Anita J. Hill, Steven J. Pas, Stephen T. Mudie, Elizabeth Van Wagner, Benny D. Freeman, David J. Cookson, "Polymers with Cavities Tuned for Fast Selective Transport of Small Molecules and Ions," Science 318, 254-258 (2007). DOI: 10.1126/science.1146744

Hyunsoo Park, Gabriel Krigsfeld, John B. Parise, "Solvothermal Synthesis and Structural Characterization of New Zn-Triazole-Sulfoisophthalate Frameworks," Cryst. Growth Des. 7 (4), 736-740 (2007). DOI: 10.1021/cg060741x

Hyun Ho Park, Emmanuelle Logette, Stefan Rausnser, Solange Cuenin, Thomas Walz, Jurg Tschopp, Hao Wu, "Death Domain Assembly Mechanism Revealed by Crystal Structure of the Oligomeric PIDDosome Core Complex," Cell 128 (3), 533-546 (2007). DOI: 10.1016/j.cell.2007.01.019

Hyun Ho Park, Hao Wu, "Crystallization and preliminary X-ray crystallographic studies of the oligomeric death-domain complex between PIDD and RAIDD," Acta Crystallogr. F 63, 229-232 (2007). DOI: 10.1107/S1744309107007889

M.J. Park, K.H. Downing, A. Jackson, E.D. Gomez, A.M. Minor, D. Cookson, A.Z. Weber, N.P. Balsara, "Increased Water Retention in Polymer Electrolyte Membranes at Elevated Temperatures Assisted by Capillary Condensation," Nano Lett. 7 (11), 3547-3552 (2007). DOI: 10.1021/nl072617l

Kamil Paruch, Michael P. Dwyer, Carmen Alvarez, Courtney Brown, Tin-Yau Chan, Ronald J. Doll, Kerry Keertikar, Chad Knutson, Brian McKittrick, Jocelyn Rivera, Randall Rossman, Greg Tucker, Thierry O. Fischmann, Alan Hruza, Vincent Madison, Amin A. Nomeir, Yaolin Wang, Emma Lees, David Parry, Nicole Sgambellone, Wolfgang Seghezzi, Lesley Schultz, Fran Shanahan, Derek Wiswell, Xiaoying Xu, Quiao Zhou, Ray A. James, Vidyadhar M. Paradkar, Haengsoon Park, Laura R. Rokosz, Tara M. Stauffer, Timothy J. Guzi, "Pyrazolo[1,5-a]pyrimidines as orally available inhibitors of cyclin-dependent kinase 2," Bioorg. Med. Chem. Lett. 17 (22), 6220-6223 (2007). DOI: 10.1016/j.bmcl.2007.09.017

S.J. Pasky, R.M. Lill, M.D. Borland, N.S. Sereno, L.L. Erwin, "Linac Automated Beam Phase Control System," Proc. of the 2006 Linear Accelerator Conference (LINAC06), SNS (2007), 241 - 243.

Georgia A. Patikoglou, Lars F. Westblade, Elizabeth A. Campbell, Valerie Lamour, William J. Lane, Seth A. Darst, "Crystal Structure of the Escherichia coli Regulator of [sigma superscript 70], Rsd, in complex with [sigma superscript 70] Domain 4," J. Mol. Biol. 372 (3), 649-659 (2007). DOI: 10.1016/j.jmb.2007.06.081

Tatjana Paunesku, Stefan Vogt, Barry Lai, Jorg Maser, Natasa Stojicevic, Kenneth T. Thurn, Clodia Osipo, Hong Liu, Daniel Legnini, Zhou Wang, Chung Lee, Gayle E. Woloschak, "Intracellular Distribution of TiO[subscript 2]-DNA Oligonucleotide Nanoconjugates Directed to Nucleolus and Mitochondria Indicates Sequence Specificity," Nano Lett. 7 (3), 596-601 (2007). DOI: 10.1021/nl0624723

Marzena Pazgier, Adam Prahl, David M. Hoover, Jacek Lubkowski, "Studies of the Biological Properties of Human [superscript beta]-Defensin 1," J. Biol. Chem. 282 (3), 1819-1829 (2007). DOI: 10.1074/jbc.M607210200

Arwen R. Pearson, Reinhard Pahl, Elena G. Kovaleva, Victor L. Davidson, Carrie M. Wilmot, "Tracking X-ray-derived redox changes in crystals of a methylamine dehydrogenase/amicyanin complex using single-crystal UV/Vis microspectrophotometry," J. Synchrotron Rad. 14 (1), 92-98 (2007). DOI: 10.1107/S0909049506051259

D. Pease, A.I. Frenkel, P. Shanthakumar, T. Huang, M. Balasubramanian, J.I. Budnick, D. Brewe, N. Abitbol, O. Odong, "Performance and Improved Design of the Log Spiral of Revolution Monochromator," AIP Conference Proceedings, B. Hedman, P. Pianetta, eds., 882, American Institute of Physics, (2007), 902 - 904.

Nino R. Pereira, Eric M. Dufresne, D.A. Arms, "A Large Aperture X-ray Refractive Lens from Lithium," SYNCHROTRON RADIATION INSTRUMENTATION: Ninth International Conference on Synchrotron Radiation Instrumentation, Jae-Young Choi, Seungyu Rah, eds., 879, Springer, (2007), 985 - 988.

V. Petkov, T. Ohta, Y. Hou, Y. Ren, "Atomic-Scale Structure of Nanocrystals by High-Energy X-ray Diffraction and Atomic Pair Distribution Function Analysis: Study of Fe[subscript x]Pd[subscript 100-x] (x) 0, 26, 28, 48) Nanoparticles," J. Phys. Chem. C 111 (2), 714-720 (2007). DOI: 10.1021/jp066166p

Janusz J. Petkowski, Maksymilian Chruszcz, Matthew D. Zimmerman, Heping Zheng, Tatiana Skarina, Olena Onopriyenko, Marcin T. Cymborowski, Katarzyna D. Koclega, Alexei Savchenko, Aled Edwards, Wladek Minor, "Crystal structures of TM0549 and NE1324—two orthologs of E. coli AHAS isozyme III small regulatory subunit," Protein Sci. 16, 1360-1367 (2007). DOI: 10.1110/ps.072793807

Taras Petrenko, Serena DeBeer George, Nuria Aliaga-Alcalde, Eckhard Bill, Bernd Mienert, Yuming Xiao, YiSong Guo, Wolfgang Sturhahn, Stephen P. Cramer, Karl Wieghardt, Frank Neese, "Characterization of a Genuine Iron(V)-Nitrido Species by Nuclear Resonant Vibrational Spectroscopy Coupled to Density Functional Calculations," J. Am. Chem. Soc. 129 (36), 11053-11060 (2007). DOI: 10.1021/ja070792y

Tatiana Petrova, Marianne E. Cuff, Ruiying Wu, Youngchang Kim, Denise Holzle, Andrzej Joachimiak, "Novel hexamerization motif is discovered in a conserved cytoplasmic protein from Salmonella typhimurium," J. Struct. Funct. Geno. 8 (1), 19-25 (2007). DOI: 10.1007/s10969-007-9028-1

Jeffrey A. Pfefferkorn, Chulho Choi, Yuntao Song, Bharat K. Trivedi, Scott D. Larsen, Valerie Askew, Lisa Dillon, Jeffrey C. Hanselman, Zhiwu Lin, Gina Lu, Andrew Robertson, Catherine Sekerke, Bruce Auerbach, Alexander Pavlovsky, Melissa S. Harris, Graeme Bainbridge, Nicole Caspers, "Design and synthesis of novel, conformationally restricted HMG-CoA reductase inhibitors," Bioorg. Med. Chem. Lett. 17 (16), 4531-4537 (2007). DOI: 10.1016/j.bmcl.2007.05.097

Jeffrey A. Pfefferkorn, Yuntao Song, Kuai-Lin Sun, Steven R. Miller, Bharat K. Trivedi, Chulho Choi, Roderick J. Sorenson, Larry D. Bratton, Paul C. Unangst, Scott D. Larsen, Toni-Jo Poel, Xue-Min Cheng, Chitase Lee, Noe Erasga, Bruce Auerbach, Valerie Askew, Lisa Dillon, Jeffrey C. Hanselman, Zhiwu Lin, Gina Lu, Andrew Robertson, Karl Olsen, Thomas Mertz, Catherine Sekerke, Alexander Pavlovsky, Melissa S. Harris, Graeme Bainbridge, Nicole Caspers, Huifen Chen, Matthias Eberstadt, "Design and synthesis of hepatoselective, pyrrole-based HMG-CoA reductase inhibitors," Bioorg. Med. Chem. Lett. 17 (16), 4538-4544 (2007). DOI: 10.1016/j.bmcl.2007.05.096

P. Pfeifer, L. Aston, M. Banks, S. Barker, J. Burress, S. Carter, J. Coleman, S. Crockett, C. Faulhaber, J. Flavin, M. Gordon, L. Hardcastle, Z. Kallenborn, M. Kemiki, C. Lapilli, J. Pobst, R. Schott, P. Shah, S. Spellerberg, G. Suppes, D. Taylor, A. Tekeei, C. Wexler, M. Wood, P. Buckley, T. Breier, J. Downing, S. Eastman, P. Freeze, S. Graham, S. Grinter, A. Howard, J. Martinez, D. Radke, T. Vassalli, J. Ilavsky, "Complex pore spaces create record-breaking methane storage system for natural-gas vehicles," Chaos 17 (4), 041108-1 (2007). DOI: 10.1063/1.2786007

Jason Phan, Joseph E. Tropea, David S. Waugh, "Structure-assisted discovery of Variola major H1 Phosphatase inhibitors," Acta Crystallogr. D D63, 698-704 (2007). DOI: 10.1016/j.cell.2007.03.040

Gabriella Piazzesi, Massimo Reconditi, Marco Linari, Leonardo Lucii, Pasquale Bianco, Elisabetta Brunello, Valerie Decostre, Alex Stewart, David B. Gore, Thomas C. Irving, Malcolm Irving, Vincenzo Lombardi, "Skeletal Muscle Performance Determined by Modulation of Number of Myosin Motors Rather Than Motor Force or Stroke Size," Cell 131 (4), 784-795 (2007). DOI: 10.1016/j.cell.2007.09.045

A. Pietryla, H. Bui, G. Decker, R. Laird, R. Lill, E. Norum, "Status of the RF BPM Upgrade at the Advanced Photon Source," Proc. of the 22nd Particle Accelerator Conference (PAC07), IEEE, (2007), 4390 - 4392.

Agustin O. Pineda, Zhi-Wei Chen, Francesca Marino, F. Scott Mathews, Michael W. Mosesson, Enrico Di Cera, "Crystal structure of thrombin in complex with fibrinogen [gamma]' peptide," Biophys. Chem. 125 (2-3), 556-559 (2007). DOI: 10.1016/j.bpc.2006.08.005

Donald J.P. Pinto, Michael J. Orwat, Stephanie Koch, Karen A. Rossi, Richard S. Alexander, Angela Smallwood, Pancras C. Wong, Alan R. Rendina, Joseph M. Luettgen, Robert M. Knabb, Kan He, Baomin Xin, Ruth R. Wexler, Patrick Y.S. Lam, "Discovery of 1-(4-Methoxyphenyl)-7-oxo-6-(4-(2-oxopiperidin-1-yl)phenyl)-4,5,6,7-tetrahydro- 1H-pyrazolo[3,4-c]pyridine-3-carboxamide (Apixaban, BMS-562247), a Highly Potent, Selective, Efficacious, and Orally Bioavailable Inhibitor of Blood Coagulation Factor Xa," J. Med. Chem. 50 (22), 5339-5356 (2007). DOI: 10.1021/jm070245n

Diana Placido, Bernard A. Brown II, Ky Lowenhaupt, Alexander Rich, Alekos Athanasiadis, "A Left-Handed RNA Double Helix Bound by the Z[alpha] Domain of the RNA-Editing Enzyme ADAR1," Structure 15 (4), 395-404 (2007). DOI: 10.1016/j.str.2007.03.001

Andrew J.R. Plested, Mark L. Mayer, "Structure and Mechanism of Kainate Receptor Modulation by Anions," Neuron 53 (6), 829-841 (2007). DOI: 10.1016/j.neuron.2007.02.025

N.V. Pletneva, Sergei V. Pletnev, D.M. Chudakov, T.V. Tikhonova, V.O. Popov, V. I. Martynov, Alex Wlodawer, Z. Dauter, V.Z. Pletnev, "Three-Dimensional Structure of Yellow Fluorescent Protein zYFP538 from Zoanthus sp. at the Resolution 1.8 A.," Bioorganisk Khimiya 33 (4), 421-430 (2007). DOI: 10.1134/S1068162007040048

Nadezhda Pletneva, Vladimir Pletnev, Tamara Tikhonova, Alexey A. Pakhomov, Vladimir Popov, Vladimir I. Martynov, Alexander Wlodawer, Zbigniew Dauter, Sergei Pletnev, "Refined crystal structures of red and green fluorescent proteins from the button polyp Zoanthus," Acta Crystallogr. D 63 (10), 1082-1093 (2007). DOI: 10.1107/S0907444907042461

V. Podgursky, V. Rose, I. Costina, R. Franchy, "Study of phase transitions within alumina grown on top of CoAl(100) surface," Surf. Sci. 601 (16), 3315-3323 (2007). DOI: 10.1016/j.susc.2007.06.003

Larissa M. Podust, Jens P. von Kries, Ali Nasser Eddine, Youngchang Kim, Liudmila V. Yermalitskaya, Ronald Kuehne, Hugues Ouellet, Thulasi Warrier, Markus Altekoster, Jong-Seok Lee, Jorg Rademann, Hartmut Oschkinat, Stefan H.E. Kaufmann, Michael R. Waterman, "Small-Molecule Scaffolds for CYP51 Inhibitors Identified by High-Throughput Screening and Defined by X-Ray Crystallography," Antimicrob. Agents Ch. 51 (11), 3915-3923 (2007). DOI: 10.1128/AAC.00311-07

M. Polacci, D.R. Baker, L. Bai, L. Mancini, "Large vesicles record pathways of degassing," B. Volcanol. online, online (2007). DOI: 10.1007/s00445-007-0184-8

J. Pollanen, S. Blinstein, H. Choi, J.P. Davis, T.M. Lippman, L.B. Lurio, W.P. Halperin, "Anisotropic Aerogels for Studying Superfluid [superscript 3]He," J. Low Temp. Phys. 148 (5-6), 579-583 (2007). DOI: 10.1007/s10909-007-9449-z

M.A. Pouchon, A.J. Kropf, A. Froideval, C. Degueldre, W. Hoffelner, "An X-ray absorption spectroscopy study of an oxide dispersion strengthened steel," J. Nucl. Mater. 362 (2-3), 253-258 (2007). DOI: 10.1016/j.jnucmat.2007.01.123

Rasmus D. Poulsen, Mads R.V. Jorgensen, Jacob Overgaard, Finn K. Larsen, Wolfgang Morgenroth, Timothy Graber, Yu-Sheng Chen, Bo B. Iversen, "Synchrotron X-Ray Charge-Density Study of Coordination Polymer [Mn(HCOO)[subscript 2](H[subscript 2]O)subscript 2]]," Chem.-Eur. J. 13 (35), 9775-9790 (2007). DOI: 10.1002/chem.200700756

L. Pradeep, I. Kurinov, S.E. Ealick, H.A. Scheraga, "Implementation of a k/k[subscript 0] method to identify long-range structure in transition states during conformational folding/unfolding of proteins," Structure 15, 1178-1189 (2007). DOI: 10.1016/j.str.2007.08.003

S.K. Pradhan, Z.T. Deng, F. Tang, C. Wang, Y. Ren, P. Moeck, V. Petkov, "Three-dimensional structure of CdX X = Se , Tenanocrystals by total x-ray diffraction," J. Appl. Phys. 102 (4), 044304-1-044304-6 (2007). DOI: 10.1063/1.2767615

Swapan Kumar Pradhan, Milen Gateshki, Markus Niederberger, Yang Ren, Valeri Petkov, "PbZrTiOby soft synthesis: Structural aspects," Phys. Rev. B 76 (1), 014114-1-014114-8 (2007). DOI: 10.1103/PhysRevB.76.014114

Swapan K. Pradhan, Yuanbing Mao, Stanislaus S. Wong, Peter Chupas, Valeri Petkov, "Atomic-Scale Structure of Nanosized Titania and Titanate: Particles, Wires, and Tubes," Chem. Mater. 19 (25), 6180-6186 (2007). DOI: 10.1021/cm7019069

Gali Prag, Hadiya Watson, Young C. Kim, Bridgette M. Beach, Rodolfo Ghirlando, Gerhard Hummer, Juan S. Bonifacino, James H. Hurley, "The Vps27/Hse1 Complex is a GAT Domain-Based Scaffold for Ubiquitin-Dependent Sorting," Dev. Cell 12 (6), 973-986 (2007). DOI: 10.1016/j.dev-cel.2007.04.013

Michael Pravica, Ognjen Grubor-Urosevic, Michael Hu, Paul Chow, Brian Yulga, Peter Liermann, "X-ray Raman Spectroscopic Study of Benzene at High Pressure," Phys. Chem. B 111 (40), 11635-11637 (2007). DOI: 10.1021/jp074321+

Michael Pravica, Zachary Quine, Edward Romano, Sean Bajar, Brian Yulga, Wenge Yang, Daniel Hooks, "Anisotropic Decomposition of Energetic Materials," Shock Compression of Condensed Matter, M. Elert, M.D. Furnish, R. Chau, N. Holmes, J. Nguyen, eds., 955, AIP, (2007), 1117 - 1120. DOI: 10.1063/1.2832914

Michael Pravica, Yongrong Shen, Zachary Quine, Edward Romano, David Hartnett, "High-Pressure Studies of Cyclohexane to 40 GPa," J. Phys. Chem. B 111 (16), 4103-4108 (2007). DOI: 10.1021/jp070052b

C. Preissner, D. Shu, T.J. Royston, "Experimental Investigation and Model Development for a Harmonic Drive Transmission," New Developments in Optomechanics, Alson E. Hatheway, 6665, SPIE, (2007), online.

Andrew J. Prongay, Zhuyan Guo, Nanhua Yao, John Pichardo, Thierry Fischmann, Corey Strickland, Joseph Myers, Jr., Patricia C. Weber, Brian M. Beyer, Richard Ingram, Zhi Hong, Winifred W. Prosise, Lata Ramanathan, S. Shane Taremi, Taisa Yarosh-Tomaine, Rumin Zhang, Mary Senior, Rong-Sheng Yang, Bruce Malcolm, Ashok Arasappan, Frank Bennett, Stephane L. Bogen, Kevin Chen, Edwin Jao, Yi-Tsung Liu, Raymond G. Lovey, Anil K. Saksena, Srikanth Venkatraman, Viyyoor Girijavallabhan, F. George Njoroge, Vincent Madison, "Discovery of the HCV NS3/4A Protease Inhibitor (1R,5S)-N-[3-Amino-1-(cyclobutylmethyl)-2,3-dioxopropyl]-3-[2(S)-[[[(1,1-dimethylethyl)amino]carbonyl]amino]-3,3-dimethyl-1-oxobutyl]-6,6-dimethyl-3-azabicyclo[3.1.0]hexan-2(S)-carboxamide (Sch 503034) II. Key Steps in Structure-Based Optimization," J. Med. Chem. 50 (10), 2310-3218 (2007). DOI: 10.1021/jm060173k

Kirstin R. Purdy, James R. Bartles, Gerard C.L. Wong, "Structural Polymorphism of the Actin-Espin System: A Prototypical System of Filaments and Linkers in Stereocilia," Phys. Rev. Lett. 98, 058105-1-058105-4 (2007). DOI: 10.1103/PhysRevLett.98.058105

Yulia Pushkar, Junko Yano, Pieter Glatzel, Johannes Messinger, Azul Lewis, Kenneth Sauer, Uwe Bergmann, Vittal K. Yachandra, "Polarized Range-Extended X-Ray Absorption Spectroscopy of Oriented Photosystem II Membranes in the S[subscript 1] State," AIP Conference Proceedings, Britt Hedman, Piero Pianetta, eds., 882, Springer, (2007), 346 - 348. DOI: 10.1063/1.2644521

Yulia Pushkar, Junko Yano, Pieter Glatzel, Johannes Messinger, Azul Lewis, Kenneth Sauer, Uwe Bergmann, Vittal Yachandra, "Structure and Orientation of the Mn[subscript 4]Ca Cluster in Plant Photosystem II Membranes Studied by Polarized Range-extended X-ray Absorption Spectroscopy," J. Biol. Chem. 282 (10), 7198-7208 (2007). DOI: 10.1074/jbc.M610505200

S.B. Qadri, M.A. Dinderman, W.J. Dressick, P.E. Schoen, P. Lubitz, J.H. He, R.J. Tonucci, J. Cross, "Structural and magnetic properties of FeB microfibers," Appl. Phys. A 89 (2), 493-496 (2007). DOI: 10.1007/s00339-007-4163-x

Ruhu Qi, Susanne Fetzner, Aaron J. Oakley, "Crystallization and diffraction data of 1H-3-hydroxy-4-oxoquinoline 2,4-dioxygenase: a cofactor-free oxygenase of the [alpha/beta]-hydrolase family," Acta Crystallogr. F 63, 378-381 (2007). DOI: 10.1107/S1744309107013760

Odayme Quesada, Brittney Gurda, Lakshmanan Govindasamy, Robert McKenna, Erik Kohlbrenner, George Aslanidi, Sergei Zolotukhin, Nicholas Muzyczka, Mavis Agbandje-McKenna, "Production, purification and preliminary X-ray crystallographic studies of adeno-associated virus serotype 7," Acta Crystallogr. F 63 (12), 1073-1076 (2007). DOI: 10.1107/S1744309107060289

D. Quock, N. Arnold, D. Dohan, J. Anderson, D. Clemons, "Applications of Interest - A Relational Database Approach to Managing Control System Software Applications," Proceedings of the 6th International Workshop on Personal Computers and Particle Accelerator Controls, JLAB-ACO-07-628, Jefferson Lab (2007), 93 - 95.

C.T. Radom, A. Banerjee, G.L. Verdine, "Structural characterization of human 8-oxoguanine DNA glycosylase variants bearing active site mutations," J. Biol. Chem. 282 (12), 9182-9194 (2007). DOI: 10.1074/jbc.M608989200

Dhanpat Rai, Dean A. Moore, Nancy J. Hess, Kevin M. Rosso, Linfeng Rao, Steve M. Heald, "Chromium(III) Hydroxide Solubility in the Aqueous K[supercript +]-H[superscript +]-OH[superscript -]-CO[subscript 2]-HCO [superscript - subscript 3]-CO [supercript 2-subscript 3] -H[subscript 2]O System: A Thermodynamic Model," J. Solution Chem. 36 (10), 1261-1285 (2007). DOI: 10.1007/s10953-007-9179-5

Andrzej Rajca, Maren Pink, Sumit Mukherjee, Suchada Rajca, Kausik Das, "1,3-Alternate calix[4]arene nitronyl nitroxide tetraradical and diradical: synthesis, X-ray crystallography, paramagnetic NMR spectroscopy, EPR spectroscopy, and magnetic studies," Tetrahedron 63 (44), 10731-10742 (2007). DOI: 10.1016/j.tet.2007.07.051

Andrzej Rajca, Suchada Rajca, Maren Pink, Makoto Miyasaka, "Annelated, Chiral [pi]-Conjugated Systems: Tetraphenylenes and Helical [beta]-Oligothiophenes," Synlett 2007 (12), 1799-1822 (2007). DOI: 10.1055/s-2007-984538

Andrzej Rajca, Kouichi Shiraishi, Maren Pink, Suchada Rajca, "Triplet (S = 1) Ground State Aminyl Diradical," J. Am. Chem. Soc. 129 (23), 7232-7233 (2007). DOI: 10.1021/ja071881d

Andrzej Rajca, Masahiro Takahashi, Maren Pink, Gaelle Spagnol, Suchada Rajca, "Conformationally Constrained, Stable, Triplet Ground State (S = 1) Nitroxide Diradicals. Antiferromagnetic Chains of S = 1 Diradicals," J. Am. Chem. Soc. 129 (33), 10159-10170 (2007). DOI: 10.1021/ja0712017

Sridhar Ramamurthy, Stewart McIntyre, Marina Fuller, Robert Klassen, Rozaliya Barabash, Rick Holt, Otto Yong, "Strain Measurements Using Synchrotron Micro-Laue Diffraction," Cold Work Workshop, AECL, COG, EPRI, (2007), online.

Arati Ramesh, Christos G. Savva, Andreas Holzenburg, James C. Sacchettini, "Crystal Structure of Rsr, an Ortholog of the Antigenic Ro Protein, Links Conformational Flexibility to RNA Binding Activity," J. Biol. Chem. 282 (20), 14960-14967 (2007). DOI: 10.1074/jbc.M611163200

Santiago Ramon-Maiques, Alex J. Kuo, Dylan Carney, Adam G.W. Matthews, Marjorie A. Oettinger, Or Gozani, Wei Yang, "The plant homeodomain finger of RAG2 recognizes histone H3 methylated at both lysine-4 and arginine-2," Proc. Natl. Acad. Sci. USA 104 (48), 18993-18998 (2007). DOI: 10.1073/pnas.0709170104

Soren G.F. Rasmussen, Hee-Jung Choi, Daniel M. Rosenbaum, Tong Sun Kobilka, Foon Sun Thian, Patricia C. Edwards, Manfred Burghammer, Venkata R.P. Ratnala, Ruslan Sanishvili, Robert F. Fischetti, Gebhard F.X. Schertler, William I. Weis, Brian K. Kobilka, "Crystal structure of the human [beta subscript 2] adrenergic G-protein-coupled receptor," Nature 450, 383-387 (2007). DOI: 10.1038/nature06325

C. Rau, V. Crecea, W. Liu, C.-P. Richter, K.M. Peterson, P.R. Jemian, U. Neuhausler, G. Schneider, X. Yu, P.V. Braun, T.-C. Chiang, I.K. Robinson, "Synchrotron-based imaging and tomography with hard X-rays," Nucl. Instrum. Methods B 261 (1-2), 850-854 (2007). DOI: 10.1016/j.nimb.2007.03.053

C. Rau, V. Crecea, C.-P. Richter, K.M. Peterson, P.R. Jemian, U. Neuhausler, G. Schneider, X. Yu, P.V. Braun, T.-C. Chiang, I.K. Robinson, "Imaging of micro- and nano-structures with hard X-rays," Micro & Nano Letters 2 (1), 1-5 (2007). DOI: 10.1049/mnl:20065060

C. Rau, W. Liu, "Cone-beam imaging with sub-100 nm focal-sized Kirkpatrick–Baez mirrors," Nucl. Instrum. Methods A 582 (1), 132-134 (2007). DOI: doi:10.1016/j.nima.2007.08.091

B. Ravel, S.D. Kelly, D. Gorman-Lewis, M.I. Boyanov, J.B. Fein, K.M. Kemner, "A pH-Dependent X-Ray Absorption Spectroscopy Study of U Adsorption to Bacterial Cell Walls," X-Ray Absorption Fine Structure - XAFS13, Britt Hedman, Piero Pianetta, 882, AIP (2007), 202 - 204. DOI: 10.1063/1.2644474

V. Ravindranath, S. Sharma, B. Rusthoven, M. Gosz, L. Zhang, J.-C. Biasci, "Thermal Fatigue Life Prediction of Glidcop Al-15," Proc. of International Workshop on Mechanical Engineering Design of Synchrotron Radiation Equipment and Instrumentation 2006 (MEDSI06), SPring-8 (2007), *.

A. Reddy, D.B. Hovis, A.H. Heuer, A.P. Paulikas, B.W. Veal, "In Situ Study of Oxidation-Induced Growth Strains in a Model NiCrAlY Bond-Coat Alloy," Oxid. Met. 67 (3/4), 153-177 (2007). DOI: 10.1007/s11085-007-9044-8

Daniel Alan Reiniger, "On Defect Detection and Residual Stress Quantification in Bonded Semiconductor Devices," Masters, University of Illinois, Champaign-Urbana, 2007.

D. Reiniger, G. Horn, T.J. Mackin, J.R. Lesniak, Y. Zhong, Y.S. Chu, Z.C. Leseman, "Experimental Residual Stress Mapping in Bonded Semiconductor," 2007 SEM Annual Conference on Experimental Mechanics, Society for Experimental Mechanics (2007), CD.

David A Reis, Aaron M. Lindenberg, "Ultrafast x-ray scattering in solids," Light Scattering in Solids IX, Topics in Applied Physics, M. Cardona and R. Merlin, eds., Springer, 2007, 371 - 422. DOI: 10.1007/b14231

S. Rendon, R.A. Bubeck, L.S. Thomas, W.R. Burghardt, A. Hexemer, D.A. Fischer, "Interrogation of 'Surface,' 'Skin' and 'Core' Orientation in Thermotropic Liquid Crystalline Copolyester Moldings by Near-Edge X-ray Absorption Fine Structure and Wide-Angle X-ray Scattering," J. Appl. Polym. Sci. 106 (4), 2502-2514 (2007). DOI: 10.1002/app.26759

S. Rendon, W.R. Burghardt, M.L. Auad, J.A. Kornfield, "Shear-Induced Alignment of Smectic Side Group Liquid Crystalline Polymers," Macromolecules 40 (18), 6624-6630 (2007). DOI: 10.1021/ma062912c

S. Rendon, W.R. Burghardt, R.A. Bubeck, "Orientation Dynamics in Commercial Thermotropic Liquid Crystalline Polymers in Transient Shear Flows," Rheol. Acta 46 (7), 945-956 (2007). DOI: 10.1007/s00397-007-0177-8

Arturo Flores Renteria, "Small-angle scattering analysis of the manufacture and thermal induced morphological changes and their influence in the thermal conductivity of EB-PVD PYSZ TBCs," Ph.D., RWTH Aachen University, Aachen, Germany, 2007.

A. Flores Renteria, B. Saruhan, J. Ilavsky, A.J. Allen, "Application of USAXS analysis and non-interacting approximation to determine the influence of process parameters and ageing on the thermal conductivity of electron-beam physical vapor deposited thermal barrier coatings," Surf. Coat. Tech. 201 (8), 4781-4788 (2007). DOI: 10.1016/j.surfcoat.2006.10.020

Pavlina Rezaova, Veronika Krejcirikova, Dominika Borek, Shiu F. Moy, Andrzej Joachimiak, Zbyszek Otwinowski, "The crystal structure of the effector-binding domain of the trehalose repressor TreR from Bacillus subtilis 168 reveals a unique quarternary assembly," Proteins 69 (3), 679-682 (2007). DOI: 10.1002/prot.21516

Timothy I. Richardson, Jeffrey A. Dodge, Gregory L. Durst, Lance A. Pfeifer, Jikesh Shah, Yong Wang, Jim D. Durbin, Venkatesh Krishnan, Bryan H. Norman, "Benzopyrans as selective estrogen receptor [beta] agonists (SERBAs). Part 3: Synthesis of cyclopentanone and cyclohexanone intermediates for C-ring modification," Bioorg. Med. Chem. Lett. 17 (17), 4824-4828 (2007). DOI: 10.1016/j.bmcl.2007.06.052

Timothy I. Richardson, Jeffrey A. Dodge, Yong Wang, Jim D. Durbin, Venkatesh Krishnan, Bryan H. Norman, "Benzopyrans as selective estrogen receptor [beta] agonists (SERBAs). Part 5: Combined A- and C-ring structure–activity relationship studies," Bioorg. Med. Chem. Lett. 17 (20), 5563-5566 (2007). DOI: 10.1016/j.bmcl.2007.08.009

Timothy I. Richardson, Bryan H. Norman, Charles W. Lugar, Scott A. Jones, Yong Wang, Jim D. Durbin, Venkatesh Krishnan, Jeffrey A. Dodge, "Benzopyrans as selective estrogen receptor [beta] agonists (SERBAs). Part 2: Structure–activity relationship studies on the benzopyran scaffold," Bioorg. Med. Chem. Lett. 17 (13), 3570-3574 (2007). DOI: 10.1016/j.bmcl.2007.04.051

Paul G. Rickert, Mark R. Antonio, Millicent A. Firestone, Karrie-Ann Kubatko, Tomasz Szreder, James F. Wishart, Mark L. Dietz, "Tetraalkylphosphonium Polyoxometalate Ionic Liquids: Novel, Organic-Inorganic Hybrid Materials," J. Phys. Chem. B 111 (18), 4685-4692 (2007). DOI: 10.1021/jp0671751

Clark Ritz, Frank Flack, Donald Savage, Douglas Detert, Paul G. Evans, Max Lagally, Zhonghou Cai, "Ordered Lattices of Quantum Dots on Ultrathin SOI Nanomembranes," ECS Transactions 6 (4), 321-326 (2007). DOI: 10.1149/1.2728877

Jeremy T. Robinson, Yifan Cao, Donald Walko, Dohn Arms, J. Alexander Liddle, Oscar D. Dubon, "Ordering and shape tuning of Ge islands on metal-patterned Si," Group IV Semiconductor Nanostructures—2006, L. Tsybeskov, D.J. Lockwood, C. Delerue, M. Ichikawa, A. W. van Buuren, eds., 958, Materials Research Society (2007), online.

J.T. Robinson, D.A. Walko, D.A. Arms, D.S. Tinberg, P.G. Evans, Y. Cao, J.A. Liddle, A. Rastelli, O.G. Schmidt, O.D. Dubon, "Sculpting Semiconductor Heteroepitaxial Islands: From Dots to Rods," Phys. Rev. Lett. 98, 106102-1-106102-4 (2007). DOI: 10.1103/PhysRevLett.98.106102

Diane J. Rodi, Suneeta Mandava, David B. Gore, Lee Makowski, Robert F. Fischetti, "Detection of Functional Ligand-Binding Events Using Synchrotron X-Ray Scattering," J. Biomol. Screen. 12 (7), 994-998 (2007). DOI: 10.1177/1087057107306104

Daniel M. Rosenbaum, Vadim Cherezov, Michael A. Hanson, Soren G.F. Rasmussen, Foon Sun Thian, Tong Sun Kobilka, Hee-Jung Choi, Xiao-Jie Yao, William I. Weis, Raymond C. Stevens, Brian K. Kobilka, "GPCR Engineering Yields High-Resolution Structural Insights into [beta subscript 2] Adrenergic Receptor Function," Science 318, 1266-1273 (2007). DOI: 10.1126/science.1150609

Richard A. Rosenberg, Gopal K. Shenoy, Matthew F. Chisholm, Li-Chia Tien, David Norton, Steven Pearton, "Getting to the Core of the Problem: Origin of the Luminescence from (Mg,Zn)O Heterostructured Nanowires," Nano Lett. 7 (6), 1521-1525 (2007). DOI: 10.1021/nl0702923

V. Rose, K. Bruggemann, R. David, R. Franchy, "Two-Dimensional Surface Magnetism in the Bulk Paramagnetic Intermetallic Alloy CoAl(100)," Phys. Rev. Lett. 98, 037202-1-037202-4 (2007). DOI: 10.1103/PhysRevLett.98.037202

V. Rose, K. Bruggemann, R. David, R. Franchy, "Oxidation-induced high-Curie-temperature ferromagnetism in CoAl(100)," Phys. Status Solidi. c. 4 (11), 4188-4196 (2007). DOI: 10.1002/pssc.200675907

V. Rose, X.M. Cheng, D.J. Keavney, J.W. Freeland, K.S. Buchanan, B. Ilic, V. Metlushko, "The breakdown of the fingerprinting of vortices by hysteresis loops in circular multilayer ring arrays," Appl. Phys. Lett. 91, 132501-1-132501-3 (2007). DOI: 10.1063/1.2786856

V. Rose, R. Franchy, "Thermal stability of Co-core-CoO-shell nanoparticles on an ultrathin [theta]-Al[subscript 2]O[subscript 3] film support," J. Appl. Phys. 101, 086104-1-086104-3 (2007). DOI: 10.1063/1.2717127

V. Rose, V. Podgursky, R. David, R. Franchy, "Growth of Co nanoparticles on a nanostructured [theta]-Al[subscript 2]O[subscript 3] film on CoAl(100)," Surf. Sci. 601 (3), 786-791 (2007). DOI: 10.1016/j.susc.2006.11.009

Budwy Rowda, Maxim Avdeev, Peter L. Lee, Paul F. Henry, Chris D. Ling, "Structures of 6H perovskites Ba[subscript 3]CaSb[subscript 2]O[subscript 9] and Ba[subscript 3]SrSb[subscript 2]O[subscript 9] determined by synchrotron X-ray diffraction, neutron powder diffraction and ab initio

calculations," Acta Crystallogr. B 64, 154-159 (2007). DOI: 10.1107/S0108768108005041

William E. Royer, Jr., Michael N. Omartian, James E. Knapp, "Low Resolution Crystal Structure of Arenicola Erythrocruorin: Influence of Coiled Coils on the Architecture of a Megadalton Respiratory Protein," J. Mol. Biol. 365 (1), 226-236 (2007). DOI: 10.1016/j.jmb.2006.10.016

J.R. Royer, E.I. Corwin, P.J. Eng, H.M. Jaeger, "Gas-Mediated Impact Dynamics in Fine-Grained Granular Materials," Phys. Rev. Lett. 99 (3), 038003-1-038003-4 (2007). DOI: 10.1103/PhysRevLett.99.038003

J. Ruan, H. Edwards, C.-Y. Tan, R. Thurman-Keup, V. Scarpine, Y. Li, J. Power, T. Maxwell, "Design of an Electro-Optical Sampling Experiment at the AWA Facility," Proc. of the 22nd Particle Accelerator Conference (PAC07), IEEE, (2007), 3901 - 3903.

Jeremy L. Ruggles, Katie M. Baldwin, Stephen A. Holt, Garry J. Foran, Ian R. Gentle, "Rigid Films of an Anionic Porphyrin and a Dialkyl Chain Surfactant," J. Phys. Chem. B 111 (20), 5651-5657 (2007). DOI: 10.1021/jp0677391

K.S. Ryan, A.R. Howard-Jones, M.J. Hamill, S.J. Elliott, C.T. Walsh, C.L. Drennan, "Crystallographic trapping in the rebeccamycin biosynthetic enzyme RebC," Proc. Natl. Acad. Sci. USA 104 (39), 15311-15316 (2007). DOI: 10.1073/pnas.0707190104

P. Ryan, D. Wermeille, J.W. Kim, J.C. Woicik, C.S. Hellberg, H. Li, "Domain ordering of strained 5 ML SrTiO[subscript 3] films on Si(001)," Appl. Phys. Lett. 90, 221908-1-221908-3 (2007). DOI: 10.1063/1.2744478

Elisabetta Sabini, Saugata Hazra, Manfred Konrad, Stephen K. Burley, Arnon Lavie, "Structural basis for activation of the therapeutic L-nucleoside analogs 3TC and troxacitabine by human deoxycytidine kinase," Nucleic Acids Res. 35 (1), 186-192 (2007). DOI: 10.1093/nar/gkl1038

Elisabetta Sabini, Saugata Hazra, Manfred Konrad, Arnon Lavie, "Nonenantioselectivity Property of Human Deoxycytidine Kinase Explained by Structures of the Enzyme in Complex with L- and D-Nucleosides," J. Med. Chem. 50 (13), 3004-3014 (2007). DOI: 10.1021/jm0700215

Kasim Sader, Michael Reedy, David Popp, Carmen Lucaveche, John Trinick, "Measuring the resolution of uncompressed plastic sections cut using an oscillating knife ultramicrotome," J. Struct. Biol. 159 (1), 29-35 (2007). DOI: 10.1016/j.jsb.2007.01.019

N. Sahai, Y.J. Lee, H. Xu, M. Ciardelli, J.-F. Gaillard, "Role of Fe(II) and phosphate in arsenic uptake by coprecipitation," Geochim. Cosmochim. Acta 71 (13), 3193-3210 (2007). DOI: 10.1016/j.gca.2007.04.008

V. Sajaev, M. Borland, Y.-C. Chae, G. Decker, R. Dejus, L. Emery, K. Harkay, A. Nassiri, S. Shastri, G. Waldschmidt, B. Yang, P. Anfinrud, V. Dolgashev, "Short X-ray Pulse Generation Using Deflecting Cavities at the Advanced Photon Source," Nucl. Instrum. Methods A 582, 57-59 (2007).

V. Sajaev, M. Borland, A. Xiao, "New Lattice Design for APS Storage Ring with Potential Tri-fold Increase of the Number of Insertion Devices," Proc. of the 22nd Particle Accelerator Conference (PAC07), IEEE, (2007), 1139 - 1141.

Deanne W. Sammond, Ziad M. Eletr, Carrie Purbeck, Randall J. Kimple, David P. Siderovski, Brian Kuhlman, "Structure-based Protocol for Identifying Mutations that Enhance Protein-Protein Binding Affinities," J. Mol. Biol. 371 (5), 1392-1404 (2007). DOI: 10.1016/jmb.2007.15.096

Lori K. Sanders, Wujing Xian, Camilo Guaqueta, Michael J. Strohman, Chuck R. Vrasich, Erik Luijten, Gerard C.L. Wong, "Control of electrostatic interactions between F-actin and genetically modified lysozyme in aqueous media," Proc. Natl. Acad. Sci. USA 104 (41), 15994-15999 (2007). DOI: 10.1073/pnas.0705898104

A.R. Sandy, K. Evans-Lutterodt, K. Fezzaa, S. Kim, S. Narayanan, M. Sprung, A. Stein, "Effect of x-ray beamline optics on x-ray photon correlation spectroscopy experiments," Advances in X-Ray/EUV Optics and Components II, A.M. Khounsary, C. Morawe, S. Goto, eds., 6705, SPIE (2007), online. DOI: 10.1117/12.734397

A. R. Sandy, X. Jiao, S. Narayanan, M. Sprung, "Contrast and Stability Improvements for XPCS Measurements at Beamline 8-ID-I at the APS," AIP Conference Proceedings, Jae-Young Choi, Seungyu Rah, eds., 879, American Institute of Physics, (2007), 898 - 901.

R. Sanishvili, C. Besnard, F. Camus, M. Fleurant, P. Pattison, G. Bricogne, M. Schiltz, "Polarization-dependence of anomalous scattering in brominated DNA and RNA molecules, and importance of crystal orientation in single- and multiple-wavelength anomalous diffraction phasing," J. Appl. Crystallogr. 40 (3), 552-558 (2007). DOI: 10.1107/S0021889807015178

L.V. Saraf, M.H. Engelhard, P. Nachimuthu, V. Shutthanandan, C.M. Wang, S.M. Heald, D.E. McCready, A.S. Lea, D.R. Baer, S.A. Chambers, "Nucleation and Growth of MOCVD Grown (Cr, Zn)O Films: Uniform Doping vs Secondary Phase Formation," J. Electrochem. Soc. 154 (3), D134-D138 (2007). DOI: 10.1149/1.2424422

S. Sarkar, S. Kababya, S. Vega, H. Cohen, J. Woicik, A. Frenkel, G. Hodes, "Effects of solution pH and surface chemistry on the post-deposition growth of chemical bath deposited PbSe nanocrystalline films," Chem. Mater. 19 (4), 879-888 (2007). DOI: 10.1021/cm060628u

S. Sasaki, I. McNulty, R. Dejus, "Undulator Radiation Carrying Spin and Orbital Angular Momentum," Nucl. Instrum. Methods A 582, 43-46 (2007).

S. Sasaki, I. McNulty, T. Shimada, "A Possibility for Using an APPLE Undulator to Generate a Photon Beam with Transverse Optical Modes," Proc. of the 22nd Particle Accelerator Conference (PAC07), IEEE, (2007), 1142 - 1144.

Kenneth A. Satyshur, Gregory A. Worzalla, Lorraine S. Meyer, Erin K. Heiniger, Kelly G. Aukema, Ana M. Misic, Katrina T. Forest, "Crystal Structures of the Pilus Retraction Motor PilT Suggest Large Domain Movements and Subunit Cooperation Drive Motility," Structure 15 (3), 363-376 (2007). DOI: 10.1016/j.str.2007.01.018

Matthew H. Sazinsky, Benjamin LeMoine, Maria Orofino, Roman Davydov, Krisztina Z. Bencze, Timothy L. Stemmler, Brian M. Hoffman, Jose M. Arguello, Amy C. Rosenzweig, "Characterization and Structure of a Zn[superscript 2+] and [2Fe-2S]-containing Copper Chaperone from

Archaeoglobus fulgidus," J. Biol. Chem. 282 (35), 25950-25959 (2007). DOI: 10.1074/jbc.M703311200

Adrian Scaffidi, Brian W. Skelton, Robert V. Stick, Allan H. White, "Structural Characterization of a Pentapeptide Derived from a Novel Carbohydrate [alpha]-Amino Acid," Aust. J. Chem. 60 (2), 93-94 (2007). DOI: 10.1071/CH06392

Kirk G. Scheckel, Rebecca Hamon, Laurence Jassogne, Mark Rivers, Enzo Lombi, "Synchrotron X-ray absorption-edge computed microtomography imaging of thallium compartmentalization in Iberis intermedia," Plant Soil 290 (1-2), 51-60 (2007). DOI: 10.1007/s11104-006-9102-7

A. Scherz, W.F. Schlotter, K. Chen, R. Rick, J. Stöhr, J. Lüning, I. McNulty, Ch. Günther, F. Radu, W. Eberhardt, O. Hellwig, S. Eisebitt, "Phase imaging of magnetic nanostructures using resonant soft x-ray holography," Phys. Rev. B 76, 214410-1-214410-5 (2007). DOI: 10.1103/PhysRevB.76.214410

C. Schlieker, W. A. Weihofen, E. Frijns, L. M. Kattenhorn, R. Gaudet, H. L. Ploegh, "Structure of a herpesvirus-encoded cysteine protease reveals a unique class of deubiquitinating enzymes," Mol. Cell 25, 677-687 (2007). DOI: 10.1016/j.molcel.2007.01.033

Norbert Schorman, Alexei Grigorian, Alexandra Samal, Raman Krishnan, Lawrence Delucas, Debasish Chattopadhyay, "Crystal structure of vaccinia virus uracil-DNA glycosylase reveals dimeric assembly," BMC Struct. Biol. 7, 45 (2007). DOI: 10.1186/1472-6807-7-45

Eric R. Schreiter, Maria M. Rodriguez, Andrzej Weichsel, William R. Montfort, Joseph Bonaventura, "S-Nitrosylation-induced Conformational Change in Blackfin Tuna Myoglobin," J. Biol. Chem. 282 (27), 19773-19780 (2007). DOI: 10.1074/jbc.M701363200

Carsten Schubert, Celine Schalk-Hihi, Geoffrey T. Struble, Hong-Chang Ma, Ioanna P. Petrounia, Benjamin Brandt, Ingrid C. Deckman, Raymond J. Patch, Mark R. Player, John C. Spurlino, Barry A. Springer, "Crystal Structure of the Tyrosine Kinase Domain of Colony-stimulating Factor-1 Receptor (cFMS) in Complex with Two Inhibitors," J. Biol. Chem. 282 (6), 4094-4101 (2007). DOI: 10.1074/jbc.M608183200

Stefan Schweizer, Anthony R. Lubinsky, Jacqueline A. Johnson, "Fluorozirconate-based glass-ceramic storage phosphors for digital mammography," Proceedings of SPIE, Medical Imagine 2007, Jiang Hsieh, Michael J. Flynn, eds., 6510, SPIE, (2007), 651046. DOI: 10.1117/12.708758

Henry P. Scott, Sabrina Huggins, Mark R. Frank, Steven J. Maglio, C. David Martin, Yue Meng, Javier Santillan, Quentin Williams, "Equation of state and high-pressure stability of Fe[subscript 3]P-schreibersite: Implications for phosphorus storage in planetary cores," Geophys. Res. Lett. 34 (6), L06302-1-L06302-5 (2007). DOI: 10.1029/2006GL029160

Dario Segura-Pena, Joseph Lichter, M. Trani, M. Konrad, A. Lavie, Stefan Lutz, "Quarternary Structure Change of a Mechanism for the Regulaton of Thymidine Kinase 1-Like Enzymes," Structure 15, 1555-1566 (2007). DOI: 10.1016/j.str.2007.09.025

Dario Segura-Pena, Stefan Lutz, Chrisitan Monnerjahn, Manfred Konrad, Arnon Lavie, "Binding of ATP to TK1-like Enzymes Is Associated with a Conformational Change in the Quaternary Structure," J. Mol. Biol. 369 (1), 129-141 (2007). DOI: 10.1016/j.jmb.2007.02.104

G.T. Seidler, T.T. Fister, J.O. Cross, K.P. Nagle, "The LERIX User Facility," AIP Conference Proceedings, B. Hedman, P. Pianetta, eds., 882, American Institute of Physics, (2007), 911 - 913.

Michelle E. Seitz, Wesley R. Burghardt, K.T. Faber, Kenneth R. Shull, "Self-Assembly and Stress Relaxation in Acrylic Triblock Copolymer Gels," Macromolecules 40 (4), 1218-1226 (2007). DOI: 10.1021/ma061993+

Nikolina Sekulic, Kristen Dietrich, Ingo Paarmann, Stephan Ort, Manfred Konrad, Arnon Lavie, "Elucidation of the Active Conformation of the APS-Kinase Domain of Human PAPS Synthetase 1," J. Mol. Biol. 367 (2), 488-500 (2007). DOI: 10.1016/j.jmb.2007.01.025

Nikolina Sekulic, Manfred Konrad, Arnon Lavie, "Structural Mechanism for Substrate Inhibition of the Adenosine 5'-Phosphosulfate Kinase Domain of Human 3'-Phosphoadenosine 5'-Phosphosulfate Synthetase 1 and Its Ramifications for Enzyme Regulation," J. Biol. Chem. 282 (30), 22112-22121 (2007). DOI: 10.1074/jbc.M701713200

N. Sereno, M. Borland, "Booster Requirements for Advanced Photon Source 1-nm Emittance Upgrade Lattices," Proc. of the 22nd Particle Accelerator Conference (PAC07), IEEE, (2007), 3438 - 3440.

N. Sereno, M. Borland, H. Friedsam, "An Energy Recovery Linac Upgrade for the Advanced Photon Source Located in the Storage Ring Infield," Proc. of the 22nd Particle Accelerator Conference (PAC07), IEEE, (2007), 1145 - 1147.

N.S. Sereno, F.R. Lenkszus, "Feedback Correction of Injection Errors Using Digital Signal-Processing Techniques," Phys. Rev. Spec. Top., Accel. Beams 10, 012803-1-012803-8 (2007). DOI: 10.1103/PhysRevSTAB.10.012803

A. Seryi, J.A. Amann, R. Arnold, F. Asiri, K.L.F. Bane, P. Bellomo, E. Doyle, A.F. Fasso, L. Keller, J. Kim, K. Ko, Z. Li, T.W. Markiewicz, T.V.M. Maruyama, M. Alabau, P. Bambade, J. Brossard, K. C. Moffeit, S. Molloy, Y. Nosochkov, N. Phinney, T.O. Raubenheimer, S. Seletskiy, S. Smith, C.M. Spencer, P. Tenenbaum, D.R. Walz, G.R. White, M. Woodley, M. Woods, L. Xiao, I.V. Agapov, G.A. Blair, S.T. Boogert, J. Carter, M. Alabau, P. Bambade, J. Brossard, O. Dadoun, M. Anerella, A.K. Jain, A. Marone, B. Parker, D.A.-K. Angal-Kalinin, C.D. Beard, J.-L. Fernandez-Hernando, P. Goudket, F. Jackson, J.K. Jones, A. Kalinin, P.A. McIntosh, R. Appleby, J.L. Baldy, D. Schulte, L. Bellantoni, A.I. Drozhdin, V.S. Kashikhin, V. Kuchler, T. Lackowski, N.V. Mokhov, N. Nakao, T. Peterson, M.C. Ross, S.I. Striganov, J.C. Tompkins, M. Wendt, X. Yang, K. Buesser, P. Burrows, G.B. Christian, C.I. Clarke, A.F. Hartin, G. Burt, A.C. Dexter, J. Carwardine, C.W. Saunders, B. Constance, H. Dabiri Khah, C. Perry, C. Swinson, O. Delferriere, O. Napoly, J. Payet, D. Uriot, C.J. Densham, R.J.S. Greenhalgh, A. Enomoto, S. Kuroda, T. Okugi, T. Sanami, Y. Suetsugu, T. Tauchi, A. Ferrari, J. Gronberg, Y. Iwashita, W. Lohmann, L. Ma, T.M. Mattison, T.S. Sanuki, V.I. Telnov, E.T. Torrence, D. Warner, N.K. Watson, H.Y. Yamamoto, "Design of the Beam Delivery System for the International Linear Collider," Proc. of the 22nd Particle Accelerator Conference (PAC07), IEEE, (2007), 1985 - 1987.

Rahul Shah, Radha Akella, Elizabeth J. Goldsmith, Margaret A. Phillips, "X-ray Structure of Paramecium bursaria Chlorella Virus Arginine Decarboxylase: Insight into the Structural Basis for Substrate Specificity," Biochemistry-US 46 (10), 2831-2841 (2007). DOI: 10.1021/bi6023447

Tsun-Kong Sham, Richard A. Rosenberg, "Time-Resolved Synchrotron Radiation Excited Optical Luminescence: Light-Emission Properties of Silicon-Based Nanostructures," Chem. Phys. Chem. 8 (18), 2557-2567 (2007). DOI: 10.1002/cphc.200700226

H.M. Shang, M. Bliss, S. Heald, T.K. Sham, F. Heigl, G.Z. Cao, "Dense and optical transparent CdWO[subscript 4] films by sol-gel processing for scintillation applications," J. Mater. Res. 22 (6), 1527-1536 (2007). DOI: 10.1557/JMR.2007.0215

Neeraj Sharma, Chris D. Ling, Grant E. Wrighter, Parry Y. Chen, Brendan J. Kennedy, Peter L. Lee, "Three-layer Aurivillius phases containing magnetic transition metal cations: Bi[subscript 2-x]Sr[subscript 2+x](Nb,Ta)[subscript 2+x]M[subscript 1-x]O[subscript 12],M=Ru[superscript 4+], Ir[superscript 4+], Mn[superscript 4+], ~0.5," J. Solid State Chem. 180 (1), 370-376 (2007). DOI: 10.1016/j.jssc.2006.10.031

Onkar Sharma, Eiki Yamashita, Mariya V. Zhalnina, Stanislav D. Zakharov, Kirill A. Datsenko, Barry L. Wanner, William A. Cramer, "Structure of the Complex of the Colicin E2 R-domain and Its BtuB Receptor: THE OUTER MEMBRANE COLICIN TRANSLOCON," J. Biol. Chem. 282 (32), 23163-23170 (2007). DOI: 10.1074/jbc.M703004200

S. Sharma, B. Adak, B. Rusthoven, "Long-Term High-Velocity Erosion of Glidcop in DI Water," Proc. of International Workshop on Mechanical Engineering Design of Synchrotron Radiation Equipment and Instrumentation 2006 (MEDSI06), SPring-8 (2007), *.

S.D. Shastri, J. Almer, C. Ribbing, B. Cederstrom, "High-energy X-ray optics with silicon saw-tooth refractive lenses," J. Synchrotron Rad. 14 (2), 204-211 (2007). DOI: 10.1107/S0909049507003962

Mouath Shatnawi, Gianluca Paglia, James L. Dye, Kevin D. Cram, Michael Lefenfeld, Simon J.L. Billinge, "Structures of Alkali Metals in Silica Gel Nanopores: New Materials for Chemical Reductions and Hydrogen Production," J. Am. Chem. Soc. 129 (5), 1386-1392 (2007). DOI: 10.1021/ja067140e

G.B. Shaw, C.D. Grant, H. Shirota, E.W. Castner Jr., G.J. Meyer, L.X. Chen, "Ultrafast Structural Rearrangement in the MLCT Excited State for Copper(I) bis-Phenanthrolines in Solution," J. Am. Chem. Soc. 129 (7), 2147-2160 (2007).

Neil Shaw, Chongyun Cheng, Wolfram Tempel, Jessie Chang, Joseph Ng, Xin-Yu Wang, Sarah Perrett, John Rose, Zihe Rao, Bi-Cheng Wang, Zhi-Jie Liu, "(NZ)CH...O contacts assist crystallization of a ParB-like nuclease," BMC Struct. Biol. 7 (46), online (2007). DOI: 10.1186/1472-6807-7-46

Neil Shaw, Min Zhao, Chongyun Cheng, Hao Xu, Juha Saarikettu, Yang Li, Yurong Da, Zhi Yao, Olli Silvennoinen, Jie Yang, Zhi-Jie Liu, Bi-Cheng Wang, Zihe Rao, "The multifunctional human p100 protein 'hooks' methylated ligands," Nat. Struct. Mol. Biol. 14 (8), 779-784 (2007). DOI: 10.1038/nsmb1269

B. Shen, Y. Li, K. Nemeth, H. Shang, Y.-c. Chae, R. Soliday, R. Crowell, E. Frank, W. Gropp, J. Cary, "Electron Injection by a Nanowire in the Bubble Regime," Phys. Plasmas 14, 053115-1-053115-5 (2007). DOI: 10.1063/1.2728773

B. Shen, Y. Li, M.Y. Yu, J. Cary, "Bubble Regime for Ion Acceleration in a Laser-Driven Plasma," Phys. Rev. E 76, 055402 (2007).

H.W. Sheng, H.Z. Liu, Y.Q. Cheng, J. Wen, P.L. Lee, W.K. Luo, S.D. Shastri, E. Ma, "Polyamorphism in a metallic glass," Nat. Mater. 6 (3), 192-197 (2007). DOI: 10.1038/nmat1839

Ju Sheng, Jun Ye, Barry P. Rosen, "Crystallization and preliminary X-ray crystallographic analysis of Escherichia coli glutaredoxin 2 in complex with glutathione and of a cysteine-less variant without glutathione," Acta Crystallogr. F F63, 280-282 (2007). DOI: 10.1107/S1744309107004204

G. Shen, H.P. Leirmann, S. Sinogeikin, W. Yang, X. Hong, C.-S Yoo, "Distinct thermal behavior of GeO2 glass in tetrahedral, intermediate, and octahedral forms," Proc. Natl. Acad. Sci. USA 104 (37), 14576-14579 (2007). DOI: 10.1073/pnas.0703098104

Qun Shen, Wah-Keat Lee, Kamel Fezzaa, Yong S. Chu, Francesco De Carlo, Peter Jemian, Jan Ilavsky, Mark Erdmann, Gabrielle G. Long, "Dedicated full-field X-ray imaging beamline at Advanced Photon Source," Nucl. Instrum. Methods A 582 (1), 77-79 (2007). DOI: 10.1016/j.nima.2007.08.169

Yong Rong Shen, Ravhi S. Kumar, Andrew L. Cornelius, Malcolm F. Nicol, "High-pressure structural studies of dysprosium using angle-dispersive x-ray diffraction," Phys. Rev. B 75, 064109-1-064109-9 (2007). DOI: 10.1103/PhysRevB.75.064109

K.W. Shepard, Z.A. Conway, J.D. Fuerst, M.P. Kelly, G.J. Waldschmidt, A.M. Porcellato, "Variable CW RF Power Coupler for 345 MHz Superconducting Cavities," Proc. of the 22nd Particle Accelerator Conference (PAC07), IEEE, (2007), 2230 - 2232.

Amy Y. Shih, Peter L. Freddolino, Stephen G. Sligar, Klaus Schulten, "Disassembly of Nanodiscs with Cholate," Nano Lett. 7 (6), 1692-1696 (2007). DOI: 10.1021/nl0706906

Atsushi Shimada, Hideaki Niwa, Kazuya Tsujita, Shiro Suetsugu, Koji Nitta, Kyoko Hanawa-Suetsugu, Ryogo Akasaka, Yuri Nishino, Mitsutoshi Toyama, Lirong Chen, Zhi-Jie Liu, Bi-Cheng Wang, Masaki Yamamoto, Takaho Terada, Atsuo Miyazawa, Akiko Tanaka, Sumio Sugano, Mikako Shirouzu, Kuniaki Nagayama, Tadaomi Takenawa, Shigeyuki Yokoyama, "Curved EFC/F-BAR-Domain Dimers Are Joined End to End into a Filament for Membrane Invagination in Endocytosis," Cell 129, 761-772 (2007). DOI: 10.1016/j.cell.2007.03.040

S. Shoaf, "Vector Processing Enhancements for Real-Time Image Analysis," Proc. of the 22nd Particle Accelerator Conference (PAC07), IEEE, (2007), 4339 - 4401.

O.G. Shpyrko, E.D. Isaacs, J.M. Logan, Yejun Feng, G. Aeppli, R. Jaramillo, H.C. Kim, T.F. Rosenbaum, P. Zschack, M. Sprung, S. Narayanan, A.R. Sandy, "Direct measurement of antiferromagnetic domain fluctuations," Nature 447, 68-71 (2007). DOI: 10.1038/nature05776

Oleg G. Shpyrko, Reinhard Streitel, V.S. K. Balagurusamy, Alexei Yu. Grigoriev, Moshe Deutsch, Benjamin M. Ocko, Mati Meron, Binhua Lin, Peter S. Pershan, "Crystalline surface phases of the liquid Au-Si eutectic alloy," Phys. Rev. B 76, 245436-1-245436-9 (2007). DOI:

10.1103/PhysRevB.76.245436

D. Shu, Z. Cai, B. Lai, "A Gas-Spring-Loaded X-Y-Z Stage System for X-ray Microdiffraction Sample Manipulation," Proc. of the Ninth International Conference on Synchrotron Radiation Instrumentation, 879, AIP, (2007), 1065 - 1068.

D. Shu, P.L. Lee, C. Preissner, M. Ramanathan, M. Beno, R.B. Von Dreele, J. Wang, R. Ranay, L. Ribaud, C. Kurtz, X. Jiao, D. Kline, P. Jemian, B.H. Toby, "Mechanical design of a high-resolution x-ray powder diffractometer at the Advanced Photon Source," New Developments in Optomechanics, Alson E. Hatheway, eds., 6665, SPIE, (2007), online. DOI: 10.1117/12.733110

D. Shu, J. Maser, M. Holt, R. Winarski, C. Preissner, B. Lai, S. Vogt, G.B. Stephenson, "A robot-based detector manipulator system for a hard X-ray nanoprobe instrument," Nucl. Instrum. Methods A 582 (1), 159-161 (2007). DOI: 10.1016/j.nima.2007.08.097

D. Shu, J. Maser, M. Holt, R. Winarski, C. Preissner, A. Smolyanitskiy, B. Lai, S. Vogt, G.B. Stephenson, "Optomechanical Design of a Hard X-ray Nanoprobe Instrument with Nanometer-Scale Active Vibration Control," Proc. of the Ninth International Conference on Synchrotron Radiation Instrumentation, 879, AIP, (2007), 1321 - 1324.

D. Shu, S. Narayanan, A. Sandy, M. Sprung, C. Preissner, J. Sullivan, "Precision Mechanical Design of an UHV-Compatible Artificial Channel-Cut X-ray Monochromator," New Developments in Optomechanics, 6665, SPIE, (2007), online. DOI: 10.1117/12.733101

D. Shu, O. Singh, M. Hahne, G. Decker, "Design Updates of the X-ray Beam Position Monitor for Beamline Front Ends," Proc. of the Ninth International Conference on Synchrotron Radiation Instrumentation, 879, AIP, (2007), 1014 - 1017.

D. Shu, T.S. Toellner, E.E. Alp, J. Maser, J. Ilavsky, S.D. Shastri, P.L. Lee, S. Narayanan, G.G. Long, "Applications of Laminar Weak-Link Mechanisms for Ultraprecision Synchrotron Radiation Instruments," Proc. of the Ninth International Conference on Synchrotron Radiation Instrumentation, 879, AIP, (2007), 1073 - 1076.

D. Shu, J. Wang, C. Preissner, "Thin, X-ray-Transparent Windows for Imaging Applications witha Pneumatically Pressurized Enclosure," Proc. of the Ninth International Conference on Synchrotron Radiation Instrumentation, 879, AIP, (2007), 1049 - 1052.

Jinfu Shu, Wendy L. Mao, Russell J. Hemley, Ho-kwang Mao, "Pressure-induced distortive phase transition in chromite-spinel at 29 GPa," Materials Research at High Pressure, M. Riad Manaa, Alexander F. Goncharov, Russell J. Hemley, Roberto Bini, eds., 987, MRS (2007), 179 - 184.

Xiaokun Shu, "Photophysics of emission color in fluorescent proteins," Ph.D., University of Oregon, 2007.

Xiaokun Shu, Karen Kallio, Xinghua Shi, Paul Abbyad, Pakorn Kanchanawong, William Childs, Steven G. Boxer, S. James Remington, "Ultrafast Excited-State Dynamics in the Green Fluorescent Protein Variant S65T/H148D. 1. Mutagenesis and Structural Studies," Biochemistry-US 46 (43), 12005-12013 (2007). DOI: 10.1021/bi7009037

Xiaokun Shu, Pavel Leiderman, Rinat Gepshtein, Nicholas R. Smith, Karen Kallio, Dan Huppert, S. James Remington, "An alternative excited-state proton transfer pathway in green fluorescent protein variant S205V," Protein Sci. 16 (12), 2703-2710 (2007). DOI: 10.1110/ps.073112007

Yu.V. Shvyd'ko, U. Kuetgens, H.D. Ruter, M. Lerche, A. Alatas, J. Zhao, "Progress in the Development of New Optics for Very High Resolution Inelastic X-ray Scattering Spectroscopy," Synchrotron Radiation Instrumentation: Ninth International Conference on Synchrotron Radiation Instrumentation, J-Y. Choi, R. Seungyu, eds., 879, AIP, (2007), 737 - 746.

H. Siebert, I. Quijada-Garrido, J. Vermant, L. Noirez, W.R. Burghardt, C. Schmidt, "Director Orientation of Nematic Side-Chain Liquid Crystalline Polymers under Shear Flow: Comparison of a Flow-aligning and a Non-flow-aligning Polysiloxane," Macromol. Chem. Phys. 208 (19-20), 2161-2172 (2007). DOI: 10.1002/macp.200700248

Edyta A.L. Sieminska, Xiaohui Xu, Alexei Savchenko, David A. R. Sanders, "The X-ray crystal structure of PA1607 from Pseudomonas aureginosa at 1.9 [Angstrom] resolution—a putative transcription factor," Protein Sci. 16 (3), 543-549 (2007). DOI: 10.1110/ps.062668207

Nathan J. Silvernail, Alexander Barabanschikov, Jeffrey W. Pavlik, Bruce C. Noll, Jiyong Zhao, E. Ercan Alp, Wolfgang Sturhahn, J. Timothy Sage, W. Robert Scheidt, "Interplay of Structure and Vibrational Dynamics in Six-Coordinate Heme Nitrosyls," J. Am. Chem. Soc. 129 (8), 2200-2201 (2007). DOI: 10.1021/ja066869k

S.B. Simon, S.R. Sutton, L. Grossman, "Valence of titanium and vanadium in pyroxene in refractory inclusion interiors and rims," Geochim. Cosmochim. Acta 71, 3098-3118 (2007). DOI: 10.1016/j.gca.2007.03.027

S.B. Simon, S. Sutton, M. Newville, L. Grossman, "The Valence of Titanium in Refractory Forsterite," Lunar and Planetary Science XXXVIII, LPI, (2007), 1892.

Anil K. Singh, Hanns-Peter Liermann, Yuichi Akahama, Haruki Kawamura, "Aluminum as a pressure-transmitting medium cum pressure standard for x-ray diffraction experiments to 200 GPa with diamond anvil cells," J. Appl. Phys. 101, 123526-1-123526-6 (2007). DOI: 10.1063/1.2734868

Mohit Singh, Omolola Odusanya, Gregg M. Wilmes, Hany B. Eitouni, Enrique D. Gomez, Amish J. Patel, Vincent L. Chen, Moon Jeong Park, Panagiota Fragouli, Hermis Iatrou, Nikos Hadjichristidis, David Cookson, Nitash P. Balsara, "Effect of Molecular Weight on the Mechanical and Electrical Properties of Block Copolymer Electrolytes," Macromolecules 40 (13), 4578-4585 (2007). DOI: 10.1021/ma0629541

S. Skanthakumar, Mark R. Antonio, Richard E. Wilson, L. Soderholm, "The Curium Aqua Ion," Inorg. Chem. 46 (9), 3485-3491 (2007). DOI: 10.1021/ic061798b

J.R. Skuza, R.A. Lukaszew, E.M. Dufresne, D.A. Walko, C. Clavero, A. Cebollada, C.N. Cionca, R. Clarke, "Real time structural modification of epitaxial FePt thin films under x-ray rapid thermal annealing using undulator radiation," Appl. Phys. Lett. 90, 251901-1-251901-3 (2007). DOI: 10.1063/1.2749426

E. Sloutskin, J. Baumert, B.M. Ocko, I. Kuzmenko, A. Checco, L. Tamam, E. Ofer, T. Gog, O. Gang, M. Deutsch, "The surface structure of concentrated aqueous salt solutions," J. Chem. Phys. 126, 54704-54710 (2007). DOI: 10.1063/1.2431361

A.J. Slowey, G.E. Brown, Jr., "Transformations of mercury, iron, and sulfur during the reductive dissolution of iron oxyhydroxide by sulfide," Geochim. Cosmochim. Acta 71 (4), 877-894 (2007). DOI: 10.1016/j.gca.2006.11.011

Paula G. Smith, "ARSENIC BIOTRANSFORMATION IN TERRESTRIAL ORGANISMS: A study of the transport and transformation of arsenic in plants, fungi, fur and feathers, using conventional speciation analysis and X-ray absorption spectroscopy," Ph.D., Queen's University, 2007.

P.G. Smith, I. Koch, K.J. Reimer, "Arsenic Speciation Analysis of Cultivated White Button Mushrooms (Agaricus bisporus) Using High-Performance Liquid Chromatography-Inductively Coupled Plasma Mass Spectrometry, and X-ray Absorption Spectroscopy," Environ. Sci. Technol. 41 (20), 6947-6954 (2007). DOI: 10.1021/es071022p

J.P. Smit, H.-S. Kim, I. Saratovsky, K.B. Stark, G. Fitzgerald, G.W. Zajac, J.-F. Gaillard, K.R. Poeppelmeier, P.C. Stair, "A Spectroscopic and Computational Investigation of the Vanadomolybdate Local Structure in the Lyonsite Phase Mg[subscript 2.5]VMoO[subscript 8]," Inorg. Chem. 46 (16), 6556-6564 (2007). DOI: 10.1021/ic7006815

Edward H. Snell, Henry D. Bellamy, Gerd Rosenbaum, Mark J. van der Woerd, "Non-invasive measurement of X-ray beam heating on a surrogate crystal sample," J. Synchrotron Rad. 14, 109-115 (2007). DOI: 10.1107/S090904950604605X

John J. Socha, Mark W. Westneat, Jon F. Harrison, James S. Waters, Wah-Keat Lee, "Real-time phase-contrast x-ray imaging: a new technique for the study of animal form and function," BMC Biology 5 (6), 1-15 (2007). DOI: 10.1186/1741-7007-5-6

Jungsan Sohn, Gregory Buhrman, Johannes Rudolph, "Kinetic and Structural Studies of Specific Protein - Protein Interactions in Substrate Catalysis by Cdc25B Phosphatase," Biochemistry-US 46 (3), 807-818 (2007). DOI: 10.1020/bi061257y

J. Sohn, R.A. Grant, R.T. Sauer, "Allosteric Activation of DegS, a Stress Sensor PDZ Protease," Cell 131 (3), 572-583 (2007). DOI: 10.1016/j.cell.2007.08.044

Emmanuel Soignard, Olga Shebanova, Paul F. McMillan, "Compressibility measurements and phonon spectra of hexagonal transition-metal nitrides at high pressure: [epsilon]TaN, [delta]-MoN, and Cr[subscript 2]N," Phys. Rev. B 75, 014104-1-014104-9 (2007). DOI: 10.1103/PhysRevB.75.014104

Inna Solomonov, Maria Osipova, Yishay Feldman, Carsten Baehtz, Kristian Kjaer, Ian K. Robinson, Grant T. Webster, Don McNaughton, Bayden R. Wood, Isabelle Weissbuch, Leslie Leiserowitz, "Crystal Nucleation, Growth, and Morphology of the Synthetic Malaria Pigment [beta]-Hematin and the Effect Thereon by Quinoline Additives: The Malaria Pigment as a Target of Various Antimalarial Drugs," J. Am. Chem. Soc. 129 (9), 2615-2627 (2007). DOI: 10.1021/ja0674183

Zhenlei Song, Richard P. Hsung, "A Formal Total Synthesis of (+)-Zincophorin. Observation of an Unusual Urea-Directed Stork-Crabtree Hydrogenation," Org. Lett. 9 (11), 2199-2202 (2007). DOI: 10.1021/ol070791a

D.J. Sordelet, M.F. Besser, R.T. Ott, B.J. Zimmerman, W.D. Porter, B. Gleeson, "Isothermal nature of martensite formation in Pt-modified [beta]-NiAl alloys," Acta Mater. 55 (7), 2433-2441 (2007). DOI: 10.1016/j.actamat.2006.11.038

D.J. Sordelet, M.F. Besser, R.T. Ott, B.J. Zimmerman, W.D. Porter, B. Gleeson, "Isothermal nature of martensite formation in Pt-modified [beta]-NiAl alloys," Acta Mater. 55 (7), 2433-2441 (2007). DOI: 10.1016/j.actamat.2006.11.038

D.J. Sordelet, X.Y. Yang, E.R. Rozhkova, M.F. Besser, M.J. Kramer, "Metastable phase formation in rapidly quenched Zr[subscript 80]Pt[subscript 20] alloys: Linkage to oxygen," J. Non-Cryst. Solids 353 (32-40), 3439-3443 (2007). DOI: 10.1016/j.jnoncrysol.2007.05.096

Jesper Sorensen, Henrik F. Clausen, Rasmus D. Poulsen, Jacob Overgaard, Birgit Schiott, "Short Strong Hydrogen Bonds in 2-Acetyl-1,8-dihydroxy-3,6-dimethylnaphthalene: An Outlier to Current Hydrogen Bonding Theory?," J. Phys. Chem. A 111 (2), 345-351 (2007). DOI: 10.1021/jp0643395

E.V. Soriano, V.C. Clark, S.E. Ealick, "Structures of Human Deoxycytidine Kinase Product Complexes," Acta Crystallogr. D 63 (12), 1201-1207 (2007). DOI: 10.1107/S0907444907048834

S.H. Southworth, D.A. Arms, E.M. Dufresne, R.W. Dunford, D.L. Ederer, C. Hohr, E.P. Kanter, B. Krassig, E.C. Landahl, E.R. Peterson, J. Rudati, R. Santra, D.A. Walko, L. Young, "K-edge x-ray-absorption spectroscopy of laser-generated Kr[superscript +] and Kr[superscript 2+]," Phys. Rev. A 76, 043421-1-043421-9 (2007). DOI: 10.1103/PhysRevA.76.043421

E.D. Specht, A. Goyal, W. Liu, "Local epitaxy of YBa[subscript 2]Cu[subscript 3]O[subscript x] on polycrystalline Ni measured by x-ray microdiffraction," J. Mater. Res. 22 (3), 664-674 (2007). DOI: 10.1557/JMR.2007.0091

S. Speziale, V.E. Lee, S.M. Clark, J.F. Lin, M.P. Pasternak, R. Jeanloz, "Effects of Fe spin transition on the elasticity of (Mg, Fe)O magnesiowüstites and implications for the seismological properties of the Earth's lower mantle," J. Geophys. Res. 112, B10212-1-B10212-12 (2007). DOI: 10.1029/2006JB004730

Julie A. Spicer, Gordon W. Rewcastle, Michael D. Kaufman, Shannon L. Black, Mark S. Plummer, William A. Denny, John Quin, III, Aurash B. Shahripour, Stephen D. Barrett, Christopher E. Whitehead, Jared B.J. Milbank, Jeffrey F. Ohren, Richard C. Gowan, Charles Omer, Heidi S. Camp, Nadia Esmaeil, Kelley Moore, Judith S. Sebolt-Leopold, Sally Pryzbranowski, Ronald L. Merriman, Daniel F. Ortwine, Joseph S. Warmus, Cathlin M. Flamme, Alexander G. Pavlovsky, Haile Tecle, "4-Anilino-5-carboxamido-2-pyridone Derivatives as Noncompetitive Inhibitors of Mitogen-Activated Protein Kinase Kinase," J. Mater. Chem. 50 (21), 5090-5102 (2007). DOI: 10.1021/jm0704548

Miguel St-Jean, Tina Izard, Jurgen Sygusch, "A Hydrophobic Pocket in the Active Site of Glycolytic Aldolase Mediates Interactions with Wiskott-Aldrich Syndrome Protein," J. Biol. Chem. 282 (19), 14309-14315 (2007). DOI: 10.1074/jbc.M611505200

Martin St. Maurice, Paola E. Mera, Maria P. Taranto, Fernando Sesma, Jorge C. Escalante-Semerena, Ivan Rayment, "Structural Characterization of the Active Site of the PduO-Type ATP:Co(I)rrinoid Adenosyltransferase from Lactobacillus reuteri," J. Biol. Chem. 282 (4), 2596-2605 (2007). DOI: 10.1074/jbc.M609557200

Martin St. Maurice, Laurie Reinhardt, Kathy H. Surinya, Paul V. Attwood, John C. Wallace, W. Wallace Cleland, Ivan Rayment, "Domain Architecture of Pyruvate Carboxylase, a Biotin-Dependent Multifunctional Enzyme," Science 317, 1076-1079 (2007). DOI: 10.1126/science.1144504

Lorenz-M. Stadler, Ross Harder, Ian K. Robinson, Christian Rentenberger, H.-Peter Karnthaler, Bogdan Sepiol, Gero Vogl, "Coherent x-ray diffraction imaging of grown-in antiphase boundaries in Fe[subscript 65]Al[subscript 35]," Phys. Rev. B 76, 014204-1-014204-9 (2007). DOI: 10.1103/PhysRevB.76.014204

G.E. Stein, E.W. Cochran, K. Katsov, G.H. Fredrickson, E.J. Kramer, X. Li, J. Wang, "Symmetry Breaking of In-Plane Order in Confined Copolymer Mesophases," Phys. Rev. Lett. 98, 158302-1-158302-4 (2007). DOI: 10.1103/PhysRevLett.98.158302

G.E. Stein, E.J. Kramer, X. Li, J. Wang, "Single-Crystal Diffraction from Two-Dimensional Block Copolymer Arrays," Phys. Rev. Lett. 98 (8), 086101-1-086101-1 (2007). DOI: 10.1103/PhysRevLett.98.086101

Gila E. Stein, Edward J. Kramer, Xuefa Li, Jin Wang, "Layering Transitions in Thin Films of Spherical-Domain Block Copolymers," Macromolecules 40 (7), 2453-2460 (2007). DOI: 10.1021/ma0625509

Gila E. Stein, Won Bo Lee, Glenn H. Fredrickson, Edward J. Kramer, Xuefa Li, Jin Wang, "Thickness Dependent Ordering in Laterally Confined Monolayers of Spherical-Domain Block Copolymers," Macromolecules 40 (16), 5791-5800 (2007). DOI: 10.1021/ma062559a

G.E. Sterbinsky, J. Cheng, P.T. Chiu, B.W. Wessels, D.J. Keavney, "Investigation of heteroepitaxial growth of magnetite thin films," J. Vac. Sci. Technol. B 25 (4), 1389-1392 (2007). DOI: 10.1116/1.2757185

E.A. Stern, D. Brewe, "Ultrafast XAFS Measurements on Laser Excited Ge Films," AIP Conference Proceedings, B. Hedman, P. Pianetta, eds., 882, American Institute of Physics, (2007), 24 - 28.

Kent D. Stewart, Kevin Steffy, Kevin Harris, John E. Harlan, Vincent S. Stoll, Jeffrey R. Huth, Karl A. Walter, Emily Gramling-Evans, Renaldo R. Mendoza, Jean M. Severin, Paul L. Richardson, Leo W. Barrett, Edmund D. Matayoshi, Kerry M. Swift, Stephen F. Betz, Steve W. Muchmore, Dale J. Kempf, Akhter Molla, "Design and characterization of an engineered gp41 protein from human immunodeficiency virus-1 as a tool for drug discovery," J. Comput. Aided Mol. Des. 21 (1-3), 121-130 (2007). DOI: 10.1007/s10822-007-9107-1

R.E. Stoller, F.J. Walker, E.D. Specht, D.M. Nicholson, R.I. Barabash, P. Zschack, G.E. Ice, "Diffuse X-ray scattering measurements of point defects and clusters in iron," J. Nucl. Mater. 367-370 (1), 269-275 (2007). DOI: 10.1016/j.jnucmat.2007.03.019

S. Stoupin, S. Chattopadhyay, T. Bolin, C.U. Segre, "High concentration manganese doping of ferroelectric PbTiO[subscript 3]," Solid State Commun. 144 (1-2), 46-49 (2007). DOI: 10.1016/j.ssc.2007.07.023

Dusan S. Strmcnik, Peter Rebec, Miran Gaberscek, Dusan Tripkovic, Vojislav Stamenkovic, Christopher Lucas, Nenad M.´Markovic, "Relationship between the Surface Coverage of Spectator Species and the Rate of Electrocatalytic Reactions," J. Phys. Chem. C 111, 18672-18678 (2007). DOI: 10.1021/jp0756146

Daniel E. Strongin, Brooke Bevis, Nhi Khuong, Maureen E. Downing, Rita L. Strack, Karthik Sundaram, Benjamin S. Glick, Robert J. Keenan, "Structural rearrangements near the chromophore influence the maturation speed and brightness of DsRed variants," Protein Eng. Des. Sel. 20 (11), 525-534 (2007). DOI: 10.1093/protein/gzm046

Wolfgang Sturhahn, Jennifer M. Jackson, "Geophysical applications of nuclear resonant spectroscopy," Advances in High-Pressure Mineralogy, E. Ohtani, eds., Geological Society of America, 2007, 157 - 174. DOI: 10.1130/2007.2421(09)

Leopoldo Suescun, Omar Chmaissem, James Mais, Bogdan Dabrowski, James D. Jorgensen, "Crystal structures, charge and oxygen-vacancy ordering in oxygen deficient perovskites SrMnO[subscript x] (x<2.7)," J. Solid State Chem. 180 (5), 1698-1707 (2007). DOI: 10.1016/j.jssc.2007.03.020

Sarah M. Sullivan, Todd Holyoak, "Structures of Rat Cytosolic PEPCK: Insight into the Mechanism of Phosphorylation and Decarboxylation of Oxaloacetic Acid," Biochemistry-US 46 (35), 10078-10088 (2007). DOI: 10.1021/bi701038x

Ping Sun, Brian P. Austin, Florian D. Schubot, David S. Waugh, "New protein fold revealed by a 1.65 Å resolution crystal structure of Francisella tularensis pathogenicity island protein IglC," Protein Sci. 16, 2560-2563 (2007). DOI: 10.1110/ps.073177307

Siyang Sun, Kiran Kondabagil, Petra M. Gentz, Michael G. Rossmann, Venigalla B. Rao, "The Structure of the ATPase that Powers DNA Packaging into Bacteriophage T4 Procapsids," Mol. Cell 25 (6), 943-949 (2007). DOI: 10.1016/j.molcel.2007.02.013

X.H. Sun, T.K. Sham, R.A. Rosenberg, G.K. Shenoy, "One-dimensional Silicon-Cadmium Selenide Heterostructures," J. Phys. Chem. C 111 (24), 8475-8482 (2007). DOI: 10.1021/jp071699z

X. Sun, O. Singh, "Tuning the Narrow-band Beam Position Monitor Sampling Clock to Remove the Aliasing Errors in APS Storage Ring Orbit Measurements," Proc. of the 22nd Particle Accelerator Conference (PAC07), IEEE, (2007), 4402 - 4404.

Y.-E Sun, D.W. Feldman, J.W. Lewellen, "Photothermal Cathode Measurements at the Advanced Photon Source," Proc. of the 2006 Linear Accelerator Conference (LINAC06), SNS (2007), 349 - 351.

Y.-E Sun, J.W. Lewellen, "Shunt Impedance Measurement of the APS BBC Injector," Proc. of the 2006 Linear Accelerator Conference (LINAC06), SNS (2007), 346 - 348.

Y.-e Sun, J.G. Power, K.-J. Kim, P. Piot, M.M. Rihaoui, "Design Study of a Transverse-to-Longitudinal Emittance Exchange Proof-of-Principle Experiment," Proc. of the 22nd Particle Accelerator Conference (PAC07), IEEE, (2007), 3441 - 3443.

M.L. Suominen-Fuller, S. Ramamurthy, N.S. McIntyre, R.J. Klassen, P.J. King, A. Gerson, W. Liu, "Texture and Residual Strain Measurements on Polished Alloy 600 Coupon Containing Two Scratches Using Synchrotron Micro-Laue Diffraction," Laue2007: International Workshop on Advanced Laue Diffraction in Frontier Science, Institut Laue-Langevin, (2007), online.

P. Swaminathan, R.A. Rosenberg, G.K. Shenoy, J.S. Palmer, J.H. Weaver, "Induced magnetism in Cu nanoparticles embedded in Co," Appl. Phys. Lett. 91, 202506-1-202506-3 (2007). DOI: 10.1063/1.2806236

Kittipong Tachampa, Helen Wang, Gerrie P. Farman, Pieter P. de Tombe, "Cardiac Troponin I Threonine 144: Role in Myofilament Length–Dependent Activation," Circ. Res. 101, 1081-1083 (2007). DOI: 10.1161/CIRCRESAHA.107.165258

Kuo-Hsiang Tang, Hongjie Guo, Wen Yi, Ming-Daw Tsai, Peng George Wang, "Investigation of the Conformational States of Wzz and the Wzz·O-Antigen Complex under Near-Physiological Conditions," Biochemistry-US 46 (42), 11744-11752 (2007). DOI: 10.1021/bi701181r

Xiaojing Tang, Stephen Orlicky, Zhenyuan Lin, Andrew Willems, Dante Neculai, Derek Ceccarelli, Frank Mercurio, Brian H. Shilton, Frank Sicheri, Mike Tyers, "Suprafacial Orientation of the SCF[superscript Cdc4] Dimer Accommodates Multiple Geometries for Substrate Ubiquitination," Cell 129 (6), 1165-1176 (2007). DOI: 10.1016/j.cell.2007.04.042

Yuanzhi Tang, Evert J. Elzinga, Young Jae Lee, Richard J. Reeder, "Coprecipitation of chromate with calcite: Batch experiments and X-ray absorption spectroscopy," Geochim. Cosmochim. Acta 71 (6), 1480-1493 (2007). DOI: 10.1016/j-gca.2006.12.010

Kunaljeet S. Tanwar, Jeffrey G. Catalano, Sarah C. Petitto, Sanjit K. Ghose, Peter J. Eng, Thomas P. Trainor, "Hydrated [alpha]-Fe[subscript 2]O[subscript 3(1102)] surface structure: Role of surface preparation," Surf. Sci. 601 (12), L59-L64 (2007). DOI: 10.1016/j.susc.2007.04.115

Kunaljeet S. Tanwar, Cynthia S Lo, Peter J. Eng, Jeffrey G. Catalano, Donald A. Walko, Gordon E. Brown, Glenn A. Waychunas, Anne M. Chaka, Thomas P. Trainor, "Surface diffraction study of the hydrated hematite (1102) surface," Surf. Sci. 601 (2), 460-474 (2007). DOI: 10.1016/j.susc.2006.10.021

R. Tappero, E. Peltier, M. Grafe, K. Heidel, M. Ginder-Vogel, K.J.T. Livi, M.L. Rivers, M.A. Marcus, R.L. Chaney, D.L. Sparks, "Hyperaccumulator Alyssum murale relies on a different metal storage mechanism for cobalt than for nickel," New Phytol. 175 (4), 641-654 (2007). DOI: 10.1111/j.1469-8137.2007.02134.x

Wolfram Tempel, Wael M. Rabeh, Katrina L. Bogan, Peter Belenky, Marzena Wojcik, Heather F. Seidle, Lyudmila Nedyalkova, Tianle Yang, Anthony A. Sauve, Hee-Won Park, Charles Brenner, "Nicotinamide Riboside Kinase Structures Reveal New Pathways to NAD[superscript +]," PLoS Biol. 5 (10), e263-1-e263-11 (2007). DOI: 10.371/journal.pbio.0050263

Karen R. Thickman, E. Allen Sickmier, Clara L. Kielkopf, "Alternative Conformations at the RNA-binding Surface of the N-terminal U2AF[superscript 65] RNA Recognition Motif," J. Mol. Biol. 366 (3), 703-710 (2007). DOI: 10.1016/j.jmb.2006.11.077

J. Thieme, I. McNulty, S. Vogt, D. Paterson, "X-Ray Spectromicroscopy - A Tool for Environmental Sciences," Environ. Sci. Technol. 41 (20), 6885-6889 (2007).

R.G. Thiessen, J. Sietsma, T.A. Palmer, J.W. Elmer, I.M. Richardson, "Phase-field modelling and synchrotron validation of phase transformations in martensitic dual-phase steel," Acta Mater. 55 (2), 601-614 (2007). DOI: 10.1016/j.actamat.2006.08.053

James B. Thoden, Hazel M. Holden, "Active site geometry of glucose-1-phosphate uridylyltransferase," Protein Sci. 16, 1379-1388 (2007). DOI: 10.1110/ps.072864707

James B. Thoden, Christopher A. Sellick, Richard J. Reece, Hazel M. Holden, "Understanding a Transcriptional Paradigm at the Molecular Level: THE STRUCTURE OF YEAST Gal80p," J. Biol. Chem. 282 (3), 1534-1538 (2007). DOI: 10.1074/jbc.C600285200

L.H. Thomas, T.R. Welberry, D.J. Goossens, A.P. Heerdegen, M.J. Gutmann, S.J. Teat, P.L. Lee, C.C. Wilson, J.M. Cole, "Disorder in pentachloronitrobenzene, C[subscript 6]Cl[subscript 5]NO[subscript 2]: a diffuse scattering study," Acta Crystallogr. B 63 (4), 663-673 (2007). DOI: 10.1107/S0108768107024305

K. Ted Thurn, Eric M.B. Brown, Aiguo Wu, Stefan Vogt, Barry Lai, Jorg Maser, Tatjana Paunesku, Gayle E. Woloschak, "Nanoparticles for Applications in Cellular Imaging," Nanoscale Res. Lett. 2 (9), 430-441 (2007). DOI: 10.1007/s11671-007-9081-5

Yunfeng Tie, Andrey Y. Kovalevsky, Peter Boross, Yuan-Fang Wang, Arun K. Ghosh, Jozsef Tozser, Robert W. Harrison, Irene T. Weber, "Atomic Resolution Crystal Structures of HIV-1 Protease and Mutants V82A and I84V with Saquinavir," Proteins 67 (1), 232-242 (2007). DOI: 10.1002/prot.21304

Vijay R. Tirumala, Rajaram A. Pai, Sumit Agarwal, Jason J. Testa, Gaurav Bhatnagar, Alvin H. Romang, Curran Chandler, Brian P. Gorman, Ronald L. Jones, Eric K. Lin, James J. Watkins, "Mesoporous Silica Films with Long-Range Order Prepared from Strongly Segregated Block Copolymer/Homopolymer Blend Templates," Chem. Mater. 19 (24), 5868-5874 (2007). DOI: 10.1021/cm070792x

J.G. Tobin, S.A. Morton, S.W. Yu, T. Komesu, G.D. Waddill, P. Boyd, "Spin Spectrometer at the ALS and APS," Nucl. Instrum. Methods A 582 (1), 162-164 (2007). DOI: 10.1016/j.nima.2007.08.098

J.G. Tobin, S.W. Yu, T. Komesu, B.W. Chung, S.A. Morton, G.D. Waddill, "Facilities for the performance of Fano measurements as a probe of electron correlation," Actinides 2006 — Basic Science, Applications and Technology, K.J.M. Blobaum, E.A. Chandler, L. Havela, M.B. Maple, M.P. Neu, eds., 986, MRS (2007), online.

J.G. Tobin, S.W. Yu, T. Komesu, B.W. Chung, S.A. Morton, G.D. Waddill, "Evidence of dynamical spin shielding in Ce from spin-resolved photoelectron spectroscopy," Europhys. Lett. 77, 17004-1-17004-6 (2007). DOI: 10.1209/0295-5075/77/17004

B.H. Toby, "A new approach for instruction in powder crystallography," Powder Diffr. 22 (1), 83-84 (2007). DOI: 10.1154/1.2472366

Elitza I. Tocheva, Federico I. Rosell, A. Grant Mauk, Michael E.P. Murphy, "Stable Copper-Nitrosyl Formation by Nitrite Reductase in Either Oxidation State," Biochemistry-US 46 (43), 12366-12374 (2007). DOI: 10.1021/bi701205jS0006-2960(70)01205-9

Tetsu K. Tokunaga, Jiamin Wan, Antonio Lanzirotti, Steve R. Sutton, Matthew Newville, William Rao, "Long-Term Stability of Organic Carbon-Stimulated Chromate Reduction in Contaminated Soils and Its Relation to Manganese Redox Status," Environ. Sci. Technol. 41 (12), 4326-4331 (2007). DOI: 10.1021/es062874c

Yufeng Tong, Preeti Chugha, Prasanta K. Hota, Rebecca S. Alviani, Mei Li, Wolfram Tempel, Limin Shen, Hee-Won Park, Matthias Buck, "Binding of Rac1, Rnd1, and RhoD to a Novel Rho GTPase Interaction Motif Destabilizes Dimerization of the Plexin-B1 Effector Domain," J. Biol. Chem. 282 (51), 37215-37224 (2007). DOI: 10.1074/jbc.M703800200

Debra S. Touw, Christer E. Nordman, Jeanne A. Stuckey, Vincent L. Pecoraro, "Identifying important structural characteristics of arsenic resistance proteins by using designed three-stranded coiled coils," Proc. Natl. Acad. Sci. USA 104 (29), 11969-11974 (2007). DOI: 10.1073/pnas.0701979104

Sharon A. Townson, James C. Samuelson, Yongming Bao, Shuang-yong Xu, Aneel K. Aggarwal, "BstYI Bound to Noncognate DNA Reveals a 'Hemispecific' Complex: Implications for DNA Scanning," Structure 15 (4), 449-459 (2007). DOI: 10.1016/j.str.2007.03.002

E. Trakhtenberg, T. Barsz, P.K. Den Hartog, G.S. Lawrence, E.R. Moog, S. Sasaki, I. Vasserman, M. White, T. Becker, S. Dufresne, W. Kummerle, R. Schuermann, G. Goldfarb, N. Lagonsky, S. Lagonsky, S. Sorsher, "LCLS Undulator Production," Proc. of the 22nd Particle Accelerator Conference (PAC07), IEEE, (2007), 1148 - 1150.

E. Trakhtenberg, G. Wiemerslage, "A Study of the Minimum Wall Thickness for an Extruded Aluminum Vacuum Chamber," Proc. of the 22nd Particle Accelerator Conference (PAC07), IEEE, (2007), 1151 - 1152.

C.Q. Tran, G.J. Williams, A. Roberts, S. Flewett, A.G. Peele, D. Paterson, M.D. De Jonge, K.A. Nugent, "Experimental Measurement of the Four-Dimensional Coherence Function for an Undulator X-Ray Source," Phys. Rev. Lett. 98, 224801-1-224801-4 (2007). DOI: 10.1103/PhysRevLett.98.224801

M.M.J. Treacy, D. Kumar, A. Rougee, G. Zhao, P.R. Buseck, I. McNulty, L. Fan, C. Rau, J.M. Gibson, "Probing medium-range structural correlations by fluctuation microscopy," J. Phys. Condens. Matter 19 (45), 455201-455211 (2007). DOI: 10.1088/0953-8984/19/45/455201

Y.C. Tseng, D. Haskel, J.C. Lang, S. Sinogeikin, Ya. Mudryk, V.K. Pecharsky, K.A. Gschneidner, Jr., "Effect of hydrostatic pressure upon the magnetic transitions in the Gd[subscript 5](Si[subscript x]Ge[subscript 1−x])[subscript 4] giant magnetocaloric compounds: X-ray magnetic circular dichroism study," Phys. Rev. B 76, 014411-1-014411-6 (2007). DOI: 10.1103/PhysRevB.76.014411

Yaroslav Tsybovsky, Henry Donato, Natalia I. Krupenko, Christopher Davies, Sergey A. Krupenko, "Crystal Structures of the Carboxyl Terminal Domain of Rat 10-Formultetrahydrofolate Dehydrogenase: Implications for the Catalytic Mechanism of Aldehyde Dehydrogenases," Biochemistry-US 46 (11), 2917-2929 (2007). DOI: 10.1021/bi0619573

Anish Tuteja, Michael E. Mackay, Suresh Narayanan, Subashini Asokan, Michael S. Wong, "Breakdown of the Continuum Stokes-Einstein Relation for Nanoparticle Diffusion," Nano Lett. 7 (5), 1276-1281 (2007). DOI: 10.1021/nl070192x

Fleur E. Tynan, Hugh H. Reid, Lars Kjer-Nielsen, John J. Miles, Matthew C.J. Wilce, Lyudmila Kostenko, Natalie A. Borg, Nicholas A. Williamson, Travis Beddoe, Anthony W. Purcell, Scott R. Burrows, James McCluskey, Jamie Rossjohn, "A T cell receptor flattens a bulged antigenic peptide presented by a major histocompatibility complex class I molecule," Nat. Immunol. 8 (3), 268-276 (2007). DOI: 10.1038/ni1432

M.H. Upton, A.C. Walters, C.A. Howard, K.C. Rahnejat, M. Ellerby, J.P. Hill, D.F. McMorrow, A. Alatas, Bogdan M. Leu, Wei Ku, "Phonons in superconducting CaC[subscript 6] studied via inelastic x-ray scattering," Phys. Rev. B 76, 220501-1-220501-4 (2007). DOI: 10.1103/PhysRevB.76.220501

Vikrant N. Urade, Ta-Chen Wei, Michael P. Tate, Jonathan D. Kowalski, Hugh W. Hillhouse, "Nanofabrication of Double-Gyroid Thin Films," Chem. Mater. 19 (4), 768-777 (2007). DOI: 10.1021/cm062136n

G. Vaitheeswaran, V. Kanchana, Ravhi S. Kumar, A.L. Cornelius, M.F. Nicol, A. Svane, A. Delin, B. Johansson, "High-pressure structural, elastic, and electronic properties of the scintillator host material KMgF[subscript 3]," Phys. Rev. B 76, 014107-1-014107-6 (2007). DOI: 10.1103/PhysRevB.76.014107

Stefan Vajda, Gregory E. Ballentine, Stephanie Mucherie, Christopher L. Marshall, Jeffrey W. Elam, Michael J. Pellin, Byeongdu Lee, Chieh-Tsung Lo, Sonke Seifert, Randall E. Winans, Joseph M. Calo, "Highly selective catalytic oxidation reactions: I. Oxidative dehydrogenation of propane (ODHP) by size-selected platinum catalysts, and II: Oxidation of alkenes on size-selected silver and gold clusters and nanoparticles," The 233rd ACS National Meeting, American Chemical Society (2007), online.

Stefan Vajda, Gregory E. Ballentine, Stephanie Mucherie, Christopher L. Marshall, Jeffrey W. Elam, Michael J. Pellin, Byeongdu Lee, Chieh-Tsung Lo, Sonke Seifert, Randall E. Winans, Joseph M. Calo, "Supported Size Selected Clusters as Model Nanocatalysts for Highly Selective and Efficient Oxidation Reactios," XXII International Symposium on Molecular Beams, A. Kleibert, K. Sell, V. von Oyenhausen, K.-H. Meiwes-Broer, eds., Universitatsplatz (2007), online.

S. Vajda, G.P. Wiederrecht, A. Bouhelier, G.Y. Tikhonov, N. Tomczyk, B. Lee, S. Seifert, R.E. Winans, "Optical Properties of Gold Nanoparticles Produced by the Assembly of Size-Selected Clusters: Covering the Full Visible Wavelength Range in the Smallest Particle Size Regime," Collect. Czech. Chem. Commun. 72 (1), 121-128 (2007). DOI: 10.1135/cccc20070121

David Vaknin, Wei Bu, SushilK. Satija, Alex Travesset, "Ordering by Collapse: Formation of Bilayer and Trilayer Crystals by Folding Langmuir Monolayers," Langmuir 23 (4), 1888-1897 (2007). DOI: 10.1021/la062672u

J. van Lierop, B.W. Southern, K.-W. Lin, Z.-Y. Guo, C.L. Harland, R.A. Rosenberg, J.W. Freeland, "Exchange bias in a columnar nanocrystalline Ni[subscript 80]Fe[subscript 20]/CoO thin film," Phys. Rev. B 76, 224432-1-224432-7 (2007). DOI: 10.1103/PhysRevB.76.224432

D.B. Varshney, S. Kumar, E.Y. Shalaev, P. Sundaramurthi, S.-W. Kang, L.A. Gatlin, R. Suryanarayanan, "Glycine Crystallization in Frozen and Freeze-dried Systems: Effect of pH and Buffer Concentration," Pharmaceut. Res. 24 (3), 593-604 (2007). DOI: 10.1007/s11095-006-9178-z

I.A. Vartanyants, I.K. Robinson, I. McNulty, C. David, P. Wochner , Th. Tschentscher, "Coherent X-ray scattering and lensless imaging at the European XFEL Facility," J. Synchrotron Rad. 14 (6), 453-470 (2007). DOI: doi:10.1107/S0909049507037600

Chrysoula Vasileiou, Soheila Vaezeslami, Rachael M. Crist, Montserrat Rabago-Smith, James H. Geiger, Babak Borhan, "Protein Design: Reengineering Cellular Retinoic Acid Binding Protein II into a Rhodopsin Protein Mimic," J. Am. Chem. Soc. 129 (19), 6140-6148 (2007). DOI: 10.1021/ja067546r

I.B. Vasserman, R.J. Dejus, S. Sasaki, J.Z. Xu, E.M. Trakhtenberg, S.V. Milton, E.R. Moog, M.M. White, N.A. Vinokurov, "LCLS undulator—recent developments: Undulator tapering to compensate for particle energy loss (simulations, continuous case). First article measurements and tuning," Nucl. Instrum. Methods A 575 (1-2), 22-28 (2007).

Dmitry G. Vassylyev, Jindrich Symersky, "Crystal Structure of Pyruvate Dehydrogenase Phosphatase 1 and its Functional Implications," J. Mol. Biol. 370 (3), 417-426 (2007). DOI: 10.1016/jmb.2007.05.002

Dmitry G. Vassylyev, Marina N. Vassylyeva, Anna Perederina, Tahir H. Tahirov, Irina Artsimovitch, "Structural basis for transcription elongation by bacterial RNA polymerase," Nature 448, 157-162 (2007). DOI: 10.1038/nature05932

Dmitry G. Vassylyev, Marina N. Vassylyeva, Jinwei Zhang, Murali Palangat, Irina Artsimovitch, Robert Landick, "Structural basis for substrate loading in bacterial RNA polymerase," Nature 448, 163-168 (2007). DOI: 10.1038/nature05931

B.W. Veal, A.P. Paulikas, B. Gleeson, P.Y. Hou, "Creep in ao, "Measuring air-water interfacial areas with x-ray microtomography and interfacial partitioning tracer tests," Environ. Sci. Technol. 41 (6), 1956-1961 (2007). DOI: 10/1021/es061474m

Susan K. Buchanan, Petra Lukacik, Sylvestre Grizot, Rodolfo Ghirlando, Maruf M.U. Ali, Travis J. Barnard, Karen S. Jakes, Paul K. Kienker, Lothar Esser, "Structure of colicin I receptor bound to the R-domain of colicin Ia: implications for protein import," EMBO J. 26 (10), 2594-2604 (2007). DOI: 10.1038/sj.emboj.7601693

P.S. Budnik, R.A. Gordon, E.D. Crozier, "The Pd/Fe Interface in the Epitaxial System Pd/Fe/GaAs(001)- 4 x 6," AIP Conference Proceedings, B. Hedman, P. Pianetta, eds., 882, American Institute of Physics, (2007), 398 - 400.

Greg Buhrman, Glenna Wink, Carla Mattos, "Transformation Efficiency of RasQ61 Mutants Linked to Structural Features of the Switch Regions in the Presence of Raf," Structure 15, 1618-1629 (2007). DOI: 10.1016/j.str.2007.10.011

T. Buonassisi, M. Heuer, A.A. Istratov, M.D. Pickett, M.A. Marcus, B. Lai, Z. Cai, S.M. Heald, E.R. Weber, "Transition metal co-precipitation mechanisms in silicon," Acta Mater. 55 (18), 6119-6126 (2007). DOI: 10.1016/j.actamat.2007.07.030

E. Sethe Burgie, James B. Thoden, Hazel M. Holden, "Molecular architecture of DesV from Streptomyces venezuelae: A PLP-dependent transaminase involved in the biosynthesis of the unusual sugar desosamine," Protein Sci. 16 (5), 887-896 (2007). DOI: 10.1110/ps.062711007

William D. Burgos, John M. Senko, Brian A. Dempsey, Eric E. Roden, James J. Stone, Ken M. Kemner, Shelly D. Kelly, "Soil Humic Acid Decreases Biological Uranium(VI) Reduction by Shewanella putrefaciens CN32," Environ. Eng. Sci. 24 (6), 755-761 (2007). DOI: 10.1089/ees.2006.0009

Leslie A. Bush-Pelc, Francesca Marino, Zhiwei Chen, Agustin O. Pineda, F. Scott Mathews, Enrico Di Cera, "Important Role of the Cys-191-Cys-220 Disulfide Bond in Thrombin Function and Allostery," J. Biol. Chem. 282 (37), 27165-27170 (2007). DOI: 10.1074/jbc.M703202200

R. Callens, C. L'abbe, J. Meersschaut, I. Serdons, W. Sturhahn, T.S. Toellner, "Determination of the magnetic spin direction from the nuclear forward-scattering line intensities," J. Synchrotron Rad. 14 (4), 366-371 (2007). DOI: 10.1107/S0909049507023229

A.J. Campbell, C.T. Seagle, D.L. Heinz, G. Shen, V. Prakapenka, "Partial melting in the iron–sulfur system at high pressure: A synchrotron X-ray diffraction study," Phys. Earth Planet. In. 162 (1-2), 119-128 (2007). DOI: 10.1016/j.pepi.2007.04.001

Elizabeth A. Campbell, Roger Greenwell, Jennifer R. Anthony, Sheng Wang, Lionel Lim, Kalyan Das, Heidi J. Sofia, Timothy J. Donohue, Seth A. Darst, "A Conserved Structural Module Regulates Transcriptional Responses to Diverse Stress Signals in Bacteria," Mol. Cell 27 (5), 793-805 (2007). DOI: 10.1016/j.molcel.2007.07.009

P.A. Candela, C.D. Crummett, D.J. Earnest, M.R. Frank, A.G. Wylie, "Low-pressure decomposition of chrysotile as a function of time and temperature," Am. Mineral. 92, 1704-1713 (2007). DOI: 10.2138/am.2007.2559

Ahmet E. Cansizoglu, Brittany J. Lee, Zi Chao Zhang, Beatriz M.A. Fontoura, Yuh Min Chook, "Structure-based design of a pathway-specific nuclear import inhibitor," Nat. Struct. Mol. Biol. 14 (5), 452-454 (2007). DOI: 10.1038/nsmb1229

A.D. Capili, C.D. Lima, "Structure and analysis of a complex between SUMO and Ubc9 illustrates features of a conserved E2-Ubl interaction," J. Mol. Biol. 369 (3), 608-618 (2007). DOI: 10.1016/j.jmb.2007.04.006

Raanan Carmieli, Todd M. Larsen, George H. Reed, Samir Zein, Frank Neese, Daniella Goldfarb, "The Catalytic Mn [superscript 2+] Sites in the

Enolase-Inhibitor Complex: Crystallography, Single-Crystal EPR, and DFT Calculations," J. Am. Chem. Soc. 129, 4240-4252 (2007). DOI: 10.1021/ja066124e

Christopher J. Carrell, Robert C. Bruckner, David Venci, Gouhua Zhao, Marilyn Schuman Jorns, F. Scott Mathews, "NikD, an Unusual Amino Acid Oxidase Essential for Nikkomycin Biosynthesis: Structures of Closed and Open Forms at 1.15 and 1.90 Å Resolution," Structure 15 (8), 928-941 (2007). DOI: 10.1016/j.str.2007.06.010

Christopher J. Carrell, John K. Ma, William E. Antholine, Jonathan P. Hosler, F. Scott Mathews, Victor L. Davidson, "Generation of Novel Copper Sites by Mutation of the Axial Ligand of Amicyanin. Atomic Resolution Structures and Spectroscopic Properties," Biochemistry-US 46 (7), 1900-1912 (2007). DOI: 10.1021/bi0619674 S0006-2960(06)01967-2

J. Carwardine, N. Arnold., F. Lenkszus, C. Saunders, B. Banerjee, B. Chase, E. Gottschalk, P. Joireman, P. Kasley, S. Lackey, P. McBride, V. Pavlicek, J. Patrick, M. Votava, S. Wolbers, K. Furukawa, S. Michizono, R.S. Larsen, R. Downing, "The ILC Control System Design," Proc. of the 22nd Particle Accelerator Conference (PAC07), IEEE, (2007), 868 - 872.

Jeffrey G. Catalano, Paul Fenter, Changyong Park, "Interfacial water structure on the (0 1 2) surface of hematite: Ordering and reactivity in comparison with corundum," Geochim. Cosmochim. Acta 71 (22), 5313-5324 (2007). DOI: 10.1016/j.gca.2007.09.019

J.G. Catalano, Z. Zhang, C. Park, P. Fenter, M.J. Bedzyk, "Bridging arsenate surface complexes on the hematite (012) surface," Geochim. Cosmochim. Acta 71 (8), 1883-1897 (2007). DOI: 10.1016/j.gca.2007.01.015

Kevin A. Cavicchi, Thomas P. Russell, "Solvent Annealed Thin Films of Asymmetric Polyisoprene-Polylactide Diblock Copolymers," Macromolecules 40 (4), 1181-1186 (2007). DOI: 10.1021/ma061163w

Derek F.J. Ceccarelli, Ivan M. Blasutig, Marilyn Goudreault, Zhiqin Li, Julie Ruston, Tony Pawson, Frank Sicheri, "Non-canonical Interaction of Phosphoinositides with Pleckstrin Homology Domains of Tiam1 and ArhGAP9," J. Biol. Chem. 282 (18), 13864-13874 (2007). DOI: 10.1074/jbc.M700505200

A.J. Celestian, J.B. Parise, R.I. Smith, B.H. Toby, A. Clearfield, "Role of the Hydroxyl-Water Hydrogen-Bond Network in Structural Transitions and Selectivity toward Cesium in Cs[subscript 0.38](D[subscript 1.08]H[subscript 0.54])SiTi[subscript 2]O[subscript 7] . (D[subscript 0.86]H[subscript 0.14)[subscript 2]O Crystalline Silicotitanate," Inorg. Chem. 46 (4), 1081-1089 (2007). DOI: 10.1021/ic0611387

M. Cetinkol, P.L. Lee, A.P. Wilkinson, "Preparation and characterization of In(I)-[beta"]-alumina," MRS Bull. 42 (4), 713-719 (2007). DOI: 10.1016/j.materresbull.2006.07.015

Y.-C. Chae, G. Waldschmidt, V. Dolgashev, "The Wakefield Effects of Pulsed Crab Cavities at the Advanced Photon Source for Short X-ray Pulse Generation," Proc. of the 22nd Particle Accelerator Conference (PAC07), IEEE, (2007), 4339 - 4341.

Y.-C. Chae, Y. Wang, "Impedance Database II for the Advanced Photon Source Storage Ring," Proc. of the 22nd Particle Accelerator Conference (PAC07), IEEE, (2007), 4336 - 4338.

Y.-C. Chae, Y. Wang, A. Xiao, "Single-Bunch Instability Estimates for the 1-nm APS Storage Ring Upgrade with a Smaller Vacuum Chamber," Proc. of the 22nd Particle Accelerator Conference (PAC07), IEEE, (2007), 4330 - 4332.

J. Chakhalian, J.W. Freeland, H.-U. Habermeier, G. Cristiani, G. Khaliullin, M. van Veenendaal, B. Keimer, "Orbital Reconstruction and Covalent Bonding at an Oxide Interface," Science 318, 1114-1117 (2007). DOI: 10.1126/science.1149338

K.-C. Chang, A. Menzel, V. Komanicky, H. You, "Electrosorbed carbon monoxide monolayers on Pt(1 1 1)," Electrochim. Acta 52 (18), 5749-5758 (2007). DOI: 10.1016/j.electacta.2007.01.070

Kinlin L. Chao, Lavanya Muthukumar, Osnat Herzberg, "Structure of Human Hyaluronidase-1, a Hyaluronan Hydrolyzing Enzyme Involved in Tumor Growth and Angiogenesis," Biochemistry-US 46 (23), 6911-6920 (2007). DOI: 10.1021/bi700382g

Karena W. Chapman, Peter J. Chupas, Charles A. Kurtz, Darren R. Locke, John B. Parise, Joseph A. Hriljac, "Hydrostatic low-range pressure applications of the Paris–Edinburgh cell utilizing polymer gaskets for diffuse X-ray scattering measurements," J. Appl. Crystallogr. 40 (1), 196-198 (2007). DOI: 10.1107/S0021889806047923

Mark A. Chappell, Kirk G. Scheckel, "Pyromorphite formation and stability after quick lime neutralisation in the presence of soil and clay sorbents," Environ. Chem. 4 (2), 109-113 (2007). DOI: 10.1071/EN06081

Joon Chatterjee, Sumeet Jain, Frank S. Bates, "Comprehensive Phase Behavior of Poly(isoprene-b-styrene-b-ethylene oxide) Triblock Copolymers," Macromolecules 40 (8), 2882-2896 (2007). DOI: 10.1021/ma062249s

S. Chattopadhyay, S.D. Kelly, T. Shibata, R. Viswanatha, M. Balasubramanian, S. Stoupin, C.U. Segre, D.D. Sarma, "EXAFS Studies of Nanocrystals of Zn[subscript 1−x]Mn[subscript x]O: A Dilute Magnetic Semiconductor Oxide System," X-Ray Absorption Fine Structure - XAFS13, Britt Hedman, Piero Pianetta, eds., 882, AIP, (2007), 809 - 811. DOI: 10.1063/1.2644672

Baoyu Chen, Michaeleen Doucleff, David E. Wemmer, Sacha De Carlo, Hector H. Huang, Eva Nogales, Timothy R. Hoover, Elena Kondrashkina, Liang Guo, B. Tracy Nixon, "ATP Ground- and Transition-States of Bacterial Enhancer Binding AAA+ ATPases Support Complex Formation with Their Target Protein, [sigma]54," Structure 15 (4), 429-440 (2007). DOI: 10.1016/j.str.2007.02.007

Bin Chen, Hengzhong Zhang, Benjamin Gilbert, Jillian F. Banfield, "Mechanism of Inhibition of Nanoparticle Growth and Phase Transformation by Surface Impurities," Phys. Rev. Lett. 98, 106103-1-106103-4 (2007). DOI: 10.1103/PhysRevLett.98.106103

Di Chen, Qiuzhi Cindy Cui, Huanjie Yang, Raul A. Barrea, Fazlul H. Sarkar, Shijie Sheng, Bing Yan, G. Prem Veer Reddy, Q. Ping Dou, "Clioquinol, a Therapeutic Agent for Alzheimer's Disease, Has Proteasome-Inhibitory, Androgen Receptor–Suppressing, Apoptosis-Inducing, and

Antitumor Activities in Human Prostate Cancer Cells and Xenografts," Cancer Res. 67 (4), 1636-1644 (2007). DOI: 10.1158/0008-5472.CAN-06-3546

Lin X. Chen, Dijia Liu, Erik C. Wasinger, Xiaoyi Zhang, Klaus Attenkofer, Guy Jennings, "Ultrafast structural dynamics of photoactive metal complexes in solar hydrogen generation," Solar Hydrogen and Nanotechnology II, Jinghua Guo, eds., 6650, SPIE (2007), 66500I-1 - 66500I-10. DOI: 10.1117/12.745507

L.X. Chen, G.B. Shaw, E.C. Wasinger, X. Zhang, K. Attenkofer, G. Jennings, "Molecular Structural Dynamics of Photoactive Transition Metal Complexes in Solar Energy Conversion Studied by Ultrafast Optical Spectroscopy and LITR-XAS," AIP Proceedings, B. Hedman, P. Pianetta, eds., 882, AIP, (2007), 844 - 848.

Lin X. Chen, Xiaoyi Zhang, Erik C. Wasinger, Klaus Attenkofer, Guy Jennings, Ana Z. Muresan, Jonathan S. Lindsey, "Tracking Electrons and Atoms in a Photoexcited Metalloporphyrin by X-ray Transient Absorption Spectroscopy," J. Am. Chem. Soc. 129, 9616-9618 (2007). DOI: 10.1021/ja072979v

Peng Chen, "Probing the Mechanism of Bacterial Metalloregulation and Virulence Regulation," Masters, University of Chicago, 2007.

X. Chen, T.D. Kim, C.V. Carman, L.Z. Mi, G. Song, T.A. Springer, "Structural plasticity in Ig superfamily domain 4 of ICAM-1 mediates cell surface dimerization," Proc. Natl. Acad. Sci. USA 104 (39), 15358-15363 (2007). DOI: 10.1073/pnas.0707406104

Vadim Cherezov, Daniel M. Rosenbaum, Michael A. Hanson, Soren G.F. Rasmussen, Foon Sun Thian, Tong Sun Kobilka, Hee-Jung Choi, Peter Kuhn, William I. Weis, Brian K. Kobilka, Raymond C. Stevens, "High-Resolution Crystal Structure of an Engineered Human [beta subscript 2]-Adrenergic G Protein–Coupled Receptor," Science 318, 1258-1265 (2007). DOI: 10.1126/science.1150577

Gary N. Chesnut, Nenad Velisavljevic, Lilliana Sanchez, "Static High Pressure X-Ray Diffraction of TI-6AL-4V," Shock Compression of Condensed Matter, M. Elert, M.D. Furnish, R. Chau, N. Holmes, J. Nguyen, eds., 955, AIP, (2007), 27 - 30. DOI: 10.1063/1.2833031

Mariya K. Chhatriwala, Laurie Betts, David K. Worthylake, John Sondek, "The DH and PH Domains of Trio Coordinately Engage Rho GRPases for their Efficient Activation," J. Mol. Biol. 368 (5), 1307-1320 (2007). DOI: 10.1016/j.jmb.2007.02.060

P. Chien, R.A. Grant, R.T. Sauer, T.A. Baker, "Structure and Substrate Specificity of an SspB Ortholog: Design Implications for AAA+ Adaptors," Structure 15, 1265-1305 (2007). DOI: 10.1016/j.str.2007.08.008

Unmesh Chinte, Binal Shah, Yu-Sheng Chen, A. Alan Pinkerton, Constance A. Schall, B. Leif Hanson, "Cryogenic (<20 K) helium cooling mitigates radiation damage to protein crystals," Acta Crystallogr. D D63 (4), 486-492 (2007). DOI: 10.1107/S0907444907005264

Catalin Chiritescu, David G. Cahill, Ngoc Nguyen, David Johnson, Arun Bodapati, Pawel Keblinski, Paul Zschack, "Ultralow Thermal Conductivity in Disordered, Layered WSe[subscript 2] Crystals," Science 315 (5810), 351-353 (2007). DOI: 10.1126/science.1136494

Malcolm H. Chisholm, Judith C. Gallucci, Hongfeng Yin, "18-Membered cyclic esters derived from glycolide and lactide: preparations, structures and coordination to sodium ions," Dalton T. 42, 4811-4821 (2007). DOI: 10.1039/b709081a

Y. Choi, J.S. Jiang, Y. Ding, R.A. Rosenberg, J.E. Pearson, S.D. Bader, A. Zambano, M. Murakami, I. Takeuchi, Z.L. Wang, J.P. Liu, "Role of diffused Co atoms in improving effective exchange coupling in Sm-Co/Fe spring magnets," Phys. Rev. B 75, 104432-1-104432-6 (2007). DOI: 10.1103/PhysRevB.75.104432

Y. Choi, J.S. Jiang, J.E. Pearson, S.D. Bader, J.J. Kavich, J.W. Freeland, J.P. Liu, "Controlled interface profile in Sm–Co/Fe exchange-spring magnets," Appl. Phys. Lett. 91, 072509-1-072509-3 (2007). DOI: 10.1063/1.2769755

Y. Choi, J.S. Jiang, J.E. Pearson, S.D. Bader, J.P. Liu, "Origin of recoil hysteresis loops in Sm–Co/Fe exchange-spring magnets," Appl. Phys. Lett. 91, 022502-1-022502-3 (2007). DOI: 10.1063/1.2752534

Y. Choi, Y.Z. Yoo, O. Chmaissem, A. Ullah, S. Kolesnik, C.W. Kimball, D. Haskel, J.S. Jiang, S.D. Bader, "Ferromagnetic Mn moments at SrRuO[subscript 3]/SrMnO[subscript 3] interfaces," Appl. Phys. Lett. 91, 022503-1-022503-3 (2007). DOI: 10.1063/1.2753100

Maria Chondroudi, Mahalingam Balasubramanian, Ulrich Welp, Wai-K. Kwok, Mercouri G. Kanatzidis, "Mixed Valency in Yb[subscript 7]Co[subscript 4]InGe[subscript 12]: A Novel Intermetallic Compound Stabilized in Liquid Indium," Chem. Mater. 19 (19), 4769-4775 (2007). DOI: 10.1021/cm071687q

Renee Chosed, Diana R. Tomchick, Chad A. Brautigam, Sohini Mukherjee, Veera S. Negi, Mischa Machius, Kim Orth, "Structural Analysis of Xanthomonas XopD Provides Insights into Substrate Specificity of Ubiquitin-like Protein Proteases," J. Biol. Chem. 282 (9), 6773-6782 (2007). DOI: 10.1074/jbc.M608730200

Jill E. Chrencik, Alexei Brooun, Michael I. Recht, George Nicola, Leila K. Davis, Ruben Abagyan, Hans Widmer, Elena B. Pasquale, Peter Kuhn, "Three-dimensional Structure of the EphB2 Receptor in Complex with an Antagonistic Peptide Reveals a Novel Mode of Inhibition," J. Biol. Chem. 282 (50), 36505-36513 (2007). DOI: 10.1074/jbc.M706340200

Peter J. Chupas, Karena W. Chapman, Guy Jennings, Peter L. Lee, Clare P. Grey, "Watching Nanoparticles Grow: The Mechanism and Kinetics for the Formation of TiO[subscript 2]-Supported Platinum Nanoparticles," J. Am. Chem. Soc. 129 (45), 13822-13824 (2007). DOI: 10.1021/ja076437p

Peter J. Chupas, Karena W. Chapman, Peter L. Lee, "Applications of an amorphous silicon-based area detector for high resolution, high sensitivity and fast time-resolved pair distribution function measurements," J. Appl. Crystallogr. 40 (3), 463-470 (2007). DOI: 10.1107/S0021889807007856

C.N. Cionca, D.A. Walko, Y. Yacoby, C. Dorin, J. Mirecki Millunchick, R. Clarke, "Interfacial structure, bonding and composition of InAs and GaSb thin films determined using coherent Bragg rod analysis," Phys. Rev. B 75, 115306-1-115306-7 (2007). DOI: 10.1103/PhysRevB.75.115306

Sara E. Cnudde, Mary Prorok, Qiuyun Dai, Francis J. Castellino, James H. Geiger, "The Crystal Structures of the Calcium-Bound con-G and con-T[K7[gamma]] Dimeric Peptides Demonstrate a Metal-Dependent Helix-Forming Motif," J. Am. Chem. Soc. 129 (6), 1586-1593 (2007). DOI: 10.1021/ja065722q

Eric N. Coker, William A. Steen, James E. Miller, "Zeolite-templated Pt/C electrocatalysts," Micropor. Mesopor. Mat. 104 (1-3), 236-247 (2007). DOI: 10.1016/j.micromeso.2007.02.044

Eric N. Coker, William A. Steen, Jeffrey T. Miller, A. Jeremy Kropf, James E. Miller, "Nanostructured Pt/C electrocatalysts with high platinum dispersions through zeolite-templating," Micropor. Mesopor. Mat. 101 (3), 440-444 (2007). DOI: 10.1016/j.micromeso.2006.12.022

Eric N. Coker, William A. Steen, Jeffrey T. Miller, A. Jeremy Kropf, James E. Miller, "The preparation and characterization of novel Pt/C electrocatalysts with controlled porosity and cluster size," J. Mater. Chem. 17 (31), 3330-3340 (2007). DOI: 10.1039/b703916f

Brian A. Collins, Yuncheng Zhong, Yong S. Chu, Liang He, Frank Tsui, "Anomalous x-ray diffraction study of disorders in epitaxial films of the Heusler alloy Co[subscript 2]MnGe," J. Vac. Sci. Technol. B 25 (3), 999-1003 (2007). DOI: 10.1116/1.2720857

Brett A. Colson, Tanya Bekyarova, Daniel P. Fitzsimonsk, Thomas C. Irving, Richard L. Moss, "Radial Displacement of Myosin Cross-bridges in Mouse Myocardium due to Ablation of Myosin Binding Protein-C," J. Mol. Biol. 367 (1), 36-41 (2007). DOI: 10.1016/j.jmb.2006.12.063

Roxana M. Coman, Arthur Robbins, Maureen M. Goodenow, Robert McKenna, Ben M. Dunn, "Expression, purification and preliminary X-ray crystallographic studies of the human immunodeficiency virus 1 subtype C protease," Acta Crystallogr. F 63, 320-323 (2007). DOI: 10.1107/S174430910701161X

Carlos Contreras-Martel, Adelio Matamala, Carola Bruna, German Poo-Caamano, Daniel Almonacid, Maximiliano Figueroa, Jose Martinez-Oyanedel, Marta Bunster, "The structure at 2 Å resolution of Phycocyanin from Gracilaria chilensis and the energy transfer network in a PC–PC complex," Biophys. Chem. 125 (2-3), 388-396 (2007). DOI: 10.1016/j.bpc.2006.09.014

David R. Cooper, Tomasz Boczek, Katarzyna Grelewska, Malgorzata Pinkowska, Malgorzata Sikorska, Michal Zawadzki, Zygmunt Derewenda, "Protein Crystallization by surface entropy reduction: optimization of the SER strategy," Acta Crystallogr. D 63 (5), 636-645 (2007). DOI: 10.1107/S907444907010931

Julio F. Cordero-Morales, Vishwanath Jogini, Anthony Lewis, Valeria Vasquez, D. Marien Cortes, Benoit Roux, Eduardo Perozo, "Molecular driving forces determining potassium channel slow inactivation," Nat. Struct. Mol. Biol. 14 (11), 1062-1069 (2007). DOI: 10.1038/nsmb1309

Julien Cotelesage, "Structural and functional studies of Phosphoenolpyruvate carboxykinase," Masters, University of Saskatchewan, 2007.

Julien J.H. Cotelesage, Jennifer Puttick, Hughes Goldie, Babak Rajabi, Brian Novakovski, Louis T.J. Delbaere, "How does an enzyme recognize CO[subscript 2]?," Int. J. Biochem. Cell B. 39 (6), 1204-1210 (2007). DOI: 10.1016/j.biocel.2007.03.015

N.P. Coussens, J.C. Mowers, C. McDonald, G. Nunez, S. Ramaswamy, "Crystal structure of the Nod1 caspase activation and recruitment domain," Biochem. Biophys. Res. Commun. 353 (1), 1-5 (2007). DOI: 10.1016/j.bbrc.2006.11.122

Jean-Francois Couture, Evys Collazo, Patricia A. Ortiz-Tello, Joseph S. Brunzelle, Raymond C. Trievel, "Specificity and mechanism of JMJD2A, a trimethyllysine-specific histone demethylase," Nat. Struct. Mol. Biol. 14 (8), 689-695 (2007). DOI: 10.1038/nsmb1273

Brett A. Cromer, Michael A. Gorman, Guido Hansen, Julian J. Adams, Marjorie Coggan, Philip G. Board, Michael W. Parker, "Expression, purification, crystallization and preliminary X-ray diffraction analysis of chloride intracellular channel 2 (CLIC2)," Acta Crystallogr. F 63 (11), 961-963 (2007). DOI: 10.1107/S1744309107049159

Brett A. Cromer, Michael A. Gorman, Guido Hansen, Julian J. Adams, Marjorie Coggan, Dene R. Littler, Louise J. Brown, Michele Mazzanti, Samuel N. Breit, Paul M.G. Curmi, Angela F. Dulhunty, Philip G. Board, Michael W. Parker, "Structure of the Janus Protein Human CLIC2," J. Mol. Biol. 374 (3), 719-731 (2007). DOI: 10.1016/j.jmb.2007.09.041

Jonathan Crowhurst, Alexander Goncharov, Babak Sadigh, Joseph Zaug, Yue Meng, Vitali Prakapenka, "Synthesis and Characterization of Nitrides of Iridium and Palladium," Materials Research at High Pressure, M.R. Manaa, A.F. Goncharov, R.J. Hemley, R. Bini, eds., 987, AIP (2007), online.

B. Roldan Cuenya, A. Naitabdi, J. Croy, W. Sturhahn, J.Y. Zhao, E.E. Alp, R. Meyer, D. Sudfeld, E. Schuster, W. Keune, "Atomic vibrations in iron nanoclusters: Nuclear resonant inelastic x-ray scattering and molecular dynamics simulations," Phys. Rev. B 76, 195422-1-195422-5 (2007). DOI: 10.1103/PhysRevB.76.195422

M.E. Cuff, H. Li, S. Moy, J. Watson, A. Cipriani, A. Joachimiak, "Crystal structure of an acetyltransferase protein from Vibrio cholerae strain N16961," Proteins 69 (2), 422-427 (2007). DOI: 10.1002/prot.21417

Yan Cui, Stefan Vogt, Neal Olson, Andrew G. Glass, Thomas E. Rohan, "Levels of Zinc, Selenium, Calcium, and Iron in Benign Breast Tissue and Risk of Subsequent Breast Cancer," Cancer Epidem. Biomar. 16 (8), 1682-1685 (2007). DOI: 10.1158/1055-9965.EPI-07-0187

Nicholas C. Cunningham, Wei Qiu, Kevin M. Hope, Hanns-Peter Liermann, Yogesh K. Vohra, "Symmetry lowering under high pressure: Structural evidence for f-shell delocalization in heavy rare earth metal terbium," Phys. Rev. B 76, 212101-1-212101-4 (2007). DOI: 10.1103/PhysRevB.76.212101

Leslie Cuthbertson, Matthew S. Kimber, Chris Whitfield, "Substrate binding by a bacterial ABC transporter involved in polysaccharide export," Proc. Natl. Acad. Sci. USA 104 (49), 19529-19534 (2007). DOI: 10.1073/pnas.0705709104

J. Alejandro D'Aquino, Judith R. Lattimer, Andrew Denninger, Katharine E. D'Aquino, Dagmar Ringe, "Role of the N-Terminal Helix in the Metal Ion-Induced Activation of the Diphtheria Toxin Repressor DtxR," Biochemistry-US 46 (42), 11761-11770 (2007). DOI: 10.1021/bi7007883

Harry A. Dailey, Chia-Kuei Wu, Peter Horanyi, Amy E. Medlock, Wided Najahi-Missaoui, Amy E. Burden, Tamara A. Dailey, John Rose, "Altered Orientation of Active Site Residues in Variants of Human Ferrochelatase. Evidence for a Hydrogen Bond Network Involved in Catalysis," Biochemistry-US 46 (27), 7973-7979 (2007). DOI: 10.1021/bi700151fS0006-2960(70)00151-4

Shaodong Dai, Rosmarie Friemann, Dominique A. Glauser, Florence Bourquin, Wanda Manieri, Peter Schurmann, Hans Eklund, "Structural snapshots along the reaction pathway of ferredoxin–thioredoxin reductase," Nature 448, 92-96 (2007). DOI: 10.1038/nature05937

Michael J. Daly, Elena K. Gaidamakova, Vera Y. Matrosova, Alexander Vasilenko, Min Zhai, Richard D. Leapman, Barry Lai, Bruce Ravel, Shu-Mei W. Li, Kenneth M. Kemner, James K. Fredrickson, "Protein Oxidation Implicated as the Primary Determinant of Bacterial Radioresistance," PLoS Biol. 5 (4), 0769-0779 (2007). DOI: :10.1371/journal.pbio.0050092

Stephen M. Danauskas, Maria K. Ratajczak, Yuji Ishitsuka, Jeffrey Gebhardt, David Schultz, Mati Meron, Binhua Lin, Ka Yee C. Lee, "Monitoring x-ray beam damage on lipid films by an integrated Brewster angle microscope/x-ray diffractometer," Rev. Sci. Instrum. 78, 103705-1-103705-9 (2007). DOI: 10.1063/1.2796147

L.R. Danielson, K. Righter, S. Sutton, M. Newville, L. Le, "The Oxidation State of Tungsten in Iron Bearing and Iron Free Silicate Glasses: Results from W L-Edge XANES Measurements," Lunar and Planetary Science XXXVIII, LPI, (2007), 2113.

Gregory Darnell, Joseph P.R.O. Orgel, Reinhard Pahl, Stephen C. Meredith, "Flanking Polyproline Sequences Inhibit [beta]-Sheet Structure in Polyglutamine Segments by Inducing PPII-like Helix Structure," J. Mol. Biol. 374 (3), 688-704 (2007). DOI: 10.1016/j.jmb.2007.09.023

Amaresh Das, Zheng-Qing Fu, Wolfram Tempel, Zhi-Jie Liu, Jessie Chang, Lirong Chen, Doowon Lee, Weihong Zhou, Hao Xu, Neil Shaw, John P. Rose, Lars G. Ljungdahl, Bi-Cheng Wang, "Characterization of a corrinoid protein involved in the C1 metabolism of strict anaerobic bacterium Moorella Thermoacetica," Proteins 67 (1), 167-176 (2007). DOI: 10.1002/prot.21094

Kalyan Das, StefanG. Sarafianos, Arthur D. Clark Jr., Paul L. Boyer, Stephen H. Hughes, Eddy Arnold, "Crystal Structures of Clinically Relevant Lys103Asn/Tyr181Cys Double Mutant HIV-1 Reverse Transcriptase in Complexes with ATP and Non-nucleoside Inhibitor HBY 097," J. Mol. Biol. 365 (1), 77-89 (2007). DOI: 10.1016/j.jmb.2006.08.097

Chen Davidovich, Anat Bashan, Tamar Auerbach-Nevo, Rachel D. Yaggie, Richard R. Gontarek, Ada Yonath, "Induced-fit tightens pleuromutilins binding to ribosomes and remote interactions enable their selectivity," Proc. Natl. Acad. Sci. USA 104 (11), 4291-4296 (2007). DOI: 10.1073pnas.0700041104

Melissa L. Davis, James B. Thoden, Hazel M. Holden, "The X-ray Structure of dTDP-4-Keto-6-deoxy-D-glucose-3,4-ketoisomerase," J. Biol. Chem. 282 (26), 19227-19236 (2007). DOI: 10.1074/jbc.M702529200

M.R. Daymond, M.L. Young, J.D. Almer, D.C. Dunand, "Strain and texture evolution during mechanical loading of a crack tip in martensitic shape-memory NiTi," Acta Mater. 55 (11), 3929-3942 (2007). DOI: 10.1016/j.actamat.2007.03.013

Martin D. de Jonge, Chanh Q. Tran, Christopher T. Chantler, Zwi Barnea, Bipin B. Dhal, David Paterson, Elliot P. Kanter, Stephen H. Southworth, Linda Young, Mark A. Beno, Jennifer A. Linton, Guy Jennings, "Measurement of the x-ray mass attenuation coefficient and determination of the imaginary component of the atomic form factor of tin over the energy range of 29–60 keV," Phys. Rev. A 75, 032702-1-032702-14 (2007). DOI: 10.1103/PhysRevA.75.032702

M.D. de Jonge, S. Vogt, D. Legnini, I. McNulty, C. Rau, D. Paterson, B. Hornberger, C. Holzner, C. Jacobsen, "A method for phase reconstruction from measurements obtained using a configured detector with a scanning transmission x-ray microscope," Nucl. Instrum. Methods A 582 (1), 218-220 (2007). DOI: 10.1016/j.nima.2007.08.111

Erik W. Debler, Gunnar F. Kaufmann, Robert N. Kirchdoerfer, Jenny M. Mee, Kim D. Janda, Ian A. Wilson, "Crystal structures of a quorum-quenching antibody," J. Mol. Biol. 368 (5), 1392-1402 (2007). DOI: 10.1016/j.jmb.2007.02.081

G. Decker, P. Den Hartog, O. Singh, G. Rosenbaum, "Progress Toward a Hard X-ray Insertion Device Beam Position Monitor at the Advanced Photon Source," Proc. of the 22nd Particle Accelerator Conference (PAC07), IEEE, (2007), 4342 - 4344.

Olga Degtyareva, Eduardo R. Hernandez, Jorge Serrano, Maddury Somayazulu, Ho-kwang Mao, Eugene Gregoryanz, Russell J. Hemley, "Vibrational dynamics and stability of the high-pressure chain and ring phases in S and Se," J. Chem. Phys. 126, 084503-1-084503-11 (2007). DOI: 10.1063/1.2433944

Olga Degtyareva, Miguel Martinez Canales, Aitor Bergara, Xiao-Jia Chen, Yang Song, Viktor V. Struzhkin, Ho-kwang Mao, Russell J. Hemley, "Crystal structure of SiH[subscript 4] at high pressure," Phys. Rev. B 76, 064123-1-064123-4 (2007). DOI: 10.1103/PhysRevB.76.064123

R. Dejus, I. Vasserman, "Phasing of Two Undulators with Different K Values at the Advanced Photon Source," Proc. of the 22nd Particle Accelerator Conference (PAC07), IEEE, (2007), 1130 - 1132.

Ranjit K. Deka, Chad A. Brautigam, Farol L. Tomson, Sarah B. Lumpkins, Diana R. Tomchick, Mischa Machius, Michael V. Norgard, "Crystal Structure of the Tp34 (TP0971) Lipoprotein of Treponema pallidum: IMPLICATIONS OF ITS METAL-BOUND STATE AND AFFINITY FOR HUMAN LACTOFERRIN," J. Biol. Chem. 282 (8), 5944-5958 (2007). DOI: 10.1074/jbc.M610215200

Shahab Derakhshan, Abdeljalil Assoud, Katja M. Kleinke, Trupti Khaire, Ahmad S. Masadeh, Simon J.L. Billinge, Holger Kleinke, "Square net distortion engineering in the ternary variants of titanium antimonide, Ti[subscript 2-delta]M[subscript delta]Sb (M=Zr Hf)," Intermetallics 15 (8), 1071-1077 (2007). DOI: 10.1016/j.intermet.2006.12.011

Darrell Desveaux, Alex U. Singer, Ai-Jiuan Wu, Brian C. McNulty, Laura Musselwhite, Zachary Nimchuk, John Sondek, Jeffery L. Dangl, "Type III Effector Activation via Nucleotide Binding, Phosphorylation, and Host Target Interaction," PLoS Pathogens 3 (3), 0456-0469 (2007). DOI: 10.1371/journal.ppat.0030048

Sanghamitra Dey, Zhiqin Hu, Xiao Lan Xu, James C. Sacchettini, Gregory A. Grant, "The Effect of Hinge Mutations on Effector Binding and Domain Rotation in Escherichia coli D-3-Phosphoglycerate Dehydrogenase," J. Biol. Chem. 282 (25), 18418-18426 (2007). DOI: 10.1074/jbc.M701174200

N. DiMonte, "The P0 Feedback Control System Blurs the Line between IOC and FPGA," Proc. of the 22nd Particle Accelerator Conference (PAC07), IEEE, (2007), 431 - 433.

Yang Ding, Rajeev Ahuja, Jinfu Shu, Paul Chow, Wei Luo, Ho-kwang Mao, "Structural Phase Transition of Vanadium at 69 GPa," Phys. Rev. Lett. 98, 085502-1-085502-4 (2007). DOI: 10.1103/PhysRevLett.98.085502

W. Dmowski, T. Egami, "Observation of structural anisotropy in metallic glasses induced by mechanical deformation," J. Mater. Res. 22 (2), 412-418 (2007). DOI: 10.15557/JMR.2007.0043

W. Dmowski, T. Egami, K. Swider-Lyons, W.-F. Yan, S. Dai, S. Overbury, "Local atomic structure in disordered and nanocrystalline catalytic materials," Z. Kristallogr. 222, 617-624 (2007). DOI: 10.1524/zkri.2007.222.11.617

Ninh Doan, Peter G.W. Gettins, "Human[alpha subscript 2]-macroglobulin is composed of multiple domains, as predicted by homology with complement component C3," Biochem. J. 407, 23-30 (2007). DOI: 10.1042/BJ20070764

Tabbetha A. Dobbins, Edward L. Bruster, Ejiroghene U. Oteri, Jan Ilavsky, "Ultrasmall-angle X-ray scattering (USAXS) studies of morphological trends in high energy milled NaAlH[subscript 4] powders," J. Alloy Comp. 446, 248-254 (2007). DOI: 10.1016/j.jallcom.2007.02.161

V. Dolgashev, M. Borland, G. Waldschmidt, "RF Design of Normal Conducting Deflecting Structures for the Advanced Photon Source," Proc. of the 22nd Particle Accelerator Conference (PAC07), IEEE, (2007), 2427 - 2429.

D. Eric Dollins, Joshua J. Warren, Robert M. Immormino, Daniel T. Gewirth, "Structures of GRP94-Nucleotide Complexes Reveal Mechanistic Differences between the hsp90 Chaperones," Mol. Cell 28, 41-56 (2007). DOI: 10.1016/j.molcel.2007.08.024

G. Dong, M. Medkova, P. Novick, K.M. Reinisch, "A Catalytic Coiled Coil: Structural Insights into the Activation of the Rab GTPase Sec4p by Sec2p," Mol. Cell 25 (3), 455-462 (2007).

J.C. Dooling, F.R. Brumwell, L.I. Donley, K.C. Harkay, R.L. Kustom, M.K. Lien, G.E. McMichael, M.E. Middendorf, A. Nassiri, S. Wang, "Observations of Rising Tune During the Injection Instability of IPNS RCS Proton Bunch," Proc. of the 22nd Particle Accelerator Conference (PAC07), IEEE, (2007), 4345 - 4347.

D.B. Drazkowski, "Characterization of the Thermodynamics and Deformation Behavior of Styrene-Butadiene-Styrene Grafted with Polyhedral Oligomeric Silsesquioxanes," Ph.D., Michigan State University, 2007.

Daniel B. Drazkowski, Andre Lee, Timothy S. Haddad, "Morphology and Phase Transitions in Styrene-Butadiene-Styrene Triblock Copolymer Grafted with Isobutyl-Substituted Polyhedral Oligomeric Silsesquioxanes," Macromolecules 40 (8), 2798-2805 (2007). DOI: 10.1021/ma062393d

T. Droubay, K.M. Rosso, S.M. Heald, D.E. McCready, C.M. Wang, S.A. Chambers, "Structure, magnetism, and conductivity in epitaxial Ti-doped [alpha]-Fe[subscript 2]O[subscript 3] hematite: Experiment and density functional theory calculations," Phys. Rev. B 75, 104412-1-104412-7 (2007). DOI: 10.1103/PhysRevB.75.104412

L. Dubrovinsky, N. Dubrovinskaia, O. Narygina, I. Kantor, A. Kuznetzov, V.B. Prakapenka, L. Vitos, B. Johansson, A.S. Mikhaylushkin, S.I. Simak, I.A. Abrikosov, "Body-Centered Cubic Iron-Nickel Alloy in Earth's Core," Science 316 (5833), 1880-1883 (2007). DOI: 10.1126/science.1142105

David M. Duda, Robert C.A.M. van Waardenburg, Laura A. Borg, Sierra McGarity, Amanda Nourse, M.Brett Waddell, Mary-Ann Bjornsti, Brenda A. Schulman, "Structure of a SUMO-binding-motif Mimic Bound to Smt3p-Ubc9p: Conservation of a Non-covalent Ubiquitin-like Protein-E2 Complex as a Platform for Selective Interactions within a SUMO Pathway," J. Mol. Biol. 369 (3), 619-630 (2007). DOI: 10.1016/j.jmb.2007.04.007

Martine C. Duff, Douglas B. Hunter, Patterson Nuessle, David R. Black, Harold Burdette, Joseph Woicik, Arnold Burger, Michael Groza, "Synchrotron X-ray Based Characterization of CdZnTe Crystals," J. Electro. Mater. 36 (8), 1092-1097 (2007). DOI: 10.1007/s11664-007-0181-x

Eric M. Dufresne, B.W. Adams, E.C. Landahl, "A study of laser-generated strain fields with X-ray microdiffraction," Nucl. Instrum. Methods A 582 (1), 205-207 (2007). DOI: 10.1016/j.nima.2007.08.138

Eric M. Dufresne, Dohn A. Arms, Eric C. Landahl, Donald A. Walko, "Impact of Pressure Regulation of Cryogenic Fluids and EPICS EPID Feedback on the Monochromatic Beam Position Stability of the 7ID Beamline at the Advanced Photon Source," SYNCHROTRON RADIATION INSTRUMENTATION: Ninth International Conference on Synchrotron Radiation Instrumentation, Jae-Young Choi, Seungyu Rah, eds., 879, American Institue of Physics, (2007), 950 - 953. DOI: 10.1063/1.2436219

Eric M. Dufresne, Dohn A. Arms, Eric C. Landahl, Donald A. Walko, "The Impact of Pressure Regulation of Cryogenics Fluids and EPICS PID Feedback on the Monochromatic Beam Position Stability," SYNCHROTRON RADIATION INSTRUMENTATION: Ninth International Conference on Synchrotron Radiation Instrumentation, Jae-Young Choi, Seungyu Rah, eds., 879, Springer, (2007), 950 - 953.

Eric M. Dufresne, Ali Khounsary, "Observation of a tilted Gaussian beam on the 7ID beamline of the Advanced Photon Source," Nucl. Instrum. Methods A 582 (1), 63-65 (2007). DOI: 10.1016/j.nima.2007.08.063

Eric M. Dufresne, Eric C. Landahl, Bernhard Adams, David Fritz, Sooheyong Lee, David Reis, "Studies of Ultrafast fs-laser Generated Strain

Fields with Coherent X-rays," SYNCHROTRON RADIATION INSTRUMENTATION: Ninth International Conference on Synchrotron Radiation Instrumentation, Jae-Young Choi, Seungyu Rah, eds., 879, Springer, (2007), 1210 - 1213.

Thomas Durek, Vladimir Yu. Torbeev, Stephen B.H. Kent, "Convergent chemical synthesis and high-resolution x-ray structure of human lysozyme," Proc. Natl. Acad. Sci. USA 104 (12), 4846-4851 (2007). DOI: 10.1073/pnas.0610630104

Michael P. Dwyer, Kamil Paruch, Carmen Alvarez, Ronald J. Doll, Kerry Keertikar, Jose Duca, Thierry O. Fischmann, Alan Hruza, Vincent Madison, Emma Lees, David Parry, Wolfgang Seghezzi, Nicole Sgambellone, Frances Shanahan, Derek Wiswell, Timothy J. Guzi, "Versatile templates for the development of novel kinase inhibitors: Discovery of novel CDK inhibitors," Bioorg. Med. Chem. Lett. 17 (22), 6216-6219 (2007). DOI: 10.1016/j.bmcl.2007.09.018

Kevin D. Dykstra, Liangqin Guo, Elizabeth T. Birzin, Wanda Chan, Yi Tien Yang, Edward C. Hayes, Carolyn A. DaSilva, Lee-Yuh Pai, Ralph T. Mosley, Bryan Kraker, Paula M.D. Fitzgerald, Frank DiNinno, Susan P. Rohrer, James M. Schaeffer, Milton L. Hammonda, "Estrogen receptor ligands. Part 16:

Advanced Photon Source
Argonne National Laboratory
9700 S. Cass Ave.
Argonne, IL 60439 USA

www.anl.gov
www.aps.anl.gov